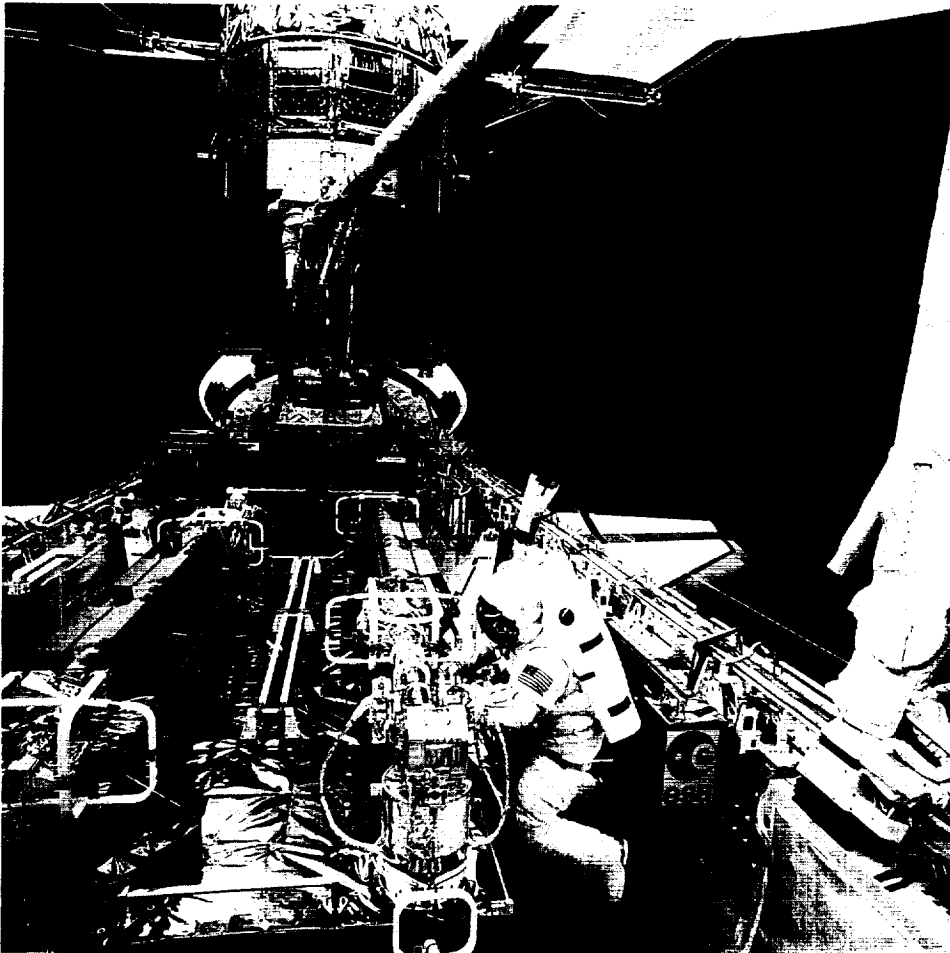


Proceedings of the First Biennial Space Biomedical Investigators' Workshop

January 11-13, 1999

League City, Texas





390995
P

Proceedings

First Biennial Space Biomedical Investigators' Workshop

**January 11-13, 1999
League City, Texas**

WORKSHOP STEERING COMMITTEE

Alfred C. Coats, M.D., Chair
John B. Charles, Ph.D.
Lauren Leveton, Ph.D.
William Paloski, Ph.D.
Judith L. Robinson, Ph.D.
Charles F. Sawin, Ph.D.
Victor Schneider, M.D.
Ronald J. White, Ph.D.

WORKSHOP LOGISTICS COMMITTEE

Terri Jones, Workshop Coordinator
Tonya Hardin
Dana Nelson
Kay Nute
Gail Pacetti

National Aeronautics and Space Administration
Lyndon B. Johnson Space Center
Houston, Texas 77058

Universities Space Research Association Division of Space Life Sciences
3600 Bay Area Boulevard
Houston, Texas 77058

Universities Space Research Association Division of Space Life Sciences operates under
Cooperative Agreement NCC9-41 with the National Aeronautics and Space Administration.

Papers in this volume may be cited as:

Author: Title of paper. Proceedings. First Biennial Space Biomedical Investigators' Workshop,
January 11-13, 1999, League City, Texas, pp. xxx.

TABLE OF CONTENTS

FOREWORD	1
PLENARY PRESENTATIONS	3
LIFE SCIENCES IN NASA'S MISSION <i>A.E. Nicogossian</i>	4
JSC, NASA LEAD CENTER: OVERVIEW OF HUMAN SPACE LIFE SCIENCES PROGRAMS OFFICE (HLSPO) <i>C. Stegemoeller</i>	12
THE HUMAN SPACE LIFE SCIENCES CRITICAL PATH ROADMAP PROJECT: A STRATEGY FOR HUMAN SPACE FLIGHT THROUGH EXPLORATION-CLASS MISSIONS <i>C.F. Sawin</i>	19
NASA JOHNSON SPACE CENTER BIOMEDICAL RESEARCH RESOURCES <i>W.H. Paloski</i>	38
HYPERGRAVITY FACILITIES: EXTENDING KNOWLEDGE OVER THE CONTINUUM OF GRAVITY <i>K.A. Souza</i>	46
TASK FORCE REPORT ON COUNTERMEASURES, FEBRUARY 1997 <i>K.A. Baldwin</i>	57
A STRATEGY FOR RESEARCH IN SPACE BIOLOGY AND MEDICINE IN THE NEW CENTURY <i>M.J. Osborn</i>	71
HUMAN HEALTH AND PERFORMANCE ASPECTS OF MARS DESIGN REFERENCE MISSION OF JULY, 1997 <i>J.B. Charles</i>	80
NATIONAL SPACE BIOMEDICAL RESEARCH INSTITUTE <i>L.R. Young</i>	94
ACCELERATOR FACILITIES FOR RADIATION RESEARCH <i>F.A. Cucinotta</i>	100
THE ROTATING ROOM FACILITY OF THE ASHTON GRAYBIEL SPATIAL ORIENTATION LABORATORY <i>P. DiZio</i>	106

SCIENTIFIC SESSIONS

BAROPHYSIOLOGY 113

BAROPHYSIOLOGY SESSION SUMMARY 114

ROLE OF INFLAMMATORY RESPONSE IN EXPERIMENTAL DECOMPRESSION SICKNESS
B.D. Butler, T. Little 116

QUANTITATIVE PREDICTION OF PULMONARY OXYGEN POISONING STRESS IN HUMAN EXPOSURES TO CHANGING DEGREES OF INSPIRATORY HYPEROXIA
C. J. Lambertsen, J. M. Clark, E. Hopkin 120

STAGED DECOMPRESSION TO A 3.5 PSI EVA SUIT USING AN ARGON-OXYGEN (ARGOX) BREATHING MIXTURE
A.A. Pilmanis, K.M. Krause, J.T. Webb, L.J. Petropoulos, N. Kannan 124

BAROPHYSIOLOGY AND BIOPHYSICS
M. R. Powell 127

AN UNDERSTANDING OF DECOMPRESSION PHYSIOLOGY LEADS TO SAFER AND MORE EFFICIENT EXTRAVEHICULAR ACTIVITY (EVA)
R.D. Vann, W.A. Gerth 132

BEHAVIOR, PERFORMANCE, AND HUMAN FACTORS I (BEHAVIOR & PERFORMANCE) 135

BEHAVIOR, PERFORMANCE, AND HUMAN FACTORS SESSION SUMMARY 136

STABILITY AND PRECISION OF PERFORMANCE DURING SPACE FLIGHT
J.V.Brady, T.H. Kelly, R.D. Hienz 139

MONITORING AND CORRECTING AUTONOMIC FUNCTION ABOARD MIR: NASA TECHNOLOGY USED IN SPACE AND ON EARTH TO FACILITATE ADAPTATION.
P. Cowings, W. Toscano, B. Taylor, C. DeRoshia, L. Kornilova, I. Koslovskaya, N. Miller 142

COGNITIVE PERFORMANCE IN SEVEN SHUTTLE ASTRONAUTS
D. R. Eddy, S. G. Schiflett, R. E. Schlegel, R. L. Shehab 145

EFFECTS OF PROMETHAZINE ON PERFORMANCE DURING SIMULATED SHUTTLE LANDINGS
D.L. Harm, L. Putcha, B. K. Sekula, K. L. Berens 148

INTERACTIONS OF CREWMEMBERS AND MISSION CONTROL PERSONNEL DURING SHUTTLE/MIR MISSIONS <i>N. Kanas, V. Salnitskiy, E. Grund, V. Gushin, O. Kozerenko, C. Marmar, A. Sled, D. Weiss</i>	150
PREDICTORS OF BEHAVIOR AND PERFORMANCE DURING LONG DURATION SPACE MISSIONS: THE ANTARCTIC – SPACE ANALOG PROGRAM (ASAP) <i>L.A. Palinkas, E.K.E. Gunderson, J.C. Johnson, A.W. Holland, C. Miller</i>	152
NASA PERFORMANCE ASSESSMENT WORKSTATION: A TOOL FOR ASTRONAUT COGNITIVE PERFORMANCE EVALUATION <i>R.E. Schlegel, R.L. Shehab, S.G. Schiflett, and D.R. Eddy</i>	154
COGNITIVE PERFORMANCE ASSESSMENT WITH A BED REST ANALOG FOR MICROGRAVITY <i>R.L. Shehab, R.E. Schlegel, S.G. Schiflett, D.R. Eddy</i>	158
REVIEW AND ANALYSIS OF DIARIES MAINTAINED BY THE LEADERS AND PHYSICIANS OF FRENCH REMOTE DUTY STATIONS <i>J. Stuster, C. Bachelard, P. Suedfeld</i>	162
PSYCHOLOGICAL ADAPTATION TO EXTREME ENVIRONMENTS: EFFECTS OF TEAM COMPOSITION ON INDIVIDUAL ADAPTATION <i>J. Wood, S.J. Hysong, D.J. Lugg, D.L. Harm</i>	164
BEHAVIOR, PERFORMANCE, AND HUMAN FACTORS II (HUMAN FACTORS).....	166
MISSION CONTROL INFORMATION FLOW ISSUES <i>Barrett S. Caldwell</i>	167
MICROGRAVITY WORKSTATION AND RESTRAINT EVALUATIONS <i>C. Chmielewski, M. Whitmore, F. Mount</i>	170
NEUROPHYSIOLOGICAL INDICES OF SUSTAINED FOCUSED ATTENTION: APPLICATION TO MONITORING COGNITIVE LOAD, OPERATIONAL FATIGUE, AND OTHER ENVIRONMENTAL STRESSORS <i>A. Gevins, M.E. Smith, L. McEvoy, H. Brown</i>	173
AN EVA SUIT FATIGUE, STRENGTH, AND REACH MODEL <i>J.C. Maida</i>	175
NONINVASIVE MOTION CAPTURE AND ANALYSIS <i>D. Metaxas</i>	176
MEASURING ASTRONAUT PERFORMANCE IN MICROGRAVITY: LOADS AND MODELING <i>D. Newman, S. Beck, A. Amir, G. Baroni, G. Ferrigno, A. Pedotti</i>	179

EVALUATIONS OF THREE METHODS FOR REMOTE TRAINING <i>B. Woolford, C. Chmielewski, A. Pandya, J. Adolf, M. Whitmore, A. Berman, J. Maida</i>	182
BONE	184
BONE SESSION SUMMARY	185
BONE DENSITY AND HIGH SALT DIETS IN A SPACE FLIGHT MODEL <i>S.B. Arnaud, M. Navidi, M.T.C. Liang, I. Wolinsky</i>	192
FEMORAL VEIN LIGATION INCREASES BONE MASS IN THE HINDLIMB SUSPENDED RAT <i>A.P. Bergula, W. Huang, J.A. Frangos</i>	194
THE EFFECT OF SKELETAL UNLOADING ON BONE FORMATION: ROLE OF IGF-I. <i>D.D. Bikle, P. Kostenuik, E.M. Holton, B.P. Halloran</i>	198
ALTERATIONS IN pQCT-DERIVED BONE GEOMETRY AND DENSITY VERSUS MECHANICAL STRUCTURAL PROPERTIES OF THE FEMORAL NECK IN SENESCENT RATS <i>S.A. Bloomfield, H.A. Hogan, E.T. Dresser, J.A. Groves</i>	200
COMPACT, HIGH PRECISION, MULTIPLE PROJECTION DEXA SCANNER FOR MEASUREMENT OF BONE AND MUSCLE LOSS DURING PROLONGED SPACEFLIGHT <i>H. K. Charles, Jr., T. J. Beck, H. S. Feldmesser, T. C. Magee, V. L. Pisacane</i>	202
THE ROLE OF CALCIUM IN THE RESPONSE OF OSTEOBLASTS TO MECHANICAL STIMULATION <i>R.L. Duncan, M.C. Farach-Carson and F.M. Pavalko</i>	205
EFFECT OF SPACEFLIGHT ON EXTRACELLULAR MATRIX IN OSTEOBLASTS GROWTH ACTIVATED UNDER MICROGRAVITY CONDITIONS <i>M.H. Fulford, V. Gilbertson</i>	208
EFFECTS OF SPACEFLIGHT ON BONE: THE RAT AS AN ANIMAL MODEL FOR HUMAN BONE LOSS <i>B. Halloran, T. Weider, E. Morey-Holton</i>	209
EFFECTS OF SPACEFLIGHT ON THE ATTACHMENT OF MUSCLES TO THE TIBIA, FIBULA AND CALCANEUS <i>R. B. Johnson, A. K. Tsao, K. R. St. John, R. A. Betcher, M. A. Tucci, D. E. Parsell, X. Dai, L. D. Zardiackas, H. A. Benghuzzi</i>	211

TRANSGENIC MARKERS OF LINEAGE PROGRESSION IN MECHANICALLY LOADED BONES <i>I. Kalajic, J. Terzic, K. Mack, D. Visnjic, A. Mapta, G. Gronowicz, S. Clark, J. Yeh, D. Rowe</i>	214
COMMON MOLECULAR EVENTS BY HORMONES AND MECHANICAL STRAIN REGULATE INSULIN-LIKE GROWTH FACTOR-I EXPRESSION IN OSTEOBLASTS <i>T.L. McCarthy, Y. Chen, C. Ji, M. Centrella</i>	215
NOVEL RECEPTOR-BASED COUNTERMEASURES TO MICROGRAVITY-INDUCED BONE LOSS <i>B.W. O'Malley, C.L. Smith, N.L. Weigel, E.M. Brown</i>	218
DEVELOPMENTAL REGULATION OF THE COLLAGENASE-3 PROMOTER IN OSTEOBLASTS <i>N.C. Partridge, Y. Yang, R.C. D'Alonzo, and S.K Winchester</i>	222
EXERCISE COUNTERMEASURES FOR BONE LOSS DURING SPACE FLIGHT: A METHOD FOR THE STUDY OF GROUND REACTION FORCES AND THEIR IMPLICATIONS FOR BONE STRAIN <i>M. Peterman, J. L. McCrory, N. A. Sharkey, S. Piazza, P. R. Cavanagh</i>	224
EXPRESSION OF NOVEL GENE PRODUCTS UPREGULATED BY DISUSE IS NORMALIZED BY AN OSTEOGENIC MECHANICAL STIMULUS: EVIDENCE FOR THE MOLECULAR BASIS OF A LOW LEVEL BIOMECHANICAL COUNTERMEASURE FOR OSTEOPOROSIS? <i>C. Rubin, J. Zhi, G. Xu, M. Cote, K. McLeod, M. Hadjiargyrou</i>	228
SKELETAL STRUCTURAL CONSEQUENCES OF REDUCED GRAVITY ENVIRONMENTS <i>C.B. Ruff, T.J. Beck, D. Newman, M. Oden, G. Shaffner, A. LeBlanc, L. Shackelford, N. Rianon</i>	232
THE EFFECTS OF PARTIAL MECHANICAL LOADING AND IBANDRONATE ON SKELETAL TISSUES IN THE ADULT RAT HINDQUARTER SUSPENSION MODEL OF MICROGRAVITY <i>L. Schultheis, J. Shapiro, S. Bloomfield, N. Fedarko, M. Thierry-Palmer, C. Ruff, J. Ruiz</i>	234
BONE LOSS IN SPACE: SHUTTLE/MIR EXPERIENCE AND BED REST COUNTERMEASURE PROGRAM <i>L.C. Shackelford, A. LeBlanc, A. Feiveson, V. Oganov</i>	235
ALTERED BONE CELL METABOLISM DURING SPACEFLIGHT <i>R.T. Turner</i>	236

NON-INVASIVE INVESTIGATION OF BONE ADAPTATION IN HUMANS TO MECHANICAL LOADING <i>R. Whalen</i>	239
RENAL STONE RISK DURING SPACE FLIGHT <i>P.A. Whitson, R.A. Pietrzyk, C.F. Sams, J.A. Jones</i>	242
BONE PROTEOGLYCAN CHANGES DURING SKELETAL UNLOADING <i>M. Yamauchi, K. Uzawa, S. Pornprasertsuk, S. Arnaud, R. Grindeland, W. Grzesik</i>	243
THE EFFECTS OF TWELVE WEEKS OF BEDREST ON BONE HISTOLOGY, BIOCHEMICAL MARKERS OF BONE TURNOVER, AND CALCIUM HOMEOSTASIS IN ELEVEN NORMAL SUBJECTS <i>J.E. Zerwekh, L.A. Ruml, F. Gottschalk, C.Y.C. Pak</i>	245
CARDIOVASCULAR	248
CARDIOVASCULAR SESSION SUMMARY	249
DIRECT CLONING OF GENES REGULATED BY MECHANICAL LOAD <i>M. Abdellatif, M.D. Schneider</i>	257
MECHANISMS FOR LOAD CONTROL OF CARDIAC MASS: CELL CULTURE STUDIES IN ADULT CARDIOMYOCYTES USING A 3-D COLLAGEN MATRIX <i>C. F. Baicu, J. H. Turner, V. D. Young, M. Barnes, M. R. Zile</i>	258
VASCULAR REACTIVITY IN A RAT MODEL OF MICROGRAVITY <i>D. Berkowitz, L. Marucci, E. Asplund, B. Winters, A. Szumski, D. Nyhan, A. Shoukas</i>	259
APPLICATION OF ACUTE MAXIMAL EXERCISE TO ENHANCE MECHANISMS UNDERLYING BLOOD PRESSURE REGULATION AND ORTHOSTATIC TOLERANCE AFTER EXPOSURE TO SIMULATED MICROGRAVITY <i>V.A. Convertino, K.A. Engelke, F. Doerr</i>	260
HEAD-OUT WATER IMMERSION IN THE PRIMATE AS A MODEL FOR THE CARDIOVASCULAR/RENAL EFFECTS OF μ G <i>K.G. Cornish, K. Hughes</i>	263
POTENTIAL MECHANISM LEADING TO IMPAIRED THERMOREGULATION FOLLOWING MICROGRAVITY EXPOSURE. <i>C.G. Crandall, R.A. Etzel</i>	267
AUTONOMIC CONSEQUENCES OF MICROGRAVITY EXPOSURE <i>D.L. Eckberg</i>	271
GENDER-RELATED DIFFERENCES IN CARDIOVASCULAR RESPONSES TO ORTHOSTATIC STRESS <i>J.M. Fritsch-Yelle, D.S. D'Aunno, W.W. Waters, S. Freeman-Perez</i>	274

HEART RATE DYNAMICS DURING MICROGRAVITY: BEDREST AND SPACEFLIGHT STUDIES <i>A.L. Goldberger</i>	276
EXERCISE TRAINING DURING +Gz ACCELERATION <i>J.E. Greenleaf, J.L. Chou, S.R. Simonson, C.G.R. Jackson, P.R. Barnes</i>	278
MECHANISMS UNDERLYING ALTERED ARTERIAL BAROREFLEX FUNCTION IN HINDLIMB UNLOADED RATS <i>E.M. Hassler, J.A. Moffitt, J.T. Cunningham, C.M. Heesch</i>	279
DIETARY CALCIUM, BLOOD PRESSURE AND VASCULAR FUNCTION FOLLOWING SPACE FLIGHT <i>D. Hatton, D. McCarron, Q. Yue, C. Rouillet, H. Xue, K. Otsuka, J. Chapman, T. Phanouvong, J. Rouillet, M. Watanabe, K. Nilan, V. Haight, J. Dierckx, J. Demerritt</i>	282
COMPUTATIONAL MODELS OF THE CARDIOVASCULAR SYSTEM AND ITS RESPONSE TO MICROGRAVITY <i>T. Heldt, E.B. Shim, R.G. Mark, R.D. Kamm</i>	283
THE EFFECT OF CARDIAC MECHANICS ON ORTHOSTATIC INTOLERANCE FOLLOWING BED REST <i>B.D. Levine</i>	286
RENAL SODIUM HANDLING AFTER EXERCISE INDUCED PLASMA VOLUME EXPANSION <i>G.W. Mack, S. A. Kavouras, K. Nagashima</i>	288
CARDIOVASCULAR SYSTEM IDENTIFICATION OF ALTERATIONS IN CARDIOVASCULAR REGULATION DURING SIMULATED SPACE FLIGHT <i>T.J. Mullen, C.D. Ramsdell, G. Sundby, G.H. Williams, R.J. Cohen</i>	290
NON-INVASIVE ASSESSMENT OF SUSCEPTIBILITY TO VENTRICULAR ARRHYTHMIAS DURING SIMULATED SPACE FLIGHT <i>T.J. Mullen, C.D. Ramsdell, G. Sundby, G.H. Williams, R.J. Cohen</i>	293
POSTURAL REGULATION OF MUSCLE SYMPATHETIC NERVE ACTIVITY BEFORE AND AFTER SIMULATED AND ACTUAL MICROGRAVITY DECONDITIONING <i>J.A. Pawelczyk, B.D. Levine, Neurolab Autonomic Team</i>	295
INFLUENCE OF GRAVITY ON BLOOD VOLUME AND FLOW DISTRIBUTION <i>D. Pendergast, A. Olszowka, E. Bednarczyk, B. Shykoff, L. Farhi</i>	297

PERIPHERAL VASCULAR HYPORESPONSIVENESS AND ELEVATED CEREBRO-VASCULAR MYOGENIC TONE IN SIMULATED MICROGRAVITY: ROLE OF NITRIC OXIDE-DEPENDENT AND -INDEPENDENT MECHANISMS <i>R.E. Purdy, Y. Ding, S.P. Duckles, G.G., Geary, D.N. Krause, N.D. Vaziri, and S.D. Sangha</i>	300
MYOCARDIAL PERFORMANCE AND METABOLISM IN MICE WITH A NULL MUTATION IN CYTOCHROME C OXIDASE SUBUNIT VIaH <i>N.B. Radford, B. Wan, L. Szczepaniak, E.E. Babcock, A. Richman, C.S. Storey, J.L. Li, K. Li, R.W. Moreadith</i>	303
CAROTID BAROREFLEX FUNCTION DURING PROLONGED EXERCISE <i>P.B. Raven</i>	305
EVALUATION OF THERMOREGULATION AFTER SPACEFLIGHT <i>S.M. Schneider, W.J. Williams, J.E. Greenleaf, S.M.C. Lee, R. Gonzalez</i>	308
HYDRAULIC AND COMPUTER MODELING OF CARDIOVASCULAR RESPONSE TO WEIGHTLESSNESS <i>M. K. Sharp, G. M. Pantalos, K. J. Gillars, K. Peterson</i>	310
SYMPATHETIC CONTRIBUTIONS TO ORTHOSTATIC TOLERANCE AND VASCULAR TONE FOLLOWING BED REST <i>J.K. Shoemaker, L.I. Sinoway</i>	314
RENAL AND CARDIO-ENDOCRINE RESPONSES IN HUMANS TO SIMULATED MICROGRAVITY <i>G.H. Williams, T. Mullen, C. Ramsdell</i>	317
IMMUNOLOGY, INFECTIOUS DISEASE, AND HEMATOLOGY	319
IMMUNOLOGY SESSION SUMMARY	320
NEOCYTOLYSIS: MECHANISMS OF MONITORING NEOCYTES <i>C.P. Alfrey, L Rice, J. Trial, P. D. Kessler, B.J. Byrne</i>	327
DETERMINATION OF WHETHER IMMUNE CLEARANCE AND PROTECTION FROM MUCOSAL VIRUS INFECTION ARE ALTERED IN GROUND-BASED MOUSE MODELS OF SPACE FLIGHT <i>M.E. Conner</i>	329
REGULATION OF EPIDERMAL GROWTH FACTOR BY GRAVITY <i>E.M. Durban</i>	331
NEW STRATEGIES FOR THE DETECTION OF E.COLI <i>N. Elayan, Y. Xu, C. Theegala, A. Suleiman</i>	334

MICROBIAL MONITORING TECHNOLOGY FOR LONG DURATION SPACE FLIGHTS	
<i>G.E. Fox, J. Wibbenmeyer, M. Larios-Sanz, K. Kourentzi, J.C. Murphy, R.C. Willson</i>	335
THE EFFECT OF ANTI-ORTHOSTATIC SUSPENSION ON DELAYED-TYPE HYPERSENSITIVITY REACTIONS	
<i>S. Kanwar, J.E. Smolen, C.W. Smith</i>	336
LATENT VIRUSES-A SPACE TRAVEL HAZARD??	
<i>P.D. Ling, R.S. Peng, D. Pierson, J. Lednicky, J.S. Butel</i>	338
RAPID ASSESSMENT OF BACTERIAL ACTIVITY IN SPACECRAFT WATER SYSTEMS	
<i>J.T. Lisle, B.H. Pyle, S.C. Broadaway, G.A. McFeters</i>	340
GENE REGULATION BY MECHANICAL FORCES IN VASCULAR CELLS	
<i>L.V. McIntire</i>	341
HEALTH HAZARDS IN CLOSED ENVIRONMENTS: THERMODEGRADATION OF WIRE INSULATION	
<i>G. Oberdörster, J.N. Finkelstein, R. Gelein, P. Mercer, N. Corson, C.J. Johnston, B. Weiss</i>	343
ANALYSIS OF MIR CONDENSATE AND POTABLE WATER	
<i>L.M. Pierre, L. Bobe, N. N. Protasov, R. L. Sauer, J. R. Schultz, Y. E. Sinyak, V. M. Skuratov</i>	345
REACTIVATION OF LATENT VIRUSES IN SPACE	
<i>D.L. Pierson, S.K. Mehta, S.K. Tyring, D.J. Lugg</i>	348
BACTERIAL BIOFILMS IN MICROGRAVITY	
<i>B.H. Pyle, S.C. Broadaway, C.K. Johnsrud, R.T. Storfa, G.A. McFeters</i>	350
STUDY DESIGN TO TEST THE HYPOTHESIS THAT LONG-TERM SPACE TRAVEL HARMS THE HUMAN AND ANIMAL IMMUNE SYSTEMS	
<i>W.T. Shearer, D.J. Lugg, H.D. Ochs, D.L. Pierson, J.M. Reuben, H.M. Rosenblatt, C. Sams, C.W. Smith, E.O. Smith, J.E. Smolen, D.F. Dinges, J.L. Mullington</i>	351
UPDATE ON THE EFFECTS OF SPACE FLIGHT ON DEVELOPMENT OF IMMUNE RESPONSES	
<i>G. Sonnenfeld, M. Foster, D. Morton, F. Bailliard, N.A. Fowler, A.M. Hakenwewerth, R. Bates, E.S. Miller</i>	354
LYTIC REPLICATION OF EPSTEIN-BARR VIRUS DURING SPACE FLIGHT	
<i>R.P. Stowe, D.L. Pierson, A.D.T. Barrett</i>	356

INHIBITION OF ERYTHROPOIESIS IN SIMULATED MICROGRAVITY <i>A.J. Sytkowski, K.L. Davis</i>	357
MUSCLE	358
MUSCLE SESSION SUMMARY	359
MYOSIN HEAVY CHAIN GENE EXPRESSION IN DEVELOPING NEONATAL SKELETAL MUSCLE: INVOLVEMENT OF THE NERVE, GRAVITY, AND THYROID STATE <i>K.M. Baldwin, G. Adams, F. Haddad, M. Zeng, A. Qin, L. Qin, S. McCue, P. Bodell</i>	363
QUANTIFYING BIOMECHANICAL CHARACTERISTICS OF JUMPING EXERCISES IN 1G AND IN SIMULATED AND TRUE MICROGRAVITY <i>B.L. Davis, S.E. D'Andrea, G. Perusek, T. Orlando</i>	365
ECTOPIC EXPRESSION OF PORCINE HV-GHRH BY A SYNTHETIC MYOGENIC VECTOR ELICITS ENHANCED GH AND IGF-1 SECRETION AND ANIMAL GROWTH <i>R. Draghia-Akli, D.R. Deaver, M.L. Fiorotto, R.J. Schwartz</i>	368
EFFECTS OF MICROGRAVITY ON THE ACCURACY OF ELBOW AND ANKLE FLEXOR AND EXTENSOR MOTOR POOLS IN MAINTAINING A TARGET TORQUE <i>V.R. Edgerton, G. E. McCall, K. O. Fleischman, G. I. Boorman, C. Goulet, R. R. Roy</i>	369
MOLEUCLAR SIGNALING IN MUSCLE PLASTICITY <i>H.F. Epstein, S. Gordon, F.W. Booth, H. Rajadurai</i>	370
ALTERATIONS IN SKELETAL MUSCLE FUNCTION WITH MICROGRAVITY, AND THE PROTECTIVE EFFECTS OF HIGH RESISTANCE ISOMETRIC AND ISOTONIC EXERCISE <i>R.H. Fitts, J.E. Hurst, K.M. Norenberg, J.J. Widrick, D.A. Riley, J.L.W. Bain, S.W. Trappe, T.A. Trappe, D.L. Costill</i>	371
IN VIVO NONINVASIVE ANALYSIS OF HUMAN FOREARM MUSCLE FUNCTION AND FATIGUE: APPLICATIONS TO EVA OPERATIONS AND TRAINING MANEUVERS <i>L.K. Fotedar, T. Marshburn, M. J. Quast, D. L. Feedback</i>	374
ACTIVATION OF THE UBIQUITIN-PROTEASOME PATHWAY IN ATROPHYING MUSCLES AND POTENTIAL INHIBITORS <i>A.L. Goldberg, D. H. Lee, V. Solomon, S. Lecker</i>	376
CO2 ACCUMULATION IN THE NON-CONFORMAL HELMET OF THE NASA LAUNCH AND ENTRY SUIT DURING SIMULATED UNAIDED EGRESS <i>M.C. Greenisen, P.A. Bishop, S.M.C. Lee, A. Moore, J. Williams</i>	377

SPACE PHYSIOLOGY STUDIES	
<i>A.R. Hargens, R.E. Ballard, W.L. Boda, A.C. Ertl, S.M. Schneider, K.J. Hutchinson, S.M. Lee, G. Murthy, L. Putcha, D.E. Watenpaugh</i>	378
INTRACELLULAR CALCIUM TRANSIENTS IN MOUSE SOLEUS MUSCLE AFTER HINDLIMB UNLOADING AND RELOADING	
<i>C.P. Ingalls, G.L. Warren, R.B. Armstrong</i>	385
IMPAIRED UTILIZATION OF EXOGENOUS SUBSTRATES BY RAT SKELETAL MUSCLE AFTER HINDLIMB SUSPENSION.	
<i>B.F. Lujan, L.A. Bertocci</i>	386
ALTERATIONS IN NEUROMUSCULAR JUNCTIONS ASSOCIATED WITH MUSCLE ATROPHY INDUCED BY HINDLIMB UNLOADING	
<i>D.R. Mosier, L. Siklós, C.L. Gooch, S. Gordon, F.W. Booth</i>	388
MUSCLE DEOXYGENATION CAUSES MUSCLE FATIGUE	
<i>G. Murthy, A.R. Hargens, S. Lehman, D. Rempel</i>	390
E PROTEINS CONTROL SKELETAL MUSCLE FIBER TYPE	
<i>C. Neville, D. Gonzales, J. Purdy, Y. Zuang, N. Rosenthal</i>	393
WEIGHTLESSNESS REDUCES SKELETAL MUSCLE GROWTH AND REGENERATION POTENTIAL	
<i>E. Schultz, P.E. Mozdziak</i>	395
MECHANICAL AND INFLAMMATORY COMPONENTS OF MUSCLE INJURY FOLLOWING MODIFIED MUSCLE LOADING	
<i>J.G. Tidball</i>	397
TISSUE ENGINEERING ORGANS FOR SPACE BIOLOGY RESEARCH.	
<i>H.H. Vandenburg, J. Shansky, M. Del Tatto, P. Lee, J. Meir</i>	400
NEUROVESTIBULAR	402
NEUROVESTIBULAR SESSION SUMMARY	403
VISUALLY-INDUCED ADAPTATION IN GRAVITY-SENSITIVE PROPERTIES OF PRIMATE VESTIBULO-OCULAR REFLEX	
<i>D.E. Angelaki, B.J.M. Hess</i>	407
ROLL-TILT PERCEPTION USING A SOMATOSENSORY BAR TASK	
<i>F.O. Black, S.W. Wade, A. Arshi</i>	409
THE EFFECTS OF LONG-DURATION SPACEFLIGHT ON POSTFLIGHT TERRESTRIAL LOCOMOTION	
<i>J.J. Bloomberg, A.P. Mulavara, P.V. McDonald, C.S. Layne, L.A. Merkle, H.S. Cohen, I.B. Kozlovskaya</i>	411

MOTOR CONTROL AND ADAPTATION IN A ROTATING ARTIFICIAL GRAVITY ENVIRONMENT <i>P. DiZio, J.R. Lackner</i>	413
SYMPATHETIC EFFERENT ACTIVITY IS DRIVEN BY OTOLITH STIMULATION <i>H. Kaufmann, I. Biaggioni, A. Voustaniuk, A. Diedrich, F. Costa, R. Clark, M. Gizzi, B. Cohen</i>	416
ANTICIPATORY POSTURAL ACTIVITY DURING LONG-DURATION SPACE FLIGHT <i>C.S. Layne, A.P. Mulavara, P.V. McDonald, C.J. Pruetz, I.B. Koslovskaya, J.J. Bloomberg</i>	418
OTOLITH-OCULAR TORSION IS MODIFIED IN NOVEL G STATES <i>C.H. Markham, S.G. Diamond</i>	420
A METHODOLOGY FOR INVESTIGATING ADAPTIVE POSTURAL CONTROL <i>P.V. McDonald, G.E. Riccio</i>	421
LOW-FREQUENCY OTOLITH FUNCTION IN MICROGRAVITY: A RE-EVALUATION OF THE OTOLITH TILT-TRANSLATION REINTERPRETATION (OTTR) HYPOTHESIS <i>S.T. Moore, B. Cohen, G. Clement, T. Raphan</i>	425
HUMAN VISUAL ORIENTATION IN UNFAMILIAR GRAVITO-INERTIAL ENVIRONMENTS <i>C. Oman, I. Howard, W. Shebilske, J. Taube, A. Beall</i>	429
MECHANISMS OF SENSORIMOTOR ADAPTATION TO CENTRIFUGATION <i>W.H. Paloski, S.J. Wood, G.D. Kaufman</i>	432
SELF-MOTION PERCEPTION: ASSESSMENT BY REAL-TIME COMPUTER-GENERATED ANIMATIONS <i>D.E. Parker</i>	435
EVIDENCE FOR A RAPID GAIN CHANGE MECHANISM THAT REGULATES HUMAN POSTURAL CONTROL DYNAMICS <i>R.J. Peterka</i>	437
VISUAL-VESTIBULAR RESPONSES DURING SPACE FLIGHT <i>M.F. Reschke, I.B. Kozlovskaya, W.H. Paloski</i>	441
CONTEXT-SPECIFIC ADAPTATION OF GRAVITY-DEPENDENT VESTIBULAR REFLEX RESPONSES (NSBRI NEUROVESTIBULAR PROJECT 1) <i>M. Shelhamer, J. Goldberg, L.B. Minor, W.H. Paloski, L.R. Young, David S. Zee</i>	443

APPLICATION OF FLOQUET STABILITY ANALYSIS TO REPEATED STEPPING IN LD AND NORMAL SUBJECTS <i>C. Wall III, D.E. Krebs</i>	447
VISION AND VISUAL-MOTOR COORDINATION IN PITCHED VISUAL ENVIRONMENTS <i>R.B. Welch</i>	449
NUTRITION	451
NUTRITION SESSION SUMMARY	452
THE COMBINED EFFECTS OF INACTIVITY AND CORTISOL ON MUSCLE PROTEIN METABOLISM <i>A.A. Ferrando, C.S. Stuart, R.R. Wolfe</i>	455
DIETARY OXALATE AND ITS INFLUENCE ON URINARY OXALATE EXCRETION <i>R.P. Holmes, D.G. Assimos</i>	456
FOOD SYSTEM CHALLENGES FOR LONG-DURATION SPACE MISSIONS <i>J.B. Hunter</i>	459
FLUID AND ELECTROLYTE NUTRITION <i>H.W. Lane, S.M. Smith, C.S. Leach, B.L. Rice</i>	461
SALIVARY PHARMACODYNAMICS AND BIOAVAILABILITY OF PROMETHAZINE IN HUMAN SUBJECTS <i>L. Putcha, D.L. Harm, R. Nimmagudda, K.L. Berens, D.W.A. Bourne</i>	462
MEASUREMENT OF BODY COMPOSTION FOR NUTRITIONAL ASSESSMENT IN SPACE FLIGHT <i>D.A. Schoeller</i>	464
CALCIUM KINETICS DURING SPACE FLIGHT <i>S.M. Smith, M.E. Wastney, K.O. O'Brien, H.W. Lane</i>	466
PROTEIN-ENERGY RELATIONSHIPS DURING SPACE FLIGHT <i>T.P. Stein</i>	467
A NONINVASIVE TEST FOR GASTRIC EMPTYING AND INTESTINAL ABSORPTION <i>L.S. Welage, G.L. Amidon, J. Rhie, B.L. Neudec, S. Choe</i>	468
RADIATION	470
RADIATION SESSION SUMMARY	471
RADIATION MEASUREMENTS ON THE RUSSIAN MIR ORBITAL STATION <i>G.D. Badhwar</i>	477

CHARACTERIZATION OF TREFOIL PEPTIDE GENES IN IRON-ION OR X-IRRADIATED HUMAN CELLS <i>E.K. Balcer-Kubiczek, G.H. Harrison, J.F. Xu, X.F. Zhou</i>	478
COMPARISON OF GAMMA AND IRON PARTICLE IRRADIATION INDUCED REMODELING OF EXTRACELLULAR MATRIX IN MURINE LIVER <i>M.H. Barcellos-Hoff, C. Wang, S.A. Ravani</i>	480
RADIATION DOSIMETRY ON MANNED SPACE MISSIONS AND AT GROUND-BASED ACCELERATORS <i>E.V. Benton, E.R. Benton, A.L. Frank, M. M. Moyers</i>	483
PROTON IRRADIATION ALTERS EXPRESSION OF FGF-2 IN HUMAN LENS EPITHELIAL CELLS <i>E.A. Blakely, K.A. Bjornstad, P.Y. Chang, M.P. McNamara, E. Chang</i>	484
HEAVY ION INDUCED GENETIC DAMAGE IN TRANSGENIC ANIMALS <i>P.Y. Chang, L. Lutze-Mann, V. Walker, D. Torous, R.A. Winegar</i>	485
SIMULATION OF CLUSTERS OF DNA DAMAGE INDUCED BY IONIZING RADIATION ENCOUNTERED IN SPACEFLIGHT <i>A. Chatterjee, W.R. Holley, I.S. Mian</i>	488
NSBRI RADIATION EFFECTS: CARCINOGENESIS IN SPRAGUE-DAWLEY RATS IRRADIATED WITH IRON IONS, PROTONS, OR PHOTONS <i>J.F. Dicello, F.A. Cucinotta, D.S. Gridley, S.P. Howard, G.R. Novak, R. Ricart-Arbona, J.D. Strandberg, M.E. Vazquez, J.R. Williams, Y. Zhang, H. Zhou, D.L. Huso</i>	490
GENETIC REGULATION OF CHARGED PARTICLE MUTAGENESIS IN HUMAN CELLS <i>A.Kronenberg, S. Gauny, C. Cherbonnel-Lasserre, W. Liu, C.Wiese</i>	493
MUTAGENIC EFFECTS OF ⁵⁶ FE RADIATION ON CULTURED MAMMALIAN CELLS <i>M. Lenarczyk, A. Ueno, D. Vannais, R. Wartens, J. Roberts, A. Kronenberg, T. Hei, C. Waldren</i>	497
PORTABLE REAL TIME NEUTRON SPECTROMETRY <i>R.H. Maurer, D.R. Roth, R. Fainchtein, J.O. Goldsten, J.D. Kinnison, A.K. Thompson</i>	500
DNA REPAIR-PROTEIN RELOCALIZATION AFTER HEAVY ION EXPOSURE <i>N.F. Metting</i>	503
ACCELERATOR-BASED STUDIES OF HEAVY ION INTERACTIONS RELEVANT TO SPACE BIOMEDICINE <i>J. Miller, L. Heilbronn, C. Zeitlin</i>	507

MOLECULAR AND CHROMOSOMAL DAMAGE AND MIS-REPAIR IN HUMAN X
CHROMOSOMES

M.C. Muhlmann-Diaz, M. Loebrich, B. Rydberg, P.K. Cooper, J.S. Bedford 511

COOPERATIVE RESEARCH IN PROTON SPACE RADIATION

G.A. Nelson, J.M. Slater, J.O. Archambeau, L.M. Green, D.S. Gridley, G.A. Abell, M.M. Moyers, G.A. Coutrakon 513

MODULATION OF RADIOGENIC DAMAGE BY MICROGRAVITY: RESULTS FROM
STS-76

G. Nelson, G. Kazarians, W. Schubert, R. Kern, D. Schranck, P. Hartman, A. Hlavacek, H. Wilde, D. Lewicki, E.V. Benton, E.R. Benton..... 515

SOME BEHAVIORAL EFFECTS OF EXPOSURE TO LOW DOSES OF ⁵⁶FE
PARTICLES

B.M. Rabin, J.A. Joseph, B. Shukitt-Hale..... 517

NON-REJOINED DNA DOUBLE-STRAND BREAKS IN HUMAN CELLS. A SHIFT IN
RBE vs LET FOR HZE IRON PARTICLES IN COMPARISON WITH LOW ENERGY
HELIUM PARTICLES

B. Rydberg, P. Cooper..... 520

QUANTITATION OF RADIATION INDUCED DELETION AND RECOMBINATION
EVENTS ASSOCIATED WITH REPEATED DNA SEQUENCES

R.R. Sinden, J.R. Ford, L.A. Braby 521

INFORMATION NEEDED TO MAKE RADIATION PROTECTION
RECOMMENDATIONS FOR TRAVEL BEYOND LOW-EARTH ORBIT

L.W. Townsend..... 524

RISK MANAGEMENT STRATEGIES DURING SOLAR EVENTS

R. Turner 525

AMINOTHIOL INDUCED MODULATION OF P53 PROTEIN ACTIVITY IN HUMAN
CELLS

R.L. Wartens, D.K. Thai, J.C. Roberts, D.K. Gaffney, A.E. Cress..... 526

CYTOGENETIC DAMAGE FROM PHOTONS, FE-IONS AND PROTONS:
MODULATION BY DOSE-RATE AND CELL TYPE.

J.R. Williams, Z. Houming, J.F. Dicello, Y. Zhang..... 528

IMPACT OF TRACK STRUCTURE EFFECTS ON SHIELDING AND
DOSIMETRY

J.W. Wilson, F.A. Cucinotta, W. Schimmerling, M.Y. Kim 529

ANALYSIS OF INCOMPLETE CHROMOSOMAL EXCHANGES USING FLUORESCENCE <i>IN SITU</i> HYBRIDIZATION WITH TELOMERE PROBES <i>H. Wu, K. George, T.C. Yang</i>	533
SLEEP/CIRCADIAN RHYTHM	534
SLEEP/CIRCADIAN RHYTHM SESSION SUMMARY	535
GENDER DIFFERENCES IN THE RESPONSES OF RHESUS MONKEYS TO 2G <i>L.K. Barger, C.A. Fuller</i>	538
DYNAMIC ASSESSMENT OF CIRCADIAN PHASE AND AMPLITUDE UNDER THE SIMULATED LIGHTING CONDITIONS OF LONG-DURATION SPACE MISSIONS <i>E.N. Brown, H.H. Luithardt, K.P. Wright Jr., C.A. Czeisler</i>	541
EFFECTIVENESS OF AN EXPERT SYSTEM FOR ASTRONAUT ASSISTANCE ON A SLEEP EXPERIMENT <i>G. Callini, S.M. Essig, D. Heher, L.R. Young</i>	543
AMBIENT LIGHT INTENSITY, ACTIGRAPHY, SLEEP AND RESPIRATION, CIRCADIAN TEMPERATURE AND MELATONIN RHYTHMS AND DAYTIME PERFORMANCE OF CREW MEMBERS DURING SPACE FLIGHT ON STS-90 AND STS-95 MISSIONS <i>C.A. Czeisler, D.-J. Dijk, D.F. Neri, R.J. Hughes, J.M. Ronda, J.K. Wyatt, J.B. West, G.K. Prisk, A.R. Elliott, L.R. Young</i>	544
ELECTROENCEPHALOGRAPHIC AND OCULAR CORRELATES OF NEUROBEHAVIORAL PERFORMANCE DECREMENTS <i>D.-J. Dijk, C. Cajochen</i>	547
COUNTERMEASURES TO NEUROBEHAVIORAL DEFICITS FROM CUMULATIVE PARTIAL SLEEP DEPRIVATION DURING SPACE FLIGHT <i>D.F. Dinges, H.P.A. Van Dongen</i>	551
THE EFFECTS OF GRAVITY ON THE CIRCADIAN TIMING SYSTEM <i>C.A. Fuller</i>	554
MELATONIN AS A COUNTERMEASURE FOR ENTRAINMENT TO THE SLEEP/WAKE SCHEDULES REQUIRED DURING SHUTTLE MISSIONS <i>B.S. S.Khalsa, D.-J. Dijk</i>	555
SLEEP AND CIRCADIAN RHYTHMS IN FOUR ORBITING ASTRONAUTS <i>T.H. Monk, D.J. Buysse, B.D. Billy, K.S. Kennedy, L.M. Willrich</i>	559
NEUROENDOCRINE AND NEUROIMMUNE MODULATION BY SLEEP DEPRIVATION <i>J. Mullington, M. Carlin, S. Kapoor, N. Price, M. Szuba, R. Schwartz, W. Shearer, J. Butel, D.F. Dinges</i>	561

BRN 3.1 KNOCKOUTS AFFECT THE VESTIBULAR, AUTONOMIC, AND CIRCADIAN RHYTHM RESPONSES TO 2G EXPOSURE. <i>D.M. Murakami, L. Erkman, M. G. Rosenfeld, and C. A. Fuller</i>	563
SLEEP RESTRICTION EFFECTS ON CARDIOVASCULAR REGULATION <i>M.L. Smith, D.E. Watenpaugh, N. Muentner, S.L. Wasmund, W.L. Wasmund, R. Carter III</i> .	565
CIRCADIAN ENTRAINMENT, SLEEP-WAKE REGULATION AND NEUROBEHAVIORAL PERFORMANCE UNDER THE SIMULATED LIGHTING CONDITIONS OF LONG-DURATION SPACE MISSIONS <i>K.P. Wright Jr., M.E. Jewett, E.B. Klerman, R.E. Kronauer, C.A. Czeisler</i>	567
TECHNOLOGY DEVELOPMENT	569
USER FRIENDLY INSTRUMENTATION FOR NON-INVASIVE ASSESSMENT OF ALTERATIONS OF CARDIOVASCULAR REGULATION ASSOCIATED WITH SPACE FLIGHT <i>R.J. Cohen, N. Iyengar, T.J. Mullen, C.D. Ramsdell, G. Sundby</i>	570
WIRELESS AUGMENTED REALITY PROTOTYPE (WARP) <i>A.S. Devereaux</i>	573
BIONA-C CELL CULTURE PH MONITORING SYSTEM <i>C. Friedericks</i>	576
PHYSIOLOGICAL SIGNAL CONDITIONER <i>C. Friedericks</i>	577
SENSORS 2000! PROGRAM: ADVANCED BIOSENSOR AND MEASUREMENT SYSTEMS TECHNOLOGIES FOR SPACEFLIGHT RESEARCH AND CONCURRENT, EARTH-BASED APPLICATIONS <i>J. Hines</i>	578
MINIATURE QUADRUPOLE MASS SPECTROMETER ARRAY <i>D. Karmon, M. Darrech, A. Chutjian, D. Jan</i>	579
BIOTELEMETRY <i>C. Mundt</i>	580
NASA AMES RESEARCH CENTER R&D SERVICES DIRECTORATE BIOMEDICAL SYSTEMS DEVELOPMENT <i>J. Pollitt, K. Flynn</i>	581
MINIATURE TIME-OF-FLIGHT MASS SPECTROMETER <i>R.S. Potember, W.A. Bryden, M. Antoine, P. Scholl, H. Ko, V.L. Pisacane, M. Leonardo, R.J. Cotter</i>	582

NEUROLAB BIOTELEMETRY SYSTEM (NBS) <i>J. Schonfeld</i>	584
NEW TECHNIQUES FOR THE NON-INVASIVE IMAGING OF TISSUE PERFUSION <i>D.A. Sherman, R.H. Rubin, R.J. Cohen</i>	585
BION-11 SPACEFLIGHT MISSION <i>M. Skidmore</i>	586
DIGITAL ECHOCARDIOGRAPHY ON THE INTERNATIONAL SPACE STATION: TECHNICAL PROGRESS AND EXPERIMENTAL PLANNING <i>J.D. Thomas, N.L. Greenberg, T. Shiota, L. Cardon, M.J. Garcia</i>	587
LASER-POLARIZED NOBLE GAS MAGNETIC RESONANCE <i>R.L. Walsworth, M.S. Albert, D.G. Cory, F.W. Hersman, D.P. Hinton, D. Hoffmann, F.A. Jolesz, R.W. Mair, S. Patz, S. Peled, V. Pomeroy, C.H. Tseng, G.P. Wong</i>	590
LIFE SCIENCES DIVISION SPACEFLIGHT HARDWARE <i>B. Yost</i>	593
 APPENDIX A	
WORKSHOP PROGRAM.....	594
 APPENDIX B	
LIST OF ATTENDEES	618
 APPENDIX C	
AUTHOR INDEX.....	647
 APPENDIX D	
KEY WORD INDEX	654

FOREWORD

The First Biennial Space Biomedical Investigators' Workshop, held January 11-13, 1999, was unique in that it assembled, for the first time, a broad cross section of NASA-funded biomedical researchers to present the current status of their projects and their plans for future investigations. All principal investigators with active, or recently-completed ground-based projects in NASA's Biomedical Research and Countermeasures Program that were funded through NASA's Office of Life and Microgravity Sciences and Applications were invited. Included were individual investigators funded through NASA Research Announcements, investigators with NASA Specialized Centers of Research and Training, investigators with the recently established National Space Biomedical Research Institute (NSBRI), and NASA civil servant investigators. Seventy-seven percent of all eligible projects were presented at the workshop. Thus, these Proceedings should provide a useful snapshot of the status of NASA-funded space biomedical research as of January 1999.

An important workshop objective was to achieve free and open communication among the presenting investigators. Therefore, presentation of new and incomplete results, as well as hypotheses and ideas for future research, was encouraged. Comments and constructive criticisms from the presenters' colleagues were also encouraged. These ground rules resulted in many lively and useful discussions, during both the presentation sessions and informal evening gatherings and breaks.

The workshop also included plenary presentations and science technology exhibits covering matters of interest to all space biomedical investigators. The plenary presentations included overviews of NASA's Space Biomedical Research Program (Nicogossian, Vernikos, Stegemoeller) and discussions of both internal NASA (Sawin) and external advisory committee (Baldwin and Osborn) attempts to establish space biomedical research priorities. The plenary presentations also included discussions of available biomedical research resources, both internal (Paloski, Souza) and external (Cucinotta, DiZio) to NASA, and discussions of specific topics of interest to space biomedical researchers (Charles, Pool, Williams, Young).

Research presentations were organized into breakout sessions divided by discipline area. The workshop steering committee appointed a session chair and co-chair for each discipline area. The session chairs were given the responsibility of (1) organizing their session's presentations into a logical order, (2) keeping the session on schedule, and (3) preparing a session summary for publication in these Proceedings. Several of the chairpersons also organized a discussion among the participants that attempted to arrive at a consensus statement of the discipline area's current overall research position and its future space biomedical research priorities. Thus, several of the session summaries include discipline area overviews.

In these Proceedings, the plenary presentations appear in their order of presentation, since this follows a logical progression from general overviews to more specific topics. In

contrast, to facilitate referral to individual abstracts, the abstracts in each discipline area (which appear after the summary) are alphabetized by author's last name.

Alfred C. Coats, MD
Steering Committee Chairman

Plenary Presentations

Life Sciences in NASA's Mission

Arnauld E. Nicogossian, MD

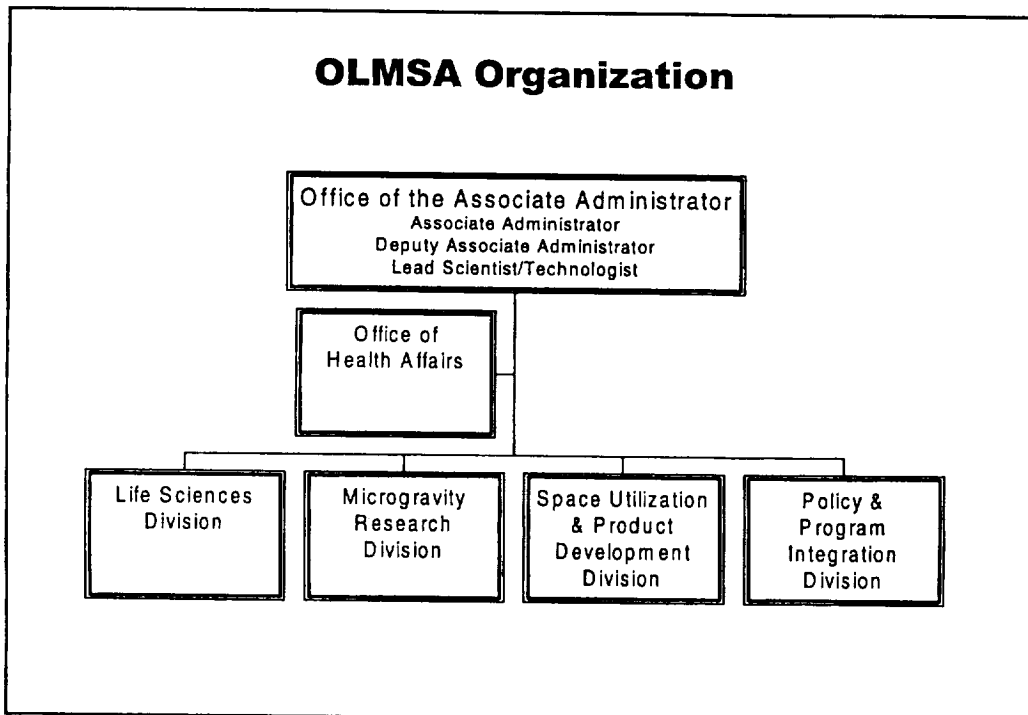
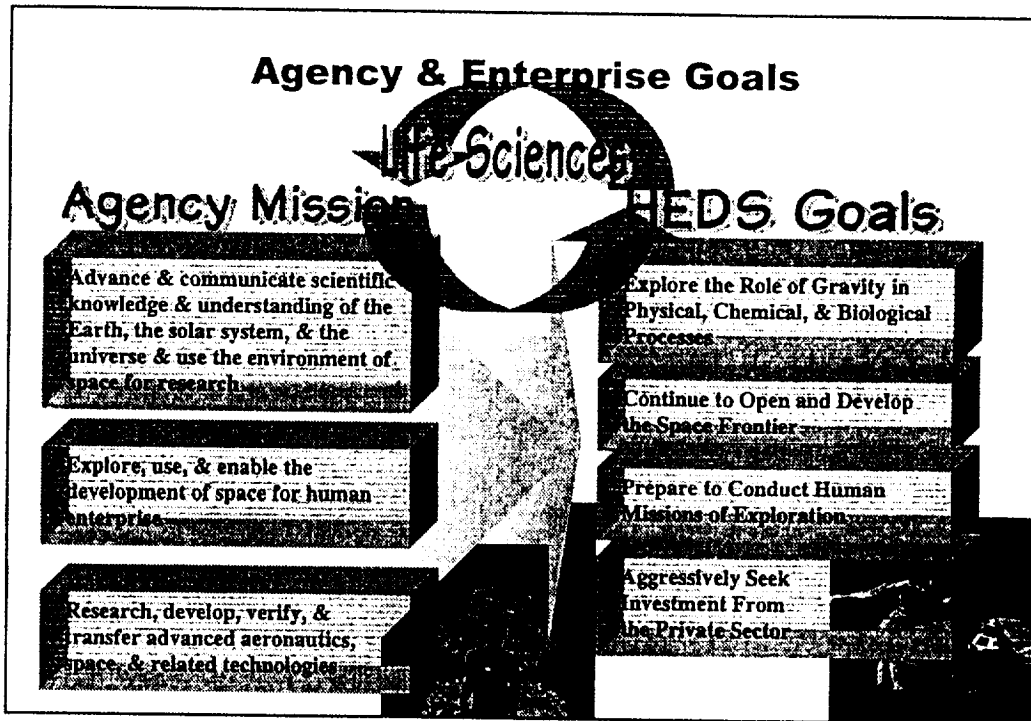
Associate Administrator

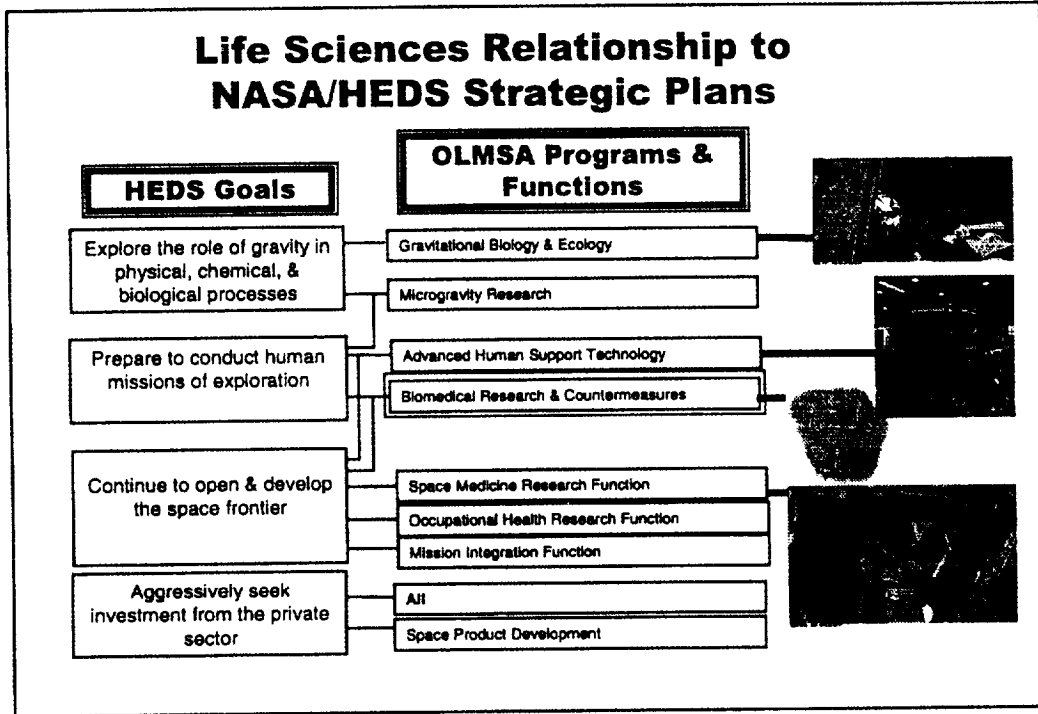
for Life & Microgravity Sciences

& Applications

National Aeronautics and Space

Administration





Budget Allocated by the HEDS Strategic Plan Goals

	FY 1999
Explore the Role of Gravity in Physical, Chemical, & Biological Processes	-82%
Continue to Open and Develop the Space Frontier	-10%
A. Develop and assemble the International Space Station & utilize it to advance scientific, exploration, engineering and commercial activities	
B. Provide safe and affordable human access to space	-1%
Prepare to Conduct Human Missions of Exploration	
Aggressively Seek Investment From the Private Sector	-7%
A. Increase the affordability of space operations through privatization and commercialization	
B. Share HEDS knowledge, technologies, and assets that promise to enhance the quality of life on Earth	

**1998 Successes
Neurolab**



Inflight Experiment



Flight Research Subjects

Neuroscience

- Culmination of Shuttle Neuroscience research
- NASA's Contribution to the Decade of the Brain

Spacelab Conclusion

- Last Spacelab flight

International Interagency

- Participation by CSA, ESA, CNES, DARA, NASDA
- Cooperation with NIH, NSF, & ONR



Flight
Launched: Apr, 1998
Landed: Apr, 1998

**1998 Successes
STS-95**

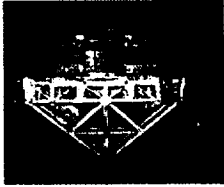



Multidisciplinary International Interagency

- Chiaki Mukai (Japan)
- Pedro Duque (Spain)

Commercial Rapidly Integrated

- Cooperation with NIH/National Institute on Aging/Baltimore Longitudinal Study on Aging
- Use of Spacehab as carrier and payload integrator
- 9 month payload integration schedule



Spartan

Flight
Launched: Oct. 29, 1998
Landed: Nov. 7, 1998

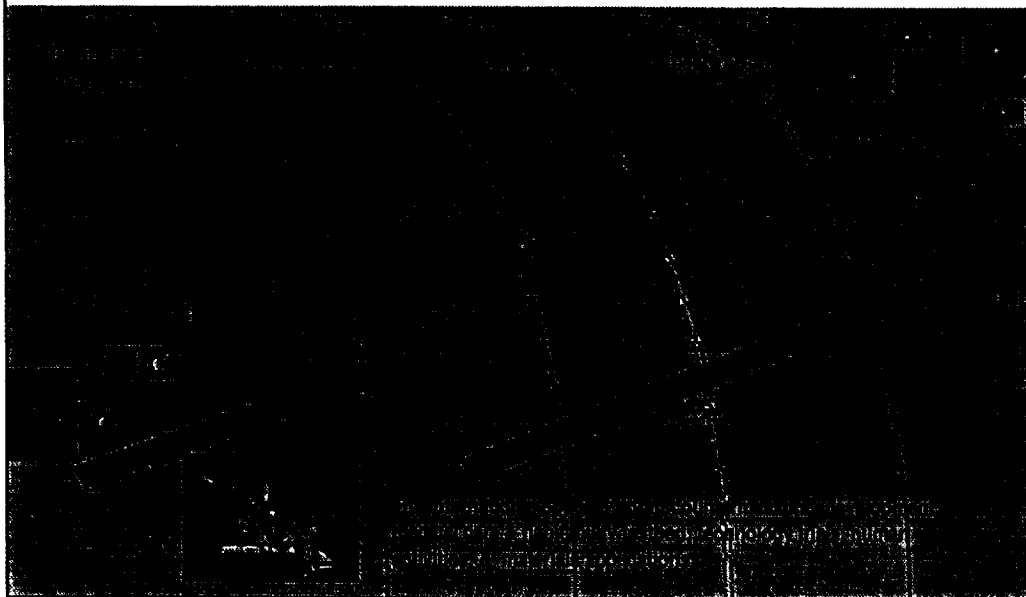
1998 Successes The Phase I Program

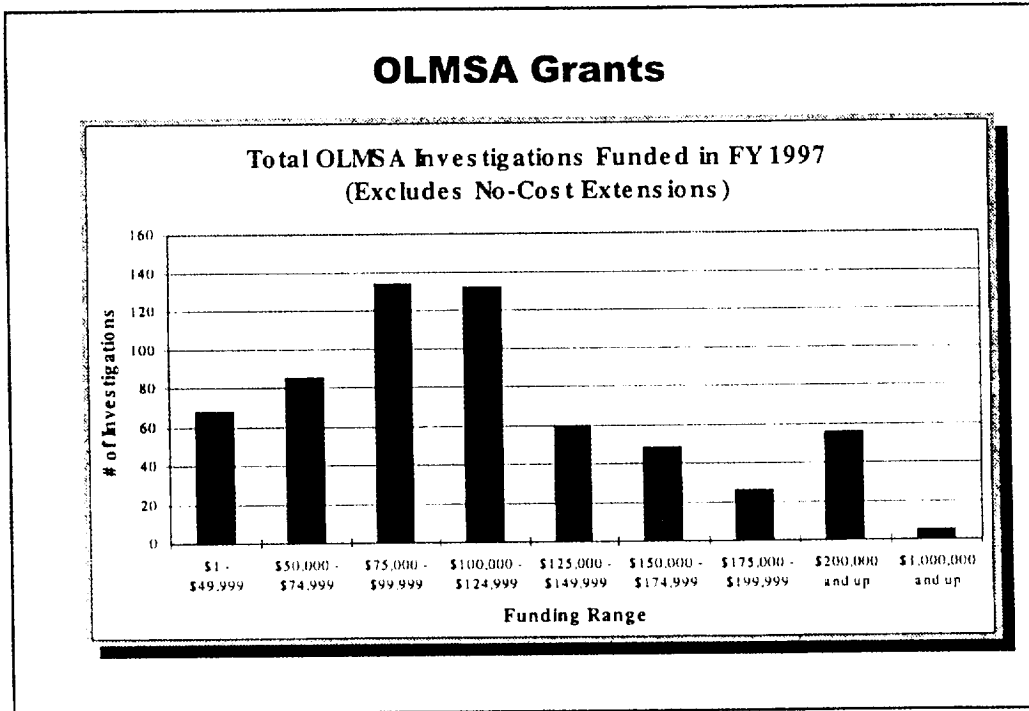
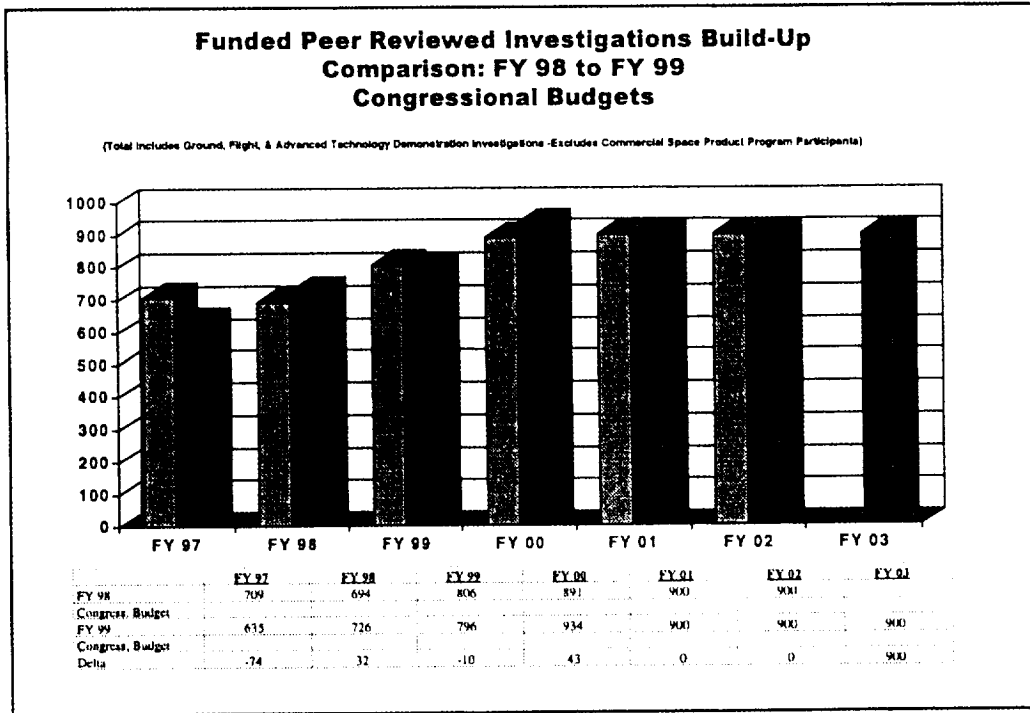


- 31 months of long-duration operational experience aboard Mir
- More than 100 distinct research & technology investigations
- Approximately 1000 pieces of equipment tested for future use on the ISS
- Nine Shuttle-Mir rendezvous
 - Four carrying Spacehab
 - One carrying Spacelab
- Studied effect of space environment on payloads and habitability
- Existing countermeasures assessed in flight



Exploration & the ISS





Biomedical Research & Countermeasures

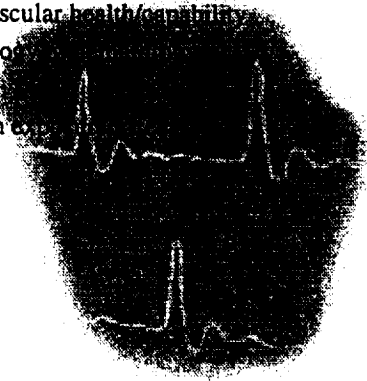
Areas of Current Emphasis

Adaptation



Pathophysiology

<ul style="list-style-type: none"> • Long-term bone loss/health • Skeletal muscle mass, strength, endurance, and performance • Sensory-motor changes • Endocrine responses • Dysbarism 	<ul style="list-style-type: none"> • Cardiovascular health/capability • Immunology • Nutrition • Radiation effects
---	--



Medical Care

- Bypass or negate deleterious effects of space travel on the human body
- Translation of terrestrial care & technologies to space
 - Pharmacology
 - μ g surgical procedures
 - Fracture healing
 - Wound healing
 - Monitoring
 - environment
 - crew member (health)



Telemedicine practices are well-established for orbital flight

Biologically-inspired Technologies

Some Areas of Current Emphasis

Smart Materials & Structures

- Anticipatory
- Collaborative
- Curious
- Self-modeling
- Adaptive
- Self-repairing
- Portable
- Sensor-fusion & sensory-guided motor control



Electronic Nose Component



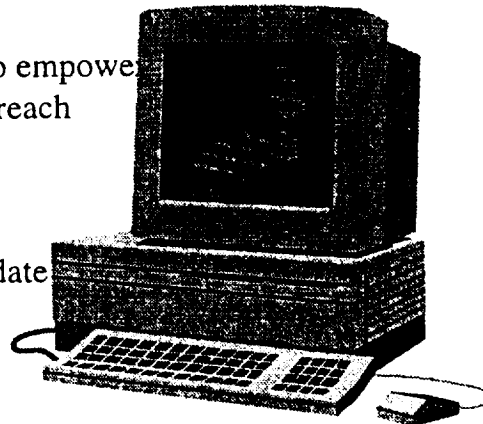
AERCam

Human-centered Systems

- Cognitive task analysis research
- Innovative human-machine interfaces
- Portable digital assistants & wearable computing research
- Just-in-time training systems & educational browsers
- Natural language understanding systems
- Performance support systems

Publication, Education, & Outreach

- Communications technologies will enable the research process
 - Peer communication
 - Cross-disciplinary interaction
- Internet technologies will also empower PI involvement with outreach
 - Online results
 - Conference proceedings
 - Interactive activities
- Future web sites will consolidate research progress
- Timely publications credit accountability



JSC, NASA Lead Center

Overview of Human Space Life Sciences Programs Office (HSLSPO)

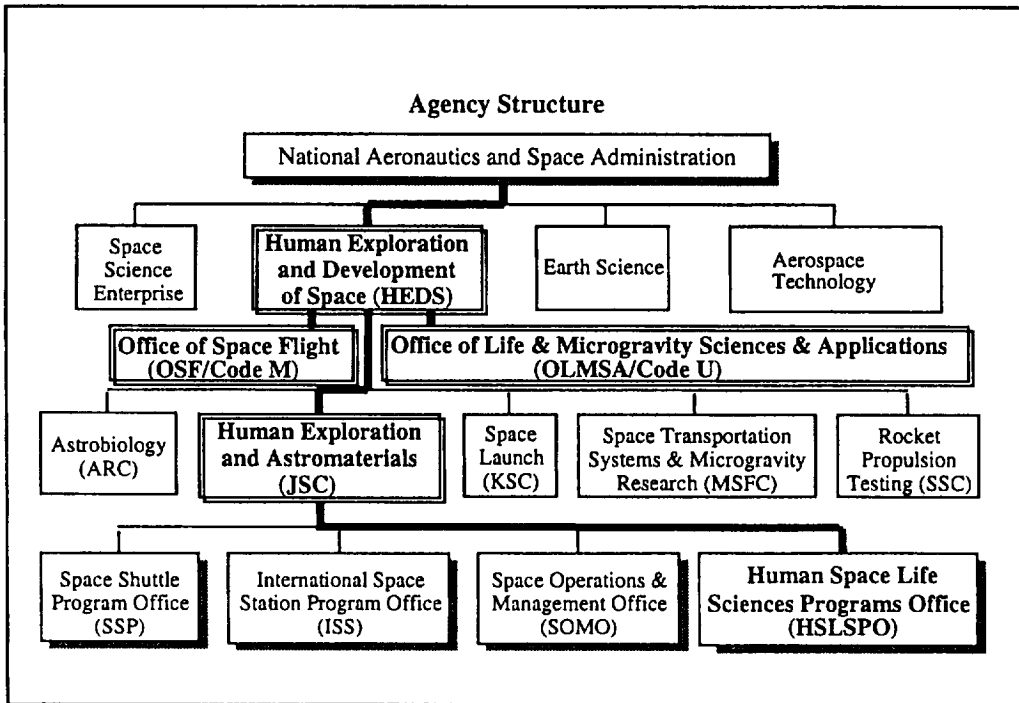
Charles Stegemoeller

Manager

JSC Human Life Sciences Programs Office

The Agency Structure

- The NASA Strategic Management Policy coordinated the Agency objectives into 4 Enterprises
- Each of the Enterprises has established their primary missions and programs consistent with the Agency's Strategic Plan
- Each of these missions and programs has been assigned to Lead Centers within the Agency
- The Johnson Space Center is the HEDS Lead Center for Human Exploration and Astromaterials
- The Human Space Life Sciences Programs Office was established to coordinate the "Human Element" of HEDS
 - Biomedical Research and Countermeasures Program (BR&C)
 - Advanced Human Support Technology Program (AHST)
 - Space Medicine - cross-cutting agency function (SMP)

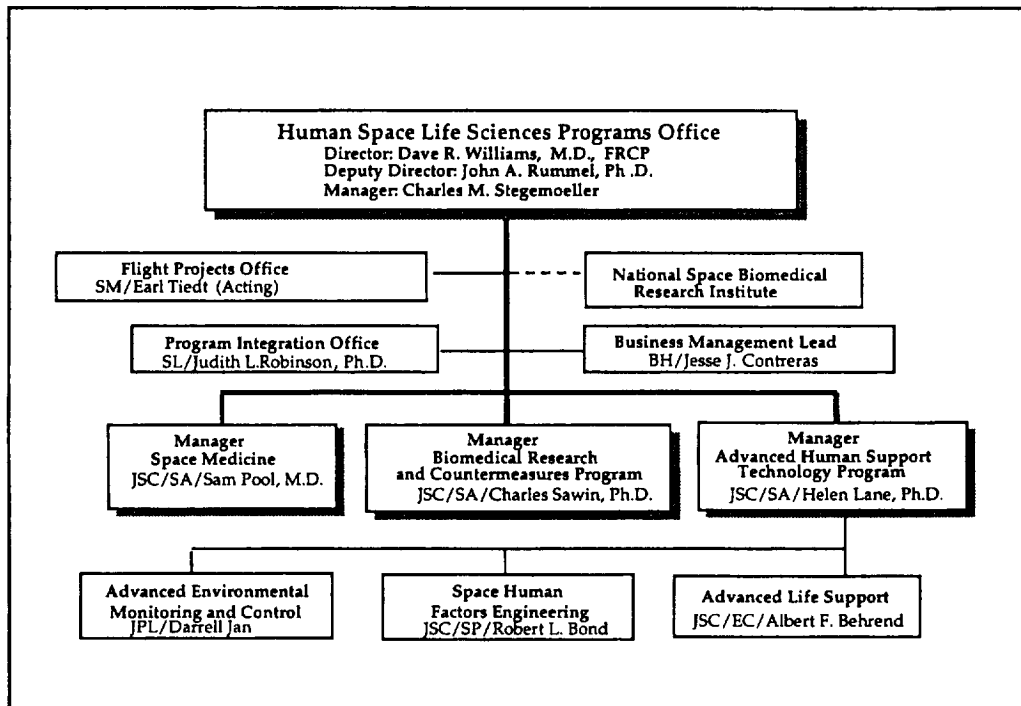


Objectives of the HSLSPO Lead Center Implementation Plan

- Bridge strategic (what/why - HQs) with the implementation (how - lead center) of human space life sciences across agency.
- Development and utilization of a "roadmap" for critical path activities that provides framework for implementation to meet agency and HEDS strategic objectives.
- Structure of HSLSPO coordinates all three program areas and includes the National Space Biomedical Research Institute (NSBRI), Flight Projects implementation, and the agency supporting Centers (ARC, KSC, JPL, GSFC, HQS).
 - Provides integrated program approach with coordinated resources

HSLSPO RELATIONSHIP TO JSC AS LEAD CENTER

- HSLSPO provides single point of contact at lead center for SMP, BR&C, AHST, and, NSBRI, across JSC, HEDS, and Code U
- Reports directly to Lead Center Director
 - Member of Lead Center Program Management Council
- HSLSPO is located within JSC Space and Life Sciences Directorate
 - Established HSLSPO Office as SLSD staff function per Center Director
 - Matrixed support from JSC line organizations and JPL to staff HSLSPO
- HSLPO coordinates all technical and financial resource management for implementing the assigned programs
 - Program Leads are responsible for the program content implementation based on agreed upon direction with OLMSA
 - Business Management Office coordinates with Headquarters and the Supporting Centers and respective Contracting Offices



HSLSPO PROGRAMS AND PROJECTS

SPACE MEDICINE	BIOMEDICAL RESEARCH AND COUNTERMEASURES	ADVANCED HUMAN SUPPORT TECHNOLOGY
<ul style="list-style-type: none"> • Spaceflight medical standards, selection and certification • Astronaut health care • Environmental health standards and monitoring • Health care systems and training (CHeCS) • Epidemiology and clinical capability development 	<ul style="list-style-type: none"> • Biomedical ground research • Countermeasures validation • Space radiation health research • Biomedical flight research (HRF) • Advanced technology • National Space Biomedical Research Institute (NSBRI) 	<ul style="list-style-type: none"> • Advanced Life Support (ALS) • Advanced Human Engineering (AHE) • Advanced Environmental Monitoring & Control (AEMC)

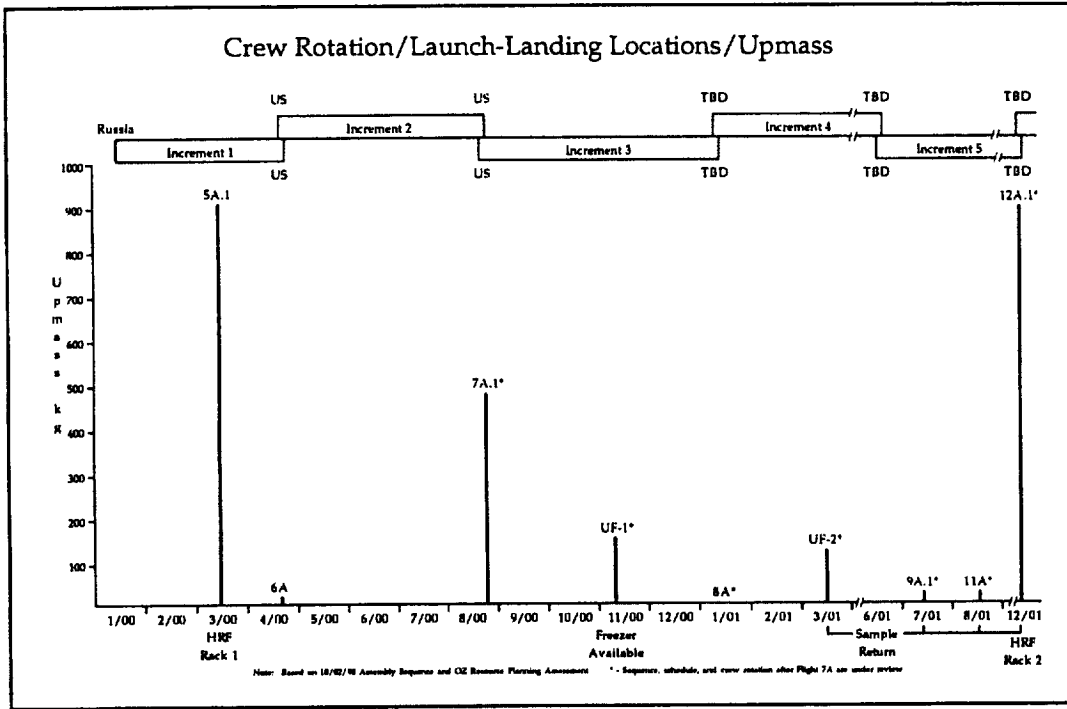
Note : Agency Program Commitment Agreements (PCA's) are in preparation for signature with NASA Administrator for AHST & BR&C.

HLSPO Relationship to International Space Station (ISS):

- HLSPO Flight Projects Office is the interface to the ISS Payloads Office and the ISS Payloads Control Board.
- Flight Projects Office coordinates HLSPO ISS flight research requirements between AHST, BRC and SMP and represents same to ISS Payloads Office.
- Note: Does not represent operational Space Medicine to ISS
- Negotiated resources from program sponsors and ISS results in implementation plan.
 - HLSPO program leads responsible for coordinating final flight implementation plan with OLMSA.
 - Flight Projects Office implements the mission research

BR&C ISS FLIGHT RESEARCH CONTENT

- Research includes US and International experiments as agreed upon with the International Space Life Sciences Working Group (ISLSWG)
- Research for ISS includes flight based and ground (pre & post flight) experiments
- Experiments include passive (non-power-crew deployed), active (powered, crew deployed), and invasive (crew interactive) requirements for implementation
- Includes sortie (Shuttle based) and long duration payloads
- Experiments use rack and non-rack resources
 - (Note: Human Research Facility is a tool for BR&C, not the Research)
- Experiments may require Russian and US ground facilities - pre and post flight
- All experiments managed via JSC Telescience Center
AND human research is very dependent on crew availability, participation and space medicine objectives and constraints.



The Human Space Life Sciences Critical Path Roadmap Project

*A Strategy for Human Space Flight
Through Exploration-class Missions*

Charles F. Sawin, PhD

Manager, JSC Biomedical Research and
Countermeasures Program

Fulfilling the HEDS Mission

In the Human Life Sciences,

In order to...

Prepare
to conduct
human missions
of exploration.....

we must...

Assess
Understand
Mitigate
Manage



Risk Management

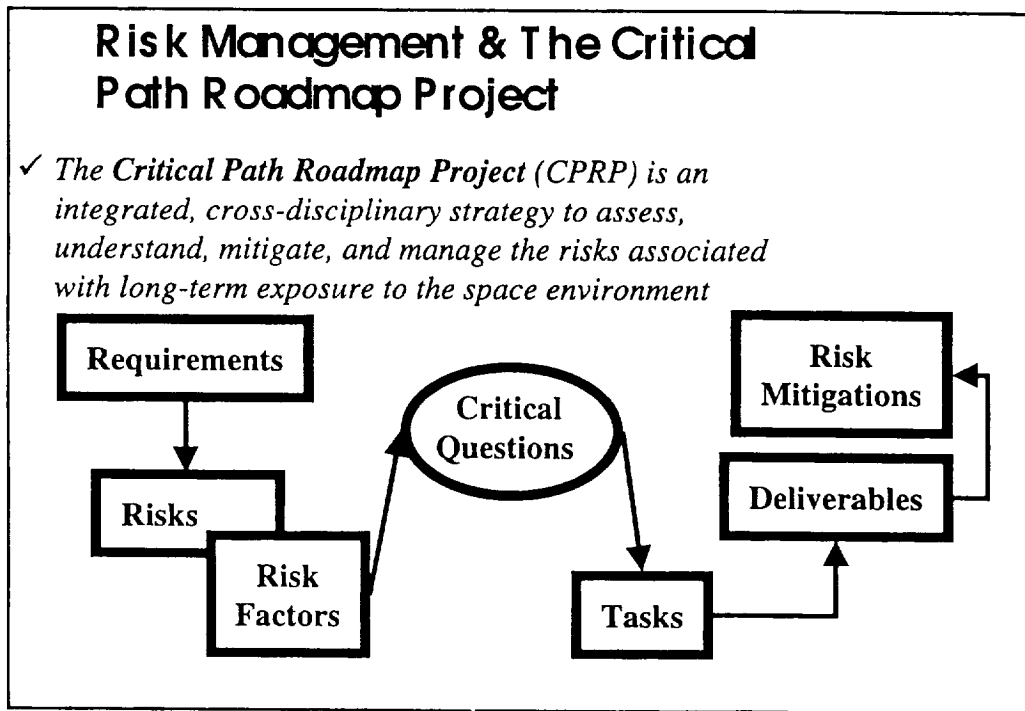
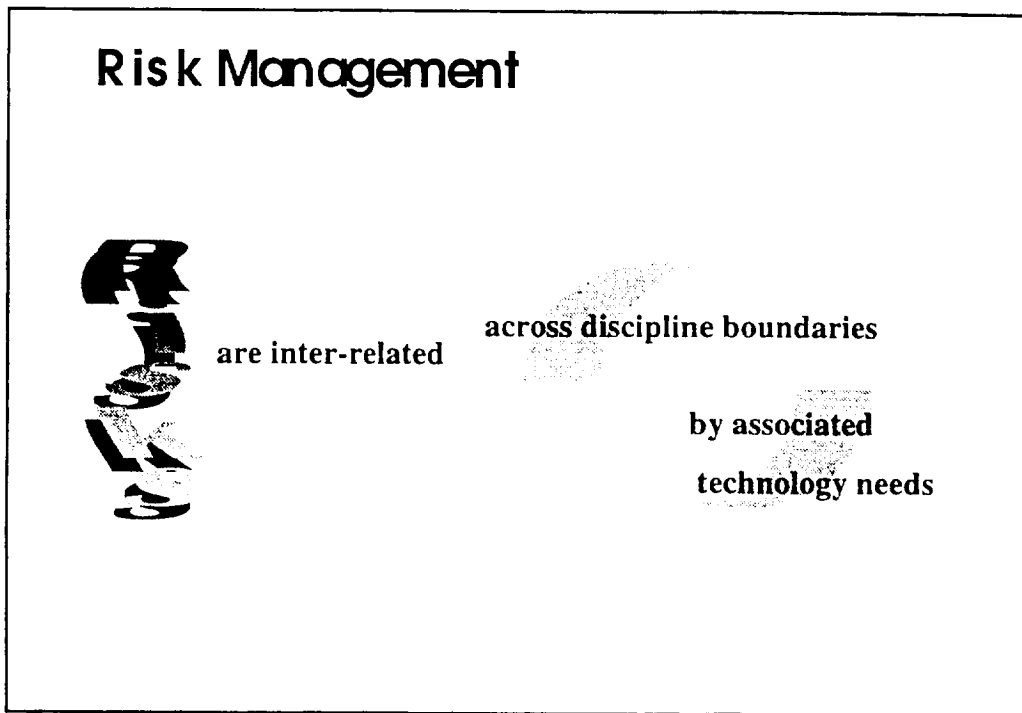
to crew performance

to crew health

crew mission contributions

attainment of mission objectives

long-term crew health



Elements of the CPRP Defined

- ✓ Risks - Likelihood of an undesirable event occurring from exposure to the space environment. Risk assessment includes the probability of the risk's occurrence, the severity of the consequences of the occurrence and the current status of the risk mitigation
 - ◆ examples: Occurrence of serious cardiac dysrhythmias
Fracture and impaired fracture healing
- ✓ Risk Factors - A condition or precipitating factor that must be present in order for the risk to occur. Such conditions can operate singly or in combination to contribute to the occurrence of the risk
 - ◆ examples: Poor nutrition
Inflight work schedule overloaded
- ✓ Critical Questions - Research and technology development needed to further assess the risk and address its mitigation
 - ◆ example: Will bone mass loss continue unabated for missions greater than six months, or will it plateau at some time consistent with absolute bone mineral density?

- ✓ Risk Mitigations - strategies, devices, interventions, requirements, etc., that need to be in place to modify the occurrence and/or impact of the risk
 - ◆ examples: Resistive exercise regimens
Medications
Preflight fitness requirements
- ✓ Critical Path Roadmap - graphic representation(s) of the essential set of research and technology development tasks required to address the critical risks associated with human space exploration-class missions, specifically denoting:
 - >relationships (causal pathway among risks, risk factors, and consequences)
 - >priorities
 - >temporal sequencing (predecessor questions/tasks)

The critical path roadmap for human exploration-class missions will illustrate

 - ◆ where we are going,
 - ◆ how we are going to get there, and
 - ◆ when we will get there

- ✓ Requirements -
 - ♦ examples:
 - Crew screening and selection requirements for minimizing bone loss
 - Habitability requirements
 - Nutritional requirements
 - Medical care systems for diagnosis, monitoring, and treatment of illness and injury

- ✓ Deliverables - specific end-items that can be identified, completed, & available at known dates
 - ♦ examples:
 - Validated, preflight training countermeasures for psychosocial adaptation
 - Validated, in-flight virtual reality-based training for emergency egress
 - Exercise countermeasures for bone loss, muscle atrophy, cardiovascular and neurovestibular adaptation

Advantages of the CPRP Approach

Optimizes Resource Allocation

- ✓ within & between disciplines
- ✓ between research & technology development
- ✓ in time

Enables Common Strategies

- ✓ takes advantage of interdependencies between risks
- ✓ recognizes short-cuts across common risks & their mitigations
- ✓ requires running dialogue between all parties

Timelines Critical Elements

- ✓ enables milestone checks
- ✓ manages interdependencies between risks

Human Mars Exploration

History

- ✓ Initiated July 1997 as internal JSC SLSD activity
 - ◆ Address HEDS strategic goals
 - ◆ Respond to Agency's advanced planning issues
- ✓ Expanded to include NSBRI participation in January 1998
- ✓ Integrates and builds on recommendations from advisory committees, task forces, and published reports
 - ◆ AMAC (1992)
 - ◆ NRC Reports
 - ◆ NASA Task Force on Countermeasures (1997)
 - ◆ Medical Policy Board Medical Policies and Requirements Document (Rev. 3)
 - ◆ Key reference documents identified for each risk

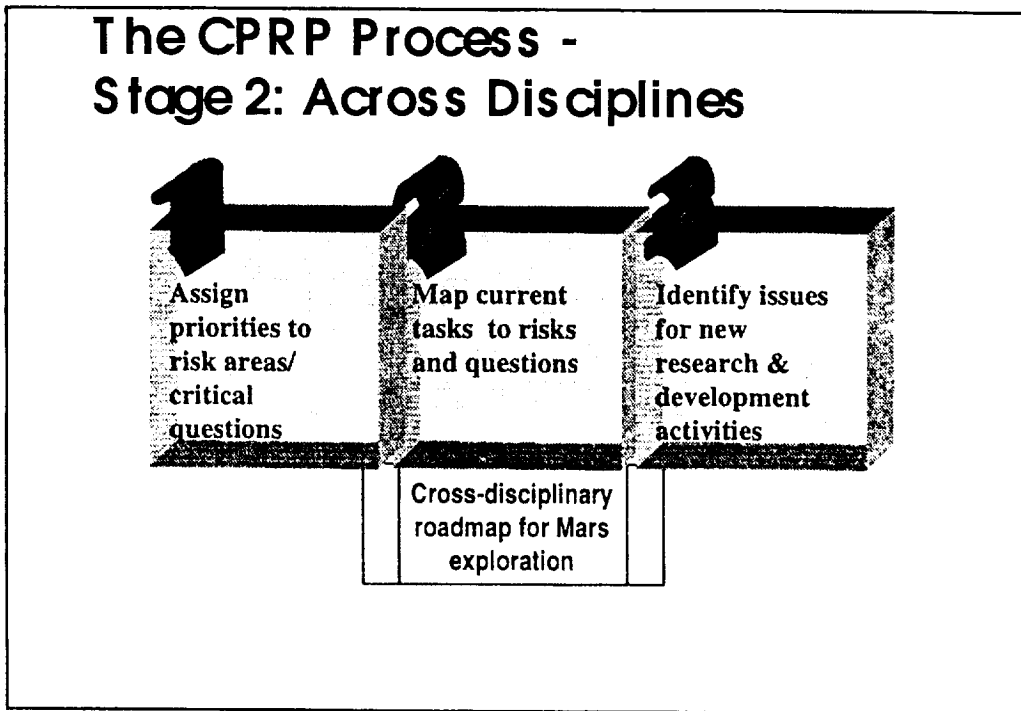
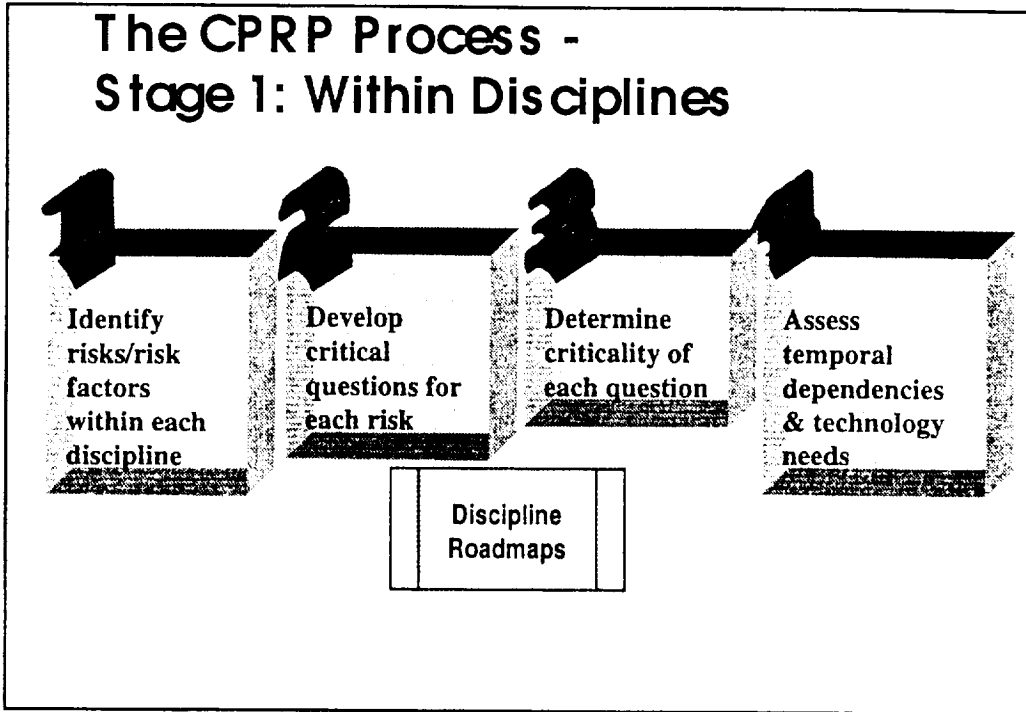
The 1st Step

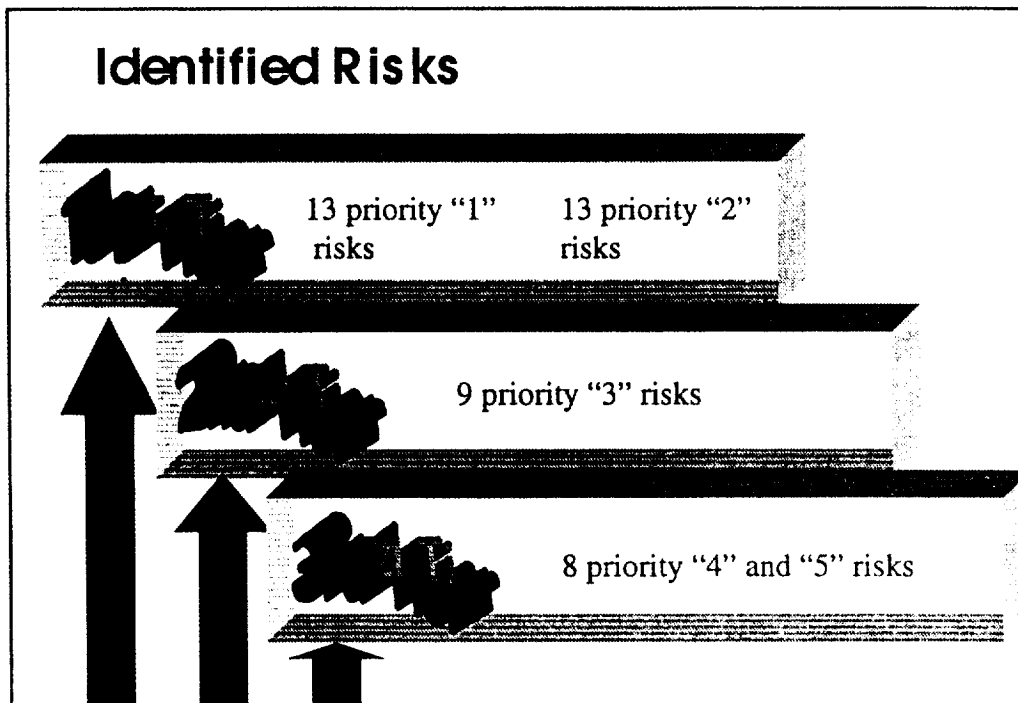
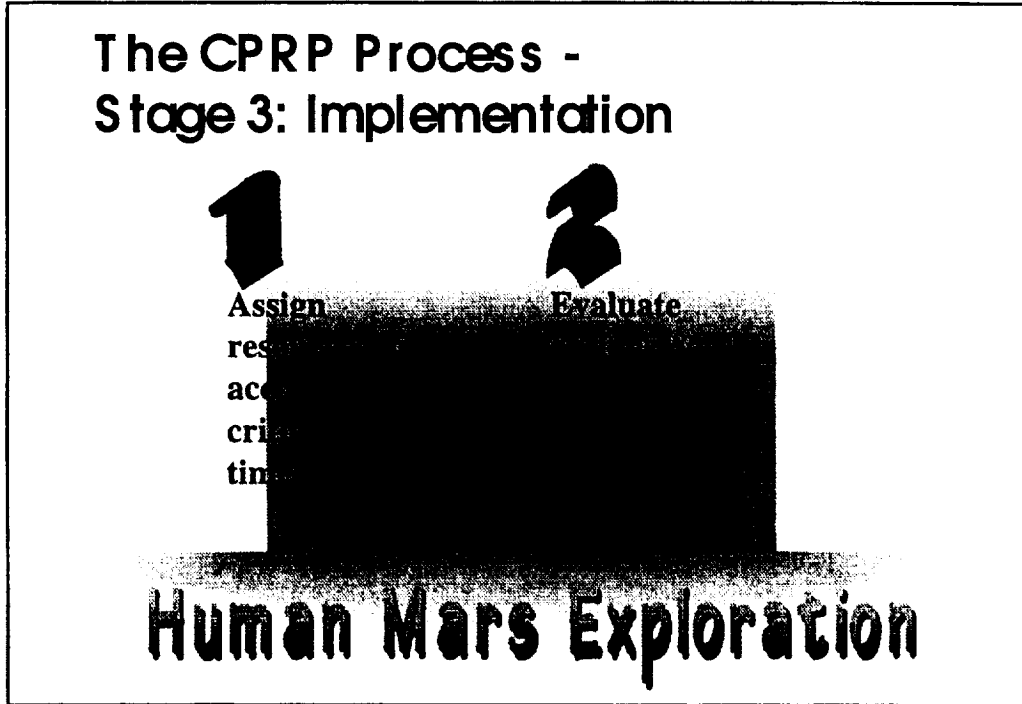
11 Discipline Risk Areas were identified

- ◆ Advanced Life Support
- ◆ Environmental Health
- ◆ Radiation Effects
- ◆ Human Performance
- ◆ Bone Loss
- ◆ Cardiovascular Alterations
- ◆ Food and Nutrition
- ◆ Muscle Alterations & Atrophy
- ◆ Immunology, Infection & Hematology
- ◆ Neurovestibular Adaptation
- ◆ Space Medicine

These Risk Areas were grouped into 4 Categories

- ◆ Environmental/Technological
- ◆ Human Behavior & Performance
- ◆ Human Health/Physiology
- ◆ Medical Care Capabilities





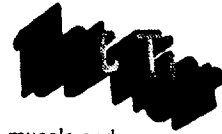
Priority "1" Risks

- ✓ Inability to maintain acceptable atmosphere in habitable areas
- ✓ Malnutrition
- ✓ Fractures and impaired fracture healing
- ✓ Occurrence of cardiac dysrhythmias
- ✓ Impaired cardiovascular response to orthostatic stress
- ✓ Human performance failure in the space environment leading to injury, accident, illness, or loss of mission objectives due to:
 - Poor psychological adaptation
 - Sleep and circadian rhythm problems
 - Human system interface problems and ineffective habitat/equipment
 - Behavioral illness (e.g., depression, anxiety, trauma, or other psychiatric dysfunction)
- ✓ Infections
- ✓ Carcinogenesis from radiation or immune system changes
- ✓ Altered hemodynamics



Priority "1" Risks

- ✓ Impacts of deficits in skeletal muscle structure and function on the homeostasis of other systems
- ✓ Loss of skeletal muscle mass, strength, and/or endurance
- ✓ Inability to adequately perform tasks due to motor performance, muscle endurance, and disruptions in structural and functional properties of soft and hard connective tissues of the axial skeleton
- ✓ Lack of appropriate inflight medical care capability, resulting in failure to provide diagnosis, treatment, and monitoring of crew illnesses and injuries during mission
- ✓ Permanent changes in balance and gaze
- ✓ Occurrences of sensory motor impairment (sensory, cognitive, perceptual, and psychomotor) affecting performance and ability to conduct a Mars landing



Priority "2" Risks

- ✓ Inability to provide and recover potable water
 - ✓ Inadequate supplies (including maintenance, emergency provisions, & edible food)
 - ✓ Renal stone formation
 - ✓ Diminished cardiac function
 - ✓ Unsafe food system
 - ✓ Altered wound healing
 - ✓ Altered host-microbial interactions
 - ✓ Inability to sustain muscle performance levels to meet demands of performing activities of various intensities (insufficient nutrition for sustaining substrate energy)
 - ✓ Damage to central nervous system from radiation exposure
 - ✓ Autonomic dysfunction
 - ✓ Post-landing alterations in cardiovascular, musculoskeletal, and neurosensory systems resulting in severe performance decrements, injuries and long-term sequelae on both planetary surfaces and on return to Earth
- 

Priority "3" Risks

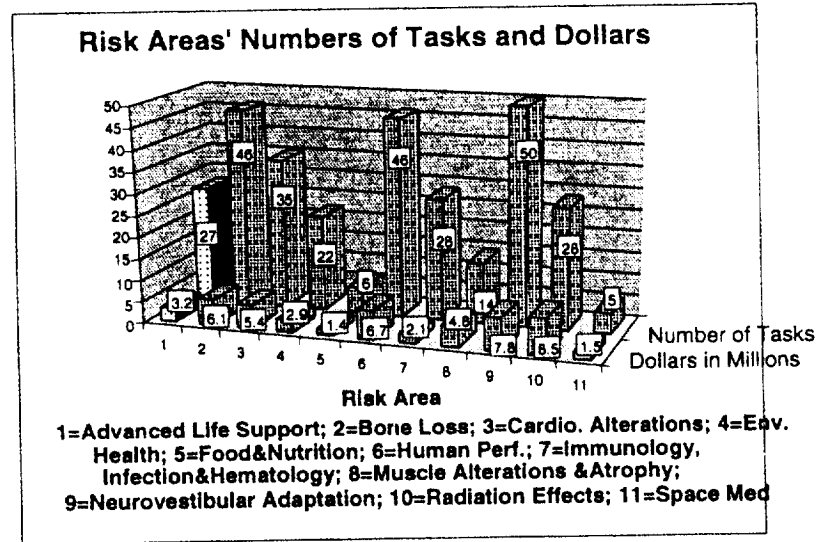
- ✓ Inability to maintain thermal balance in habitable areas
 - ✓ Inability to adequately process solid wastes
 - ✓ Injury to soft connective tissue, joint cartilage, intervertebral rupture, with or without neural complications
 - ✓ Manifestation of previously asymptomatic cardiovascular disease
 - ✓ Allergies and hypersensitivities
 - ✓ Propensity to develop muscle injury, connective tissue dysfunction, and bone fractures due to deficiencies in motor skill, muscle strength, and muscular fatigue
 - ✓ Decreased neuromuscular strength upon return to positive g environment
 - ✓ Synergistic effects from radiation exposure and microgravity
 - ✓ Development and treatment of decompression illness
- 

Priority "4" & "5" Risks

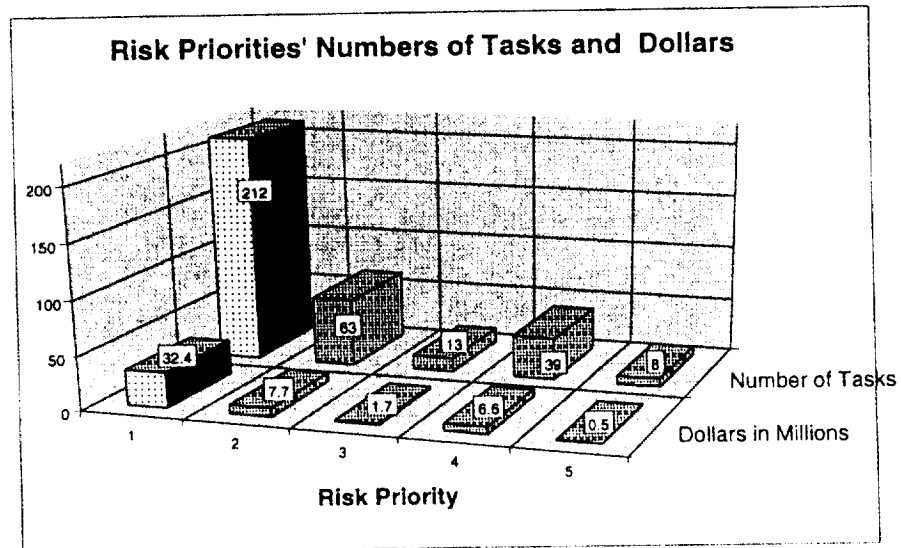
- ✓ Inadequate stowage and disposal facilities for solid and liquid trash generated during the mission
- ✓ Acceleration of age-related osteoporosis
- ✓ Impaired cardiovascular response to exercise stress
- ✓ Inability to rehabilitate
- ✓ Adverse drug reactions
- ✓ Space motion sickness
- ✓ Early or acute effects from radiation exposure
- ✓ Radiation effects on fertility, sterility, and heredity

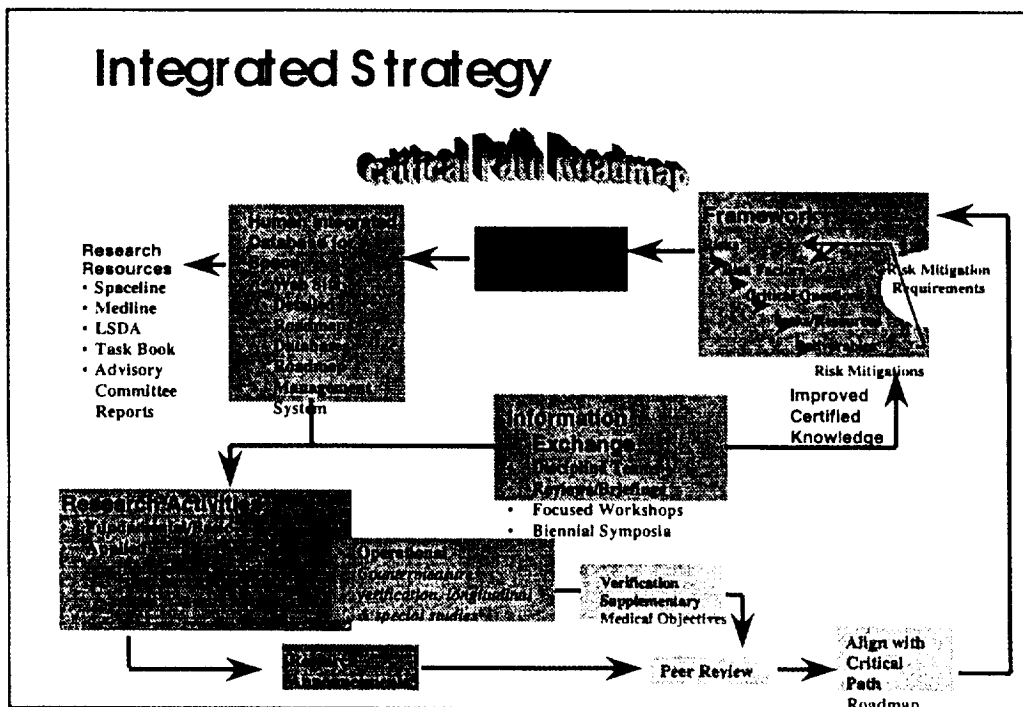
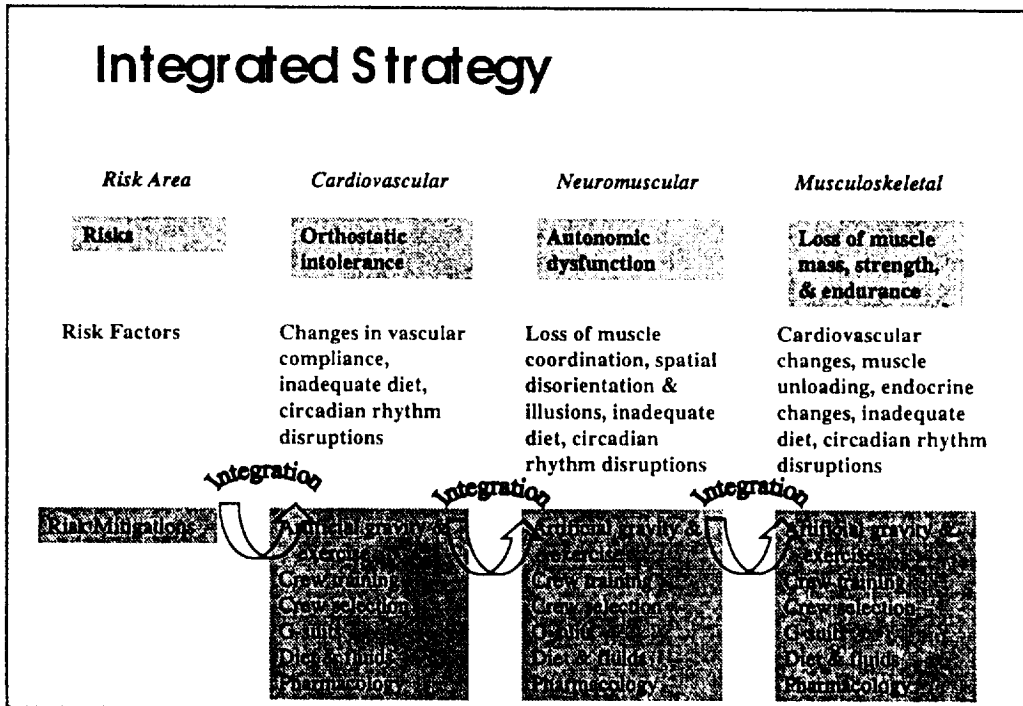


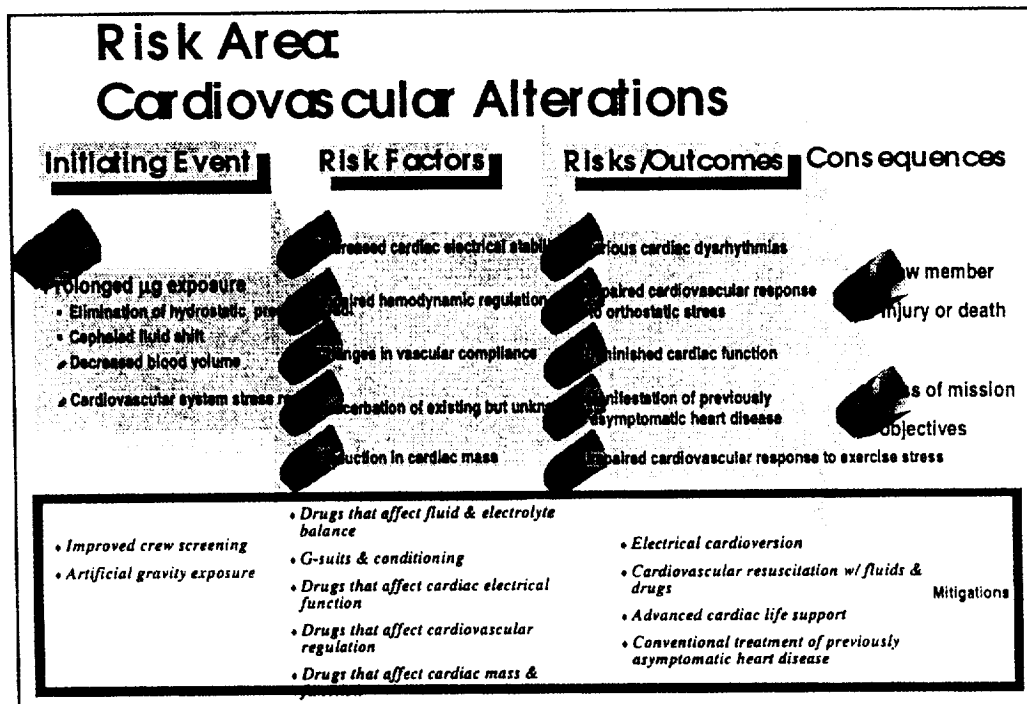
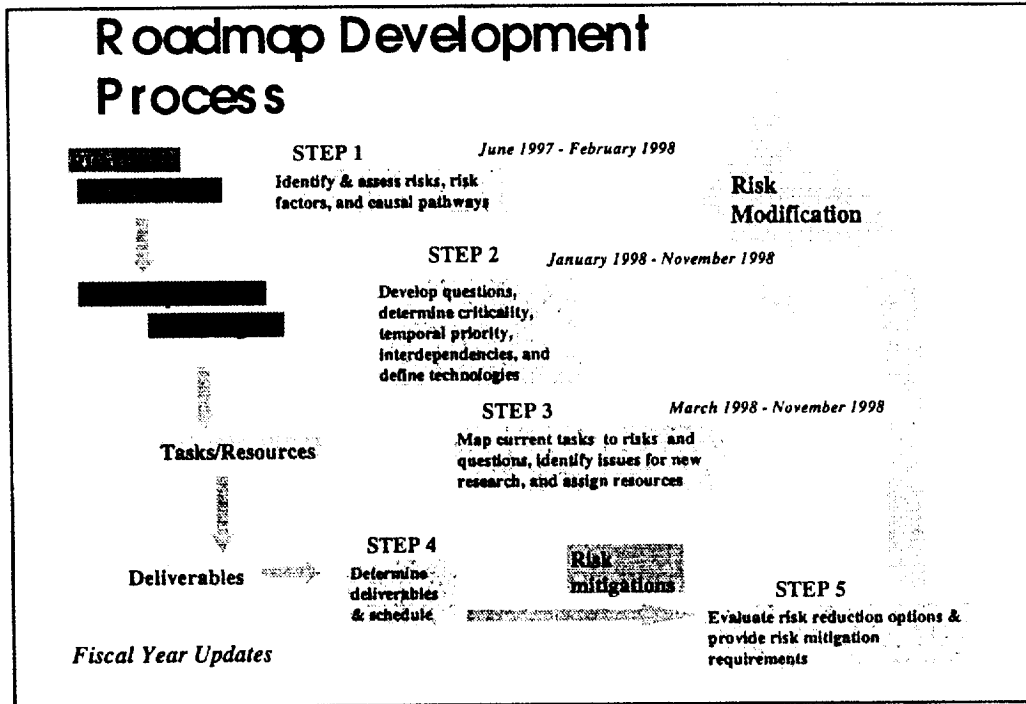
Risk Areas - Tasks & \$

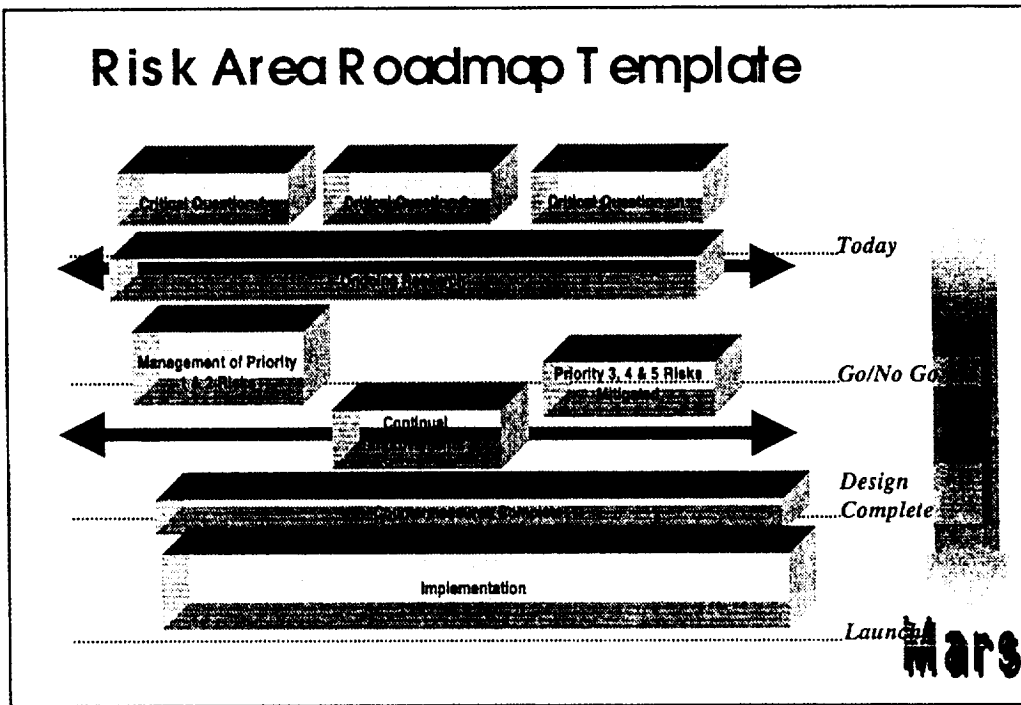
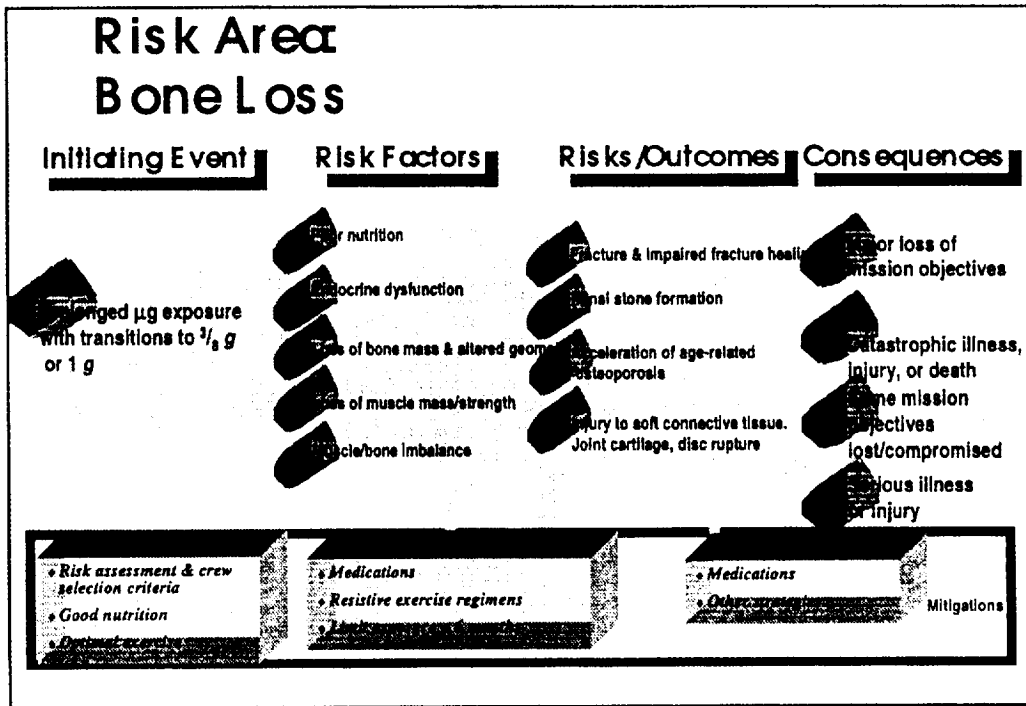


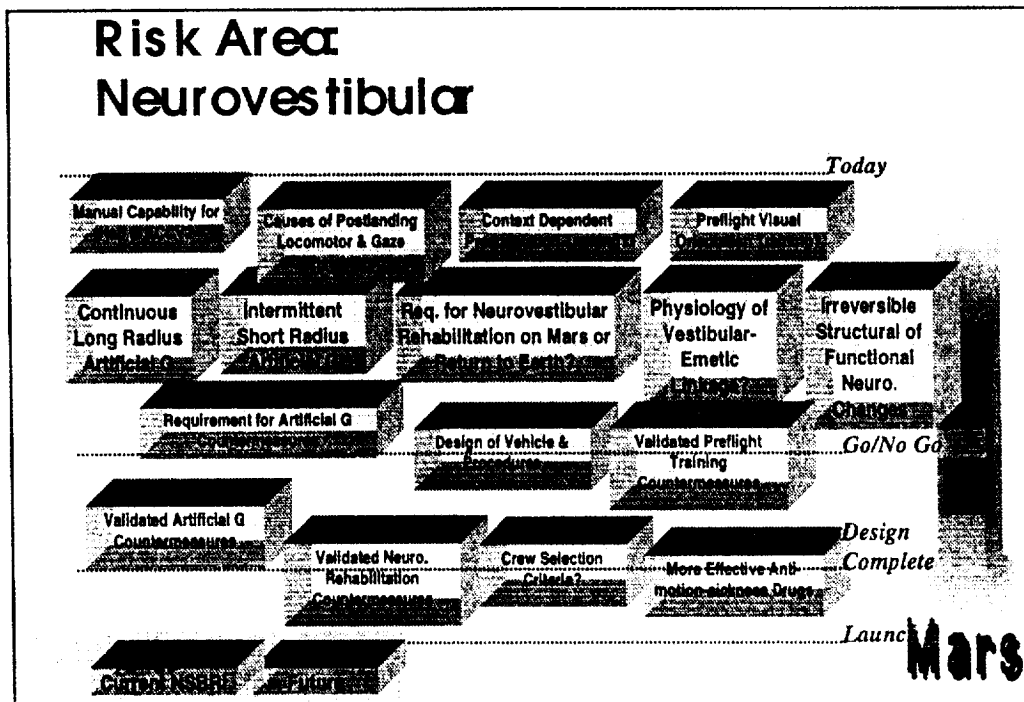
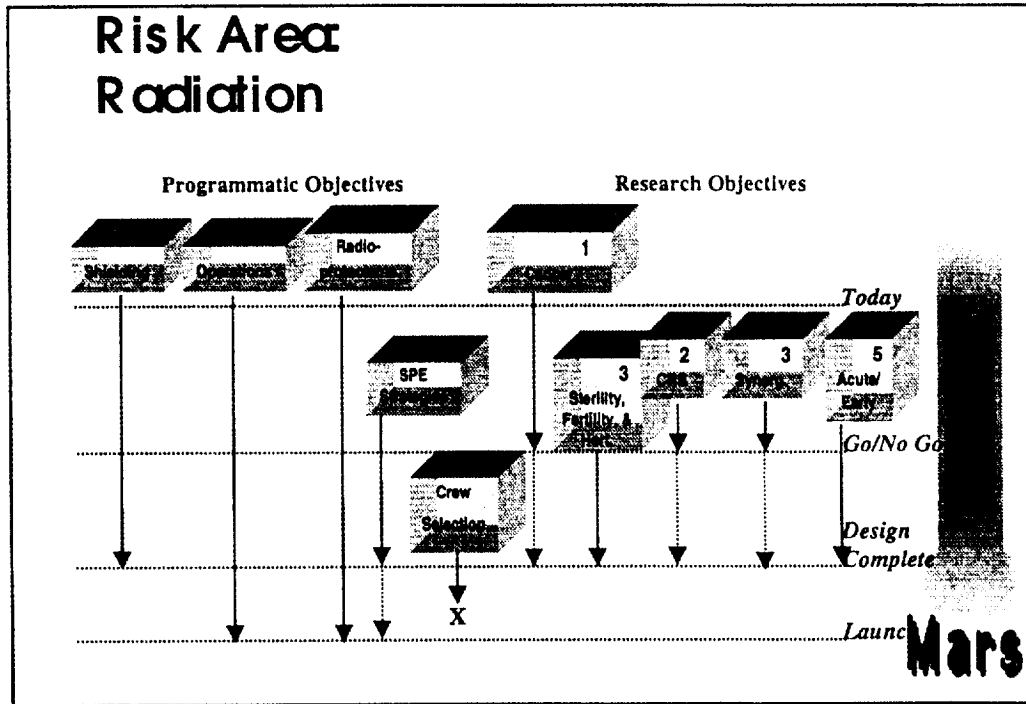
Risk Priorities - Tasks & \$







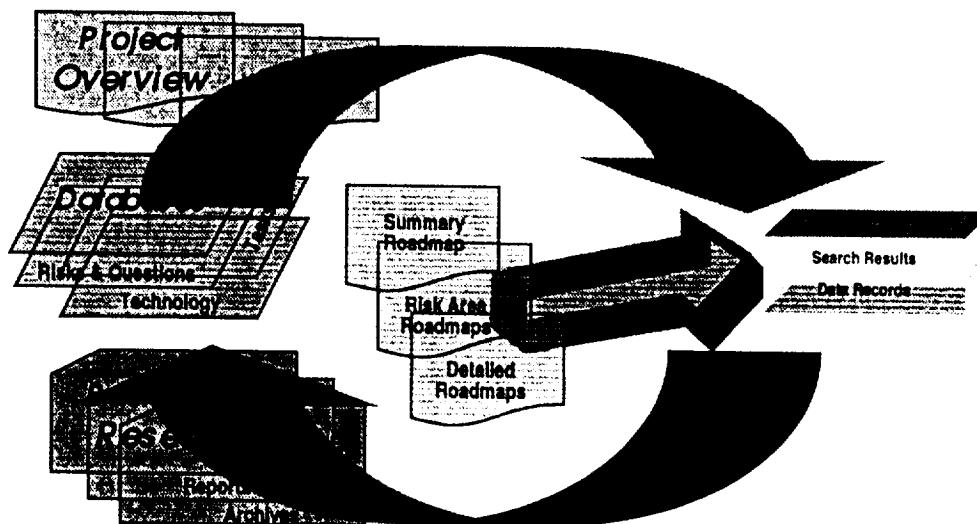




The CPRP Website

- ✓ Vision: to communicate CPRP to a diverse community of potential users
 - Scientists
 - Senior managers & project managers
 - Engineers
- ✓ Purpose
 - Provide scientific and technology information needed to address Agency's exploration goals
 - Facilitate dialogue and input about those needs
- ✓ Elements
 - Relational database of risk areas, risks, risk factors, critical questions, tasks, & technologies
 - Background research reports (e.g., FASEB, Task Force on Countermeasures, Spaceline)
 - Roadmaps (within risk areas, within risks, across risk areas)
 - Project management tools and data (resources, schedules)

Website Concept Overview



Status of Key Activities

- | | |
|--|------------------------|
| ✓ Identify risks within discipline | Completed |
| ✓ Rate risk severity, probability, and mitigation status | Completed |
| ✓ Rate or rank order risks within disciplines | Completed |
| ✓ Rate or rank order risks across disciplines | <i>Ongoing</i> |
| ✓ Identify and schedule future projects | <i>Ongoing</i> |
| ✓ Integrate current research results into critical path | <i>Ongoing</i> |
| ✓ Plan for biennial biomedical investigators workshop | Completed |
| ✓ Plan for artificial gravity workshop | Completed |
| ✓ Input to NRA process | February 1999, ongoing |
| ✓ Deliver finalized, integrated critical path roadmap | January 2000 |

Next Steps

- ✓ Continue to develop and refine temporal roadmaps for each risk area (Ongoing)
- ✓ Identify technologies required for critical questions (Ongoing, First iteration completed)
- ✓ Identify research projects/tasks and resources needed to address critical path risks and questions (e.g., Countermeasure Task Force Report) (Ongoing)
- ✓ Develop overarching/integrated roadmap across all risks (Jan - May 1999)
- ✓ Develop working prototype of Critical Path Roadmap Web Site (Ongoing)
- ✓ Perform NASA Headquarter's and Advisory Committee Reviews (Ongoing)
- ✓ Identify all deliverables and end-items (July, 1999)

Summary

- ✓ The product of the critical path roadmap project is an integrated strategy for mitigating the risks associated with human exploration class missions
- ✓ It is an evolving process that will assure the ability to communicate the integrated critical path roadmap
- ✓ Unlike previous reports, this one will not sit on a shelf - it has the full support of the JSC Space and Life Sciences Directorate (SA) and is already being used as a decision making tool (e.g., budget and investigation planning for Shuttle and Space Station mission)
- ✓ Utility of this product depends on many efforts, namely: providing the required information (completed risk data sheets, critical question information, technology data)
- ✓ It is essential to communicate the results of the critical path roadmap to the scientific community - this meeting is a good opportunity to do so
- ✓ The web site envisioned for the critical path roadmap will provide the capability to communicate to a broader community and to track and update the system routinely

NASA Johnson Space Center Biomedical Research Resources

W. H. Paloski, Ph.D.

Chief, NASA Johnson Space Center Life
Sciences Laboratories

JSC Medical Sciences Laboratories

Purpose

These laboratories constitute a national resource for support of medical operations and life sciences research enabling a human presence in space.

Role

They play a critical role in evaluating, defining, and mitigating the untoward effects of human adaptation to space flight.

Primary Tasks

- Over the years they have developed the unique facilities and expertise required to perform:
- biomedical sample analyses and physiological performance tests supporting medical evaluations of space flight crew members,
 - scientific investigations of the operationally relevant medical, physiological, cellular, and biochemical issues associated with human space flight.

Staffing

They currently support 20 civil servants and approximately 100 contractor personnel.

JSC Medical Sciences Laboratories

- **Bone and Muscle Lab**
 - Linda Shackelford, M.D.
- **Cardiovascular Lab**
 - Janice Yelle, M.S.
- **Cellular/Molecular Research Lab**
 - Clarence Sams, Ph.D.
- **Clinical Lab**
 - Daniel Feedback, Ph.D.
- **Environmental Physiol/Biophysics Lab**
 - Michael Powell, Ph.D.
- **Exercise Physiology Lab**
 - Michael Greenisen, Ph.D.
 - Suzanne Schneider, Ph.D.
- **Microbiology Lab**
 - Duane Pierson, Ph.D.
- **Muscle Research Lab**
 - Daniel Feedback, Ph.D.
- **Neurosciences Labs**
 - Deborah Harm, Ph.D.
 - Millard Reschke, Ph.D.
 - Jacob Bloomberg, Ph.D.
 - William Paloski, Ph.D.
 - Todd Schlegel, M.D.
- **Nutritional Biochemistry Lab**
 - Scott Smith, Ph.D.
- **Pharmacology Lab**
 - Lakshmi Putcha, Ph.D.
- **Radiation Biophysics Lab**
 - Open
- **Test Subject Facility**
 - Todd Schlegel, M.D.
- **Toxicology Lab**
 - John James, Ph.D.
- **Water and Food Analytical Lab**
 - Richard Sauer, P.E.

JSC Laboratory Activities

medical operations

- crew selection
- medical monitoring
- environmental monitoring
- sample analyses
- performance testing
- occupational health
- risk analyses
- countermeasures
- rehabilitation
- anomaly assessment

biomedical research

- operational studies
- clinical studies
- countermeasures
- flight experiments
- ground-based studies
- modelling
- analog studies
- hardware development
- data archival
- critical path

education/outreach

- K-12
- university
- public affairs
- corporate

service

- other JSC orgs
- other NASA orgs
- extramural scientists
- international partners

Unique Features of JSC Laboratories

Location

- Colocation with each other—rapid response to anomalies.
- Proximity to astronauts, flight surgeons, crew trainers, flight engineers, timeliners, etc.
 - Satellite laboratories at KSC (Florida), DFRF (California), and GCTC (Russia).

Experience

- Familiarity with flight experiment operational constraints (crew, equipment, timeline, etc.).
 - Familiarity with mission operations procedures, manifesting, and control boards.
 - First-hand knowledge of space adaptation syndrome—multiple landing experiences.
 - Scientific collaborations with local, national, and international investigators.
- Programmatic collaboration with Russian, European, French, German, and Japanese Space Agencies.

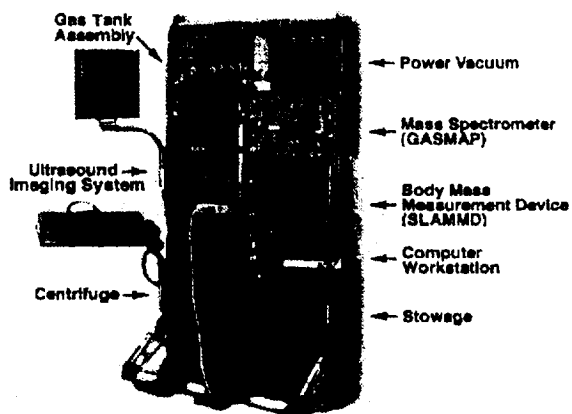
Corporate Knowledge

- Single location for non-volatile memory of NASA life/medical sciences experiences.
 - Continuous support provided since the beginning of human space flight in the US.
 - Repository of historical space flight data and samples.

ISS Human Research Facility (HRF)

one-rack facility equipped to:

- assess crew health
- conduct operational research
- develop countermeasures
- conduct basic human research



HRF Cardiopulmonary Research Capabilities

- **Echocardiograph**: for cardiac and peripheral vascular measurements
- **ADAS, Holter Monitor, Portapres, Heart Rate and Blood Pressure Monitors**: heart rate and blood pressure variability and response to stress
- **Handgrip, LBNP, Infusion Supplies, Blood and Urine Sampling**: tests of autonomic function
- **Treadmill and Cycle Ergometer**: studies of cardiopulmonary function during exercise
- **GASMAP/Pulmonary Function System**: respiratory studies
- **Pulse Oximeter**: arterial oxygen saturation during sleep, exercise, prebreathe

HRF Musculoskeletal Research Capabilities

- **Echocardiograph**: muscle volume, tendon and connective tissue assessments
- **Resistance Exercise Device**: countermeasures to muscle atrophy, strength loss and bone demineralization
- **Blood and Urine Collection Kits**: bone and muscle markers
- **Handgrip and Pinch Force Dynamometer**: hand muscle strength and endurance
- **Strength Measurement Device (Muscle Atrophy Research and Exercise System)**: muscle strength, endurance and neuromotor function
- **Foot-Ground Interface Device**: assessment of the role of ground impact forces during countermeasure exercises on bone loss

HRF Neurosensory Research Capabilities

- **Strength Measurement Device**: neuromotor responses such as reaction times, motor reflex responses, muscle recruitment
- **Range of Motion Goniometer**: locomotion studies, neurosensory control
- **Force Plate**: postural stability
- **ADAS**: EMG measurements for neuromotor assessment
- **Workstation**: complex cognitive and visual performance tests

HRF Biochemistry/Integrative Physiology Research Capabilities

- **Blood and Urine Collection Systems, Centrifuge, Infusion Systems, Freezer:** endocrine, immune, pharmacological studies
- **Body Mass Measurement Device:** nutritional balance
- **GASMAP:** metabolic measurements during rest and exercise
- **Core Temperature Device:** circadian studies
- **Activity Monitor:** nutrition/metabolic, sleep studies

HRF Radiation Research Capabilities

- **Dosimeters**
- **Blood Collection System:** to monitor changes in chromosome mutations

ISS Crew Health Care System (CHeCS)

Clinical/Health Care Equipment:

- Ambulatory Medical Pack (AMP)** - Used for routine assessment of each crew member's general health and as diagnosis and treatment of illnesses and minor injuries
- Advanced Life Support Pack (ALSP)** - Provides a collection of emergency medical instruments and supplies for initial care and stabilization of a critically injured crewmember
- Crew Contamination Protection Kit (CCPK)** - Provides gear for protection of the crew during or after a contamination event
- Medical Equipment Computer (MEC)**
- Treadmill with Vibration Isolation System (TVIS), Ergometer with Vibration Isolation System**
- Resistive Exercise Device (RED)** - Used for exercising and testing the major muscle groups in the isometric, isotonic, and isokinetic modes
- Heart Rate Monitor, Blood Pressure/ECG Monitor**
- Defibrillator**
- Crew Medical Restraint System (CMRS)** - Provides a restraint surface and a transport mechanism for an ill or injured crewmember
- Crew Contamination Protection Kit (CCPK)** - Provides gear for protection of the crew

ISS Crew Health Care System (CHeCS)

Radiation Monitoring Equipment:

- Tissue Equivalent Proportional Counter (TEPC)** - Portable radiation exposure monitor used to monitor the internal radiation doses absorbed by ISS crews
- Total Organic Carbon Analyzer/Ion Selective Electrode Assy. (TOCA/ISE) Dosimeter Set** - Contribute to the monitoring of the radiation dose levels inside the ISS
- Intra Vehicular Charged Particle Directional Spectrometer (IVCPDS)** - Portable device which monitors radiation fluxes to determine the penetrating ability of radiation
- Extra Vehicular Charged Particle Direction Spectrometer (EVCPS)** - To measure the flux of trapped, secondary, and galactic cosmic rays as a function of time in three directions

ISS Crew Health Care System (CHeCS)

Environmental Monitoring Equipment:

Compound Specific Analyzer- Combustion Products (CSA-CP) - Detects and quantifies specific toxicological compounds in the ISS atmosphere

Compound Specific Analyzer- Hydrazine (CSA-H)

Microbial Air Sampler (MAS)

Fungal Spore Sampler (FSS)

Volatile Organic Analyzer (VOA)

Water Microbiology Kit (WMK) - Detects, enumerates, and selectively identifies the microbial load of ISS water

Water Sampler & Archiver (WS&A) - Collect and store ISS water samples for both in-flight and ground-based analyses

Spectrophotometer - Used to measure iodine, color, turbidity, and general spectrophotometric analysis of ISS water samples

Surface Sampler Kit (SSK) - Detects and quantifies the microbial load of internal surfaces of ISS habitable modules

Incubator

Slide Staining Apparatus (SSA)

Hypergravity Facilities: Extending Knowledge over the Continuum of Gravity

Kenneth A. Souza

Chief, Life Sciences Division

NASA Ames Research Center

Historical Perspectives

● 1960's

Life Sciences Program initiated at ARC with emphasis on fundamental aspects of space biology and biomedicine

- Laboratories, centrifuges and bedrest facilities constructed and research started
- Spaceflight research and projects begun (Biosatellites 1, 2, 3)

● 1970's

Centrifuges and simulation facilities used to characterize biological responses to hypergravity and unloading

- Long term hypergravity effects of rodent physiology and reproduction
- Rat hind-limb suspension model developed
- First female bedrest study conducted
- Vestibular Research Facility developed

● 1980's

Flight activities increase: facilities used for "applied research"

- Launch and landing simulations
- Biomedical countermeasures; fluid loading, resistive exercise, autogenic feedback

● 1990's

Refocus facilities as a national resource: Center for Gravitational Biology Research (CGBR)

- Facility upgrades and new capabilities
 - ISS Testbed Centrifuge
 - Hypergravity Facility for Cell Culture (HyFaCC)
 - Human-Powered Centrifuge
 - Chronic Live-Aboard Centrifuge (CLAC)
 - Construction of new support areas
- Biocomputation Center established

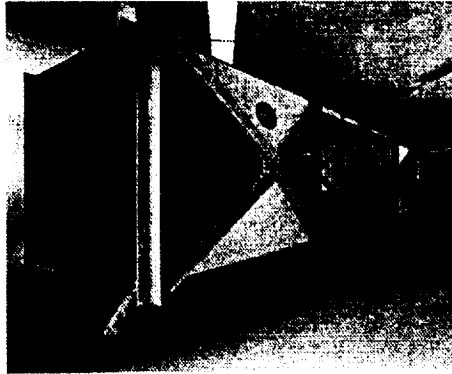
Why A Center for Gravitational Biology Research?

- Stimulate research in gravitational biology
 - Familiarize the scientific community with the use of centrifuges both on the ground and in space
- Utilize unique suite of existing facilities
- Support development, conduct and interpretation of flight experiments
- Facilitate flight simulation studies e.g., bedrest, hind-limb suspension, launch/landing stress
- Provide testbed for ISS flight hardware development
- Provide control environment for various flight experiments

Centrifuges as Research Tools Key Questions

- Effects of altered gravity on:
 - Reproduction and Development
 - Aging
 - Behavior and Performance
 - Structure and Function
 - Physiological and Immunological function
- Time course of adaptation to new g-level
- Centrifugation in space
 - Countermeasures? "Artificial Gravity" What level and frequency?
 - 1-g onboard control? Rotational effects? Stopping frequency?
 - Gravity threshold

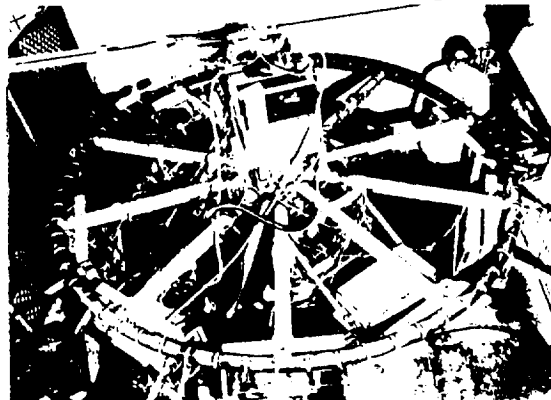
20-G Centrifuge



◆ Facility Scientist: Dr. Malcolm Cohen

- Radius - 29 foot (fixed)
- Payload - 16,000 G-lbs
- Max G - 20 (human-rated to 12.5G)
- Max RPM - 50
- Acceleration - 1G/sec to 12G;
0.5G/sec 12 to 20G
- Drive - 300 HP DC motor
- Cabs - 91 inch L x 71 inch W x 82 inch H (Cab A - Swing chair, Cab B - Treadmill installation)
- Exposure - Acute exposure (minutes to hours)
- Specimens - Humans, rodents, rhesus and squirrel monkeys

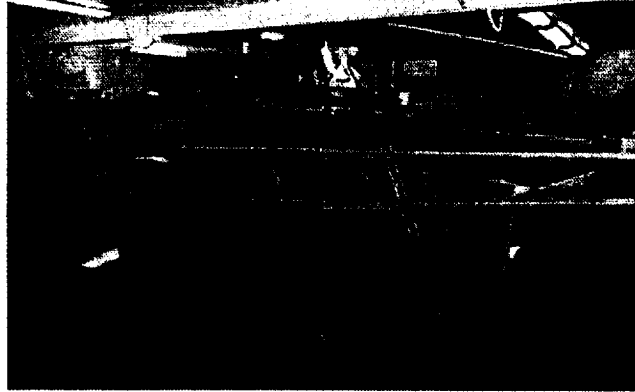
8-Foot Centrifuge



◆ Facility Scientist: Dr. Charles Wade

- Radius - 4 foot (fixed)
- Payload - 10 animal enclosures (1/radial arm)
- Max G - 10
- Max RPM - 85
- Gravity Onset - Adjustable
- Drive - 10 HP DC motor
- Specimens - Rodents, small primates, snakes
- ISS habitat compatible

24-Foot Centrifuge



◆ Facility Scientist: Ms. Meryl Corcoran (Acting)

- Radius - 12 foot (variable from 4-12 ft at 6 inch intervals)
- Payload - 20 animal enclosures (2/radial arm)
- Max G - 4.15
- Max RPM - 30.5
- Gravity Onset - 0.0370 rad/sec²
- Drive - 25 HP DC motor
- Specimens - Rodents, guinea pigs, rabbits, primates

Vestibular Research Facility

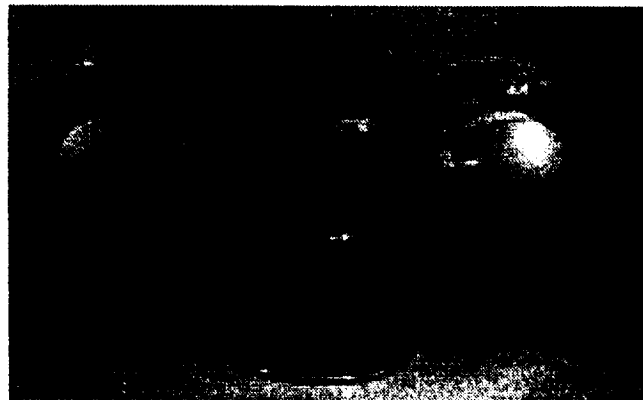
◆ Science Manager: Dr. Larry Hoffman (Acting)

● Vestibular Research Facility (VRF) enables study of responses to smooth linear motion or to combinations of linear and angular motion

- Multi-axis ground-based centrifuge
- 12-foot Linear Spring Sled
- 30-foot Linear Sled
- 8-foot Programmable Linear Sled

Vestibular Research Facility

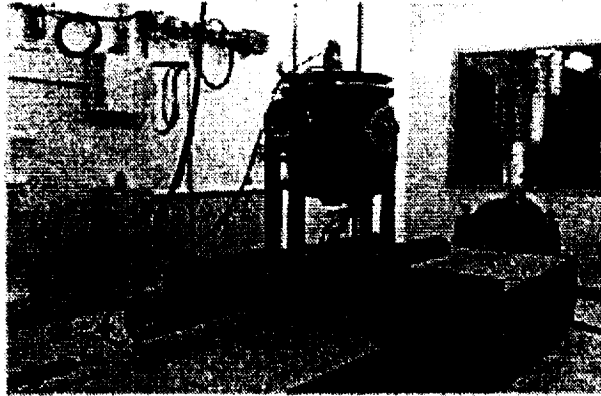
Multi-Axis Ground-Based Centrifuge



- Radius - 3.9 foot
- Payload - 54 pound (each STC)
- Max G - 1.75
- Max RPM - 40 (main axis); 83 rpm (Inner yoke and STC axes)
- Gravity Onset - 8.72 rad/sec^2
- Specimens - Small primates, rodents

Vestibular Research Facility

12-Foot Linear Spring Sled



- Size - 12 foot long
- Payload - 300 pound
- Drive - Harmonically tuned springs driven by a linear actuator
- Range - 0.25, 0.50, 1.5 and 5.0 Hz
- Specs response - Max 0.6G acceleration, 1.0G deceleration and 5 Hz
- Specimens - Small primates, rodents, chicks

Vestibular Research Facility

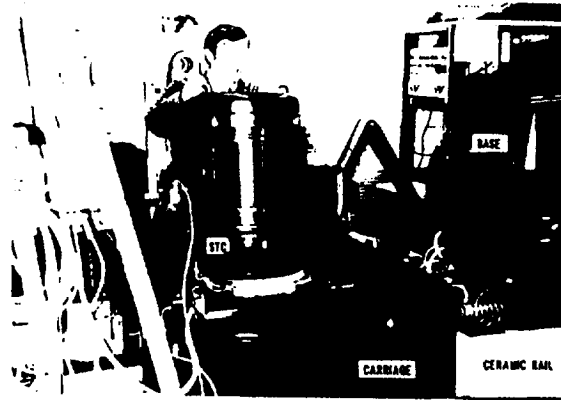
30-Foot Linear Sled



- Size - 30 foot long
- Payload - 300 pounds
- Drive - Linear motor
- Range - Sinusoids of >0.2 ; Peak over 0.2-10 Hz
- Specs response - Max 1.0G acceleration, planned 1.0G deceleration
- Specimens - Humans, small primates, rodents, chicks

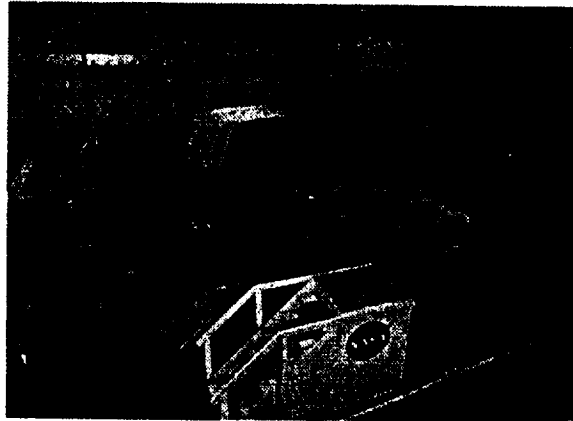
Vestibular Research Facility

8-Foot Programmable Linear Sled



- Size - 8 feet long, with max displacement 20 inches (horizontal or vertical operations)
- Payload - 650 pounds
- Drive - Linear motor
- Range - 1.0 - 5.0 Hz
- Specs response - Max 1.0G acceleration, 0.7G deceleration
- Specimens - Small primates or other small animals

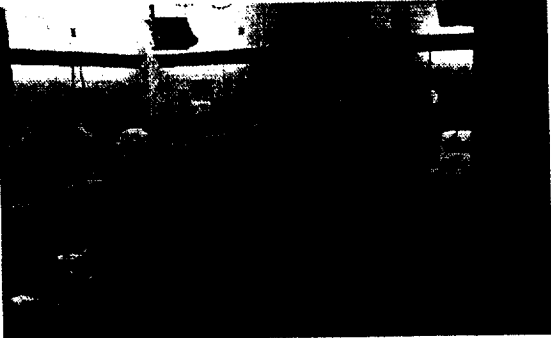
Hypergravity Facility for Cell Culture



◆ Facility Scientist : Dr. Ruth Globus

- Radius - 9 foot
- Payload - 500 pounds
- Max G - 6
- Max RPM - 45
- Gravity Onset - 0.007 to 0.52 rad/sec²
- Drive - 20 HP DC motor
- Exposure - Acute exposure
- Specimens - Cells, tissues

Human Research Facility



◆ Facility Scientist: Dr. Sara Arnaud

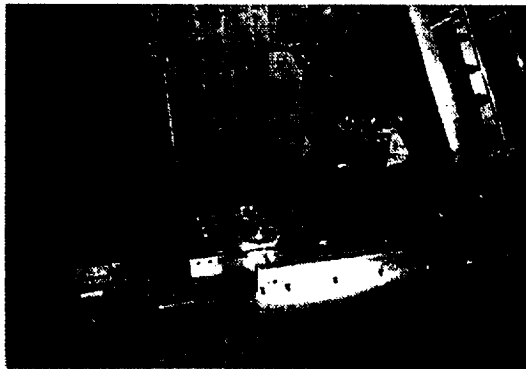
- 4100 square foot facility
 - Supports up to 12 bedrest subjects; 6 degree head-down capability
 - Four bedrooms, 3 bathrooms - one horizontal shower
 - Recreation/dining area
 - Test and support area
 - Central data station/nurses station

Human Research Facility



- Test area provides lower-body negative pressure device, upright and supine bicycle ergometry, upright treadmill, isokinetic exercise devices, and a tilt table to test orthostatic intolerance
- Horizontal shower

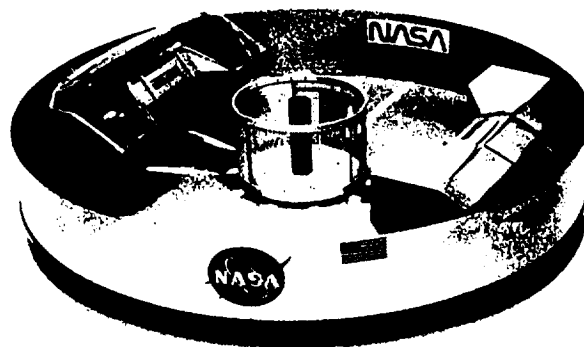
Human-Powered Centrifuge



◆ Facility Scientist : Dr. John Greenleaf

- Diameter - 12.5 foot (fixed)
- Payload - 500 kilograms (rider/disc weight)
- Max G - Up to 5G at the on-board rider's foot
- Angular Velocity at 1G Centripetal Acceleration - 2.3 rad/second
- Gravity Onset - Variable for rider at .05 hp
- Drive - Manual pedaling
- Exposure - Short exposure (minutes to hours)
- Specimens - Humans

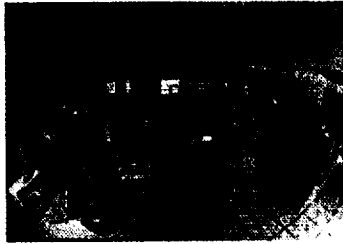
Chronic Live-Aboard Centrifuge



◆ Facility Scientist: Dr. Malcolm Cohen

- Radius - 13.4 - 22.2 foot (fixed)
- Payload - 5000 pounds
- Max G - 2.0
- Max RPM - 18.6
- Gravity Onset - Nominal
- Drive - 75 HP DC motor
- Cab - 21 inch L x 8 inch W x 8 inch H
- Exposure - Chronic (weeks to months)
- Specimens - Humans, rodents, small primates and plants

Center for Bioinformatics



◆ Science Manager: Dr. Muriel Ross

- Three dimensional, serial section reconstruction (image processing)
- Advanced Visualization (graphics/virtual environments)
- Modeling/Simulation (finite element/neuronal networks/electrophysiology)
- Neurotechnology (from biological neuronal circuits and systems to chips, processors and computer architectures)

Access to CGBR

● General Information

-Center for Gravitational Biology Research

◆ Website: <http://lifesci.arc.nasa.gov/CGBR/CGBR.html>

-Facility Use Questionnaire

◆ Website: <http://lifesci.arc.nasa.gov:100/facilities>

-Point of contact:

◆ Mr. James Connolly

(650) 604-6483 - jconnolly@mail.arc.nasa.gov

● NASA Research Announcement (<http://peer1.idi.usra.edu>)

-Standard Companion Document

Task Force Report on Countermeasures February 1997

Kenneth M. Baldwin, PhD
Professor
Department of Physiology & Biophysics
University of California Irvine
School of Medicine

CHARGE TO THE COMMITTEE:

- **SURVEY EFFICACY AND APPROPRIATENESS OF EXISTING COUNTERMEASURES, INCLUDING CURRENT RESEARCH**
- **EVALUATE ADEQUACY OF EXISTING DATA BASES**
- **EVALUATE CURRENT PLANS AND ONGOING COUNTERMEASURES, INCLUDING NASA AND RUSSIAN PROGRAMS: PROPOSE INNOVATIVE RESEARCH AND ASSOCIATED METRICS**
- **PROVIDE SHORT TERM AND LONG TERM RECOMMENDATIONS**
- **PROVIDE FEEDBACK ON QUALITY AND DIRECTION OF CURRENT MEDICAL POLICIES**

COMMITTEE MEMBERS

KENNETH M. BALDWIN, UC IRVINE (CHAIR)
JEFFREY BORER, CORNELL SCHOOL OF MEDICINE
V. REGGIE EDGERTON, UC LOS ANGELES
MARTIN J. FETTMAN, COLORADO STATE UNIVERSITY
MICHAEL HOLICK, BOSTON UNIV. SCHOOL OF MEDICINE
RONALD C. MERRELL, YALE UNIV. SCHOOL OF MEDICINE
ALAN SCHILLER, MOUNT SINAI SCHOOL OF MEDICINE
ARTHUR C. VAILAS, UNIVERSITY OF HOUSTON
***ELLEN BAKER, JOHNSON SPACE CENTER**
***ROGER BILICA, JOHNSON SPACE CENTER**
***VICTOR CONVERTINO, BROOKS AIR FORCE BASE**
***CRAIG FISCHER, PALM SPRINGS, CA.**
***JERE MITCHELL, UNIV. OF TEXAS SOUTHWEST. MED. CTR**
***EMILY HOLTON, NASA AMES RESEARCH CENTER**
***CHARLES SAWIN, JOHNSON SPACE CENTER**
***PEGGY WHITSON, JOHNSON SPACE CENTER**
***RHEA SEDDON, JOHNSON SPACE CENTER**
*** CONSULTANT**

TIMELINE OF COMMITTEE ACTIVITIES

- **COMMITTEE MEMBERSHIP FORMED, FALL, 1995**
- **JANUARY 31, 1996: COMMITTEE TELECONFERENCE TO ORGANIZE INTO DISCIPLINE SUBCOMMITTEES AND TO FORM DATA BASES**
- **FEBRUARY-MARCH, 1996: SUBCOMMITTEE TELECONFERENCES TO ORGANIZE DATA BASES AND TO IDENTIFY AREAS OF PROGRAMMATIC BRIEFING**
- **APRIL, 1996: MEETING AT JSC; COMMITTEE REVIEWED COUNTERMEASURE STATUS OF TARGETED DISCIPLINES VIA INTERACTIONS WITH PROGRAM DIRECTORS AND SCIENTISTS AT JSC; ADDITIONAL PRESENTATIONS ON CROSS-CUTTING AREAS**
- **JUNE, 1996: SECOND MEETING AT JSC; FURTHER REVIEW OF COUNTERMEASURES PROGRAM; REVIEW REPORTS OF VESTIBULAR AND BEHAVIOR AND PERFORMANCE TASK FORCES; FORMULATE STRATEGY, FORMAT, AND TIME TABLE FOR FINAL REPORT**
- **SEPTEMBER, 1996: ORAL PRESENTATION OF REPORT TO LIFE AND MICROGRAVITY SCIENCES & APPLICATIONS ADVISORY SUBCOMMITTEE (LMSAAS)**
- **OCTOBER/NOVEMBER, 1996: FINAL DOCUMENT SUBMITTED TO NASA**

COMMITTEE/SUBCOMMITTEE BRIEFING TOPICS

- **THE RUSSIAN AND NASA EXPERIENCE IN SPACE**
- **COUNTERMEASURE ACTIVITIES FOR MUSCLE AND MOTOR DEFICITS**
- **MICROGRAVITY EFFECTS ON THE CARDIOVASCULAR SYSTEM AND STATUS OF COUNTERMEASURES**
- **MICROGRAVITY AND BED REST EFFECTS ON BONE**
- **NUTRITIONAL ISSUES FOR ASTRONAUTS**
- **PHARMACOKINETICS OF DRUG THERAPY IN SPACE**
- **CREATING ARTIFICIAL GRAVITY: NEW TECHNOLOGY**
- **STATUS OF DISCIPLINE REPORTS**
- **OVERARCHING ISSUES: NUTRITION, EXERCISE MODALITIES, STANDARDIZATION OF ASTRONAUT PERFORMANCE CAPABILITIES, ARTIFICIAL GRAVITY**

REPORT FORMAT

- **INTRODUCTION AND CHARGE**
- **BACKGROUND**
- **EXECUTIVE SUMMARY AND CONSENSUS FINDINGS**
- **INDIVIDUAL DISCIPLINE REPORTS: CARDIOVASCULAR, BONE AND CONNECTIVE TISSUE, MUSCLE AND MOTOR PERFORMANCE, VESTIBULAR, BEHAVIOUR AND PERFORMANCE, CLINICAL MEDICAL ISSUES**
- **STATEMENT OF PROBLEM—MICROGRAVITY EFFECT**
- **CONCERNS RELATIVE TO COUNTERMEASURES**
- **RECOMMENDATIONS**
- **APPENDIX NARRATIVE—BACKGROUND INFORMATION**

SKELETAL MUSCLE AND MOTOR PERFORMANCE

ISSUES/CONCERNS

MICROGRAVITY INDUCES STRUCTURAL AND FUNCTIONAL DEFICITS:

- **MUSCLE MASS, CHIEFLY LEG EXTENSOR GROUPS AND POSTURAL MUSCLES OF TRUNK**
- **STRENGTH AND POWER CAPACITY, STRUCTURAL AND NEURAL**
- **SHIFT TO FASTER CONTRACTILE PHENOTYPES, LESS EFFECTIVE AT 1 G FOR POSTURE AND LOCOMOTION**
- **FATIGUE DURING SUSTAINED ACTIVITY**
- **POTENTIAL TO DEPEND ON CARBOHYDRATES FOR ENERGY SOURCE, FACILITATES MUSCLE AND BODY FATIGUE**
- **MOTOR SKILLS FOR GROSS AND FINE MOVEMENT SKILLS (NEURO-MOTOR AND NEURO-SENSORY DEFICITS)**

POTENTIAL PROBLEMS DERIVED FROM MUSCLE/MOTOR DEFICITS

- **EXTRAVEHICULAR WORK CAPACITY AND MOTOR SKILL IN MICROGRAVITY**
- **EMERGENCY EGRESS IN GRAVITY FIELDS – STRENGTH, POWER, ENDURANCE**
- **LONG TERM DEFICITS IN MOTOR CONTROL (?)**

STATUS OF COUNTERMEASURES

- **CURRENT PROGRAM IS LARGELY AEROBIC (CYCLING, ROWING; TREADMILL); INEFFICIENT ACTIVITIES FOR CONSERVING MASS AND MAINTAINING A POSITIVE PROTEIN SYNTHESIS/DEGRADATION RATIO**
- **INSUFFICIENT FORCE STIMULI TO CONSERVE MASS AND MAINTAIN SLOW CONTRACTILE PHENOTYPES**
- **DON'T HAVE DATABASE TO KNOW EFFECTIVENESS OF CURRENT STRATEGIES; I.E., NO BASELINE DATA ON HUMAN EXPERIENCE IN SPACE**

RECOMMENDATIONS

- **RESISTANCE TRAINING A HIGH PRIORITY IN EXERCISE PRESCRIPTION**
- **SKELETAL MUSCLE AND HEART MASS**
- **CONTINUE AEROBIC ACTIVITIES BUT MINIMIZE RELATIVE AMOUNT**
- **INCLUDE ACTIVITIES TO MAINTAIN MOTOR SKILLS AND POSTURE**
- **INCORPORATE CURRENTLY AVAILABLE RESISTANCE EQUIPMENT FOR STRESSING MUSCLE RATHER THAN DESIGNING DE NOVO DURING SHORT TERM**
- **NASA NEEDS TO DEFINE FITNESS STANDARDS FOR ASTRONAUTS, ACCEPTABLE SKILLS AND PERFORMANCE CRITERIA**
- **PROGRAMS NEED TO BE CREATIVE AND CHALLENGING TO INSURE COMPLIANCE**
- **NUTRITION: INSURE ADEQUATE PROTEIN AND CARBOHYDRATE COMPOSITION RELATIVE TO APPETITE**
- **DEVELOP TECHNOLOGY FOR GENERATING INTERMITTENT GRAVITY COUPLED TO EXERCISE STIMULUS, GRAVITY CYCLE**

BONE AND CONNECTIVE TISSUE

ISSUES/CONCERNS

BONE MASS, CALCIUM, AND SKELETAL CHANGES OCCUR DURING SPACE FLIGHT (1 WEEK TO 312 DAYS)

- **DEFICITS IN THE FOLLOWING**
 - **BONE LOSS IS SITE-SPECIFIC—LUMBAR, CALCANEAL**
 - **URINARY CALCIUM MARKEDLY INCREASES**
 - **BONE MINERAL LOSS TRACKS ↓ IN BODY WEIGHT**
- **HORMONAL IMBALANCE LIKELY CAUSES CALCIUM RESORPTION**
- **CALCIUM BALANCE BECOMES NEGATIVE**
- **EXERCISE DOES NOT PREVENT BONE/URINARY CALCIUM LOSS**
- **POTENTIAL TO FORM RENAL STONES BY ↑ URINARY CALCIUM**
- **SPINAL LENGTHENING MAY LEAD TO BACK PAIN**
- **DIET COMPOSITION MAY INTERFERE WITH MINERAL BALANCE**

RECOMMENDATIONS

- **ASTRONAUT DIET NEEDS MODIFICATION TO INSURE ADEQUATE CALORIC INTAKE AND APPROPRIATE MINERAL BALANCE (SODIUM CONTENT)**
- **SIMULATED SUNLIGHT TO AFFECT VITAMIN D METABOLISM**
- **EXERCISE PARADIGM NEEDS TO CREATE HIGH LOADING AND IMPACT ON BONE**
- **RESEARCH/CLINICAL TRIAL WITH BISPHOSPHONATES**
- **BASIC AND APPLIED RESEARCH TO IDENTIFY MECHANISM OF URINARY CALCIUM ELEVATION, ENDOCRINE CHANGES, BONE AND CONNECTIVE DEFICITS, AND MORE EFFECTIVE COUNTERMEASURES**
- **INTERMITTENT ARTIFICIAL GRAVITY WITH IMPACT LOADING**

CARDIOVASCULAR

ISSUES/CONCERNS

- **HYPOVOLEMIA INDUCED BY SPACEFLIGHT CONTRIBUTES TO ORTHOSTATIC HYPOTENSION**
- **REDUCED PHYSICAL STRESS AND ACTIVITY IN MICROGRAVITY CAUSE REDUCED AEROBIC FITNESS**
- **LONG TERM EXPOSURE TO MICROGRAVITY LIKELY CAUSES HEART ATROPHY AND REDUCED COMPLIANCE**
- **LOWER BODY NEGATIVE PRESSURE HAS NOT PROVEN TO BE AN EFFECTIVE COUNTERMEASURE**
- **RE-ENTRY ANTI-G SUIT MAY CAUSE HEAT STRESS AND CONTRIBUTE TO ORTHOSTASIS**
- **GRAVITY FORCES DURING RE-ENTRY MAY CONTRIBUTE TO ORTHOSTASIS**

RECOMMENDATIONS

- **IDENTIFY COUNTERMEASURE TO ACUTELY INCREASE CENTRAL VENOUS PRESSURE SET POINT –COMBINE WITH FLUID LOADING**
- **USE FLUID LOADING IN COMBINATION WITH MAXIMAL AEROBIC EXERCISE STIMULUS BEFORE RE-ENTRY TO MAINTAIN NEAR NORMAL PLASMA VOLUME**
- **CONTINUE RESEARCH TO IDENTIFY OPTIMAL EXERCISE PRESCRIPTION TO PROVIDE GREATEST CARDIOVASCULAR BENEFIT –MAINTAIN FITNESS AND REDUCE ORTHOSTASIS**
- **DISCONTINUE LBNP AS A COUNTERMEASURE –USE IN TESTING CARDIOVASCULAR HOMEOSTASIS**
- **CONTINUE TO USE ANTI-G SUIT BUT DETERMINE AMOUNT OF TIME IT IS NEEDED**
- **CONTINUE TO USE THE LIQUID COOLING GARMENT BUT MODIFY DESIGN TO FOCUS ON UPPER BODY TORSO**

- **CONTINUE TO USE SUPINE POSITION IN MID DECK DURING RE-ENTRY**
- **CONTINUE RESEARCH ON PENGUIN SUIT – AUTONOMIC REFLEXES**
- **ENDORSES RESISTANCE TRAINING – SKELETAL MUSCLE AND CARDIOVASCULAR BENEFIT**
- **USE MAX EXERCISE TEST COUPLED WITH FLUID LOADING AS COUNTERMEASURE FOR INCREASING PLASMA VOLUME PRIOR TO RE-ENTRY**

CLINICAL MEDICINE

ISSUES/CONCERNS:

- **BASIC BACKGROUND AND DESCRIPTIVE DEFINITIONS ARE LACKING AND THE RESEARCH COMMUNITY HAS NOT ENGAGED IN AN ALL-ENCOMPASSING CLINICAL APPROACH TO THE PROBLEM OF COUNTERMEASURES**

RECOMMENDATIONS

- **CRITICALLY REVIEW ALL LABWORK AND STUDIES DONE ROUTINELY DURING THE SHUTTLE PROGRAM, E.G., INCLUDING SELECTION, ANNUAL PHYSICAL, AND FLIGHT RELATED EXAMS, TO ASSESS WHICH STUDIES SHOULD CONTINUE TO BE MONITORED**
- **DETERMINE WHICH STUDIES ARE NECESSARY TO MAKE REAL-TIME DECISIONS AND TO PRACTICE PREVENTIVE MEDICINE ON FLIGHTS OF ALL DURATIONS**
- **CAREFULLY DESCRIBE ENTRY AND LANDING SYNDROME THROUGH A REVIEW OF MEDICAL RECORDS AND EXISTING PERFORMANCE DATA AS WELL AS VIA COLLECTION OF PROSPECTIVE DATA**
- **DEFINE AND ACCEPT (BY NASA PROGRAM MANAGEMENT) THE REQUIREMENTS FOR PERFORMANCE OF CREW EGRESS IN NORMAL AND EMERGENCY SITUATIONS**
- **DEVELOP COUNTERMEASURE RESEARCH PLAN TO INTEGRATE ALL RESEARCH DISCIPLINES EFFICIENTLY**
- **WORK CLOSELY (MEDICAL OPERATIONS STAFF) WITH THE RESEARCH TEAM TO ENSURE A CLINICAL AND OPERATIONAL FOCUS TO THE DEVELOPMENT OF COUNTERMEASURES**
- **ENSURE THAT RESEARCH AND COUNTERMEASURES ARE COMPATIBLE WITH THE SPACECRAFT ENVIRONMENT AND CREW SCHEDULE TO OBTAIN MAXIMUM CREW COOPERATION AND COMPLIANCE**

VESTIBULAR

ISSUES/CONCERNS:

- **NUMEROUS MEASURABLE SENSORIMOTOR ALTERATIONS THAT OCCUR DUE TO SPACE FLIGHT MAY RESULT IN OPERATIONAL PROBLEMS**
- **SOME PROBLEMS MAY BE CREW MEMBER-SPECIFIC DEPENDING ON THEIR ROLE IN THE FLIGHT AND THE FLIGHT SCENARIO**
- **A LARGE BODY OF OPERATIONAL DATA IN THIS AREA HAVE NOT YET BEEN ANALYZED**
- **EFFECTIVE COUNTERMEASURES:**
 - **PROMETHAZINE INJECTIONS**
 - **CREW TRAINING BRIEFING**
 - **TIME LINE ADJUSTMENTS**
 - **REGENCY OF TRAINING PRIOR TO MISSION**
 - **IN-FLIGHT EXERCISES**
 - **ASSISTED EGRESS**

RECOMMENDATIONS

- **EVALUATE EFFICACY OF COUNTERMEASURES TO FOCUS ON THE FUNCTIONAL LINK BETWEEN SENSORIMOTOR ALTERATIONS AND REAL OPERATIONAL DEFICITS (EYE-HEAD COORDINATION AND DYNAMIC VISUAL ACUITY)**
- **TAILOR COUNTERMEASURES TO CREW MEMBER'S DUTY**
- **INCLUDE COLLATION, REVIEW, AND EVALUATION OF EXISTING COUNTERMEASURE OPERATIONAL AND EXPERIMENTAL DATA BASES**
- **FURTHER EVALUATE PROMETHAZINE ROUTE OF ADMINISTRATION, IN-FLIGHT SIDE EFFECTS, AND DEVELOPMENT OF ALTERNATIVE DRUG INTERVENTIONS THAT ARE CLOSER TO 100% EFFECTIVE**
- **CONTINUE AND IMPROVE CREW TRAINING, BRIEFING, AND TIME LINE ADJUSTMENTS**

- **DEVELOP PREDICTORS TO IDENTIFY INDIVIDUALS WHO MIGHT BENEFIT FROM ADDITIONAL OR ALTERNATIVE INTERVENTIONS**
- **DEVELOP COPING PROCEDURES FOR THE FEW INDIVIDUALS WHO FAIL TO ADAPT FOR PROLONGED PERIODS**
- **DEVELOP MORE EXTENSIVE PREFLIGHT ADAPTIVE TRAINING DEVICES**
- **TRAIN CREW TO ADOPT HEAD MOVEMENT STRATEGIES TO DECREASE SPACE MOTION SYNDROME TO AVOID NEED FOR MEDICATIONS**
- **PROVIDE FUNDING FOR ARTIFICIAL GRAVITY RESEARCH AND DEVELOPMENT**
- **EVALUATE MECLEZINE/PHENEGRAN TREATMENT**
- **PROVIDE PROCEDURES AND EQUIPMENT ON ORBIT THAT ALLOW PRACTICE OF HEAD AND BODY MOVEMENTS THAT APPROXIMATE THE TERRESTRIAL ADAPTED STATE TO MINIMIZE PROBLEMS DURING LANDING AND EGRESS**
- **DEVELOP ULTRALIGHT, MINIATURIZED HEAD MOVEMENT MONITORING SYSTEM FOR TRAINING AND DYNAMIC RESTRAINT**

BEHAVIOR AND PERFORMANCE

ISSUES/CONCERNS:

- **TAKE ADVANTAGE OF LITERATURE FROM ISOLATED AND UNIQUE ANALOGUE ENVIRONMENTS THAT HAVE A HIGH CORRELATION POTENTIAL WITH SPACEFLIGHT**
- **THOROUGHLY REVIEW THE RUSSIAN EXPERIENCE**
- **ESTABLISH ASTRONAUT SELECTION AND CREW COMPOSITION RESEARCH WITH PRIMARY EMPHASIS ON ASSEMBLING OPTIMAL CREWS FOR LONG DURATION MISSIONS RATHER THAN ON SELECTING INDIVIDUALS**

RECOMMENDATIONS

- **UNDERTAKE CRITICAL REVIEW OF ANALOGUE STUDIES**
- **REVIEW THE RUSSIAN EXPERIENCE**
- **COMPREHENSIVELY RESEARCH ASTRONAUT SELECTION AND CREW COMPOSITION**
- **MAINTAIN THE PRESENCE OF BEHAVIOR AND PERFORMANCE SPECIALISTS IN ALL PHASES OF SPACE MISSION DESIGN**
- **SELECT FULL MISSION CREWS AND CRITICAL GROUND PERSONNEL AS A TEAM**
- **EMBED TESTS OF COGNITIVE, EMOTIONAL, AND BEHAVIORAL PERFORMANCE IN FUNCTIONING MISSION HARDWARE AND EXPERIMENTS**
- **INCREASE THE USE OF SIMULATORS FOR TRAINING ON BOARD THE MISSION**
- **DEVELOP VIRTUAL ENVIRONMENTS AND TELESCIENCE TO ADDRESS MISSION BEHAVIOR AND PERFORMANCE**
- **USE GROUND-BASED ANALOGUES AND SIMULATORS FOR SELECTION AND TRAINING**
- **DEVELOP FURTHER SELF REPORT TOOLS**

OVERARCHING ISSUES

SUBGROUP AND DISCIPLINE CONSENSUS CONCERNING:

- **DEFINE (NASA PROGRAM MANAGEMENT) THE FITNESS STANDARDS AND/OR LEVELS OF ACCEPTANCE OF PHYSIOLOGICAL HOMEOSTASIS RELATIVE TO THE 1 G ENVIRONMENT**
- **REVIEW AND IMPROVE ASTRONAUT DIETS TO INSURE ADEQUATE CALORIC INTAKE AND APPROPRIATE COMPATIBILITY FOR MINERAL BALANCE**
- **MODIFY THE EXERCISE PRESCRIPTION, WHICH SHOULD ALSO IMPACT CARDIOVASCULAR HOMEOSTASIS, TO FOCUS MORE ON MUSCLE AND BONE CONSERVATION**
- **NUMEROUS DISCIPLINES STRONGLY ENDORSE THE DEVELOPMENT OF A HUMAN-POWERED GRAVITY CYCLE**
- **INTEGRATE RESEARCH AND OPERATIONAL MEDICAL ISSUES INTO THE COUNTERMEASURES PLAN**
- **DESIGN COUNTERMEASURE STRATEGIES THAT ARE EFFECTIVE, INTEGRATIVE, AND APPEALING TO INSURE ASTRONAUT COMPLIANCE**

A Strategy for Research in Space Biology and Medicine in the New Century

Mary Jane Osborn, PhD
Chair, Committee on Space Biology and Medicine
Space Studies Board
National Academy of Sciences

Professor and Chair,
Department of Microbiology
University of Connecticut Health Center

GOALS OF SPACE LIFE SCIENCES

- 1. To describe and understand human adaptation to the space environment and readaptation upon return to earth**
- 2. To use the knowledge so obtained to devise procedures that will improve the health, safety, comfort and performance of the astronauts**
- 3. To understand the role that gravity plays in biological processes in both plants and animals**
- 4. To determine if any biological phenomenon is better studied in space than on earth**

HIGH PRIORITY AREAS OF RESEARCH

PHYSIOLOGICAL AND PSYCHOLOGICAL EFFECTS OF SPACEFLIGHT

1. Loss of weight-bearing bone and muscle

- **Studies should provide mechanistic insights into development of effective countermeasures against bone and muscle deterioration during and after flight.**
- **Ground-based model systems should be used to investigate mechanisms of changes.**
- **A database on the natural history of the microgravity-related bone loss and its reversibility in humans should be established in preflight, inflight and postflight recordings of bone mineral density.**
- **Hormone profiles should be obtained on humans before, during and following spaceflight.**
- **The relationship should be investigated between exercise activity levels and protein energy balance inflight.**

2. Vestibular function, the vestibular ocular reflex and sensorimotor integration.

- **Highest priority should be given to experiments to determine the basis for compensatory mechanisms on earth and in space.**
- **Inflight recordings of signal processing following otolith afferent stimulation should be made by a trained physiologist serving as payload specialist.**
- **Future studies should determine if and how exposure to microgravity affects mechanisms whereby new motor patterns are learned in response to sensory perturbations.**

3. Orthostatic intolerance upon return to earth gravity

- **Extend knowledge of magnitude, time course and mechanisms of cardiovascular adjustments to include long duration spaceflight.**
- **Determine the specific mechanisms underlying inadequate total peripheral resistance during postflight orthostatic stress.**
- **Identify and validate appropriate methods for referencing intrathoracic vascular pressures to systemic pressures in microgravity, given the observed changes in cardiac and pulmonary volume and compliance.**
- **Re-evaluate current anti-orthostatic countermeasures to refine those that offer protection and eliminate those that do not. Priority should be given to interventions that may provide simultaneous bone and/or muscle protection.**

4. Radiation hazards

- **Determine carcinogenic risks following irradiation by protons and HZE particles.**
- **Determine if exposure to heavy ions at levels encountered in deep-space missions of long duration pose a risk to integrity and function of the central nervous system.**
- **Determine how spacecraft design affects the radiation environment of the crew.**
- **Determine effects of radiation exposures expected during long-term spaceflight beyond low earth orbit on the immune system and resistance to infection.**
- **Determine whether combined effects of radiation and stress on the immune system in spaceflight could produce additive or synergistic effects on host defenses.**

5. Physiological effects of stress

- **Analyze interactions between the hypothalamic-pituitary-adrenal (HPA) axis and the immune system during spaceflight to determine the role that host response to stressors plays in alterations in host defenses.**

6. Psychological and social issues

- **Conduct research on neurobiological (circadian, endocrine) and psychosocial (individual, group, organizational) mechanisms underlying the effects of physical and psychosocial environmental stressors on performance. Such research should be interdisciplinary and conducted in ground-based analogue settings as well as inflight.**
- **The efficacy of existing countermeasures should be determined.**
- **Both of the above will require development of noninvasive techniques for ongoing assessment of behavior and performance.**

SCIENCE POLICY ISSUES

PEER REVIEW

- **Establishment of peer review panels and funding decisions should remain a function of the Headquarters Division of Life Sciences.**
- **Ensure that scientific review panels have appropriate expertise to appropriately evaluate feasibility of proposed flight experiments.**

INTEGRATION OF RESEARCH ACTIVITIES

- **PIs and NASA managers and design engineers should function as an integrated team throughout the life of the project.**

FUNDING AND GUIDING OF INTERDISCIPLINARY RESEARCH

- **Review and evaluate the NSCORT program to determine whether this mechanism provides the best way to foster interdisciplinary research.**
- **Regularly review and evaluate the performance of the National Space Biomedical Research Institute and the impact of its funding on the overall life sciences research program and budget.**

HUMAN FLIGHT DATA: COLLECTION AND ACCESS

- **Initiate an ISS-based program to collect detailed physiological data on astronauts before, during and after flight.**
- **Promote mechanisms for making complete data from studies on astronauts accessible to qualified investigators in a timely manner.**

PUBLICATION AND OUTREACH

- **Provide funding for data analysis of flight experiments for a sufficient period to ensure timely publication of the results.**
- **Insist on timely publication and dissemination of results of space life sciences research.**

PROFESSIONAL EDUCATION

- **Develop a small, highly competitive program of individual postdoctoral fellowships for training by NASA-supported investigators in academic and research institutions outside NASA centers.**

PROGRAM ISSUES

SPACE-BASED RESEARCH

CRITERIA FOR FLIGHT EXPERIMENTS

DEVELOPMENT OF ADVANCED INSTRUMENTATION, METHODS

- **Work with research community and industry to facilitate needed development.**
- **Take advantage of advanced instrumentation developed in foreign countries**
- **Make real-time direct access between flight crew and PIs' home laboratories a priority**

UTILIZATION OF ISS

- **Bring external user community into planning, design**
- **Make every effort to mount additional Spacelab flight**
- **Determine whether shuttle missions should be continued after opening of ISS**

RECOMMENDED APPROACHES

MULTIDISCIPLINARY STUDIES ON FUNDAMENTAL MECHANISMS

**CELLULAR, MOLECULAR BIOLOGY
GENETICS
TISSUE AND ORGAN SYSTEM
INTACT ORGANISM**

**USE OF MODEL SYSTEMS
GROUND-BASED RESEARCH: MECHANISTIC HYPOTHESES
FLIGHT EXPERIMENTS: CRITICAL TESTS OF HYPOTHESES**

DEVELOPMENT OF COUNTERMEASURES

**MECHANISM-BASED DESIGN
EXPERIMENTAL VALIDATION**

SETTING PRIORITIES IN RESEARCH

HIGHEST PRIORITY TO:

- **PROBLEMS THAT MAY LIMIT SURVIVAL OR FUNCTION IN PROLONGED SPACE FLIGHT**

Include basic as well as applied research.

Include ground-based as well as flight experiments.

Emphasize NASA capabilities

Take into account funding patterns of other agencies

- **FUNDAMENTAL BIOLOGICAL PROCESSES IN WHICH GRAVITY IS KNOWN TO PLAY A DIRECT ROLE**

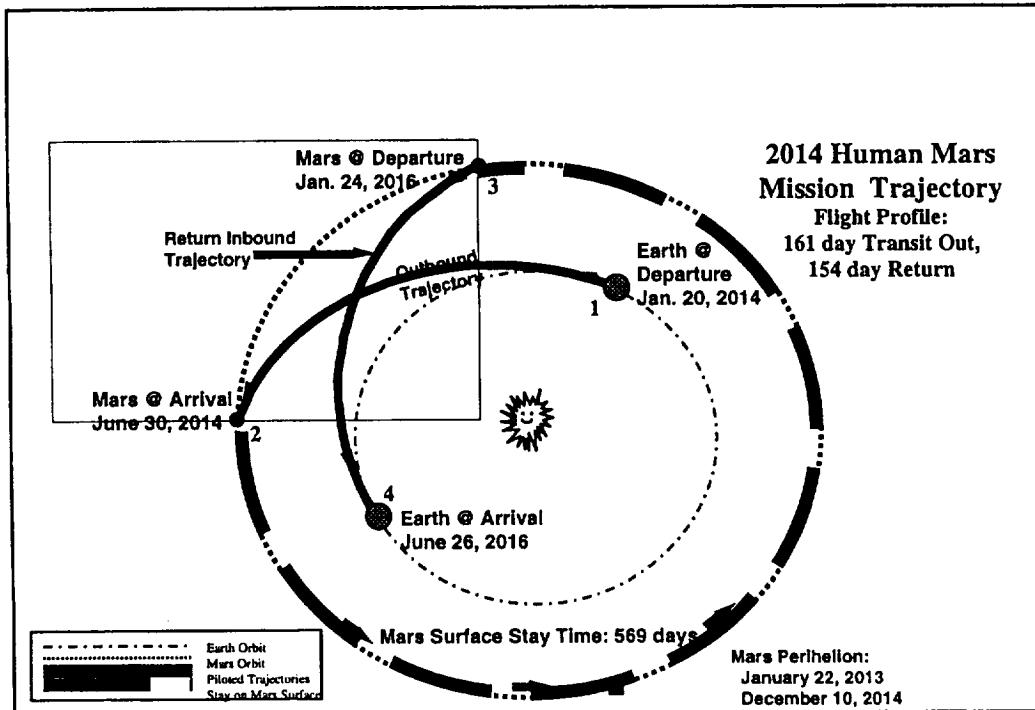
Human Health and Performance Aspects of Mars Design Reference Mission of July, 1997

John B. Charles, PhD
NASA Johnson Space Center
Human Space Life Sciences Programs Office
(HLSPO)

DISCLAIMER

NASA does not now have authority to undertake a piloted Mars mission. No claim to the contrary can be inferred from this presentation.

This presentation is based upon the Mars Design Reference Mission (NASA Special Publication 6107, July, 1997). This document summarizes the work of NASA scientists, engineers, and planners, who have defined the Reference Mission. This work forms a basis for comparing different approaches and criteria involving new or improved technologies, in order to select from among them at the appropriate time.



“Triconic Aeroshell”

- sized to “Magnum” booster
- defines the size and shape of the Mars vehicles.

Piloted Transit Habitat vehicle:

- outbound transit habitat
- Mars crew landing vehicle
- Mars surface habitat

Cargo vehicle:

- arrives at Mars before crew
- delivers Mars Ascent Vehicle and ISRU plant to Mars surface

Trans-Earth vehicle:

- Earth Return Vehicle
- arrives at Mars before crew
- waits in orbit around Mars to transport crew home

L. Kos (MSFC)

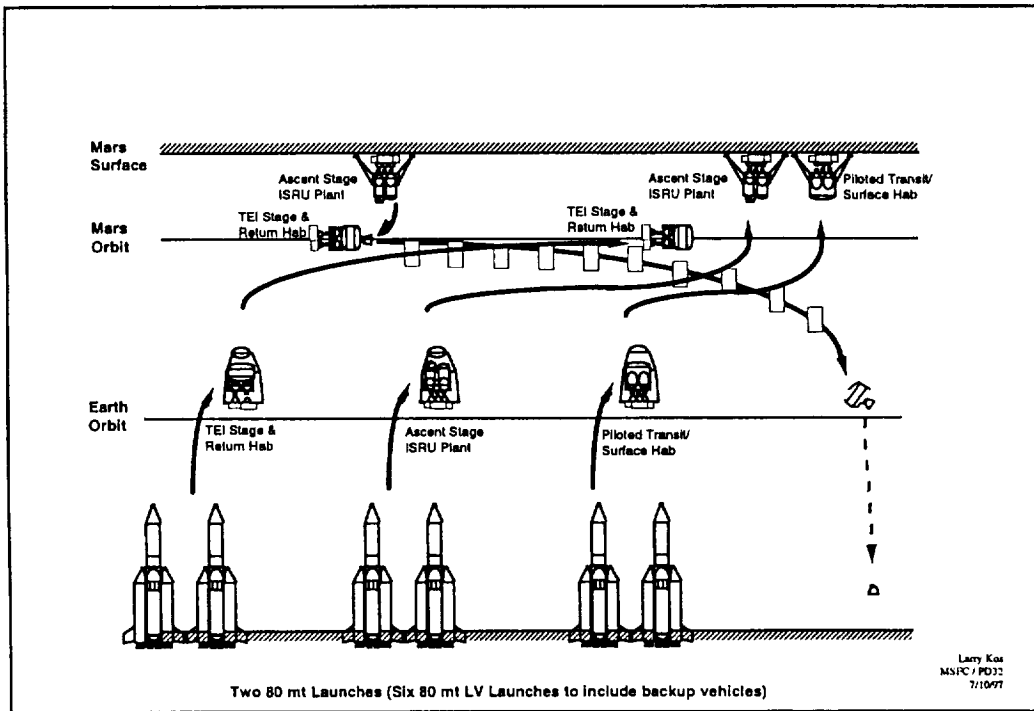
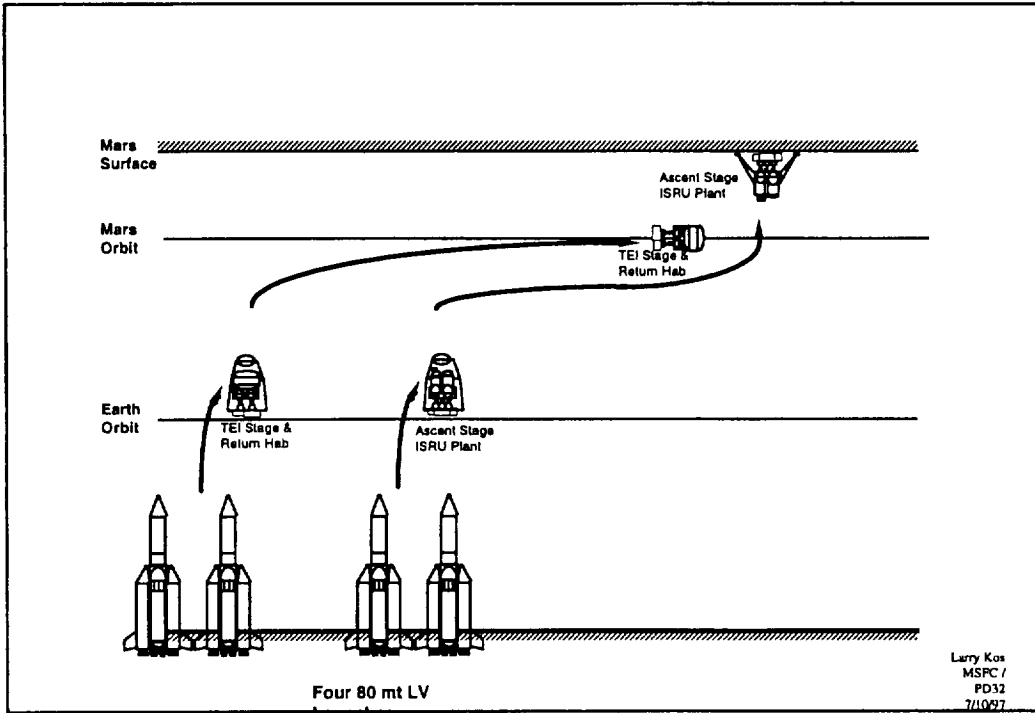
Conceptual interior layout
(including crew seating within Transit Habitat) for Mars arrival:

- $+g_x$ during aerobraking (seatbacks 23 degrees forward of vertical)
- $+g_z$ during landing (seatbacks vertical)

NOTE: Interior layout of Transit Habitat is undefined at this time

Pilot's field of view (conceptual)

artwork from: Larry Kos and Paul Wercinski



Mission Abort Scenarios

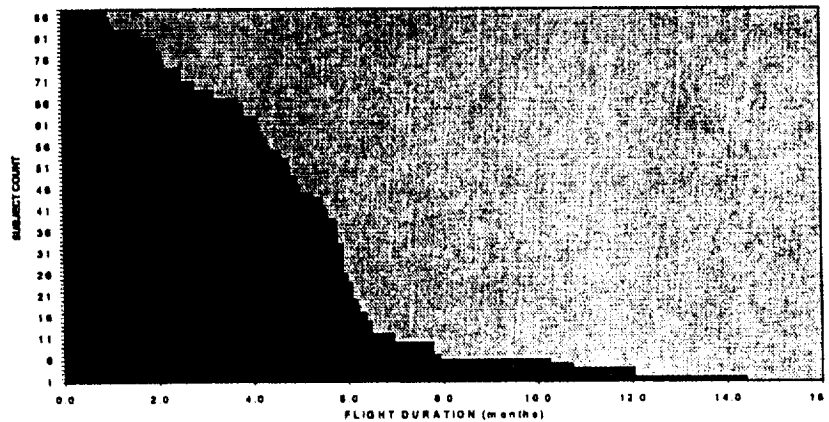
“Abort to Earth” very limited

- Trans-Mars Injection (Earth-departure maneuver)
 - NTR (or other impulsive maneuver) option: “abort-to-Earth” progressively more difficult after half-way through the mission – over half of fuel is already expended
 - SEP (or other low-thrust, long-duration maneuver) option: limited spacecraft maneuvering fuel, long time required
- Missed Mars orbit insertion or direct entry
 - Mars flyby may result in 2-year return to Earth -- not much different than completed mission

“Abort to Mars”

- life support, other resources already emplaced
- next to Earth, Mars is safest place to be (radiation-shield; partial gravity)

Human Space Flight Experience Greater Than 30 Days (as of 1 Jan. 98)



Physical Challenges to HHP: Gravity and Acceleration

	Earth Launch	Transit	Mars Landing	Mars Surface	Mars Launch	Transit	Earth Landing
G-Load	up to 3 g	0 g	3-5 g	1/3 g	TBD g	0 g	3-5 g
Notes	boost phase, 8 min.; TMI, minutes	4-6 months	aero-braking, minutes; parachute braking, 30 sec.; powered descent, 30 sec.	18 months	boost phase, minutes; TEI, minutes	4-6 months	aero-braking, minutes; parachute braking, minutes
Cumulative hypo-g	0		4-6 months		22-24 months		26-30 months
G Transition	1 g to 0 g		0 g to 1/3 g		1/3 g to 0 g		0 g to 1 g

“Artificial Gravity” as Countermeasure to Extended Weightlessness

Question: Can artificial gravity (“AG”) preserve physiological function on long-duration missions?

Implications:

- How much AG is enough (1 g, 1/3 g, 1/6 g, or 1/100 g)?
- How often (whole transit or brief exposures)?
- Can AG be offset by other countermeasures (such as exercise)?
- How will NASA validate approach?
 - ISS small-animal centrifuge not available before CY 2003
 - larger centrifuge not currently planned at all!
- Can Mars DRM afford weight, power, cost of AG?
 - require dual systems for 0 g and AG phases of transits?
 - require rotating whole vehicle, or just a small part of it?

Physical Challenges to HHP: Radiation

	Earth Launch	Transit	Mars landing	Mars Surface	Mars Launch	Transit	Earth Landing
Source	van Allen (trapped radiation) belts	GCR (quiet Sun); SPE (active Sun); nuclear power reactor		GCR (quiet Sun); SPE (active Sun); nuclear power reactor		GCR (quiet Sun); SPE (active Sun); nuclear power reactor	
Exposure	SEP option: 3 passages or more	4-6 months		18 mon.; shielded by Mars' bulk and atmos.		4-6 months	
Cum. Exp.	hours-days		4-6 months		22-24 months		26-30 months

HHP Mars Transit Requirements

Mostly Autonomous (one-way Earth-Mars comm. time: 3-22 min.)

- Medical care
- Nutrition
- Psychological support
 - meaningful work
 - simulations of Mars entry/landing, contingencies
 - refresher training/continuing education
 - rover ops/landing site prep
 - housekeeping
 - cruise science (microgravity, astronomy, biomedical, etc.)
 - communications capability
 - reliable contact with mission control, family, friends

Habitat Facilities

- maintenance/housekeeping
 - workshop
- exercise - conditioning for Mars surface activities
- recreation
- privacy

Human Factors and Habitability

The following require engineering solutions to optimize HHP:

- clean air
- clean water
- particulate analyzer
- microbial analyzer
- waste management/recycling
- adequate food
 - long-duration storage
 - processing of flight-grown foodstuffs
- adequate fresh clothing (clothes washer)
- lighting
 - Intensity (threshold level)
 - periodicity (circadian rhythmicity)

Peak Physical Challenges for HHP: Mars Surface Phase (Post-Landing through Pre-Launch)

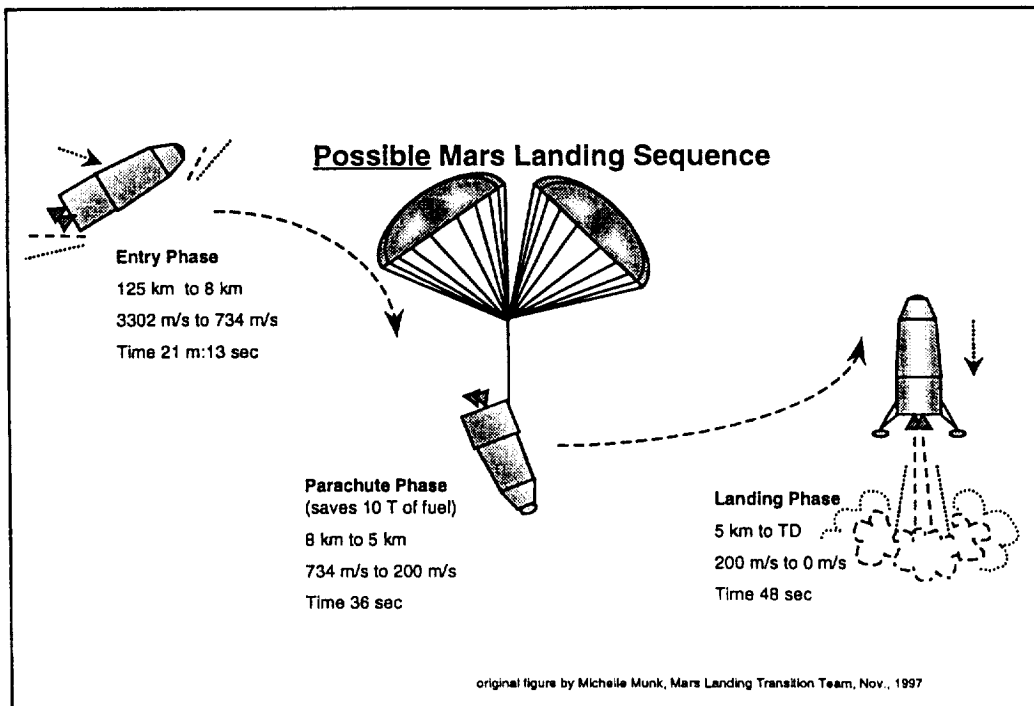
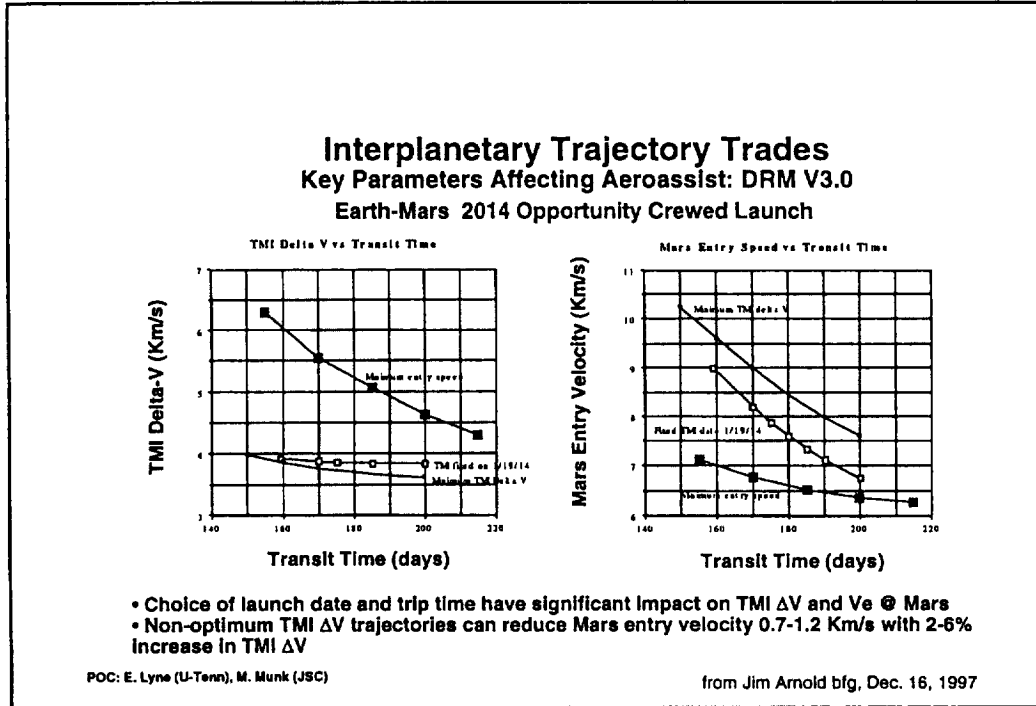
Assumption

Mars surface gravity

- too *low* to be beneficial (bone integrity, etc.)
- too *high* to be ignored (g-transition vestibular symptoms)

Challenges

- physical
 - g-transition (first few days only?)
 - prolonged exposure to 1/3 g
 - high-intensity surface activity
 - EMU hypobaric environment
 - 70 kg EMU (partially self-supporting)
 - surface trauma risk
- no real-time MCC support (one-way comm: 3-22 min.)
 - crew highly autonomous
 - Earth monitoring for trend analysis only



Peak Physical Challenges for HHP: Strategy for Mars Surface Ops

Background: anecdotal evidence suggests only ~50% of Russian Mir crewmembers are ambulatory with assistance immediately after landing, increasing to nearly 100% within hours

Assume: only 3 out of 6 Mars crewmembers ambulatory immediately after landing

Strategy: start with passive IVA tasks; progress to strenuous EVA tasks

- first 1-3 days limited to IVA reconfig of lander/habitat, surface recon
- then, first EVA(s) in vicinity of lander (umbilical instead of PLSS?)
- next, use unpressurized rover for early, shorter excursions
- after a week or more, extended excursions possible

HHP Mars Surface Stay Requirements

Autonomous (one-way Earth-Mars comm. time: 3-22 min.)

- Medical care
- Nutrition
- Psychological support
 - meaningful work
 - surface science
 - planetary
 - biomedical
 - simulations of Mars launch, TEI, contingencies
 - progressive debriefs, sample processing, etc.
 - housekeeping
 - communications capability

Habitat Facilities

- maintenance/housekeeping
 - workshop
- exercise - supplemental to Mars surface activities
- recreation
- privacy

Life Sciences on Mars Surface

Periodic (monthly?) health checks:

- bone integrity
- cardiovascular/cardiopulmonary function
- musculoskeletal fitness
- blood work

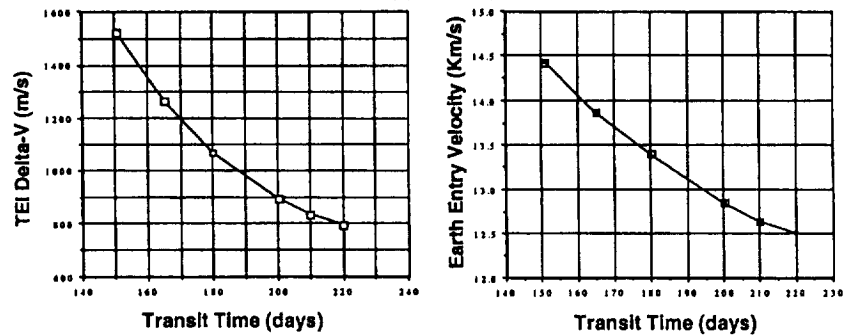
Assessments will also serve as applied research:

- probably longest period away from Earth to date
- probably longest exposure to hypogravity (1/3 g) environment to date

Interplanetary Trajectory Trades

Key Parameters Affecting Aeroassist: DRM V3.0

Mars-Earth Return 2016 Opportunity, Minimum TEI Conditions



- Choice of launch date and trip time have significant impact on TEI ΔV and V_e @ Mars
- Increasing trip time reduces both TEI ΔV and Earth entry velocity
- DRM conditions -> 13.0 - 13.5 Km/s entry velocity
- Further analysis needed to look at synodic period effects on Earth entry velocity

POC: E. Lyne (U-Tenn), M. Munk (JSC)

from Jim Arnold bfg, Dec. 16, 1997

HHP Earth Return Transit Requirements

Autonomous (one-way Earth-Mars comm. time: 3-22 min.)

- Medical care
- Nutrition
- Psych support
 - meaningful work
 - simulations of Earth aerobraking, contingencies
 - debriefs, reporting, consultation with PI
 - housekeeping
 - cruise science
 - Mars sample analysis?
 - microgravity, astronomy, other?
 - communications capability

Habitat Facilities

- maintenance/housekeeping
 - workshop
- exercise - preparatory to Earth reambulation
- recreation
- privacy

data from R. Billica, Jan., 1998, and D. Hamilton, June, 1998

Space Medicine Issues

Based on US and Russian space flight data, and US astronaut longitudinal data, submarine experience, Antarctic winter-over experience, and military aviators:

Significant Illness or Injury = 0.06 per person per year (or PYE)

- requiring emergency room (ER) visit or hospital admission
- by US standards

For DRM of 6 crewmembers and 2.5 year mission, expected incidence is 0.90, about one person per mission

Subset requiring intensive care support (ICU) = 0.02 per PYE

Expected incidence is 0.30, about once per three missions

(~80% of ICU admissions last only 4-5 days)

Note: any such occurrences will also preoccupy onboard care-giver.

Why Mars (from the Life Sciences perspective)?

Mars design reference mission is a "strawman" chosen to represent exploration-class missions because it requires a more rigorous life sciences critical path than any other mission in the foreseeable future.

Mars DRM

- 30 months round-trip: 6 months 0g, 18 months 1/3 g, 6 months 0g
- four g-transitions: 1g to 0g; 0g to 1/3g; 1/3g to 0g; 0g to 1g
- two episodes of high (up to 5) g-load: Mars aerobrake; Earth aerobrake
- high physical demands of Mars surface EVA, possibly daily
- exposure to spacecraft, terrestrial and extraterrestrial toxins

Current Experience and ISS Requirements

- longest flight to date: 14 months
ISS tours: 3-6 months
- two g-transitions:
1g to 0g; 0g to 1g
- one episode of low (1.5-2) g-load:
Earth aerobrake (via Shuttle)
- infrequent orbital EVA;
regular daily exercise
- exposure to spacecraft and
terrestrial toxins only

Conclusions

- The human element is the most complex element of the mission design
- Mars missions will pose significant physiological and psychological challenges to crew members
- Some challenges (human engineering, life support) must be overcome (potential "non-starters")
- Some challenges (bone, radiation) may be show-stoppers
- ISS will only indirectly address Mars questions before any "Go/No Go" decision
- Significant amount of ground-based and specialized flight research will be required -- Critical Path Roadmap project will direct HSLSPO's research toward Mars exploration objectives

Background

HSLSPO determines critical areas of research and development to assure human health and performance capability to explore and develop space.

Mars Design Reference Mission is benchmark for determining content and direction of mid- and long-term research activities.

Near-term focus continues on tasks and techniques to expand human performance on Shuttle and ISS missions.

Bibliography

Human Exploration of Mars: The Reference Mission of the NASA Mars Exploration Study Team (Stephen J. Hoffman and David I. Kaplan, eds.) NASA Special Publication 6107 (July, 1997).

The author has augmented the information in the primary source with additional insights from many formal briefings, informal conversations, and personal musings, some based on the following works:

Oberg, James E. Mission to Mars : Plans and Concepts for the First Manned Landing. Harrisburg, PA: Stackpole Books, 1982.

Collins, Michael. Mission to Mars: An Astronaut's Vision of Our Future in Space. New York: Grove Weidenfeld, 1990.

Zubrin, Robert. The Case for Mars: The Plan to Settle the Red Planet and Why We Must. New York: The Free Press, 1996.

National Space Biomedical Research Institute

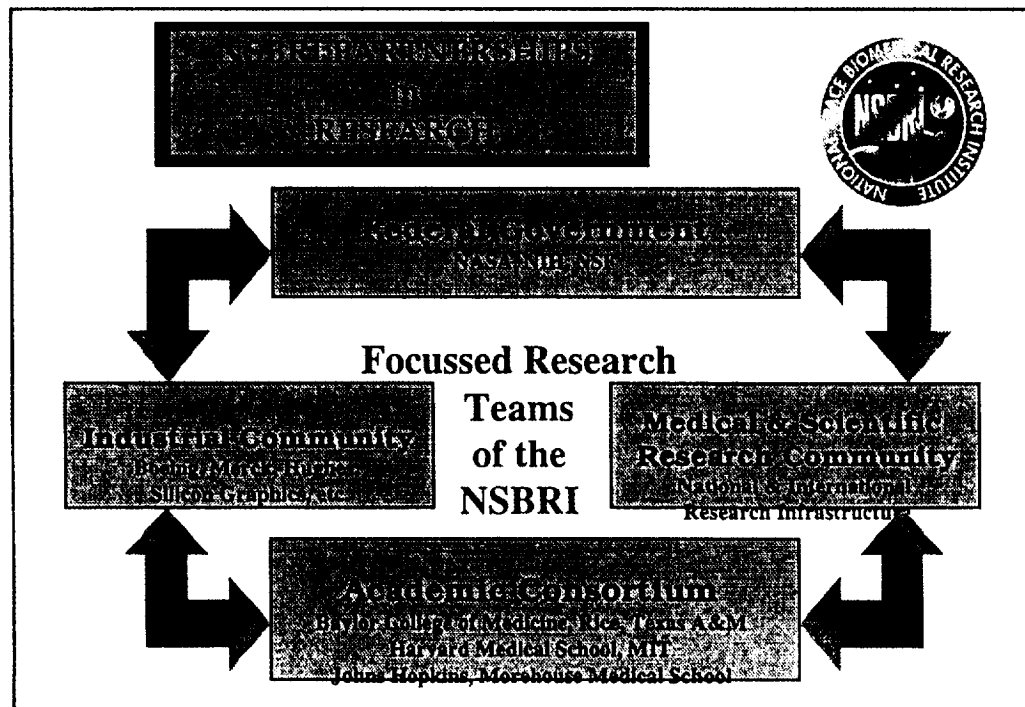
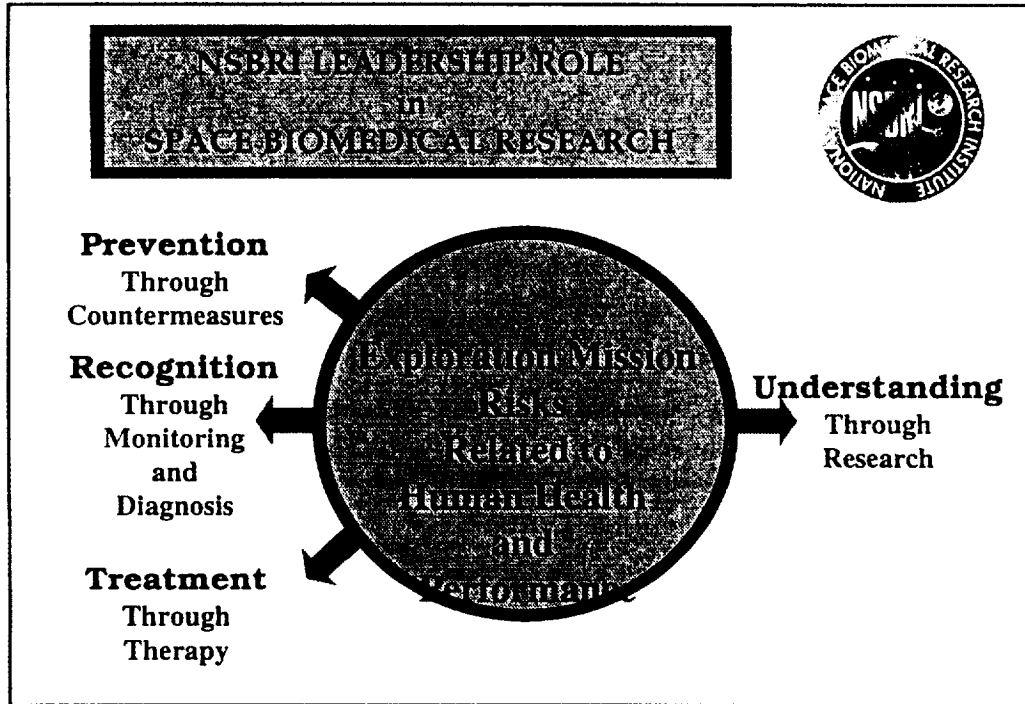
Laurence R. Young, ScD
Apollo Program Professor of Astronautics
Massachusetts Institute of Technology
Director, National Space Biomedical
Research Institute

Key Personnel

- **Chairman of the Board:**
Bobby R. Alford, M.D.
Executive Vice President and Dean of Medicine
Baylor College of Medicine
- **Director:**
Laurence R. Young, Sc.D.
Apollo Program Professor of Astronautics
Massachusetts Institute of Technology
- **Associate Director:**
Ronald J. White, Ph.D.
Professor
Baylor College of Medicine.

Institute Mission Statement

The NSBRI will lead a world-class, **National effort**
in integrated, critical path, **space biomedical research**
that supports NASA's
Human Exploration and Development of Space (HEDS) Strategic
Plan
by focusing on the
enabling of long-term human presence
in, development of, and exploration of space.



Mission Implementation

Involves:

- **Developing countermeasures;**
- **Defining and integrating the molecular, cellular, organ-level and whole-body responses to space flight;**
- **Establishing and developing appropriate biomedical support technologies;**
- **Transferring advances in knowledge and technology to the benefit of mankind in space and on earth; and**
- **Ensuring open involvement in the Institute's activities.**

Consortium Institutions

- **Baylor College of Medicine**
- **Harvard Medical School**
- **The Johns Hopkins University**
- **Massachusetts Institute of Technology**
- **Morehouse School of Medicine**
- **Rice University**
- **Texas A&M University**

Active Institute Associates

Andersen Consulting
Australian Antarctic Division
Brookhaven National Laboratory
Brooklyn College
Dartmouth College
Loma Linda University Medical Center
Mayo Clinic
NASA Johnson Space Center
SmithKline Beecham Pharmaceuticals
Uniformed Services University of the Health Sciences

University of California, Irvine
University of Florida
University of Houston
University of Pennsylvania
University of Texas Health Science Center at Houston
University of Texas M.D. Anderson Cancer Center
University of Washington
University of Wisconsin
York University



Human Health J. F. Dicello, Ph.D. Johns Hopkins	Human Performance R. J. Schrago, Ph.D. MIT
Human Adaptation C. A. Barger, M.D., Ph.D. Johns Hopkins	Human Nutrition & Hematology W. J. Schurman, M.D., Ph.D. MIT
Muscle Atrophy R. J. Schrago, Ph.D. MIT	Neurovestibular Adaptation G. M. Oman, Ph.D. MIT
Radiation Effects J. F. Dicello, Ph.D. Johns Hopkins	Technology Development V. L. Pisarcu, Ph.D. Johns Hopkins Applied Physics Laboratory

Cooperative National Research Initiatives

PARTNER: National Institute on Deafness and Other
Communication Disorders (NIDCD)

PROGRAM: Basic Vestibular Research Grants Program

- \$800,000 Annual Budget, Equally Shared (NSBRI Portion from Private Sources)
- Periodic Joint Program Announcements Developed by Both & Issued by NIH
- First Announcement Published in NIH Guide, June 16, 1998 Calling for Proposals by September 28, 1998
- Focus on Basic Vestibular Research Applicable to Health Care of Space Travelers and Vestibular Disorders on Earth
- NIH Supports Peer Review & Selection

International Research Affiliation

PARTNER: Institute of Aerospace Medicine of the German
Aerospace Center (DLR)

AGREEMENT:

- Signed January 21, 1998
- Enables Joint Projects in Research, Technology Development, or Education/Outreach
- Encourages Exchange of Scientists, Materials, Publications, and Students
- Funding of German Activities Responsibility of DLR

Accelerator Facilities for Radiation Research

Francis A. Cucinotta, PhD
NASA Johnson Space Center

Glossary of Terms

- AGS- alternating gradient synchrotron
- BAF- Booster Application Facility
- BNL- Brookhaven National Laboratory
- CNS- central nervous system
- GCR- galactic cosmic ray
- H(<E)- Dose equivalent from ions with energy less than E
- HIMAC- heavy ion accelerator in Chiba, Japan
- HZE- high charge and energy
- ISS- International Space
- LLU- Loma Linda University
- MeV/amu- million electron volts per atomic mass unit
- MOA- memorandum of agreement
- NAS- National Academy of Sciences
- NRC- National Research Council
- SPE- solar particle event
- SRHP- Space Radiation Health Project
- TEPC- tissue equivalent proportion counter

HSRP Goals in Accelerator Use and Development

- Need for ground-based heavy ion and proton facility to understand space radiation effects discussed most recently by NAS/NRC Report (1996)
- Strategic Program Goals in facility usage and development:
 - Operation of AGS for approximately 600 beam hours/year
 - Operation of Loma Linda University (LLU) proton facility for approximately 400 beam hours/year
 - Construction of BAF facility
 - Collaborative research at HIMAC in Japan and with other existing or potential international facilities
- MOA with LLU has been established to provide proton beams with energies of 40-250 important for trapped protons and solar proton events
- Limited number of beam hours available at Brookhaven National Laboratory's (BNL) Alternating Gradient Synchrotron (AGS)

NASA-Loma Linda University (LLU) Memorandum of Agreement (MOA)

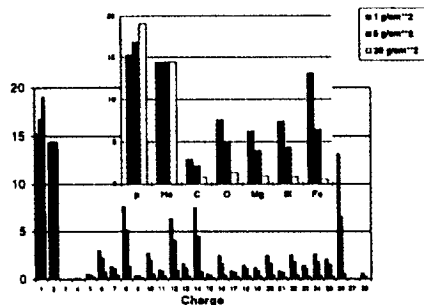
Proton and heavy ion contributions to dose equivalent behind shielding



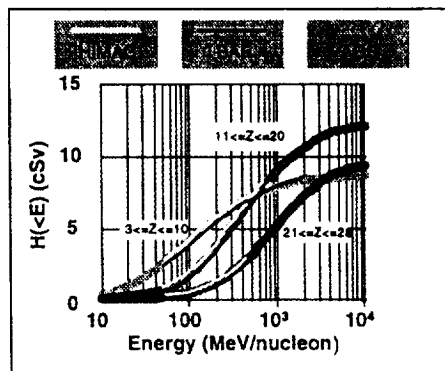
- Accelerator Facilities at LLU provide proton beams that allow for simulation of solar particle effects, trapped protons and portion of GCR spectrum
- NASA-LLU MOA Highlights:
 - to enhance basic knowledge of living systems and their response to radiation
 - apply of this knowledge to radiation protection, risk assessment, diagnosis, and treatment of cancer
 - exploit the synergy between NASA research requirements and charged particle therapy to establish a collaborative peer-reviewed research base which benefits the Loma Linda academic community

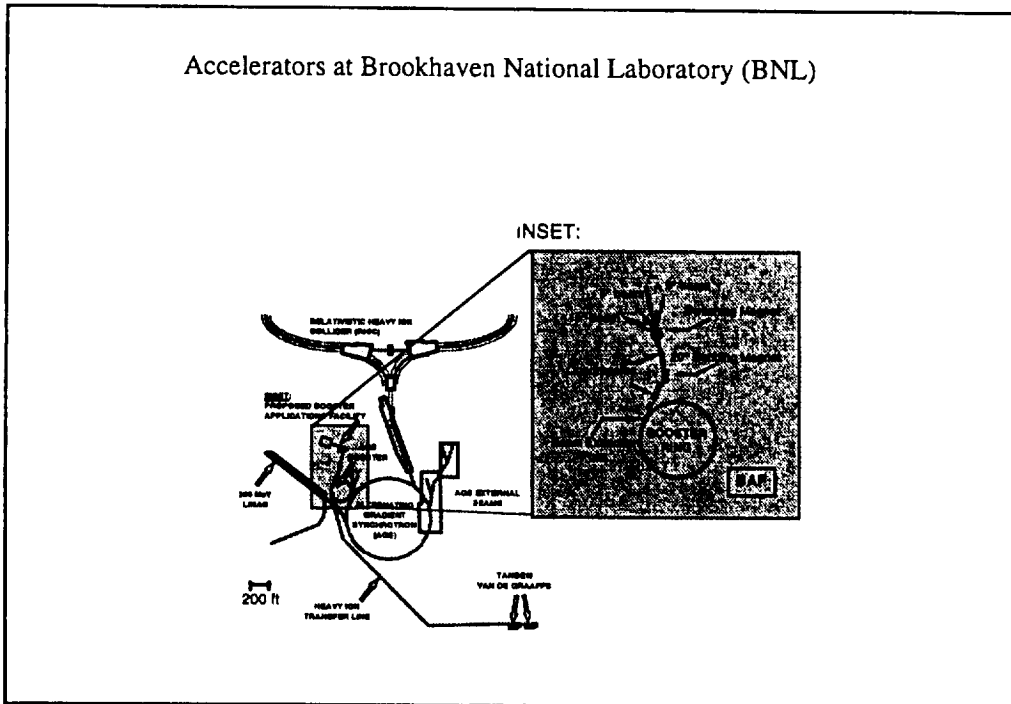
Space Radiation Charge and Energy Components

Relative contribution of various charge groups to Eye dose equivalent behind shielding



Accelerator Energy Ranges and GCR Doses Equivalent (H) contributions from energy, E

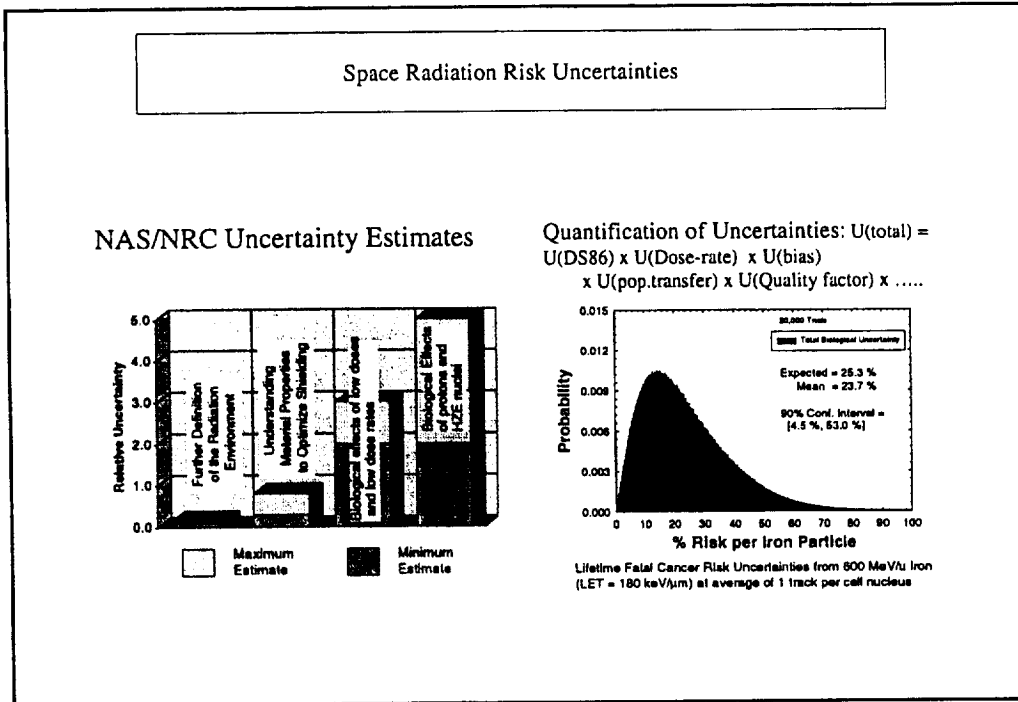




BNL Accelerator Facilities

- Alternating Gradient Synchrotron (AGS) provides relativistic heavy ion beams for study of high energy GCR components. NASA use in competition with high energy physics community
- Booster application facility (BAF) a dedicated facility under construction for NASA to perform radiobiology and shielding research, and for space dosimetry calibrations
- Major deliverables from BAF
 - Example beam energy and charges

Proton	730-3100 MeV	Oxygen	120-1500 MeV/amu
Silicon	90-1200 MeV/amu	Iron	100-1100 MeV/amu
 - Ability for rapid beam switching allowing for mixed ion fractionation studies
 - Construction includes major modifications to tandem, beam transport, and booster systems
 - Adequate experimental buildings for animal, cellular biology and shielding studies
- First experiments at BAF to occur in 2002 or 2003
- Plans to include compatible dosimetry and support labs at LLU and BAF



Validation: Physical and Biological Dosimetry

Comparisons to measurements for dose- and dose equivalent rate on Mir-18.

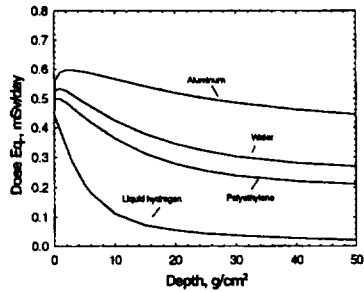
	GCR		Trapped Protons		TOTAL	
	Dose mGy/day	Dose Eq. mSv/day	Dose mGy/day	Dose Eq. mSv/day	Dose mGy/day	Dose Eq. mSv/day
TEPC	0.142	0.461	0.153	0.298	0.299	0.781
HZETRN						
Naussica	0.138	0.535	0.191	0.295	0.329	0.830
TEPC	0.141	0.526	0.140	0.219	0.281	0.745
Location						
Lyulin	0.134	0.547	0.254	0.391	0.388	0.938

Comparisons of Calculations to Measurements for Fraction of lymphocytes with chromosome aberration (dicentric) from Mir-18 Crew Member

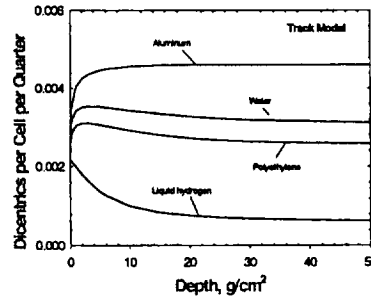
Shielding	Model	GCR	Trapped p+	Total
Naussica	LET	2.20×10^{-3}	2.19×10^{-3}	4.39×10^{-3}
Naussica	Track	2.78×10^{-3}	2.66×10^{-3}	5.44×10^{-3}
Lyulin	LET	2.23×10^{-3}	2.46×10^{-3}	4.69×10^{-3}
Lyulin	Track	2.76×10^{-3}	3.02×10^{-3}	5.78×10^{-3}
Mir-18-Crew Member	Biodos.			$6.4(\pm 2) \times 10^{-3}$

Risk Mitigation through Shielding?

GCR Dose Equivalent on ISS

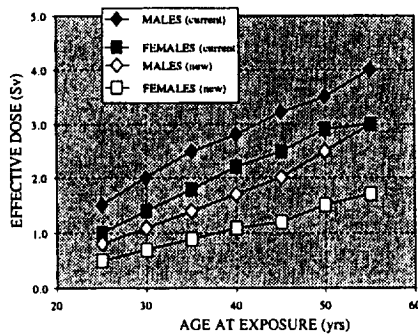


Chromosome aberrations on ISS



Issues in Risk Limits, Bioethics, and Flight Rules

Draft NCRP Limits for ISS



- Issues:
 - Differences in dose limits by NASA and International partners
 - Ethics of limiting cancer mortality versus cancer incidence

Tissue	Lethality factor
Leukemia	0.95
Breast	0.55
Colon	0.5
Thyroid	0.10

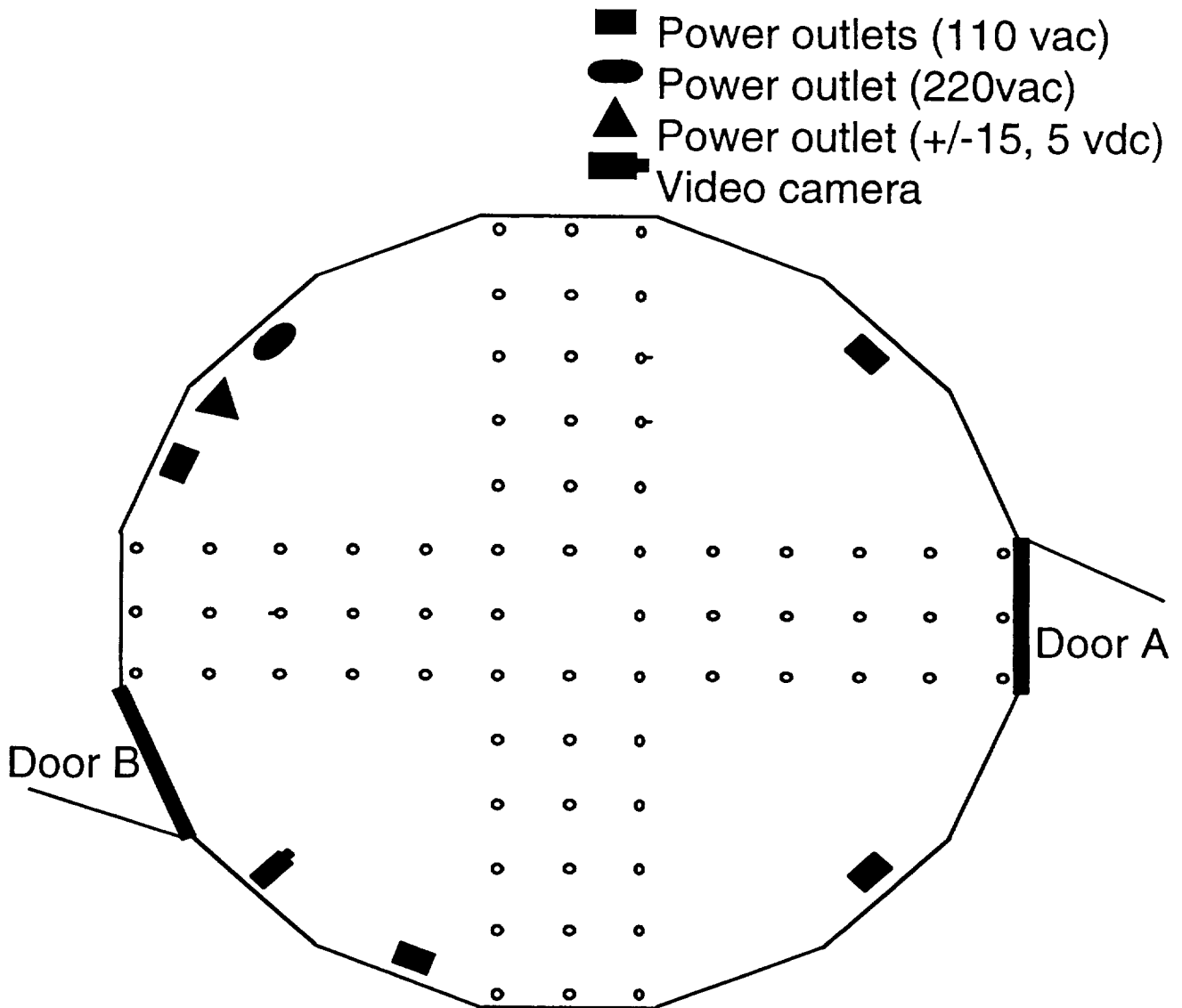
- Inability to assess CNS risk and cancer risk for exploration limits
- Long-term planning for including role of individuals genetic pre-disposition
- Ground-based facilities for proper dosimetry calibrations

The Rotating Room Facility of the Ashton Graybiel Spatial Orientation Laboratory

Paul DiZio, PhD

Volen Center for Complex Systems

Brandeis University



Room inside diameter= 22'

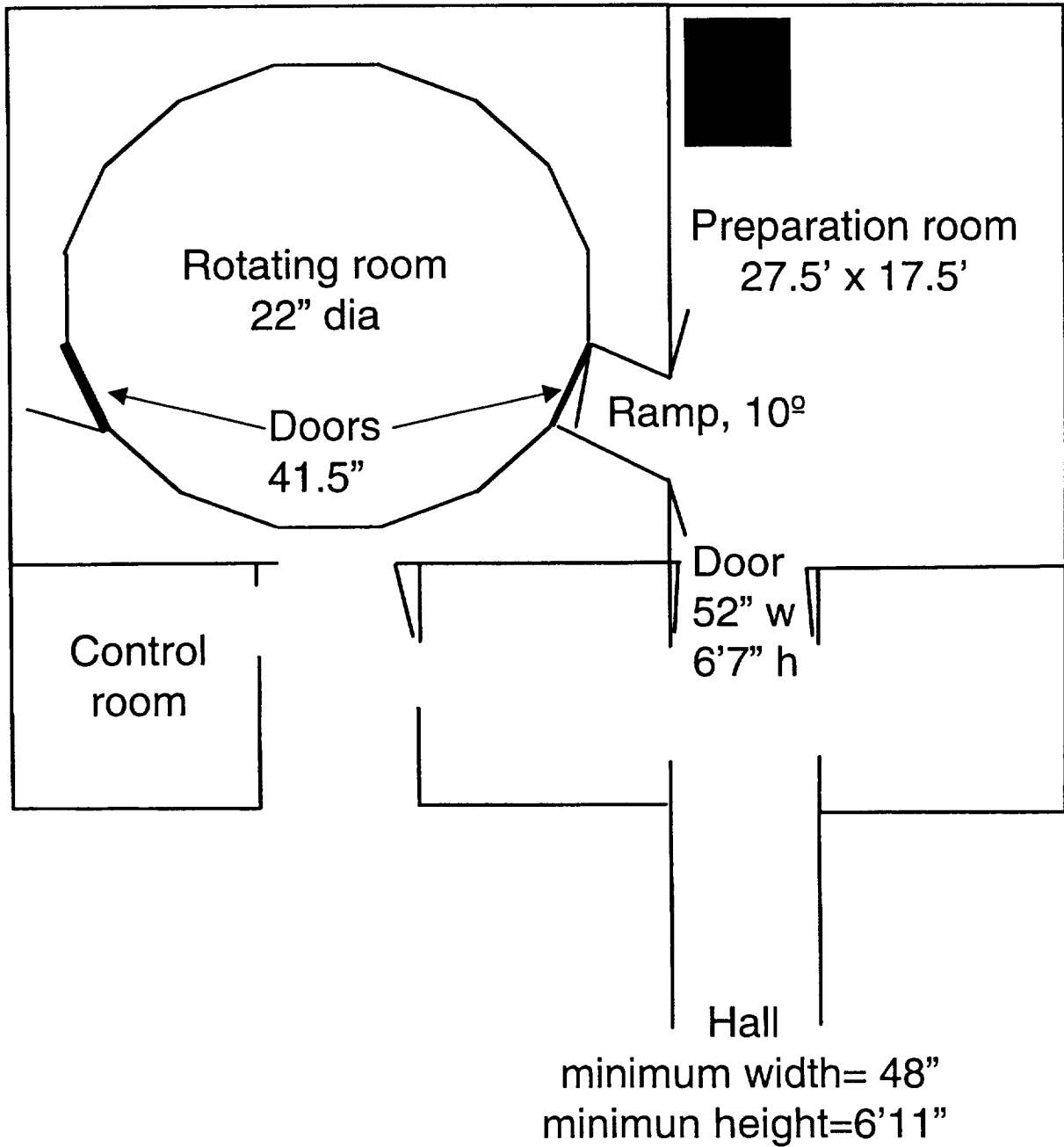
Ceiling height= 94" at center, 88.7" at walls

Door width= 41.5", height= 77.5"

Tie-down grid

Spacing = 20" x 20"

Holes = 3/8-16



Resources

- Motion profiles
 - Maximum rotation speed = 35 rpm
 - Maximum angular acceleration = $15^\circ/\text{s}^2$
 - Maximum linear acceleration = 4.7 g
- Operating Modes
 - Linear induction motors for high acceleration
 - Belt drive for low vibration and backup

- Schedule
 - Emphasis is placed on putting back-to-back studies that would not require major re-configuration of the slow rotation room and providing appropriate blocks of time to complete studies expeditiously.
- Personnel
 - Graybiel Laboratory supplies two operators whose job is to ensure safety and to provide the desired motion profile.

Resources

- Power
 - 110 vac single phase, 40 amp
 - 220 vac single or three phase, 80 amp
 - \pm 12-18 vdc, 6 amp, 5 vdc, 4 amp
 - backup generator, 120 vac, 10 amp
- Space
 - 22 foot inside diameter
 - ceilings 94" at center, 88.7" at walls

- Lighting
 - Incandescent light, remote controlled
- Temperature
 - Ambient temperature linked dependent on building thermostat
- Payloads
 - Up to 6000 lbs with COG within bearing
- Data
 - Users supply onboard data storage
 - Video and audio available

Terms of Use

- Investigators with NASA/NIH funding to cover costs may apply for use time.
- The Graybiel Laboratory supplies space, power, time, and room operators.
- Visiting team supplies all stimulation and measurement equipment, test subjects, and test conductors.

- All protocols and equipment must meet the approval of the director and associate director of the Ashton Graybiel Spatial Orientation Laboratory.

Investigator Requirements

- Investigators provide a written description of protocols and equipment: Power, Space, Weight, Protocol description, Schedule, Stress analysis, Hazard analysis.
- PI or senior scientist must be present during all rotation experiments.
- All personnel going aboard require medical certification: Air Force Flying Class III or equivalent.

- IRB approval is required from home institution, NASA, and Brandeis University.

Barophysiology

Chair

Michael R. Powell, Ph.D.

Co-Chair

Richard D. Vann, Ph.D.

BAROPHYSIOLOGY SESSION SUMMARY

Barophysiology is the science of the effects that the atmospheric components oxygen, carbon dioxide, inert gas, and barometric pressure have on living organisms. Deleterious effects or risks relevant to space exploration include hypoxia from insufficient oxygen, oxygen toxicity from too much oxygen, decompression sickness (DCS) from the formation of nitrogen bubbles, and ebullism from the vaporization of body fluids upon exposure to near total vacuum. These risks can be mitigated and the deleterious effects treated by careful selection of the atmospheric components and by manipulation of factors such as gravity, exercise, and temperature.

Astronauts performing extravehicular activity (EVA) do not seem to develop decompression sickness, but 20-50% of experimental subjects in previous ground-based EVA simulations developed mild DCS, and 2-3% developed moderate to serious DCS. Recent ground-based studies have shown that subjects not exercising the anti-gravity muscles have significantly less DCS than standing subjects suggesting that gravity may be a DCS risk factor (**Powell**). A possible explanation for this finding is that standing and walking in 1-g gravity generates microbubbles that grow after depressurization and cause DCS. If this is correct, DCS risk may be greatest in ground-based EVA simulations, less in the reduced gravity of Mars or the moon, and least in low-earth orbit or inter-planetary travel where gravity is minimal. The possible effects of gravity on DCS risk warrant further experimental investigation.

A common method for reducing DCS risk is to breathe 100% oxygen to eliminate nitrogen from the tissues so that fewer bubbles form after depressurization. In ground-based studies, exercise during oxygen breathing has been found to accelerate nitrogen elimination thereby allowing shorter periods of oxygen breathing (**Pilmanis et al.**).

In the Space Shuttle, astronauts occasionally breathed oxygen at the 14.7 psia cabin pressure for 4 hrs before depressurization to the space suit pressure of 4.3 psia, but this prebreathe procedure was unpopular as it limited their mobility. A more common practice during Shuttle EVA is to depressurize the entire craft to 10.2 psia for 24 hrs or longer. The 10.2 psia decompression "stage" is followed by a short period of oxygen breathing (40 minutes) prior to depressurization to suit pressure. During construction of the International Space Station, stage decompression will be impractical because, with the exception of a small equipment lock, the cabin pressure must remain at 14.7 psia. A potential solution to this problem is for astronauts to exercise during oxygen breathing at 14.7 psia to increase the rate of nitrogen elimination. In recent ground-based tests in which subjects simulated microgravity by reclining, there was no DCS in 50 trials of subjects who exercised during part of a two-hour oxygen breathing period. These experiments were conducted under the auspices of Johnson Space Center in a multi-center trial involving Hermann Hospital, Duke Medical Center, and the Defence Civil Institute of Environmental Medicine (DCIEM of Canada). Further studies are planned to investigate exercise dosage and to determine if the oxygen breathing period can be reduced to less than two hours (**Vann and Gerth**).

While DCS is clearly initiated by bubbles, the mechanisms that give rise to the various signs and symptoms are by no means well understood. Treatment involves breathing hyperbaric oxygen to compress and dissolve the bubbles, but optimal treatment regimens are not fully established, and useful pharmacological agents are yet to be identified. To improve the safety and effectiveness of

oxygen therapy, human trials were conducted to develop the relationships of oxygen dose to the signs and symptoms of pulmonary and central nervous system toxicity (**Lambertsen et al.**). Potential targets for pharmacological therapy are under investigation in animal models of DCS. Venous gas emboli (VGE) in the lungs have been found to cause pulmonary edema secondary to inflammatory response possibly mediated by nitric oxide inactivation (**Butler and Little**).

The recent concept of the inflatable spacecraft (e.g., the “Trans-Hab”) has the potential for reducing vehicle weight and cost. Cabin pressure can have an important role to this end since, for example, the radius of a spherical vehicle would vary indirectly with the internal pressure. Thus, halving the pressure would approximately double the permissible radius. This presents a unique opportunity for redesigning the spacecraft atmosphere to achieve additional benefits in cost and weight reduction. A sub-atmospheric cabin pressure would also decrease gas leakage and DCS risk during EVA. A lower cabin pressure, moreover, would permit a lower space suit pressure and improved suit flexibility. For an excursion to Mars, savings in consumables could be achieved by replacing nitrogen from the Earth’s atmosphere with argon present in the Martian atmosphere. Reduced fire hazard is another benefit of argon as a diluent gas, and further reductions in fire hazard and still lower cabin pressures might be achieved by decreasing the oxygen partial pressure and allowing the carbon dioxide partial pressure to rise within physiologically tolerable limits. Thus, a normobaric air environment is not necessarily the optimal atmosphere for space travel. In planning for an improved atmosphere, all aspects that would be affected by pressure and gas composition should be considered including structural design, cooking, plant cultivation, heat transfer, and DCS risk.

Chair, Michael Powell; Co-Chair, Richard Vann

ROLE OF INFLAMMATORY RESPONSE IN EXPERIMENTAL DECOMPRESSION SICKNESS

B.D. Butler, T. Little

Baromedical Laboratory and Hermann Center for Environmental, Aerospace and Industrial Medicine, Dept. Anesthesiology, Univ. of Texas Medical School, 6431 Fannin, 5020 MSB Houston, TX 77030

INTRODUCTION

Decompression to altitude can result in gas bubble formation both in tissues and in the systemic veins. The venous gas emboli (VGE) are often monitored during decompression exposures to assess risk for decompression sickness (DCS). Astronauts are at risk for DCS during extravehicular activities (EVA), where decompression occurs from the Space Shuttle or Space Station atmospheric pressure of 14.7 pounds per square inch (PSI) to that of the space suit pressure of 4.3 PSI.

DCS symptoms include diffuse pain, especially around joints, inflammation and edema. Pathophysiological effects include interstitial inflammatory responses and recurring injury to the vascular endothelium. Such responses can result in vasoconstriction and associated hemodynamic changes. The granulocyte cell activation and chemotaxin release results in the formation of vasoactive and microvascular permeability altering mediators, especially from the lungs which are the principal target organ for the venous bubbles, and from activated cells (neutrophils, platelets, macrophages). Such mediators include free arachidonic acid and the byproducts of its metabolism via the cyclooxygenase and lipoxygenase pathways (see figure). The cyclooxygenase pathway results in formation of prostacyclin and other prostaglandins and thromboxanes that cause vasoconstriction, bronchoconstriction and platelet aggregation. Leukotrienes produced by the alternate pathway cause pulmonary and bronchial smooth muscle contraction and edema. Substances directly affecting vascular tone such as nitric oxide may also play a role in the response to DCS.

We are studying the role and consequent effects of the release inflammatory bioactive mediators as a result of DCS and VGE. More recent efforts are focused on identifying the effects of the body's circadian rhythm on these physiological consequences to decompression stress.

METHODS

The studies are divided into five categories using several animal models. Hyperbaric and hypobaric decompression and direct venous air embolization were evaluated in a dog model simulating the bubble load observed in ground-based EVA decompression studies. Rodent models involve decompression from hyperbaric exposures to determine the effectiveness of mediator inhibition on DCS symptoms and inflammatory response as well as the role of the circadian time structure.

In the canine studies, hemodynamic assessment was carried out before, during and following decompression or VGE infusion. DCS evaluation included VGE characterization using echo ultrasound; gross symptoms; pulmonary edema (gravimetric analysis); collection of arterial blood, urine, pleural fluid and bronchial alveolar lavage (BAL) for protein analysis; differential

cell counts and eicosanoid (thromboxane B2 [TxB2], 11-dehydro TxB2 [11dhTxB2] and leukotriene E4 [LKE4]) analysis using ELISA techniques. Changes in plasma nitric oxide levels were determined in both canine and rodent samples using chemoluminescence.

Protocols:

- 1) Hyperbaric DCS: Anesthetized dogs were decompressed from 184 kPa after 120 mins.
- 2) Hypobaric DCS: Anesthetized dogs were decompressed to 40,000 ft (4.3PSI) for 180 mins.
- 3) VGE: Venous air infusions of 0.15, 0.25 and 0.35 ml/kg/min for 180 mins.
- 4) Rodent DCS / Eicosanoid Inhibition Studies: Sprague-Dawley rats pretreated with drug (Dibutyryl cAMP[DBcAMP], ziluton or accolate) were decompressed from 616 or 683 kPa after 60 mins.
- 5) Circadian Rhythm influences on DCS risk and response in a rodent model using 6 time points in a 24 hr. cycle.

RESULTS

- 1) The canine **hyperbaric decompression exposures** resulted in VGE formation at a level of Spencer Grade 4 using a 0-4 scoring method as well as moderate increases in pulmonary artery pressure and systemic vascular resistance. These increases paralleled a decrease in plasma nitric oxide levels. Similarly, increases occurred with pulmonary edema and BAL protein levels as well as arterial and BAL white blood cell (WBC) and neutrophil counts. Increases in eicosanoid levels included; arterial, lung tissue and BAL LKE4, and urinary TxB2 and 11dhTxB2 levels.
- 2) **Hypobaric decompression exposures** resulted in VgE formation (Spencer Grade 1-4), increases in pulmonary edema, arterial and BAL WBC's and neutrophils. Urinary TxB2 and 11-dhTxB2 levels were increased.
- 3) **VGE TxB2 and LKE4 levels** were increased with the larger air dose in both urine and BAL, as were WBC counts and myeloperoxidase levels. Hemodynamic and pulmonary edema changes were increased over baseline in all groups, with no difference between groups. Plasma nitric oxide levels were decreased in the 0.15 and 0.35 ml/kg/min groups immediately after VGE and remained depressed following recovery in all three groups.
- 4) In the **rodent hyperbaric decompression exposures** urine and arterial levels of TxB2, 11-dhTxB2 and LKE4 increased in the 683 kPa group over controls as did BAL 11-dhTxB2 and LKE4 levels. With DBcAMP treatment the increases in arterial, BAL and urinary 11-dhTxB2 and LKE4 were attenuated. DBcAMP also attenuated the increases ($p < 0.05$) over controls in; pulmonary edema formation, BAL and pleural protein levels and BAL WBC counts (683 kPa group). Pretreatment with the leukotriene antagonist accolate or the 5-lipoxygenase inhibitor ziluton, failed to show any significant change in DCS outcome in two additional studies.
- 5) With the **circadian rhythm studies** preliminary results indicated circadian rhythm dependencies ($p < 0.05$) in pleural protein and neutrophils, BAL WBC, and arterial and BAL LKE4 using a 24 hour cosine fit. A 12 hour pattern showed significance with BAL neutrophils, urinary TxB2 and BAL 11-dhTxB2. Pulmonary edema and DCS symptoms had greatest effects at 14 and 18 hours after lights on.

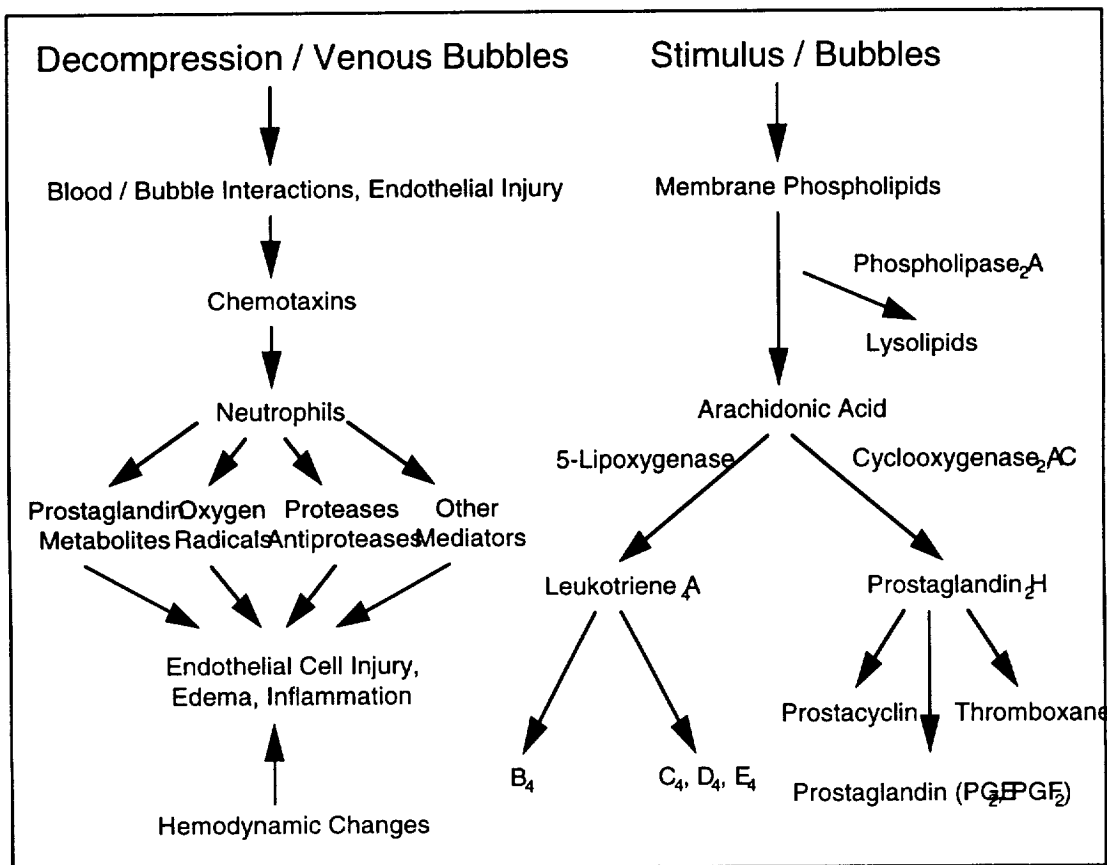
CONCLUSIONS

These studies demonstrate an inflammatory-type of response to DCS-induced venous bubble formation and elucidate some of the underlying mechanisms of DCS symptoms. Microvascular endothelial injury and subsequent changes in vessel wall tone and permeability can account for

some of the localized edema formation and the concomitant release of bioactive mediators that may be involved with pain sensation and associated cellular activation. Increased numbers and activation of neutrophils likely play an additional role in the production and release of arachidonic acid and its byproducts of metabolism including the eicosanoids. Plasma nitric oxide levels were consistent with observed changes in vascular resistance. Increased microvascular permeability manifesting as edema was further verified by the elevated protein levels in the BAL and pleural fluids. The protective effects of exogenous DBcAMP (increases intracellular AMP) are attributable to such factors as; positive inotropic and chronotropic effects, pulmonary vasodilation, reduction in intracellular calcium and therefore reduced phospholipase A2 and eicosanoid production, and inhibition of intercellular gap formation or endothelial cell contraction. The more recent data demonstrate that there is likely a circadian-rhythm dependent outcome to DCS and should therefore also be considered with regards to operational concerns where DCS is a risk factor.

FUTURE STUDIES

Future studies will concentrate on further defining the circadian rhythm dependency of DCS outcome, as well as the use of inflammatory inhibitors and their role in symptom attenuation, especially with regards to dose variation and time dependencies.



REFERENCES

- 1) Butler BD, Little T, Smolensky M: Circadian rhythm influences on decompression outcome in rats. In: Biol Clocks Mech and Applications, ed. Touitou Y. Excerpta Medica Int Cong Ser (ICS1152) Elsevier Amsterdam, 1998, pp 541-544.
- 2) Little T, Butler BD: Dibutyryl cAMP effects on thromboxane and leukotriene production in decompression-induced lung injury. Undersea and Hyperbaric Med 24: 185-191, 1997.
- 3) Butler BD, Little T, Powell M, Robinson R: Biomedical studies relating to decompression stress with simulated EVA; overview. NASA 12th Man in Space Symp, Wash D.C., 1997
- 4) Butler BD, Powell M, Little T: Dose response levels of 11-dehydrothromboxane B2 (TxB2) and leukotriene E4 (LTE4) with intravenous air embolism. Undersea and Hyperbaric Med 22, supp.40, 1995

ACKNOWLEDGMENTS

Supported in part by NASA NAG-9-215, NAG-W-4479, NAG-5-6176, NAG-9-1040

QUANTITATIVE PREDICTION OF PULMONARY OXYGEN POISONING STRESS IN HUMAN EXPOSURES TO CHANGING DEGREES OF INSPIRATORY HYPEROXIA

C. J. Lambertsen, J. M. Clark, E. Hopkin, Environmental Biomedical Research Data Center, Institute for Environmental Medicine, University of Pennsylvania Medical Center, Philadelphia, PA 19104

INTRODUCTION

Redevelopment and improved validity have been accomplished, for graphic and mathematical modeling of rates and magnitudes of pulmonary mechanical function decrements, in varied degrees and duration of hyperoxic exposures. The original (1968) IFEM predictive model of Unit Pulmonary Toxic (O_2) Dose and Cumulative Pulmonary Toxic Dose (1, 2, 3), in use over 30 years, was derived with the then limited usable data of two experiment series at .83 and .98 ATA O_2 and one series at 2.0 ATA (2). The present redevelopment program has included extensive additional data for series of prolonged exposures at 1, 1.5, 2.0, 2.5 and 3.0 ATA O_2 , involving use of 101 subjects overall (Table 1).

METHODS AND RESULTS

In all stated series of exposures of normal men to hyperoxia at rest, multiple measures of pulmonary mechanical functions were performed (2, 4). In each series, the functions most consistently demonstrating statistically significant reductions with extended O_2 exposure duration were Slow or Fast Vital Capacity. Slow Vital Capacity (SVC) was used in analytic modeling of Pulmonary O_2 Tolerance, reserving other measures (e.g. alveolar-arterial O_2 gradient, CO diffusion coefficient) for related analytic processes, including recovery rates.

Analytic processes initially included use of duration/effect averages to compare the higher rates of decrease in vital capacity at the higher degrees of inspired O_2 (1, 1.5, 2.0, 2.5 ATA O_2). Measurements at 3.0 ATA were so heavily devoted to neurological effects that serial pulmonary function studies were not practical. The average data were pooled for analysis by Multiple Log Probit Linear Regression, illustrated by the curves and mean data of Fig 1. This method in turn provided for parallel linear log-log plots (hyperbolic) of different durations and oxygen pressures combinations showing the "same" degree of reduction in the pulmonary vital capacity. Fig. 2 shows the family of O_2 pressure/duration hyperbolae representing 2% to 20% predicted vital capacity decrement, with a superimposed hyperbolic representation of observed "first neurologic effect" at each designated O_2 pressure.

The hypothesis of an hyperbolic relationship of O_2 Exposure Pressure and Duration to toxic effect was utilized in the initial model of pulmonary O_2 tolerance prediction (1, 2, 3). The present and the linked original modeling concept include hyperbolae asymptotes at zero time for infinite exposure PO_2 , and a borderline pulmonary toxicity asymptote of 0.5 ATA at infinite exposure duration (1, 2, 3).

The present stage of predictive model development allows graphic tracking of accumulating pulmonary effect induced in transits of varied durations, among different oxygen pressures. It also provides the desired mathematical model for computation of predictive Cumulative Pulmonary O_2 Toxic Dose and Effect.

CONCLUSION

Refinement of a descriptive predictive model has been accomplished for degree of pulmonary toxic effect of continuous exposures to stable or varied degrees of hyperoxia. Refinement required new data on subject groups at 1, 1.5, 2.0 and 2.5 ATA inspired PO₂, and use of pulmonary vital capacity as the only indicator of significant changes occurring in association with increasing exposure pressure and duration. The model system allows use of combined exposure durations and oxygen exposure pressures as indices of a pulmonary mechanical effect, and as a quantitative index of toxic oxygen stress.

REFERENCES

1. Lambertsen, C.J. Basic requirements for improving diving depth and decompression tolerance. In: *Underwater Physiology. Proceedings of the Third Symposium*. C.J. Lambertsen, Ed. Williams and Wilkins Co., Baltimore, 1967.
2. Clark, J. M., and C. J. Lambertsen. *Pulmonary Oxygen Tolerance in Man and Derivation of Pulmonary Oxygen Tolerance Curves*. IFEM Report No. 1-70. Philadelphia, PA: Institute for Environmental Medicine, University of Pennsylvania, 1970.
3. Wright, W. B. *Use of the University of Pennsylvania Institute for Environmental Medicine Procedure for Calculation of Cumulative Pulmonary Oxygen Toxicity*. U.S. Navy Experimental Diving Unit Report 2-72. Washington, DC, 1972.
4. Clark, J. M., C. J. Lambertsen, R. Gelfand, N. D. Flores, J. B. Pisarello, M. D. Rossman, and J. A. Elias. Effects of prolonged oxygen exposure at 1.5, 2.0, or 2.5 ATA on pulmonary function in man (Predictive Studies V). *J. Appl. Physiol.* 1998 (In Press).

FIGURES AND TABLES

Table 1

REDEVELOPMENT OF OXYGEN TOLERANCE MODEL
Pulmonary and CNS Hyperoxia Effects Data Base
(Individual Subjects, Repetitive Measurements)

Maximum Exposures		Number of Subjects	
PO ₂ ATA	Duration (HRS)	Pulmonary Database	CNS Database
3.0	3.5	18	18
2.5	6	8	8
2.0	12	44	32
1.5	18	9	9
1.0	48	22	-
		101	67

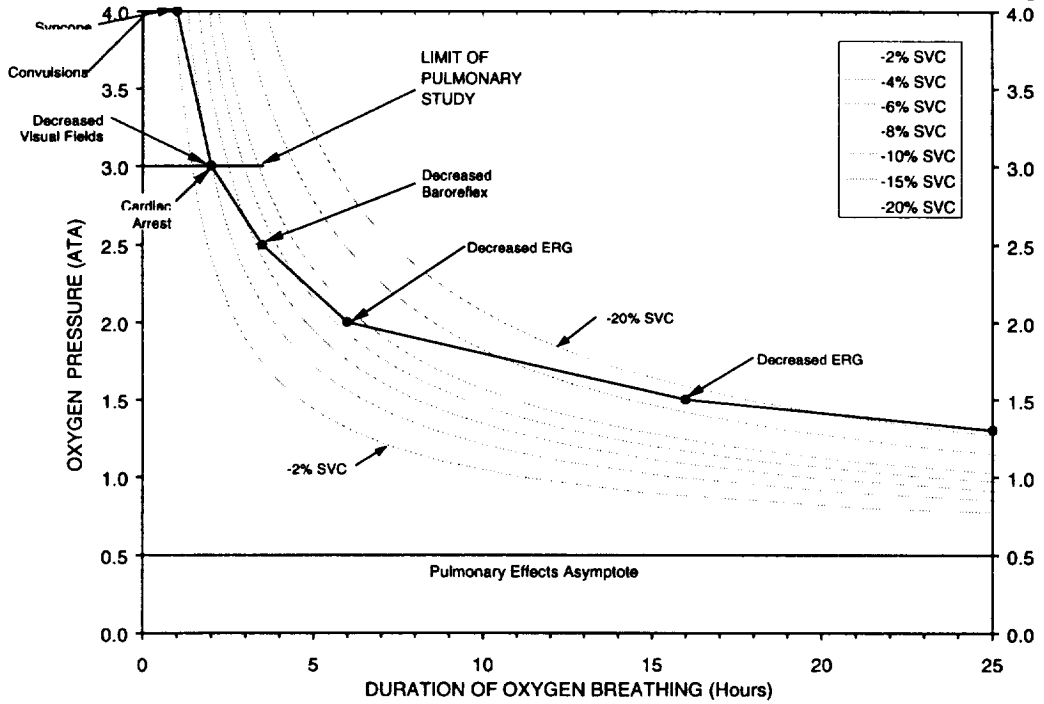


Fig. 1. Relations of Pulmonary and Neurological O₂ Tolerance. Neurologic Incidents Prediction. Neurologic Incidents (First Objective Neurological Effect) Superimposed on Pulmonary Oxygen Tolerance Prediction.

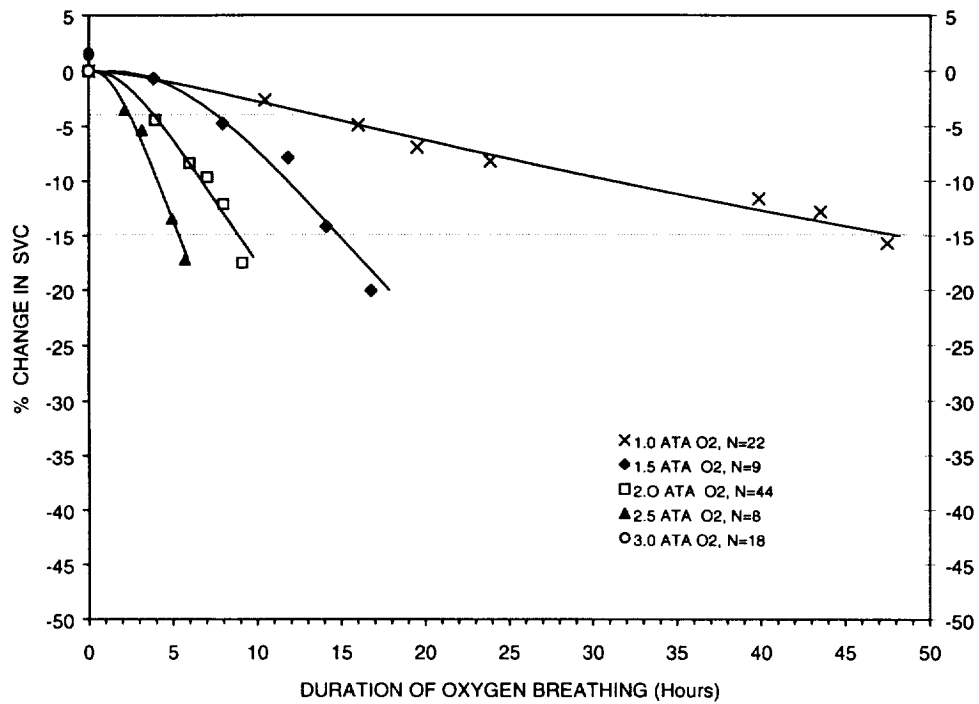


Fig. 2. Effect of Oxygen Pressure-Duration Exposure On Decrease In SVC (Multiple Log Probit Linear Regression Analysis). Plotted points are duration-effect means for the subject groups. Dose-Response Curves for the different Oxygen Pressures are Multiple Log Probit. Linear Regression analysis of Exposure Duration vs. Effect. Horizontal dashed lines illustrate durations producing equal effect at different exposure pressures.

STAGED DECOMPRESSION TO A 3.5 PSI EVA SUIT USING AN ARGON-OXYGEN (ARGOX) BREATHING MIXTURE

A.A. Pilmanis, K.M. Krause, J.T. Webb, L.J. Petropoulos, N. Kannan,
AF Research Laboratory/HEPR, Brooks AFB, Tx 78235. , Wyle Laboratories, San
Antonio, TX 78235. University of Texas at San Antonio, San Antonio, Tx 78249

INTRODUCTION

Long-term NASA goals include permanent occupation of the International Space Station (ISS) and missions to both the moon and Mars. One of the critical issues for reaching these goals is the definition of an optimum pressure for extravehicular activity (EVA) suits. Currently, a 4.3 psia pressure suit is used for space shuttle EVAs. This suit, in combination with current preoxygenation schedules, is effective for decompression sickness (DCS) prevention. However, at 4.3 psia, the astronauts experience hand and arm fatigue. Also, due to the gravitational forces that exist on the moon and Mars, the current suit will be too heavy for planetary EVA. A 100% oxygen breathing gas at an ambient pressure of 2.8 psia, is physiologically equivalent to breathing air at 10,000 feet altitude. However, because there will be some minimal performance decrement from mild hypoxia at that pressure and to provide a margin of safety, we propose a lower limit for the suit pressure of 3.5 psia. A soft, lower pressure suit requires a trade-off between preoxygenation time and suit weight and mobility. Development of a new 3.5 psia EVA pressure suit would reduce structural complexity, leak rate, and weight while increasing mobility, comfort, and maintainability. The trade-off for these advantages will be an increase in decompression time.

Due to fire hazard, a "shirt sleeve" module containing 100% oxygen for preoxygenation is unacceptable. A fire safe mixture of oxygen and nitrogen in the module would greatly reduce the denitrogenation rate and therefore require breathing on an oxygen mask. In addition, air breaks in preoxygenation would be required while donning the EVA suit. Air breaks in preoxygenation necessitate additional preoxygenation time. A "shirt sleeve" environment must utilize a breathing mixture which is fire safe and provides hypoxia and DCS protection. Argon is an inert gas with properties similar to nitrogen. It is relatively inexpensive and available. In terms of fire protection, a 38% oxygen - 62% argon mixture at 7.34 psia will provide an equivalent burn rate of paper strips as sea level air. In terms of hypoxia prevention, this mixture, at this pressure, is the equivalent of breathing air at an altitude of 2,728 feet. The Martian atmosphere has argon as a constituent that will appear in the breathing mixture unless costly and heavy systems are provided to separate it from the nitrogen. In addition, the option of transporting nitrogen from earth is not attractive.

Preoxygenation with ARGOX will be effective for nitrogen elimination, because a large nitrogen pressure gradient will exist between the body and the breathing gas. Argon however, will be loaded during this period. At the proposed stage of 7.34 psia, with a 38% oxygen - 62% argon mixture, the driving pressure for the loading of argon will be 235 mmHg, as compared to 600 mmHg for a fire safe ARGOX mixture at atmospheric pressure. This will result in relatively less on-gassing of argon. In addition, the duration of argon breathing at the stage is 4 hours. In this time frame, the argon will only be loaded to what are termed "fast and medium tissues." During

the 100% oxygen breathing 1,000 ft/min ascent to the 3.5 psia suit pressure”, the argon will be eliminated, while nitrogen continues to be off-gassed.

The overall objective of this project is to provide data on concepts necessary for the development of advanced EVA decompression schedules. This effort will accomplish two specific goals: 1. determine the optimum decompression requirements for a low-pressure EVA suit, 2. determine the DCS implications of breathing an oxygen and argon mixture during decompression prior to EVA.

METHODS

Forty (40) subjects will complete three hypobaric exposures each. Figure 1 shows the details of the three exposure profiles. Exposure A is a 5-hour preoxygenation routine for exposure to 3.5 psia. Exposure B is a 5-hour preoxygenation routine for exposure to 3.5 psia, utilizing a 7.34 psia stage. Finally, Exposure C is a 5-hour preoxygenation routine for exposure to 3.5 psia, utilizing a 7.34 psia stage with an ARGOX breathing mixture. To simulate microgravity, subjects are supine on a gurney for the entire preoxygenation following exercise, ascent, exposure to simulated altitude, and descent. All ascents are at 1,000 ft/min. Echo-imaging is accomplished at approximately 15-min intervals throughout the exposures using a Hewlett Packard SONOS 1000 Echo-Imaging System. The VGE are graded by the Spencer Scale and used as an indication of relative severity of exposure. This method also detects arterial gas emboli, since both ventricles are observed, and can allow visualization of gas emboli in other areas of the vasculature. The experiments are terminated with the completion of the 3 hour exposure to 3.5 psia or the occurrence of signs or symptoms of DCS.

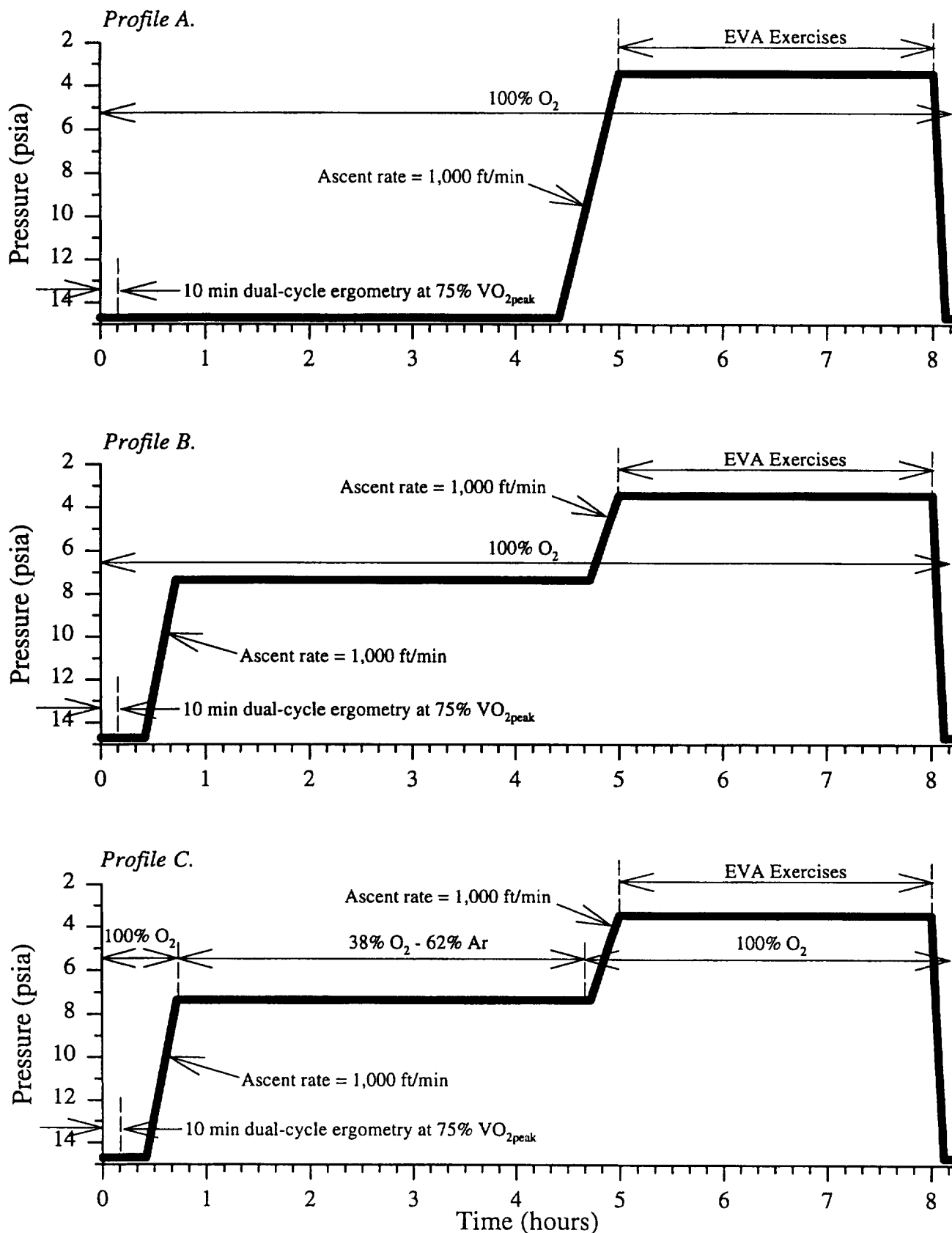
CURRENT STATUS

Partial funding (NRA 96-HEDS-04 and 96-HEDS-05) was received in July 1998 and experimental exposures of human subjects initiated the same month. The research protocol had previously been approved by the AFRL institutional review board and the USAF Surgeon General's Office. Modifications to the hypobaric chamber and exercise equipment were accomplished to allow the simulation of microgravity. Subject recruitment was initiated and 17 subject-exposures were completed in FY98. The study is on schedule, and it is expected that the 120 subject-exposures will be completed within the 3-year funding timeframe.

FUTURE PLANS

No attempt will be made in this study to define an operational preoxygenation schedule, nor to determine an operationally acceptable level of DCS risk. The data obtained from this study will provide a crucial starting point, from which future experiments can be designed to determine an operationally specific preoxygenation schedule for a 3.5 psia pressure suit using staged decompression with 100% Oxygen or ARGOX.

Figure 1. Description of experimental exposures.



BAROPHYSIOLOGY AND BIOPHYSICS

Michael R. Powell, Ph.D. Head, Environmental Physiology/Biophysics Group
NASA/Johnson Space Center, Houston, Texas 77586

INTRODUCTION

Decompression is an important aspect of extravehicular activity (EVA). Errors can result in decompression sickness (DCS) if the protective measures are too liberal, while valuable on-orbit time is dissipated in prophylactic methodologies that are excessively conservative. Nucleation is an important consideration in many natural events, and its *control* is very important in many industrial procedures. The amount of Extravehicular Activity (EVA) that will be required during the construction of the International Space Station exceeds all of the other activity combined. The requirements in astronaut time and consumables (breathing oxygen and air) will be considerable. In an attempt to mitigate these requirements, *Project ARGO* was instigated in 1990 to investigate the effects of gravitational forces on the musculoskeletal system. This work has led to the present plans for the reduction of prebreathe duration. Over the past decade, research has been directed towards an understanding of the biophysical basis of the formation and growth of the decompression gas phase with the goal of improving the efficiency of the EVA process. In the past, we have direct work towards a more complete understanding of gas bubble formation and growth and exercise-enhanced washout during oxygen prebreathe.

Theories of decompression have been based primarily on the concept originated by J. S. Haldane at the turn of the century, i.e., limited, stable supersaturation. NASA/JSC models have developed along the lines of the "Tissue Bubble Dynamics Model" devised originally by Dr. Michael Gernhardt. The original model has been revised and certain new parameters have been, or will be, inserted to allow for the changes in micronuclei prior to depress. Some primary concepts are [1.] There is not a mixture of aqueous and lipid tissues. 2. Supersaturation occurs in the tissue responsible for decompression sickness but is not the sole determinant of DCI. and 3. Several factors influence bubble growth. "Microbubble intermediates" (MBI) are performed by a mechanism involving musculoskeletal activity. The MBI appear in a size distribution described by a power law function $n = n_0 K r^{-D}$.

Critical Radii In decompression work, the failure of decompression tables has been dealt with almost solely by supersaturation control, accomplished by the tracking and control of inert gas uptake and elimination in body "compartments". As a general topic, however, nucleation and gas micronuclei has been discussed by virtually everybody in the field of hyper- and hypobaric decompression over the past several decades, but actual control of this parameter has not been thought possible. Efforts at JSC have been directed towards utilizing the concept of the critical radius R_c . The equation for the critical radius of a bubble with surface tension σ at the time of decompression for a pressure change ΔP is given by $R_c = 2\sigma / \Delta P$. The control of growth is dependent upon σ which is controlled by the biochemical composition of the cellular milieu, the temporal change of interfacial surfactants (the *Vroman effect* which is depended upon relative rates of bulk diffusion, adsorption and desorption, and convection). Many aspects of this can be studied with the oscillating bubble surfactometer.

Nucleation Of Bubbles There may exist small volumes of a gas phase ("micronuclei"), or "seed" micronuclei, in hydrophobic crevices exposed to the aqueous environment. It is commonly

observed *in vitro* (in instances not involving decompression) that gas bubbles do arise from micropores in hydrophobic materials previously exposed to the air. These surfaces lose their ability to promote bubble formation when subjected to hydrostatic pressure since, it is surmised, their nuclei collapse.

Micronuclei (that is, microbubble intermediates) may exist prior to decompression and be created by several mechanisms (*vide infra*). These nuclei would have lifetimes probably on the order of hours (and possibly a day). The most telling evidence that we have concerning the presence of these tiny gas volumes is the production of visible gas bubbles by the mechanism of isobaric gas countertransport reported by Lambertsen and Idacula in 1975. These microbubble intermediates are probably generated by "spontaneous" nucleation mechanisms.

Spontaneous Nucleation "Spontaneous" refers to the ability for a gas phase to form without the prior condition of the presence of a stable gas micronucleus. It is necessary that sufficient energy be deposited in a small volume within the liquid such that phase separation can result. In living (i.e., moving) systems, these energy density fluctuations are the result of musculoskeletal kinetic activity.

In decompression and *in vivo* phase transitions, kinetic activity has been postulated to assist in the cavity formation. Phase transformations proceed more easily when "assisted," and this is often accomplished in real, physical systems by the presence of either impurities or mechanical forces. Some form of "stress assisted", or mechanical, mechanism is postulated to be responsible for the genesis of *critical microbubble intermediates* from which arises the large decompression gas phase in tissue. While micronuclei ($100 < r < 200$ angstroms) might always be present, and probably are, we would postulate the larger microbubble intermediates ($R \approx 1$ micron) arise by one of two mechanisms: [a] They represent the short-lived entities generated *de novo* from e.g. stress assisted mechanisms. They will in a short time decay in size to again become micronuclei. [b] They are the enlargement of a subset of the population of micronuclei constantly present *in vivo* (though this concentration will vary depending on the kinetic activity level of the particular tissue. They will have a short lifetime and decay to the status of micronuclei. Several mechanisms are known that could generate these bubbles.

We can postulate that the microbubble intermediates are generated by hydrodynamic cavitation mechanisms. Microturbulence is well known in hydraulic engineering as one form. Pressure or shock waves might be produced in the lower appendages when walking. *Tribonucleation* can effect the formation of a gas phase when two surfaces separated by a fluid are brought into near contact with one another and then parted, a process also termed "tacky" or "viscous adhesion". Negative, dilatative forces capable of overcoming the tensile strength of water are generated when adjoining surfaces are separated. Dean stated that "...bubbles can always be produced by stirring or turbulent circulation of the liquid."

Most biological fluids can be classified as *viscoelastic* and behave more as an elastic body than as water. It is possible that it varies to some degree from individual to individual and would therefore play a role in the tendency to acquire decompression sickness. Viscosity would play a role in cavitation from microturbulence and tribonucleation.

Reduction of DCS Incidence Joint-pain decompression sickness ("the bends") occurs from the formation of a gas phase in connective tissue of joints. Astronauts appear to have a reduced risk of DCS following exposure to 0-g compared to other experimental subjects who have ambulated at 1-g before decompression. Continuing trends in the reported outcomes of decompression during EVA indicate that the incidence is still zero.

Astronauts have performed more than 100 manned-excursions for extravehicular activity that required significant decompression immediately preceding the activity, and not even mild DCS has apparently occurred. Possibilities for this reduction are: 1. unnoted joint pain or soreness; 2. cluster phenomenon; 3. improved gas exchange at the lungs; 4. tissue perfusion increases; 5. use of analgesics; 6. extensions to the oxygen prebreathe protocols; and 7. reduction of stress-assisted nucleation

It is known that the supersaturation limits for the production of a decompression gas phase in vitro in quiescent fluids exceeds by several orders of magnitude that for in vivo systems. Altitude decompression sickness overwhelmingly involves the lower extremities because these are the most stress by gravitation. Straining has long been known to foster certain sites for DCS formation while the absence of kinetic activity has resulted in few bubbles being produced by decompression. The reduction in the effects of stress-assisted nucleation and/or the number of tissue gas micronuclei may explain the reduction of DCS during EVA. Such reduction could result a decrease in activity (hypokinesia) in space of the lower limbs and the lack of weight-bearing loads (adynamia) on the legs.

For the past several years, evidence has been accumulating from several laboratories around the world that adynamia can substantially aid in the reduction of the duration of oxygen prebreathe prior to EVA. It has not been clear, however, how to quantify the effects.

Blood Flow Changes with Exercise Examination of decompression data by Loftin and Conkin implicates changes in blood flow as they affect decompression outcome, and the effects are profound. While it has been known for decades that blood flow is modified by exercise, in barophysiology this effect has generally *not* been ascribed to modifying the compartment half times by more than $\pm 20\%$. These flow changes have never really been incorporated into decompression algorithms, because the conditions are so varied under which any decompression table would be employed. Such variability is not present in NASA EVA operations, however. Because the conditions in space can be quite controlled, at least at the present time, NASA decompression procedures can be more specific. The variety of situations in space is currently very limited, the number of participants is limited and the depressurizations are of a very specialized type (as contrasted with tables for deep sea divers which must have a wide latitude).

It is known that a change in blood flow in muscle tissue with exercise is about ten-fold. Local blood flow and functional compartment half times can change approximately ten fold (0.04 to 0.4 l/kg-min.) while flow to bones and joints change little (0.03 to 0.06).

Blood Flow and Oxygen Consumption Oxygen consumption is a reflection of muscle activity and thus can be used to indicate the degree of local blood flow (which naturally carries oxygen to the tissues). Resting muscle has a very low blood perfusion rate, and this rises very rapidly with

but very modest amounts of physical activity (“functional hyperemia”). This rapid rise can be a very potent adjunct to the *in vivo* modification of inert gas partial pressures, especially during prebreathe when it is desired to eliminate as much dissolved inert gas as possible from tissues.

The salient point for inert gas washout with exercise in barophysiology is that the *fraction of blood flow to muscle increases considerably with the onset of even very little physical exercise*. The perfusion increases locally because a larger fraction of the cardiac output is shunted to muscle tissue (and supposedly tendon and ligament). Thus, it is not totally an effect of increased pumping action of the heart.

Half Times and Blood Flow It has been debated as to what is the actual meaning of the Haldanian halftimes. The original concept traced them to *actual, distinct tissue types* with rather narrow limits of perfusion. They could exceed their supersaturation limits and evolve gas bubbles which would be released into the blood stream. In the analytical system here, it appears that the tissue is one which has a highly variable blood flow that can vary within a factor of ten. This is similar to what has been proposed for muscle tissue. Wherever is the locus of gas bubble generation (and apparently also those tissue types related to DCI pain), it appears that a factor of ten is possible for blood flow.

It is possible to construct a relationship between the blood flow and the compartment half times through the standard Haldane perfusion equation. The blood flows, as measured in classical physiology, will produce half times that are too short in comparison to those derived from analysis of decompression data in barophysiology. (It is currently not known why this is the case.) To yield values of half times that are commensurate with experience, it is necessary to have a partition coefficient k equal to 1.96×10^3 (derived from resting blood flow = 360 minute half time). This is a very small value and does not appear to correspond to a true blood/tissue partition coefficient.

Effective Half Times Various altitude chamber tests have been performed over the past years where decompression illness rates have been modified by physical activity during oxygen prebreathe. From an analysis of the data concerning decompression illness, it is possible to determine how the body responded to the depressurization conditions. That is, the system behaves effectively as if the TR is lower. One can calculate what half time was required to reduce the inert gas loads from the initial to final state. This is designated as the “effective” half time.

Exercise and Decompression Illness Work by Henry, where weights were lifted by the arms, indicates that decompression illness in the upper limbs is proportional to the exercise level. The results were reported for different experiments in which the weights were lifted slowly, rapidly, in a jerking fashion, and simply hold a weight out in front of the subject. The incidence of DCI was related to the work load and not so much to the type of activity, at least within the confines of the experimental conditions. This needs further clarification. Similar results were found by Ferris and Engel where stair stepping exercise was used. It appears that the energy expenditure rather than the type of exercise, within limits, governs the incidence of joint pain decompression illness. The physical activity levels encountered during prebreathe are typically quite low as is seen in the figure.

Exercise, Effective Half Time and Adynamia It is possible to measure the oxygen consumption of a group of individuals and relate to the effective half-time according to the following equation $t_{1/2} = 1,741 ([O_{2\text{Consump}}] - 427.7)^{-0.5133}$. It has been shown that adynamia during the prebreathe period as well as during exposure to altitude, reduces the risk of bubble formation and DCS. An empirical relationship between TR_{ady} and TR is: $TR_{\text{ady}} = 0.7171 [TR]^{1.19}$

Future Methods of Improvement The other effects which could be employed to reduce the Tissue Ratio (increase prebreathe efficiency) could include:

1. carbon dioxide in prebreathe mixture,
2. increased exercise in final phase,
3. "scaling" of EVA participants (or creation of individual prebreathe prescriptions).

They will require considerable development before they can be placed into operational use.

AN UNDERSTANDING OF DECOMPRESSION PHYSIOLOGY LEADS TO SAFER AND MORE EFFICIENT EXTRAVEHICULAR ACTIVITY (EVA)

R.D. Vann and W.A. Gerth

F.G. Hall Hypo/Hyperbaric Center and Department of Anesthesiology, Box 3823, Duke University Medical Center, Durham, NC 27710

INTRODUCTION

Extravehicular activity (EVA) in the U.S. space program requires decompression from a sea level cabin pressure to an oxygen-filled space suit with a pressure equivalent to an altitude of 30,000 feet. Immediate decompression to this altitude would result in incapacitating or fatal DCS from the formation of nitrogen bubbles in blood and tissue. To avoid this problem, astronauts breathe oxygen at sea level or remain at an intermediate decompression stage of 10,000 feet to eliminate dissolved tissue nitrogen prior to further decompression for EVA. In ground-based EVA simulations, the DCS incidence has been 20-30% pain and 2-3% chokes or cerebral symptoms. This is despite breathing oxygen at sea level for 3.5-4 hours or remaining at 10,000 feet for 12 hours. Results from mathematical simulations of decompression are in agreement with these tests and indicate that a 12-hour decompression stage at 10.2 psia is inadequate to avoid significant DCS risk. DCS has not been reported during actual Shuttle EVAs, on the other hand, but these operations generally stayed at 10,000 feet for longer than one day (mean 37.8 hrs in 59 EVAs from Shuttle through February 1996). Such procedures are too long for construction of the International Space Station (ISS) where fast and frequent EVA will be required. A solution to this practical problem was found as a direct result of studies that addressed the fundamental mechanisms of decompression sickness.

INVESTIGATIONS OF DECOMPRESSION PHYSIOLOGY

METHODS

Our initial studies investigated the effects of environmental and physiological conditions on DCS risk and precordial Doppler bubbles. We measured respiratory nitrogen elimination during 2.5 or 3.5 hours of preflight oxygen breathing and monitored subjects for Doppler bubbles after ascent to 30,000 feet. The subjects remained at altitude for four hours or until developing DCS. We investigated the following prebreathe conditions: body position (seated, supine, head-down tilt), exercise, pharmacological vasodilation, and thermoneutral water immersion. We also studied weightlifting before prebreathing and micro-gravity simulation while at altitude.

RESULTS

DCS occurred in one third of 213 studies. Analysis indicated that prebreathe exercise, prebreathe duration, and immersion during prebreathe significantly enhanced respiratory nitrogen elimination and reduced the incidence of DCS and precordial bubbles. High body weight and terrestrial gravity, on the other hand, increased DCS risk suggesting DCS risk might be inherently lower in micro-gravity than on earth.

DEVELOPMENT OF AN ISS PREBREATHE REDUCTION PROTOCOL

METHODS

Brooks Air Force Base found independent support for the beneficial effect of prebreathe exercise while Johnson Space Center found independent support for the detrimental effect of gravity. The

separate and corroborating results of three institutions suggested that a reduced prebreathe protocol might be feasible for rapid EVA during construction of the International Space Station based on the concepts:

- (a) removing gravitational stresses from the legs ("adynamia" or microgravity simulation) decreases the incidence of DCS and Doppler-detected bubbles; and
- (b) exercise during prebreathe accelerates nitrogen elimination and reduces DCS risk.

Accordingly, a pre-EVA protocol with a 2.5-hour duration was targeted by Johnson Space Center as optimal for ISS construction. Micro-gravity was simulated by maintaining subjects in a semi-recumbent position beginning at 100 min before oxygen breathing and extending to the end of the study. The challenge was to find a pattern of prebreathe exercise for which the DCS incidence would be acceptably low. A new EVA exercise simulation developed at Johnson Space Center was used to more accurately reflect the work performed during actual EVAs. Various 2.5-hour prebreathe protocols were tested in a multi-center trial at Duke University Medical Center, Hermann Hospital, and the Canadian Space Agency.

RESULTS

Three different 2.5-hr prebreathe protocols were tested.

Phase I. Ten minutes of exercise at 75% maximum oxygen consumption was performed at the beginning of prebreathe. Forty-nine trials were conducted with an 18% DCS incidence.

Phase II. Ten minutes of exercise at 75% maximum oxygen consumption was performed at the beginning of prebreathe with 40 minutes of light exercise added shortly before ascent to 30,000 feet to simulate the activity of pre-EVA preparation. Fifty trials were conducted without incident. The statistical uncertainty of the Phase II protocol (an upper 95% binomial confidence limit of 5.8%) was sufficiently low to recommend it for operational use during ISS construction.

Phase III. The only prebreathe activity in Phase III was 40 minutes of light exercise shortly before ascent. There was a 20% DCS incidence in 10 trials. The second of these incidents involved serious neurological symptoms that resolved completely with hyperbaric oxygen therapy. A subsequent echocardiograph with micro-bubble contrast injection found that this subject had a patent foramen ovale at rest.

CONCLUSION

A 2.5-hr prebreathe protocol suitable for operational use has been successfully developed, but important questions remain concerning both the physiology of decompression sickness and the practical applications of this physiology to operational procedures. We do not fully understand how exercise duration, placement, and severity affect nitrogen elimination and DCS risk. In addition, Johnson Space Center has demonstrated that severe exercise can precipitate bubble formation suggesting that exercise may also increase DCS risk. An understanding of these effects is needed to address the ultimate operational goal of a 1-hr prebreathe procedure.

The serious incident of Phase III is unprecedented in its severity in nearly 4,000 altitude exposures over the past 20 years. Many of these exposures were more extreme than the Phase III protocol. It seems less likely that the protocol was of high risk than that the subject was highly susceptible. Additional Phase III tests are needed to resolve this issue as well as to define the effects of prebreathe exercise.

Decompression sickness (DCS) is not a mishap but an expected event of low probability whether in diving, compressed air work, aviation, or space. Fortunately, the likelihood that DCS will be serious is small during hypobaric exposure, unlike hyperbaric exposure where neurological DCS is common.

Behavior, Performance, and Human Factors I (Behavior and Performance)

Chair

Nick Kanas, M.D.

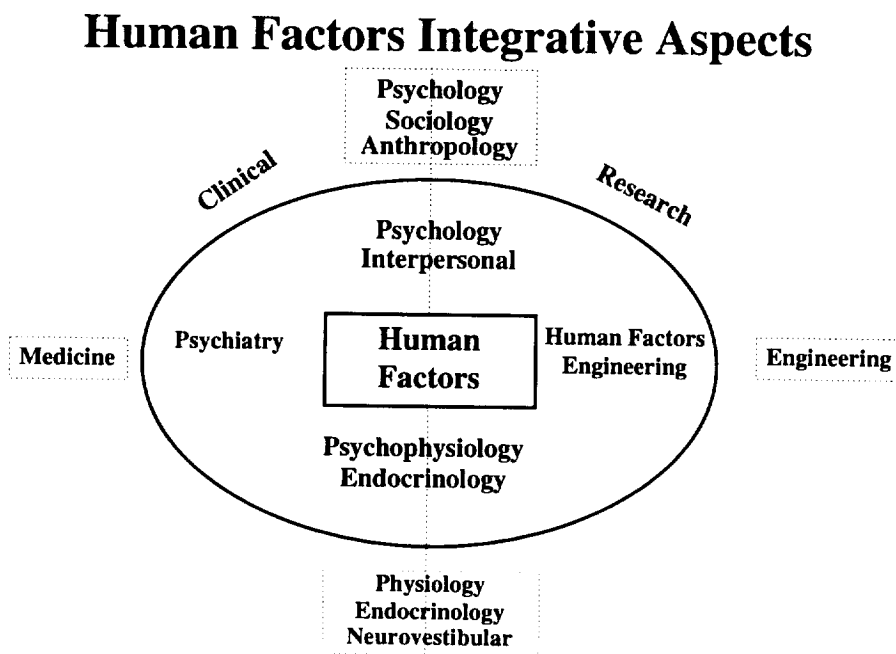
Co-Chair

Barbara Woolford

BEHAVIOR, PERFORMANCE, AND HUMAN FACTORS SESSIONS SUMMARY

Scope of the field

Human factors is a broad area that encompasses a number of specialized fields that work together to enhance space crew health, safety, and performance. As the Figure below shows, four major areas comprise human factors. The first is psychology and interpersonal relationships. This area includes cognitive psychology, personal growth resulting from meaningful work and leisure time activities, group dynamics, gender and cultural factors, and issues involving crewmember screening and selection. The second area is psychiatry. Examples include abnormal stress responses affecting astronauts and cosmonauts in space, asthenia, effects of psychotropic medications, and counseling/psychotherapy. The third area is human factors engineering, or ergonomics. Examples include tool development, human-automation interaction, human-machine interfaces, and virtual reality. The fourth area is psychophysiology and endocrinology. This includes sleep and circadian rhythms, hormonal effects, autonomic monitoring and training, physiological effects of drugs, and food and nutrition.



As the Figure illustrates, major components of human factors interface in both clinical and research areas. For example, psychology has obvious research ramifications but also merges with psychiatry in clinical areas affecting crewmembers. Also, these four human factor areas interface with broader scientific and technological fields: psychology and interpersonal relationships with academic psychology, sociology, and anthropology; psychiatry with medicine; human factors engineering with the broad area of engineering; and psychophysiology and endocrinology with academic physiology, endocrinology, and neurovestibular sciences.

Because of the wide scope that defines human factors, it is difficult to isolate specific questions or problems and to focus available resources on these issues. Each of the four major areas described above has several concerns related to it, which have important behavioral, performance, and research implications. In fact, one could argue that each of the four human factors divisions is equivalent to other scientific areas presented in this Workshop, such as bone or cardiovascular. On the other hand, the four human factors areas are closely integrated, as indicated in the Figure, and it makes sense to keep these four divisions interrelated under the broad field of human factors. Perhaps the most reasonable approach is to consider each of the four human factors areas as separate for research funding and resource allocation purposes, while at the same time acknowledging their integration as being important operationally to overall human behavior, performance, and well-being in space.

Overview of the Behavior, Performance, and Human Factors Scientific Session

Keeping in mind the above divisions, a number of interesting papers were presented during this session. In the area of psychology and interpersonal relationships, issues were discussed concerning: measuring performance with a computerized battery of cognitive and psychomotor tasks (**Brady et al.**); using the Performance Assessment Workstation (PAWS) to evaluate cognitive performance in a bedrest study (**Shehab et al.**) and in space (**Eddy et al.**); studying crew and ground control group tension, cohesion, and leadership roles during Shuttle/Mir missions (**Kanas et al.**); and studying psychological and interpersonal issues in polar space analog environments using psychometric tests (**Palinkas et al.**), diary content analysis (**Stuster et al.**), and computerized questionnaires (**Wood et al.**).

No papers were presented in the field of psychiatry. It is recognized that this certainly is an area for future research, particularly concerning stress and asthenic reactions, psychotropic medication effects, and counseling and psychotherapy.

In the area of human factors engineering (ergonomics), papers were presented related to: the development of a computer-based battery of tasks to evaluate cognitive performance on the PAWS (**Schlegel et al.**); measuring and analyzing mission control room communication modes for complex situations (**Caldwell**); identifying salient features in information presentation for remote training (**Woolford et al.**); and identifying and evaluating critical design features of workstations and restraints as a function of task type and duration, and crew anthropometry (**Chmielewski et al.**, presented by Whitmore). Additional papers were related to the development of: instrumentation and models of crew kinetics in order to provide information on performance in microgravity (**Newman et al.**); new techniques for tracking complex 3D motions of humans and changes in body contours (**Metaxas**); and models of EVA suit effects on strength, reach, and fatigue (**Maida**).

Many of the psychophysiology and endocrinology papers related to circadian rhythms and sleep were presented in a separate scientific session that is reported elsewhere in the Proceedings. In our session, there were papers related to: enhancing physiological state and task performance through Autogenic Feedback Training Exercise™ (**Cowings et al.**); measuring the effect of promethazine on performance using a simulated Shuttle landing test (**Harm et al.**); and developing and validating EEG measures of sustained focused attention to assess cognitive load

from environmental stressors (**Gevins et al.**). It is noted that there is a need to coordinate papers presented in our session with sleep and circadian rhythm presentations in future conferences so that we all can benefit from each other's work.

Implications for Future Research

A number of issues came up that have ramifications for future research in human factors. There is a need to integrate research proposals across disciplines to prevent duplication and to allow researchers to understand and interface with each other. Opportunities for interacting with outside groups and international partners need to be provided. Finally, human factors research should be aimed at operational relevance, such as the development and evaluation of various countermeasures to assure optimal behavior and performance in the space environment

In terms of countermeasures, the state of human factors research allows us currently to identify and study important risk factors and to use existing knowledge and tools to evaluate countermeasure effectiveness in a number of important areas. The ultimate goal is to enhance crew health, safety, and operational efficiency. The optimal performance of mission control personnel responsible for space missions also needs to be assessed. Countermeasures should be used and evaluated in both space and in ground simulation environments. Examples of possible studies include the following: 1) Assessment of the impact of countermeasures (both human factors-related and those related to other scientific disciplines) on general operational cognitive and psychomotor performance status; 2) Assessment of the effectiveness of crew training modules that focus on group dynamics and interpersonal coping strategies on subsequent behavior and performance; 3) Assessment of biomechanical and visual performance models in different space analog environments; and 4) Assessment of preflight and inflight Autogenic Feedback Training Exercise™ to facilitate adaptation. Although these four examples address important countermeasure issues, the list is not meant to be exhaustive but to illustrate the breadth of work that needs to be done in the human factors area.

Nick Kanas and Barbara Woolford

STABILITY AND PRECISION OF PERFORMANCE DURING SPACE FLIGHT

J.V.Brady¹, T.H. Kelly², and R.D. Hienz¹

¹Johns Hopkins University School of Medicine, ²University of Kentucky

INTRODUCTION

The success of long-term spaceflights with humans depends critically upon the development of a technology that can effectively manage the imposing behavioral and social complexities inherent in such undertakings. Development of an ecosystem to accomplish these objectives will proceed most effectively with an experimentally-derived database focused upon the prediction and functional management of the behavior of individuals. Of primary importance is the development of a means for behavioral support during prolonged exposure to confined micro-society environments such as those associated with long-term space travel. Investigations of the performance of small groups over the past two decades have convincingly demonstrated that the consequences of any single individual's behavior is a critical determinant of both individual and group behavior under conditions of prolonged social and cultural isolation.

In the course of ground-based laboratory studies, computerized procedures were developed for engendering and maintaining stable measures of a range of complex human behaviors, including cognitive and psychomotor performances, under conditions that require only minimum training. In studies involving continuous performance monitoring, human participants have been shown to work productively and energetically with this computerized task battery over extended time intervals. The stability and sensitivity of the measures generated have made it possible to assess both decrements in and enhancements of performances that are affected by meal macronutrient content, sleep deprivation, medications, and stressful conditions. The demonstrated sensitivity and utility of these procedures for long-term repetitive assessment of the stability and precision of multiple human behavior dimensions provided the basis for their application to an evaluation of crewmember performance during a space flight mission.

METHODS

Four crewmembers (3 males and 1 female) of Space Shuttle Mission STS 89 participated in the study. The computerized task battery was administered to each crewmember in the course of multiple daily sessions during the Pre-, In-, and Postflight phases of the study on a Macintosh 170 Powerbook Computer with attached Kensington Keypad. The performance battery required approximately 20 minutes to complete and consisted of the following components:

1. A 72 item research version of the Profile of Mood States (POMS) requiring a 1 ("not at all") to 5 ("extremely") keypad rating of adjectives associated with 8 empirically derived "mood" scales.
2. An 11 item Visual Analogue Scale (VAS) requiring use of the computer tracking ball to move an indicator to a place on the line between the labels "not at all" on the left and "extremely" on the right in response to words on the computer display screen representing the crewmember's "feeling" at the time of presentation.

3. A Time Estimation Task (timing measure) requiring that repeated presses on the keypad be spaced by a fixed time interval to advance a point counter and an increasing monitoring gauge on the computer display screen.
4. A Repeated Acquisition Task (learning measure) requiring that the crewmember learn to press four designated keys on the keypad to complete a 10 response sequence. Feedback for correct and incorrect responses is provided on the computer display screen. A new order for pressing the four designated keys must be learned each time the task is presented. Across sessions, the efficiency with which these sequences are learned remains stable in the absence of any conditions that affect learning ability.
5. A Number Recognition Task (memory measure) requiring the crewmember to hold down two keys simultaneously on the key pad, one of which has been designated a "yes" key and the other a "no" key. An array of numbers presented on the computer display screen disappears after a brief exposure and a single test number appears. If the test number had been presented in the previous array, the finger is lifted from the "yes" key and if not, the "no" key finger is lifted.
6. A Digit Symbol Substitution Task (psychomotor performance measure) requiring presses on a 3x3 keypad pattern corresponding to the location of the filled squares in signaled boxes in 3x3 patterns of boxes which appear on the computer display screen. The location of the filled squares and the 3x3 signaled boxes on the computer display screen are changed frequently to prevent memorization of the patterns.

A Daily Log was also completed in association with performances on the computerized task battery during the Preflight, Inflight, and Postflight phases of the study to provide information from participating crewmembers on sleep, diet, exercise, and medication usage. In addition, Debriefing Reports were obtained during postflight interviews conducted with each crewmember individually.

Following completion of initial training and practice on the computerized task battery, performance data were collected from each crewmember during three study phases, including (1) Preflight, (2) Inflight, and (3) Postflight. Performances were recorded on separate individualized computer diskettes for each participating crewmember. The time and duration of each human performance data take was recorded on the individualized diskette along with rating scale responses and the number of correct and incorrect responses to each of the programmed tasks. The number of performance data take sessions during each phase of the study varied somewhat between crewmembers but each had 6 or more training sessions followed by 5 or more Preflight baseline sessions, 5 or more Inflight sessions, and 6 or more Postflight sessions.

RESULTS

All four crewmembers learned the computerized task battery without difficulty and maintained stable levels of performance during the Preflight Baseline Data Collection phase of the study. Results obtained with the self-report "mood" (POMS) and "feelings" (VAS) scales reliably reflected changes in selected items as a function of study phase. For example, on measures of "fatigue" from both the POMS and the VAS, increased ratings obtained Inflight (relative to

Preflight baselines) were significantly decreased during Postflight performance sessions. Data obtained from individual crewmembers on the POMS and VAS self-report tasks also showed consistency in the relationship between scale items reflecting progressive changes during the Inflight phase of the study.

The timing performances for all four crewmembers as measured by the Time Estimation Task remained stable and accurate throughout the study with no evident perturbations during either the Preflight, Inflight, or Postflight phases. Learning performances as measured by the Repeated Acquisition Task were also found to hold up well throughout the study with no identifiable changes related to the Preflight, Inflight, or Postflight phases. Within-session acquisition of the correct 10-response sequence was rapid for all four crewmembers, and there was evidence of an increase in efficiency of the learning performance across the Preflight, Inflight, and Postflight phases of the study.

The results obtained with the Number Recognition Task measure of short-term memory performance were consistent with the outcome of preliminary studies showing differences in information processing response times associated with determining whether the matching stimulus number was ("yes") or was not ("no") in the sample display on the one hand, and whether the number of digits in the sample display was large (4 to 6) or small (1 to 3). In addition, however, there were evident increases in the response times recorded during the Inflight phase of the study and there was a significant three-way interaction between the "yes"/"no" response times, the number of digits in the sample display array, and the phase of the study. There was a selective and significant ($p < .01$) increase in "no"-trials reaction times with sample display arrays of 4-6 digits Inflight compared to the performances during the Preflight and Postflight phases of the study.

Psychomotor performances as measured by the Digit Symbol Substitution Task showed selective Inflight changes in the context of a general increase in performance effectiveness over the entire Preflight through Postflight course of the study. While modest performance rate increases were apparent between Preflight and Postflight testing phases, significant decreases in performance rates were observed during Inflight testing sessions.

Preliminary examination of the Daily Logsheets and the Debriefing Reports has been undertaken to identify factors of potential relevance to the outcome of the study.

CONCLUSION

The results of this study show clearly that the stability and precision of human performance during spaceflight can be reliably and sensitively assessed with a computerized battery of cognitive and psychomotor tasks requiring only minimal training. Although the research findings identified significant changes in the performances of crewmembers during the Inflight phase of the study, no mission-impairing decrements were apparent. The nature of the changes during the Inflight phase of the study however, do suggest that some elements of performance are sensitive to microgravity environments. There is evident need for additional research to further delineate the nature of these effects, and to assess the potential value of such measures as an index of other mission-critical dimensions of behavior over more extended space flight intervals.

MONITORING AND CORRECTING AUTONOMIC FUNCTION ABOARD MIR: NASA TECHNOLOGY USED IN SPACE AND ON EARTH TO FACILITATE ADAPTATION

P. Cowings¹, W. Toscano², B. Taylor³, C. DeRoshia¹, L. Kornilova⁴, I. Koslovskaya⁴ and N. Miller⁵

¹ Space Life Sciences Division, NASA Ames Research Center, Moffett Field, California 94035;

²Department of Psychiatry, University of California at Los Angeles; ³Department of Biomedical Engineering, University of Akron, Ohio; ⁴Institute for Biomedical problem, Moscow;

⁵Department of Psychology, Yale University.

INTRODUCTION

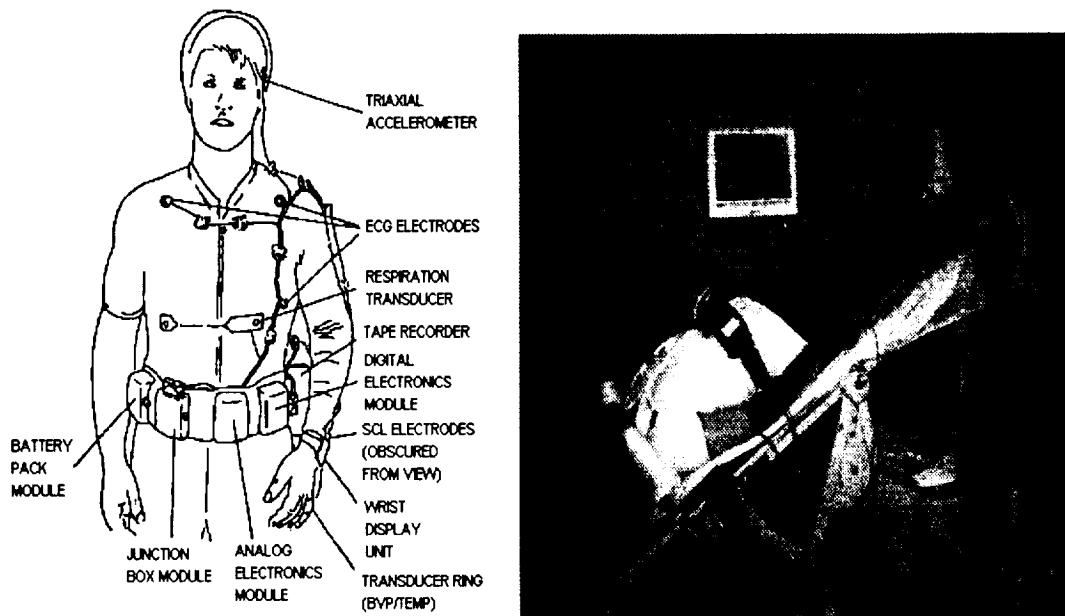
The broad objective of the research was to study individual characteristics of human adaptation to long duration spaceflight and possibilities of their correction using autonomic conditioning. The changes in autonomic state during adaptation to microgravity can have profound effects on the operational efficiency of crewmembers and may result in debilitating biomedical symptoms. Ground-based and inflight experiment results showed that certain responses of autonomic nervous system were correlated with, or consistently preceded, reports of performance decrements or the symptoms. Autogenic-Feedback-Training Exercise (AFTE) is a physiological conditioning method that has been used to train people to voluntary control several of their own physiological responses. The specific objectives were: 1) To study human autonomic nervous system (ANS) responses to sustained exposure to microgravity; 2) To study human behavior/performance changes related to physiology; 3) To evaluate the effectiveness of preflight autonomic conditioning (AFTE) for facilitating adaptation to space and readaptation to Earth; and 4) To archive these data for the NASA Life Sciences Data Archive and thereby make this information available to the international scientific community.

METHODS

Overview. Four cosmonauts (men, ages 43-47) participated in this study. Preflight training was performed at Star City, Russia prior to the MIR missions 23 and 25. Preflight baseline data were collected (tilt-table) and training in autonomic control administered within 4 months prior to launch. Inflight, eight data collection days were distributed throughout the 6-month missions. Inflight crew activities included: 8-hour ambulatory monitoring, and performing computer-based performance task batteries, mood assessment and symptom diagnostic scales three times per day on test days. Flight data were returned to the investigators post-flight.

Apparatus. The Autogenic Feedback System-2 (AFS-2) is a self-contained ambulatory monitoring system designed to monitor human physiological responses. The system includes a garment, transducers, signal-conditioning amplifiers, a microcontroller, a wrist-worn feedback display and a cassette tape recorder. This system was developed and tested on astronauts during a space shuttle mission in 1992. Data collected with the AFS-2 was used to evaluate physiological responses to microgravity during the mission. This technology is also currently in use by the U.S. Army for evaluating environmental effects of motion within command and control vehicles on soldier performance and by physicians at the University of Tennessee for diagnoses of nausea and syncope incidents in patient populations (see Figure 1).

Figure 1. AFS-2: Drawing, and as worn by a cosmonaut during preflight tests



The physiological parameters currently monitored with this system include: (1) electrocardiography ; (2) respiration rate; (3) finger pulse volume; (4) skin temperature; (5) skin conductance level; and (6) triaxial accelerometer to measure head and upper-body movements.

Autogenic Clinical Laboratory System (ACLS). During preflight training and post flight tests, physiological signals are collected and displayed using a Pentium computer with custom display and acquisition software referred to as the Autogenic Clinical Laboratory System (ACLS). The system provides real-time acquisition and display of 16 input variables, 20 digitally-displayed output variables and printed averages, plus coupled audible tones, voice commands and respiratory pacing signals. The system contains an analog to digital converter (A/D) and a video controller, which allows four monitors, two for the operator’s console and two for subject displays.

Autogenic-Feedback Training Exercise (AFTE). Each subject received 6 hours of AFTE, which is administered in twelve 30-min sessions. Following a 6-min pretest baseline, each 30 min. session was divided into ten 3-min. trials during which subjects were instructed to alternately increase and decrease their response levels (e.g., heart rate accelerations and decelerations, peripheral vasodilatation and constriction, etc.). There was a 6-min resting baseline following each session (total 42 min). The purpose of the training sessions was to provide subjects with the ability to recognize bodily sensations associated with both increases and decreases in their physiological response levels and with practice to improve their skill in controlling these responses. Subjects eventually learn to maintain their physiological response levels at or near their own resting baseline levels and improve their tolerance to environmental stressors (e.g., tilt-table, conditions of microgravity, etc.).

Performance Task Batteries, Symptom and Mood/Alertness Scales were administered using a PC system. Crewmembers received training in the use of these assessment tools on the same days as preflight AFTE. The performance battery included tests of reaction time, manual

dexterity and spatial transformation. A computer program was used by subjects to rate their own symptoms using a standardized symptom diagnostic scoring procedure. Mood was assessed using a visual analog scale in which crewmembers self-reported their levels of "ease of concentration", motivation, and emotional state.

RESULTS

Crewmembers (prime and alternate) for the first mission participated in only 3.5 to 4 hours of training. Only one crewmember showed significant control of autonomic responses. This crewmember was given an additional 4 hours of training prior to the second mission (one year interval) and his performance continued to improve (see figure 2). Based on preflight learning rate and retention, it was predicted that AFTE effects would be most beneficial for this subject.

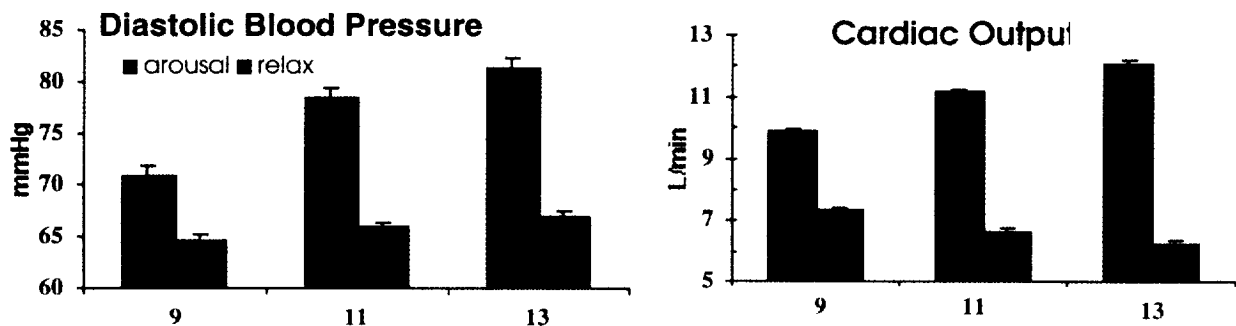


Figure 2: Average diastolic blood pressure and cardiac output levels during AFTE sessions 9, 11, and 13 (year two) for one cosmonaut during preflight training.

A total of 110 hours of data were obtained from flight. The crewmember whose preflight data are shown in figure 2, showed similar control of physiological responses during flight. This crewmember reported no space motion sickness and showed significant resistance to post-flight orthostatic intolerance.

CONCLUSIONS

Flight data are currently being analyzed and will be discussed in the final report. These data will be made available for access from the NASA Life Sciences Archive. The objectives of this study were successfully met. The use of three converging indicators: physiological responses, self-rated symptom reports, and task performance was an effective means of evaluating the incidence of space motion sickness and the impact of sustained exposure to microgravity on overall crew operational capacity. AFTE may be a valuable supplement to crew training/exercise protocols.

COGNITIVE PERFORMANCE IN SEVEN SHUTTLE ASTRONAUTS

D. R. Eddy¹, S. G. Schiflett², R. E. Schlegel³, and R. L. Shehab³

¹NTI, Inc., PO Box 35482, Brooks AFB, Texas 78235, ²Principal Investigator, AFRL/HEAS, Brooks AFB, ³School of Industrial Engineering, University of Oklahoma

INTRODUCTION

The impact of microgravity and other stressors on cognitive performance need to be quantified before long duration space flights are planned or attempted since countermeasures may be required. Two cooperative USAF/NASA experiments were flown aboard Space Shuttle Columbia to investigate cognitive performance in space. One was a part of the payload for the Second International Microgravity Laboratory (IML-2) in July 1994 (STS-65) and the other was aboard the Life and Microgravity Spacelab (LMS) in June 1996 (STS-78). Cognitive performance tests were selected from the DOD Unified Tri-Service Cognitive Performance Assessment Battery (UTC-PAB) to assess the types of skills required of astronauts working on space-based tasks. A Performance Assessment Workstation (PAWS) was developed and validated for space flight to present the tasks and collect the cognitive performance data. The tests measured working memory, spatial processing, directed attention, tracking, and dual task timesharing.

The PAWS battery included the following tests: a Mood Scale, Unstable Tracking, Spatial Matrix Rotation, Sternberg Memory Search, Continuous Recognition Memory, Directed Attention--Manikin and Mathematical Processing, Dual Task, and a Fatigue Scale. Complete descriptions of the tests can be found in Schlegel, Shehab, Gilliland, Eddy and Schiflett (1995).

METHODS

The IML-2 experiment studied the interactive effects of microgravity and fatigue on cognitive functioning of three male astronauts for 13 days on a dual-shift mission. Referenced to earth time, two subjects were on the day shift, one was on the night shift. All three astronauts completed 40, 20-minute sessions of PAWS containing 6 cognitive performance tests and 2 subjective scales (fatigue and mood) on a laptop computer. Twenty-four sessions were preflight, 13 sessions were in-orbit, and 3 sessions were postflight. On the single-shift, LMS mission, four male astronauts completed 38 sessions of the same PAWS test battery on a laptop computer. Twenty-four sessions were preflight, 9 sessions were in-orbit, and 4 sessions were postflight.

The IML-2 subjects were tested once every day in-orbit; the LMS subjects were tested approximately every other day. With continued practice, performance tends to improve with each testing session causing the data from each flight to be differentially affected by learning. To counter this potential problem, mathematical models of learning were fit to each subject's preflight data for each of 14 dependent variables (Eddy, Schiflett, Schlegel and Shehab, 1998). Assuming continued improvement, expected values were generated from the models and were subtracted from the actual performance data. The difference scores were then averaged across blocks of days (Periods) so that the data from the two flights could be pooled. The average difference scores were then used in comparing in-orbit conditions with pre- and postflight conditions.

RESULTS

Analysis of Variance of the Mood and Fatigue Scales revealed no significant effects among the periods. Using Dunnett's statistic, two tests showed significant ($p < 0.05$) performance degradation between baseline (BL) and the first block of flight days (F1) with the six, day-shift subjects. Figure 1 shows a plot of the Directed Attention—Manikin correct reaction time (RT), $F(11,51) = 2.64$, $p = .01$, and Figure 2 shows the Dual Task control losses (CL), $F(11,51) = 2.25$, $p = .03$. The Unstable Tracking showed overall significance, but no Period was significantly different than BL. In each figure, the asterisked point shows performance on the first session in-orbit was degraded compared to preflight baseline values. Figure 2 further shows that for the one night shift subject tested, performance was degraded throughout several testing sessions during the flight on the Dual Task. Performance for over half of the other tests showed a similar trend.

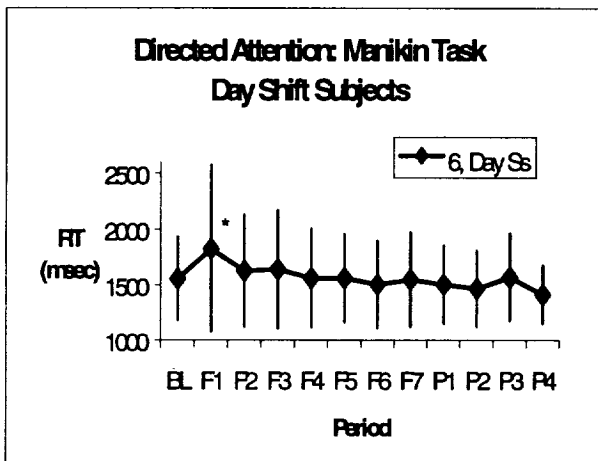


Figure 1. The average correct reaction time for six subjects on the Manikin portion of the Directed Attention test is plotted across blocks of days. BL is an average of the last four preflight sessions, F1, F2, etc. are blocks of flight days, and P1, P2, etc. are postflight days. F1 was significantly different than BL. Error bars represent one standard deviation.

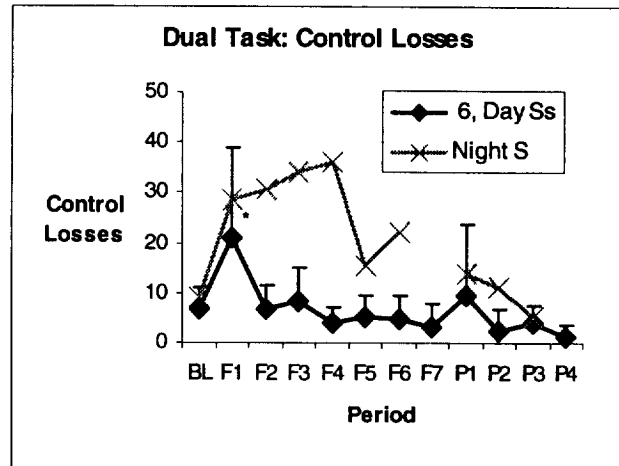


Figure 2. The average number of tracking control losses for six subjects on the Tracking portion of the Dual Task is plotted across blocks of days. All labels and error bars are the same as Figure 1. F1 was significantly different than BL. Data for the single, night-shift subject are shown with the X symbol. The IML-2 mission ended prior to F7.

The factors causing the deterioration in the six, day-shift subjects can not be determined without appropriate ground-based control groups. With only one night shift subject on can not conclude that the circadian rhythm was disrupted by the shifting work/rest schedule of the night shift.

CONCLUSIONS

1. Cognitive performance is degraded when measured after launch across two of six cognitive performance tests (Directed Attention and Dual Task).
2. Astronauts quickly adapted to the microgravity environment and performed within the limits of learning model predictions.
3. Night shift astronauts may be more degraded than their day shift counterparts. Performance is degraded across many more cognitive skills and appears to be more severe compared with astronauts on the day shift. However, this conclusion is based on only one subject.
4. Without appropriate ground control groups these cognitive performance decrements can not be associated with a single in-orbit stressor.

REFERENCES

- Eddy, D. R., Schiflett, S. G., Schlegel, R.E., and Shehab, R.L. (1998). Cognitive performance aboard the life and microgravity spacelab, *Acta Astronautica*, 43, pp. 193-210.
- Schlegel, R.E., and Shehab, R.L., Gilliland, K., Eddy, D. R., Schiflett, S. G. (1995). *Microgravity effects on cognitive performance measures: Practice schedules to acquire and maintain performance stability*, ALJCF-TR-94-0040, Brooks AFB, TX.

EFFECTS OF PROMETHAZINE ON PERFORMANCE DURING SIMULATED SHUTTLE LANDINGS

D.L. Harm¹, L. Putcha¹, B. K. Sekula², K. L. Berens³

¹NASA Johnson Space Center, Houston, TX 77058, ²Enterprise Advisory Services Inc., Houston, TX 77058, ³Wyle Laboratories, Houston, TX 77058

INTRODUCTION

Promethazine (PMZ) is the antimotion sickness drug of choice in the U.S. Space Shuttle program; however, virtually nothing is known about the bioavailability and performance effects of this drug in the microgravity environment. PMZ has detrimental side effects on human performance on Earth that could affect Shuttle operations. In a recent ground-based study we examined: 1) the effects of promethazine (PMZ) on Shuttle landing performance using the portable inflight landing operations trainer (PILOT), and 2) saliva and urine samples to determine the pharmacokinetics of PMZ. The PILOT performance data is presented here.

METHODS

Nine subjects participated in the study (6 commercial pilots and 3 Shuttle landing simulator trainers). The study was a double-blind crossover design where each subject received PMZ 50 mg IM in one session and Placebo IM in the other session; the drug/placebo order was counterbalanced across subjects. Subjects completed 4 training sessions (6-7 landings in each session) to achieve stable performance before drug/placebo sessions began. Six landings were performed, and saliva samples were collected, before and at 1,2,4,8,24,32 and 48 hours after drug/placebo administration (all urine was collected from the first morning void to the 48 hr period; one additional saliva sample was collected at 36 hrs.). For all sessions, the PILOT was configured for completely nominal conditions (i.e., no crosswinds, and daytime landing at KSC), and subjects performed the landing task in a quiet room to minimize distractions.

RESULTS

There are a number of parameters that can be analyzed to measure performance on the PILOT at specific times during the approach and landing. In addition, the system provides a composite score (the JNM score) at the end of each landing. We found no significant effect of PMZ on the JNM composite score and no significant correlation between the JNM score and the Stanford Sleepiness Scale. However, there were a number of points during the approach and landing where pitch and roll errors were significantly larger following PMZ compared to Placebo-saline (at 2-4 after drug administration). Unfortunately, due to hardware problems, approximately 50% of the individual parameter data were lost and unavailable for repeated measures analyses. Nonetheless, despite the loss of a large portion of this data differences between PMZ and Placebo in X and Y runway position approached significance.

CONCLUSION

Overall, the data support the conclusion that PMZ affects landing performance. Moreover, it is important to note that the participants were all highly skilled at approach and landing tasks and that the conditions were all nominal. Under these conditions, it is expected that much higher doses of medications or alcohol are required to significantly disrupt performance. This leads us to suggest that PMZ (50mg IM) would be expected to produce greater disruption of task

performance if the individual is not over-trained in the task, or if task performance occurs under off-nominal conditions. We plan to test the hypothesis that PMZ will produce greater decrements in performance under off-nominal conditions than under nominal conditions in a future investigation. In addition, we expect to perform the ground-based study, described above, during space flight on a mission late in 1999.

INTERACTIONS OF CREWMEMBERS AND MISSION CONTROL PERSONNEL DURING SHUTTLE/MIR MISSIONS

N. Kanas¹, V. Salnitskiy², E. Grund¹, V. Gushin², O. Kozerenko², C. Marmar¹, A. Sled¹, and D. Weiss¹

¹University of California and V.A. Medical Center, San Francisco, CA, USA; ²Institute for Biomedical Problems, Moscow, Russia

INTRODUCTION

Reports from space and space analog studies on Earth have suggested that interpersonal issues play an important role in how crewmembers relate with one another and with people on the ground during long-duration space missions. These sources, along with our previous work (i.e., a questionnaire study of 54 astronauts and cosmonauts who had flown in space; an investigation of psychosocial factors affecting a three-man crew confined for 135 days in the Mir space station simulator in Moscow), have suggested that crew tension, cohesion, and leadership role are important issues warranting further study in the space environment. We also found evidence to support a biphasic model where psychosocial issues are manifested differently in the 2nd half versus the 1st half of a typical mission involving people secluded together for a long period of time. It is important to study such issues, since interpersonal problems can lead to decreased morale and compatibility, withdrawal and territorial behavior, scapegoating and subgrouping, and disruptive crew-ground communication. This paper will present findings from a four-year NASA-funded study that examined how tension, cohesion, and leadership role affect space crews and members of mission control on Earth and how these factors change over time.

METHODS

After signing informed consent, astronauts, cosmonauts, and U.S. and Russian ground support personnel stationed in Russia who were assigned to participate in Shuttle/Mir missions were trained to complete a questionnaire that included items from the Profile of Mood States (POMS), the Group Environment Scale (GES), the Work Environment Scale (WES), a coping measure, and a critical incident log. These measures were intended to characterize the interpersonal environment on the Mir and in mission control in Russia, and they included subscales that assessed group tension, cohesion, and leadership role. The questionnaire was completed each week on Wednesdays by all subjects four times before the mission began, every week during the mission, and two times after the mission ended. Subjects in space used a computerized questionnaire; their encrypted responses were saved on disk and returned to Earth during space shuttle missions. Subjects on the ground filled out a hard-copy questionnaire; their responses were mailed along with the disks from space to the Principal Investigator in San Francisco.

RESULTS

The data collection phase of this study ended in August 1998. Five U.S. and four Russian space crews and their ground support personnel were studied during Shuttle/Mir missions that took place from 1994 to 1998. The number of subjects who participated included 6 astronauts, 11 cosmonauts, and 41 U.S. and 18 Russian mission control personnel. The overall compliance rate was 80%. To test hypotheses related to psychosocial issues affecting the 1st half versus the 2nd half of a typical mission, all of the subject responses were arrayed in terms of the midpoint of each subject's mission for each subscale of the POMS, GES, and WES. Preliminary analyses of

the GES data showed that crewmembers reported significant declines in the 2nd half of the missions on measures of cohesion, leader support, and task orientation. Crew self-discovery dropped throughout the missions. There also were significant differences between the Mir crews and personnel in mission control on five of the six POMS subscales, with astronauts and cosmonauts reporting less dysphoria than ground support personnel. On the WES, Mir crewmembers scored significantly higher than did mission control personnel on measures of perceived managerial control and comfort with their physical environment. Significant differences also were found between U.S. and Russian subjects on a number of subscales, suggesting possible cultural differences.

CONCLUSIONS

Preliminary analyses of the data using a biphasic model supported some but not all of the study hypotheses regarding the effects of the phase of a space mission on crew tension, cohesion, and leadership role. As predicted, crew cohesion and perceived leader support declined significantly in the 2nd half of the missions, possibly indicating asthenic changes and disruptions in interpersonal relationships. The significant crew-ground differences in measures of dysphoria might be more reflective of the low POMS scores reported from space than of a problem on the ground, since both groups of subjects scored below typical adult norms. Further analyses are being performed to see if a triphasic model is more appropriate, such as has been suggested by Rohrer in Antarctic and submarine studies and by anecdotal reports involving cosmonauts during previous long-duration space missions. The findings from this study suggest a number of important countermeasures that can be developed for use in future manned space missions. These will be discussed in terms of pre-flight selection and training; in-flight monitoring and support; and post-flight readaptation to the social environment on Earth.

PREDICTORS OF BEHAVIOR AND PERFORMANCE DURING LONG DURATION SPACE MISSIONS: THE ANTARCTIC – SPACE ANALOG PROGRAM (ASAP)

L.A. Palinkas¹, E.K.E. Gunderson², J.C. Johnson³, A.W. Holland⁴, and C. Miller¹

¹ Department of Family and Preventive Medicine, University of California, San Diego, La Jolla, CA 92093-0807, ² Naval Health Research Center, ³ East Carolina University, ⁴ NASA Johnson Space Center.

INTRODUCTION

It is generally acknowledged that long duration space missions will require crewmember personality and social characteristics that differ substantially from those required for short duration missions. However, small sample sizes and relatively few long duration missions have made the identification of such characteristics in astronaut personnel somewhat problematic. Studies of personnel in analog environments such as Antarctic research stations allow for a determination of the characteristics of ideal candidates for long duration missions.

METHODS

The influence of crewmember personality and social characteristics, station size and severity of station environment on measures of behavior and performance at the end of the austral winter was examined in 657 American men who wintered over as members of 42 different expeditions at 8 Antarctic research stations between 1963 and 1974. Personality characteristics were based on subscales of a survey designed for winter-over personnel that assessed the following: 1) attitudes toward the antarctic environment (motivation, job importance, boredom, confidence in organization, confidence in medical care); 2) common psychological needs (achievement, autonomy, nurture, and orderliness); 3) self-descriptions (decisiveness, excitability, bluntness, and absentmindedness), and 4) desired characteristics of friends (efficiency, sympathy, conservatism, optimism, dignity, cynicism, adventurousness). The FIRO-B scale was used to measure two aspects (expressing and wanting) of three interpersonal needs (inclusion, control and affection). Social characteristics included age, marital status, military/civilian status, education, and years in occupation. Station environment was determined on the basis of crew size, latitude, altitude, and mean annual temperatures. Performance was assessed by means of self reports of depressive symptoms, based on RDC criteria; peer nominations of crewmembers to winter-over at a small station; and combined peer-supervisor evaluations of task performance (ability), emotional well-being (stability), participation in social relations (compatibility), leadership, and overall performance. Predictors were entered into two-step hierarchical regression models with forced entry of social-demographic characteristics and stepwise selection of psychological and environmental variables.

RESULTS

Significant independent predictors of depression at the beginning of the austral winter included the following: high levels of boredom ($r = .14$, $p < 0.01$); desired cynicism in friends ($r = .12$, $p < 0.05$); small crew size ($r = -.11$, $p < 0.05$); and being currently married ($r = .24$, $p < 0.001$). Significant independent predictors of depression at the end of winter included the following: depression at the beginning of winter ($r = .51$, $p < 0.001$); less severe station environments ($r = -.11$, $p < 0.05$); and high levels of boredom ($r = .21$, $p < 0.001$) and motivation ($r = .09$, $p < 0.05$).

Significant predictors of the percent of station crew who nominated an individual to winter-over again included: size of crew ($r = -.47, p < 0.001$); high desire for optimism ($r = .18, p < 0.001$) and low desire for efficiency ($r = -.12, p < 0.05$) in friends; low levels of boredom ($r = -.14, p < 0.01$) and high levels of motivation ($r = -.10, p < 0.05$); a need to be controlled by others ($r = .11, p < 0.05$); and military service ($r = .13, p < 0.05$). Combined peer-supervisor evaluations of task ability were independently associated with a low need for affection from others ($r = -.17, p < 0.001$) and orderliness ($r = -.14, p < 0.01$); low levels of boredom ($r = -.12, p < 0.05$); and a high desire for optimism ($r = .18, p < 0.01$) but a low desire for efficiency ($r = -.12, p < 0.05$) in friends. Evaluations of emotional stability were independently associated with a low need for affection from others ($r = -.12, p < 0.05$); military service ($r = .13, p < 0.05$); and low levels of boredom ($r = -.10, p < 0.05$). Evaluations of social compatibility were independently associated with a low need for achievement ($r = -.15, p < 0.001$) and affection from others ($r = -.11, p < 0.05$); military service ($r = .13, p < 0.05$); low levels of boredom ($r = -.10, p < 0.05$); and a desire for optimism ($r = .14, p < 0.01$) in friends. Evaluations of leadership were independently associated with marital status ($r = .16, p < 0.01$); low absentmindedness ($r = -.13, p < 0.01$); a need to control others ($r = .10, p < 0.05$); and high levels of motivation ($r = .12, p < 0.05$). Evaluations of overall performance were independently associated with military service ($r = .16, p < 0.01$); a low need for affection from others ($r = -.13, p < 0.01$) and orderliness ($r = -.13, p < 0.01$); and low levels of boredom ($r = -.11, p < 0.05$).

CONCLUSION

Ideal candidates for long-duration missions appear to have the following characteristics: low levels of depression at the beginning of winter, boredom, and a desire for affection from others; a low need for achievement and orderliness; a high need for optimism but a low need for efficiency in others; and military service. Leaders of such missions should be married, highly motivated, and express a need for control over others. The low need for personal achievement and orderliness, affection from others and efficiency in friends may reflect characteristics that are uniquely suited to the prolonged isolation, confinement, and unique environmental characteristics of Antarctic research stations. Highly motivated personnel in small stations may also experience depressive symptoms at various points during an extended mission in an isolated, confined environment due to the absence of opportunities and resources to meet social and psychological needs. The emphasis placed on military service in the evaluations by peers and supervisors may reflect a bias inherent in small groups where military or civilian personnel comprise the majority of both station leaders and crewmembers.

NASA PERFORMANCE ASSESSMENT WORKSTATION: A TOOL FOR ASTRONAUT COGNITIVE PERFORMANCE EVALUATION

R.E. Schlegel¹, R.L. Shehab¹, S.G. Schiflett², and D.R. Eddy³

¹University of Oklahoma, Norman, OK 73019, ²USAF Armstrong Laboratory, Brooks AFB, TX 78235, ³NTI Incorporated, San Antonio, TX 78239

INTRODUCTION

The NASA Performance Assessment Workstation (PAWS) is a laptop computer-based battery of tasks designed to evaluate astronaut cognitive performance during space flight. The tasks were selected to examine attention shifting, spatial, mathematical, and memory skills, and tracking ability. The subjective scales were selected to assess overall fatigue and mood state. PAWS was flown on the Second International Microgravity Laboratory (IML-2) and the Life and Microgravity Spacelab (LMS) missions to study the combined effects of microgravity and fatigue on cognitive performance. This paper provides a background on the PAWS battery of tasks, including descriptions of the tasks and information on task reliability, stability and learning curves.

PAWS TASK DESCRIPTIONS

Several factors were considered in selecting tasks for the NASA PAWS. One of the most important of these is the restrictive time available during flight for performance assessment. Another critical factor is the specific information processing skills necessary for mission success. The final and most relevant issue is the information provided by a specific test that could aid in identifying the cognitive processes or information processing stages affected by microgravity. These and other factors were taken into account in reviewing a large number of human performance task batteries. As a result, six performance tests and two subjective scales from these various batteries were selected for inclusion in the NASA PAWS. Different mood assessment instruments were used on the two missions, the Mood Scale II for IML-2 and Monk's Visual Analog Mood Scale for LMS. Descriptions of the performance tests and subjective rating scales follow in the order in which the tasks are presented in the battery.

Mood Scale II is a variation of the Profile of Mood States. The task has 36 descriptive adjectives which address Activity, Happiness, Depression, Anger, Fatigue, and Fear and involves pressing a numbered key to indicate the level of agreement with each adjective. The test takes approximately 1 minute.

In the Visual Analog Mood Scale, the subject moves a horizontal cursor on a scale from "very little" to "very much" to show agreement with each of eight mood categories represented by the following adjectives: alert, sad, tense, effort, happy, weary, calm, and sleepy. The categories are combined to provide indications of the dimensions of global vigor and affect.

Critical Tracking provides a measure of visual-motor coordination by requiring the subject to maintain an unstable target (cursor) in the center of a horizontal line. A trackball is used to nullify the input disturbance whose magnitude is affected by the instability parameter (λ). In this version of the task, λ increases regularly during the course of the two-minute task until cursor control is lost. The parameter is then reset to a lower level and the task continues.

The number of control losses, the value of lambda at each control loss, and the maximum lambda achieved are all measures of task performance.

The Matrix task provides a measure of spatial rotation ability using 100 basic patterns. Each pattern is a 5 by 5 matrix with five illuminated cells selected at random. At the beginning of each trial series, the subject views a pattern. After studying the pattern, the subject presses a response key and a new pattern is presented. The subject must decide as quickly as possible if the new pattern is identical (except for a 90 degree rotation) to the preceding pattern. After memorizing the current pattern, the subject presses one key for "same" or another key for "different." As soon as a response is made, the next pattern appears and the subject must now compare this new pattern to the immediately preceding pattern. This process continues for 1.5 minutes. Mean reaction time (RT) for correct responses, percentage correct (PC), and throughput (TP) are used as performance measures.

In the Sternberg Memory Search task, subjects indicate as rapidly and accurately as possible whether a visually presented letter is the same as one of those in a previously memorized set. Prior to the 2-minute trial series, a different set of four letters drawn randomly from a restricted alphabet is presented to the subject for memorization. The set of letters (positive set) stays on the screen for a maximum of five seconds, the screen is cleared, and a series of single test letters is presented. If the presented letter matches one of the letters in the previously memorized positive set, the subject responds with a "yes" key press. If a different letter appears (negative set), then the subject responds with a "no" key press, indicating a non-matching letter was presented. Mean RT for correct responses, PC, and TP are the performance measures.

The Continuous Recognition task assesses the ability to maintain attention and to carry out repetitive cognitive processes over a 2-minute period of time. In this task, the subject views two numbers, one above the other as in a fraction. The subject is asked to memorize the bottom number. When the next stimulus appears, the subject is to determine if the new top number is the same as the previous bottom number. Before responding, the subject must note the new bottom number for comparison with the next stimulus. Thus, the subject must exercise short-term memory, and also inhibit the response until the new bottom number is committed to memory. Mean RT for correct responses, PC, and TP are the measures.

The Directed Attention (or Performance Switching) task assesses the ability to shift attention and resource allocation in response to rapidly changing and unpredictable external demands. On each trial in this task, the subject is directed by an on-screen indicator to perform one of two distinct and discrete tasks. One is a spatially-based task, and the other is a mathematically-based task. Both tasks appear, side-by-side, simultaneously on the screen on every trial. The subject must make an exclusive response to the active task, where reaction time and percent correct data are obtained only for that task. The switching from task to task for each trial is random with restrictions. Therefore, the subject must remember to watch the indicator on each trial, allocate the appropriate resources to respond to that trial, and make the appropriate response.

The two tasks selected to exercise this paradigm in PAWS are the Manikin task and the Mathematical Processing task. In the Manikin task, a "stick figure" is presented facing either forward or backward. In addition, the figure can be either upright or upside-down. The figure is

standing on a box and inside the box is either a rectangle or a circle. In the figure's two hands are a rectangle and a circle. The subject's task is to note which symbol is inside the box, and then to determine which of the manikin's hands (left or right) is holding the designated symbol. In the Mathematical Processing task, the subject presses a key to indicate whether an expression involving the sums and differences of three single-digit numbers is greater or less than 5. The test lasts 4 minutes. In addition to mean RT, PC, and TP as performance measures, importance is given to responses made on "switched" trials where the current task is different from the immediately preceding task.

The Dual Task, involving simultaneous Tracking and Memory Search, provides a measure of the ability to allocate attentional resources among several tasks. The tracking task defined above is presented in the middle of the screen and the letters of the Memory Search task (also defined above) appear in a fixed location directly above the center null point. The Tracking task has a constant difficulty (fixed λ), which is set at 2.0 during training and adjusted upward based on subject ability for actual testing. The task lasts 3 minutes and provides performance measures similar to those for each of the component tasks with the addition of RMS error for tracking.

The Fatigue Scale assesses the level of fatigue experienced by the subject on a scale of 1 to 7. The subject responds by selecting the statement that best describes the current level of fatigue.

TEST METHODS

Combined studies involving 101 ground-based subjects were used to evaluate the differential stability and reliability of the PAWS performance measures, and to provide a comparative data base for classifying astronaut performance changes. In addition, PAWS has been used to collect data on three astronauts on IML-2, eight bed rest subjects in a pilot study for LMS, and four astronauts on LMS.

RESULTS

Typical patterns of performance improvement are observed during task training. For discrete response tasks, response times become faster and percent correct improves. Throughput, the number of correct responses processed per minute, shows a corresponding increase. Improvement in the critical tracking task is reflected in increases in the instability parameter λ , indicating an improved ability to control a more unstable cursor. Improvement in the dual tracking task results in fewer control losses and a decrease in RMS error even as the difficulty increases. In most tasks, the majority of learning is accomplished during the first six sessions.

Stable task performance measures are essential for the determination of performance change as a function of exposure to any stressor, including microgravity. Intertrial correlations and Lord and Novick (1968) reliabilities were computed to evaluate the stability and reliability of the PAWS measures (Table 1). Lord and Novick (1968) reliabilities, computed as the ratio of (Between-subject Variability minus Within-subject Variability) divided by Between-subject Variability, were of similar magnitude and paralleled the intertrial correlations.

Table 1. PAWS Intertrial Correlations and Lord & Novick Reliabilities.

Task	Measure	Correlation	Reliability
Critical Tracking	Maximum Lambda	0.74	0.73
	Mean Lambda	0.78	0.77
	Control Losses	0.66	0.66
	RMS Error	0.73	0.72
Matrix Task	Mean RT for Correct Responses	0.89	0.89
	Percent Correct	0.65	0.62
	Throughput	0.92	0.91
Memory Search	Mean RT for Correct Responses	0.77	0.73
	Percent Correct	0.39	0.38
	Throughput	0.79	0.74
Continuous Recognition	Mean RT for Correct Responses	0.92	0.91
	Percent Correct	0.73	0.72
	Throughput	0.91	0.90
Directed Attention - Manikin Task	Mean RT for Correct Responses	0.92	0.90
	Percent Correct	0.62	0.60
	Mean Transition RT	0.89	0.88
	Transition Percent Correct	0.50	0.50
Directed Attention - Math Processing Task	Mean RT for Correct Responses	0.91	0.89
	Percent Correct	0.59	0.52
	Mean Transition RT	0.87	0.84
	Transition Percent Correct	0.47	0.42
Dual Task - Tracking	Control Losses	0.70	0.70
	RMS Error	0.83	0.80
Dual Task - Memory Search	Mean RT for Correct Responses	0.84	0.84
	Percent Correct	0.42	0.36
	Throughput	0.85	0.84
Fatigue	Response	0.47	0.59
	Mean RT	0.44	0.47

CONCLUSIONS

The NASA PAWS provides very good to excellent levels of differential stability and reliability (0.78 to 0.92) for at least one measure on all tasks. In addition, the tasks are sensitive to a variety of stressors and have been successfully used on multiple space shuttle missions.

COGNITIVE PERFORMANCE ASSESSMENT WITH A BED REST ANALOG FOR MICROGRAVITY

R.L. Shehab¹, R.E. Schlegel¹, S.G. Schiflett², and D.R. Eddy³

¹University of Oklahoma, Norman, OK, 73019, ²USAF Armstrong Laboratory, Brooks AFB, TX, 78235, ³NTI Incorporated, San Antonio, TX, 78239

INTRODUCTION

The NASA Performance Assessment Workstation (PAWS) is a computer-based battery of tasks designed to evaluate astronaut cognitive performance during space flight. Each PAWS session requires subjects to complete six performance tasks and two subjective scales. The tasks were selected to examine attention shifting, spatial, mathematical, and memory skills, and tracking ability. The subjective scales were selected to assess overall fatigue and mood state. PAWS was flown on the Second International Microgravity Laboratory (IML-2) and the Life and Microgravity Spacelab (LMS) missions to study the combined effects of microgravity and fatigue on cognitive performance.

The LMS mission assembled twelve experiments designed to evaluate the impact of space flight on a broad range of human abilities. The experiments examined three general areas: 1) muscle structure and function, 2) metabolism, and 3) performance. The NASA PAWS was included as a performance experiment to evaluate cognitive performance changes during and after flight.

One-year prior to the flight of LMS, a bed rest analog was used in a ground-based study to examine the host of proposed life sciences experiments. The bed rest microgravity analog restricts subjects to a prone, 6°, head-down posture for the duration of the study. The physiological effects of this postural restriction simulate the physiological effects of a microgravity environment. The bed rest study followed the planned flight schedule and procedures for LMS and served to evaluate the combined sequence of experiments prior to the actual flight. The bed rest study provided the opportunity to identify and resolve conflicts and incompatibilities within the schedule, refine experimental procedures, and optimize proposed timelines. The bed rest study also provided ground-based control group data for comparison with the flight data. As part of the LMS payload, PAWS was included in the LMS bed rest study. This paper details the PAWS bed rest experiment.

METHODS

The bed rest study was conducted in the Human Research Facility (HRF) at the NASA Ames Research Center, Moffet Field, California. The HRF was designed to handle the unique needs of bed rest research. Eight male subjects (average age = 42.3 years) participated in the study. Subjects passed rigorous screening requiring no smoking, medication or drug use, and passing a physical examination. Seven of the subjects had participated in previous bed rest research.

The experimental procedures planned for the LMS mission were followed as closely as possible in the bed rest study. This included restrictions such as PAWS testing within the first four hours of waking and at approximately the same time each day, no food consumption or exercise immediately prior to PAWS testing, and minimal external distractions during PAWS testing.

The 36 PAWS sessions were collected in four phases: orientation, control period, bed rest, and recovery. During orientation, subjects trained extensively on PAWS, completing eight sessions across two days. The remaining phases of the study were consecutive and spanned approximately one month. The eight-day control period was three weeks after orientation and involved sixteen additional PAWS sessions (two sessions per day) for practice and stabilization of performance and establishing individual baselines. Immediately following, subjects were confined to 6° head down tilt bed rest for sixteen days. During the eight-day recovery phase, subjects were again ambulatory. One PAWS session was performed every other day during the bed rest and recovery phases.

The standard testing posture for the PAWS was seated at a workstation. However, after eight control period sessions had been completed, subjects were transitioned to the bed rest testing posture. This allowed subjects to adapt to the constraints of the modified posture prior to bed rest testing. This posture positioned the subject face-down on a gurney, with the head extended over the end and resting on a padded “doughnut”, and the arms extended beyond the edge of the gurney to the test apparatus below.

RESULTS

Figures 1 and 2 depict orientation and control period performance for the Critical Tracking and Directed Attention tasks, respectively. Typical patterns of improvement were observed during the eight orientation sessions. For discrete response tasks, response time became faster and percent correct improved. Throughput, the number of correct responses processed per minute, showed a corresponding increase. Improvement in the tracking task was reflected in fewer control losses and a decrease in RMS error. In all tasks, the majority of learning was accomplished by Session 6.

In the control period phase, performance demonstrated a moderate level of continued learning. Examination of the throughput measure for the simpler tasks indicated continued improvement in spite of the change in test posture. However, the change in test posture negatively impacted performance of the tracking and directed attention tasks. The horizontal gurney posture actually impaired tracking performance on the Dual task and the Critical Tracking task (Figure 1). Tracking performance did recover to the seated-posture level by the end of the control period, but there was no continued improvement as may have been expected if all testing was seated. A similar phenomenon was observed for the Directed Attention task (Figure 2). The change of test posture terminated improvement and may have produced slight decreases in performance.

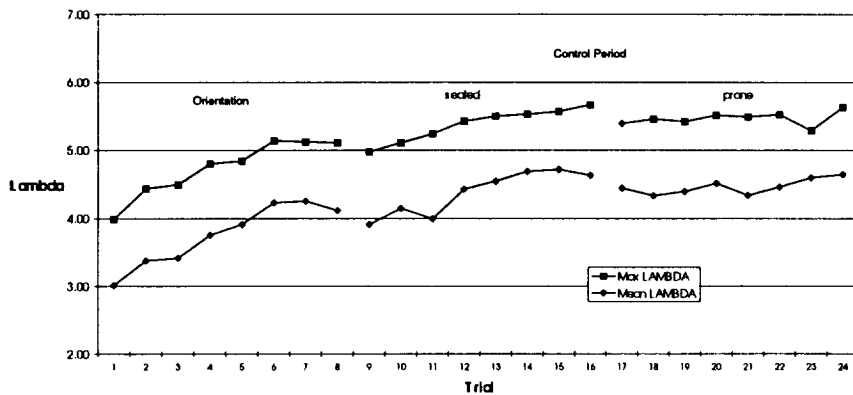


Figure 1. Critical Tracking Task.

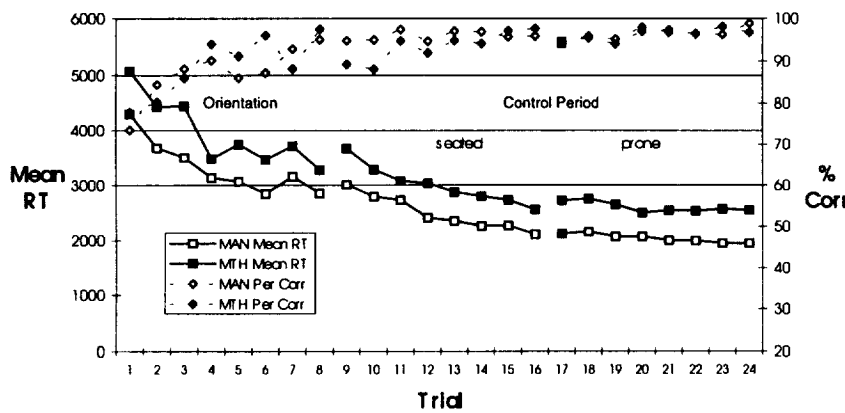


Figure 2. Divided Attention Task.

Performance data acquired during bed rest did not indicate any cumulative effects of bed rest. After a short period of performance stabilization, the observed trend of a moderate level of continued learning resumed (Figure 3). In most tasks, this trend continued through recovery. However, Dual Task performance (both Tracking and Memory Search) was somewhat erratic throughout bed rest and did not restabilize until recovery. Parametric analyses were unable to identify statistically significant differences between bed rest and control period performance.

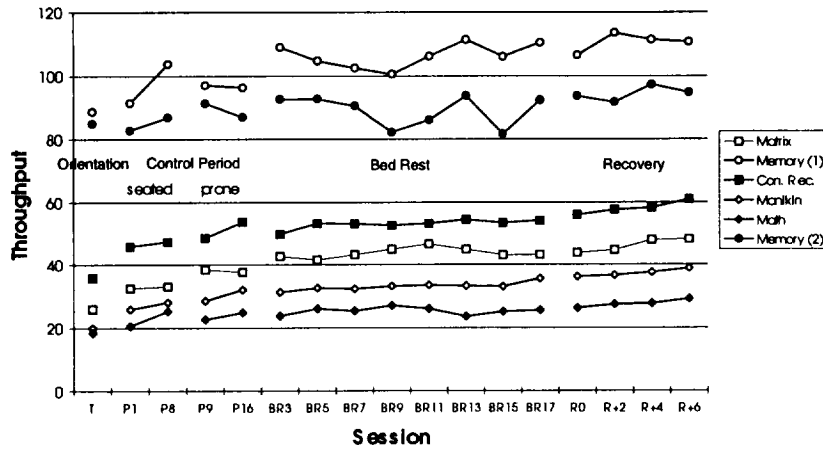


Figure 3. Throughput Measure for All Discrete Response Tasks.

CONCLUSION

In general, the impact of bed rest on cognitive performance was minimal. When noted, effects were manifested as a decrease in the slight rate of improvement rather than overall performance impairment. More specific effects were noted on the motor control tasks. However, it is likely that the change in testing posture confounded these effects. It was interesting to note that the tasks that revealed the greatest sensitivity to bed rest effects were the more complex tasks, Directed Attention and Dual Task. Perhaps the simpler tasks demanded so little effort that sufficient resources were available to compensate for the additional stress imposed by bed rest. Based on the bed rest analog, it was predicted that the physiological changes associated with space flight would only minimally impact cognitive performance.

REVIEW AND ANALYSIS OF DIARIES MAINTAINED BY THE LEADERS AND PHYSICIANS OF FRENCH REMOTE DUTY STATIONS

J. Stuster¹, C. Bachelard², and P. Suedfeld³

¹Anacapa Sciences, Inc., Santa Barbara, California 93102, ²Territoire des Terres Australes et Antarctiques Françaises and Institut Française Pour La Recherche Et La Technologie Polaires,

³University of British Columbia

INTRODUCTION

In previous studies of space analogue conditions it has been impossible to support with objective evidence any scheme that attempts to assign relative priority to the many behavioral issues that must be considered when designing procedures and equipment for long duration isolation and confinement. Psychologist, Peter Suedfeld, voiced the concern of behavioral scientists and perplexed aerospace managers when he commented that a particular study, "...does not communicate judgments about the relative importance of the various problems, so the reader is often left wondering about what design or preparation or intervention goals should have priority if one has to make choices--as one often does because of restrictions of time, space, payload capacity, personnel, funds, and so forth." Using data derived from the experiences of actual leaders and physicians during expeditions in remote, isolated, and hostile environments, the current study identifies the major categories of behavioral issues associated with isolation and confinement, and provides quantitative data on which to base judgments concerning the relative importance of the categories and their constituent themes.

METHODS

A content analysis was performed of nine personal journals that were maintained for this purpose by the leaders and physicians at French remote duty stations in Antarctica and on small islands in the South Indian Ocean. The diaries were maintained during the 1993-1994 expedition as part of the International Antarctic Psychological Program (IAPP). All diary entries were assigned to a primary category and more than half of the entries also were assigned to a secondary category, based on content. Major themes (clusters of entries on similar topics) were identified from the diary entries within each category of behavioral issues. All entries also were coded as positive, negative, or neutral in tone, to permit analyses using a metric defined as net positivity-negativity.

RESULTS

Group Interaction was found to be the most salient of the 22 categories to emerge from the analysis of diary entries, followed by Outside Communications, Workload, Recreation and Leisure, Medical Support, Adjustment, Leadership, Event, and Food. Substantial evidence of a third quarter phenomenon was found in all expeditions, regardless of duration or location (i.e., shorter and longer duration, Antarctic and insular stations); leaders, however, experienced their greatest negativity during the second quarters of their missions, rather than in the third quarters. Some of the study results were contrary to the expectations of many experts. For example, shorter missions (69 to 180 days) generated greater negativity than the longer missions (230 to 363 days), especially concerning issues related to workload and outside communications; this was a response to tighter work schedules, overly optimistic goals for the relatively brief time spent at a remote base, and problems arising from communications with headquarters. Similarly, the diaries from the insular stations were more negative than the diaries from the Antarctic base,

largely as a consequence of the disruption caused by frequent visits to the more accessible insular stations by scientists and others who were not a part of the main expeditions. Outside communications were found to be the sources of considerable negativity (problems with headquarters, negative news), but became a source of positivity during the third quarters of the missions, a period during which all other categories declined. Recreation and leisure activities were the greatest sources of positivity during the missions, with excursions away from the stations and special meals playing key roles in this category. More than 100 specific themes emerged from the analysis in 22 categories of behavioral issues.

CONCLUSION

This research identifies the behavioral issues associated with long duration isolation and confinement and places the issues in order of importance, using quantitative means. Study results provide clear indications of the priority that should be placed on the various behavioral issues to prepare for long duration orbital missions, and lunar and planetary expeditions.

PSYCHOLOGICAL ADAPTATION TO EXTREME ENVIRONMENTS: EFFECTS OF TEAM COMPOSITION ON INDIVIDUAL ADAPTATION

J. Wood¹, S.J. Hysong², D.J. Lugg³, & D.L. Harm⁴

¹Baylor College of Medicine, ²Department of Psychology, Rice University, ³Australian Antarctic Division, ⁴Neuroscience Laboratories, Johnson Space Center

INTRODUCTION

This study is part of an ongoing program of research examining the psychological effects of isolation and confinement on individual adaptation, productivity and group relations in Antarctic winter personnel. This environment is used as an analogue for long-duration space mission scenarios, such as a space station sojourn, or a mission to Mars. Earlier results from this and other environments have demonstrated that: (1) most changes in psychological well-being are event-related and of relatively short duration; and (2) the greatest problem facing most individuals is interpersonal conflict. Content analysis of responses to open-ended questions has identified the numerous enjoyable aspects of Antarctic living, and confirmed that many of the problems reported were interpersonal in nature, and that problems varied significantly by station. Current work is exploring the effects of team assignment on the self-reported psychological changes and self-evaluations of members of isolated teams. This work includes identifying the dimensions by which subjects determine how well they are functioning. These dimensions (e.g., work, social life, internal emotional state) appear to play an important role in how subjects evaluate many aspects of life in isolation. It is expected that groups with many

METHODS

116 subjects were recruited from the Australian National Antarctic Research Expeditions (ANARE) winter personnel in 11 winter-station expedition groups over the course of three years. Participants completed a computer-administered questionnaire once a week, for as long as they were at the stations. The questionnaire contained items that measured mood, cognitive state, social and work relationships. Open-ended questions also allowed respondents to elaborate on matters that were not otherwise included in the questionnaire. Demographic information was collected for all the participants, and, personality data, as measured by the 16 Personality Factor Questionnaire were obtained for 72 of the Australian participants.

A set of variables on which the subjects evaluate themselves (reflecting mood, morale, productivity, and sense of belonging to the group) will be analyzed with Multidimensional Scaling to identify the important dimensions around which subjects self-evaluate. An individual differences model will be utilized to account for differences in the importance of each dimension to the various subjects.

Cluster analysis will be used to identify subgroups of subjects with similar importance ratings on the self-evaluation dimensions.

Categorical regression analysis will be used to examine the roles of team membership, degree of isolation, and selected personality traits on self-evaluation subgroups.

RESULTS

Preliminary results will be presented. The importance of team composition and its effect on individual adaptation will be discussed. A subset of the data, from those subjects who provided data during multiple years will be presented.

Behavior, Performance, and Human Factors II (Human Factors)

Chair

Barbara Woolford

Co-Chair

Nick Kanas, M.D.

MISSION CONTROL INFORMATION FLOW ISSUES

Barrett S. Caldwell, Principal Investigator, University of Wisconsin-Madison

INTRODUCTION

The NASA funded research project, "Control-Crew Network Communication During Routine and Non-Routine Events: Effects on Mission Control-Crew Performance," has only been active since May, 1998. However, the current research is also able to draw on prior work conducted in the PI's research group since 1995. Much of this related research has significant impacts on several biomedical and human performance assessment topics, especially in the area of task coordination and performance enhancement in cognitively demanding tasks. This presentation will provide a brief overview of past studies, outline of the current research, and plans for future investigations from this early research perspective.

One human performance concern in supervisory control tasks is the interaction of changes in task demands (workload transitions) and cycles of operator alertness during system monitoring or supervisory system management. The combination of sudden workload transitions with lowered alertness can result in hazardous states of awareness, which may significantly impair the operator's ability to respond effectively to a degraded situation or environmental condition. Hazardous states of awareness can present problems both for mission control console operators, and the astronaut crews themselves, depending on phase of flight and the need for coordinated information flow and task performance. In order to reduce potential performance degradation associated with hazardous states of awareness, research effort has been devoted to identify physiological or behavioral correlates of reduced alertness associated with reduced task performance.

Two studies conducted in the PI's Group Performance (GROUPER) research group have addressed the impact of workload transitions on operators at varying states of alertness as measured by EEG and EKG data. One study, conducted at SPAWAR in San Diego, evaluated operators in an air defense task over 96 person-hours (N=12, four two-hour task sessions over two days) of varying alertness. The second study, conducted at the Sleep Research Center at UW-Madison, evaluated performance in a NASA MATB resource management task after a period of low task demands, collecting approximately 50 person-hours (N~100, one 30-minute session) of data. Analysis of both data sets is ongoing. However, initial results from the SPAWAR study indicated that variations in alertness in the single minute prior to workload transitions could significantly predict variance in task performance during the 5-7 minute high task demand phase following the transition. Initial results of the Sleep Research Center study indicated that persons with serious measured sleep apneas were significantly more impaired in their performance responses to a workload transition after a period of low task demands.

The results of these studies clearly indicate that effective information flow regarding operator alertness, as well as increased task coordination support during workload transitions, will be of importance in managing distributed supervisory control task performance between mission control operators and astronaut crews. The current research does not examine operator alertness variables, but focuses instead on the changes in communication patterns associated with routine and non-routine events. Both types of events may represent workload transitions for the crew

and mission control, and may require new techniques for adaptive bandwidth allocation to support mission success.

CURRENT STATUS OF RESEARCH

The current research project is still in initial stages of project formulation and data collection. The research data consists of audio data (obtained from DVIS data logs), video data (from NASA Select / Public Affairs video tapes of the Flight Director and CAPCOM consoles), and mission telemetry data from STS mission simulations. No effective means currently exist for systematically obtaining these data in a consistent and compatible format, due to the history of the data collection infrastructures for audio, video, and telemetry data. Of primary importance is the change in communication network structure and activity after mission events, including the changes in console monitoring and active participation in various DVIS audio loops. DVIS logs can easily recognize a console operator selecting a DVIS loop for active participation; however, selection of passive monitoring of a loop is less clearly identified in the log data.

ANALYSIS METHODS

Analysis of the audio and video data of communication loop activity is expected to utilize a combination of coding and statistical methods. Video data will be coded behaviorally, focusing on the unmediated ("air loop") communications between Flight, CAPCOM, and other console stations. Audio data will be coded both according to communications behavior patterns and the network linkages of those participating. Statistical analysis of these data will examine the dynamic properties of the communications loops, particularly from the perspective of perturbed time series and dynamical systems behavior. Dependent variables in the mission simulations will focus on achievement of ordinal levels of mission accomplishment (survival, recovery of major mission continuation capability, recovery / completion of required mission tasks, performance of desirable, but not mission required, tasks).

Of direct relevance to the above alertness and operator performance studies are the issues of what makes an event "routine," and the cognitive processing associated with monitoring and participating in multiple communications loops. Much of the research in high-reliability organizations discusses task performance in response to events, but does not reliably distinguish the characteristics of routine and non-routine events. In the current research, we are assuming that "non-routine" events have four dimensions relevant to effective operator response and successful recovery performance: expectation or advance warning of the event's onset; preparedness for contingencies associated with the event; impact of the event progression if appropriate responses are not made; and the time scale of event progression. Operator alertness and response capabilities are clearly related to the expectation and time scale dimensions, with impaired performance most likely with unexpected events occurring at periods of low alertness and progressing at rates on an order similar to the recovery times required for re-establishing effective operator performance. Expectation in itself will provide forestallment of hazardous awareness states, because of the operator's ability to pre-plan activities to permit greater alertness when the event is due to occur.

From a cognitive standpoint, simultaneous attention to several communication loops is clearly a resource intensive process, which is sensitive to fatigue, pre-task alertness, and stress effects. Studies of expertise acquisition in divided attention resource tasks are still quite limited and

rudimentary, although more real-world cognitive science research of this type would greatly benefit the design of mission control communications systems. Mission control operators' and crew members' ability to process multiple communication loops during critical mission events represent a principal resource limitation for communication, coordination and distributed task performance.

PLANS FOR FUTURE INVESTIGATIONS

The early stage of the current research makes planning for future investigations problematic. As mentioned above, however, the goal of this study will be to identify hardware, software, and organizational methods of adaptive communications and bandwidth allocations to support enhanced mission control - crew performance, especially in the era of multiple space vehicles and crews. The current study only focuses on "front room" communications loops. Future work will help to identify methods for improving communications dynamics between front rooms and back rooms, and tools for enhancing information flow both within console specialties across mission support groups, and within mission support groups across console specialties.

MICROGRAVITY WORKSTATION AND RESTRAINT EVALUATIONS

C. Chmielewski¹, M. Whitmore¹, and F. Mount²

¹ Lockheed Martin, ² NASA, JSC

INTRODUCTION

Confined workstations, where the operator has limited visibility and physical access to the work area, may cause prolonged periods of unnatural posture. Impacts on performance, in terms of fatigue and posture, may occur especially if the task is tedious and repetitive or requires static muscle loading. The glovebox design is a good example of the confined workstation concept.

Within the scope of the 'Microgravity Workstation and Restraint Evaluation' project, funded by the NASA Headquarters Life Sciences Division, it was proposed to conduct a series of evaluations in ground, KC-135 and Shuttle environments to investigate the human factors issues concerning confined/unique workstations, such as gloveboxes, and also including crew restraint requirements.

As part of the proposed integrated evaluations, two Shuttle Detailed Supplementary Objectives (DSOs) were manifested; one on Space Transportation System (STS)-90 and one on STS-88. The DSO on STS-90 evaluated use of the General Purpose Workstation (GPWS). The STS-88 mission was planned to evaluate a restraint system at the Remote Manipulator System (RMS). In addition, KC-135 flights were conducted to investigate user/workstation/restraint integration for long-duration microgravity use. The scope of these evaluations included workstations and restraints to be utilized in the ISS environment, but also incorporated other workstations/ restraints in an attempt to provide findings/requirements with broader applications across multiple programs (e.g., Shuttle, ISS, and future Lunar-Mars programs). In addition, a comprehensive electronic questionnaire has been prepared and is under review by the Astronaut Office which will compile crewmembers' lessons learned information concerning glovebox and restraint use following their missions.

These evaluations were intended to be complementary and were coordinated with hardware developers, users (crewmembers), and researchers. This report is intended to provide a summary of the findings from each of the evaluations.

BACKGROUND

Based on the literature, internet searches, and personal discussions with points of contact, a list of current and planned space gloveboxes was generated. Two of the Shuttle gloveboxes were previously evaluated under DSO-904 (Space Human Factors Evaluations) by Johnson Space Center (JSC) Usability Testing and Analysis Facility (UTAF) personnel. The user interface, crew posture, and comfort were the human factors issues addressed for the GPWS on STS-58 and Spacelab microgravity glovebox (GBX) on STS-50 and STS-73. Although no DSO-904 human factors evaluations were conducted on Biorack and the Middeck glovebox, it was determined that both designs were very similar, if not identical, to the GBX in terms of user interface. Therefore, the human factors issues were also anticipated to be similar among these three gloveboxes.

In an attempt to obtain information on the Standard Interface Glovebox (SIGB) developed by Ames Research Center, a presentation on its development efforts and use on Mir was attended at the 27th International Conference on Environmental Systems (ICES) in 1997. It was found that the SIGB user

interface in terms of gloveport location and orientation, work volume, and viewing window placement was very similar to that of the design concept recommended by the UTAF after previous human factors evaluations (Whitmore, McKay and Mount, 1995). In addition, during one of the NASA-Mir Long Duration Mission post-flight debriefs, the U.S. crewmember commented that his experiences with the glovebox were positive and did not report any discomfort or design concerns.

Finally, based on the discussions held during a July 1997 NASA JSC Human Factors Technical Interchange Meeting on the Microgravity Sciences Glovebox (MSG), human factors issues such as accommodation of crew anthropometry, crew restraint requirements and lighting were identified. A preliminary review of the Life Sciences Glovebox (LSG) was conducted and human factors issues were identified. Human factors issues were also identified for the ISS Maintenance Work Area (MWA).

METHOD

The first set of workstation and restraint evaluations was performed on the KC-135 microgravity aircraft in March 1998. The type of workstation focused on was gloveboxes due to their confined nature and their multitudes of use on both the Shuttle and Mir. The main goal was to identify glovebox and restraint issues that can aid in the best utilization of the current items to enhance operator comfort, efficiency, and safety, as well as to benefit the design of future gloveboxes and restraints.

A set of criteria to identify the gloveboxes and crew restraints for the KC-135 evaluations was created which would facilitate a positive impact on design and be the most effective utilization of the available resources.

Based on the criteria, the ISS MSG, the GBX flown on USML-1, and the SIGB concepts were included within the scope of the KC-135 evaluations. The objectives included the evaluation of glovebox design issues such as:

- 1) gloveport size
- 2) distance between gloveports
- 3) size and angle of the viewing window
- 4) airlock operations (MSG only), and
- 5) work volume.

In addition, the KC-135 evaluations focused on crew restraint requirements for the selected workstations.

The General Purpose Workstation (GPWS) is a glovebox which has flown on previous Shuttle Spacelab missions. It is a multi-functional facility that supports animal experimentation and microscope use within its volume. As part of the workstation and restraints integrated evaluations project, DSO-904 was conducted onboard the Shuttle during STS-90/ Neurolab in April 1998. The purpose of these microgravity evaluations was to evaluate the GPWS in terms of the following:

- 1) usability, adjustability, and accessibility;
- 2) use of restraint systems and mobility aids; and
- 3) experiment procedures including temporary stowage.

All four Neurolab payload crewmembers participated in the evaluation, via in-flight video at the GPWS and/or questionnaire. A questionnaire addressing workstation and restraint design issues,

as well as crew comfort, was available to the crew in-flight. Selected mission activities were recorded for postflight video analysis of crew posture. The video captured the crewmember's posture on their left side from head to toe while working at the front of the GPWS. The video did not capture the activities inside the GPWS. The questionnaire was to be filled out by all four Neurolab payload crewmembers on a late Flight Day (FD) after much of their activities in the GPWS were completed.

The posture categories emphasized in this evaluation were with the lower body. It was found that upper body positions varied only a small amount; crewmembers maintained either hunched shoulders or extended reach for the duration of the GPWS activities. It is believed this was due to the large size of the GPWS interior and the fine motor control needed for the activities, as well as the uniqueness of the crewmembers' heights (all were over 6 feet tall).

STS-88, scheduled to fly in December 1998, was identified as another mission where a Shuttle human factors assessment could be manifested. A modified design of the Advanced Lower Body Extremities Restraint Test (ALBERT) named the Foot Restraint Equipment Device (FRED) is planned to be used at the remote manipulator system (RMS) workstation during ISS assembly tasks (EVA operations). It is anticipated that this evaluation will provide valuable information on restraint use during robotics and earth observation activities.

CONCLUSIONS

Comments from crewmembers and Astronaut Office representatives, as well as workstation and restraint design engineers and management indicate that the primary project goal was achieved successfully. That is, to facilitate the awareness of integrated evaluations and provide means to transfer findings and lessons learned from the past into future work.

Main issues of concern in the design and use of gloveboxes and restraints have been outlined and can now be addressed for future design efforts. Presentations were given to management personnel in the JSC FCSD and ISS Payloads Integration in order to demonstrate the capabilities and limitations of the different glovebox and restraint concepts and their potential applications. In addition, project personnel have been requested to provide comments on other payloads, such as the Life Sciences Glovebox (LSG), Window Observational Research Facility (WORF), and Fluids Combustion Facility (FCF) based on their experience in this area.

NEUROPHYSIOLOGICAL INDICES OF SUSTAINED FOCUSED ATTENTION: APPLICATION TO MONITORING COGNITIVE LOAD, OPERATIONAL FATIGUE, AND OTHER ENVIRONMENTAL STRESSORS

Alan Gevins, Michael E. Smith, Linda McEvoy, Halle Brown
EEG Systems Laboratory, One Rincon Center, 101 Spear St., Suite 204, San Francisco, CA 94105

INTRODUCTION

In complex work environments, any cognitive overload imposed by high task demands can lead to performance errors and inefficiencies in the acquisition of new procedures. Similarly, personnel who are experiencing a transient cognitive impairment (because of fatigue or sleep loss, illness or medication, intoxication or hangover, etc.) may be error prone in situations that tax the limits of their reduced mental capacity. Such conditions have frequently been implicated in major accidents. Neurophysiological (EEG) measures can provide sensitive indices of an individual's ability to focus and sustain attention and to hold information in working memory (Gevins et al., 1997). We are evaluating the feasibility of using such measures of brain function to detect changes in cognitive status associated with environmental stressors. Preliminary studies provided initial evidence that multivariate combinations of task-related EEG variables can provide sensitive indices of cognitive load and transient cognitive impairment. Our current NASA-sponsored effort aims to further verify and extend these results.

METHODS

We are in the final stages of data collection of an experiment in which 16 healthy normal subjects (average age 25.5 years, equal number of men and women) were tested on 7 different occasions. In the first session, subjects were trained on behavioral tasks and familiarized with EEG recording procedures. The tasks included versions of a continuous working memory test and of the NASA Multi-Attribute Task Battery (MATB -- a multi-tasking, flight-simulation style task). During the second session, data were collected while subjects performed versions of MATB that varied in difficulty. These data will permit an assessment of whether EEG measures can index variations in cognitive load during a task that better approximates real world activities than our working memory task. During the subsequent four sessions, subjects were tested in a double-blind fashion after receiving moderate doses of alcohol, caffeine, antihistamine, or placebo. During a seventh session designed to mimic operational fatigue, subjects performed tasks from the evening of one day until 0700 the next morning. These latter datasets will allow us to evaluate the sensitivity of EEG variables to mild forms of transient cognitive impairment or enhancement.

RESULTS

Analyses on the data described above are currently underway. We previously (Gevins et al, 1998) found that multivariate combinations of EEG features in the alpha and theta bands can be used to discriminate data obtained in a high cognitive load test condition from data obtained in a low cognitive load test condition with a cross-validation accuracy > 95% ($p < .001$). Those data were collected during a highly controlled laboratory test of working memory with minimal perceptuomotor requirements. Preliminary analyses of the data recorded with the NASA Multi-Attribute Task Battery suggest that we will also be able to detect variations in cognitive load under the more realistic demands that it imposes. Similarly, in another preliminary study (Gevins & Smith, submitted), we found that multivariate combinations of EEG features in the alpha and theta bands

can be used to discriminate between alert and drowsy states, and between alert and mildly intoxicated states. More specifically, an average cross-validation classification accuracy of >95% was obtained in the alert versus intoxicated comparison, and >92% in the alert versus drowsy comparison (for both comparisons, $p < .001$). Preliminary results from the current experiment suggest that effects of similar magnitude will be obtained.

CONCLUSION

In sum, preliminary results suggest that it is feasible to use EEG measures of sustained focused attention to measure cognitive load or transient cognitive impairment associated with environmental stressors. Further experimental studies are planned to verify and extend these findings. Practical application of these measures will require further efforts to develop recording and analysis technologies suitable for use in operational environments.

REFERENCES

- Gevins, A., Smith, M.E., McEvoy, L., & Yu, D. (1997). High resolution EEG mapping of cortical activation related to working memory: Effects of task difficulty, type of processing, and practice. *Cerebral Cortex*, 7, 374-385.
- Gevins, A., Smith, M.E., Leong, H., McEvoy, L., Whitfield, S., Du, R., & Rush, G. (1998). Monitoring working memory load during computer-based tasks with EEG pattern recognition. *Human Factors*, 40, 79-91.
- Gevins, A., & Smith, M.E. (1998). Detecting transient cognitive impairment with EEG pattern recognition. *Aviation, Space, and Environmental Medicine*, submitted.

AN EVA SUIT FATIGUE, STRENGTH, AND REACH MODEL

James C. Maida, NASA Johnson Space Center

The number of EVAs performed will increase dramatically with the up-coming Space Station assembly missions. It is estimated that up to 900 EVA hours may be required to assemble the Space Station with an additional 200 hours per year for maintenance requirements. Efficient modeling tools will be essential to assist in planning these EVAs. Important components include strength and fatigue parameters, multi-body dynamics and kinematics. This project is focused on building a model of the EVA crew member encompassing all these capabilities. Phase 1, which is currently underway, involves collecting EMU suited and unsuited fatigue, strength and range of motion data, for all major joints of the body. Phase 2 involves processing the data for model input, formulating comparisons between the EMU suits and deriving generalized relationships between suited and unsuited data. Phase 3 will be formulation of a multi-body dynamics model of the EMU capable of predicting mass handling properties and integration of empirical data into the model. Phase 4 will be validation of the model with collected EMU data from the Neutral Buoyancy Laboratory at NASA/JSC.

Engineers and designers will use the EVA suit database to better understand the capabilities of the suited individuals. This knowledge will lead to better design of tools and planned operations. Mission planners can use the modeling system and view the animations and the visualizations of the various parameters, such as overall fatigue, motion, timelines, reach, and strength to streamline the timing, duration, task arrangement, personnel and overall efficiency of the EVA tasks. Suit designers can use quantifiable data at common biomechanical structure points to better analyze and compare suit performance.

Major Participating Institutions:

NASA/JSC, Houston TX.

Lockheed Martin Engineering and Sciences Company, Houston, TX.

NONINVASIVE MOTION CAPTURE AND ANALYSIS

Dimitris Metaxas, Department of Computer and Information Science, University of Pennsylvania
200 South 33rd St. Philadelphia, PA 19104-6389. email: dnm@central.cis.upenn.edu WWW: <http://www.cis.upenn.edu/~dnm>

INTRODUCTION

Noninvasive computer-vision methods have begun to play an increasingly important role in applications like anthropometry, human factors design, ergonomics, teleconferencing, virtual reality and performance measurement of both athletes and patients with psychomotor disabilities. All of these areas require the identification of the parts of a human body and/or the estimation of their shape and motion parameters. The main difficulties in developing algorithms for human shape and motion analysis stem from the complex 3D non-rigid motions of humans and the occlusion among body parts.

The solution to the above problems requires the development of an algorithm that: (1) integrates the processes of segmentation and fitting, (2) allows reliable shape description of the parts, (3) estimates the true location of the joints between the parts, (4) detects multiple joints, (5) copes with the problem of occlusion, (6) makes no assumptions of a prior model or part segmentation, and (7) obviates the need for markers and special equipment.

We have developed physics-based vision techniques for the development of algorithms to automatically capture human motion from multiple single and multiple cameras. Using the captured data we can analyze the motions of humans during a variety of applications.

CURRENT STATUS OF RESEARCH

Most of the existing approaches that employ a human body model use non-deformable models that can only approximate the human body and cannot adapt to different body sizes. To overcome this limitation other researchers assume prior segmentation of the given data into parts and then fit deformable models. Therefore, the process of segmentation and the process of shape and motion estimation are decoupled leading to possible inaccuracies and lack of robustness.

In contrast to previous methods, our approach allows the automatic recovery of a human's shape and motion based on occluding edge information and the integration of optical flow information within a deformable model framework using the method of Lagrange multipliers.

METHODS

We have developed an algorithm that segments the apparent body contour of a moving human into the constituent parts. Initially, a single deformable model is used in order to fit the image data. As the model deforms to fit the changes in (due to the motion of the human) subsequent image contours, a novel Human Body Part Identification Algorithm (HBPIA) is developed to identify all the body parts. To be able to represent compactly large deformations in the model we define a new shape representation for deformable models based on the composition of geometric primitives. Replacing the initial model with the composed one, not only allows us to represent the shape of an apparent contour in a compact way, but also to hypothesize an underlying body

part structure. This hypothesis is verified by monitoring the relative motion of the defining primitives of the composed deformable model. By applying the HBPIA iteratively over the subsequent frames, all the moving parts are identified. Thus, we formally automate the task of deciding how many deformable models should be used in fitting the apparent contours of a human whose body parts are in motion.

In addition, we have developed an algorithm to estimate the 3D shape of a subject's body parts. Information from images taken from three cameras placed orthogonally is integrated. A subject is requested to perform a set of movements according to a protocol that allows the integration of information from multiple views. First, the image data from each active view are fitted using 2D deformable models. During the movement new parts are detected based on the HBPIA. Depending on whether the new part is a previously unseen body part or a subpart of a part whose 3D model has already been recovered, two different algorithms are employed to estimate its 3D shape. At the end of all the movements, the 3D shape of all the major parts of the human body is available.

Finally, we have recently developed an algorithm to integrate optical flow information within a deformable model framework using the method of Lagrange multipliers. This approach has allowed us to successfully track complex nonrigid motions such as facial motion with expressions.

RESULTS

We present experiments which demonstrate the ability of our method to track complex 3D motions of humans and faces including their expressions. The input to the system are image sequences from single/multiple cameras. We demonstrate our results using videosequences with our deformable models superimposed on the image data.

CONCLUSION

We have developed a deformable model-based approach to estimate the 3D shape and motion of humans from single/multiple camera images sequences. The use of deformable models allows the applicability of the method to humans of different size, race and gender. The method is particularly suited for monitoring and tracking human activities in space as well as in general biomedical applications.

REFERENCES

- 1) "3D Human Body Model Acquisition from Multiple Views". I. Kakadiaris and D. Metaxas. Accepted for publication to the International Journal of Computer Vision.
- 2) "Inferring Object Structure in 2D from the Deformation of Apparent Contours". I. Kakadiaris, D. Metaxas and R. Bajcsy. Journal of Computer Vision and Image Understanding, February, 1997.
- 3) "Deformable model-based shape and motion analysis from images using motion residual error". D. DeCarlo and D. Metaxas. Procs 6th International Conference on Computer Vision, India, January 1998.

4) "The integration of optical flow and deformable models with applications to human face shape and motion estimation". D. DeCarlo and D. Metaxas. In Procs. CVPR '96, pp. 231-238, June 1996.

MEASURING ASTRONAUT PERFORMANCE IN MICROGRAVITY: LOADS AND MODELING

D. Newman¹, S. Beck², A. Amir¹, G. Baroni³, G. Ferrigno³, A. Pedotti³

INTRODUCTION

Quantitative analysis of human performance in microgravity is important for both scientific investigations and spacecraft engineering design. By collecting and evaluating the kinematics and kinetics data of astronauts in space, it becomes possible to characterize human motor strategies, postural behavior in weightlessness (Massion, 1992), improve the design of orbital modules, help maintain a quiescent microgravity for acceleration-sensitive material science and life science experiments (NASA JSC, 1996), and optimize the human operative capabilities during long-duration space missions (Griffin et al., 1978; Wichsman and Donaldson, 1996). Hence, there is a need for a precise measurement of the forces and moments exerted by the astronauts on the space station and their postures and movements.

METHODS

The advanced load sensors are an instrumented version of the crew restraint devices and mobility aids to be provided on the International Space Station (ISS). In particular, the functionality of a hand hold, a foot restraint, and a push-off pad are provided while measuring forces and moments in three axes (6 degrees of freedom). The processing of the acquired data is conducted in real-time to provide immediate feedback on the load level applied to the crew restraint. To maximize the mobility and flexibility of the load sensors, the objective was to miniaturize the system as much as possible with current technology. ELITE-S2 will be an automatic opto-electronic system for real-time 3-D motion analysis using video image processing for detecting multiple passive markers in the environment. The architecture of the system has two levels: Level 1 consists of the Interface with The Environment (ITE) and of a Fast Processor for Shape Recognition (FPSR). The components of the ITE are CCD video cameras as well as a set of reflective markers. The identification of markers in each camera image is performed by the custom-designed FPSR electronics hardware. Level 2 of the architecture is a laptop computer with special software.

RESULTS

The completed work under this research grant includes load sensor, electronics and motion analysis equipment design. Each load sensor consists of two parts: the Sensor Restraint Unit (SRU) and the Sensor Electronics Unit (SEU). The former contains, as the name implies, the astronaut restraint mechanism (either a handle or a foot loop) as well as the load cells to measure forces and moments. The latter contains all the necessary electronics for data processing, storage, data display, etc. The SRU is attached to standard ISS hand rails or so-called seat track anchor interfaces. The measurement of forces and torques is accomplished with three custom-designed load cells (flexures) in a circular arrangement placed 120° apart. Each load cell is equipped with two full wheatstone strain gage bridges consisting of four foil strain gages. Full bridges are used to nearly double the measurement sensitivity and to compensate for temperature effects. Three signals are from bridges on the center beams and three signals are from bridges on the side beams. Each SRU is connected via a cable to a corresponding Sensor Electronics Unit, measuring centimeters. The SEU has been designed around the PowerPAQ handheld

¹ Massachusetts Institute of Technology, Department of Aeronautics and Astronautics, Cambridge, MA.

² NASA Langley Research Center, Langley, VA.

³ Polytechnic of Milan University, Department of Bioengineering, Milano, Italy.

reference design. Developed by Motorola Inc.'s Semiconductor Division, the PowerPAQ is a reference platform for embedded systems with applications such as image capture, wireless connectivity, speech recognition, and Global Positioning System receivers (Motorola, 1998).

The SRU is connected to the 6-channel signal conditioning board of the SEU that supplies the excitation voltage to the load cells and conditions the voltage signal returned from the load cells. The signal is sampled with a commercial PCMCIA Type II 16-bit A/D Converter housed in one of the two PCMCIA card readers of the modified PowerPAQ. Data will be recorded with a 250 Hz sampling frequency, written to PCMCIA Type III 520 Mbytes hard disks, and processed by the MPC823 PowerPC™ processor to provide real-time feedback on the load applied. The SEU incorporates a 16.3 cm color TFT display with a touch screen for input supplemented with an internal microphone to digitally record crew comments. A modified Windows CE™ operating system is used for operating the sensors. Time synchronization with other load sensors, the ELITE-S2 motion analysis system, and the space station as a whole is accomplished with a Bancomm time card using the IRIG timer signal. A Universal Serial Bus port is included for communication between load sensors and the ELITE-S2 system (Amir, 1998).

The ELITE-S2 system can handle up to eight cameras and 100 markers, provide real-time data acquisition for several minutes, and operates with in working volume of at least meters. Since the markers are recognized by their shape, a very high reliability of recognition even in “disturbed and uncontrolled” environments can be achieved. The shape recognition is accomplished by a two-dimensional cross correlation which increases the accuracy of the motion analysis by more than a hundred times above the resolution of the CCD sensor.

The cameras of the system use solid state frame transfer CCD sensors with good sensitivity in the near infra-red region and are equipped with flashes coaxial with the lenses. The flash is generated by near infra-red (870 nm) LEDs arranged in concentric circles around the camera lens. The sensors are driven by a special circuitry reaching a sampling rate of 200 Hz. The other hardware-allowable sample rates are 50, 60, 100, and 120 Hz. Using the software it is possible to reduce the sampling rate by an integer factor. The sensors are discharged one millisecond before the data transfer takes place, and implement a fast shuttering function which minimizes shape distortions for high speed motion. The camera synchronization is driven by ELITE-S2 itself, which acts as a master. In this way all the data readings are synchronous.

The markers are made of plastic hemispheres coated with 3M Scotchlite reflecting the impinging light within a narrow angle with respect to the provenience direction and thus allow to obtain very bright marker images with the coaxial flashes.

The identification of markers is performed by dedicated pattern recognition hardware—the FPSR. The processor implements a two-dimensional cross correlation between the incoming image and a reference kernel, which maximizes the correlation when a marker-shaped object is in the scene and minimizes the error in the presence of background noise including bright spots (Ferrigno et al., 1990). The data processing is performed by a laptop computer with an Intel Pentium® processor. The capabilities of the ELITE software include resolution enhancement, marker labeling, distortion correction (and 2-D calibration), 3-D Intersection (and 3-D calibration), real-time 2-D and 3-D graphics representation, and real-time saving of data to a storage medium. These functions can be performed automatically in real-time or in several steps when the system is off-line.

The advanced instrumentation described herein will provide hardware and techniques to quantify astronaut performance on board the space station.

CONCLUSION

An integrated system of advanced kinematic and kinetic instruments to make these measurements within the space station is being developed jointly by MIT, NASA, and Polytechnic of Milan University. Crew-induced forces and moments will be measured by an advanced version of the Dynamic Load Sensors that have flown on the Space Shuttle (Newman et al., 1996) and on the Russian Orbital Complex Mir. Crew motion will be captured by the ELITE-S2 system, an enhanced version of the real-time opto-electronic motion analyzer ELITE-S which has flown on Mir as part of the EuroMir '95 Mission (Ferrigno and Pedotti, 1985; Baroni et al., 1996).

REFERENCES

- A. R. Amir, "Design and Development of Advanced Load Sensors for the International Space Station," E.A.A. Thesis, Massachusetts Institute of Technology, 1998.
- G. Baroni, G. Ferrigno, G. Andreoni, F. Bracciaferri, and A. Pedotti, "Accuracy Assessment in Microgravity Human Movement Analysis," Proceedings of the VIth European Symposium on Life Sciences Research in Space, Trondheim, Norway, ESA SP-390, pp.129-134, 1996.
- N. A. Borghese and G. Ferrigno "An Algorithm for 3D Automatic Movement Analysis by Means of Standard TV Cameras," IEEE Transactions on Biomed. Eng., BME 37, 1221-1225, 1990.
- G. Ferrigno and A. Pedotti, "ELITE: A Digital Dedicated Hardware System for Movement Analysis via Real-Time TV-Signal Processing," IEEE Trans. Biomed. Eng., BME 32, 943-950, 1985.
- G. Ferrigno, N. A. Borghese and A. Pedotti "Pattern Recognition in 3D Human Motion Analysis," ISPRS Journal of Photogramm. Remote Sensing, 45, 227-246, 1990.
- J. Massion, "Movement, Posture, and Equilibrium: Interaction and Co-ordination." Progress in Neurobiology, 38:35-36, 1992.
- Motorola Consumer Systems Group, "Product Information: PowerPAQ Handheld Reference Design," 1998.
- NASA Johnson Space Center, "Microgravity Control Plan," SSP 50036, Revision A, Type 2, NASA, 29 February 1996.
- D. J. Newman, M. Tryfonidis, and M. C. van Schoor, "Astronaut-Induced Disturbances in Microgravity," Journal of Spacecraft and Rockets, Vol. 34, No. 2, March-April 1997.
- H. A. Wichman and S. I. Donaldson, "Remote Ergonomics Research in Space: Spacelab Findings and a Proposal," Aviation Space and Environmental Medicine, Vol. 67, No. 2, pp. 171-175, 1996.

EVALUATIONS OF THREE METHODS FOR REMOTE TRAINING

B. Woolford¹, C. Chmielewski², A. Pandya², J. Adolf ², M. Whitmore², A. Berman², and J. Maida¹

¹Flight Crew Support Division, Johnson Space Center, Houston, TX 77058; ²Lockheed Martin, 2400 NASA Road I, Houston, TX 77058

INTRODUCTION

Long duration space missions require a change in training methods and technologies. For Shuttle missions, crew members could train for all the planned procedures, and carry documentation of planned procedures for a variety of contingencies. As International Space Station (ISS) missions of three months or longer are carried out, many more tasks will need to be performed for which little or no training was received prior to launch. Eventually, exploration missions will last several years, and communications with Earth will have long time delays or be impossible at times. This series of three studies was performed to identify the advantages and disadvantages of three types of training for self-instruction: video-conferencing; multimedia; and virtual reality. These studies each compared two types of training methods, on two different types of tasks. In two of the studies, the subjects were in an isolated, confined environment analogous to space flight; the third study was performed in a laboratory.

METHODS

All subjects were civil service or contractor employees of NASA's Johnson Space Center (JSC), and all had technical backgrounds and several years' experience in scientific or engineering positions. The first study was carried out during the Lunar-Mars Life Support Test Project (LMLSTP) Phase IIa. In it, video-conferencing using CU-SeeMe was used for half the training sessions, and self-paced instruction from a multimedia training program was used for the other half. The second study was carried out during the LMLSTP Phase III study, and in this case, multimedia training packages with and without a self-test (simulation) were compared. Finally, the third study was carried out in the Graphics Research and Analysis Facility at JSC. In this case, the multimedia training material with interactive self-test from the previous study was compared with similar training material and a self-test presented through a virtual reality system. In all studies, one task required assembling a piece of equipment (i.e., a leg restraint, body worn blood pressure device, or laptop computer) which the subjects first saw in the disassembled state. The other task required operating an electronic instrument: in the first study, a 1/3 Octave Sound Level Meter was used; in the other two, a Fluke ScopeMeter was used. In all three studies, a 2x2 within subjects design was used, where training method and type of task were counterbalanced.

RESULTS

Both objective and subjective data were collected. In all cases, training time and task performance time were recorded. In all multimedia sessions, the order and frequency with which different features (e.g., diagrams, photos, text, and video) were accessed was recorded automatically. In all cases the performance of the actual task, after training, was observed and videotaped, and number of errors in performing the task was counted. Subjective data included ratings of the instructions, self-test, physical comfort and usability of the virtual reality equipment, and the various ways in which information was conveyed (photos, video, audio, etc.)

In the first test, subjective ratings and performance time both showed 2-way audio-visual training to be superior; however, subjects' comments during debriefs indicated that they felt that they would remember the multimedia training better and longer. In the second test, the self-test option was rated highly. In the third test, significant differences were found in training time and number of errors in the multimedia - virtual reality study, but not in the time to complete the task. Subjects spent more time training with multimedia than with virtual reality, but made fewer errors in the actual task. Subjective ratings and debriefings identified many strengths and weaknesses of training materials in multimedia, and the lack of maturity in virtual reality hardware and software.

CONCLUSION

Remote training will become more and more important in human space flight. Identifying the effectiveness of different features of procedures organization and presentation for individual learning styles and various types of tasks will enable the flight crews to learn to perform new tasks in less time and with less effort. Further evaluations which identify relative benefits of current and new training methods and technologies for different types of tasks and different types of learners should be carried out to prepare for long duration missions.

Bone

Chair

Jay Shapiro, M.D.

Co-Chair

Edward Brown, M.D.

BONE SESSION SUMMARY

Introduction

With the launch of the first components of the International Space Station, the United States enters a new era of extended spaceflight that may eventuate in human exploration of Mars. A considerable, flight-derived database in animals and humans describing the negative response of bone to weightlessness focuses on the risks to astronauts engendered by a progressive loss of skeletal mass. This risk is strengthened by data gained from bed rest studies on earth as well as flight and ground-based studies involving animals or cultured cell lines, several of which were presented in this Workshop. Bone loss in humans averages 1-2%/month during flight. However, the range of the observed loss is wide; the reasons individuals differ in their skeletal response to this alteration in normal gravitational forces is unknown. Age, gender, race, hormone levels and hormone responsiveness and previous patterns of bone strain may determine rates of loss (**Turner**). The early loss of muscle mass and strength is considered to be an important factor leading to bone loss. Moreover, calcium mobilization from skeletal tissues occurs early in flight and increases the risk of renal stone formation. Although analyses of biochemical alterations in serum and urine related to stone formation have been carried out by **Whitson et al.** (presented by Jones), proposed countermeasures to calculus formation have not yet been widely tested.

The broad range of observed bone loss reported during exposure to microgravity raises significant questions about the mechanisms involved in modulating bone remodeling and their susceptibility to control by various factors. Are these likely to be constant from one individual to another, or are different mechanisms involved, perhaps mediated by genetic background or other factors? Research presented at the first Biennial Space Investigators Workshop by 24 principal investigators has concentrated on: 1) enhancing our understanding of the basic mechanisms of bone loss in the setting of weightlessness, which, in turn, will facilitate the development of effective countermeasures, and 2) an evaluation of the efficacy of certain countermeasures that will be available for testing in the near future.

Critical path/ risk outcomes

Four major critical path issues, each associated with significant risk factor outcomes, have been defined by NASA staff in collaboration with NSBRI investigators: These emphasize important questions requiring effective countermeasures before human flight to Mars is realized.

1. Acceleration of age-related osteoporosis.
2. Fracture and impaired fracture healing.
3. Injury to soft connective tissue, joint cartilage and disc rupture.
4. Renal stone formation.

In addition, while not a critical path issue per se, symposium participants expressed concern about the delay in recovery of bone mass following return to earth. Estimates of the risks stated above have not been defined. The following is a crude estimate based on data derived from 6 month Mir flights and applied to a three year flight to Mars, including 2 years of Mars habitation

at 0.38 g: loss in bone density is related to fracture risk as derived at 1G. Estimates may or may not apply to structural alterations aside from bone density per se during extended space flight.

	<u>Bone Loss</u>	<u>% Fracture Risk</u>
Fracture risk outward to Mars	0-12%	5-10%
Fracture risk on Mars	6%	5%
Fracture risk on return flight	0-12%	5-10%
Fracture risk on Earth 1 year post flight	0%	0-20%

Methods of risk assessment

To date, rates of bone loss have been based on comparisons of pre- and post-flight data. Bone loss appears to be site-specific and progressive with continued weightlessness. The return of lost bone following return to earth is delayed in many individuals. Site-specific analysis of bone loss will require the development of new instrumentation to: 1) permit the accurate and sequential determination of bone mass during extended space flight and, 2) to provide information on the effectiveness of countermeasures and their application in a timely manner related to the individual rates of loss. It will also be useful to compare changes in bone density during extended space flight with non-invasive markers of bone turnover and with bone turnover measurement as determined by stable isotopic methods (**Shackelford et al.**).

Techniques based on peripheral quantitative computerized tomography (pQCT) are used to sequentially measure bone mass in hindquarter suspended, rodent models (**Ruff et al.** [reported by Beck], **Bloomfield et al.**). This has facilitated evaluating the effects of mechanical loading as well as those of the bisphosphonate, ibandronate, on bone mass (**Schultheis et al.**, **Ruff et al.** [reported by Beck]). Additional methods presented for evaluating bone changes during rodent hindquarter elevation are histomorphometry and biomechanical testing, including an assessment of the susceptibility to fracture of the femur neck (**Bloomfield et al.**).

The Dual Energy X-ray Absorptiometry (DEXA) project is aimed at design and construction of an advanced x-ray scanner that will measure the effects of microgravity on both bone and muscle during flight and during habitation on extraterrestrial surfaces (**Charles et al.**). Unlike commercial scanners, this instrument will have improved spatial resolution and will avoid the use of two-dimensional projections of three-dimensional bones that limit the precision and accuracy of current scanning systems. This whole body fan-beam DEXA scanner incorporates rotational capability to permit measurements of three-dimensional cross-sectional geometry that are important for estimating fracture risk. Of critical importance are the weight and size of the instrument that is planned for use during flight as well as the radiation dose received by crew during prolonged flight.

Conventional DEXA measurements of BMD has been obtained from astronauts and cosmonauts before and after Mir flights as well as from subjects during 17 weeks of bed rest (**Ruff et al.** [reported by Beck], **Shackelford et al.**). Analysis of geometric properties of the mid-femur in normal aging compared to the Mir crew demonstrated an increased periosteal bone growth during normal aging that did not occur during exposure to microgravity. 3-D finite element analysis is in progress to validate the results of DEXA data in predicting changes in geometry

and structure of bone (**Ruff et al.** [reported by Beck]). Analysis of bone density following the Mir flights has emphasized the difficulty that some crew members experience in regaining bone mass after return to earth's gravity (**Shackelford et al.**).

Studies of the calcaneus have permitted identification of mechanical stimuli, e.g., peak cyclic forces, numbers of loading cycles and loading rate, as contributors to the regulation of bone density (**Whalen**). Furthermore a balloon pressure device has been developed to simulate gravitational force on the lower extremities. This theoretical model points to understanding the effects of earth-equivalent loading and its potential for the maintenance of bone mass during extended space flight. Studies have also focused on measuring mechanical strain threshold for the prevention of bone loss during space flight (**Peterman et al.** [reported by Cavanagh]). External ground reaction forces during 1G and simulated 0-G exercise have been studied using the Penn State zero-G locomotion simulator. A cadaver-based model containing strain gauges has been developed to measure tibial strains during simulated 1-G walking in 1/20th real time speed. Ground reaction forces in human subjects ambulating under simulated zero-G conditions were lower than their 1G equivalents during walking and running. Tibial strains measured in cadaver legs during simulated 1G walking were within the range of physiological strains previously reported by Lanyon et al. (*Acta Ortho Scandinav* 46: 256, 1975). These sophisticated models should provide important information related to the results expected from different exercise regimens during space flight.

Two widely accepted earth bound models for fracture risk assessment are the hindquarter suspension rat and chronic bed rest studies using healthy human volunteers (**Halloran et al.**). As detailed below, the rat model is used extensively in studies of growth factors and hormones (**Bikle et al.**), as well as the effects of alterations in venous flow on bone mass (**Frangos et al.**) and the effects of varied mechanical loading on bone mass in the weighted forelimb and the weightless hindlimb of suspended adult rats (**Schultheis et al.**). Discussion of suitable models included increased utilization of the mouse, which has advantages related to the development of transgenic and knockout models, as well as saving space when caged in space flight (**Kalajic et al.** [reported by Rowe]).

Basic mechanisms

1. Changes in bone formation vs. resorption. Animal studies, especially in male rats, have shown an important contribution of reduced bone formation to microgravity-induced bone loss. **Turner** found, however, that ovariectomized rats exhibit excess resorption that is exacerbated by microgravity and associated with site-specific loss of bone (e.g., from metaphysis but not epiphysis). Thus microgravity-induced bone loss has sex-specific components that must be accounted for in optimizing countermeasures. **Zerwekh et al.** examined the effects of 12 weeks of bedrest on bone histology and markers of bone turnover and calcium homeostasis in 12 normal subjects. In addition to decreases in trabecular osteoblast surface, significant increases occurred in trabecular and cortical eroded surfaces and active osteoclast surface. Markers of resorption increased while those for formation did not change. BMD decreased in lumbar spine, femoral neck and greater trochanter, serum calcium rose slightly and serum iPTH and 1,25(OH)₂D₃ levels fell. Urinary calcium increased by 40%. **Shackelford et al.** made similar observations in their bed rest studies. Thus in humans, increased bone resorption likely

contributes importantly to microgravity-induced bone loss, supporting the use of antiresorptive countermeasures.

2. How do bone and bone cells sense changes in gravitational and other physical forces?

Understanding how bone “senses” physical loading could lead to novel therapies for microgravity-induced bone loss. **Duncan et al.** showed that increased fluid shear elevates the cytosolic calcium concentration (Ca_i) in osteoblasts, in part, by activating a mechanosensitive, cation-selective Ca^{2+} channel. Changes in Ca_i then modify the actin cytoskeleton and, in turn, gene expression. Unexpectedly, maneuvers inhibiting release of intracellular calcium and not calcium channel activity reduced these biological responses. How changes in shear are linked to release of intracellular calcium (i.e., does it involve a cell surface “sensing” mechanism?), however, remains to be identified. **Bergula et al.** (reported by Frangos) explored the role of increased interstitial fluid flow (IFF), e.g., by producing greater fluid shear stresses, as a bone anabolic factor. They used unilateral femoral venous ligation to increase intramedullary pressure and IFF in hindlimb-suspended (HS) rats. Venous ligation substantially increased bone mineral content (BMC) (by ~12%) in the HS rats, supporting a role for IFF in regulating bone remodeling.

3. Microgravity-induced changes in key bone proteins and hormones. What are the consequences of altered physical forces for bone cell function? **Turner** showed that the reduced bone formation in male rats after 9 but not 4 days of space flight is associated with reduced RNA levels for osteocalcin, type 1 collagen and transforming growth factor- β (TGF- β) but not for IGF-1, tumor necrosis factor- α and interleukin-6. These changes are site-specific and reversible - more dramatic reductions occurring in proximal femoral metaphysis than in diaphysis, for example. **Bikle et al.** showed that hindlimb suspension either increases or has no effect on the levels of mRNA and protein for IGF-1, suggesting possible resistance to this skeletal growth factor. In fact, IGF-1 infusion only stimulated bone growth in normally loaded bones. There was similar resistance to growth hormone, while the anabolic effect of PTH persisted in unloaded animals. PTH, however, did not increase the osteoprogenitor pool arising from bone marrow stromal cells (BMSC) of unloaded animals, perhaps because this requires normal IGF-1 action. **Fulford and Gilbertson** found no consistent differences in fibronectin mRNA and protein expression by MC3T3-E1 osteoblasts flown aboard the space shuttle from control, 1G cells aboard the shuttle or ground controls after 27.5 hours. Thus alterations in transcription, translation or extracellular assembly of fibronectin could not explain reduced bone formation in microgravity. **Yamauchi et al.** examined bone proteoglycans in male rats hindlimb-suspended for 1, 4 and 8 weeks. Most proteoglycans were more abundant in suspended bones, including the small collagen-binding proteoglycans, fibromodulin and/or lumican, and might therefore contribute to the reduced mineralization of bone in microgravity. Studies such as those just described may elucidate molecular mechanisms by which the skeletal “mechanostat” modifies bone cell function(s) and bone properties under microgravity.

Several workers presented investigations of the mechanisms controlling osteoblast differentiation/function as a possible basis for reversing reduced osteoblastic function in microgravity. **Partridge et al.** studied the molecular basis for tissue specific and developmental control of collagenase-3 in osteoblasts. Factors regulating this gene include AP-1 and RD binding sites and the osteoblast-specific factor 2 (Osf2) transcriptional regulator. **McCarthy et**

al. studied how hormones raising cAMP (i.e., PGE₂ and PTH) and mechanical loading increase IGF-1 expression via the same transcription factor, C/EBP. Mechanical loading elicits increased PGE₂ production as a key mediator for upregulating IGF-1. **Kalajic et al.** (reported by Rowe) are developing transgenic mouse models expressing a marker gene (e.g., CAT or green fluorescent protein) under the control of fragments of the collagen 1A1 gene (COL1A1) promoter. This approach might enable assessment of transcriptional activities in vivo in specific osteoblastic cell populations. The authors showed the utility of this approach in their analysis of osteoblastic activity in the OIM mouse model of osteogenesis imperfecta.

4. Identification of novel genes whose expressions are altered by microgravity. **Rubin et al.** used differential display polymerase chain reaction (DD-PCR) on RNA from tibiae of 10-day tail-suspended rats to identify two genes upregulated by skeletal unloading. One, S-14, is a known liver gene not previously shown to be expressed in bone; the second, OPO-1 (osteoporosis 1), is a novel gene of unknown function. Thus DD-PCR may enable identification of genes involved in the response of bone to microgravity.

5. Impact of unloading on tendinous insertions of muscle on bone. **Johnson et al.** found increased resorption of cortical bone at tendinous insertions in the hindlimbs of pregnant rats after 11 days of space flight that reduced Sharpey fiber density and decreased cortical thickness, without reducing bone density per se. These changes may weaken tendon-bone junctions of the hindlimbs of pregnant but presumably not those of non-pregnant female or male rats during spaceflight.

6. Additional factors impacting on microgravity-induced bone loss. **Halloran et al.** showed in retrospective studies of flown rats that animals housed singly lost more bone than those housed in groups. Older animals also lost more bone than young, growing rats. The use of Fischer rats and longer space flights were likewise associated with greater bone loss. Future studies must control for such factors as age, single vs. group housing and genetic factors that contribute to microgravity-induced bone loss.

7. Impact of microgravity-induced bone loss on other physiological systems. **Whitson et al.** (reported by Jones) showed that the negative skeletal calcium balance due to microgravity increases urinary calcium excretion by 100 or more mg/day. Risk of renal stone formation during space flight is increased further by reduced fluid intake and resultant diminished urine output as well as decreased urinary pH and citrate, thereby substantially augmenting the risk of forming calcium oxalate, calcium phosphate and, potentially, uric acid stones. Vigorous hydration to increases urinary volume to >2 liters/day reduces stone risk but additional maneuvers preventing net bone loss will be essential to reduce urinary calcium excretion and, presumably, stone risk to preflight levels.

Countermeasures

1. Resistive exercises as well as varying frequency and intensity of loading. **Shackelford et al.** are studying intensive resistive exercises as a countermeasure for bone loss during bed rest. Such exercise regimens mitigate but do not totally prevent bone loss, decreasing loss more in lumbar spine, femoral neck and calcaneus than in greater trochanter. Their

retrospective analysis of bone loss occurring during the Mir flights suggested the importance of vigorous exercise regimens and regaining full muscle strength following return to 1G in maximizing recovery of lost bone. Several investigators are testing novel means of exercising during space flight that mimic partial or full gravitational forces on earth. **Peterman et al.** (reported by Cavanagh) are testing a 0-G locomotion simulator that enables attainment of ground reaction forces within about 30% of those on earth. They are also developing a treadmill suitable for use in space that isolates the spacecraft from the ground reaction forces generated while walking and running. **Whalen** discussed the testing of an apparatus enabling exercise on a treadmill in space under conditions approaching 1G by applying positive pressure to the upper body. Thus there is significant progress in developing exercise regimens that achieve forces approaching 1G that can be maintained during prolonged space flight and would be expected to reduce microgravity-induced bone loss.

Rubin et al. have shown that high frequency, low amplitude mechanical strains may be an effective “surrogate” for musculoskeletal ground reaction forces and could lead to novel countermeasures that do not depend upon the low frequency, high magnitude loading traditionally used to mitigate microgravity-induced bone loss. **Kalajic et al.** (reported by Rowe) also found a non-traditional physical force on the skeleton-shaking rats for 30 minutes daily in an orbital shaker-improved histomorphometric indices in bone. Similarly, **Schultheis et al.** are exploring the efficacy of regimens with varying frequency and amplitudes of ground reaction forces on the forelimbs of hindlimb suspended rats in mitigating bone loss related to skeletal unloading.

2. Pharmacological approaches.

Because of the increased bone resorption during microgravity-induced bone loss, at least in humans, several trials are assessing the impact of inhibitors of bone resorption. **Shackelford et al.** found that the bisphosphonate, alendronate (10 mg/day), essentially totally prevented bone loss in subjects at bed rest for 17 weeks and produced actual increases in BMD in some regions of the skeleton (i.e., spine). In hindlimb-suspended rats, **Schultheis et al.** showed in preliminary results that the bisphosphonate, ibandronate, partially prevented bone loss. **O'Malley et al.** (reported by Brown) are testing the hypothesis that novel pharmacological agonists of the calcium-sensing receptor, vitamin D receptor or estrogen receptor, alone or in combination, increase bone formation and/or reduce bone resorption in models of microgravity, permitting the development of novel receptor-based countermeasures. Studies are planned in hindlimb-suspended animals to test the efficacy of various combinations of these receptor agonists. **Turner** showed that programmed administration of PTH upregulated mRNAs for bone-matrix proteins and exerted an anabolic action that reduced cancellous osteopenia in hindlimb suspended rats. Similar observations were made by **Bikle et al.** in their own studies using PTH infusion; In contrast, these latter workers found that IGF-1 failed to exert an anabolic action in hindlimb suspended rats.

3. Dietary factors.

Increased urinary excretion of sodium can aggravate urinary calcium loss. Therefore, **Arnaud et al.** examined the impact of varying intakes of dietary calcium and salt on BMD in hindlimb suspended rats. Excess dietary salt only reduced total body mineral content when dietary calcium

was restricted, emphasizing the importance of interactions between dietary salt and calcium under specific circumstances with regard to bone health.

Unresolved problems

Extensive discussion at the workshop highlighted several important topics about which new information is required.

1. Basic Mechanisms of Bone Loss:
 - a. Mechanisms of mechanosensing and signal transduction in bone: interaction of mechanical strain and biochemical factors
 - b. Muscle/ bone interaction in strain signal transduction
 - c. Data required on osteoblast/osteoclast function and coupling factors: balance of bone formation and resorption
2. Selection of animal models: sex, age, strain, inbred vs. outbred strains, caging effects on bone loss.
3. Preflight bone profiles: impact on crew selection
 - a. Importance of preflight mechanical strain histories. Applicable risk factors: family history
 - b. Entry bone mineral density
4. Countermeasure Development:
 - a. Magnitude, duration and frequency of mechanical loading required to limit bone loss
 - b. Studies of possible interactions among countermeasures utilized by various teams.
5. Nutrition as an effective countermeasure
6. Mechanisms limiting recovery of bone mass after return:
 - a. applicability to the aging process
7. Technology advances:
 - a. Real time biochemical measurements of bone related and endocrine parameters
 - b. Assessment of structural and biomechanical properties of bone pre- and postflight
8. Artificial Gravity: Can this be developed in time to mitigate bone loss during extended space flight.
9. Investigator access to flight opportunities: The initiation of the International Space Station directs attention validating proposed countermeasures.
10. Access to data on previously completed studies: Many investigators indicate the benefit to be gained when full access to flight data is obtained.

Jay Shapiro and Edward Brown

BONE DENSITY AND HIGH SALT DIETS IN A SPACE FLIGHT MODEL

S. B. Arnaud¹, M. Navidi², M.T.C.Liang³ and I. Wolinsky⁴,

¹Life Sciences Division, NASA Ames Research Center, Moffett Field, California 94035, ²Lockheed Martin Engineering and Science Services, ³Bowling Green State University, Bowling Green, Ohio 43403, ⁴University of Houston, Texas 77204.

INTRODUCTION

High salt diets accelerate bone loss with aging in patients with postmenopausal osteoporosis except when calcium supplementation is provided (Devine et. al. Am. J. Clin. Nutr.,62, 1995). We have observed that the decrease in mineral content of growing femurs in juvenile rats, exposed to a space flight model which unloads the hind limbs, is substantially less in animals fed excess salt (Navidi et. al., J. Applied Physiol. 68,1995). To determine whether excess dietary salt has the same effect on the skeleton of the mature animal whose response to unloading is increased resorption and bone loss rather than impaired growth, we carried out a metabolic study in mature rats with hindlimbs unloaded by tailsuspension.

METHODS

Male Sprague Dawley rats, 6 mo. old and weighing 450-520 g were housed in metabolic cages designed for monitoring food intake, urine and feces (Harper et. al., Lab Animal Science 44, 1994). In the first experiment, half the animals had their hindlimbs unloaded by tail-suspension (S) for 4 weeks and half served as ambulatory controls (C). One set of rats was fed normal dietary salt, 0.26% Na (NC and NS) and a second set was fed 8% dietary salt (HiC and HiS). Dietary calcium (Ca) was 0.5% and phosphorus (P), 0.6%. A second experiment identical to the first was carried out with lower levels of dietary Ca (0.1%) and P (0.3%). Measurements of body weight were determined twice a week and calcium balance each week from dietary, urine and fecal calcium assay. Total body bone mineral content (BMC) was determined by dual photon absorptiometry (Lunar DPXL) and femoral BMC by ash weight of the bone heated to 600° C for 24 H at the end of the week experiments.

RESULTS

Mature rats with unloaded hindlimbs showed 5-9% lower body weights than ambulatory controls irrespective of the level of dietary salt or calcium. Total body BMC was the same in controls fed normal salt diets at each level of dietary calcium, but was 10 percent lower in rats fed 8% salt than in normal. Total body BMC was lower in unloaded than loaded rats only in animals fed 0.1% calcium diets (10.56±0.5 vs. 9.87±0.7g, p<.05). Calcium balances in high salt groups differed according to the level of dietary Ca, averaging -7 to -2 mg/day @0.1% and +17 to +20 mg/day @0.5%. Femoral BMC was less in S than C in each group fed normal dietary salt, irrespective of the level of dietary calcium. However, in rats fed 8% salt diets, femoral BMC was nearly the same in unloaded and control bones (0.511±.04 vs. 0.499±.07g @0.5% and 0.545±.02 vs. 0.535±.05g @0.1%), respectively.

CONCLUSION

In a mature rat model for space flight, excess dietary salt is associated with lower calcium balance and with lower whole body bone mineral content in animals whose dietary calcium is restricted, but not in those fed adequate dietary calcium. The level of dietary calcium does not appear to influence the slightly protective effect of high salt diets on the mineral density in the unloaded femur. There are

differences in the effects of dietary salt on bone which are a function of the level of dietary calcium, an important consideration for protecting bone mass from high dietary salt during spaceflight.

FEMORAL VEIN LIGATION INCREASES BONE MASS IN THE HINDLIMB SUSPENDED RAT

A.P. Bergula¹, W.Huang¹, and J.A. Frangos¹

¹Department of Bioengineering, University of California, San Diego, 9500 Gilman Drive, La Jolla, CA 92093-0412

INTRODUCTION

Bone remodeling in response to changing mechanical demands is well recognized. While it is generally accepted that the local mechanical environment contributes to the physiological maintenance of bone, several studies have suggested a role for interstitial fluid flow (IFF) in bone remodeling. Bone contains a porous network of canaliculi that has been shown to facilitate substantial and rapid transcortical IFF. Flow is steady in the absence of mechanical strain, but bending or compressive loads create pressure gradients which drive fluid from areas of compression to areas of tension. *In vitro* investigations of flow effects on bone demonstrate that fluid shear rapidly stimulates the release of nitric oxide and prostaglandin E₂, two autocrine/paracrine factors associated with remodeling. These results suggest that the fluid shear stresses induced by increased IFF in bone may stimulate bone growth. Consequently, it has been hypothesized that changes in IFF due to intraosseous pressure changes influence bone remodeling. The goal of this study was to investigate the role of IFF in bone *in vivo*; the effect of venous ligation as a means to increase intramedullary pressure and IFF was observed in a model independent of mechanical strain, the hindlimb suspended rat.

METHODS

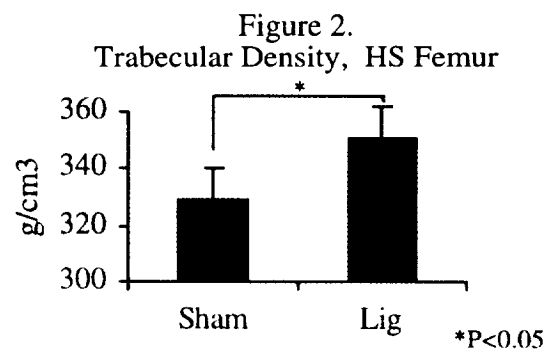
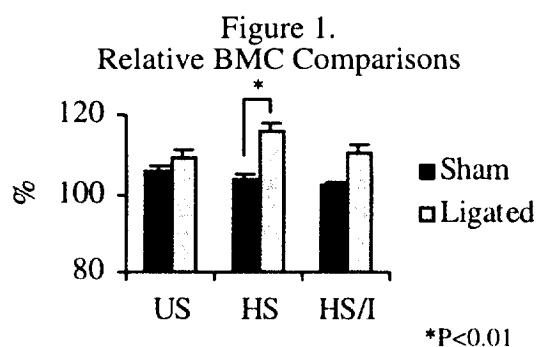
The animal use protocols for these studies were approved by the Animal Subjects Committee at the University of California, San Diego. Forty-one female Sprague Dawley rats were divided into three experimental groups: sixteen rats were hindlimb suspended (HS), sixteen remained unsuspended (US), and nine others were suspended, given indomethacin (a prostaglandin production inhibitor) via drinking water daily (HS/I, 16 µg/ml). For all groups, ligation of one femoral vein was performed on Day (0); the contralateral limb was sham-operated as control. Animals were transferred to suspension cages on Day (2) where they remained, whether subject to suspension or not, for nineteen days. HS and HS/I animals were tail-suspended according to established and widely accepted methodology. Bone mineral content (BMC) and bone mineral density (BMD) were assessed on Days (-2) and (19) using dual energy x-ray absorptiometry. Changes in bone dimensions were monitored with high resolution x-rays taken on Days (-3) and (18). Suspension on Days (18) and (19) was interrupted for as brief a time as possible by periods of anesthesia required for DEXA and x-ray procedures; the animals were immediately resuspended following recovery. Femurs and tibias were excised at the time of sacrifice on Day (21). Trabecular density of the HS femurs was subsequently analyzed by Skeletech, Inc. (Seattle, WA). Marrow pressure in the venous ligated and control femurs was also measured just prior to sacrifice in five US rats to confirm an increase in intramedullary pressure induced by the venous ligation procedure. Tasks were separated to ensure that all measurements and statistical analyses were performed blind. Two-way ANOVA was used for the comparison of multiple independent groups. Paired T-tests were used where appropriate, as in direct comparison of sham vs experimental limbs within particular groups. Significance was defined as $P < 0.05$.

RESULTS

Marrow pressure in the ligated femur (27.8 ± 3.1 mm Hg) at the time of sacrifice was consistently and significantly greater versus the contralateral sham (unligated) femur (16.4 ± 3.1 mm Hg). Histological examination of the surrounding thigh muscles revealed no evidence of swelling or compartment syndrome due to venous ligation. No qualitative morphological difference between the muscle tissue from the sham and venous ligated limbs was noted, suggesting that the effect of venous ligation was limited to the increase in marrow pressure.

Two-way ANOVA was used to determine the relative changes occurring in the femurs with regard to the effects of suspension and venous ligation. No interaction effect was observed for any comparison of relative change in any measured parameter; thus, any significant effect induced by ligation was independent of suspension. Suspension significantly decreased relative BMD ($P < 0.01$), relative proximal width ($P < 0.01$) and relative diaphyseal width ($P < 0.01$). Suspension also significantly decreased BMC. Relative BMC for the sham femur of the HS rat was smaller in comparison to the relative BMC of the US rat, suggesting bone loss induced by suspension. Venous ligation, on the other hand, appeared to have a stimulatory effect, associated with significant increases in body weight-adjusted BMC ($P < 0.05$) and length ($P < 0.01$).

The most pronounced changes induced by venous ligation were observed in the HS rat. When normalized to body weight, the relative BMC of the venous ligated limb was significantly greater than the contralateral sham limb ($115.9 \pm 15.6\%$ vs $103.8 \pm 13.2\%$, Figure 1). Furthermore, the BMC increase of the venous ligated femur in the HS rat was greater than the increases observed for both the venous ligated ($109.1 \pm 14.5\%$) and sham ($105.8 \pm 16.8\%$) femurs of the US rat (Figure 1). Relative length ($106.2 \pm 2.1\%$ vs $104.5 \pm 2.1\%$, $P < 0.05$) and relative distal width ($110.8 \pm 10.3\%$ vs $106.2 \pm 8.2\%$, $P < 0.05$) of the venous ligated limb in the HS rat were also significantly greater compared with the sham limb. Trabecular density as assessed by pQCT was found to be significantly greater in the femur with venous ligation than the contralateral sham limb (351 ± 12 g/cm³ vs 329 ± 11 g/cm³, Figure 2).



Two-way ANOVA was also performed to determine the effect of indomethacin in the HS group. No significant differences were observed. Indomethacin did not appear to affect bone adaptation in the HS rat. However, while indomethacin did not block a relative increase in BMC (Figure 1), the length increase for the venous ligated femur relative to the sham limb was eliminated by drug treatment ($104.4 \pm 2.8\%$ • $104.5 \pm 2.2\%$).

CONCLUSION

The aim of our study was to determine if IFF changes in bone could influence skeletal adaptation independent of mechanical strain. Femoral vein ligation was performed to increase femoral marrow pressure and IFF. The animals were suspended to eliminate load-induced strain on the hindlimbs. Bone adaptation was assessed by direct measurements of BMC, BMD, trabecular density, and femur dimensions. These mass, density and morphological changes were used as indicators of bone remodeling activity. Our results show that femoral vein ligation stimulated increases in BMC, trabecular density, length, and distal width in the femurs of HS rats. These stimulated increases were consistent with observed increases in intramedullary pressure.

In this study, the increases in IFF are likely to have resulted from an increase in marrow pressure induced by venous ligation. Femoral vein occlusion has previously been shown to result in an increase in intramedullary pressure. We found that bone marrow pressure in the femur with venous ligation was significantly greater relative to the contralateral sham control. This suggests a significant increase in marrow pressure and IFF induced by venous ligation that was sustained over the course of the experiment. The observed differences between sham and venous ligated limbs can be related to the difference in bone marrow pressure influencing IFF. Histological examination of the surrounding muscle tissue revealed no evidence of pooling or similar qualitative pathology (i.e. compartment syndrome) in the venous ligated limb relative to sham. This indicated that there was no pooling of fluids or edema in the venous ligated limb and provides indirect evidence that venous ligation did not affect the pressure in the surrounding muscle tissue and on the periosteal surface of the bone. While pressure at the bone surface remained constant, marrow pressure in the venous ligated limb was significantly increased. It follows, therefore, that IFF in the venous ligated limb relative to the sham limb was significantly increased due to the increased pressure drop across the bone. Increased IFF has been suggested as a mediator by which a mechanical stimulus is transduced into a mitogenic signal for remodeling.

The role of IFF in bone adaptation independent of mechanical strain was examined with the HS rat. Hindlimb suspension has long been used as a model of disuse and simulation of weightlessness in spaceflight. Skeletal unloading has been shown to result in marked bone loss, impairment of BMD increase, and reduction in trabecular bone volume. Two-way ANOVA comparisons between HS and US rats revealed that suspension led to significant decreases in relative BMC and BMD. Protection from suspension-induced bone loss, however, was provided by venous ligation. Venous ligation promoted growth and/or maintenance of both cortical and trabecular (cancellous) bone despite the effects of suspension. Increases in BMC, length, width, and trabecular density associated with venous ligation occurred independent of suspension effects. The increases measured in the venous ligated femur of the HS rat strongly suggest a role for IFF in bone remodeling.

This study has demonstrated that venous ligation increases bone mass in the hindlimb suspended rat. Venous ligation was performed as a means to increase IFF in bone. This study is the first to investigate the effects of IFF uncoupled from mechanical strain on bone adaptation *in vivo*. Venous ligation in a hindlimb suspended rat was able to restore and exceed the normal relative BMC observed in an age-matched ambulatory animal. Trabecular density of the venous ligated femur in the HS rat was also found to be significantly greater than the contralateral sham control. Furthermore, venous ligation influenced bone shape (length, width). The protective effect of venous ligation was seen in the absence of mechanical strain and appears to be fluid flow-mediated. The mechanism of fluid flow effects should be evaluated in further experiments. The

current study suggests that IFF can directly influence bone adaptation independently of mechanical loading and supports the hypothesis that fluid flow modulates bone remodeling.

THE EFFECT OF SKELETAL UNLOADING ON BONE FORMATION: ROLE OF IGF-I

D.D. Bikle¹, P. Kostenuik¹, E.M. Holton², B.P. Halloran^{1,2}

¹Veterans Affairs Medical Center and University of California, San Francisco, CA and ²NASA-Ames, Moffett Field, CA

INTRODUCTION

The best documented change in bone during space flight is the near cessation of bone formation. Space flight leads to a decrease in osteoblast number and activity, likely the result of altered differentiation of osteoblast precursors. The net result of these space flight induced changes is weaker bone. To understand the mechanism for these changes poses a challenge. Space flight studies must overcome enormous technical problems, and are necessarily limited in size and frequency. Therefore, ground based models have been developed to evaluate the effects of skeletal unloading. The hindlimb elevation (tail suspension) model simulates space flight better than other models because it reproduces the fluid shifts seen in space travel, is reversible, and is well tolerated by the animals with minimal evidence of stress as indicated by continued weight gain and normal levels and circadian rhythms of corticosterone. This is the model we have used for our experiments.

Skeletal unloading by the hindlimb elevation method simulates a number of features of space flight in that bone formation, mineralization, and maturation are inhibited, osteoblast number is decreased, serum and skeletal osteocalcin levels fall, the ash content of bone decreases, and bone strength diminishes. We and others have shown that when osteoblasts or osteoprogenitor cells from the bones of the unloaded limbs are cultured in vitro they proliferate and differentiate more slowly, suggesting that skeletal unloading causes a persistent change in cell function which can be assessed in vitro. In contrast to the unweighted bones of the hindlimbs, no significant change in bone mass or bone formation is observed in the humeri, mandible, and cervical vertebrae during hindlimb elevation. The lack of effect of hindlimb elevation on bones like the humeri, mandible, and cervical vertebrae which are not unloaded by this procedure suggests that local factors rather than systemic effects dominate the response of bone to skeletal unloading.

We have focussed on the role of IGF-1 as the local factor mediating the effects of skeletal unloading on bone formation. IGF-I is produced by bone cells and chondrocytes; these cells have receptors for IGF-I, and respond to IGF-I with an increase in proliferation and function (e.g. collagen, and glycosaminoglycan production, respectively). IGF-I production by bone is under hormonal control, principally by GH and PTH, and IGF-I is thought to mediate some if not all of the effects of GH and PTH on bone growth.

Thus, systemic changes in hormones such as GH and PTH may still have effects which vary from bone to bone depending on the loading history.

METHODS AND RESULTS

When we measured the effects of skeletal unloading on IGF-I we observed that the mRNA and protein levels of IGF-I are either increased or unchanged during hindlimb elevation. This was a surprise, but we also observed similar changes in IGF-I mRNA levels in the bones of flight rats.

The increase in IGF-I mRNA and protein during skeletal unloading suggested to us the possibility that skeletal unloading leads to an initial resistance of the bone to IGF-I. Infusion of IGF-I was then shown to stimulate bone growth only in the normally loaded bones. Similar resistance was found to GH during skeletal unloading, although GH was at least as effective in stimulating the mRNA levels of IGF-I, alkaline phosphatase, osteocalcin and procollagen in the unloaded bones as in the normally loaded bones. PTH, on the other hand, stimulated bone formation even in the unloaded animals. However, its ability to increase the osteoprogenitor pool in subsequently isolated bone marrow stromal cells (BMSC) was blocked by skeletal unloading. Since PTH does not directly stimulate BMSC proliferation when added to BMSC cultures in vitro, unlike IGF-I, we hypothesized that PTH increased the osteoprogenitor population in vivo via a mechanism requiring IGF-I. In support of this hypothesis we found that BMSC from unloaded bones were resistant to the proliferative action of IGF-I. Thus skeletal unloading alters different aspects of the anabolic effects of PTH and GH on bone, but the common denominator may be skeletal resistance to IGF-I.

CONCLUSION

Resistance to IGF-I during skeletal unloading may account for the reduction in bone formation during skeletal unloading, and explain the resistance of bones to the anabolic actions of PTH and GH during the unloaded state.

ALTERATIONS IN pQCT-DERIVED BONE GEOMETRY AND DENSITY VERSUS MECHANICAL STRUCTURAL PROPERTIES OF THE FEMORAL NECK IN SENESCENT RATS

S.A. Bloomfield¹, H.A. Hogan², E.T. Dresser¹, and J.A. Groves²

Departments of ¹Health & Kinesiology and ²Mechanical Engineering, Texas A&M University, College Station, TX 77843-4243

INTRODUCTION

Few data are available on the relationship of bone morphometry and bone mineral density (BMD) to mechanical properties of the femoral neck in senescent rats. Therefore, we studied femoral neck bone excised from young adult and senescent male Fischer rats using peripheral quantitative computed tomography (pQCT), followed by 3-point bending to failure to determine structural mechanical properties.

METHODS

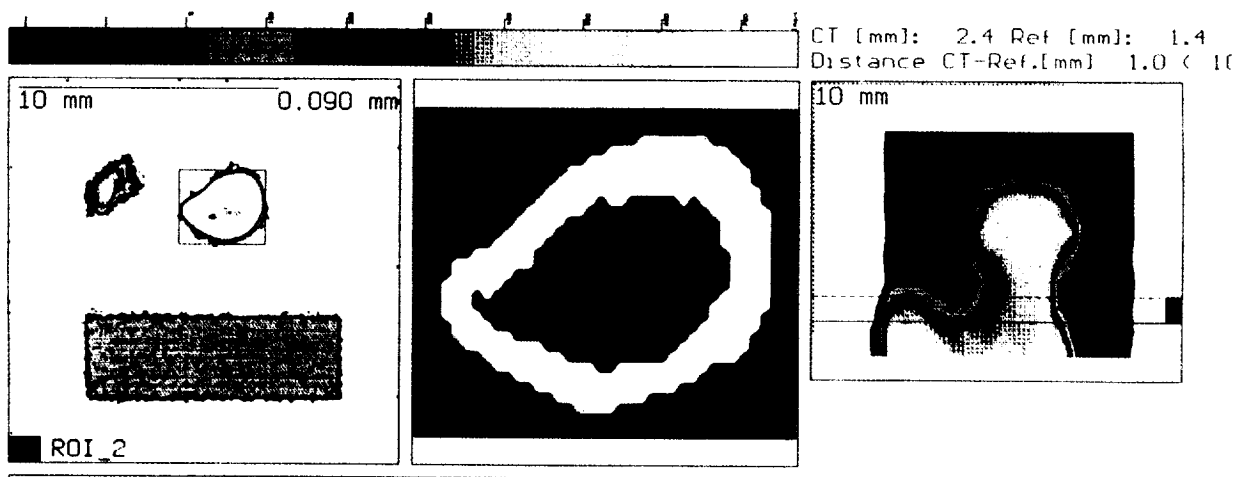
We studied 6-month-old (n=8) and 24-month-old (n=8) male Fischer rats using peripheral quantitative computed tomography (pQCT; Stratec XCT-Research SA, Norland Corp.). A single slice located at the center of the femoral neck perpendicular to its long axis (see figure below) was assessed for volumetric BMD (in mg/cm^3) and for area of the entire bone as well as for cortical and trabecular bone areas. Polar strength-strain index (SSI_p ; estimates torsional bone strength), section modulus, and polar cross-sectional moment of inertia for total bone were calculated from area and density values. Bones were then subjected to mechanical testing with an Instron 1125 device. With the femoral shaft fixed vertically, quasi-static loading was applied to the femoral head parallel to the femur's long axis at 2.54 mm/min. Maximal load at fracture and stiffness were calculated from the load-displacement curve. Means (\pm S.E.) for the two groups were compared by unpaired t-tests.

Figure: pQCT analysis of femoral neck of 24-month-old male Fischer rat

A. Region of interest box: femoral neck slice

B. Cortical shell of femoral neck

C. Scout view: slice taken at dotted line



RESULTS

Detailed in the table below are results of the pQCT and mechanical testing of femoral necks in adult and senescent male rats.

Variable	6-mo-old	24-mo-old	p value	
CRT BMD (mg/cm ³)	1209 ± 22	1220 ± 32	0.79	
CRT area (mm ²)	2.99 ± 0.12	3.35 ± 0.17	0.11	
TRB BMD (mg/cm ³)	822 ± 17	650 ± 43	0.002	
TRB area (mm ²)	1.26 ± 0.05	1.35 ± 0.10	0.42	
Total BMD (mg/cm ³)	1098 ± 16	1048 ± 29	0.16	
Total bone area (mm ²)	4.62 ± 0.13	5.12 ± 0.18		0.04
SSI _p (mg/cm ³)	1.98 ± 0.06	2.20 ± 0.14	0.16	
Section modulus (mm ³)	2.38 ± 0.10	2.67 ± 0.12	0.09	
CSMI _p (mm ⁴)	3.36 ± 0.16	4.12 ± 0.19	0.009	
MAX load (N)	105.8 ± 3.5	130.3 ± 4.8	0.002	
Stiffness (N/mm)	102.7 ± 10.3	155.8 ± 7.9		0.004

CRT= cortical; TRB=trabecular; BMD=bone mineral density; SSI_p = polar strength-strain index; CSMI_p = polar cross-sectional moment of inertia; MAX= maximal.

Direct measurement of structural properties shows that maximal load is higher by 23% and stiffness by 52% in older rats, even as trabecular volumetric BMD declines by 21%. Multiple linear regression analyses of pooled data suggest that variations in femoral neck morphometry (i.e., CSMI_p) are largely responsible for the higher maximal load and stiffness of femoral necks in aged male rats, and that alterations in trabecular bone mineral density of the femoral neck minimally affect its strength.

CONCLUSIONS

Because many of the changes observed with prolonged spaceflight parallel those observed with aging, these data pose the intriguing question: can bone strength be maintained effectively in the face of significant declines in bone mineral density, given mechanically advantageous changes in bone geometry? Certainly, the timeline with even long-term spaceflight is quite a bit shorter than the decades of time that might be required to produce significant increases in CSMI. We also do not know if there is a gender difference in geometry of bone in aging rats, as has been suggested for humans^{1,2}. These techniques will be applied to adult male rats subjected to 3-28 days of hindlimb unloading to follow changes in cortical and trabecular components of femoral neck bone, total bone geometry, and structural mechanical properties with simulated microgravity.

REFERENCES

1. Beck TJ, Beck CB, Scott WW Jr., Plato CC, Tobin JD and Quan CA. Sex differences in geometry of the femoral neck with aging: a structural analysis of bone mineral data. *Calcif. Tissue Int.* 50: 24-29, 1992.
- Mosekilde L and Mosekilde L. Sex differences in age-related changes in vertebral body size, density and biomechanical competence in normal individuals. *Bone* 11:67-73, 1990.

COMPACT, HIGH PRECISION, MULTIPLE PROJECTION DEXA SCANNER FOR MEASUREMENT OF BONE AND MUSCLE LOSS DURING PROLONGED SPACEFLIGHT

H. K. Charles, Jr.¹, T. J. Beck,² H. S. Feldmesser,¹ T. C. Magee,¹ and V. L. Pisacane¹

¹The Johns Hopkins University Applied Physics Laboratory, Laurel, Maryland 20723-6099

²The Johns Hopkins University School of Medicine, Baltimore, Maryland 21287

INTRODUCTION

The purpose of the Dual Energy X-ray Absorptiometry (DEXA) project is to design, build, and test an advanced X-ray absorptiometry scanner capable of being used to monitor the deleterious effects of weightlessness on the human musculoskeletal system during prolonged spaceflight. The instrument is based on the principles of dual energy X-ray absorptiometry and is designed, not only to measure bone mineral density and volume and to decompose soft tissue into measurements of fat and lean mass but also, to use those measurements to derive structural properties (cross sections, moments of inertia) permitting an assessment of the biomechanical consequences of microgravity on bone and/or muscle mass and the potential risk upon returning to planetary gravity levels. Multiple projection technology, coupled with axial translation, will be employed to provide geometric properties in three dimensions suitable for a three-dimensional structural analysis of the scanned region. The structural analysis will then be combined with bone models and projected loading scenarios to determine risk of fracture. The instrument will employ advanced fabrication techniques to minimize volume and mass (100 kg current target with a long-term goal of 60 kg) of the scanner as appropriate for the space environment, while maintaining the required mechanical stability for high-precision measurement. The unit will have the precision required to detect changes in bone mass and geometry as small as 1% and changes in muscle mass as small as 5%.

RESEARCH STATUS

From the earliest experience with prolonged weightlessness, it has become known that the elimination of gravitational effects on the human body produces an adaptation response resulting in the wasting of body skeletal muscle and bone mass. These musculoskeletal effects are somewhat complex because the stimuli for maintaining homeostasis of muscle and bone appear to be different; moreover, there also appear to be differences between losses in weight bearing and non-weight bearing body regions. Bone mass lost from the vertebrae, pelvis, and proximal femur average between 1 and 1.6% per month. This loss magnitude should be contrasted to the loss from these sites of about 0.8 to 1.3% per year in postmenopausal women, and it is highly associated with increased bone fragility. The ultimate concern is that the loss of mass will lead to degradation in mechanical competence and possible failure. With restricted access to medical treatment during prolonged space travel, bone fracture may prove to be catastrophic, especially since healing rates in the absence of mechanical stimulus (load) are believed to be degraded. Clearly, effective countermeasures to stem the loss as well as some method for dynamically monitoring countermeasure effectiveness are required.

METHODS

While measurements of bone and muscle mass are statistically correlated with mechanical strength, they are not direct measurements of strength and cannot be directly employed in any

conventional engineering analysis. As currently configured, bone and muscle mass measurements (via conventional DEXAs or ultrasound) involve regional averaging which obscures structural details. Clearly, the mechanical consequences of lost bone and muscle mass are exhibited in the structure. To directly assess the biomechanical consequences of weightlessness, some absolute determination of skeletal mechanical competence is needed to supplement the conventional mass measurements. Engineering properties of the bones can be derived from bone mass data using DEXA techniques. The method is based on geometrical methods (cross-sectional areas, moments of inertia, and bending moments) derived from the bone mass image.

RESULTS

Work in our laboratory using commercial DEXA scanners has shown that bone strength defining details underlying observed changes in bone mass due to age, disuse, and microgravity are evident in the structural geometry; i.e., the quantification of bone size and shape. Commercial DEXA scanners can be used to measure geometry from mass data and image dimensions but are optimized for measurement of bone mass, not geometry. Poor spatial resolution and constraints of two-dimensional projections of three-dimensional bones limit precision and accuracy of current systems. A whole body fan-beam DEXA scanner was therefore designed specifically for bone geometry measurements. The scanner is based on a kV/filter switching X-ray generator and a high resolution, high quantum efficiency detector. Several different detector schemes are under consideration, including a conventional fan-beam scintillator-photodiode array, a high-quantum efficiency scintillator-coupled array of charge-coupled devices (CCDs), and a flat-panel detector based on amorphous silicon diode arrays.

The design incorporates rotational capability to provide multiple projections so that complex cross-sectional geometry can be evaluated in three dimensions. Algorithms for the derivation of three-dimensional geometry from as few as three projections have been implemented. A theoretical analysis of performance indicates that bone mass precision will exceed that of commercial DEXA systems, and spatial resolution should be better than three-line pairs/mm in the patient. Scanning attributes are incorporated to make measurement precision nearly independent of patient thickness.

A full-size bench-top test bed of the scanner has been constructed for testing of principles and experimental verification of simulations. The prototype incorporates a high-precision rotation and translation stage to provide scanning capability. Full-scale performance with a field width of 35 cm will require completion of the multi-module detector array, but assembly of a single CCD module has been completed and testing has begun. The single CCD will permit optimization of signal performance under simulated patient conditions, as well as experimental verification of theoretical performance characteristics. System performance data has been collected and is compared to both theoretical predictions and commercial scanner performance. Images of human cadaver hip and spine specimens together with mass and geometric measurements under simulated in vivo conditions will also be presented.

CONCLUSION

A compact, high precision, multiple projection DEXA scanner system is being built to accurately measure bone and muscle loss during prolonged spaceflight. The availability of such a system

offers significant potential for fostering future musculoskeletal research in a number of disciplines.

FUTURE PLANS

Evaluation of other detector designs will be completed during the next few months. Finalization of the high-voltage, power supply design will also be accomplished. Completion of these two items will allow detail design of the structure and control hardware and software to be developed. While final electronic and mechanical designs are being completed and construction of the hardware prototype is continuing, the test bed will be used to (1) further develop analysis algorithms, (2) develop the appropriate inputs for bone modeling software, and (3) validate the inputs and links to the risk of fracture information development activity.

The ready availability of a highly accurate DEXA will significantly aid in the development of countermeasures. The real-time feedback available to the astronauts and ground-based doctors from the spaceflight version would be a significant help to today's clinician trying to assess the efficacy of a particular countermeasure. Because of the accurate quantitative measurements made by our DEXA, even small improvements in remediation could be observed.

Since it is likely that people in long-term spaceflight might need additional diagnostic imaging capabilities, we will attempt to include additional features in the DEXA scanner. Conventional planar radiographic capability could be built into the scanner and would assist astronauts and earth-based medical personnel in diagnosing and monitoring fractures and other disease states that are imageable. Further work could be done to build in CT capability to extend this unit's utility.

Commercially, if cost projections could be realized, there is a significant market for population screening and treatment monitoring of osteoporosis in postmenopausal women. It is believed that a compact, easy-to-use, portable instrument could be developed for the small clinic or doctor practice. The market for this is several hundred to several thousand units, depending on final cost. We intend to continue our discussions with medical device and instrumentation firms regarding the commercial potential. Structuring the scanner as a ground-based, transportable unit has large implications for use as a tool in nursing homes, clinics, and medical offices.

THE ROLE OF CALCIUM IN THE RESPONSE OF OSTEOBLASTS TO MECHANICAL STIMULATION

R.L. Duncan^{1,2}, M.C. Farach-Carson³ and F.M. Pavalko²

Dept. of ¹Orthopaedic Surgery, ²Physiology and Biophysics, Indiana University Medical Center, Indianapolis, IN and ³Dept. of Biological Sciences, University of Delaware, Newark, DL.

INTRODUCTION

A major biomedical concern in the exploration and development of space is the rapid loss of bone associated with extended periods of spaceflight. Mineral content, bone formation, matrix protein production and total body calcium are all reduced during long-term periods of weightlessness. These effects of weightlessness appears to be due to decreases in the anabolic function of osteoblasts and osteocytes rather than changes in the resorptive activity of osteoclasts. Conversely, subjecting the skeleton to exogenous mechanical loading increases matrix protein synthesis and bone formation rate, a process which also appears mediated through osteogenic cells. Osteoblasts have been shown to respond to a number of types of mechanical stimulation. However recently we have demonstrated that osteoblasts respond to fluid shear, but not physiologic levels of mechanical strain, with increases in expression of the matrix protein, osteopontin. We have also shown similar responses in other markers for the anabolic response in bone. The expression of the early response gene, c-fos, and the inducible-isoform of the prostaglandin synthetic enzyme, cyclooxygenase-2 (COX-2), both increase rapidly in response to fluid shear, but not strain.

How osteoblasts and osteocytes perceive mechanical stimuli and convert this stimulus into a biochemical event within the cell is still unknown. However, examination of the cellular events following mechanical stimulation indicate that two of the earliest responses are a rapid increase in intracellular calcium ($[Ca^{2+}]_i$) and a reorganization of the actin cytoskeleton. The increase in $[Ca^{2+}]_i$ is dependent on the presence of extracellular Ca^{2+} , suggesting the activation of membrane Ca^{2+} channel. We have previously characterized a mechanosensitive, cation-selective channel (MSCC) in osteoblast-like clonal cells, which we postulate is important in this early response to mechanical loading. Using an antisense oligodeoxynucleotide strategy, we have tentatively identified this channel as an isoform of the α_{1C} subunit of the dihydropyridine-sensitive, voltage sensitive Ca^{2+} channel (VSCC). However, a major component in this mechanically induced rise in $[Ca^{2+}]_i$ is the release of Ca^{2+} from intracellular stores. The actin cytoskeleton also rapidly responds to fluid shear with an increase in stress fiber formation and a realignment of the cell parallel to the direction of flow. To ascertain whether these two observations are related and how they effect shear-induced gene expression, we examined the role of Ca^{2+} channels and intracellular Ca^{2+} release on cytoskeletal reorganization and the resultant increases in the expression and production of c-fos and COX-2 in response to fluid shear.

METHODS

Application of fluid shear: MC3T3-E1 cells, an osteoblast-like, non-transformed cell line, were grown on fibronectin-coated glass slides. Once the cells had reached confluency, the slide was mounted on a parallel plate chamber which subjects the cells to uniform laminar flow across the plate. During the flow experiments, cells were maintained at 37°C with the flow media pH held constant by aeration with 95% air/5% CO₂. Flow was kept constant at 12 dynes/cm² for the duration of the experiment.

Determination of membrane Ca^{2+} channel functional and molecular expression: Following 1, 2 and 3 hours of shear, slides were removed from the flow chamber and broken to fit into the patch chamber. Slide shards were bathed in normal Na^+ Ringers' containing 5 mM TEA to suppress K^+ channel activity and MC3T3-E1 cells were patched using the whole cell patch configuration to determine whole cell currents. Once basal whole cell currents were determined, the cell was hypotonically challenged with an hypotonic Na^+ Ringers' solution and whole cell current changes ascertained. The MSCC component of this current was determined by adding 10 μ M $GdCl_3$ to the Ringer solutions 5 min prior to hypotonic challenge. The VSCC component was determined by addition of the dihydropyridine antagonist of the VSCC, nifedipine (5 μ M). Calcium entry into the sheared cells were tested with an intracellular imaging system using fura-2 loaded cells, which fluorescently detects $[Ca^{2+}]_i$.

To determine the molecular expression of the VSCC α_{1C} subunit in response to various intervals of shear, primers were designed to amplify a 246 bp region of the α_1 subunit cDNA called +2514/-2759. This region is located 5' to the isoform specific region of the cDNA encoding the IV transmembrane segment. An internal standard cDNA is used routinely for competitive, quantitative PCR. This standard was generated by PCR using an upstream primer of 40 bp designed to anneal to two 20 bp regions of the α_1 subunit cDNA located 100 bp apart. By performing PCR under low stringency conditions (50°C annealing) the cDNA generated by this mutagenic method contains sequences identical to the target (VSCC) cDNA, each of which are recognized by both the +2514 and the -2759 primers, thus serving as a competitor to the endogenous target. The competitor cDNA, denoted M146, and the target cDNA amplification products can then be readily distinguished by size on autoradiographs of polyacrylamide gels. Plots of competitor/target vs. competitor concentration provide linear data for regression analysis that can be used to quantitate and compare mRNA levels encoding VSCC α_1 subunit present in various samples.

Determination of c-fos and COX-2 and actin cytoskeletal changes following shear: Following application of shear, cells were fixed in 4% paraformaldehyde and processed for immunofluorescence using 1^o and 2^o antibodies against c-fos and COX-2, rhodamine-phalloidin or FITC-phalloidin. Images were recorded on Tmax 400 film using a Nikon Optiphot II microscope. To determine the expression of c-fos and COX-2, tRNA was isolated immediately following application of shear and Northern analyses conducted. To determine the effects of Ca^{2+} channels and intracellular Ca^{2+} release, various channel and release inhibitors were introduced 30 min prior to application of shear and kept in the shear solution for the duration of loading.

RESULTS

Functional and molecular expression of Ca^{2+} channels: Whole cell patch clamp studies found that non-loaded control MC3T3-E1 cells exhibit very small, voltage insensitive currents when challenged with hypotonic Ringers'. However, when MC3T3-E1 cells were subjected to shear, a 7-fold increase in whole cell currents were observed. When Gd^{3+} was added prior to hypotonic challenge, approx. 68% of the hypotonically-induced whole cell currents were inhibited. Less than 10% of the hypotonic-induced current could be inhibited with nifedipine. Intracellular Ca^{2+} measurements using fura-2 correlated with these data to show that approx. 50% of non-loaded MC3T3-E1 cells (54/106) responded to hypotonic challenge with a peak $[Ca^{2+}]_i$ transient of 180nM. Sheared MC3T3-E1 cells were significantly more responsive, with 88% (67/76) of the

cells responding to challenge. Peak $[Ca^{2+}]_i$ transients were also substantially higher ($[Ca^{2+}]_i = 240nM$). These increases in $[Ca^{2+}]_i$ were in response to increased MSCC activity since addition of $10 \mu M Gd^{3+}$ totally abolished the transient response.

Examination of the molecular expression of the α_{1C} subunit of the VSCC using rt-PCR techniques found low levels in expression of this subunit in non-loaded cells. However when MC3T3-E1 cells were sheared for 2-24 hours, α_{1C} expression was increased 3-5 fold within four hours of initiation of shear.

Ca²⁺ regulation of actin cytoskeletal reorganization and gene expression: As we have shown previously, MC3T3-E1 cells subjected to shear maximally expressed c-fos and COX-2 at 0.5 and 3 hr, respectively. Accompanying this increase in expression is a dramatic increase in actin stress fiber formation. Disruption of stress fiber formation using a variety of means completely abrogates this increase in gene expression. To determine the role of $[Ca^{2+}]_i$ in this response to shear, the intracellular Ca^{2+} chelating agent, BAPTA-AM was introduced to the cell prior to application of shear. This treatment completely abolished the actin stress fiber formation and c-fos and COX-2 expression in MC3T3-E1 cells subjected to shear. However, inhibition of channel activity with either Gd^{3+} or nifedipine failed to block either the cytoskeletal response or the increase in gene expression. When intracellular Ca^{2+} stores were depleted with thapsigargin, actin stress fiber formation and gene expression was ablated. Inhibition of IP_3 -induced intracellular Ca^{2+} release via block of the phospholipase C pathway by neomycin also inhibited these responses.

CONCLUSIONS

These data indicate that fluid shear increases both MSCC activity and expression. However, these studies also demonstrate IP_3 -mediated intracellular Ca^{2+} release is essential to the shear-induced increase in expression of factors associated with anabolic responses in bone. It is unclear how the phospholipase C pathway is activated by shear. It is also unclear what role mechanosensitive channels play in mechanotransduction, since these data indicate that Ca^{2+} entry via these channels has no effect on marker expression. However, activation of these channels could be important in the signal amplification of mechanical stimulus by increasing secretion of factors to stimulate surrounding cells.

(Supported by NASA: NAG5-4917)

EFFECT OF SPACEFLIGHT ON EXTRACELLULAR MATRIX IN OSTEOBLASTS GROWTH ACTIVATED UNDER MICROGRAVITY CONDITIONS

M.H. Fulford and V. Gilbertson, Laboratory of Cell Growth, Department of Medicine, University of California and VA Medical Center, San Francisco, CA 94121

INTRODUCTION

To determine critical molecular events in osteoblast growth in spaceflight MC3T3-E1 osteoblasts were used to examine fibronectin (FN) mRNA levels, protein synthesis and FN extracellular matrix accumulation after growth activation in microgravity. FN is known to regulate adhesion, differentiation and function in adherent cells. We paid particular interest to the extracellular matrix since several investigators have reported in vivo and in vitro changes in osteoblast growth and cell shape in flight. To characterize fibronectin's role in these changes, quiescent osteoblasts were sera activated in microgravity with or without a 1-G gravity field. After activation and collection in spaceflight, samples were analyzed on ground. We were able to measure both transcription and translation of extracellular matrix genes in flown 0-g, 1-g conditions and in ground samples.

METHODS

Early passage quiescent MC3T3-E1 osteoblasts were launched on the shuttle and then sera activated in microgravity. Cells were grown on coverslips in Biorack Plunger boxes. Cells were placed in guanidium thiocyanate (GITC) solution after 2.5 and 27.5 hours. GITC lysates were then placed in the freezer for later ground analysis. Analysis included isolation and rtPCR of RNA as well as collection of protein and identification of protein on Western blot. Cell matrix morphology was also examined.

RESULTS

Two and a half hours after activation there were significant reductions in both FN mRNA synthesis and total protein when compared to either the on-board 1-G or ground control samples. After 27.5 hours, there were no significant differences between the various gravity conditions for either the FN message or protein. However, at 27.5 hours the FN message was increased 2 fold and the protein increased 4 fold over the 2.5 hour samples. Using immunofluorescence, we found no significant differences in the amount or orientation of the FN matrix after 27.5 hours in microgravity.

CONCLUSION

These results demonstrate that FN is made routinely in growth activated osteoblasts during exposure to microgravity. These data also suggest that in long term spaceflight fibronectin transcription, translation or altered matrix assembly is not responsible for the altered cell shape or altered matrix formation of osteoblasts.

EFFECTS OF SPACEFLIGHT ON BONE: THE RAT AS AN ANIMAL MODEL FOR HUMAN BONE LOSS

B. Halloran¹, T. Weider¹, and E. Morey-Holton²

¹University of California, San Francisco, CA 94121, ²NASA-Ames Research Center, Moffett Field, CA 94035

INTRODUCTION

The loss of weight bearing during spaceflight results in osteopenia in humans. Decrements in bone mineral reach 3-10% after as little as 75-184 days in space. Loss of bone mineral during flight decreases bone strength and increases fracture risk. The mechanisms responsible for, and the factors contributing to, the changes in bone induced by spaceflight are poorly understood.

The rat has been widely used as an animal model for human bone loss during spaceflight. Despite its potential usefulness, the results of bone studies performed in the rat in space have been inconsistent. In some flights bone formation is decreased and cancellous bone volume reduced, while in others no significant changes in bone occur. In June of 1996 Drs. T. Wronski, S. Miller and myself participated in a flight experiment (STS 78) to examine the effects of glucocorticoids on bone during weightlessness. Technically the 17 day flight experiment was flawless. The results, however, were surprising. Cancellous bone volume and osteoblast surface in the proximal tibial metaphysis were the same in flight and ground-based control rats. Normal levels of cancellous bone mass and bone formation were also detected in the lumbar vertebrae and femoral neck of flight rats. Furthermore, periosteal bone formation rate was found to be identical in flight and ground-based control rats. Spaceflight had little or no effect on bone metabolism! These results prompted us to carefully review the changes in bone observed in, and the flight conditions of, previous spaceflight missions.

METHODS

We conducted a thorough study of the rats used, the experimental conditions and the bone changes induced by spaceflight in 16 flight missions from 1975-1996. These included both Russian and American flights. The strain of the animals used, their sex and age, housing and dietary conditions, flight duration, and bone processing techniques were examined.

RESULTS

Our analysis shows that the changes in bone induced by spaceflight in the rat were influenced by: 1) how the animals were housed during flight, 2) the age of the animals, 3) the particular strain (genetic background) of the rat used in the study, and 4) the flight duration. When animals are housed singly (as opposed to in groups), regardless of age or animal strain bone formation is inhibited and cancellous bone volume is reduced. In Space Life Sciences-1, animals were housed both singly and in groups. Periosteal bone formation was significantly reduced in the singly housed but not in the group housed animals.

An identifiable pattern also emerged for age. For the 16 missions analyzed, animals ranged in age from 34-105 days of age at launch. Despite the limited age range, older animals tended to show a greater inhibition of bone formation than younger animals. Regression of change in bone

formation onto age produced a regression coefficient of $r = 0.71$, $p < .01$. No study has been conducted comparing animals of different ages under identical flight conditions. Oddly, no skeletal studies have been conducted in adult rats, only young growing animals have been used. Thus the effects of age can not be clearly defined until further studies are conducted.

Although housing and age appear to account for much of the variation in skeletal response in the rat to spaceflight, animal strain or genetic background also appears to be important. In the group housed missions ($n=6$), bone formation was significantly inhibited only when F344 rats (2 of 6 missions) were used. That genetic background can play a role in bone responsiveness to loading is supported by recent findings in mice and suggests the exciting possibility that specific genes maybe responsible for sensing and/or responding to mechanical loading. Predictably, flight duration is also an important determinant of the response of bone to spaceflight. Longer duration missions tend to result in greater decrements in bone mass.

DISCUSSION

Our analysis of existing flight data has shown that the skeletal response of the rat does indeed mimic the skeletal response of the human to spaceflight. The rat remains a useful and valuable model to study the mechanisms by which osteopenia in the human develops during weightlessness. Our analysis also indicates, however, that experimental conditions can dramatically influence the magnitude of the bone response to loss of weight bearing. This is exciting! It suggests that bone loss in the human may also be influenced by environmental conditions, age and genetic factors. Indeed the loss of bone in astronauts and cosmonauts during spaceflight has been surprisingly variable.

EFFECTS OF SPACEFLIGHT ON THE ATTACHMENT OF MUSCLES TO THE TIBIA, FIBULA AND CALCANEUS

R. B. Johnson¹, A. K. Tsao², K. R. St. John², R. A. Betcher², M. A. Tucci², D. E. Parsell¹, X. Dai¹, L. D. Zardiackas¹, and H. A. Benghuzzi³. ¹Schools of Dentistry, ²Medicine, and ³Health Related Professions, University of Mississippi Medical Center, Jackson, MS.

INTRODUCTION

Microgravity significantly reduces transmission of ground-reaction forces to bones, promoting atrophy. There is little information available concerning the effects of microgravity on bones at sites where anti-gravity muscles are attached (tendon-bone junctions). This study evaluates the effects of microgravity on the origin and insertion sites of anti-gravity muscles on the rat tibia, fibula and calcaneus. Changes in the strength of those tendon-bone junctions could predispose the animal to injury following spaceflight.

METHODS

The sites of origins and insertions of the anti-gravity muscles on the femur, tibia and fibula were studied by light and scanning electron microscopy and densitometry techniques.

Animals. 30 pregnant female rats were placed into each of three groups: a) flight, b) synchronous control, and c) vivarium control. Flight animals flew in the mid-deck of Atlantis for 11 days during the NIH.R1 mission. Vivarium controls were housed in a vivarium during the period of spaceflight. Synchronous control animals experienced 1-3 Gs in a centrifuge with launch noise simulation (108dB, 31.5-2500 Hz), at 22°C for 8 minutes to simulate launch. Animals were then returned to the vivarium and maintained at 26°C during the period of spaceflight. To simulate landing, animals experienced 1-2 Gs in a centrifuge for 16 minutes at 26°C.

Tissue removal. Animals were euthanized and hindlimbs removed by blunt dissection. The left leg was cleaned of muscles and fixed in 100% ethanol for SEM and bone densitometry. The right leg was fixed by immersion in Karnovsky's fixative and was prepared for LM. Scanning electron microscopy. The tibia, fibula and calcaneus were radiographed (with density wedges) and then dehydrated in acetones, dried and mounted on aluminum stubs. Prior to dehydration, a section was removed for density assessments. Specimens were coated with 200 nm gold-palladium and examined by SEM. Images were captured onto computer disk and histomorphometric analysis performed on the bone at the tibial and calcaneal tuberosities. Changes in mineralization were determined by assessment of bone ash from pulverized bones and densitometric analysis of radiographs. Light microscopy. Hindlimbs were dehydrated in ethanols and embedded in paraffin wax. Serial sections (6µm in thickness) were collected and stained with hematoxylin and eosin. Images were captured onto computer disk and histomorphometric analysis performed on the muscle and bone at the tibial tuberosity, posterior tibia and fibular head and the calcaneal tuberosity.

Collection of endpoint data To assess bone strength, cortical thickness, porosity and density were determined at the sites of muscle attachments using computerized histomorphometric and densitometry techniques from LM and SEM images and from digitized radiographs. Changes in mineralization were determined by a Vickers' microhardness test using intact bone and

thermoanalysis of pulverized bones. To assess strength of the tendon-bone junction, Sharpey fiber density, diameter and perimeter were similarly determined from SEM images. To assess muscle strength, muscle fiber density, perimeter and diameter were measured from LM images.

Statistical analysis. Mean parameters were calculated for flight, vivarium controls and flight simulation controls and parametric data were compared by factorial analysis of variance and a post-hoc Tukey's test. Cortical porosity and radiographic density was compared using the Wilcoxon matched-pairs sign ranked test. $P < 0.05$ was used to reject the null hypothesis.

RESULTS

There were no significant differences in endpoint data between vivarium and synchronous control groups; thus, these data have been pooled and titled "controls". There were significant increases in sites exhibiting enhanced cortical porosity and endosteal and periosteal resorption throughout the bones of the flight animals; resorption of cortical bone at the tendon insertion sites significantly reduced Sharpey fiber density (Table 3). Cortical thickness at muscle attachments was reduced in flight animals; however, bone density was not affected (Tables 1 and 2). Although radiographic bone density was not affected by spaceflight, bone microhardness was significantly reduced in flight animals (58.3 ± 6.77 , control; 37.7 ± 4.06 , flight). There were no significant differences in exothermal data between groups, suggesting no chemical changes in the bone structure. There were no significant changes in Sharpey fiber or muscle histomorphometric parameters with spaceflight.

Table 1. Tibial cortical thickness and density at the site of origin of the soleus muscle in flight and control animals used in this experiment.

PARAMETER	FLIGHT	CONTROL
Cortical thickness (mm ²)	10.81±0.48*	13.79±0.57
Bone density (% control)	97.92±1.21	100.00±1.11

Significantly different from control: * $p < 0.01$

Table 2. Calcaneal cortical thickness and density at the tuberosity of flight and control animals used in this experiment.

PARAMETER	FLIGHT	CONTROL
Cortical thickness (mm)	0.48±0.02*	0.58±0.02
Bone density(%Control)	98.99±0.09	100.00±1.03

Significantly different from control: * $p < 0.05$

Table 3. Fibular cortical thickness and density at the origin of the soleus muscle in flight and control animals used in this experiment.

PARAMETER	FLIGHT	CONTROL
Cortical thickness (head) ($\text{mm} \times 10^1$)	10.04 \pm 0.83**	14.10 \pm 0.76
Sharpey's fibers (#/1000 μ m^2)	3.73 \pm 0.52*	10.69 \pm 1.24
Bone porosity (% area)	14.69 \pm 1.82*	5.06 \pm 0.91

Significantly different from control: * $p < 0.001$, ** $p < 0.01$

CONCLUSION

The data suggest significant and deleterious changes in bone mass (but not density) at the tendon-bone junction in flight animals coincident to microgravity. These changes are likely caused by the spaceflight itself and not muscle weakness, as muscle histomorphometric parameters were not different between control and flight animals. Sharpey fiber density was significantly decreased in flight animals. Taken together with enhanced cortical porosity and reduced cortical thickness and microhardness, this data suggests significant weakness in the tendon-bone junctions of the hindlimbs coincident to spaceflight. Weakened tendon-bone attachments could result in injury following return to Earth. (Supported by NASA: NCC 2-863).

TRANSGENIC MARKERS OF LINEAGE PROGRESSION IN MECHANICALLY LOADED BONES

I. Kalajic, J. Terzic, K. Mack, D. Visnjic, A. Mapta, G. Gronowicz, S. Clark, J. Yeh and D. Rowe. Departments of Pediatrics, Orthopedics and Medicine, University of Connecticut Health Center, Farmington, CT 06030 and Dept. of Medicine, Winthrop University Hospital, Mineola, NY 11501

Bone formation and remodeling reflects the control of recruitment of osteo-progenitor cells to preosteoblasts, osteoblasts and osteocytes. These same cells also modify the osteoclast pathway. As a first step of appreciating the osteoprogenitor pathway, we have developed transgenic mice expressing a marker gene (CAT or GFP) under control of fragments of the COL1A1 promoter. This promoter appears to have a modular organization such that fragments can be utilized to produce transcriptional activity that is restricted to various connective tissues. As expressed in bone, Col3.6CAT is active in osteoblasts, periosteal cells and osteocytes, but not vascular smooth muscle cells, while the activity of Col2.3CAT is restricted to mature osteoblast. Preliminary data suggests that the pOBCol3.6CAT and pOBCol3.6GFP activity is restricted to the preosteoblast.

The advantage of using transgenes to assess osteoblastic activity has been demonstrated in the OIM mouse. This model of human OI has high bone turnover due to defective matrix production as judged by diminished bone volume, low bone formation but high mRNA levels for Col1A1, BSP and OC extracted from OIM bone and high urinary excretion of DPD crosslinks. The ColCAT3.6 transgene was bred into the OIM line and its enzymatic and mRNA level assessed in the three genotypes. There was excellent correlation between the enzyme activity and mRNA levels facilitating easy assessment of osteoblastic activity in intact bone. Relative to the +/+ littermates, the CAT activity was increased 4x in oim/oim and 2x in the oim/+ mice. This contrasts with less than a 2x increase in endogenous mRNA levels of Col1A1, BSP or OC in the oim/oim mice and no significant increase in the oim/+ genotype. The CAT levels are highly reflective of bone formation rates characteristic of growing and mature mice and demonstrate that in growing oim/oim mice maximal bone formation cannot exceed that of normal mice. This may explain why bone fractures are highest in rapidly growing children. The osteoprogenitor lineage cannot meet the concomitant demand of high turnover inherent to OI and the additional demand for longitudinal skeletal growth.

We have been frustrated by our inability to apply this approach of bone formation to normal mice exposed to protocols designed to increase bone growth. A variety of attempts to increase formation histomorphometrically by treadmill exercising, a method with demonstrated success when applied to rats, have not resulted in similar changes in mice irregardless of their genotype (CD1, C57B6 or C3H). It appears that the nocturnal burrowing activity of mice cannot be superseded by additional daytime exercise. Recently we have discovered that lateral mechanical stress to the bone in the form of an orbital shaker (30 min/day for 4 weeks) does significantly increase histomorphometric measures although at that time a concomitant increase in mRNA levels of Col1A1, BSP and OC was not observed. This protocol is currently being applied to mice bearing the Col2.3CAT transgene at shorter intervals of shaking with the expectation that the sensitivity of the transgene will validate this approach for assessment of osteoblastic activity.

COMMON MOLECULAR EVENTS BY HORMONES AND MECHANICAL STRAIN REGULATE INSULIN-LIKE GROWTH FACTOR-I EXPRESSION IN OSTEOBLASTS

T.L. McCarthy, Y. Chen, C. Ji, M. Centrella

Yale University School of Medicine, Department of Surgery, Section of Plastic Surgery, New Haven, CT 06520-8041

INTRODUCTION

Mechanical load, hormones and growth factors control bone metabolism *in vivo* and *in vitro*. Often, small changes in any of these elements can disrupt balanced bone remodeling and skeletal integrity. Because mechanical load helps to maintain bone mass, bone integrity can diminish from disuse or loss of mechanical stimulation in microgravity. Insulin-like growth factor-I (IGF-I) is an important skeletal growth factor. Expression of IGF-I by osteoblasts is increased by activators of protein kinase A (PKA) like parathyroid hormone (PTH) or prostaglandin E₂ (PGE₂). PGE₂ is made by bone cells in response to certain hormones or mechanical load. We previously showed an important role for IGF-I on collagen matrix synthesis in coupled bone remodeling induced by PTH. In support of this, recent *in vivo* studies indicate that anabolic effects of PTH or its analogs occur by way of cAMP. Furthermore, a direct correlation between bone mass and serum IGF-I levels was noted in middle aged men with idiopathic osteoporosis, and among inbred strains of mice with significant differences in bone density. Whereas serum IGF-I principally derives from liver, a general decrease in the capability to express IGF-I also may be imposed on skeletal cells. This in effect produces a resistance to normal control mechanisms that occur in response to hormones and mechanical strain.

Microgravity is thought to decrease bone formation without significantly altering resorption. Several research groups have predicted that loss of mechanical strain in microgravity may alter the synthesis or activity of local bone growth factors within the skeleton. Consistent with the quick induction of IGF-I by cAMP inducing hormones, work from the Chambers lab identified IGF-I as an early response gene stimulated by short duration compressive strain. Indomethacin, an inhibitor of PGE₂ synthesis, blocked both the induction of IGF-I and the subsequent increase in skeletal collagen synthesis. These results indicate a key role for both factors in the anabolic response of the skeleton to mechanical loading. We recently defined a molecular link among cAMP, PKA, and IGF-I in hormone activated osteoblasts, predicting that shared mechanisms and downstream effectors may function in both hormone and strain activated IGF-I expression, which then directly influence new collagen synthesis and bone formation.

METHODS

Culture Model Primary osteoblast-enriched cultures were prepared from parietal bones of 22 day old Sprague-Dawley rat fetuses (Charles River Laboratories) by methods approved by the Yale Animal Care and Use Committee. Cranial sutures were eliminated by dissection, and bones were digested with collagenase for 5 sequential 20 min intervals. Cells released during the last 3 digestions, exhibiting biochemical characteristics associated with differentiated osteoblasts, were plated at 4,800 per cm² in DMEM, 20 mM HEPES (pH 7.2), 0.1 mg/ml ascorbic acid, penicillin and streptomycin, and 10% fetal bovine serum (FBS).

Mechanical Strain Model Strain was applied to cell cultures with the Flexercell[®] FX-3000, which uses computer controlled solenoids to regulate vacuum pressure and rate. Osteoblast

cultures were plated on collagen coated silastic membrane cluster dishes. Biaxial strain was applied by vacuum distention at defined amplitude (% elongation) and rate (cycles per minute; Hz). Cultures also experience fluid shear because mechanical distortion of the membrane agitates the culture medium. We found that a moderate flex rate of 0.1 Hz (6 cycles per min) gives the best induction of IGF-I expression, whereas 1 Hz (60 cycles per min) is less effective.

IGF-I promoter constructs For IGF-I gene activation studies, we examined reporter gene expression directed by the fully active IGF-I promoter construct IGF1711b, with 1711 bp of upstream DNA and all of exon 1 sequence, or the synthetic construct 4x HS3D/Luc, with 4 tandem copies of the C/EBP binding sequence (+202 to +209 of exon 1) found in the IGF-I gene. Studies to examine the essential role of this C/EBP binding sequence utilized mutated or truncated promoter constructs that eliminated this element.

Plasmid Preparation and Transfection studies Plasmids were propagated in *E. coli*, and purified with Qiagen Midiprep columns. Promoter/reporter plasmids were co-transfected with vector carrying the • -galactosidase gene to normalize for transfection efficiency. Cultures at 50% confluence were rinsed and exposed to plasmids and transfection reagent. After incubation, solutions were replaced with medium + 5% FBS. Cultures were grown to confluence for 48 h, rinsed, and treated for varying intervals with PGE₂ or mechanical strain in serum free medium. In some studies cells were pre-exposed to ibuprofen to inhibit local PGE₂ expression. After treatment, cells were rinsed and lysed. Reporter gene expression was then measured in nuclear free extracts and corrected for protein content by the Bradford assay.

Cytoplasmic and Nuclear Protein Extracts Cultures were rinsed, treated with vehicle or test agent, and cells were harvested by scraping. Cytoplasmic and nuclear extracts were prepared by the method of Lee et al. with minor modifications. Cells were lysed in hypotonic buffer with phosphatase and protease inhibitors, and 1% Triton X-100. Nuclei were separated from cytoplasm by centrifugation. Nuclear proteins were released by extraction in hypertonic buffer with phosphatase and protease inhibitors, and nuclear extracts were separated from insoluble material by centrifugation.

Gel Mobility Shift Assay Radiolabeled double-stranded (ds) probes were prepared by annealing complementary oligonucleotides, followed by fill-in of single-stranded overhangs with dCTP, dGTP, dTTP and [³²P]dATP using the Klenow fragment of DNA polymerase I. Nuclear protein was incubated for 20 min on ice with poly(dI:dC) with or without unlabeled specific or nonspecific competitor DNAs in 60 mM KCl, 25 mM Hepes, pH 7.6, 7.5% glycerol, 0.1 mM EDTA, 5 mM DTT, and 0.025% BSA. After adding the radiolabeled DNA probe (0.1-0.2 ng) for 30 min, samples were applied to a 5% nondenaturing polyacrylamide gel pre-electrophoresed for 30 min at 12.5 V/cm at 25 C in 45 mM Tris, 45 mM boric acid, 1 mM EDTA. Electrophoresis was for 2.5 h. The dried gel was exposed to X-ray film at -80 C with an intensifying screen.

RESULTS

In osteoblasts, PGE₂ is a potent inducer of cAMP, which activates PKA by the release of regulatory subunits. Subsequent effects by PKA rapidly increase IGF-I gene expression. Using transient transfection methods and native or synthetic IGF-I promoter/reporter constructs, we identified a binding element in the transcribed but non-coding exon 1 of the IGF-I gene that is

critical for PKA dependent activation of the IGF-I promoter. We then identified a transcription factor, termed CCAAT/enhancer binding protein • (C/EBP•) as the essential factor for this event in osteoblasts. PKA directly or indirectly activates C/EBP• which then translocates to the nucleus, and binds to its cognate DNA binding sequence in exon 1, and stimulates IGF-I gene transcription. Inhibition of protein synthesis by cycloheximide does not diminish IGF-I transcription induced in this way. Therefore, C/EBP• is a pre-existing factor in osteoblasts. However, PGE₂ not only activates endogenous C/EBP• , but also induces new C/EBP• expression. This apparently can replenish the transcription factor pool, and prolong IGF-I gene expression in response to a single inducing event.

Having established this process, we then examined IGF-I promoter activity in osteoblasts experiencing mechanical strain. Osteoblasts were plated on collagen coated flexible bottom (silastic membrane) cluster dishes. Subconfluent cultures were transfected with an active IGF-I promoter construct (IGF1711b), or a truncated fragment lacking the C/EBP binding sequence (IGF1711c). Cultures were grown to confluence in serum containing medium, and then tested for their response to moderate amplitude (15% elongation), low frequency (0.1 Hz) mechanical strain of varied duration in serum-free medium. Strain was applied using a Flexercell[®] FX-3000. Control cultures were plated on comparable plates, but do not experience mechanical strain. Some static cultures were treated with 1 μM of PGE₂, which optimally activates IGF-I transcription, as a positive control. Mechanical strain induced a 6-fold activation of the functional IGF1711b promoter fragment within 6 hr of initiating the strain protocol. Loss of the PGE₂ sensitive C/EBP binding sequence in promoter fragment IGF1711c reduced this response to 2-fold. In parallel static cultures, PGE₂ caused an 11-fold stimulation of IGF1711b and a 1.7-fold stimulation of IGF1711c. The stimulatory effect of strain was inhibited by 40% when cultures were treated with ibuprofen to inhibit new PGE₂ synthesis throughout the strain protocol.

CONCLUSION

Our results show that cAMP inducing hormones such as PGE₂ and PTH, as well as mechanical loading, can increase IGF-I expression by way of the same C/EBP binding sequence. This reveals a pivotal role for pre-existing C/EBP• , and perhaps other C/EBP family members, in bone formation induced by hormone exposure or strain. Importantly, cyclooxygenase inhibitor studies show that PGE₂ appears to have an integral role in the process by which mechanical strain activates new IGF-I expression, consistent with *in vivo* results from other investigators. Time course studies show that both C/EBP• and IGF-I are both early response genes that can account for the anabolic response of osteoblasts to hormonal and mechanical stimuli. Therefore, understanding how to enhance their expression and activation will provide a novel avenue to limit and reverse bone loss from disuse, microgravity or age related events.

NOVEL RECEPTOR-BASED COUNTERMEASURES TO MICROGRAVITY-INDUCED BONE LOSS

B.W. O'Malley¹, C.L. Smith¹, N.L. Weigel¹, and E.M. Brown², Department of Cell Biology
¹Baylor College of Medicine, Houston TX 77030 and ²Endocrine-Hypertension Division, Brigham & Women's Hospital, Boston, MA 02115.

INTRODUCTION

Manned space flight has opened new frontiers for human exploration, but humans in a microgravity environment for an extended time experience numerous physiological changes, including bone loss. Weight-bearing exercise contributes significantly to bone health, and it is likely reduced mechanical load is a major cause of microgravity-induced osteopenia. However, changes in the levels of systemic factors regulating bone formation and resorption [growth factors, calcium, steroids and 1,25-dihydroxyvitamin D (1,25-D)] occur in humans and animals in microgravity, and it is likely that these alterations also negatively influence bone. The biological actions of these hormones are mediated by their receptors [estrogen receptor (ER), vitamin D receptor (VDR) and Ca²⁺_o-sensing receptor (CaR)], which play key roles in the normal bone turnover that is necessary for skeletal health. These receptors control: (1) differentiation of osteoblast (OB) and osteoclast (OC) precursors, (2) functions of mature OBs and OCs and/or (3) other cells within the bone and bone marrow microenvironment controlling (1) and (2) (*e.g.* stromal cells and monocytes). Thus, we hypothesize that appropriate use of novel ER-, VDR- and CaR-based therapeutics will mitigate the reduced bone formation and increased bone resorption that contribute to microgravity-induced bone loss. Indeed, synergistic interactions among these receptors may enhance the actions of any one used alone.

METHODS

Our studies utilize various model bone cell preparations, including the osteoblastic cells described below as well as osteoclast-like cells generated in culture that resemble *bona fide* osteoclasts isolated from bone. We investigate the expression of receptors for the CaR, ER, and VDR in these various types of cells and assess the capacity of various agonists of these receptor to activate receptor-mediated biological responses detailed in RESULTS. Our goal is to extend these studies subsequently to the STLV bioreactor as a ground-based model of microgravity and, eventually, to the hind limb suspension rat model of microgravity to determine the impact of our receptor-based therapies on bone loss in this situation.

RESULTS

We used RT-PCR and Northern analysis to demonstrate CaR transcripts and immunocytochemistry and Western analysis with CaR-specific antisera to document expression of CaR protein in the OB-like cell lines, murine MC3T3-E1, rat UMR-106, and human SAOS-2 and MG-63. Furthermore, raising Ca²⁺_o stimulates proliferation and chemotaxis of MC3T3-E1 cells. We also used the same techniques to document CaR mRNA and protein expression in the ST-2 mouse stromal cell line. Stromal cells could either communicate with OBs via paracrine or direct interactions or serve as OB precursors. As with MC3T3-E1 cells, high Ca²⁺_o stimulated proliferation and chemotaxis of ST-2 stromal cells. To study the CaR's role in modulating cells of the OC lineage, we examined the mouse monocytic cell line, J774, and human peripheral blood monocytes for CaR expression, since a subset of monocytes are thought to serve as OC

precursors. Most (80-85%) monocytes express abundant CaR protein and mRNA, as does the J774 monocytic cell line. In addition, mouse marrow cultures form OCs *in vitro* upon treatment with 1,25-D. When we examined such cultures for CaR expression during *in vitro* osteoclastogenesis, we found expression by both mononuclear cells that formed aggregates and then fused to form multinucleated, OC-like cells expressing tartrate-resistant acid phosphatase (TRAP) and calcitonin receptors (OC markers) as well as multinucleated cells themselves. Moreover, high Ca^{2+}_o , potentially through activation of the CaR, inhibited the formation of these TRAP-positive, multinucleated giant cells.

We also examined the role of the VDR and ER in controlling OB function in preparation for our future studies of the impact of unit gravity and microgravity on bone cell function. Since our initial studies showed that bone cells could not be transfected with high efficiency using conventional, lipid-based transfection methods, we adapted our lysine-coupled adenovirus transfection procedure for this purpose. Using this adenovirus transfection technique, we can readily detect the activity of the endogenous VDR in MG-63, ROS 17/2.8 and MC-3T3-E1 cells. We have then performed hormone titration curves with 1,25-D and the less calcemic analog, EB1089, using osteocalcin-based reporters as well as synthetic reporters. EB1089 is both more potent and efficacious than 1,25-D in inducing osteocalcin expression. One nM EB1089 induces maximal osteocalcin levels whereas 100 nM 1,25-D was required for its maximal effect. Inductions were 50-100 fold. Under these conditions we also can detect the activity of the endogenous VDR using either CAT or luciferase reporters. In each case hormone-dependent inductions are 10-20 fold. Using a VDREtkCAT reporter containing a vitamin D responsive element, we found good induction with EB1089. In each case, EB1089 is more potent than 1,25-D. Because VDR acts as a heterodimer with retinoid X receptor (RXR), we measured the effect of its ligand, 9-cis retinoic acid on VDR function. Even at suboptimal doses of VDR agonist, 9-cis retinoic acid had no effect. This is consistent with several reports that, in most cases, RXR ligands do not alter VDR function. Finally, for reporter activation, we see no effects of estradiol on VDR function. However, we expect that more complex biological actions will be affected by estradiol.

Using synthetic target genes with 1-3 copies of an estrogen response element linked to a minimal promoter and the luciferase target gene, we also assessed endogenous ER activity in MG-63 cells. No activation of target gene expression was detected in cells treated with either estradiol or 4-hydroxytamoxifen. However, when ER α was expressed in this cell line via a constitutively active mammalian expression vector, luciferase gene expression was increased 3- to 12-fold, depending on the target gene examined (1 vs. 3 EREs, respectively). Taken together, these data suggest that there are insufficient functional ERs in MG-63 cells to mediate transcriptional activity, and this apparent insensitivity can be overcome by expressing exogenous ER α . We also introduced ER β into these cells via expression vector and can upregulate its activity ~3-fold with estradiol. For both ER α and ER β , estradiol stimulates reporter gene expression in a dose-dependent fashion, with maximal stimulation at 10 nM estradiol. We also assessed the ability of ER agonists to modulate osteocalcin in this cell line and found that estradiol alone did not stimulate osteocalcin secretion. This was not unexpected, and we will examine whether ER agonists modulate VDR regulation of osteocalcin. The effects of estradiol and various Selective estrogen receptor modulators (SERMs) are currently being assessed in the other two OC cell lines, ROS17/2.8 and MC3T3-L1. The experiments to date indicate insufficient ER expression in

ROS 17/2.8 cells to measure the transcriptional activity of endogenous ERs, even with reporter genes delivered by our adenovirus methodology. Western blots also failed to detect ER α in these cells. While ER expression in ROS 17/2.8 cells has been reported (Migliaccio et al, *Endocrinology* 130(5): 2617-2624, 1992), the level is very low (200-500 binding sites/cell). We recently obtained a cell line from Dr. Kenneth Korach (NIEHS, Research Triangle, NC) in which ROS 17/2.8 cells are stably transfected with an ER α expression vector, and we will use this line to continue our characterization of SERM activity in OBs. With respect to MC3T3-E1 cells, our initial synthetic target gene expression experiments indicate that these cells express functional ERs of unknown subtype. We are currently expanding these studies to examine the effectiveness of SERMs, and characterizing ER α /ER β protein expression. As stated above, one of our objectives is to assess the combined activities of VDR, CaR and ER agonists, and studies of the expression of ERs in these cell lines are an important step towards this goal.

We have established conditions in the STLV bioreactors permitting us to grow three dimensional arrays of MG-63 cells in rotating vessels under conditions that partially simulate microgravity. Using the optimal rotation rate (8 rpm), we compared the responses of MG-63 cells in bioreactors with those at unit gravity. Our goal is to determine whether the differences detected by Carmeliet et al. (*J. Bone Miner Res* 1997:786-794) when MG-63 cells were exposed to microgravity aboard the Foton 10 satellite would be reproduced in the bioreactor. Carmeliet et al. measured alkaline phosphatase activity and mRNAs for a number of marker genes. In microgravity, induction of alkaline phosphatase by TGF β and 10^{-7} M calcitriol was only 1.8-fold. In agreement with this, we find a similar increase. Their studies showed that microgravity reduced osteocalcin mRNA levels to about 15-20% of control. They were unable to measure osteocalcin secretion for technical reasons. We measured osteocalcin by immunoassay and found that while there are very low levels of osteocalcin in the uninduced conditions, osteocalcin increased 100-fold upon treatment in unit gravity whereas no increase occurred in the bioreactor. Measurements of mRNA levels are ongoing. However, our initial assessment is that the bioreactors mimic microgravity. To begin to understand the lack of response to calcitriol in microgravity, we measured VDR levels in cells grown in the bioreactor versus control cells. Our initial immunoblots suggest that VDR levels are substantially reduced in the bioreactor. To determine whether cells exposed to microgravity alter their basal signaling responses, we utilized phosphorylation site-specific antibodies to measure activated mitogen activated protein kinases (MAPK) and stress-activated protein kinases (SAPK). There was little change in activation of MAPK, but SAPK activity was greatly increased indicating that MG-63 cells respond to microgravity as a stress. If these findings are confirmed, then a major defect in osteoblasts exposed to microgravity may be downregulation of the VDR. We will seek to upregulate the vitamin D receptor using selective estrogen modulators (SERMs) and/or CaR agonists and determine whether this alters the response of the cells. In addition, we will ask whether the downregulation of the VDR is observed in the rat hind limb suspension model.

CONCLUSIONS

The presence of CaR transcripts and/or protein in OB cell lines and OC-like cells generated in vitro indicates that the CaR is a strong candidate for mediating the known actions of Ca $^{2+}$ on OB and OC function. These effects of Ca $^{2+}$ could stimulate bone formation by increasing the proliferation of pre-OBs and their chemotaxis to sites of bone resorption and to inhibit the generation and, perhaps, the function of OCs. To date, however, we have not directly proven that

the actions of Ca^{2+}_o on OBs and OCs are mediated by the CaR. An important goal, therefore, will be to utilize dominant negative CaR constructs to prove the CaR's role in mediating the actions of Ca^{2+}_o on these bone cells. Assuming these studies show a mediatory role of the CaR, this would provide a strong foundation of pursuing further the possible use of CaR agonists, alone or in combination with SERMs and VDR agonists, in treating microgravity-induced bone loss. Our experiments with VDR agonists suggest that a vitamin D analog may be useful in maintaining VDR activity and, therefore, in potentially reducing microgravity-induced bone loss. We now have in place cell-based models enabling us to assess the relative potencies of various SERMs in OB-like cells. The STLV bioreactors are operational and we anticipate verifying their ability to mimic microgravity in 2 months. We will then determine whether the ability of OBs to respond to VDR and ER agonists varies as a function of gravitational force. We will also examine the effects of these agonists on additional markers of OB functions (protein and mRNA expression levels), and study the effects of VDR and ER agonists on osteoclastogenesis and mature OC function. Although *in vivo* microgravity experiments are beyond the scope of this proposal, a future goal is to assess the ability of hormonal countermeasure(s) to maintain bone density and strength in hind limb-suspended rats in collaboration with Dr. Susan Bloomfield of the Bone Team (NSBRI). As soon as we identify a promising receptor agonist(s), we will begin to evaluate these compounds in the hind limb suspension model. Collectively, our data will provide the foundation for future studies on the ability of these compounds to maintain bone density and strength in rats housed in microgravity conditions (*e.g.* aboard a space shuttle and/or station), and human bed rest studies.

DEVELOPMENTAL REGULATION OF THE COLLAGENASE-3 PROMOTER IN OSTEOBLASTS

N.C. Partridge, Y. Yang, R.C. D'Alonzo, and S.K Winchester

Department of Pharmacological and Physiological Science, Saint Louis University School of Medicine, St. Louis, MO 63104

INTRODUCTION

Previously, we have shown that collagenase-3 mRNA is developmentally expressed in normal, differentiating rat osteoblasts. In vivo, the gene is expressed in a tissue-specific fashion in hypertrophic chondrocytes and osteoblasts and developmentally regulated. Our studies aim at determining the promoter elements and proteins binding to the promoter responsible for tissue and developmental regulation of collagenase-3.

METHODS

In vitro, normal rat and mouse osteoblasts are cultured in a differentiation protocol whereby the cells proliferate through day 7 of culture, then cease proliferation, differentiate and mineralize an extracellular matrix. Various reporter constructs of the rat collagenase-3 promoter are transfected into the proliferating cells, either transiently or stably. Expression of the reporter gene is then assessed at different stages of differentiation. This is modulated by co-transfection of transcription factors in expression vectors. In this way, we can assess the promoter elements and proteins involved in regulation of collagenase-3 during osteoblast differentiation. In vivo, we are determining the DNA elements involved in tissue specific expression of the gene by attaching portions of the collagenase-3 promoter to a reporter gene and injecting these into mouse blastocysts and then assessing the expression of the reporter gene in all the tissues of the resultant transgenic mice.

RESULTS

Collagenase-3 mRNA is not detectable during osteoblast proliferation (day 5), but expression increases as the osteoblasts begin to differentiate and mineralize an extracellular matrix (days 14 and 21). We demonstrated by nuclear run-on analysis that this increase in expression is due to an increase in transcription of the collagenase-3 gene. Through transient transfection into cultured osteoblasts of deletion and mutated collagenase-3 promoter constructs, we demonstrated that the activator protein-1 (AP-1) and runt domain (RD) binding sites are responsible for transcription of the collagenase-3 gene. Mutation of either the AP-1 or the RD binding sites resulted in a loss of collagenase-3 promoter activity. The AP-1 and RD binding sites have been shown to bind members of the activator-protein-1 family of transcription factors and Acute Myelogenous Leukemia (AML) family of transcription factors, respectively. Overexpression of both c-Fos and c-Jun into proliferating osteoblasts or overexpression of osteoblast-specific factor 2 (Osf2) resulted in an increase in collagenase-3 promoter activity. Furthermore, overexpression of c-Fos, c-Jun and Osf2 into osteoblasts resulted in a synergistic increase in collagenase-3 promoter activity. However, mutation of either the AP-1 or the RD binding site resulted in the inability of c-Fos and c-Jun or Osf2 to increase collagenase-3 promoter activity suggesting that both the AP-1 and RD binding sites and proteins are required for expression of collagenase-3 in differentiating osteoblasts. In vivo, we have found that the same promoter region (-148 bp

upstream of the transcriptional start site) appears to retain some tissue specificity, being expressed in bone and teeth, but, as well in muscle.

CONCLUSION

The RD binding site and AP-1 site and the transcription factors Osf2 and JunD appear important in regulating expression of collagenase-3 in differentiating osteoblasts. The -148 bp region of the promoter appears also to regulate bone-specific expression of collagenase-3 but other elements further upstream may be necessary for expression in hypertrophic chondrocytes. These experiments are currently ongoing.

(Supported by NASA: NAG-4538, NCC2-884, and GSRP-98-087).

EXERCISE COUNTERMEASURES FOR BONE LOSS DURING SPACE FLIGHT: A Method for the study of Ground Reaction Forces and their Implications for Bone Strain

M. Peterman, J. L. McCrory, N. A. Sharkey, S. Piazza, and **P. R. Cavanagh**
The Center for Locomotion Studies, Penn State University, University Park, PA 16802

INTRODUCTION

Effective countermeasures to prevent loss of bone mineral during long duration space flight remain elusive. Despite an exercise program on MIR flights, the data from LeBlanc et al. (1996) indicated that there was still a mean rate of loss of bone mineral density in the proximal femur of 1.58% per month (n=18, flight duration 4-14.4 months). The specific mechanisms regulating bone mass are not known, but most investigators agree that bone maintenance is largely dependent upon mechanical demand and the resultant local bone strains (Frost, 1986; Jaworski and Uthoff, 1986; Rubin and Lanyon, 1985; Jee and Li, 1990). A plausible hypothesis is that bone loss during space flight, such as that reported by LeBlanc et al. (1996), may result from failure to effectively load the skeleton in order to generate localized bone strains of sufficient magnitude to prevent disuse osteoporosis.

A variety of methods have been proposed to simulate locomotor exercise in reduced gravity (Davis et al. 1993). In such simulations, and in an actual microgravity environment, a gravity replacement load (GRL) must always be added to return the exercising subject to the support surface and the resulting skeletal load is critically dependent upon the magnitude of the GRL. To our knowledge, GRLs during orbital flight have only been measured once (on STS 81) and it is likely that most or all prior treadmill exercise in space has used GRLs that were less than one body weight. McCrory (1997) has shown that subjects walking and running in simulated zero-G can tolerate GRLs of 1 if an appropriate harness is used.

Several investigators have attempted to measure in vivo strains and forces in the bones of humans, but have faced ethical and technical limitations. The anteromedial aspect of the tibial midshaft has been a common site for the placement of strain gauges (Lanyon et al., 1975; Milgrom et al., 1996; Burr et al., 1996); one reason to measure strains in the anterior tibia is that this region is surgically accessible (Lanyon et al., 1975). Aamodt et al. (1997) were able to measure strains on the lateral surface of the proximal femur only because their experimental subjects were already scheduled for hip surgery. Lu et al. (1997) used an instrumented massive proximal femoral prosthesis along with electromyographic measurements to demonstrate that femoral forces depend on muscular activity. These analyses of in vivo bone mechanics are valuable. The invasive nature of the procedures involved, however, limits both the number of subjects and the number of strain gauge locations. Further, the results of these studies may be confounded by the inclusion of subjects with pathological conditions. Gross et al. (1992) measured strain at three locations on the equine third metacarpal and used those data to construct a computer model of the internal strain environment of the bone. An analogous placement of multiple gauges in living humans would be difficult and potentially hazardous because of the depth of soft tissue overlying the tibia and femur.

The purpose of the present study was to present a method to measure external ground reaction forces in human subjects during 1G and simulated zero-G exercise and to measure internal bone strains under similar conditions using a unique cadaver model.

METHODS

The Penn State zero-G locomotion simulator used in this study (Fig. 1) has been previously described by Davis et al. (1996). Briefly, the limbs of the subject are suspended from long elastic cords that act as quasi-constant force springs to offset the weight of the suspended segments. GRLs are applied through waist and shoulder harnesses, and ground reaction forces are measured by a force platform located under the belt of a vertically mounted treadmill. Subjects also performed the same exercises during level 1G locomotion over a Kistler force platform.

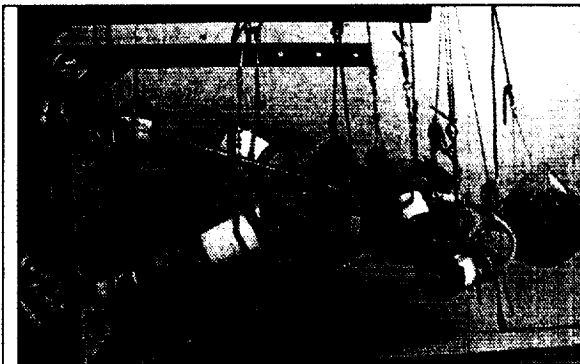


Figure 1: A subject walking in the zero-Gravity Locomotion simulator which has a vertically mounted force measuring treadmill.

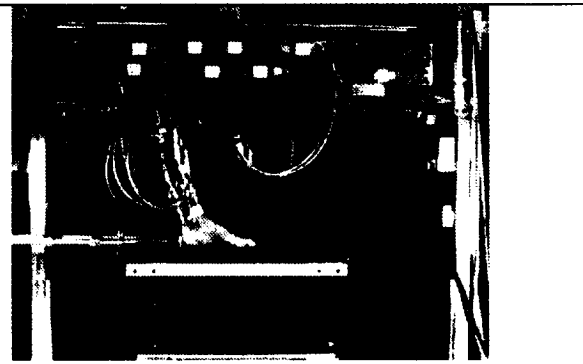


Figure 2: The cadaver simulator showing the muscle forces being applied as the limb moves through the appropriate kinematic trajectory.

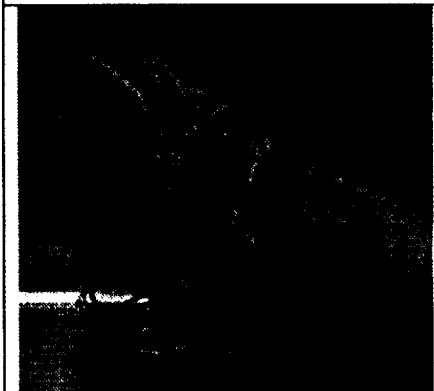


Figure 3: Strain gauges bonded to the distal tibia of a cadaver limb. The cut ends of the Achilles tendon are clamped to a force actuator.

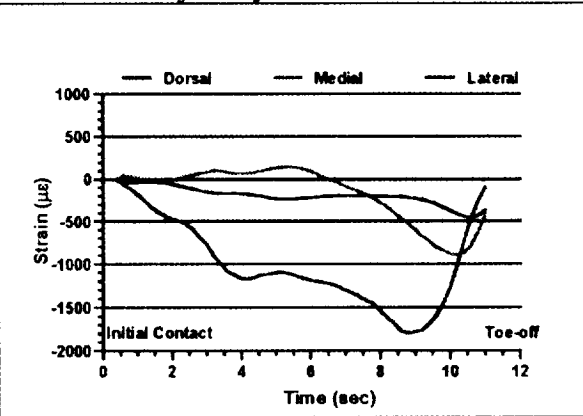


Figure 4: Metatarsal strains measured during simulated 1-G walking in 1/20th real time speed.

Each cadaver foot was mounted into an apparatus described by Sharkey and Hamel (1998) that dynamically loads the limb preparations and mimics the kinetics and kinematics of the tibia, foot, and ankle during the stance phase of gait from heel-strike to toe-off (Fig. 2). Physiologic actions of the extrinsic foot muscles are simulated using force feedback controlled linear actuators

interfaced with the tendons of the specimen. Previous studies have shown that the ground reaction forces and plantar pressures under the specimens are well within physiologic ranges and demonstrate inter-subject variation consistent with that seen in live subjects. The timing and force output of six separate muscle groups (constituting the major dorsi- and plantar flexors of the foot) were independently controlled with stepper motor powered linear actuators. Each muscle force profile was shape-matched to its corresponding mean EMG activity profile. Stacked epoxy-phenolic encapsulated rosette strain gauges (Micro-Measurements Group, Inc. WA-06-060WR-120) were attached at four transversely co-planar locations on the distal tibia of the cadaver limbs using M-Bond 200 cyanoacrylate adhesive and Catalyst-C (Fig. 3). Specimen surfaces were prepared in the following manner: a small region of the periosteum was removed by lightly sanding the region which was then cleaned and degreased with an acetone swab. The gauges, leadwires, and strain relief terminals were sealed with silicon rubber.

RESULTS

Ground reaction forces in the human subjects ambulating under zero-G conditions were significantly lower than their 1G equivalents (active force peaks 87.8 %BW vs. 124.4 BW % during walking, 180% BW vs 240% BW during running). This was apparently due to a bent-knee or "Groucho" running style which subjects used to minimize the applied load. Metatarsal strains measured in cadaver feet during simulated 1G walking were within the physiological ranges that have been previously reported (Fig 4). Data on tibial strains will also be presented.

CONCLUSION

The human zero-gravity locomotion simulator and the cadaver simulator offer a powerful combination for the study of the implications of exercise for maintaining bone quality during space flight. Such studies, when compared with controlled in-flight exercise programs, could help in the identification of a strain threshold for the prevention of bone loss during space flight.

This work was supported in part by NASA grant NAGW-4421.

REFERENCES:

- Aamodt, A., Lund-Larsen, J., Eine, J., et al. 1997, *In vivo* measurements show tensile axial strain in the proximal lateral aspect of the human femur. *Journal of Orthopaedic Research*, 15: 927-31.
- Burr, D. B., Milgrom, C., Fyhrie D., et al. 1996, *In vivo* measurement of human tibial strains during vigorous activity. *Bone*, 18: 405-10.
- Davis, B. L., Cavanagh, P. R., 1993, Simulating reduced gravity: a review of biomechanical issues pertaining to human locomotion. *Aviation, Space, and Environmental Medicine*, 64(6): 557-566.
- Davis, B. L., Cavanagh, P. R., Sommer, H. J., III, Wu, G., 1996, Ground reaction forces during locomotion in simulated microgravity. *Aviation, Space and Environmental Medicine*, 67(3): 235-242.
- Frost H.M., 1986, *Intermediary Organization of the Skeleton*. CRC Press, Boca Raton.
- Gross, T. S., McLeod, K. J., and Rubin, C. T., 1992, Characterizing bone strain distributions *in vivo* using three triple rosette strain gauges. *Journal of Biomechanics*, 25: 1081-7.
- Jaworski Z.F.G., and Uthoff H.K., 1986, Reversibility of nontraumatic disuse osteoporosis during its active phase. *Bone*. 7: 431-439.

- Jee W.S.S., and Li X.J., 1990, Adaptation of cancellous bone to overloading in the adult rat: a single photon absorptiometry and histomorphometric study. *Anatomical Record*, 227: 418-426.
- Lanyon, L. E., Hampson, W. G., Goodship, A. E., and Shah, J. S., 1975, Bone deformation recorded *in vivo* from strain gauges attached to the human tibial shaft. *Acta Orthopaedica Scandinavica*, 46: 256-68.
- LeBlanc A; Schneider V; Shackelford LL; et al. 1996, Bone mineral and lean tissue loss after long duration spaceflight. *J. Bone Mineral Research*, 11: S323.
- Lu, T. W., Taylor, S. J., O'Connor, J. J., and Walker, P. S., 1997, Influence of muscle activity on the forces in the femur: an *in vivo* study. *Journal of Biomechanics*, 30: 1101-6.
- Milgrom, C., Burr, D., Fyhrie, D., et al. 1996, The effect of shoe gear on human tibial strains recorded during dynamic loading: a pilot study. *Foot & Ankle International*, 17: 667-71.
- McCrorry J.L., 1997, A biomechanical comparison of 1-G and fully loaded simulated Zero-gravity locomotion. Ph.D. Thesis. Penn State University.
- Rubin C.T., and Lanyon LE., 1985, Regulation of bone mass by mechanical strain magnitude. *Calcified Tissue International*. 37: 411-417
- Sharkey N.A., and Hamel, A.J., 1998, A dynamic cadaver model of the stance phase of gait: performance characteristics and kinetic validation. *Clinical Biomechanics*, 13: 420-433.

**EXPRESSION OF NOVEL GENE PRODUCTS UPREGULATED BY DISUSE IS
NORMALIZED BY AN OSTEOGENIC MECHANICAL STIMULUS: EVIDENCE FOR
THE MOLECULAR BASIS OF A LOW LEVEL BIOMECHANICAL
COUNTERMEASURE FOR OSTEOPOROSIS?**

C. Rubin, J. Zhi, G. Xu, M. Cote, K. McLeod & M. Hadjiargyrou
Musculo-Skeletal Research Laboratory, Program in Biomedical Engineering
State University of New York at Stony Brook, 11794-8181

INTRODUCTION

The National Research Council's report entitled: A Strategy for Space Biology and Medical Science (Goldberg et. al., 1987), highlighted several areas of fundamental scientific investigation which must be addressed to make long-term space exploration not only feasible, but safe. This "Goldberg Strategy," as well as several subsequent reports published by the NRC's Space Studies Board (e.g., Assessment of Programs in Space Biology and Medicine, Smith et. al., 1991), suggests that the principal hurdle to man's extended presence in space is the osteopenia which parallels reduced gravity. Ironically, the most significant risk to the skeleton may only be realized on return to normal gravitational fields, and full recovery of bone mass may never occur. Effective counter-measures to this microgravity induced bone loss are thus essential. Considering the similarities of space and aging induced osteopenia, an indisputable benefit of such a prophylaxis would be its potential as a treatment for the bone loss which plagues over 25 million people in the U.S.

The osteogenic potential of mechanical strain is strongly frequency dependent, with sensitivity increasing up through at least 60 Hz (cycles per second). One hundred seconds per day of a 1 Hz cyclic loading will inhibit disuse osteopenia only if sufficient in magnitude to engender 1000 microstrain ($\mu\epsilon$) in the tissue (Rubin & Lanyon, 1987). When loading is applied at 30 Hz, however, mechanical strains on the order of $50\mu\epsilon$ (~1% of the peak strains which occur in bone during vigorous functional activity), can stimulate bone formation in a duration dependent manner (Qin et. al., 1998). In longer term animal studies, strains of less than $10\mu\epsilon$, induced non-invasively via a whole body vibration, will stimulate bone formation on the surfaces of trabeculae, increase bone density, and improve strength (Rubin et. al. 1998a). Finally, preliminary results from a double blind prospective clinical trial shows promise in inhibiting the bone loss which parallels the menopause (Rubin et. al., 1998b). Based on these observations, we propose that these high frequency, low magnitude, mechanical strains effectively serve as a "surrogate" for musculoskeletal ground reaction forces, and thus represent an ideal countermeasure to the osteopenia which parallels microgravity conditions. The specific goal of this NASA funded work is to identify genes in bone upregulated by disuse, and to determine the efficacy of an osteogenic mechanical stimulus to downregulate their expression.

METHODS

In the first phase of this study, functionally normal rats were used to histomorphometrically characterize the osteogenic interdependence of frequency (22, 45 & 90 Hz), intensity (0.25 & 0.5g), and duration (10, 40 & 80min) of a very low magnitude biomechanical stimulus. In the second phase of this study focussing on the rat-tail suspension model of disuse osteopenia (Morey-Holton & Wronski, 1981), differential mRNA display (DD-PCR) was used to isolate and

identify genes that were activated by removal of function. In phase three, it was then determined if genes upregulated by disuse were downregulated by a mechanical intervention which stimulated bone formation. It is clear from our preliminary work that the magnitude of mechanical strain necessary to promote osteogenesis is sufficiently low that whole body vibration of the standing animal will be sufficient to stimulate bone formation in the weight-supporting skeleton. Whole body vibration was achieved using a small, low force (18N), but highly linear, moving coil actuators (BEI model LA18-18, San Marcos, CA) to impose acceleration of up to 0.6g on animals of up to 90 Kg over the frequency range of 1 to 400 Hz (Fritton et. al., 1997). With accelerometer feedback from the plate surface, control circuitry eliminates non-translational modes of vibration due to motion or positional changes of the animal. An identical apparatus has been successful in partial body vibration of the hindquarters of sheep, as well as total body vibration for turkeys and humans.

Retired female breeder Sprague-Dawley rats, 180-240 days old were, used in each phase of this study. Mechanical stimulation was performed 5 days per week for 28 days. The rats remain free to roam in their cages during the stimulation. Tail suspension was evaluated at ten days. The measurements of dynamic indices of bone modeling and/or remodeling sites in either cancellous or cortical bone were performed on the proximal tibial metaphysis of the right tibia. The left tibia was immediately frozen in liquid nitrogen to be used for the extraction of RNA, which was isolated using the acid-guanidinium thiocyanate-phenol-chloroform extraction method (Chomczynski & Saachi, 1987). The differential expression of genes was analyzed using the differential mRNA display method (Liang & Pardee, 1992) utilizing polymerase chain reaction (PCR) and RNA image kits (GenHunter Corp.). Any bands clearly present under one condition (i.e., disuse, mechanical stimulation) and absent in the other, was subsequently excised from the gel and reamplified, cloned and sequenced using standard procedures in order to determine its identity. Northern blots were performed to verify that such cDNA fragments were differentially expressed. Six animals were evaluated in each group, and each animal was evaluated independently (RNA was not pooled).

RESULTS

Histomorphometric evaluation of the cortical and trabecular response demonstrated that the ability of low magnitude mechanical strain to stimulate bone formation was strongly dependent on the characteristics of the signal. Several distinct stimuli (e.g., MS1: 90 Hz, 0.5g, 80min; MS2: 90Hz, 0.25g, 40min) were anabolic, while other signals slowed bone growth (e.g., MS3: 45Hz, 0.5g, 10min). This is shown in trabeculae by percent labeled surface (Fig. 1a) and bone formation rate per bone volume (Fig. 1b).

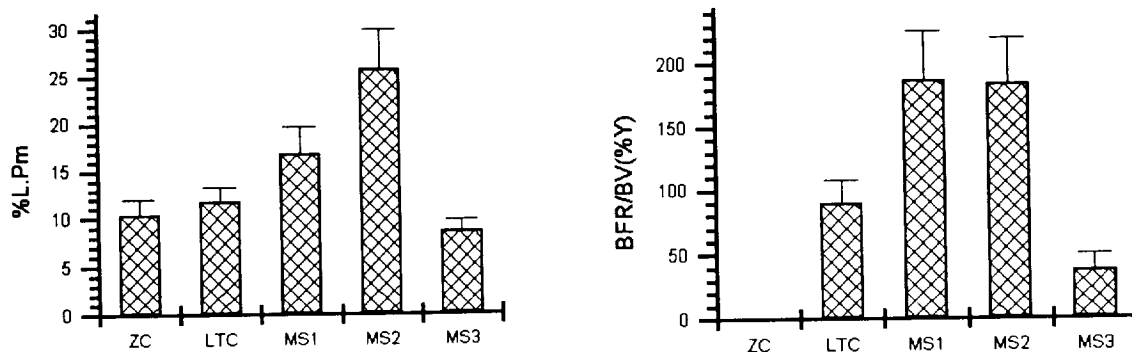


Fig. 1a (left) shows the percent of surface of the trabeculae of the proximal tibial metaphysis, distal to the growth plate, with active deposition of bone over the course of the protocol. While long term control (LTC) shows no significant difference from zero time control (ZC), there is a significant increase in labeled surface in both MS-1 and MS-2, and a decrease in MS-3 ($p < 0.05$). Fig. 1b shows bone formation rate per bone volume. The osteogenic specificity of the signals is also seen in this analysis. BFR/BV cannot be performed on zero-term controls, as only a single label is given (N=6).

DD-PCR of RNA from the tibiae of the tail suspended animals successfully identified several gene candidates with increased expression following 10d of disuse, as compared to long term controls (Table 1). Northern blots confirmed these observations. Discussed here are two specific genes, one known, and one unknown. S-14 was first isolated from liver (Liaw & Towle, 1984), and is believed to participate in adipose synthesis. S-14 has not previously been shown to be expressed in bone. The second, OPO-1 (Osteoporosis 1) is a novel gene, and the full-length clone has been isolated and sequenced (1.8 Kb). Interestingly, both osteogenic mechanical stimuli (MS-1 & MS-2) downregulated expression of both candidate genes, and to a certain extent, even below control levels. RNA analysis is not yet available from MS-3.

	CONTROL	DISUSE	MS-1	MS-2
S-14	++	+++	++	+
OPO-1	++	+++	+	++

Table 1. The relative expression of two genes, one known but not previously identified in bone (S-14), and one novel (OPO-1). Northern blots were used to confirm the differential expression of these genes, and their relative expression determined using optical density methods normalized to GAPDH expression. Relative to long term control, the expression of both S-14 and OPO-1 was elevated by disuse, but downregulated by two distinct, low level mechanical stimuli.

CONCLUSIONS

Preliminary evidence from these studies suggests that a low level biomechanical stimulus can significantly influence the patterns of bone formation and resorption in the rat tibia. The specific components of the mechanical signal, or rather the critical interdependence of frequency, magnitude and duration of the signal which makes it osteogenic, is not known. Disuse, as modeled by tail-suspension of the rat, is known to cause a retardation of growth, and here it is demonstrated to upregulate the expression of several genes, some known and some novel. That the osteogenic mechanical stimulation downregulates the expression of these genes, even below the level seen in "normal" bone, suggests that these genes play a role in the recruitment and activity of osteoclasts. As our studies begin to focus on determining the function of these genes, it is encouraging that a non-invasive, non-pharmacogenic intervention can serve as a "surrogate" for weightbearing, and that the discovery of novel genes may help identify new modalities to biophysically or biochemically control the bone loss which plagues long term space flight.

This work was funded by NASA NAG 53950. Exogen, Inc kindly provided the mechanical stress devices.

Chomczynski, P. & Sacchi, N. (1987) *Anal. Biochem* 162:156-159.

Fritton, J., Rubin, C., Qin, Y-X, & McLeod. *J. Biomed. Eng.* 25:831-839

Goldberg, J.M. et. al. (1987) Space Studies Board, National Academy Press, Washington, D.C.

Liang, P & Pardee, A.B. (1992) *Science* 257:967-971.

Liaw, C & Towle, H. (1984) *J. Biol. Chem.* 259: 7253-7260

Morey-Holton, E & Wronski, T (1981) Animal models for simulating weightlessness. *Physi.*24:545-548

Qin, Y.-X., Rubin, C. & McLeod, K. (1998) *J. Orth. Res.* 14:482-489

Rubin, C. & Lanyon, L. (1987) *J Orth. Res.* 5:300-310

Rubin, C., Turner, S., Jerome, C., Bain, S., & McLeod, K. (1998a) *ASBMR: Bone*: 23: 1126

Rubin, C., Recker, R., Cullen, A., Ryaby, J., & McLeod, K. (1998b) *ASBMR: Bone*: 23:1106

Smith, L.D., et. al. (1991) Space Studies Board, National Academy Press, Washington, D.C.

SKELETAL STRUCTURAL CONSEQUENCES OF REDUCED GRAVITY ENVIRONMENTS

C.B. Ruff, T.J. Beck, D. Newman, M. Oden, G. Shaffner, A. LeBlanc, L. Shackelford, and N. Rianon

INTRODUCTION

Human physical activity in terrestrial environments is enabled by muscle forces acting through the levers of the long bones to move the body's mass against the earth's gravitational field. The loading forces generated in the skeleton are believed to be the stimulus for structural adaptation of bone to maintain skeletal strains within certain intrinsic limits. Exceeding strain set limits with consistent strenuous exercise is believed to stimulate new bone formation while strains consistently below set limits, as in disuse or microgravity, cause bone loss. The removal of mechanical stimulus in disuse or exposure to microgravity results in the rapid loss of muscle mass followed by the slower but inexorable loss of bone. In prolonged space-flight, astronauts and cosmonauts experience highly variable patterns of bone loss, probably because of variations in the effects of microgravity as well as local variations in the efficacy of exercise countermeasures. The main consequence of loss of bone is an increase in bone fragility, but the structural consequences of bone loss, i.e., the risk of catastrophic failure, cannot be ascertained by conventional metrics of skeletal bone mass. The principle goals of this project are to use engineering methods to assess the structural consequences of prolonged weightlessness. Work involves the extraction of structural information from bone mass data on astronauts, cosmonauts and bed-rest subjects as well as the use of x-ray computed tomography on the tail suspended rat model.

METHODS

There are three separate sub-projects in this study.

In sub-project 1 rats subjected to a 35 day period of tail suspension in the NSBRI study of Schultheis and Shapiro are periodically scanned with a small animal CT scanner (XCT Research SA, Norland Inc. Fort Atkinson WI). Scans are to be done in both the unloaded femur and in the humerus which will be either partially or fully weight bearing, or with or without treatment with a bisphosphonate (ibandronate) depending on the study group. High resolution CT scans require scan times on the order of 20 minutes per slice, hence rats are anesthetized and positioned in a special immobilizing device.

In subproject 2, data from a conventional dual energy x-ray absorptiometry (DEXA) scanner are analyzed with a program to extract geometric properties permitting the application of engineering analysis. DEXA data for analysis includes research subjects undergoing 17 weeks of bed-rest as well as astronaut and cosmonaut data acquired before and after Mir missions. Most of the data includes scans of the hip, although a special scan at the mid-thigh in bed-rest subjects is also provided. The mid-thigh scan permits the quantification of both muscle and bone geometry from a single data set.

In the third subproject, 3-dimensional finite element models of the human femur are being compared with 2-dimensional engineering models derived from DEXA data. 3D models are

being constructed from high resolution CT data on a young male cadaver femur, and models derived from *in vivo* CT data acquired pre and post bed rest is in planning.

RESULTS

Significant advances have taken place over the past several months in all three subareas of this project: pQCT measurements of suspended rats, DEXA scan analyses of bedrest/Mir subjects, and finite element modeling of human femora. The first group of eight animals in the suspended rat study (done in collaboration with Drs. Schultheis and Shapiro) have been pQCT scanned at four skeletal locations and baseline values for both trabecular density and cortical bone geometry determined. They are now undergoing treatment with combinations of full suspension, partial suspension, ibandronate, periodic weightbearing, or normal weightbearing. A new positioning and anesthetization procedure (the scanning can take several hours per animal) was successfully implemented on these animals. Further validation of these procedures through repeated scanning of live non-study animals has also been carried out.

In the second subarea of the project, a total of 73 serial DEXA scans acquired at the mid-thigh on 9 Baylor University bed-rest subjects have been obtained. The purpose of this procedure is to permit the quantitative assessment of changes in cortical bone geometry and muscle size from the DEXA data. The thigh scan procedure was developed and validated using a different DEXA scanner for an unrelated project. For the Hologic scanner used on the bedrest subjects, thigh scanning involves a non-standard scanning protocol not supported by the manufacturer; thus the calibrations are not available and must be derived. Special software for calibration, conversion of scan data into image files, and analysis of the resulting images has been written for this project, and testing of the software on the 73 scan files is currently in process. On this same subproject, hip data on bed-rest subjects has been analyzed showing that strength related dimensional changes in the cortex do occur. These changes are inconsistent with those observed in the aging process, and suggest that exposure to microgravity produces a greater degradation in bone strength for a given loss of bone mass, than is associated with the aging process. A series of Mir cosmonaut hip scans are currently being analyzed at Baylor University. Results from that study as well as the data from the mid-thigh in the bed-rest subjects will be presented.

The primary goal of the finite element analysis (FEA) portion of this project is to validate the 2-D curved beam analysis performed on DEXA images in the second part of the study project. A human femur has been scanned using pQCT and used to create a 3-D finite element model. A convergence study has been conducted using four different mesh densities and it appears that a mesh with approximately 2,000 elements will yield sufficient accuracy for this study. We have developed a protocol and are currently negotiating to obtain permission to CT scan two or more subjects in the Baylor bedrest study, to develop 2-D to 3-D conversion techniques on a sample more appropriate for application to astronaut data.

THE EFFECTS OF PARTIAL MECHANICAL LOADING AND IBANDRONATE ON SKELETAL TISSUES IN THE ADULT RAT HINDQUARTER SUSPENSION MODEL OF MICROGRAVITY

Lex Schultheis*, Jay Shapiro⁺, Sue Bloomfield[#], Neal Fedarko*, Myrtle Thierry-Palmer[^], Christopher Ruff*, Jennifer Ruiz*: *Johns Hopkins University, ⁺Walter Reed Army Medical Center, [#]Texas A & M University and the [^]Morehouse School of Medicine.

The elimination of weight bearing force in microgravity uncouples bone formation from bone resorption resulting in net bone loss. Gravity imposed mechanical loading can mitigate these effects of diminished mechanical strain. However quantitative assessment of gravity titration as a mechanical countermeasure in a ground-based animal model has not yet been studied. We will determine the level of mechanical loading required to maintain bone remodeling in the face of weightlessness as well as the role of antiresorptive agents under this condition.

Graded mechanical loading on forepaws starting at 50% body weight vs. unloaded hindlimbs is applied through a novel servo-controlled platform that is the floorplate of each cage. An infrared optical system quantitatively resolves a total displacement of 2 mm caused by a 100 gram weight to within 5%. The activity of the animals is monitored continuously. The relationship between ground reaction forces and humerus bone strain is being concurrently investigated. Critical parameters under investigation include the magnitudes, repetition rates and frequency (Fourier) spectrum of applied forces and their associated bone strain history. Antiresorptive agents have been shown to decrease bone resorption and to increase bone mass. Ibandronate is a third-generation bisphosphonate which can be administered intravenously at 3 month intervals with little systemic toxicity. Using the rat adult (250-300 gm) hindquarter 35- day suspension model, parameters of bone biomechanics, bone mineral density, bone histomorphology and biochemistry are measured. Assessment includes vitamin D metabolites, and 24 hour urine catecholamine production and dry adrenal mass as parameters of stress.

Ten simultaneous animal suspension systems are operational. Continuously monitored impact profiles have been recorded during suspension with 50% weight bearing and in free roaming controls. Bone mineral density has been recorded using peripheral quantitative computed tomography (pQCT). Bone marrow stromal fibroblasts (osteoprogenitor cells) have been isolated from suspended and control animals.

We hypothesize that the combination of a critical amount mechanical loading and an antiresorptive agent will maintain normal bone remodeling in the face of microgravity.

BONE LOSS IN SPACE: SHUTTLE/MIR EXPERIENCE AND BED REST COUNTERMEASURE PROGRAM

L.C. Shackelford¹, A. LeBlanc², A. Feiveson¹, V. Oganov³

¹NASA Johnson Space Center, ²Baylor College of Medicine, ³Institute of Biomedical Problems

Loss of bone mineral during space flight was documented in the 1970's Skylab missions. The USSR space program made similar observations in the 1980's. The Institute of Biomedical Problems in Moscow and NASA JSC in 1989 began to collect pre- and post-flight bone mineral density (BMD) using Hologic QDR 1000 DEXA scanners transferred from JSC to Moscow and Star City. DEXA whole body, hip, and lumbar spine scans were performed prior to and during the first week after return from 4- to 6-month missions (plus one 8-month mission and one 14-month mission) on the Mir space station. These data documented the extent and regional nature of bone loss during long duration space flight. Of the 18 cosmonauts participating in this study between 1990 and 1995, seven flew two missions. BMD scans prior to the second flight compared to the first mission preflight scans indicated that recovery was possibly delayed or incomplete. Because of these findings, NASA and IBMP initiated the study "Bone Mineral Loss and Recovery After Shuttle/Mir Flights" in 1995 to evaluate bone recovery during a 3-year post-flight period. All of the 14 participants thus far evaluated lost bone in at least one region of the spine and lower extremities during flight. Of the 14, only one to date has exhibited full return to baseline BMD values in all regions. The current study will continue until the last participant has reached full bone recovery in all regions, has reached a plateau, or until three years after the flight (2001 for the last mission of the program).

Bone mineral density losses in space and difficulty in returning to baseline indicate a need for countermeasure development. In late 1996 NASA JSC and Baylor College of Medicine were approved to conduct two countermeasure studies during 17 weeks of bed rest. In 1997 the studies were begun in the bed rest facility established by NASA, Baylor College of Medicine, and The Methodist Hospital in Houston. To date, three bed rest controls, five resistive exercisers, and four subjects taking alendronate (a bisphosphonate that inhibits osteoclastic resorption of bone) have completed 17 weeks bed rest. In contrast to information currently available from space flight (n=28) and bed rest (n=12) in which all individuals experienced bone loss in at least one region, one of four subjects taking alendronate and one of five subjects performing heavy resistive exercise at bed rest fully maintained bone density in all regions of the spine and lower extremities. Overall results of both countermeasures which will be presented are encouraging. The study will be completed by mid to late 2000 with 10 subjects in each of three groups.

ALTERED BONE CELL METABOLISM DURING SPACEFLIGHT

Russell T. Turner, Departments of Orthopedics and Biochemistry and Molecular Biology, Mayo Clinic, Rochester, MN 55905

INTRODUCTION

My laboratory performs research which is directed toward understanding the cellular and molecular mechanisms by which mechanical usage influences bone mass, architecture and turnover. The goal of this research is to develop countermeasures to prevent disuse-induced bone fractures.

CURRENT STATUS OF RESEARCH

A) Methods

We perform studies on laboratory animals, primarily rats, and cultured human bone cells (hFOB). The endpoints generally consist of bone histomorphometry and gene expression (in vivo), and protein synthesis and gene expression (cell culture).

B) Results

Cortical and cancellous osteopenia occur in normal male rats following spaceflight. These abnormalities were due to decreased osteoblast activity (Backup, et al. 1994; Turner, et al. 1995; Westerlind and Turner, 1995). Furthermore, the decreased cellular activity was associated with reductions in steady-state mRNA levels for bone matrix proteins and TGF- β (Westerlind and Turner, 1995; Evans, et al. 1998).

Interestingly, spaceflight resulted in cancellous bone loss in ovariectomized rats with established osteopenia in excess of that due to estrogen deficiency (Cavolina, et al. 1997). This additional bone loss was due to increased bone resorption, indicating that gonadal hormones have a profound effect on the skeletal response to reduced mechanical usage. This conclusion was confirmed using ground based models for increasing as well as decreasing mechanical usage (Turner, et al. 1998).

We have established a time-course for changes in bone histomorphometry during spaceflight. No significant changes in cancellous or cortical bone volume were detected following a 4-day spaceflight (Backup, et al. 1994; Turner, 1995) and bone formation rate was not decreased. In contrast, decreases in bone formation rate and bone volume were observed in long bone metaphysis after 9 and 10 day spaceflights (Backup, et al. 1994; Turner, et al. 1995). Similarly, the periosteal bone formation rate in the diaphysis was decreased following a 9-day flight (Backup, et al. 1994).

Ovariectomy results in site-specific loss of cancellous bone. Although the long bone metaphysis (distal femur or proximal tibia) is highly sensitive to estrogen deficiency the corresponding epiphysis does not undergo bone loss as evaluated by conventional histomorphometry and micro QCT. Dynamic bone histomorphometry, measurement of eroded trabecular surfaces and Northern analyses of steady-state mRNA levels for bone matrix proteins revealed that bone turnover was dramatically increased in the epiphysis of estrogen-deficient rats. We concluded from these studies that the epiphysis is an estrogen target site and that estrogen determines the

rate of bone turnover but not necessarily the balance between bone formation and bone resorption. Finite element analysis established that trabeculae in the epiphysis are subjected to higher strain energies than those in the metaphysis (Westerlind, et al. 1997). We tested the hypothesis that mechanical strain determined the sensitivity of trabeculae to estrogen deficiency by manipulating strain levels. As predicted, increasing strain levels by treadmill exercise ameliorated the bone loss at the metaphysis whereas decreasing strain during spaceflight and following unilateral sciatic denervation resulted in bone loss from the epiphysis (Westerlind, et al. 1997). Similarly, resistance exercise increased cortical and cancellous bone volume in normal female rats (Westerlind, et al. 1998).

Recent collaborative studies in the laboratories of Dr. Turner and Dr. Emily Morey-Holton (NASA-Ames Research) have focused on the effects of mechanical unloading and the response to acute reweighing on gene expression in skeletal tissues. Results from these studies in rats flown in space or undergoing hindlimb elevation have consistently shown that unloading the skeleton results in a decrease in steady-state mRNA levels for the bone matrix proteins osteocalcin and type 1 collagen but has no effect on glyceraldehyde-3-phosphate dehydrogenase. These changes in gene expression preceded histological evidence for depressed bone formation and the values quickly returned to normal levels following reloading (unpublished). Of relevance to the proposed research was the finding that the upregulation of TGF- β mRNA levels preceded changes in matrix proteins. Additionally, we discovered that the effects of spaceflight on mRNA levels for bone matrix proteins in the femur are bone compartment-specific; the most dramatic reductions were observed in the proximal metaphysis whereas minimal changes were observed in the diaphysis (Evans, et al. 1998).

The effects of disuse and reloading on mRNA levels for skeletal signaling molecules appear to be gene specific; we have not detected changes in IGF-1 and fibroblast growth factor (FGF), TGF- β_2 , tumor necrosis factor- α (TNF- α), and interleukin-6 (IL-6). On the other hand, spaceflight resulted in decreased TGF- β_1 in males and increased interleukin-1 β (IL-1 β) and interferon- γ (IFN- γ) in ovariectomized rats (Zhang, et al. 1998).

Our studies have shown that programmed administration of hPTH using osmotic pumps can reproduce the anabolic effects on bone derived from daily sc administration of the hormone. This discovery provides a practical method of delivering PTH to rats during spaceflight. Ground-based studies have demonstrated that programmed administration of PTH is effective in reducing cancellous osteopenia in hindlimb elevated rats (Dobnig, et al. 1997; Turner, et al. 1998).

Time-course studies have revealed that daily sc administration of hPTH increases bone formation and results in upregulation of mRNA levels for bone matrix proteins within 12 hr. hPTH was shown to increase mRNA levels for early response genes (*c-fos* and *c-jun*) within 30 minutes. We are presently evaluating the time course changes in mRNA levels for skeletal signaling molecules and bone matrix proteins following treatment with hPTH (unpublished).

Cultured hFOB cells grew normally and expressed normal differentiated function during orbital spaceflight. There were, however, transient abnormalities in the expression of cytokines and growth factors by these cells following their return to earth (unpublished).

C) Conclusions

Our results suggest that regulation of bone cell metabolism by mechanical usage is mediated, in part, by osteoblast-derived cytokines and growth factors. The signaling pathways induced by weight bearing appear to overlap with the pathways induced by estrogen.

PLANS FOR FUTURE INVESTIGATION

Our future investigations will focus on the development of countermeasures which take advantage of the ability of target cell specific estrogen agonists to increase the sensitivity of bone cells to prevailing mechanical strain energies. We will also perform further evaluation of the potential of parathyroid hormone to maintain normal bone formation during spaceflight.

PUBLICATIONS

Backup P, Westerlind K, Harris S, Spelsberg T, Kline B, Turner R: Spaceflight results in reduced mRNA levels for tissue-specific proteins in the musculoskeletal system. Am J Physiol 266:E567-E573, 1994.

Turner RT: Effects of short-term spaceflight and recombinant human growth hormone (rhGH) on bone growth in young rats. Aviat Space Environ Med 66:763-769, 1995.

Turner RT, Evans GL, Wakley GK: Spaceflight results in depressed cancellous bone formation in rat humeri. Aviat Space Environ Med 66:770-774, 1995.

Westerlind KC, Turner RT: The skeletal effects of spaceflight in growing rats: Reduced steady-state mRNA levels of TGF- β . J Bone Miner Res 10(6):843-848, 1995.

Cavolina JM, Evans GL, Harris SA, Zhang M, Westerlind KC, Turner RT: The effects of orbital spaceflight on bone histomorphometry and mRNA levels for bone matrix proteins and skeletal signaling peptides in ovariectomized growing rats. Endocrinology 138:1567-1576, 1997.

Westerlind KC, Wronski TJ, Luo Z-P, An K-N, Bell NH, Turner RT: Estrogen regulates the rate of bone turnover but bone balance in ovariectomized rats is modulated by prevailing mechanical strain. Proc Natl Acad Sci 94:4199-4204, 1997.

Westerlind KC, Fluckey JD, Gordon SE, Kraemer WJ, Farrell PA, Turner RT: Effect of resistance exercise training on cortical and cancellous bone in mature male rats. J Applied Physiol 84:459-464, 1998.

Dobnig H, Turner RT: The effects of programmed administration of human parathyroid hormone fragment (1-34) on bone histomorphometry and serum chemistry in rats. Endocrinology 138:4607-4612, 1997.

Zhang M, Turner RT: The effects of spaceflight on mRNA levels for cytokines in proximal tibia of ovariectomized rats. Aviat, Space, Environ Med 69:626-629, 1998.

Evans GL, Morey-Holton E, Turner RT: Spaceflight has compartment and gene specific effects on mRNA for bone matrix proteins in rat femur. J Appl Physiol 84:2132-2137, 1998.

Turner RT, Evans GL, Cavolina JM, Halloran B, Morey-Holton E: Programmed administration of parathyroid hormone increases bone formation and reduces bone loss in hindlimb-unloaded ovariectomized rats. Endocrinology 139:4086-4091, 1998.

NON-INVASIVE INVESTIGATION OF BONE ADAPTATION IN HUMANS TO MECHANICAL LOADING

R. Whalen

NASA Ames Research Center, Moffett Field, CA 94035

INTRODUCTION

Experimental studies have identified peak cyclic forces, number of loading cycles, and loading rate as contributors to the regulation of bone metabolism. We have proposed a theoretical model that relates bone density to a mechanical stimulus derived from average daily cumulative peak cyclic 'effective' tissue stresses (Whalen, Beaupré, Carter). In order to develop a non-invasive experimental model to test the theoretical model we need to (1) monitor daily cumulative loading on a bone, (2) compute the internal stress state(s) resulting from the imposed loading, and (3) image volumetric bone density accurately, precisely, and reproducibly within small contiguous volumes throughout the bone.

We have chosen the calcaneus (heel) as an experimental model bone site because it is loaded by ligament, tendon and joint contact forces in equilibrium with daily ground reaction forces that we can measure; it is a peripheral bone site and therefore more easily and accurately imaged with computed tomography; it is composed primarily of cancellous bone; and it is a relevant site for monitoring bone loss and adaptation in astronauts and the general population.

This paper presents an overview of our recent advances in the areas of monitoring daily ground reaction forces, biomechanical modeling of the forces on the calcaneus during gait, mathematical modeling of calcaneal bone adaptation in response to cumulative daily activity, accurate and precise imaging of the calcaneus with quantitative computed tomography (QCT), and application to long duration space flight.

METHODS

At the NASA Ames Research Center we have developed the NASA Ground Reaction Force (GRF) Activity Monitor to record the vertical component of ground reaction forces (GRFz) during daily activity. Peak cyclic GRFz are filtered and stored along with their time of occurrence, as well as the time of initial foot-ground contact and foot lift-off (Breit, Quintana). We have recently used the GRF Activity Monitor to quantify the range in (three-day) non-exercising daily activity in 24 subjects in terms of histograms of subject-specific peak cyclic GRFz (Bowley).

The calcaneus is loaded almost exclusively during stance-phase of gait by joint, ligament and tendon forces in equilibrium with the ground reaction force. We constructed a 2D sagittal plane contact-coupled finite element model of the foot to estimate these forces and the internal stress states throughout stance-phase of walking and running (Giddings). Experimental kinematic data of foot skeletal structures and simultaneous GRF recordings were collected with high-speed cineradiography synchronized to a force plate in the Gait Analysis Laboratory at the Henry Ford Hospital. Results from the GRF Activity Monitor and the biomechanical model were then applied to the Stanford time-dependent mathematical model of bone adaptation to simulate sagittal plane calcaneal bone remodeling in response to normal daily activity. Boundary forces

imposed at the point of peak cyclic loading during walking and running were applied along with a subject daily history of GRFz.

We have recently developed and partially validated state-of-the-art algorithms to register serial QCT images and correct for beam hardening using single energy computed tomography (Yan). To test registration accuracy and precision, we scanned in helical mode excised calcanei in different orientations secured to a custom-made fiducial frame surrounded by water. To test our beam hardening correction algorithms, we scanned phantoms containing known concentrations of potassium phosphate in a cow bone cylinder surrounded by water with dense objects in the field.

RESULTS

Analysis of individual daily peak cyclic GRFz histograms of 24 subjects recorded over the three-day period identified a wide range in the 'intensity and duration' of daily activity and lower limb skeletal loading encompassing normal 'non-exercising' activity. A three-fold difference in number of daily loading cycles of greater than 0.95 body weight (BW) was observed with individual peak cyclic GRFz ranging from a few cycles of approximately 1.6 BW to peak force magnitudes over 2.5 BW.

The biomechanical model showed that the highest internal stresses in the calcaneus occur during mid- to late-stance, at approximately 70 percent of stance phase during walking and 60 percent of stance phase during running. Very little stress was generated in the calcaneus at heel strike. Walking and running differed only significantly in the magnitude of the internal stresses, not in the distribution of the stress or strain field. The magnitude of the internal stress state was scaled by the moment about the ankle. These results imply that monitoring peak GRFz with our monitor provides a good measure of the cumulative peak loading imposed on the calcaneus during walking and running. Our mathematical model of bone adaptation predicted many features of (sagittal plane) calcaneal bone distribution including a Ward's triangle, a cortical shell and a region of lower density in the central posterior calcaneus.

We obtained sub-voxel registration accuracy throughout the entire volume of the calcaneus (voxel size 0.30 mm x 0.30 mm x 0.50 mm). The mean error for all points within the calcaneus from six surface-based registrations was 0.20 mm (SD ± 0.02 mm), i.e., on average, points within the calcaneus were registered to within 200 microns of their true location. Following beam hardening correction of our phantom images, the maximum mean percent error in determining potassium phosphate concentration was approximately 1.5% (SD $\pm 1.5\%$) within the 34 mm cow bone cylinder. Concentrations tested ranged from zero (distilled water) to 800 mg/cc K₂HPO₄.

CONCLUSION

We believe it is possible to maintain the musculoskeletal system in space during long duration space flight with Earth-equivalent daily cumulative tissue loading. Monitoring daily ground reaction forces on Earth gives us a method of determining Earth-equivalent loading in space as well as a way of monitoring space flight exercise. We hope also to gain insight into the mechanical loading component of bone metabolism and bone density regulation by examining with our QCT methods and mathematical modeling the time-course of changes in volumetric bone density within small contiguous regions within the calcaneus in response to chronic (spinal cord injury) and acute (space flight without exercise) disuse, exercise, drug therapy and aging.

ACKNOWLEDGMENTS

NASA GRF Activity Monitor: Greg Breit, PhD; Jason Quintana, MS; Susan Bowley, MS. QCT bone imaging: Chye Yan, PhD (Thesis, Stanford University); Sandy Napel, PhD; Gary Beaupré, PhD, Cliff Les, PhD; Tammy Cleek, MS. Biomechanical modeling: Virginia Giddings, PhD (Thesis, Stanford University); Gary Beaupré, PhD; Dennis Carter, PhD.

This work has been supported by NASA Cooperative Agreements NCC2-5088, NCC2-5186, Department of Veterans Affairs Merit Review project B802-RA, and NASA grant 199-26-12-35. We would like to thank Dr. Scott Tashman, Bone and Joint Center, Henry Ford Hospital, for his expert advice, help and facilities.

RENAL STONE RISK DURING SPACE FLIGHT

Peggy A. Whitson, Ph.D., NASA/JSC, Robert A. Pietrzyk, M.S., Wyle Life Sciences, Clarence F. Sams, Ph.D., NASA/JSC and Charles Y.C. Pak, M.D. Univ of Texas Health Science Center. Presented by **Jeffrey A. Jones**, M.D., NASA/JSC.

Space flight produces a number of metabolic and physiological changes in the crewmembers exposed to microgravity. Following launch, body fluid volumes, electrolyte levels, and bone and muscle undergo changes as the human body adapts to the weightless environment. Changes in the urinary chemical composition may lead to the potentially serious consequences of renal stone formation.

Previous data collected immediately after space flight indicate changes in the urine chemistry favoring an increased risk of calcium oxalate and uric acid stone formation (n = 323). During short term Shuttle space flights, the changes observed include increased urinary calcium and decreased urine volume, pH and citrate resulting in a greater risk for calcium oxalate and brushite stone formation (n = 6). Results from long duration Shuttle/Mir missions (n = 9) followed a similar trend and demonstrated decreased fluid intake and urine volume and increased urinary calcium resulting in a urinary environment saturated with the calcium stone-forming salts. The increased risk occurs rapidly upon exposure to microgravity, continues throughout the space flight and following landing.

Dietary factors, especially fluid intake, or pharmacologic intervention can significantly influence the urinary chemical composition. Increasing fluid intake to produce a daily urine output of 2 liters/day may allow the excess salts in the urine to remain in solution, crystals formation will not occur and a renal stone will not develop. Results from long duration crewmembers (n = 2) who had urine volumes > 2.5 L/day minimized their risk of renal stone formation. Also, comparisons of stone-forming risk in short duration crewmembers clearly identified greater risk in those who produced less than 2 liters of urine/day. However, hydration and increased urine output does not correct the underlying calcium excretion due to bone loss and only treats the symptoms and not the cause of the increased urinary salts. Dietary modification and promising pharmacologic treatments may also be used to reduce the potential risk for renal stone formation. Potassium citrate is being used clinically to increase the urinary inhibitor levels to minimize the development of crystals and the growth of renal stones. Bisphosphonates are a class of drugs recently shown to help in patients with osteoporosis by inhibiting the loss of bones in elderly patients. This drug could potentially prevent the bone loss observed in astronauts and thereby minimize the increase in urinary calcium and reduce the risk for renal stone development.

Results of NASA's renal stone risk assessment program clearly indicate that exposure to microgravity changes the urinary chemical environment such that there is an increased risk for supersaturation of stone-forming salts, including calcium oxalate and brushite. These studies have indicated specific avenues for development of countermeasures for the increased renal stone risk observed during and following space flight. Increased hydration and implementation of pharmacologic countermeasures should largely mitigate the in-flight risk of renal stones.

BONE PROTEOGLYCAN CHANGES DURING SKELETAL UNLOADING

M. Yamauchi¹, K. Uzawa¹, S. Pornprasertsuk¹, S. Arnaud², R. Grindeland², W. Grzesik¹

¹ Dental Research Center, University of North Carolina, Chapel Hill, NC 27599-7455

² NASA Ames Research Center, Moffett Field, CA94035-1000

INTRODUCTION

Skeletal adaptability to mechanical loads is well known since the last century (Wolff 1892). Disuse osteopenia due to the microgravity environment is one of the major concerns for space travelers. Several studies have indicated that a retardation of the mineralization process and a delay in matrix maturation occur during the space flight (Simmons et al., 1990).

Mineralizing fibrillar type I collagen possesses distinct cross-linking chemistries and their dynamic changes during mineralization correlate well with its function as a mineral organizer (Yamauchi 1996). Our previous studies suggested that a certain group of matrix proteoglycans in bone play an inhibitory role in the mineralization process through their interaction with collagen (Cheng et al., 1996, 1998). Based on these studies, we hypothesized that the altered mineralization during spaceflight is due in part to changes in matrix components secreted by cells in response to microgravity. In this study, we employed hindlimb elevation (tail suspension) rat model to study the effects of skeletal unloading on matrix proteoglycans in bone.

METHODS

Four month-old male albino rats (about 425 g) were hindlimb unweighted for 0, 1, 4 and 8 weeks using the procedure reported by Wronski and Holton (1987). Groups of 8-10 suspended and similar numbers of control (ambulatory) rats were killed at each time period and bones (femurs and tibiae) were collected. Some bones were sectioned and fixed for routine histological as well as immunohistochemical studies. The antibodies that are specific to various glycosaminoglycans (chondroitin-4-sulfate, chondroitin-6-sulfate, keratan sulfate and dermatan sulfate) were used for the latter studies. Tibiae were obtained from five rats that were subjected to 8 week suspension and from five control rats. The middle third of bones were cut, pulverized and lyophilized. Certain amounts of dried bone powder were subjected to sequential extraction using 6M guanidine-HCl and then 0.5M EDTA at 4°C in order to separate mineral-unbound and -bound matrix molecules (Cheng et al., 1996). Each extract was dialyzed, lyophilized and weighed. Equal amounts of dried matrix molecules (100 µg) were then subjected to Western blot analyses using the panel of antibodies described above.

RESULTS

In these preliminary studies, we found that the amounts of guanidine-HCl extract (mineral-unbound fraction) in 8 week-suspended bones were significantly larger than that of control (approximately 30 % larger). The amounts of EDTA extractable matrix (mineral-bound) were not significantly different between the two groups. Various proteoglycans were found to be enriched in the guanidine-HCl extract when compared to the EDTA extract in both suspended and control bones. The Western blot analyses demonstrated that most proteoglycans examined are more abundant, on a dry weight basis, in the suspended bones when compared to control. Based on the molecular size, the keratan sulfate containing molecules were likely small collagen-binding proteoglycans, fibromodulin and/or lumican. Interestingly, the molecular weight of the chondroitin-6-sulfate proteoglycans that exhibited a high molecular weight (more than 220 kDa, possibly versican) in the suspended bones was slightly higher than that of control.

CONCLUSION

These preliminary studies indicate that the proteoglycan composition (quantity as well as quality) in bone changes in response to skeletal unloading. This type of matrix alteration could be associated with a mineralization defect of bone observed during space flight.

Supported by NASA grant NAG 2-1188.

THE EFFECTS OF TWELVE WEEKS OF BEDREST ON BONE HISTOLOGY, BIOCHEMICAL MARKERS OF BONE TURNOVER, AND CALCIUM HOMEOSTASIS IN ELEVEN NORMAL SUBJECTS

J.E. Zerwekh¹, L.A. Ruml¹, F. Gottschalk², and C.Y.C. Pak¹

¹Center for Mineral Metabolism and Clinical Research and ²Department of Orthopaedic Surgery, University of Texas Southwestern Medical Center at Dallas, Dallas, TX 75235-8885

INTRODUCTION

Gravity is recognized as an important factor in the normal growth and maintenance of the skeletal system. The mechanism(s) by which gravity affects skeletal growth and remodeling are not known, but in its absence, such as during space flight or prolonged immobilization, the result is a rapid loss of bone mineral. If of sufficient duration and magnitude, such losses of bone mineral could lead to fracture. In addition, increased urinary concentration of stone-forming salts would increase the risk for kidney stone formation. In order to prevent such losses during skeletal unloading, effective countermeasures must be directed at preventing the underlying defect in bone metabolism. In order to better understand the nature of the skeletal defect(s) which contribute to this loss of bone mineral, we examined the effects of twelve weeks of bedrest on bone metabolism and calcium homeostasis in eleven normal volunteers. This was accomplished via the use of bone histomorphometry and measurement of calcitropic hormones and biochemical markers of bone turnover.

METHODS

This study was approved by the University institutional review board. All subjects were admitted to the Clinical Research Center after giving informed consent. The subjects ranged in age from 20 to 53 (34•11) years. There were seven Caucasian and two African-American men as well as one Hispanic and one Caucasian woman. All volunteers underwent an initial ambulatory phase, an 84-day bed rest phase, and a reambulation phase. Subjects were evaluated while under constant metabolic diet regimen during each phase. Fasting venous blood samples were collected for measurement of serum chemistries, intact parathyroid hormone (iPTH), vitamin D metabolites, osteocalcin, bone-specific alkaline phosphatase (BSAP), type I procollagen extension peptide (PICP), and carboxyl telopeptide of type I collagen (ICTP). Three consecutive 24 hr urine collections were obtained and analyzed for calcium, phosphorus, hydroxyproline (OHPro), N-telopeptide (NTx) and free deoxypyridinoline (Dpd) cross-links of type I collagen. Intestinal calcium absorption was determined using fecal recovery of ⁴⁷Ca prior to bed rest and again prior to reambulation. Bone mineral density (BMD) of the lumbar spine, femoral neck, and trochanteric regions of the hip and at the radius were also performed. Bed rest commenced after tetracycline labeling and procurement of the baseline bone biopsy. Bloods and urine were obtained each week during bed rest for the tests listed above. Prior to reambulation a second bone biopsy was obtained and BMD determinations again performed.

RESULTS

Following 12 weeks of bed rest, BMD declined at the lumbar spine (-2.9%), femoral neck (-1.1%), and greater trochanter (-3.8%, p=0.002). It did not change at the radius. Bed rest resulted in a small but significant increase in serum Ca and no significant change in serum P (Table 1). Serum iPTH and 1,25-dihydroxyvitamin D declined significantly during bedrest and rose during

reambulation. Both urinary calcium and phosphorus rose significantly during bedrest and declined towards normal during reambulation. Overall, there was no significant change in fractional intestinal Ca absorption during bedrest. Trabecular bone histology demonstrated significant increases in eroded surface ($2.1 \cdot 1.1$ SD to $4.7 \cdot 2.2$ %, $p=0.002$) as well as for active osteoclast surface ($0.2 \cdot 0.2$ to $0.4 \cdot 0.4$ %, $p=0.02$) following 12 weeks of bed rest. In addition, there was a significant decrease in osteoblastic surface ($3.1 \cdot 1.3$ to $1.9 \cdot 1.5$ %, $p=0.014$). The remaining static and dynamic parameters did not change significantly. Cortical bone also demonstrated significant changes in eroded surface ($3.5 \cdot 1.1$ to $7.3 \cdot 4.0$ %, $p=0.018$) and in osteoclast surface ($0.2 \cdot 0.3$ to $0.7 \cdot 0.7$ %, $p=0.021$). There were no other significant changes observed for cortical bone. Table 2 summarizes the changes in the biochemical markers of bone turnover. The bone formation serum markers osteocalcin and BSAP demonstrated no consistent significant change during bedrest or following reambulation. However, there was a significant interaction between bedrest and PICP as disclosed by the repeated measures ANOVA. Changes in the markers of bone resorption were more marked. Significant increases in serum ICTP and in urinary NTx and Dpd were observed during the first 4 weeks of bed rest. These values remained elevated throughout bedrest and declined towards normal following reambulation.

Table 1. Effect of 12 weeks bed rest and reambulation on serum and urinary parameters of calcium homeostasis in 11 normal subjects.

Parameter	Bed rest phase					Normal range
	Pre	Weeks 1-4	Weeks 5-8	Weeks 9-12	Reambulation	
Serum						
Ca (mmol/l)	2.32•0.05*	2.37•0.07 ⁺	2.37•0.07 ⁺	2.37•0.05 ⁺	2.35•0.10 (p=0.015) [^]	2.12-2.57
P (mmol/l)	1.42•0.14	1.42•0.16	1.45•0.16	1.45•0.16	1.42•0.16	0.81-1.45
iPTH (ng/l)	31•15	25•10	24•8	23•6	31•12 (p=0.015) [^]	10-65
25OHD (nM)	40•17	37•17	40•20	37•15	35•17	20-105
1,25(OH) ₂ D (pM)	70•14	53•12 ⁺	48•12 ⁺	46•10 ⁺	53•17 ⁺ (p<0.0001) [^]	43-125
Urine						
Ca (mmol/d)	5.3•1.5	6.4•1.8 ⁺	7.3•2.5 ⁺	7.0•2.1 ⁺	4.5•0.9 ⁺ (p<0.0001) [^]	<5.0
P (mmol/d)	26•5	28•6 ⁺	30•7 ⁺	28•7	24•7 (p<0.0001) [^]	
Fract. Intest.	47•11	-	-	43•10	-	40-60
Ca absorp. (%)						

*All values expressed as mean • SD.

⁺Value significantly different from pre-bed rest value by Bonferroni adjusted paired-t using • =0.0125 (0.05/4) level of significance.

[^]p value for repeated measures of analysis to assess differences among the five phases.

CONCLUSION

Using a ground-based model of skeletal unloading we have observed that during 12 weeks of immobilization there is a marked increase in cortical and cancellous bone resorption. This increase in bone resorption is further supported by the significant increases in the biochemical markers of bone resorption during bed rest and their decrease following reambulation. Furthermore, the small but significant increase in serum calcium, hypercalciuria, iPTH suppression, and decline are all sequelae of this increased bone resorption. However, despite a significant decline in osteoblast numbers and a general trend for decreased cancellous osteoid surface and reduced tetracycline uptake, the biochemical markers failed to disclose marked

changes in bone formation activity. Taken together these observations would indicate that antiresorptive therapy might serve as a useful countermeasure to microgravity-induced bone loss.

Table 2. Effect of 12 weeks bed rest and reambulation on serum and urinary biochemical markers of bone turnover in 11 normal subjects.

Parameter	Bed rest phase					Normal range
	Pre	Weeks 1-4	Weeks 5-8	Weeks 9-12	Reambulation	
Formation-serum						
Osteocalcin (• mol/l)	7.1•2.5*	7.5•2.0	7.7•2.1	7.4•1.6	7.7•1.9	2.4-11.7
BSAP (U/l)	21•9	19•6	19•5	20•5	21•6	12-40
PICP (• g/l)	117•48	107•29	115•30	110•22	140•36 (p=0.013) [^]	38-202
Resorption-serum						
ICTP (• g/l)	4.9•1.6	6.3•2.0*	6.1•2.2*	5.8•2.2	5.5•1.9 (p=0.003) [^]	1.8-5.0
Resorption-urine						
OH-Pro (• • mol/d)	190•61	244•69*	275•84*	275•69*	221•53* (p<0.0001) [^]	<198
Dpd (nmol/d)	55•21	61•22	75•27*	87•28*	76•26* (p=0.0001) [^]	20-144
NTx (nmolBCE/d)	366•199	476•250*	553•270*	547•262*	421•219 (p=0.0002) [^]	45-803

*All values expressed as mean • SD.

[^]Value significantly different from pre-bed rest value by Bonferroni adjusted paired-t using • =0.0125 (0.05/4) level of significance.

[^]p value for repeated measures of analysis to assess differences among the five phases.

Cardiovascular

Chair

Peter Raven, Ph.D.

Co-Chair

Sue Schneider, Ph.D.

CARDIOVASCULAR SESSION SUMMARY

Within the two and one half days there were twenty-six presentations ranging across four major areas of cardiovascular space biology:

- Effects of microgravity on the cardiovascular and thermoregulatory systems
 - Countermeasures
 - Molecular biology
 - New approaches of assessment
- I. Microgravity effects on the cardiovascular and thermoregulatory systems. Ground based investigations

Human studies - bedrest

1.
 - a. Cardiac atrophy is observed after bedrest deconditioning. Prolonged bed rest or space flight may increase the amount of atrophy.
 - b. Plasma volume is reduced after bed rest and when combined with the cardiac atrophy, diastolic volume and stroke volume in the upright position are reduced and appear related to post-bed rest orthostatic hypotension.
 - c. When arterial and cardiopulmonary baroreflexes are calculated as a function of change in stroke volume both heart rate and muscle sympathetic nerve activity appear to be appropriately regulated after bed rest and spaceflight. It was concluded that the countermeasure to the cardiac atrophy decreased stroke volume and decreased plasma volume would be exercise training. A bed rest exercise training study is underway. (**Levine**)
2.
 - a. Orthostatic intolerant (OI) individuals following 14 days of -6° head down tilt bed rest were characterized by
 - (i) elevated supine muscle sympathetic nerve activity (MSNA)
 - (ii) a blunted increase in MSNA at 60° head up tilt (HUT).
 - b. The OI individuals had a reduced norepinephrine response, a smaller increase in total peripheral resistance to HUT suggesting an inadequate sympathetic vasoconstriction.
 - c. The increase in resting supine MSNA and blunted MSNA response in the OI group following the head-down bed rest suggest arterial baroreflex dysfunction, resetting or central dysregulation in some subjects. (**Shoemaker and Sinoway**)
3. Two weeks of bed rest with a constant sodium and potassium intake induced (n):
 - a. Sodium retention and potassium loss
 - b. Enhanced renin and aldosterone responses to upright posture.
 - c. Enhanced aldosterone response to angiotensin II infusion.
 - d. Reduced the nighttime melatonin surge.
 - e. Sleep deprivation dissociation of the renin and aldosterone responses to the upright position.

It was suggested that simulated microgravity did not produce a natriuresis but activated the sodium retaining hormonal mechanisms. A possible countermeasure include a

- time/dose dependent melatonin administration; a matching of electrolyte intake and/or administration of a aldosterone receptor antagonist. (**Williams et al.**)
4.
 - a. Thermoregulatory responses to simulated microgravity or spaceflight are impaired.
 - b. Cutaneous vasodilation during a thermal stress after simulated or actual microgravity exposure is reduced probably due to an increased threshold of internal temperature for cutaneous dilation and reduced slope of response. The mechanisms of this response are unknown but may be related to a greater decrease in central venous pressure due to heating following bed rest.
 - c. Sweating responses were also diminished following spaceflight. (**Schneider et al., Crandall and Etzel**)
 5.
 - a. Cardiac output at rest, low and moderate exercise is elevated in early and late bed rest as compared to the erect posture on earth.
 - b. In simulated microgravity pulmonary blood flow is increased and central blood flow is reduced.
 - c. The distribution of blood volume in microgravity is independent of gravity suggesting lower pulmonary vascular resistance is a reason for increased pulmonary blood flow and a myogenic constriction of the large cerebral artery results in a reduced cerebral blood flow via PET scanning. (**Pendergast et al.**)

Animal Studies

1.
 - a. Head-out water immersion of the non-human primate produced a consistent increase in blood pressure, cardiac output, renal blood flow, urine flow, central venous pressure and a decrease in heart rate.
 - b. De-immersion causes a rapid decrease in blood pressure, cardiac output, renal blood flow and urine flow with a reflex tachycardia.
 - c. The arterial baroreflex is reset during and after immersion. However, during immersion there is a (n).
 - i Negative water balance; and
 - ii Increased sensitivity to acute volume expansion. (**Cornish and Hughes**)
2. Hind limb unweighting in rats resulted in:
 - a. Decreased baroreflex activation of renal and lumbar sympathetic nerve activity in response to hypotension or hemorrhage.
 - b. Changes in baroreflex function appear to be due to altered central nervous system processing of baroreceptor afferent input with normal afferent input from aortic baroreceptors.
 - c. The rostral ventrolateral medulla (RVLM) appears to be involved in altered sympathetic control.
 - d. Reduced FOS expression in RVLM during hypotension was consistent with sympathoexcitation.
 - e. Increased GABAergic mediated inhibition of the RVLM.
 - f. The increased GABAergic inhibition involves GABAergic inputs from regions of the central nervous system other than the caudal ventrolateral medulla (CVLM). (**Hasser et al.**)
3.
 - a. Hind limb unweighting caused a(n): vascular hyporesponsiveness by an upregulation of endothelial nitric oxide synthase (e NOS) in the carotid artery.

- b. Upregulation of inducible nitric oxide synthase (iNOS) in the femoral artery.
- c. Marked increase in middle cerebral artery myogenic tone by the downregulation of eNOS.
- d. iNOS inhibition markedly elevated blood pressure in the hind limb unweighted rat. (**Purdy et al.**)

B. Space Flight

Human Data

1. a. Data from the recent neurolab mission involving the cardiovascular responses to the Valsalva maneuver suggest that autonomic nervous system (vagal) control of blood pressure was altered and that the sympathetic responses were not proportional to reductions in blood pressure as noted in ground based studies. (**Eckberg**)
2. a. Other data from the recent neurolab mission using muscle sympathetic nerve activity (MSNA) response to lower body negative pressure suggest that the sympathetic response was appropriate given the reductions in cardiac size and plasma volume.
 - b. The lack of presyncopal episodes in this group of astronauts limits the conclusions that could be drawn. (**Pawelczyk et al.**)
3. a. The evidence of presyncope during the upright position is several fold greater after four to five months of spaceflight compared to 4-18 days of spaceflights.
 - b. Presyncope after spaceflight is related to autonomic dysfunction.
 - c. Non-pilot trained (aircraft) women appear more susceptible to presyncope after spaceflight compared to non-pilot trained men.
 - d. Pressor responses to phenylephrine on landing day are equal to or greater than pre-flight responses.
 - e. Preliminary findings suggest that presyncopal subjects may have normal norepinephrine release to tyramine injections but subnormal norepinephrine release in response to the upright position on landing day. (**Fritsch-Yelle et al.**)

Rats

- a. Calcium diet induced differences in blood pressure are maintained by microgravity.
- b. Blood pressure regulation is altered by microgravity.
- c. Vascular responsiveness of mesenteric resistance vessels are reduced by microgravity.
- d. Basal free intracellular calcium is reduced but thrombi stimulated calcium values and intracellular calcium stores appear to be normal. (**Hatton et al.**)

Countermeasures

1. a. The development of a human powered centrifuge provides artificial gravity to the subject while exercising.

- b. The human powered centrifuge which was designed for exercise to produce acceleration - has a linear response between oxygen uptake, heart rate and ventilation with exercise load (**Greenleaf et al.**)
 2. a. Graded workload cycle ergometer exercise designed to elicit maximal physical effort has been successful in restoring orthostatic tolerance and maintaining the capacities of physiological mechanisms that contribute to blood pressure regulation following exposure to ground analogs of low gravity. (**Convertino et al.**)
 3. a. Plasma volume expansion following high intensity exercise is associated with an increased renal retention of sodium and water.
 - b. Increase renal sodium retention occurs in the proximal tubules.
 - c. Plasma volume expansion following intense exercise is limited in the supine posture. (**Mack et al.**)
 4. a. Baroreflex resetting to the higher exercise blood pressure is directly related to active muscle mass and intensity of exercise.
 - b. The operating point of the baroreflex is directly related to the intensity of the exercise and is relocated towards the threshold of the reflex as work intensity increases and/or central command increases.
 - c. During prolonged exercise the carotid baroreflex is progressively reset upwards and rightwards with the operating point moving to a point below threshold in relation to the increasing central command as the exercising muscle fatigues and recruits more fiber.
 - d. By applying external compression to the legs using LBPP or MASTrousers an intramuscular mechanoreceptor reflex activation of the sympathetic nervous system results in a marked increase of mean arterial blood pressure of 8-10mmHg during rest and exercise to maximum. (**Raven**)

Molecular Biology

1. a. Alterations in gene expression in cyochrome oxidase subunit VIaH results in a cardiac phenotype of diastolic dysfunction in the isolated working mouse heart.
 - b. Although this gene mutation is not associated with differences in overall ATP production reduced myocardial oxygen consumption is present.
 - c. Use of transgenic models can be used to study underlying metabolic and transcriptional origins of cardiac phenotypes resulting from microgravity. (**Radford et al.**)
2. a. Electrical stimulation of isolated cardiac myocytes with medium conditions in a 3-D collagen matrix can mimic altered conditions of pre-load and afterload.
 - b. Progressive increase in either preload or afterload produced progressive increases in all protein synthesis rates.
 - c. Preload and afterload are primary determinants of cardiomyocyte gravity. (**Baicu et al.**)
3. a. Genes directly involved in the mechanical load induction of hypertrophy can be identified and cloned. (**Abdellatif and Schneider**)

Assessment: New Approaches

1.
 - a. The measurement of microvolt level T-wave alternans (TWA) is a non-invasive technology for the assessment of susceptibility to ventricular tachyarrhythmias which has been developed over the past decade with NASA support.
 - b. TWA has proven to be a promising accurate non-invasive predictor of cardiac arrest and sudden cardiac death from ventricular tachyarrhythmias both in animal studies, and in human studies in a variety of patient populations.
 - c. Preliminary data from four subjects in a 14 day bed-rest study indicates that bed-rest tends to induce microvolt level TWA in same subject.
 - d. This preliminary finding needs to be confirmed in additional healthy subjects as well as in longer term bedrest studies, and in astronauts pre- and post-flight.
 - e. TWA may potentially provide a marker for the development of countermeasures to mitigate the risk of sustained ventricular tachyarrhythmias during long term spaceflight. Its utility has been shown in patients at significant risk of arrhythmias, but this predictive power has not been shown in healthy subjects. **(Mullen et al.)**
2.
 - a. Quantification of beat-to-beat fluctuation in heart rate dynamics, including the use of nonlinear dynamics methods, may i) provide a new approach to non-invasively evaluate cardiovascular regulation. It is unknown whether this can provide predictive power for space motion sickness or cardiovascular deconditioning.
 - b. Cardiac arrhythmogenesis is a perceived concern during long-term space flight and warrants further, systematic evaluation.
 - c. Comprehensive databases that achieve continuous electrocardiographic and other physiological recordings during spaceflight and microgravity simulations should be annotated to provide correlations with other variables such as activity, pharmacology, and subjective symptomology (e.g. space motion sickness). **(Goldberger)**
3.
 - a. Cardiovascular System Identification (CSI) is a new technique developed under NASA support for the assessment of closed-loop cardiovascular regulation.
 - b. CSI involves the mathematical analysis of beat-to-beat variability in physiologic signals such as heart rate, blood pressure, respiration, and cardiac output to construct an individualized closed-loop model of cardiovascular regulation.
 - c. CSI can quantify alterations in cardiovascular regulation associated with changes in posture, pharmacologic autonomic blockade, and sub-clinical diabetic autonomic neuropathy.
 - d. CSI is being applied to study alterations in cardiovascular control during a 14-day bed-rest study. Preliminary results indicate that bed-rest results in diminished autonomic reflexes (including the heart rate baroreflex) as well as alterations in circulatory mechanics. **(Ramsdell et al.)**
4.
 - a. A novel technique for assessing left ventricular filling dynamics (intraventricular pressure gradients) developed to avoid much of the load dependency can be used during spaceflight and bed-rest microgravity when alterations in load occur.
 - b. The technique can be used to assess diastolic suction.
 - c. Myocardial relaxation can be assessed using tissue Doppler echocardiography. **(Thomas et al.)**

5.
 - a. Microgravity induced elimination of hydrostatic pressure is the primary response involved in stimulating the secondary physiological, neurological and endocrinological responses.
 - b. Hydraulic and computer models can be used to isolate and study individual response mechanisms.
 - c. These same hydraulic and computer models can be used to predict the effectiveness of countermeasures for post-flight orthostatic intolerance. (Sharp et al.)

It was apparent from the number of diverse presentations and findings and the limited discussion time available to the group, that the obtaining of consensus of where the results are heading to suggest future work was fraught with diametrically opposed opinions. We (Chair and Co-chair) have attempted to provide a succinct summary of the findings and to identify topics of future investigations.

Underlying this summary is the recognition that two philosophies appeared to pervade our thinking. These being:

- i Because space flight deconditioning appears duration dependent in many organ systems, in flight countermeasure protocols need to be established at the outset and continued throughout flight. This could mean continuous artificial gravity or intermittent artificial gravity using human powered or motor powered centrifuges. However, the protocols and engineering required along with cost factors in terms of development monies and astronaut time commitments need to be determined.
- ii If one views the cardiopulmonary system in isolation, then it appears that the adaptations the system undergoes during microgravity exposure are appropriate for survival during prolonged spaceflight. The crux of the physiological problem occurs on re-entry into a gravitational field and therefore results in our focus being on entry employed countermeasures to the microgravity-induced adaptations. However, when dealing with the human organism it appears that some of the organ systems (e.g. bone) continue to deteriorate over the duration of the flight and do not achieve some adaptive steady state to microgravity, such that in flight countermeasures need to be established for these organ systems.

Summary

It was apparent that the bed-rest and spaceflight data indicated that decreases in plasma volume and cardiac atrophy along with cardiac remodeling were fundamental changes which predisposed many astronauts to post flight orthostatic intolerance. Despite the recently acquired in-flight and post-flight muscle sympathetic nerve activity findings suggesting that the sympathetic nerve responses were appropriate there remains significant contrary data from bed-rest studies, post-flight stand tests and hind-limb unweighted rat studies that suggest that the vasoconstrictive responses were compromised at least insufficient in susceptible individuals. The key issues raised is whether a diminished increase in sympathetic activity from baseline without changes in

peak response or receptor adaptations is an abnormal response or is an individual variance of response to the accentuated decrease in stroke volume.

Data relating autonomic neural control of heart rate were presented to suggest that the vagal and sympathetic control of heart rate was attenuated. Also, bed-rest and space flight induced attenuated baroreflex control of heart rate was shown to be restored to pre-bedrest function by one bout of maximal dynamic exercise. However, these data were confounded by relying on the use of R-R interval as a measure of efferent responses of the baroreflex during a condition in which the baseline heart rate was changed. Clearly the idea that the autonomic control of heart rate may be changed by microgravity needs further investigation. This direction is suggested despite the fact that in the triple product ($HR \times SV \times TPR = MAP$) assessment of the regulation of arterial blood pressure during orthostasis the role of the HR reflex may be less influential than that associated with cardiac atrophy (SV changes) and aberrant sympathetic vasoconstriction (resistance) changes.

Although sympathetic nerve activity responses in-flight and post-flight on neurolab appeared appropriate, enough bed-rest and post-flight stand test data, along with animal model data suggest that vasoconstriction was compromised. The mechanism of this compromised vasoconstriction needs to be delineated.

Other major findings concerning microgravity and physiological regulatory systems are that:

1. Thermoregulatory adaptation appear to suggest some decrements in the control of cutaneous vasodilation and sweating;
2. Calcium resorption and dietary calcium need to be defined for differing durations of spaceflight, especially as the effects of excess calcium on vasomotor function appears to be detrimental;
3. Neurohumoral mechanisms of microgravity induced changes in neural function and the regulation of plasma volume and total body water, bone resorption and autonomic neural control of the circulation need further delineation;
4. As performance of work tasks become prolonged, the mechanisms of blood pressure regulation in microgravity needs to be obtained to determine whether in-flight countermeasures need to be used in the recovery period from prolonged work tasks.

The use of the hind-limb unweighted rat model in evaluating cardiovascular adaptation and blood pressure regulation responses needs to be reviewed in context that from a heart function perspective the heart is acutely loaded in the head down position. However, whether the model truly reflects the microgravity environment of space needs to be verified with space flight before the elegant findings regarding central nervous system control of arterial baroreflexes are accepted as a consequence of microgravity.

From the data presented viable countermeasures include maximal exercise bouts and its consequent plasma volume expansion and the possible changes in baroreflex regulation of heart rate control. Inflation of the "anti g-suit,, increasing intramuscular pressure and reflexly increasing arterial blood pressure, which along with whole body surface cooling to translocate cutaneous blood volume centrally and counteract aberrant cutaneous vasodilation and sweating

responses to heat stress should be considered a prerequisite of re-entry procedures and initial recovery period in 1 "G,,. The role of in-flight artificial gravity developed by a human powered centrifuge or a motor driven centrifuge or a total space craft centrifuge need to be evaluated. Specifically, the time and duration of the cardiovascular responses to the artificial gravity and its benefits need to be determined.

In flight monitoring using non-linear dynamic measures of cardiovascular function, electrocardiogram analysis of T-wave alternans, color-flow Doppler echocardiography and models of cardiovascular function need to be brought on-line and evaluated as to their effectiveness to provide real time assessments of cardiovascular function during space flight.

Ground based molecular biologic models of cardiac atrophy, cardiac metabolism, altered ion channel control of heart rate and differences in ventricular pre-load and after-load adaptations, vascular smooth muscle and neuroendocrine control of the cardiovascular system as result of microgravity need to be developed to investigate the molecular events explaining the adaptation to microgravity.

Peter Raven and Sue Schneider

DIRECT CLONING OF GENES REGULATED BY MECHANICAL LOAD

M. Abdellatif, M.D. Schneider
Baylor College of Medicine

In an attempt to identify genes that are regulated during pressure overload hypertrophy; we resorted to subtraction hybridization between hearts from sham operated and aortically banded mice. In parallel, we also performed a subtraction between an adult and a neonatal heart, for comparison of pressure overload-induced and normal growth of the heart. This led to the identification of several known (75%) and unknown (25%) genes that were upregulated during both normal and pathological growth of the heart. In general, about 50 % of the known genes belong to one of three functional groups. 1- Genes related to transcription, such as: histone H2A.Z, cardiac ankyrin-repeat protein (CARP), Bop2, high mobility group 2, and CDC10. 2- Genes related to translation, such as: quaking protein, p68 RNA helicase, mitochondrial rRNA and tRNA, ribosomal proteins L23a, L7a, S18, and L3, Heterogenous ribonucleoprotein C and F, elongation factor 1-alpha, and RNA helix-destabilizing protein. 3- Genes related to the cytoskeleton and regulation of its structure, such as: thymosin beta-4, Pr22, Cyr61, desmin, OSF-2, collagen, Mena+, tropoelastin, and integrin-linked kinase. The remainder of the genes included, ~25% repeats of the known genes and ~25% of genes belonging to other functional groups, which included the Ras related signaling molecule, Rap1B, whose function is still unclear. While all genes tested by Northern analysis, were expressed at higher levels in both neonatal and hypertrophy hearts versus normal adult heart, the CARP was one exception that was upregulated during hypertrophy but had lower levels in the neonatal compared to the adult heart. In general, the subtraction method helped identify several genes, previously unknown for their role in hypertrophy, and some previously unknown even for their presence in the heart, such as the extra-cellular matrix protein, osteoblast specific factor-2. It also helped identify novel cardiac isoforms, as in the case of the quaking protein. The functional role of these genes in hypertrophy await further investigation.

MECHANISMS FOR LOAD CONTROL OF CARDIAC MASS: CELL CULTURE STUDIES IN ADULT CARDIOMYOCYTES USING A 3-D COLLAGEN MATRIX

C. F. Baicu, J. H. Turner, V. D. Young, M. Barnes, and M. R. Zile

Medical University of South Carolina, Gazes Cardiac Research Institute, Charleston, SC 29403

INTRODUCTION

Growth regulation in the adult myocardium is controlled by a complex interaction of mechanical, neurohormonal and growth factors. The purpose of this study was to use *in-vitro* primary cell culture techniques to isolate hemodynamic and mechanical determinants of cardiac muscle cell growth without making simultaneous changes in other potential factors.

METHODS

Cardiomyocytes were embedded in a 3-dimensional collagen matrix which mimics *in-vivo* myocardial composite conditions. This model allowed isolated changes in individual mechanical determinants to be made. Isolated adult feline cardiomyocytes were embedded in a 3-D collagen-type I matrix and cultured in a mitogen-free medium. Protein Synthesis Rate (PSR [*nmol PHE/g protein/hr*]) was measured using tritium-labeled phenylalanine over a 4 hour period. PSR was measured in quiescent and electrically stimulated cells. 140 V, 1 Hz and 5 msec pulse characterize the applied electric field. Afterload (AL) was altered by varying the constitutive properties of the gel matrix, i.e. changing the collagen concentration.

RESULTS

Cardiomyocyte shortening extent (SE) decreased as collagen % increased (SE=5.74±0.35% for collagen 2%, SE = 3.44±0.28% for collagen 8%, p<0.05). Preload (PL) was altered by varying sarcomere length (SL) by stretching the composite collagen-embedded cells. Cardiomyocyte SL increased from 1.8 • m to 2.1 • m, as cell strain was increased from 0% to 10%. PSR in quiescent cells did not significantly change as the collagen concentration was increased (PSR = 175.5±4.34 for collagen 2%, PSR = 182.4±5.4 for collagen 4%). However, PSR increased in electrically stimulated cells and increased as the collagen concentration increased (PSR = 207.7±3.7 for collagen 2%, PSR = 254.7±7.0 for collagen 4%, p<0.05). Compared to non-stretched quiescent cells, PSR in stretched quiescent cells increased (PSR stretched quiescent = 203.9±4.6, p<0.05 vs. PSR non-stretched quiescent = 170.8±4.7). PSR was further increased in stretched and stimulated cells (PSR = 374.9±4.6, p<0.05 vs. non-stretched and stimulated). An increase in either AL or PL caused an increase in PSR of 50±4% and 19±3%, respectively. Additionally, the combined effect of increased AL and PL caused a 119±5% increase in PSR. Thus, both PL and AL are primary determinants of cardiomyocyte growth.

VASCULAR REACTIVITY IN A RAT MODEL OF MICROGRAVITY

Dan E. Berkowitz, Leo Marucci, Esther Asplund, Bradford Winters, Annette Szumski, Daniel Nyhan, Artin Shoukas
Departments of Anesthesiology and Critical Care Medicine and Biomedical Engineering, Johns Hopkins University School of Medicine

Orthostatic intolerance is a major problem following exposure to prolonged bedrest and microgravity. The etiology of attenuated cardiac output (CO) and blood pressure (BP) responses is incompletely understood. Normal or accentuated norepinephrine (NE) response to an orthostatic challenge suggest that the abnormality may be in the end organ (vessels). To test the hypothesis that changes in vascular reactivity may be responsible for hypotension in vitro vessel responses were studied in vessel rings from normal and hind-limb unweighted (HLU) rats. Although the model is well accepted ground based model of microgravity we have verified in chronically instrumented rats (aortic flow probe and arterial line), that redistribution of blood volume/orthostatic stress (70° tilt) results in appropriate baroreceptor mediated responses (~10% decrease in CO, ~8% increase in BP and ~5-10% increase in heart rate). Animals were euthanized following 21 days of HLU and 5mm aortic rings (just below the aortic arch), renal (500mm), carotid and femoral arteries were harvested and placed in vessels chambers containing Krebs solution. Dose responses to KCl and NE, phenylephrine (PE), U46619 (U4) (thromboxane analogue) were performed in 1/2 log doses. The starting diameter of the vessel rings was similar in all animals. There was a significant rightward shift in the KCl, NE, PE and U4 dose response with a decrease in the maximal response in aortic rings. While renal artery responses to KCl were similar, there were accentuated responses to alpha-1AR agonists NE and PE in HLU animals. There are significant differences in the EC50 to agonists between carotid and femoral arteries but no differences between control and HLU animals has been demonstrated. Radioligand binding of [125I] HEAT, an alpha-1AR specific ligand to membranes prepared from rat aorta showed a ~60% reduction in receptor number in HLU animals. The change in both receptor dependent and independent contractile activity in aorta suggests that the vascular abnormality observed may be secondary to abnormalities of Ca²⁺ mobilization or may represent abnormalities in the contractile machinery involved in excitation contraction coupling. (e.g. vessel atrophy). The reduction in alpha-1 AR receptor number may suggest a mechanism. This is provocative in light of the attenuated sympathetic traffic observed during microgravity/bedrest exposure, and the importance of NE in smooth muscle hypertrophy. The increase in alpha-1 AR specific responses in renal arteries suggests differential regulation of alpha-1 AR's in different vascular beds.

APPLICATION OF ACUTE MAXIMAL EXERCISE TO ENHANCE MECHANISMS UNDERLYING BLOOD PRESSURE REGULATION AND ORTHOSTATIC TOLERANCE AFTER EXPOSURE TO SIMULATED MICROGRAVITY

V.A. Convertino, K.A. Engelke, and D.F. Doerr

US Army Institute of Surgical Research, Ft Sam Houston, Texas 78234, Biomedical Operations Office, Kennedy Space Center, Florida 32899

INTRODUCTION

Development of orthostatic hypotension and intolerance in astronauts who return to earth following a spaceflight mission represents a significant operational concern to NASA. Reduced plasma volume, vascular resistance, and baroreflex responsiveness following exposure to actual and ground-based analogs of microgravity have been associated with orthostatic instability, suggesting that these mechanisms may contribute alone or in combination to compromise of blood pressure regulation after spaceflight. It therefore seems reasonable that development of procedures designed to reverse or restore the effects of microgravity on regulatory mechanisms of blood volume, vascular resistance and cardiac function should provide some protection against postflight orthostatic intolerance. Several investigations have provided evidence that a single bout of exhaustive dynamic exercise enhances functions of mechanisms responsible for blood pressure stability. Therefore, the purpose of our research project was to conduct a series of experiments using ground-based analogs of reduced gravity (i.e., prolonged restriction to the upright standing posture) in human subjects to investigate the hypothesis that a single bout of dynamic maximal exercise would restore blood volume, vascular resistance and cardiac function and improve blood pressure stability.

METHODS

We conducted a series of 3 experiments. In the first experiment, we evaluated carotid-cardiac baroreflex responses in 8 normotensive ambulatory men on two different test days, each separated by at least one week. On one day, baroreflex response was tested before and at 3, 6, 12, 18 and 24 h after graded supine cycle exercise to volitional exhaustion. On another day, this 24-h protocol was repeated with no exercise (control). In a subsequent experiment, we measured cardiovascular responses during 15 minutes of 70° head-up tilt (HUT) and assessed arterial baroreceptor stimulus- response relationships in 10 paraplegic subjects 24 hours after arm-crank exercise designed to elicit maximal effort, and during a control (no exercise) condition. One week separated the treatments. The wheelchair confinement of these patients represented a low gravity posture compared to normal upright ambulatory subjects. In the third experiment, cardiovascular responses during exposure to a protocol of graded, presyncopal-limited lower body negative pressure (LBNP), alterations in blood volume, and autonomic responses associated with blood pressure regulation were assessed in 7 male subjects before and after two periods of 6° head-down tilt (HDT) separated by 11 months. On the last day of one HDT period, subjects performed a single bout of maximal ergometry (exercise). Exercise consisted of supine cycling with graded work rates increasing by 16 W/min to volitional fatigue and required an average of 16 min. Subjects did not exercise after the other HDT period (control). In all experiments, carotid-cardiac baroreflex sensitivity was evaluated by measurement of R-R interval during external application of graded pressures to the carotid sinuses from 40 to -65 mmHg using a neck collar device; changes of R-R intervals were plotted against carotid pressure

(systolic pressure minus neck chamber pressure). Integrated baroreflex function was assessed by recording beat-to-beat heart rate (HR) and mean arterial blood pressure (MAP) during a 15-sec Valsalva maneuver (VM) at a controlled expiratory pressure of 30 mmHg. The ratio of change in HR to change in MAP (\bullet HR/ \bullet MAP) during phases II and IV of the VM was used as an index of cardiac baroreflex sensitivity. Baroreflex-mediated vasoconstriction was assessed by measuring the late phase II rise in MAP. Heart rate, blood pressure, vascular resistance, and vasoactive hormones were measured during HUT and LBNP protocols. In the third experiment, plasma volume, fluid intake (ad libitum), urine output, renal function, and hormones associated with fluid homeostasis were measured before HDT, 24 h before the end of HDT just prior to exercise, and at the end of HDT 24 h after exercise. A standard cross-over design was used in all experimental protocols in which the order of treatment (exercise or control) was counterbalanced across all subjects.

RESULTS

In the 8 ambulatory subjects, the maximum slope of the carotid-cardiac baroreflex stimulus-response relationship increased ($P < 0.05$) from preexercise to 12 hr (3.7 ± 0.4 to 7.1 ± 0.7 msec/mmHg) and remained significantly elevated through 24 h. No significant differences were observed during the control 24-h period. In the paraplegic subjects, the maximum slope of the carotid-cardiac baroreflex response was increased ($P = 0.049$) by exercise (6.2 ± 1.7 msec/mmHg) compared to control (3.3 ± 0.6). During control HUT, HR increased from 61 ± 1 to 90 ± 7 bpm ($P = 0.001$) while SBP decreased from 118 ± 5 to 106 ± 9 mmHg ($P = 0.025$). During HUT 24 hours after exercise, HR increased from 60 ± 2 to 90 ± 4 bpm ($P = 0.001$), but the reduction in SBP was essentially eliminated (116 ± 5 to 113 ± 5 mmHg). The reduction in SBP during control HUT (-12.0 ± 4.6 mmHg) was four-fold larger ($P = 0.017$) than during HUT following exercise (-3.1 ± 3.9 mmHg). A single bout of intense, dynamic arm-crank exercise eliminated orthostatic hypotension in the paraplegic patients. Equal HR response with smaller reduction in SBP during HUT after exercise was consistent with a measured increased sensitivity of the carotid-cardiac baroreflex. The post-exercise increase in forearm vascular resistance (FVR) from supine to HUT of 17.0 ± 2.4 to 24.8 ± 3.2 PRU was greater ($P = 0.042$) than the increase observed during control (18.3 ± 3.7 to 19.5 ± 3.1 PRU). Responses in norepinephrine, vasopressin, and plasma renin-angiotensin induced by HUT were similar for control and post-exercise and there was no difference in either leg compliance or plasma volume between the two conditions. Additionally, HR and SBP responses to phases II and IV of the Valsalva maneuver, indices of integrated baroreflex sensitivity, were enhanced ($P < 0.05$) following maximal exercise compared to control. In the third experiment, a reduction of LBNP tolerance time after HDT from pre-HDT levels was greater ($P = 0.041$) in the control condition (-2.0 ± 0.2 min) compared to the exercise condition (-0.4 ± 0.2 min). At presyncope after HDT, FVR and plasma norepinephrine were higher ($P < 0.05$) following exercise compared to control while MAP, HR, leg volume, and other plasma hormone responses were similar in both conditions. Following HDT, carotid-cardiac baroreflex sensitivity was reduced (2.8 to 2.0 msec/mmHg; $P = 0.05$) as was \bullet HR/ \bullet MAP during phase II of the VM (-1.5 to -0.8 beats/mmHg; $P = 0.002$). After exercise, isolated carotid baroreflex activity and phase II \bullet HR/ \bullet MAP returned to pre-HDT levels but remained attenuated in the control condition. The late phase II increase of MAP was 71% greater following exercise

compared to control (7 mmHg vs. 2 mmHg; $P = 0.041$). Heightened baroreflex function was associated with maintenance of orthostatic tolerance following HDT in the exercise condition. HDT reduced PV by 16% in both control and exercise conditions. Maximal exercise completely restored plasma volume within 24 h to 3.9 ± 3.2 % of pre-HDT levels despite continued HDT. Compared to control, exercise induced a 660-ml larger positive fluid balance due to greater fluid intake and reduced urine volume during the 24 h after exercise.

CONCLUSIONS

The development of orthostatic hypotension and the possibility of frank syncope in astronauts following their return from spaceflight and procedures to counteract this adverse adaptation has been an operational concern to NASA for more than a quarter century. We tested the hypothesis that one bout of maximal exercise performed at the conclusion of prolonged exposure to low gravity would improve blood pressure stability during an orthostatic challenge. Maintenance of orthostatic tolerance by application of acute intense in our experiments was associated with greater circulating levels of NE, vasoconstriction, cardiac function, baroreflex sensitivity, and plasma volume. Therefore, these results support our hypothesis and indicate that any procedure that can reverse hypovolemia and baroreflex impairment should be effective in restoring orthostatic tolerance following spaceflight. The observation that acute exercise designed to elicit maximal physical effort restored the responsiveness of baroreflex control of cardiac function and vascular resistance as well as plasma volume in individuals who had undergone prolonged exposure to groundbased analogs of low gravity supports the notion that its application to astronauts following prolonged spaceflight may be effective in improving orthostatic stability. Operationally, the use of less frequent and more intense exercise as a possible countermeasure against postflight orthostatic hypotension is attractive because its use within 24 h of orbiter reentry would be maximally cost effective by enhancing crew safety and postflight rehabilitation while minimizing inflight use of work time, food, water and oxygen usually utilized during longer exercise regimens repeated during numerous days of the mission. Additional experiments are underway to continue the investigation of mechanisms underlying the effects of acute maximal exercise. The results from this series of experiments provide a physiological basis for future spaceflight testing of acute maximal exercise as a protective measure against postflight orthostatic instability in astronauts.

HEAD-OUT WATER IMMERSION IN THE PRIMATE AS A MODEL FOR THE CARDIOVASCULAR/RENAL EFFECTS OF μ G

Kurtis G. Cornish*, Ph.D., Kathryn Hughes, M.D. Dept. of Physiology and Biophysics. University of Nebraska College of Medicine. Omaha, NE. 68198-4575.

INTRODUCTION

The objectives of this research were: 1) Develop a non-human primate model that simulates the cardiovascular deconditioning that is exhibited by the astronauts; 2) Determine how in the baroreflex control of blood pressure is altered during and after 72 hrs of simulated microgravity; 3) Determine if there is an alteration in the control of blood volume during simulated microgravity; 4) Investigate possible counter measures that could be used in order to prevent the orthostatic hypotension that has been observed in the astronauts.

METHODS

This study has involved the use of 8 chronically instrumented Rhesus monkeys. Cardiovascular instrumentation included arterial and venous catheters and aortic and renal Doppler flow probes. After training the animals to the restraint chair, they were placed in a water tight suit and then immersed in the upright position to the level of the mid chest. The immersion period lasted for 72 hrs and was preceded and followed by two hours of control. The animals tolerated this well and eating and drinking normally during the procedures. Renal and cardiovascular data were recorded continually and urine was collected hourly. The psychological well-being of the animal was ensured by having someone with them continually as well as being provided with soft music and a variety of fruits.

The control immersion consisted of 72 hrs with no additional volume supplement. Catheter lines were maintained patent by infusing lactated Ringer's solution at a rate of 3 ml/hr/catheter. The baroreflex was determined by injecting phenylephrine and nitroprusside before immersion, 4 hours into the immersion and then at 28, 52, and 70 hrs of immersion and then after the immersion. Potential countermeasures studied were 1) continuous volume maintenance (VM) to prevent negative water balance, and 2) isotonic/isooncotic volume expansion prior to de-immersion. VM was achieved by continuously infusing 51 ml lactated Ringer's solution/hr. Alterations in the control of blood volume were determined by volume expanding (VE) the animals with 6% isoconic/isooncotic dextran (15% EBV). The control volume expansion was done on a day other than the immersion day. VE was repeated on the last day of the immersion. This was done with and without the VM.

RESULTS

Control cardiovascular and renal changes are presented in **Table 1**. Immersion caused an increase in blood pressure associated with a reflex bradycardia and resetting of the baroreflex. After the immersion there was a significant tachycardia with a decrease in blood pressure. These were partly attenuated by VM. A diuresis and natriuresis resulted during the immersion that was potentiated VM. The response to acute VE was potentiated during immersion suggesting that countermeasures involving volume loading may potentiate the diuresis observed during weightlessness.

Immersion with and without volume maintenance.

Table 1. The effect of immersion on Renal and cardiovascular variables. IMM= average during immersion period; P-DI = the time after post de-immersion. For Cont vs Imm * = $p < 0.05$, ** = $p < 0.01$; For Cont vs P-DI † = $p < 0.05$; For Imm vs D-Imm # = $p < 0.05$

	Control	IMM	P-DI		Cont	IMM	P-DI
<u>CVP (mmHg)</u>				<u>U_{Na}V (mEq/hr)</u>			
Avg	-1.87	4.56*	-1.22#	Avg	1043.57†	1905.40*	1509.00
SE	0.92	1.77	0.39	SE	387.42	65.27	514.24
<u>ABP (mmHg)</u>				<u>CO (ml/min)</u>			
Avg	106.44	119.82*	112.67	Avg	97.70	172.73	129.80
SE	4.59	5.62	3.92	SE	37.40	4.66	24.12
<u>HR (bpm)</u>				<u>U_{Osm}(mOsm)</u>			
Avg	177.38†	157.58*	220.35 #	Avg	533.29	461.25 *	475.33
SE	8.88	0.88	6.71	SE	65.78	16.43	150.52
<u>Renal Flow</u>				<u>UV ml/min</u>			
Avg	12.63	9.08	14.94	Avg	9.06 †	34.13 **	23.23
SE	3.59	0.23	5.72	SE	2.28	1.34	5.04

In response to immersion there was:

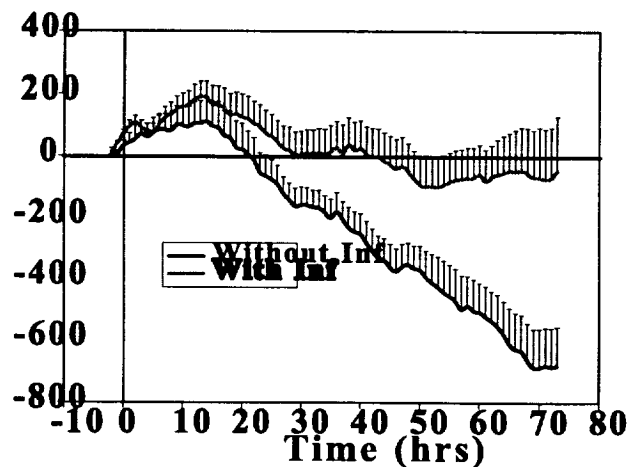
An upward and rightward shift in the baroreflex curve.

A gradually hypotensive developing during the first hr post de-immersion.

A significant negative water balance early in the immersion and that increased throughout the immersion. During VM the animals become adipsic and need to be encouraged to drink (Figure 1).

An initial increase in ANF during the immersion which returned to normal or below after 24 hrs of immersion. It increased above control levels post de-immersion, probably due to the tachycardia.

An increase in urine output within the 2 hour of immersion that continued throughout the immersion. This was associated with a similar increase in sodium excretion.



With VM there was:

1. A greater increase in CVP. After de-immersion the blood pressure tended to be at or above the pre-immersion control levels.
2. A continued shift in the baroreflex, possible with greater sensitivity. There was a decreased

hypotension with nitroprusside.

3. No tendency for the animals to become hypotensive during the post de-immersion period even though they still exhibited a significant tachycardia.
4. A negative water balance that was less than without VM (Figure 1).
5. A similar change in ANF when compared to the control immersions.
6. A greater diuresis and natriuresis throughout the immersion.

VE during Immersion without VM.

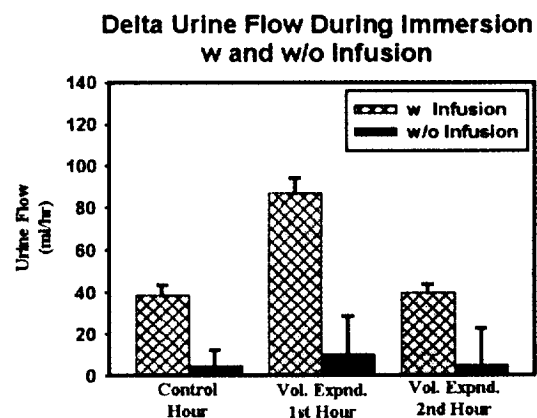
The volume expansion was intended to simulate current counter measures and to examine the reflex control of blood volume during the immersion. The following were observed with VE.

7. VE during the last 6 hours of immersion did not cause a significant diuresis (Figure 2).
8. The baroreflex curve was shifted upwards with the same saturation. However there was still tachycardia as seen in the control immersions.
9. The animals did not become hypotensive to any degree during post immersion period. They were also less sensitive to nitroprusside and more responsive to phenylephrine.

VE during Immersion with VM.

With VE there was:

10. A significant diuresis in response to the dextran infusion given just before de-immersion. In some instances this exceeded the volume given during the expansion (Figure 2).
11. An upward and rightward shift in the baroreflex curve.
12. A decreased tachycardia post immersion.
13. A relative insensitivity to nitroprusside post immersion and very sensitive to phenylephrine.



CONCLUSIONS

Head-out water immersion of the non-human primate simulates the cardiovascular and renal responses to microgravity reported in astronauts. Our results support a diuresis during exposure to microgravity, the degree being related to the level of hydration of the astronaut. Volume maintenance before and during microgravity may actually increase the diuresis during microgravity but would also decrease the degree of post flight orthostatic hypotension. It would appear that the control of blood volume is enhanced during exposure to microgravity. Therefore volume loading immediately prior to re-entry may actually enhance the diuresis associated with increased fluid volume. As would be expected VM would decrease the sensitivity to interventions that produce hypotension by restoring vascular and extra vascular volumes. However, these interventions do not completely restore post immersion changes in the baroreflex.

FUTURE DIRECTIONS:

Examine the possibility of using Growth Hormone as a countermeasure to cardiovascular and renal deconditioning effects of microgravity. Results from a single animal.

14. GH decreased in the negative water balance.
 15. GH increased the range of the baroreflex.
- GH decreased hypotension post de-immersion.

POTENTIAL MECHANISM LEADING TO IMPAIRED THERMOREGULATION FOLLOWING MICROGRAVITY EXPOSURE

C.G. Crandall^{1,2} and R.A. Etzel¹

¹Institute for Exercise and Environmental Medicine at Presbyterian Hospital of Dallas, and

²Department of Internal Medicine at University of Texas Southwestern Medical Center, Dallas, TX 75231

INTRODUCTION

Prolonged exposure to microgravity or its analogues impairs thermoregulation in humans evidenced by higher internal temperatures following the exposure during a thermal challenge (3, 5). Although the mechanism leading to this response has not been clearly delineated, we identified that prolonged head-down tilt (HDT) markedly impairs thermoregulatory reflex control of skin blood flow, as demonstrated by an increased internal temperature threshold for cutaneous vasodilation, and by a reduced slope of the relationship between the elevation in skin blood flow relative to the elevation in internal temperature (2). Recently, Fortney et al. (4) identified similar responses in two individuals following 115 days of microgravity exposure. One possible mechanism leading to altered cutaneous vasodilation during a thermal challenge following actual or simulated microgravity exposure may be associated with baroreflex-mediated attenuation in the elevation of skin blood flow.

During a heat stress the elevation in skin blood flow is accomplished through a combination of increased cutaneous vascular conductance and cardiac output, both of which result in central venous pressure (CVP) decreasing 2-6 mmHg (7). Reductions in CVP of this magnitude in normothermia decrease muscle blood flow (6) and skin blood flow (8) presumably through unloading the cardiopulmonary baroreceptors. It is unclear whether the reduction in CVP, and accompanying cardiopulmonary baroreceptor unloading, during passive heating buffers the elevation in skin blood flow. That is, would the elevation in skin blood flow be greater if CVP did not decrease, or decreased to a lesser extent during the heat stress? Conversely, if CVP decreased to a greater extent during a thermal challenge following a perturbation such as prolonged HDT, would the elevation in skin blood flow be attenuated during that thermal challenge? Given that prolonged HDT decreases plasma volume and central venous pressure (1, 2), such a finding would provide a plausible hypothesis to explain why skin blood flow does not increase to the same extent during a heat stress following simulated (2) or actual microgravity exposure (4). Thus, the purpose of this project was to identify whether cardiopulmonary baroreceptor unloading coincident with heat stress buffers the elevation in skin blood flow.

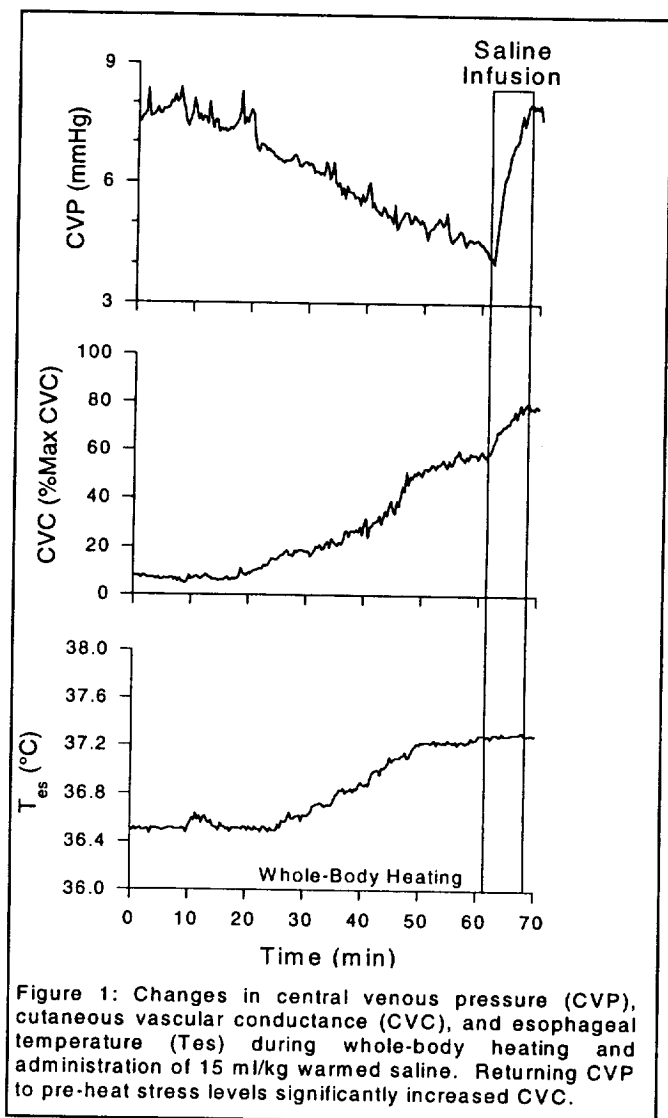
METHODS

Seven subjects (4 men, 3 women) participated in the project. Each subject was instrumented for the measurement of esophageal (T_{es}) and mean skin temperatures (T_{sk}). Mean arterial pressure (MAP; Finapres), heart rate (HR; electrocardiogram), and forearm skin blood flow (laser-Doppler flowmetry) was also monitored. An index of cutaneous vascular conductance was calculated from the ratio of laser-Doppler derived skin blood flow to MAP. Central venous pressure was measured from a catheter placed in the subject's antecubital vein and advanced to the superior vena cava.

The subject was placed in a tube-lined suit that permitted the control of T_{sk} by changing the temperature of the water perfusing the suit. The suit covered the entire body surface with the exception of the head, feet, and the forearm where skin blood flow was monitored. A plastic garment was placed over this suit to impede sweat evaporation. In the supine position, neutral ($\sim 34^{\circ}\text{C}$) water was perfused through the tube-lined suit. After approximately 10 minutes, baseline data were collected. Following this baseline period, T_{sk} was increased to 38.5°C by perfusing the tube-lined suit with warm water. Once cutaneous vascular conductance was elevated and stable, 15 ml/kg warmed (37°C) isotonic saline was rapidly administered (7-10 min) through a catheter previously placed in an antecubital vein to return CVP to pre-heat stress pressures (see Fig 1). Following the infusion, T_{sk} was returned to pre-heat stress levels by perfusing the suit with cool water. A heater surrounding the laser-Doppler flow probe was used to raise local skin temperature to 42°C . Local temperature was held at this level for 30 min to elicit maximal cutaneous vasodilation. Values for cutaneous vascular conductance were then converted to percentages of maximum for that site.

RESULTS

Whole-body heating significantly increased T_{es} , HR, and cutaneous vascular conductance, while decreasing CVP and MAP (see Table 1). Saline infusion returned CVP to pre-heat stress pressures without significantly changing MAP, pulse pressure, or T_{es} . Skin blood flow immediately prior to saline infusion was significantly less than skin blood flow following 5 min of saline infusion (57 ± 3 versus 75 ± 6 % max cutaneous vascular conductance units; $P<0.001$). This difference was due to an increased rate of elevation in cutaneous vascular conductance during the first 5 min of saline infusion when compared with the period just prior to saline infusion (0.5 ± 0.2 to 2.8 ± 0.4 %max cutaneous vascular conductance units/min, $P<0.001$; see Fig. 1). If the rate of increase in cutaneous vascular conductance had not increased as a result of saline infusion (i.e. remained at 0.5 % max cutaneous vascular conductance units/min), the predicted cutaneous vascular conductance after 5 minutes of saline infusion would be 59 ± 4 % max cutaneous vascular conductance units. This predicted value was significantly less than the value achieved after 5 minutes of saline infusion (i.e. 75 ± 6 % max cutaneous vascular conductance



units; $P < 0.001$). The profound increase in cutaneous vascular conductance during saline infusion was not due to an increase in internal temperature as neither the rate of elevation in T_{es} (0.03 ± 0.01 to 0.02 ± 0.01 °C/min; $P = 0.12$) nor absolute T_{es} (37.0 ± 0.1 to 37.1 ± 0.1 °C; $P > 0.05$) significantly changed during saline administration. Plasma osmolality (P_{osm}) did not change during whole body heating but increased significantly following saline infusion (see Table 1). This increase was likely due to the administration of saline that had an osmolality slightly greater than the subjects' plasma osmolality.

Table 1: Responses to passive heating and saline infusion

	Pre-Heat Stress	Heat Stress	Saline Infusion
CVC (% max CVC)	13±2	54±5*	70±8*†
CVP (mmHg)	7.7±0.6	4.9±0.5*	7.9±0.6†
MAP (mmHg)	88±4	75±4*	73±4*
Heart Rate (bpm)	66±4	89±4*	98±4*†
Pulse Pressure (mmHg)	-	47±2.2	47±2.0
T_{es} (°C)	36.5±0.1	37.2±0.1*	37.3±0.1*
Posm (mosm/kg)	286±1.5	286±0.9	291±1.8*†

CVC: cutaneous vascular conductance, CVP: central venous pressure, MAP: mean arterial pressure, T_{es} : esophageal temperature, Posm: plasma osmolality. CVC is expressed as (laser-Doppler flux/mmHg)*100. *: Significantly different from pre-heat stress stage ($P < 0.05$).

†: Significantly different from heat stress stage ($P < 0.05$).

CONCLUSION

These data provide evidence that cardiopulmonary baroreceptor unloading coincident with passive heating attenuates the elevation in cutaneous vascular conductance. Moreover, these data provide a possible explanation for attenuated elevations in skin blood flow during a thermal challenge following exposure to simulated or actual microgravity (2, 4).

REFERENCES

1. Convertino, V.A., D.F. Doerr, D.A. Ludwig, J. Vernikos. Effect of simulated microgravity on cardiopulmonary baroreflex control of forearm vascular resistance. *Am. J. Physiol.* 266: R1962-R1969, 1994.
2. Crandall, C.G., J.M. Johnson, V.A. Convertino, P.B. Raven, K.A. Engelke. Altered thermoregulatory responses after 15 days of head-down tilt. *J. Appl. Physiol.* 77: 1863-1867, 1994.
3. Fortney, S.M. Thermoregulatory adaptations to inactivity. In: *Adaptive Physiology to Stressful Environments*, edited by S. Samueloff, M.K. Yousef. Boca Raton, FL: CRC, 1987, p. 75-83.
4. Fortney, S.M., V. Mikhaylov, S.M.C. Lee, Y. Kobzev, R.R. Gonzalez, J.E. Greenleaf. Body temperature and thermoregulation during submaximal exercise after 115-day spaceflight. *Aviat. Space Environ. Med.* 69: 137-141, 1998.
5. Greenleaf, J.E., J.D. Reese. Exercise thermoregulation after 14 days of bed rest. *J. Appl. Physiol.* 48: 72-78, 1980.
6. Johnson, J.M., L.B. Rowell, M. Niederberger, M.M. Eisman. Human splanchnic and forearm vasoconstrictor responses to reduction of right atrial and aortic pressures. *Circ. Res* 34: 515-524, 1974.

7. Rowell, L.B., G.L. Brengelmann, J.A. Murray. Cardiovascular responses to sustained high skin temperature in resting man. *J. Appl. Physiol.* 27: 673-680, 1969.
8. Tripathi, A., E.R. Nadel. Forearm skin and muscle vasoconstriction during lower body negative pressure. *J. Appl. Physiol.* 60: 1535-1541, 1986.

Supported by NASA grants: NAGW3582 and NAG9-1033.

AUTONOMIC CONSEQUENCES OF MICROGRAVITY EXPOSURE

Dwain L. Eckberg, M.D., Professor of Internal Medicine and Physiology, Medical College of Virginia at Virginia Commonwealth University, Richmond, Virginia, and Co-Investigators from around the world

INTRODUCTION

Human autonomic stretch and chemical receptors continuously sense changes of body position, arterial pressure, blood volume, blood chemistry, metabolic activity, and exercise, and orchestrate finely tuned changes of efferent sympathetic and vagal nerve traffic to diverse organs. When astronauts enter microgravity, the quality and quantity of receptor inputs change in major ways. Immediately, distension of the heart and arteries in the upper body increases. As exposure to microgravity continues, however, blood volume and distension of the heart and upper body decrease. Upon return to gravity, most astronauts experience difficulty standing: their heart rates increase to levels above those experienced before exposure to microgravity, their arterial pressures may fall, and they may even lose consciousness.

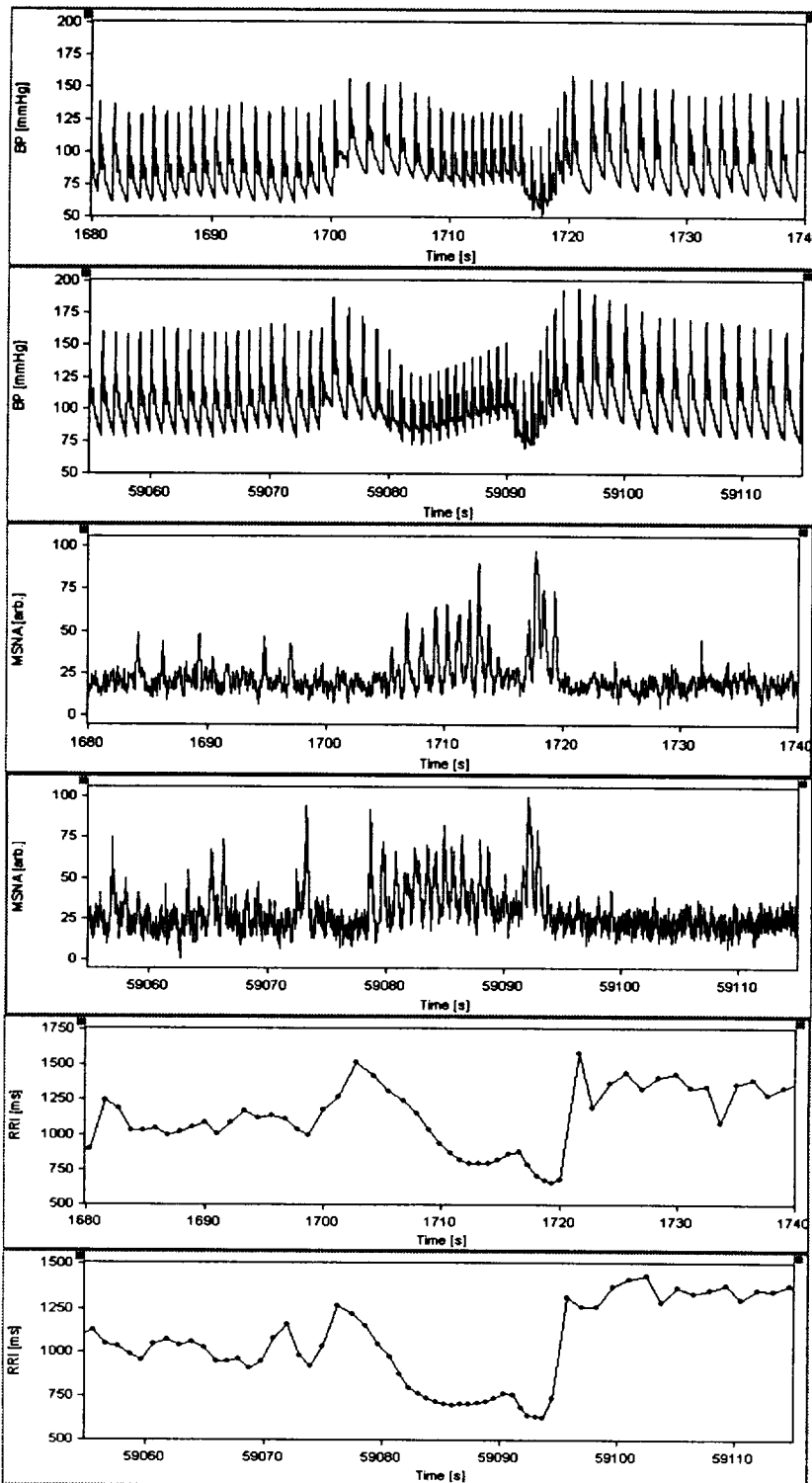
My laboratory has longstanding interest in these autonomic changes, and has over many years sought to characterize them before, during, and after space missions. Space studies have been complemented by ground based research in healthy volunteers and patients with orthostatic syncope. This total effort has helped to define basic human physiological mechanisms. In particular, recent efforts have helped to delineate autonomic mechanisms involved with interventions that may lead to hypotension, including major exercise, and standing.

METHODS

We have used a variety of interventions in studies conducted in space, including (but not limited to) controlled breathing, Valsalva straining, and lower body suction. In studies performed before and after space missions, we also have used passive upright tilt. We have measured many parameters, including electrocardiographic R-R intervals, beat-by-beat finger photoplethysmographic pressure, and muscle sympathetic nerve activity.

RESULTS

The most recent data from space research, including studies performed on the Russian Space Station, Mir, and studies performed during the April – May, 1998 Neurolab Space Shuttle Mission are being analyzed. The figure illustrates autonomic responses to Valsalva straining, obtained from one astronaut before and during the Neurolab Mission.



This graph illustrates two panels for each measurement. The first of each pair was made ~ 60 days before the Neurolab Space Shuttle Mission, and the second was made during Mission Day 13. BP = Blood Pressure; MSNA = Muscle Sympathetic Nerve Activity; RRI = R-R Interval.

CONCLUSIONS

These data document beyond argument, that sophisticated, state-of-the art research can be conducted on astronauts during space missions. They provide a variety of clues (to be explored as definitive analyses are performed) regarding human autonomic physiology in microgravity. First, baseline arterial pressure and sympathetic nerve activity are increased, and responses to Valsalva straining are exaggerated in space. Second, vagally-mediated R-R interval responses to Valsalva straining are intact in space. Full analysis of such data from space, interpreted through the lens of ground-based research may yield profound insights into how exposure to microgravity alters human autonomic physiology.

GENDER-RELATED DIFFERENCES IN CARDIOVASCULAR RESPONSES TO ORTHOSTATIC STRESS

Janice M. Fritsch-Yelle¹, Dominick S. D'Aunno², Wendy W. Waters², Sondra Freeman-Perez³

¹Life Sciences Research Laboratories, National Aeronautics and Space Administration, Johnson Space Center, Houston, Texas, ²National Space Biomedical Research Institute, Baylor College of Medicine, Houston, Texas, ³WYLE Laboratories, Houston, Texas

INTRODUCTION

There is evidence that men and women have different cardiovascular responses to standing, and that women are more susceptible to orthostatic hypotension than men. The present study seeks to determine if decreased orthostatic tolerance in women is caused by diminished vasoconstrictive responses.

METHODS

In men (n=5) and premenopausal women (n=5), ECG, arterial pressure, stroke volume (SV), cardiac output (CO), and total peripheral resistance (TPR) were continuously measured before and during 15 minutes of passive upright tilt. Women were tested once during the follicular phase (high estrogen) and once during menses (low estrogen) of their menstrual cycles. Differences in cardiovascular parameters were analyzed using Mann-Whitney Rank Sum Test and unpaired t-tests. Results are reported as means \pm standard errors.

RESULTS

Cardiovascular parameters are presented in the tables below.

Parameter	Baseline		
	Menses	Follicular Phase	Men
HR	64.0 \pm 2.72*	71.0 \pm 6.20*	53.8 \pm 2.48
SV	70.61 \pm 8.43	63.27 \pm 2.68	63.83 \pm 7.39
CO	4.57 \pm 0.50	4.54 \pm 0.41	3.50 \pm 0.32
TPR	18.58 \pm 2.64	17.43 \pm 1.26*	23.57 \pm 2.01

* = p<0.05 vs. men

HR, heart rate, beats/min. SV, stroke volume, ml. CO, cardiac output, l/min. TPR, total peripheral resistance, mmHg/l/min.

Parameter	Response to Tilt		
	Menses	Follicular Phase	Men
Δ HR	30.80 \pm 4.51	27.2 \pm 4.64	20.4 \pm 7.81
Δ SV	- 41.26 \pm 9.19	- 38.26 \pm 1.62*	- 20.86 \pm 6.91
Δ CO	- 2.02 \pm 0.54*	- 2.12 \pm 0.34*	- 0.49 \pm 0.24

Δ TPR	7.75 ± 3.10	$11.67 \pm 1.66^{**}$	0.57 ± 1.81
--------------	-----------------	-----------------------	-----------------

* $p < 0.05$ vs. men ** $p < 0.01$ vs. men

HR, heart rate, beats/min. SV, stroke volume, ml. CO, cardiac output, l/min. TPR, total peripheral resistance, mmHg/l/min.

A greater susceptibility to orthostatic intolerance was observed in women ($p < 0.05$). Women display higher baseline resting heart rates in both the follicular and menstrual phase than men. Women in the follicular phase had a significantly lower TPR than men. No other cardiovascular parameters were different between men and women regardless of the menstrual phase.

Cardiovascular responses to tilt reveal that women in both the follicular and menstrual phase had greater falls in CO than men. Women in the follicular phase had a greater decrease in SV and a greater increase in TPR with tilt than men. No other changes in cardiovascular parameters with tilt testing were significantly different between men and women.

CONCLUSION

These findings support previous observations that women and men have different cardiovascular strategies for handling orthostatic stress. The decreased orthostatic tolerance in women may not be caused by a diminished arteriolar vasoconstriction, as previously reported. In this study, women had a greater increase in resistance than men did with orthostatic stress. Women appear to increase TPR at the expense of CO while men appear to increase venous return and maintain CO. This does not appear to be as effective a strategy, as evidenced by the greater incidence of presyncope in the women.

Estrogen is known to have vasodilatory effects, both directly and indirectly. Estrogen has been shown to upregulate nitric oxide synthase (NOS) and increase production of the vasodilator nitric oxide. In addition, the vasodilatory effects of nitric oxide donors, such as nitroprusside and nitroglycerin, are more pronounced in veins than arteries. Based on these observations, estrogen may diminish venoconstriction and arteriolar constriction differentially, thereby altering women's cardiovascular response to orthostatic stress.

HEART RATE DYNAMICS DURING MICROGRAVITY: BEDREST AND SPACEFLIGHT STUDIES

A.L. Goldberger

Margret and H.A. Rey Laboratory for Nonlinear Dynamics in Medicine, Beth Israel Deaconess Medical Center/Harvard Medical School, Boston, MA 02215

INTRODUCTION

In collaboration with investigators at NASA (J. Fritsch-Yelle, S. Fortney Schneider, J. Charles) and the Russian Space Program (R. Baevsky), we have been involved with a series of collaborative studies on analysis of heart rate dynamics during both terrestrial bedrest deconditioning studies and long-duration spaceflight aboard Mir. Our objectives are:

- 1) To compile and analyze digitized databases (preflight, during flight, and postflight) of continuous ECG recordings from de-identified crew members from U.S. Spacelab Life Sciences and Shuttle missions, as well as Russian Mir missions.
- 2) To test the hypotheses that i) loss of complex heart rate variability is a useful new index of cardiac deconditioning and space sickness during space flight, as well as during microgravity simulations with bedrest; and ii) to quantitatively assess the effects of countermeasures such as LBNP and exercise.
- 3) To analyze electrocardiographic data from spaceflight and microgravity simulations for evidence of potentially serious cardiac electrical instability and its precursors.
- 4) To analyze subtle alterations in diurnal cycle dynamics in order to better understand the "restorative" function of sleep.

METHODS

Our analytic techniques are based on standard waveform and variability analysis of electrocardiographic data, as well as on newer measures of complex variability derived from nonlinear dynamics ("chaos theory"). These measures allow detection of hidden information in noisy, nonstationary time series (1-6).

RESULTS

Our findings include:

- 1) The detection of a loss of complex heart rate variability in healthy young women during short-term bedrest studies (7).
- 2) The report of a case of non-sustained ventricular tachycardia during long-term spaceflight (8).
- 3) The description of cardiovascular responses, including evidence for increased adrenergic tone during inflight transfer between space vehicles (9).
- 4) The detection of an increase in fractal heart rate complexity during sleep, both in healthy subjects on earth and in Mir crew members (10).

CONCLUSION

Detailed analysis of both ECG waveforms and beat-to-beat heart rate dynamics in microgravity studies may have important implications for understanding integrated physiology during bedrest deconditioning and spaceflight, as well as for monitoring crew members' health and assessing

the efficacy of countermeasures. These studies also have implications for the compilation of useful databases.

SELECTED REFERENCES

1. Goldberger AL, Bungo MW, Baevsky RM, Bennett BS, Rigney DR, Mietus J, Nikulina GA, Charles JB. Heart rate dynamics during long-term spaceflight: report on Mir cosmonauts. *Am Heart J* 1994;128:202-204.
2. Lipsitz LA, Hashimoto F, Lubowsky LP, Mietus J, Moody G, Appenzeller O, Goldberger AL. Heart rate and respiratory rhythm dynamics on ascent to high altitude. *Br Heart J* 1995;74:390-396.
3. Ivanov PCh, Rosenblum MG, Peng C-K, Mietus J, Havlin S, Stanley HE, Goldberger AL. Scaling behavior of heartbeat intervals obtained by wavelet-based time series analysis. *Nature* 1996;383:323-327.
4. Pincus SM, Goldberger AL. Physiological time-series analysis: what does regularity quantify? *Am J Physiol* 1994;266(Heart Circ Physiol):H1643-H1656.
5. Ho KKL, Moody GB, Peng C-K, Mietus JE, Larson MG, Levy D, Goldberger AL. Predicting survival in heart failure case and control subjects by use of fully automated methods for deriving nonlinear and conventional indices of heart rate dynamics. *Circulation* 1997;96:842-848.
6. Goldberger AL. Nonlinear dynamics for clinicians: chaos theory, fractals, and complexity at the bedside. *Lancet* 1996;347:1312-1314.
7. Goldberger AL, Mietus JE, Rigney DR, Wood ML, Fortney SM. Effects of head-down bedrest on complex heart rate variability: response to lower body negative pressure testing. *J Appl Physiol* 1994;77:2863-2869.
8. Fritsch-Yelle JM, Leuenberger UA, D'Aunno DS, Rossum AC, Brown TE, Wood ML, Josephson ME, Goldberger AL. An episode of ventricular tachycardia during long-duration spaceflight. *Am J Cardiol* 1998;81:1391-1392.
9. Fritsch-Yelle JM, Brown TE, Charles JB, Mietus JE, D'Aunno DS, Goldberger AL. Effects of long-duration spaceflight on autonomic and cardiovascular dynamics. Submitted for publication.
10. Ivanov PCh, Bunde A, Amaral LAN, Havlin S, Fritsch-Yelle J, Stanley HE, Goldberger AL. Sleep-wake differences in scaling behavior of the human heartbeat: analysis of terrestrial and spaceflight data. Submitted for publication.

EXERCISE TRAINING DURING +Gz ACCELERATION

J.E. Greenleaf¹, J.L. Chou², S.R. Simonson², C.G.R. Jackson³, and P.R. Barnes⁴

¹Ames Research Center, Moffett Field CA, 94035; ²Lockheed Martin Co.; ³Fresno State University, CA 93740; ⁴San Francisco State University, CA 94132

INTRODUCTION

The overall purpose is to study the effect of passive (without exercise) and active (with exercise) +Gz (head-to-foot) acceleration training, using a short-arm (1.9m radius) centrifuge, on post-training maximal oxygen uptake (VO_2 max, work capacity) and 70° head-up tilt (orthostatic) tolerance in ambulatory subjects to test the hypothesis that (a) both passive and active acceleration training will improve post-training tilt-tolerance, and (b) there will be no difference in tilt-tolerance between passive and active exercise acceleration training because increased hydrostatic and blood pressures, rather than increased muscular metabolism, will provide the major adaptive stimulus. The purpose of the pilot study was to test the hypothesis that there would be no significant difference in the metabolic responses (oxygen uptake, heart rate, pulmonary ventilation, or respiratory exchange ratio) during supine exercise with moderate +Gz acceleration.

METHODS

In the pilot study seven men (24-39 yr) exercised supine on the 1.9m human-powered centrifuge (HPC). Each subject performed maximal and submaximal exercise at 42%, 61%, 89% of VO_2 max (100%) under two conditions: exercise only (EX) and exercise + acceleration (EXA, +2.20 ± 0.02 Gz, 50% of max Gz from the HPC mode).

RESULTS

There were no significant differences in oxygen uptake, heart rate, or pulmonary ventilation at the submaximal or maximal levels between the exercise only and exercise + acceleration conditions. Mean (±SE) VO_2 max for EX was $2.86 \pm 0.12 \text{ L}\cdot\text{min}^{-1}$ ($35 \pm 2 \text{ ml}\cdot\text{min}^{-1}\cdot\text{kg}^{-1}$) and for EXA was $3.09 \pm 0.14 \text{ L}\cdot\text{min}^{-1}$ ($37 \pm 2 \text{ ml}\cdot\text{min}^{-1}\cdot\text{kg}^{-1}$); maximal heart rate EX = $169 \pm 6 \text{ b}\cdot\text{min}^{-1}$ and EXA = $180 \pm 5 \text{ b}\cdot\text{min}^{-1}$; maximal pulmonary ventilation EX = $119.6 \pm 6.8 \text{ L}\cdot\text{min}^{-1}$ and EXA = $134.9 \pm 8.0 \text{ L}\cdot\text{min}^{-1}$; and maximal respiratory exchange ratio EX = 1.3 ± 0.1 and EXA = 1.3 ± 0.1 .

CONCLUSION

Moderate +Gz acceleration does not significantly affect the normal exercise regression curves between oxygen uptake, heart rate, pulmonary ventilation, or respiratory exchange ratio and the relative exercise load.

MECHANISMS UNDERLYING ALTERED ARTERIAL BAROREFLEX FUNCTION IN HINDLIMB UNLOADED RATS

E.M. Hasser, J.A. Moffitt, J.T. Cunningham and C.M. Heesch

Dept. of Veterinary Biomedical Sciences, Dept. of Physiology and Dalton Cardiovascular Research Center, University of Missouri, Columbia, MO 65211

INTRODUCTION

Following prolonged periods of exposure to microgravity subjects experience a number of adverse cardiovascular consequences, including orthostatic intolerance. Several possible mechanisms could account for this orthostatic intolerance, including alterations in body fluid volumes, changes in vascular or cardiac responsiveness, and alterations in reflex control of the circulation. Normally, the primary adjustments to an orthostatic challenge require arterial baroreflex mediated increases in peripheral resistance, which are elicited through activation of the sympathetic nervous system to the vasculature. We therefore hypothesized that hindlimb unloading to simulate exposure to microgravity in rats would result in attenuated baroreflex control of the sympathetic nervous system. A corollary hypothesis was that reflex control of sympathetic nerve activity to the viscera and to skeletal muscle would be impaired in a differential manner. We therefore conducted studies to evaluate arterial baroreflex control of renal (RSNA) and lumbar sympathetic nerve activity (LSNA) following hindlimb unloading in conscious rats. Additional experiments were carried out to evaluate the afferent and/or central nervous system mechanisms involved in alterations in baroreflex function.

METHODS

Baroreflex Control of Sympathetic Nerve Activity in Conscious Hindlimb Unloaded Rats. Male Sprague Dawley rats were either hindlimb unweighted by attachment of a tail harness, or served as cage controls. Following 13 days of HU or normal cage activity, rats were implanted with femoral catheters and electrodes for recording either renal sympathetic nerve activity (RSNA) or lumbar sympathetic nerve activity (LSNA) and allowed to recover 24 hours. Thus, there were four groups of rats: control RSNA (n = 8), HU RSNA (n = 8), control LSNA (n = 8) and HU LSNA (n = 8). Reflex changes in RSNA or LSNA and heart rate (HR) were recorded in response to changes in arterial pressure. Mean arterial pressure (MAP) was increased or decreased by ramp infusions of phenylephrine and nitroprusside, respectively. Data relating RSNA or LSNA and HR to MAP were fit to a sigmoid logistic function, and curve parameters generated.

Evaluation of Baroreceptor afferent function and central processing of baroreceptor afferent information Rats were either hindlimb unweighted (n=8) as described above, or served as cage controls (n=8). Following 14 days of HU or control activity, rats were anesthetized with Inactin, and implanted with arterial and venous femoral catheters. Electrodes were placed on the aortic depressor nerve (ADN, an arterial baroreceptor afferent nerve), and on a branch of the renal nerve RSNA. Changes in ADN activity and RSNA were recorded in response to increases and decreases in mean arterial pressure (MAP) due to ramp infusions of phenylephrine and nitroprusside, respectively. Data relating RSNA to MAP were used to assess overall baroreflex function; data relating ADN activity to MAP were used to assess baroreceptor afferent function; and data relating RSNA to ADN activity were used to assess central processing of baroreceptor

afferent information. All data were fit to a sigmoid logistic function. Curve parameters were generated for each animal and averaged.

Fos expression in the brainstem of hindlimb unloaded rats after hypotension. This study examined Fos-like immunoreactivity in the brainstem following 14 days of HU. Rats were either HU (n=5) as above, or served as cage controls (C) (n=4). Following 12 days of HU or C, rats were implanted with chronic arterial and venous femoral catheters and allowed 2 days to recover. Mean arterial pressure (MAP) was recorded in conscious animals for a 30-min baseline period and then for 90 min following intravenous injection of hydralazine (HDZ; 10 mg/kg) or the isotonic saline vehicle. Rats were then perfused with paraformaldehyde and brains were removed and processed for Fos immunoreactivity (c-fos Ab, Oncogene).

GABAergic Influences on Rostral Ventrolateral Medulla following Hindlimb Unloading. This study tested the hypothesis that the attenuation in baroreflex mediated sympathoexcitation in hindlimb unloaded rats is due to increased GABAergic influences on rostral ventrolateral medulla (RVLM) neurons. Rats were either HU (n=8) or served as cage controls (C) (n=7). Following 14 days of HU rats were anesthetized with Inactin (100 mg/kg) and instrumented with femoral catheters and a renal sympathetic nerve electrode. Rats were ventilated and placed in a Kopf stereotaxic apparatus. The RVLM and caudal ventrolateral medulla (CVLM) were functionally identified using typical stereotaxic coordinates and by observing a pressor or depressor response, respectively, to microinjection of glutamate (10mM, 30nl). Changes in mean arterial pressure (MAP) heart rate (HR), and RSNA were recorded in response to bilateral microinjection of the GABAA antagonist Bicuculline (BIC; 5mM, 90nl). To evaluate the source of any change in GABAA influence in the RVLM, changes in hemodynamic parameters and RSNA were recorded in response to bilateral microinjection of the depolarization blocking agent kainic acid (5mM, 90nl) into the CVLM. At the peak of CVLM inhibition, BIC; 5mM, 90nl was bilaterally microinjected into the RVLM to block additional GABAA influences originating from sources other than the CVLM.

RESULTS

Baroreflex function in conscious rats

Resting MAP was not altered by HU, while HR was significantly increased (HU: 423.8 ± 10.5 , C: 365.4 ± 7.3). Maximal RSNA in response to decreases in MAP (HU: $249 \pm 12\%$ control, C: $455 \pm 34\%$ control) and gain of baroreflex control of RSNA (HU: -5.1 ± 0.2 , C: -15.0 ± 4.0) were significantly reduced. In addition, maximal LSNA in response to decreases in MAP (HU: $204 \pm 12\%$ control, C: $342 \pm 31\%$ control) and gain of baroreflex control of LSNA (HU: -4.0 ± 0.6 , C: -7.8 ± 1.3) were also significantly reduced. Baroreflex control of HR was not different between groups. Thus, HU attenuated baroreflex control of both RSNA and LSNA.

Baroreceptor afferent function and central processing

As in the previous study, HU reduced the maximum activation of RSNA in response to a decrease in arterial pressure. Hindlimb unweighting did not significantly alter the ADN activity in response to changes in arterial pressure. The threshold pressure for activation of baroreceptor afferent activity and the pressure at which afferent activity was saturated also were not different between control and HU rats. However, the slope of the efferent RSNA response to similar decreases in baroreceptor afferent activity was reduced by HU.

Fos expression

Resting MAP (C: 121 vs. HU: 122 mmHg), and MAP following hydralazine administration (C: 50 vs. HU :53 mmHg), were similar in both groups. Numbers of Fos-positive nuclei in the RVLM after isotonic saline administration were comparable in both groups (C: 2.8 vs. HU: 3.2); however, after hydralazine treatment the number of Fos-positive nuclei in the RVLM were less in HU rats compared to C rats (C: 18.3 vs. HU: 7.7).

GABAA in the RVLM

The increase in MAP and RSNA in response to BIC microinjection into the RVLM was significantly greater in HU rats compared to control (MAP; C: 74 + 6.2 vs. HU: 100 + 1.8 mm/Hg; $p < .02$ and RSNA; C:250 + 57 vs. HU: 488 + 92 % baseline $p < .07$); however there was little difference in the increase in HR between groups (C: 32 + 7 vs HU: 40 + 9.4 bpm; $p < .4$). There was no difference in the increase in MAP (C:76 + 4.7 vs. HU:80 + 6.2 mmHg), HR (C:43 + 11 vs HU:35 + 11 bpm) and RSNA (C:256 + 33 vs. HU:323 + 53 %baseline) between groups in response to CVLM blockade. However, during CVLM blockade the additional increase in MAP and RSNA due to BIC microinjection in the RVLM was greater in HU rats (MAP:C, 24 + 5.0 vs.HU: 44 + 5.5 mmHg; RSNA:C, 171 + 35 vs. HU: 311 + 39 %baseline).

CONCLUSION

These data suggest that arterial baroreflex control of sympathetic nerve activity is impaired after hindlimb unloading in rats. The data are consistent with the concept that impaired baroreflex function could be a contributing factor to orthostatic intolerance following exposure to microgravity. In addition, the attenuation in baroreflex function is likely to involve a central nervous system mechanism rather than a change in baroreceptor afferent function alone. The central dysfunction appears to be associated with decreased neural activation in the RVLM. Reduced activation of the RVLM during hypotensive stimuli may involve an alteration in GABAA mediated inhibition at the RVLM, apparently due to sources of GABA other than the CVLM.

DIETARY CALCIUM, BLOOD PRESSURE AND VASCULAR FUNCTION FOLLOWING SPACE FLIGHT.

D. Hatton, D. McCarron, Q. Yue, C. Rouillet, H. Xue, K. Otsuka, J. Chapman, T. Phanouvong, J. Rouillet, M. Watanabe, K. Nilan, V. Haight, J. Dierckx, J. Demerritt
Division of Nephrology and Hypertension, Oregon Health Sciences University, Portland, OR 97201

INTRODUCTION

Deficits in calcium intake are associated with increased blood pressure, decreased bone mineralization and impaired calcium metabolism. Calcium losses due to exposure to microgravity may result in a similar constellation of outcomes.

METHODS

To test that hypothesis, fourteen 7-week-old, male spontaneously hypertensive rats (SHR) were flown on STS-80, an 18 day shuttle mission. Beginning at 3 weeks of age, half the rats were fed a low calcium diet (0.2%) and half were fed a high calcium (2.0%) diet. The animals were maintained on the diets throughout the experiment.

RESULTS

Preliminary results indicate that systolic blood pressure, measured in conscious SHR 3 hours after landing using an indirect tail cuff method, was somewhat lower in the flight animals relative to concurrent ground controls ($p=.053$). When anesthetized with halothane (2% in O₂) just prior to catheterization for blood sampling, direct arterial blood pressure was found to be significantly higher ($p<.0001$) in the flight animals than the control animals in both diet groups (+18 mmHg on average). The differences in blood pressure may have been related to variations in vascular smooth muscle function. Mesenteric resistance vessels from flight animals had smaller maximal contractions to norepinephrine than control animals ($p<.0001$) and showed poorer relaxation to acetylcholine, calcium and sodium nitroprusside ($p<.0001$). Ionized calcium values between diet groups were much closer together in the flight animals (1.34 vs 1.38 mmol/L, $p<.01$) than the controls (1.24 vs 1.36 mmol/L, $p<.0001$). Parathyroid hormone values for flight animals were 198 vs 127 pg/ml for the low and high calcium groups respectively ($p<.05$). Vivarium control values were 145 vs 46 pg/ml ($p<.001$). These values indicate that microgravity increased PTH levels while preserving the dietary difference. Basal free intracellular calcium values were decreased in platelets from flight animals ($p<.05$) while thrombin and ionomycin stimulated calcium levels did not differ from control animals.

CONCLUSIONS

Overall, the preliminary data indicate that exposure to microgravity had a profound effect on blood pressure regulation, vascular function, and calcium metabolism.

COMPUTATIONAL MODELS OF THE CARDIOVASCULAR SYSTEM AND ITS RESPONSE TO MICROGRAVITY

Thomas Heldt, Eun B. Shim, **Roger G. Mark**, and Roger D. Kamm
 Massachusetts Institute of Technology, Room E25-505, Cambridge, MA 02139

INTRODUCTION

The primary objective of this project is to develop a general, modular model of cardiovascular function that contains the essential features associated with the effects of gravity, and to use this model to investigate the short term response to orthostatic stress in normal and micro-gravity adapted cardiovascular systems. The model provides an intellectual framework with which to interpret experimental observations and to evaluate alternative physiologic hypotheses of the cause of orthostatic intolerance. Furthermore, the model can potentially guide the development of screening methods that might be used to identify individuals who are at high risk of developing orthostatic intolerance.

METHODS

To investigate the effects of microgravity, we developed and refined a six compartment, lumped parameter cardiovascular model (Fig. 1). It provides for real time display of all major hemodynamic variables, such as pressures and flows, on a user friendly graphical user interface implemented under UNIX and LINUX.

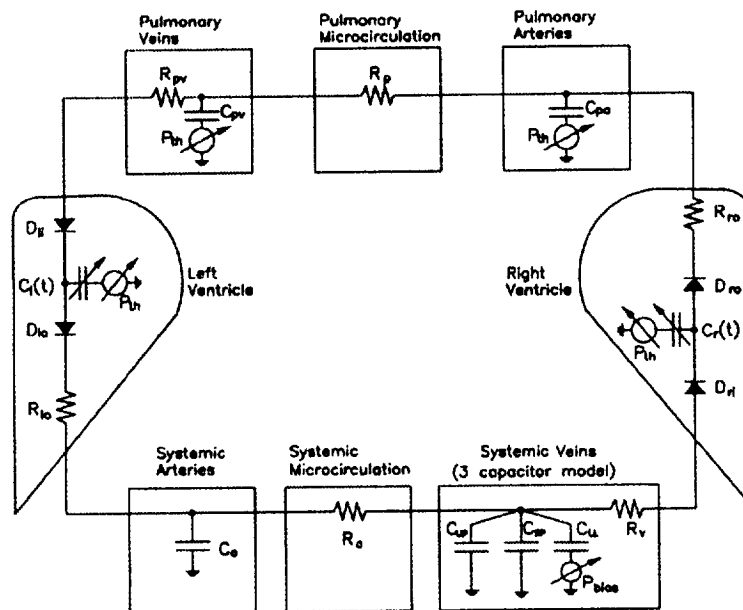


Figure 1: Block diagram of the lumped parameter model.

The control system consists of an arterial baroreflex and a cardiopulmonary reflex limb and provides for interactions between the two (Fig. 2). The model, in its present version, is capable of simulating the response to orthostatic stress such as tilt or lower body negative pressure (LBNP), and model parameters may be modified to account for the postulated effects of microgravity.

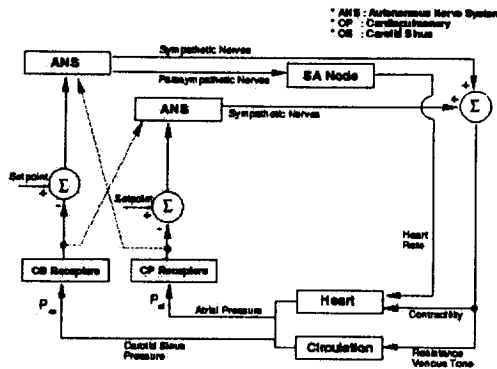


Figure 2: Diagram of the control system.

RESULTS

The model was used to simulate tilt table and LBNP interventions in normals, and the simulation results were compared with actual data from the literature.

Tilt Table Experiments:

To simulate the physiologic response to a tilt table experiment, we implemented (1) changes in hydrostatic pressure at the carotid sinus baroreceptor due to changes in posture, (2) a rapid change in venous transmural pressure which leads to blood pooling in the dependent veins, and (3) changes in total blood volume due to increased capillary filtration into the interstitial space. The comparison of simulation to experimental data of the heart rate response to a 70 degree head up tilt are shown in figure 3 (data taken from Bräuer, G. et al. Acta biol. med germ. 34: 1153-1157, 1975):

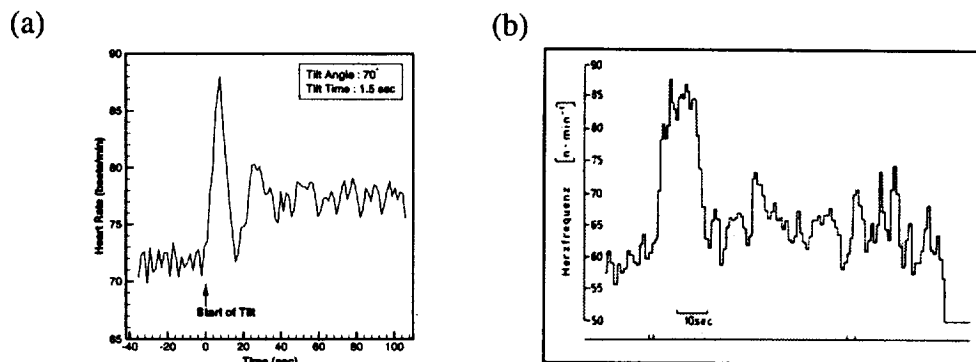


Figure 3: (a) simulation of a 70 degree head up tilt and (b) experimental result.

LBNP Procedure:

In order to simulate an LBNP procedure, we implemented (1) an increased (time varying) venous transmural pressure due to the externally applied negative pressure and (2) the leakage of blood plasma into the interstitium by appropriate time-varying modification of the total blood volume. In our simulations, the negative pressure was ramped linearly from 0 to -50 mmHg over a time course of 50 minutes. Figure 4 shows the results of our simulation in comparison to experimental data found in the literature (Johnson, J.M. et al. *Circ. Res.*, 34: 515-524, 1974):

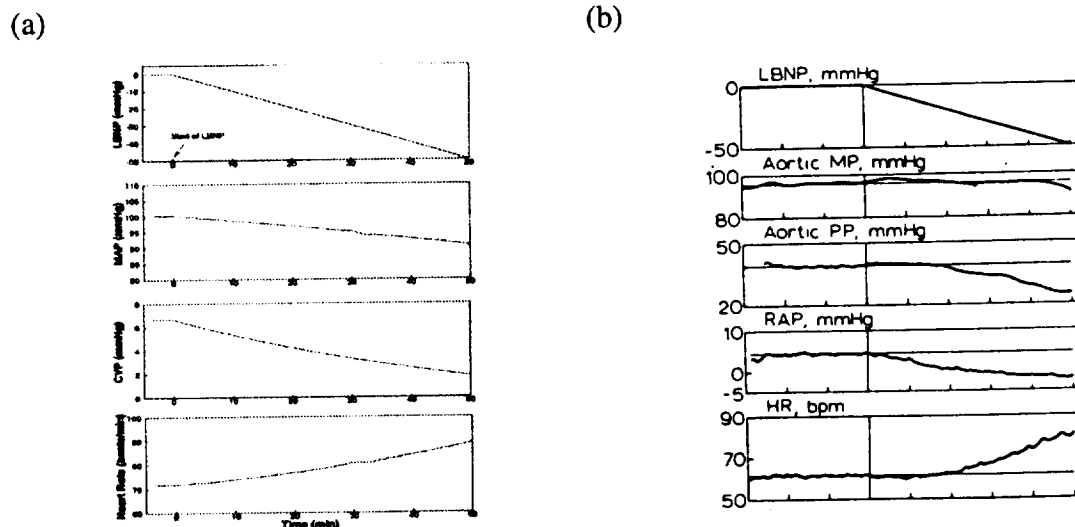


Figure 4: (a) simulation of a LBNP procedure and (b) experimental observation (horizontal axis is time in units of 10 min).

CONCLUSIONS AND OUTLOOK

We successfully completed the first stage of our modeling efforts, namely the faithful simulation of short-term cardiovascular responses to orthostatic stress in normal humans. Future modeling efforts will include further enhancements of the control system such as inclusion of hormonal control loops and adapting the model to simulate rodent experiments. The project will also integrate and evaluate data taken from human and animal studies which are currently being conducted by several teams of NSBRI.

THE EFFECT OF CARDIAC MECHANICS ON ORTHOSTATIC INTOLERANCE FOLLOWING BED REST

Benjamin D. Levine, M.D., Director, Institute for Exercise and Environmental Medicine, Presbyterian Hospital and Associate Professor of Medicine, University of Texas Southwestern Medical Center at Dallas

Gravitational and hydrostatic gradients play an essential role in determining the distribution of pressure and volume within the cardiovascular system. When these gradients are removed or minimized, such as during spaceflight or its ground-based simulations (head-down tilt bed rest), a central fluid shift occurs, initiating a neurohumorally mediated reduction in both blood/plasma and ventricular volume. Diastolic wall stress is thereby decreased and the volume load of the left ventricle is reduced compared to the supine position at 1G. This adaptation is rapid, and appears to be substantially complete within the first 24-48 hours of microgravity exposure. Compounding these hemodynamic changes is a reduction in physical activity associated with confinement, which minimizes chronotropic and pressure work compared to more freely ambulatory periods. Within a few weeks of real or simulated microgravity, the heart appears to atrophy, presumably in response to reduced myocardial work. This cardiac atrophy results in impaired diastolic function characterized by decreased ventricular distensibility, and possibly by loss of diastolic suction leading to reduced ventricular filling. The combination of atrophy and hypovolemia results in a prominent reduction in stroke volume in the upright position at 1G, which is the essential stimulus for microgravity induced orthostatic hypotension.

Although the hypovolemia of spaceflight or bed rest appears to plateau after 24-48 hours of real or simulated microgravity, preliminary data obtained by the PI in three subjects who have completed 12 weeks of bed rest has failed to identify a plateau in the loss of cardiac mass measured by MRI. Moreover, 2 additional subjects have been studied through 6 weeks of supine bed rest (total n=5) allowing statistical analysis at this time point. These data are shown in Table 1. A reduction in cardiac mass was clearly evident after 6 weeks of supine bed rest. Moreover this reduction in mass was accompanied by a reduction in mean wall thickness, suggesting that it was a normal adaptive response of the myocardium to maintain wall stress.

Table 1	<u>Baseline</u>	<u>2 weeks</u>	<u>6 weeks</u>
LVEDV (ml)	139±11	120±10*	116±11*
LV mass (gm)	252±23	250±23	231±21*#
MWT (cm) (mean wall thickness)	1.49±0.09	1.49±0.07	1.39±0.07*#

(* = p<0.05 compared to baseline, # = p<0.05 compared to 2 weeks, using ANOVA with Newman-Keuls post-hoc test for multiple comparisons; mean wall thickness (MWT) calculated as average wall thickness over the entire heart)

In animal models, cardiac atrophy is associated with increased chamber stiffness. Because of the curvilinear nature of the left ventricular pressure-volume relationship, cardiac stiffness is

dynamic with the instantaneous stiffness, defined as dP/dV , dependent on the specific value of left ventricular volume. Cardiac stiffness, LVEDV and consequently SV may therefore be altered by either: 1) shifting up (hydrated state) or down (dehydrated state) on any individual pressure-volume curve, or; 2) changing the underlying pressure-volume relationship. These changes may occur acutely: with either an alteration in intravascular volume, or a sudden change in extracardiac influences (pericardial or pulmonary mechanical restraint); or more chronically via a specific cardiac adaptation.

Not only is SV easily altered by mechanical and hydrostatic effects, but it serves as the primary stimulus to baroreflex regulation of arterial pressure during an orthostatic stress as part of the "triple product" of blood pressure control: $BP = HR \times SV \times TPR$. Orthostatic hypotension thus will ensue if the fall in stroke volume is of sufficient magnitude to overwhelm normal compensatory mechanisms, or if the reflex increase in HR and/or TPR is impaired by disease states, or by a specific adaptation of the autonomic nervous system. After adaptation to real or simulated microgravity, virtually all individuals studied have an excessive fall in stroke volume in the upright position. Although there are conflicting data regarding changes in baroreflex regulation of heart rate and vascular resistance that may limit the compensatory response to orthostasis, it is this excessive fall in stroke volume that is the *sine qua non* of microgravity induced orthostatic hypotension. Ultimately in some individuals, reflex compensatory mechanisms appear to be overwhelmed by this excessive fall in stroke volume. A corollary to this argument is that if this excessive fall in stroke volume could be eliminated, then orthostatic intolerance should be eliminated as well. This hypothesis is currently being tested in ongoing experiments that will be discussed.

RENAL SODIUM HANDLING AFTER EXERCISE INDUCED PLASMA VOLUME EXPANSION

G. W. Mack, S. A. Kavouras, and K. Nagashima The John B. Pierce Laboratory and Dept. of Epidemiology and Public Health, Yale Univ. Sch. of Med., New Haven, CT 06519

INTRODUCTION

It is generally agreed that reduced orthostatic tolerance post space flight in astronauts is due, in part, to a reduction in plasma volume. It is also believed that exercise will be a critical component of any remedy used counter the "maladaptive" response to prolonged space flight. Within this context it is believed that exercise training and its accompanying hypervolemia could be used to offset the reduction on plasma volume associated with space flight. Thus, it is essential that the basic mechanisms responsible for plasma volume expansion be elucidated. Plasma volume expansion during exercise training is essentially isotonic. It has been proposed that increased salt retention could account for the elevation in plasma volume during exercise training yet little direct data supporting this hypothesis exists. The purpose of this investigation was to examine the role of renal sodium handling on exercise induced plasma volume expansion.

METHODS

Five subjects rested in upright posture for 6.5 h in two separate conditions: 24 h after exercise (EX) and after no exercise (CON). After 3 h of rest 15 ml/kg of isotonic saline was infused over a 30-min period to challenge the fluid regulating system with a volume and sodium load. The renal clearance of inulin and PAH was used to calculate glomerular filtration rate (GFR) and effective renal plasma flow, respectively. Lithium clearance was used to differentiate distal and proximal tubular sodium clearance. The exercise protocol used to elicit plasma volume expansion consisted of eight 4-min bouts of exercise at 85% of peak O₂ uptake with 5-min recovery between bouts.

RESULTS

The exercise protocol induced a $6.1 \pm 3.4\%$ ($p < 0.05$, 2.43 ± 1.21 ml/kg body wt) plasma volume expansion within 24-h. Saline infusion expanded plasma volume by an additional 3.56 ± 0.59 and 3.79 ± 0.36 ml/kg body wt ($p < 0.05$) in CON and EX. Plasma volume remained elevated until the end of the 2-h recovery period ($p < 0.05$, 2.86 ± 0.48 and 2.35 ± 0.46 ml/kg body wt). GFR was unaffected by the saline infusion (see Figure 1). The filtered load of sodium, lithium clearance and proximal tubular sodium output following saline infusion were greater for the CON than the EX trial ($p < 0.05$). No differences were found in distal tubular sodium handling. Urinary sodium excretion and sodium clearance tended to be higher during the CON trial following the infusion ($p < 0.05$). Plasma renin activity and aldosterone levels were decreased after the infusion and remained lower ($p < 0.05$), but no differences between the CON and EX trials were found. Atrial natriuretic peptide level remained unchanged during the experiment.

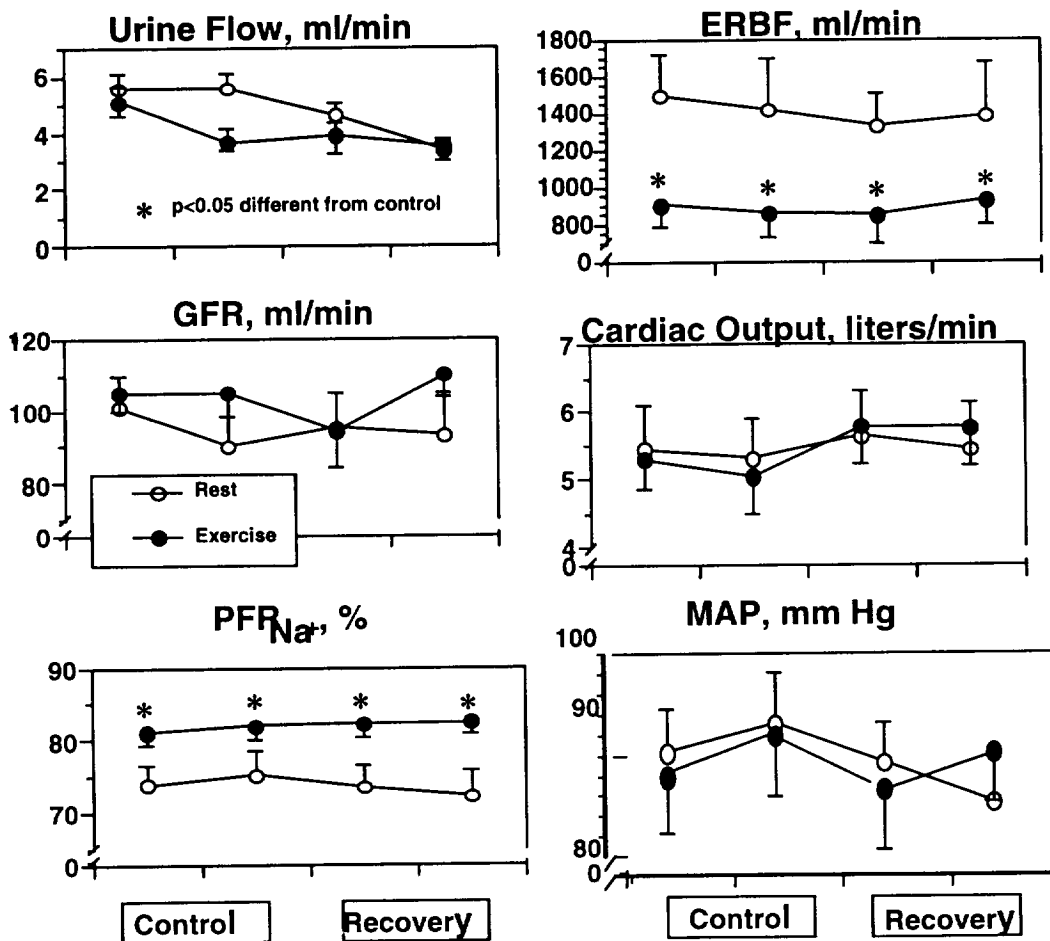
CONCLUSION

These data indicate that during exercise induced hypervolemia sodium sparing is mediated by an increase in proximal tubular sodium reabsorption. This increase in proximal tubular sodium reabsorption is likely the result of a reduction in renal blood flow and increased filtration fraction which act to increase peritubular capillary colloid osmotic pressure and thereby increase sodium

reabsorption. The mechanism responsible for the reduction in renal blood flow 24-h following exercise is unknown but may be related to increased renal sympathetic nerve activity or circulating vasoactive hormones. We detected an increase in vasopressin or plasma renin activity 24-h following exercise suggesting a role of for renal sympathetic nerve. In support of this hypothesis we have observed that renal blood flow is higher 24-h after exercise in the supine posture when volume loading of cardiopulmonary baroreceptors should provide inhibition of renal sympathetic nerve activity. The potential for the supine posture to limit plasma volume expansion following exercise suggests similar limitations may exist during space flight.

FIGURE 1. Where: GFR is glomerular filtration rate measured by inulin clearance; PFR_{Na^+} is proximal tubular fractional reabsorption of sodium; ERBF is effective renal blood flow measured by the clearance rate of para-amin0-hippuric acid and hematocrit; and MAP is mean arterial blood pressure taken from the brachial artery using an automated arm cuff system. * $P < 0.05$ different from rest. Control represents the pooled data from collection period 1 & 2 and 3 & 4 before saline infusion and Recovery represents the pooled data from collection periods 6 & 7 and 8 & 9 following saline infusion.

Renal and cardiovascular function in the upright posture before (control) and after (recovery) saline loading at rest and 24-h following exercise.



CARDIOVASCULAR SYSTEM IDENTIFICATION OF ALTERATIONS IN CARDIOVASCULAR REGULATION DURING SIMULATED SPACE FLIGHT

T.J. Mullen², C.D. Ramsdell², G. Sundby², G.H. Williams², R.J. Cohen¹,
¹Massachusetts Institute of Technology, Cambridge, Massachusetts, 02139, ²Harvard Medical
School, Boston, Massachusetts, 02115

INTRODUCTION

Alterations in cardiovascular regulation and function that occur during and after space flight have been reported. These alterations are manifested, for example, by reduced orthostatic tolerance upon reentry to the earth's gravity from space. However, the precise physiologic mechanisms responsible for these alterations remain to be fully elucidated. Perhaps, as a result, effective countermeasures have yet to be developed. In this study we apply a powerful, new method – cardiovascular system identification (CSI) – for the study of the effects of space flight on the cardiovascular system so that effective countermeasures can be developed.

CSI involves the mathematical analysis of second-to-second fluctuations in non-invasively measured heart rate, arterial blood pressure (ABP), and instantaneous lung volume (ILV – respiratory activity) in order to characterize quantitatively the physiologic mechanisms responsible for the couplings between these signals. Through the characterization of all the physiologic mechanisms coupling these signals, CSI provides a model of the closed-loop cardiovascular regulatory state in an individual subject. The model includes quantitative descriptions of the heart rate baroreflex as well as other important physiologic mechanisms. With an additional non-invasive measurement of stroke volume (SV – ultrasound Doppler method), the model may be extended to also include the characterization of the peripheral resistance baroreflex – which may play a central role in the development of orthostatic intolerance – and measures of systolic and diastolic function.

We apply CSI in conjunction with the two general protocols of the human studies core. The first protocol involves ground-based, human bed-rest to simulate microgravity and standing to provide an orthostatic challenge. The second protocol is the same as the first but with the addition of circadian rhythm disruption to determine whether such disruption contributes to cardiovascular alterations. In these studies, we focus on the basic physiologic mechanisms responsible for the alterations in cardiovascular regulation and function during the simulated microgravity in order to formulate hypotheses regarding what countermeasures are likely to be most effective.

In future studies, we plan to apply CSI to test the potential countermeasures in conjunction with the same bed-rest model. We also anticipate applying CSI for studying astronauts before and after space flight and ultimately, during space flight. The application of CSI promises to provide information relevant to the development and evaluation of effective countermeasures allowing humans to adapt appropriately upon reentry to the earth's gravity and to live and work for longer periods of time in microgravity.

METHODS

CSI quantifies the feedforward and feedback relationships between cardiovascular variables that play an integral role in maintaining cardiovascular homeostasis. Many of these relationships are mediated by the autonomic nervous system, and therefore the technique provides insight into the state of autonomic cardiovascular control mechanisms.

A CSI model used to analyze fluctuations in heart rate (HR), arterial blood pressure (ABP), and instantaneous lung volume (ILV) about their mean values is illustrated in Figure 1. The fluctuations in these variables are interrelated through five coupling mechanisms: CIRCULATORY MECHANICS, the arterial blood pressure response to a single heartbeat; HR BAROREFLEX, the baroreceptor coupling between changes in arterial blood pressure and heart rate; sinoatrial (SA) node, the instantaneous heart rate; ILV→HR, the neurally mediated coupling between respiratory activity and heart rate; and ILV→ABP, the mechanical coupling between variations in lung volume and arterial blood pressure. Each of the five coupling mechanisms may be characterized in an individual from a single recording of ECG, ILV and ABP. We apply a system identification technique based on autoregressive-moving average equations [Mullen *et al.*, 1997].

CIRCULATORY MECHANICS represents the relationship between cardiac contraction and the generation of the ABP waveform. The input to CIRCULATORY MECHANICS is pulsatile heart rate (PHR) which is defined to be a train of impulses occurring at the times of contraction of the ventricles. PHR may be constructed from the times of occurrence of the QRS complexes in the electrocardiogram (ECG). The output from CIRCULATORY MECHANICS is the pulsatile ABP signal. The CIRCULATORY MECHANICS transfer function represents the ABP wavelet generated with each cardiac contraction. The contractile properties of the heart as well as the mechanical properties of the great vessels and the peripheral circulation determine CIRCULATORY MECHANICS. CIRCULATORY MECHANICS may also encompass the reflex adjustment of vascular mechanical properties mediated by the α -sympathetic, β -sympathetic and renin-angiotensin systems (the resistance baroreflex).

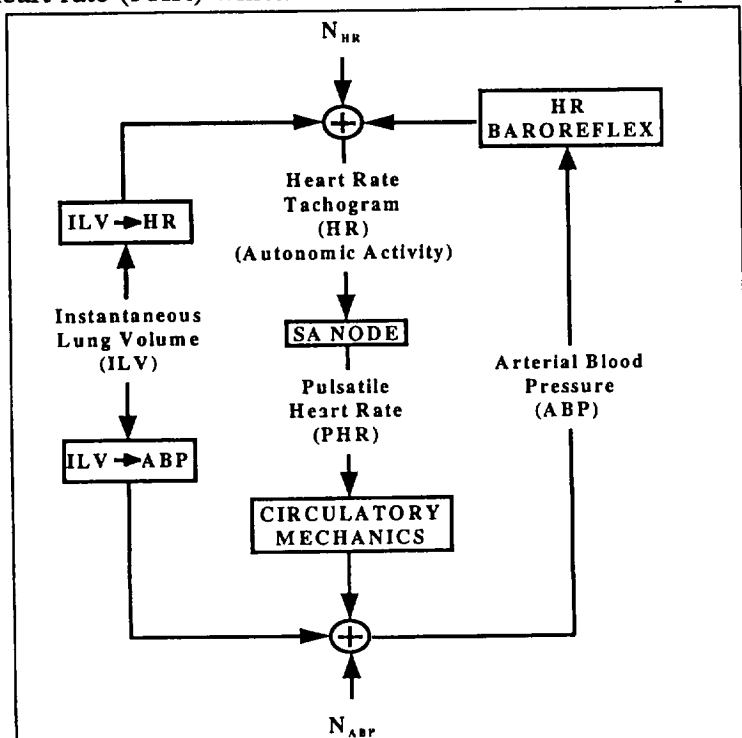


Figure 1. Cardiovascular System Identification model used to characterize short-term cardiovascular control mechanisms. ILV→HR, instantaneous lung volume (ILV) to heart rate (HR) transfer relation; ILV→ABP, ILV to arterial blood pressure (ABP) transfer relation. HR BAROREFLEX and CIRCULATORY MECHANICS, causal transfer relations from ABP to HR and HR to ABP respectively. N_{HR} and N_{ABP} , those components (noise sources) of HR and ABP, respectively, not correlated with other inputs. SA, sinoatrial [adapted from Mullen *et al.*, 1997].

HR BAROREFLEX represents the autonomically mediated baroreflex coupling between fluctuations in ABP and fluctuations in heart rate. Here heart rate is represented by the heart rate tachogram (HR) rather than PHR. HR is defined to be a stepwise continuous process whose value corresponds to the reciprocal of the current inter-beat interval for the time period corresponding to the duration of that interval [Berger *et al.*, 1986]. Unlike PHR, HR has no periodic component at the mean heart rate frequency and is closely related to the net autonomic input signal modulating sinoatrial node activity. SA NODE represents the coupling between HR and PHR. The SA NODE in this model is an "integrate and fire" device; such a device precisely relates the input HR to the output PHR.

ILV→HR represents the autonomically mediated coupling between respiration and heart rate. ILV→HR is responsible for the respiratory sinus arrhythmia. ILV→ABP represents the mechanical effects of respiration on ABP due to the alterations in venous return and the filling of intrathoracic vessels and heart chambers associated with the changes in intrathoracic pressure.

In addition to the five coupling mechanisms, the model incorporates two perturbing noise sources, N_{HR} and N_{ABP} . N_{HR} represents the fluctuations in HR not caused by fluctuations in ABP or ILV.

In this study, data for CSI analysis is acquired from normal, healthy human subjects in the supine, 30° head-up tilt, 60° head-up tilt, and standing position both before and after a two week period of head-down tilt bedrest to simulate weightlessness.

PROGRESS

The personnel for this project were identified and hired. All equipment needed to conduct the studies was identified, purchased, assembled and tested. Six subjects have completed the bed-rest protocol. Data from these subjects is currently being analyzed at the Massachusetts Institute of Technology (MIT). We will continue to collect data throughout this fiscal year until fourteen subjects have been studied, at which time we will begin the sleep deprivation bed-rest protocol.

As preparations for the bed-rest study proceeded during the first three quarters of this past year, we worked in conjunction with the National Space Biomedical Research Institute Instrumentation Team and the NASA Center for Quantitative Cardiovascular Physiology, Modeling and Data Analysis at MIT to extend the CSI method to utilize non-invasive, beat-to-beat measurements of SV. In particular, our laboratory has been developing identification algorithms, which require these measurements along with beat-to-beat measurements of ABP and heart rate, to quantify left ventricular contractility, in terms of left ventricular end-systolic compliance, and the control of total peripheral resistance. With these algorithms, we may test our hypotheses that alterations in left ventricular contractility and the arterial resistance baroreflex occur as a result of exposure to simulated microgravity and contribute to reduced orthostatic tolerance.

NON-INVASIVE ASSESSMENT OF SUSCEPTIBILITY TO VENTRICULAR ARRHYTHMIAS DURING SIMULATED SPACE FLIGHT

T.J. Mullen², C.D. Ramsdell², G. Sundby², G.H. Williams², R.J. Cohen¹

¹Massachusetts Institute of Technology, Cambridge, Massachusetts, 02139, ²Harvard Medical School, Boston, Massachusetts, 02115

INTRODUCTION

There are numerous anecdotal reports that suggest that space flight may increase the incidence of ventricular tachyarrhythmias, including one documented episode of a 14 beat run of ventricular tachycardia during a Mir mission. However, it is not known whether space flight actually does decrease ventricular electrical stability. It is extremely important to assess whether long duration space flight predisposes the heart to life-threatening ventricular arrhythmias – particularly with regard to planning a possible mission to mars. However, experience in clinical medicine on earth has shown that commonly used non-invasively risk stratifiers (e.g. signal averaged electrocardiogram (SAECG), QT dispersion, heart rate variability, baroreceptor sensitivity, left ventricular ejection fraction, and the presence of non-sustained ventricular tachycardia on Holter monitoring) are not very accurate predictors of the occurrence of sudden cardiac death (SCD), sustained ventricular tachycardia (VT), or ventricular fibrillation (VF). It is generally believed that invasive electrophysiologic testing (EP) is more accurate, but this procedure is highly invasive and not risk free. Recently, with NASA support, a new technique – the measurement of microvolt level T wave alternans (TWA) – has been developed. In a series of clinical studies in varied patient populations this technique has proven superior to other non-invasive risk stratifiers as a predictor of SCD, VT and VF. TWA has been found in various studies to be equivalent to or superior to EP. In this project we apply the measurement of TWA, along with other risk stratifiers, to determine whether simulated microgravity increases the risk of ventricular tachyarrhythmias.

METHODS

Volunteers participating in a 14 day head down bed-rest study, will have microvolt level T wave alternans measured before and after the bed-rest period during exercise bicycle stress to 70% of maximum predicted heart rate. Measurements will be made using a CH 2000 (Cambridge Heart, Inc., Bedford, MA) system. Electrocardiographic recordings will be made using multi-contact electrodes placed at locations which enable recording both vector and precordial electrograms. TWA will be measured using the Spectral Method. The resulting trend plots will be reviewed to determine whether sustained alternans occurs during the period of the test and, if present, to determine the onset heart rate. Sustained alternans is defined as TWA which is consistently present above a subject-specific onset heart rate. The hypothesis being tested is that bed-rest increases the incidence of sustained alternans, and decreases its onset heart rate. In addition, the recorded ECGs will be recorded to perform signal averaged electrocardiography and measure QT dispersion. Holter monitoring will be performed before, during and after the period of bed-rest to assess changes in heart rate variability, the presence of non-sustained ventricular tachycardia and the frequency of premature ventricular beats. Cardiovascular system identification will be used to non-invasively assess changes in baroreceptor sensitivity.

Similar sets of analyses will be performed prior to, during and following bed-rest in the context of a separate four month bed-rest study. During this study, measurements will be made on a monthly basis; the exercise will be conducted with a supine bicycle.

RESULTS

Data has been collected on the first three subjects in the 14 day bed-rest study. The data are currently being analyzed.

CONCLUSION

The measurement of microvolt level TWA in conjunction with bed-rest studies may help resolve whether space flight increases susceptibility to life threatening ventricular tachyarrhythmias. The TWA technology is already having important spinoff applications on earth for the identification of individuals at risk for sudden cardiac death.

POSTURAL REGULATION OF MUSCLE SYMPATHETIC NERVE ACTIVITY BEFORE AND AFTER SIMULATED AND ACTUAL MICROGRAVITY DECONDITIONING

J.A. Pawelczyk¹, B.D. Levine², and the Neurolab Autonomic Team

¹Noll Physiological Research Center, Pennsylvania State University, University Park, PA 16802

²Institute for Exercise and Environmental Medicine, Presbyterian Hospital and University of Texas Southwestern Medical Center, Dallas, TX 77058

INTRODUCTION

The etiology of orthostatic intolerance after spaceflight is multifaceted. Morphological adaptations, in particular cardiac atrophy, are likely to magnify the decrease in stroke volume that occurs with reductions in cardiac filling pressure when standing. Neural adaptations may be inferred as well, as reductions in carotid-cardiac baroreflex responsiveness have been reported following bedrest deconditioning and spaceflight.

Neural control of vascular resistance has not been studied directly when orthostatic intolerance is florid in the hours following spaceflight. However, the increases in systemic vascular resistance and plasma catecholamines during orthostatic stress are inappropriately low in orthostatically intolerant subjects following spaceflight, suggesting that deficits in the regulation of vascular resistance may be associated with hypoadrenergic function. The studies described in this abstract were designed to test this hypothesis.

METHODS

Cardiovascular reflex responsiveness was assessed under simulated microgravity conditions using an 18-day bedrest deconditioning paradigm with -6° head-down tilt using 12 men and women 18-35 years old. Before and after bedrest muscle sympathetic nerve activity (MSNA) was recorded from stainless steel microelectrodes inserted in the peroneal nerve at the fibular head or the popliteal fossa. Changes in MSNA were characterized during increases in cardiac filling pressure using lower-body negative pressure (LBNP, -15 and -30 mmHg) and rapid infusion of warm isotonic saline ($+15$ and $+30$ ml/kg body weight). Cardiac filling pressures were determined using a Swan-Ganz catheter to determine pulmonary capillary wedge pressure (PCWP).

Similar experiments were performed before and after the STS-90 Neurolab mission using six crewmembers 37-46 years old. MSNA was recorded in the supine and 60° head-up tilt positions from five of the volunteers 60 days prior to flight and 1.5-4 hours after landing. Volume infusion was not performed. Cardiac filling pressures were not determined directly; rather, changes in cardiac filling were inferred from the changes in stroke volume determined by C_2H_2 rebreathing.

RESULTS

The combination of LBNP and rapid saline infusion allowed us to characterize reflex responsiveness over a range of PCWP from 4-20 mmHg. Prior to bedrest, MSNA increased to more than 200% of control (supine) values during LBNP, and decreased to 30% of control values with saline infusion ($P < 0.01$). After bedrest deconditioning, baseline MSNA, quantified as

sympathetic discharges per minute, was not statistically different from the pre-bedrest state. However, the increase with LBNP was greater, reaching 350% of baseline ($P<0.05$). Though the fall in PCWP was not different following bedrest, the reduction in stroke volume was significantly greater.

Following spaceflight both supine and standing MSNA were increased, while SV was reduced ($P<0.05$). The linear relationship between MSNA and SV did not change during 18 days of spaceflight.

CONCLUSIONS

Though MSNA responses to orthostatic stress were greater after simulated and actual spaceflight deconditioning, these responses were consistent with reductions in stroke volume associated with hypovolemia and cardiac atrophy. We conclude that these two factors alter the neural response to orthostatic stress appropriately, increasing sympathetic activity without a change in sympathetic reflex stimulus-response characteristics. This increase in sympathetic activity is presumably directed to the heart as well as suggested by greater orthostatic heart rates following spaceflight and bedrest deconditioning. The combination of diminished cardiac mass, hypovolemia, and a hyperadrenergic state is similar to that often observed in patient populations presenting with orthostatic intolerance and may predispose individuals to aberrant ventricular mechanoreceptor stimulation ("empty heart syndrome"). Future investigations should focus on ameliorating the cardiac and volume adaptations to spaceflight to preserve orthostatic tolerance.

ACKNOWLEDGEMENTS

The Neurolab Autonomic Team is comprised of scientists represented by four STS-90 principal investigators: Friedhelm Baisch (DLR, Germany), C.G. Blomqvist (U.T. Southwestern), D. Eckberg (Medical College of Virginia), and D. Robertson (Vanderbilt). The outstanding dedication of the numerous investigators, technicians, and volunteers participating in these investigations is recognized and greatly appreciated. This work was funded in part by NSCORT NAGW3582 (C.G. Blomqvist, B.D. Levine and J.A. Pawelczyk), NAGW4389 (J.A. Pawelczyk), NAS 9-19429 (C.G. Blomqvist), and NAS 9-19573 (J.A. Pawelczyk).

INFLUENCE OF GRAVITY ON BLOOD VOLUME AND FLOW DISTRIBUTION

D. Pendergast¹, A. Olszowka¹, E. Bednarczyk², B. Shykoff¹, and L. Farhi¹

¹Departments of Physiology and Biophysics and ²Nuclear Medicine, Buffalo, NY 14214

INTRODUCTION

In our previous experiments during NASA Shuttle flights SLS 1 and 2 (9-15 days) and EUROMIR flights (30-90 days) we observed that pulmonary blood flow (cardiac output) was elevated initially, and surprisingly remained elevated for the duration of the flights. Stroke volume increased initially and then decreased, but was still above 1 Gz values. As venous return was constant, the changes in SV were secondary to modulation of heart rate. Mean blood pressure was at or slightly below 1 Gz levels in space, indicating a decrease in total peripheral resistance. It has been suggested that plasma volume is reduced in space, however cardiac output/venous return do not return to 1 Gz levels over the duration of flight. In spite of the increased cardiac output, central venous pressure was not elevated in space. These data suggest that there is a change in the basic relationship between cardiac output and central venous pressure, a persistent "hyperperfusion" and a re-distribution of blood flow and volume during space flight.

Increased pulmonary blood flow has been reported to increase diffusing capacity in space, presumably due to the improved homogeneity of ventilation and perfusion. Other studies have suggested that ventilation may be independent of gravity, and perfusion may not be gravity-dependent. No data for the distribution of pulmonary blood volume were available for flight or simulated microgravity. Recent studies have suggested that the pulmonary vascular tree is influenced by sympathetic tone in a manner similar to that of the systemic system. This implies that the pulmonary circulation is dilated during microgravity and that the distribution of blood flow and volume may be influenced more by vascular control than by gravity.

The cerebral circulation is influenced by sympathetic tone similarly to that of the systemic and pulmonary circulations; however its effects are modulated by cerebral autoregulation. Thus it is difficult to predict if cerebral perfusion is increased and if there is edema in space. Anecdotal evidence suggests there may be cerebral edema early in flight. Cerebral artery velocity has been shown to be elevated in simulated microgravity. The elevated cerebral artery velocity during simulated microgravity may reflect vasoconstriction of the arteries and not increased cerebral blood flow.

The purpose of our investigations was to evaluate the effects of alterations in simulated gravity (\pm), resulting in changes in cardiac output (\pm), and on the blood flow and volume distribution in the lung and brain of human subjects. The first hypothesis of these studies was that blood flow and volume would be affected by gravity, but their distribution in the lung would be independent of gravity and due to vasoactivity changing vascular resistance in lung vessels. The vasodilatation of the lung vasculature (lower resistance) along with increased "compliance" of the heart could account for the absence of increased central venous pressure in microgravity. Secondly, we postulate that cerebral blood velocity is increased in microgravity due to large artery vasoconstriction, but that cerebral blood flow would be reduced due to autoregulation.

METHODS

Simulated gravity was produced by combinations of lower-body negative or positive pressure, the head-down tilt position (6°), graded head-out immersion in water of thermal neutral temperature, or human centrifugation. Gravity was altered progressively or studied as a function of time, up to 6 hr.

Six series of experiments were conducted using 6-10 young health volunteers in each protocol. Data were analyzed by multivariate analysis of variance for repeated measures. During all experiments heart rate was determined from a continuous ECG recording, blood pressure was determined by automated auscultation, oxygen consumption by open circuit spirometry and pulmonary blood flow by CO₂ re-breathing. Diffusing capacity (D_L) was determined using CO and NO during re-breathing. Blood flow and volume measurements in the heart and lung were determined by nuclear imaging. Global cerebral blood flow and regional blood flow distribution were determined by Positron Emission Tomography (PET).

RESULTS

Cardiac output and stroke volume increased in simulated microgravity (up to 40%) and decreased in +Gz (by 40%) in all forms of simulation. These changes were associated with decreases in heart rate and total peripheral resistance during 0 Gz and increase during +Gz, while mean blood pressures were not different from 1 Gz values. These changes resulted from alterations in sympathetic tone, mediated by the baroreceptors. The changes observed initially in all gravity simulations, persisted through out the time of the experiments.

The changes in pulmonary blood flow and total lung volume paralleled the changes in cardiac output during changes in simulated gravity. The distribution of blood flow and volume in the lung are shown as % of the total in the right lung in Table 1.

Table 1. Percentage of blood flow and volume in lung sections 1-9 during changes in gravity.

	-----Top-----Lung Layer-----Apex-----								
Cond.	1	2	3	4	5	6	7	8	9
1Gz	7.1	7.1	8.5	9.9	12.4	13.1	13.8	13.9	14.2
0Gz	5.2	5.7	8.3	10.2	10.7	13.0	13.1	15.6	18.2
+Gz	6.8	7.6	8.4	9.6	10.0	13.5	14.3	14.7	15.1

The percentage of blood flow and volume in the vertical segments of the lung (1-9) were not affected by gravity. This implies all segments of the lung vasodilate or vasoconstrict in parallel. The initial changes in lung blood flow and volume persisted throughout the time period of the experiments, up to six hours.

Cardiac volume measures during simulated gravity demonstrated that end-diastolic volume, end-systolic volume and stroke volume increased in 0 Gz and decreased progressively in +Gz. The rate of change of volume during systole and particularly during diastole increased in +Gz and decreased in 0 Gz. These data are consistent with changes in "compliance" associated with the sympathetically mediated changes in inotropic state of the heart resulting from changes in Gz. Increased cardiac "compliance", when combined with decreased pulmonary resistance, could

explain the absence of increase in central venous pressure in space.

Previous investigators have suggested that the increased cardiac output and cerebral perfusion pressure would result in increased cerebral blood flow and could cause edema. We have determined cerebral blood flow using $H_2^{15}O$ and PET during 0.5 hrs erect and 3.0 hrs in the head-down tilt position. In a separate series of experiments, we have examined the effect of nitroglycerin (NG) administration on cerebral blood flow over 3 hrs in the supine position (SUP). The data for global cerebral blood flow (CBF, ml/min/100g) are presented in Table 2 along with similar data collected with the transcranial Doppler technique (TCD) reported in the literature.

Table 2. Cerebral blood flow and velocity are shown for selected time periods.

Protocol	Erect	Time, Hrs.		
		1.0	2.0	3.0
CBF-HDT-PET	53	38	42	40
CBV-HDT-TCD	49	58	57	55
CBF-SUP-NG	49	62	57	56

Cerebral blood flow decreased and cerebral blood flow velocity increased initially during head-down tilt. These data are consistent with a vasoconstriction of the large arteries and autoregulation in the brain, presumably due to myogenic responses to increased cardiac output and perfusion pressure. Over the three hours in the head-down tilt position cerebral blood flow was modulated toward control levels and cerebral blood velocity began to fall. There were regional changes in blood flow distribution and a two-fold increase in scalp flow, perhaps due to a "stealing". Assuming the cerebral blood flow data in 0 Gz are correct, a vasodilator like nitroglycerin could serve as a "countermeasure". Cerebral blood flow in the supine position was increased with nitroglycerin and remained elevated for 3 hrs.

CONCLUSION

The results of this series of experiments demonstrated that the lung vasculature is vasodilated and vasoconstricted by alterations in sympathetic tone in response to decreasing or increasing gravity, respectively. The reduction in pulmonary vascular resistance, when combined with the increased cardiac compliance, may account for the absence of an increase in central venous pressure in space. The increased perfusion pressure and reduced sympathetic tone in 0 Gz is offset by autoregulation, resulting in reduced cerebral blood flow with a re-distribution of flow to the scalp and within the brain. The absence of an increase in central venous pressure and modifications in cerebral blood flow may contribute to the sustained elevation of cardiac output, facial edema, motion sickness and other problems in and after space flight.

These studies were supported in part by NASA grants:NAS916042 and NAGW3937.

PERIPHERAL VASCULAR HYPORESPONSIVENESS AND ELEVATED CEREBRO-VASCULAR MYOGENIC TONE IN SIMULATED MICROGRAVITY: ROLE OF NITRIC OXIDE-DEPENDENT AND -INDEPENDENT MECHANISMS

R. E. Purdy¹, Y. Ding², S. P. Duckles¹, G. G., Geary¹, D. N. Krause¹, N. D. Vaziri², and S. D. Sangha¹

Departments of Pharmacology¹ and Medicine², College of Medicine, University of California, Irvine, Irvine, California 92697

INTRODUCTION

Microgravity was simulated in the present study using hindlimb unweighting (HU) in rats. We have shown previously that 20 days of HU causes hyporesponsiveness of peripheral arteries to norepinephrine (NE; 1). This was explored further by investigating the role of both nitric oxide dependent and independent mechanisms. Reduced contraction to NE can be due to up-regulation of a vasodilator mechanism, for example, increased activity of either endothelial constitutive nitric oxide synthase (ecNOS) or inducible nitric oxide synthase (iNOS). Such changes were studied in the carotid and femoral arteries. Reduced contraction to NE may also be caused by a decrease in coupling at one or more steps between alpha adrenoceptor stimulation and activation of the contractile apparatus. Coupling was studied in the abdominal aorta in which nitric oxide mechanisms have been shown to have no role in HU-mediated hyporesponsiveness to NE (1).

In both real and simulated microgravity, there is an acute cephalad fluid shift and an increase in cerebral perfusion pressure. Adaptation to this increased pressure was studied using isolated middle cerebral arteries from control and HU rats (2). Myogenic tone was increased in HU vessels, consistent with the development of a protective mechanism to prevent overperfusion of the brain vasculature. It is suggested (see Discussion) that peripheral vascular hyporesponsiveness and elevated cerebrovascular myogenic tone interact synergistically to cause postural intolerance.

METHODS

Male Sprague Dawley rats, 200 to 250 g, were randomly divided into caged control and HU groups. HU was achieved by placing a harness in the tail of the rat and elevating the hindlimbs 0.5 cm above the cage floor via a tether to the top of the cage. This tilted the body of the rat ~35° from horizontal. The rats were otherwise freely moving. After twenty days, peripheral arteries were isolated, cleaned and 3 mm rings mounted on luminal wires for the measurement of isometric contraction. Middle cerebral artery segments, 2mm, were cannulated at both ends and mounted in an apparatus for no flow pressurization with continuous superfusion. Lumen diameter was measured by video microscopy.

RESULTS

The role of nitric oxide dependent mechanisms on the vascular hyporesponsiveness to NE was investigated in carotid and femoral arteries. Mechanical removal of the endothelium from carotid, but not femoral, artery rings of HU rats restored the contractile response to NE toward control. A 10-fold increase in sensitivity to acetylcholine was observed in phenylephrine (PHE) precontracted carotid, but not femoral, artery rings from HU rats. In the presence of the nitric oxide synthase substrate, L-arginine, the iNOS inhibitor, aminoguanidine (AG), restored the

contractile responses to NE to control levels in the femoral, but not carotid, artery rings from HU rats. *In vivo* blood pressure measurements revealed that the peak blood pressure increase to NE was significantly greater in the control compared to the HU rats, but that to AG was less than half in control compared to HU rats. These results indicate that the endothelial vasodilator mechanisms may be upregulated in the carotid artery while the iNOS expression/activity may be increased in the femoral artery from HU rats. Upregulation of iNOS may occur in a large enough component of the vasculature to have a hemodynamically important vasodilator effect. These HU-mediated changes could produce a sustained elevation of vascular nitric oxide levels that, in turn, could contribute to the vascular hyporesponsiveness to NE.

Studies using the isolated abdominal aorta revealed that HU treatment made this blood vessel hyporesponsive to NE by nitric oxide synthase-independent mechanisms. It was also found that while HU treatment reduced the contractile response to NE, it had no effect on the contraction to serotonin. This afforded the opportunity to explore possible differences in the signal transduction pathways for NE versus serotonin stimulation of the aorta to determine which might be sensitive to HU. To this end, vasoconstriction to both agonists was measured in the presence and absence of the following second messenger antagonists: indomethacin to block the synthesis of vasoconstrictor cyclooxygenase products, genistein to block tyrosine kinase and the vasoconstrictor contribution of the MAP kinase pathway, and nifedipine to block L-type calcium channels. All three antagonists inhibited the contractions to serotonin equally in control and HU aorta rings. In contrast, all three antagonists markedly inhibited the contractile response to NE in control aorta rings but had no effect in rings from HU treated rats. Additional signal transduction pathways remain to be investigated. If it is found that HU treatment inhibits all pathways, it suggests that HU treatment has an inhibitory effect on alpha adrenoceptor function at a step earlier than coupling to individual second messenger pathways.

Adaptation of the cerebral circulation to simulated microgravity was investigated using rat middle cerebral arteries. Myogenic responses were measured in isolated, pressurized arteries from HU and control animals. Maximal passive lumen diameters, obtained in the absence of extracellular calcium plus EDTA, were not significantly different between groups. In physiological salt solution containing calcium, arteries from both HU and control animals maintained a constant lumen diameter when subjected to incremental increases in transmural pressure (20-80 mm Hg). However, the diameters of arteries from HU animals was significantly smaller than those of arteries from control animals at all pressures. This difference could be eliminated by exposure to the nitric oxide synthase inhibitor, N(g)-nitro-L-arginine methyl ester; i.e., the control vessels constricted to match the diameter of the HU vessels. After HU treatment, transient distensibility of the artery wall in response to pressure was also significantly decreased, whereas the frequency and amplitude of vasomotion were increased. The latter changes were not affected by N(g)-nitro-L-arginine methyl ester. Thus, simulated microgravity increases cerebral artery myogenic tone through both nitric oxide synthase-dependent and -independent mechanisms. In turn, the increased myogenic tone likely underlies an upward shift of the autoregulatory pressure range of the cerebrovasculature.

DISCUSSION

The results of this study demonstrate that the peripheral vascular adaptation to simulated microgravity results in vasoconstrictor hyporesponsiveness to NE. In the carotid artery and,

possibly, in other vessels of the upper body, this may be due in part to elevated ecNOS activity. In the femoral artery and, possibly, in other vessels of the lower body, this may be due in part to elevated iNOS activity. In the abdominal aorta, hyporesponsiveness to NE is independent of nitric oxide mechanisms and involves reduced coupling of the alpha adrenoceptor to several second messenger pathways.

In both real and simulated microgravity, there is an acute cephalad fluid shift and an increase in cerebral perfusion pressure. The cerebrovascular adaptation of increased myogenic tone described above is likely to represent a protective shift of the cerebrovascular autoregulation to a higher systemic blood pressure range. However, that autoregulatory shift may work synergistically with the peripheral vascular hyporesponsiveness to cause postural intolerance on re-exposure to gravity. When microgravity-adapted astronauts stand in Earth's gravity, they tend to exhibit postural hypotension due, in part, to an impaired ability to increase peripheral resistance. In turn, the hypotension may yield a cerebrovascular perfusion pressure below the microgravity-adapted, higher pressure range of the cerebral autoregulation. As a consequence, cerebral blood flow declines, potentially leading to symptoms of postural intolerance including syncope.

REFERENCES

1. Purdy, R.E. Duckles, S.P., Krause, D.N., Rubera, K.M. and Sara, D. Effect of simulated microgravity on vascular contractility. *J. Appl. Physiol.* 85(4): 1307-1315, 1998.
2. Geary, G.G., Krause, D.N., Purdy, R.E. and Duckles, S.P. Simulated microgravity increases myogenic tone in rat cerebral arteries. *J. Appl. Physiol.* 85(5): 1615-1621, 1998.

MYOCARDIAL PERFORMANCE AND METABOLISM IN MICE WITH A NULL MUTATION IN CYTOCHROME C OXIDASE SUBUNIT VIAH

N. B. Radford, B. Wan, L. Szczepaniak, E. E. Babcock, A. Richman, C. S. Storey, J. L. Li, K. Li and R.W. Moreadith.

The Rogers Magnetic Resonance Center, The University of Texas Southwestern Medical Center, Dallas, TX 75235 USA

INTRODUCTION

Several lines of evidence suggest that cytochrome c oxidase (COX) subunit VIaH may modulate COX activity, thus exerting regulatory control over oxidative energy production with potential consequences for myocardial mechanical performance. To test this hypothesis in the intact heart, a murine line with a null mutation in COXVIaH was created and an assessment of systolic, diastolic and metabolic performance was made.

METHODS

A murine line with a null mutation in COXVIaH was created using gene-targeting technology *via* homologous recombination in pluripotential embryonic stem cells. A single female chimera was found to transmit the mutation to her offspring. Heterozygote mutants were bred to each other to generate wild type (VIaH+/+), heterozygote (VIaH+/-) and homozygote (VIaH-/-) offspring. There was no evidence of embryonic loss of mutant mice. A northern blot confirmed the absence of COXVIaH mRNA in VIaH-/- heart and skeletal muscle. Cross sections from myocardial tissue were stained with hematoxylin/eosin and examined for general morphology. There were no pericardial abnormalities nor increase in myocardial fibrosis in the mutant hearts. Hearts from wild type and mutant animals were also examined using scanning electron microscopy. There were no differences noted in mitochondrial morphology, size or number per cell.

RESULTS

Myocardial performance was examined using the isolated perfused, working mouse heart preparation. With increasing left atrial filling pressure, hearts from VIaH+/- and VIaH-/- mice were unable to generate equivalent stroke work compared to hearts from VIaH+/+ mice. Direct measurement of left ventricular end-diastolic volume using magnetic resonance imaging in this preparation, suggests that this impaired performance is a consequence of impaired left ventricular filling or diastolic dysfunction. Ejection fraction, measured in the isolated working heart preparation, was similar in hearts from VIaH+/+ and VIaH+/- mice. Total myocardial ATP, measured using both ³¹P nuclear magnetic resonance spectroscopy in the working mouse heart and traditional biochemical methods in tissue extracts, was not different in hearts from VIaH+/+, VIaH+/- and VIaH-/- mice. However, cytochrome c oxidase activity, measured spectro-photometrically in homogenized tissue, was reduced in hearts from VIaH-/- mice while citrate synthase activity was increased. Myocardial oxygen consumption was also reduced in mutant hearts.

CONCLUSION

These findings suggest that altered expression of COXVIaH has a measurable impact on myocardial diastolic performance rather than systolic performance but the underlying metabolic derangements associated with this phenotype require are not yet clearly defined.

CAROTID BAROREFLEX FUNCTION DURING PROLONGED EXERCISE

P.B. Raven, NASA GRANT #NAG4668, University of North Texas Health Science Center, Fort Worth, TX 76107.

INTRODUCTION

Astronauts are often required to work (exercise) at moderate to high intensities for extended periods while performing extra-vehicular activities (EVA). Although the physiologic responses associated with prolonged exercise have been documented, the mechanisms involved in blood pressure regulation under these conditions have not yet been fully elucidated. An understanding of this issue is pertinent to the ability of humans to perform work in microgravity and complies with the emphasis of NASA's Space Physiology and Countermeasures Program.

Prolonged exercise at a constant workload is known to result in a progressive decrease in mean arterial pressure (MAP) concomitant with a decrease in stroke volume and a compensatory increase in heart rate. The continuous decrease in MAP during the exercise, which is related to the thermoregulatory redistribution of circulating blood volume to the cutaneous circulation, raises the question as to whether there is a loss of baroreflex regulation of arterial blood pressure. We propose that with prolongation of the exercise to 60 minutes, progressive increases on central command reflect a progressive upward resetting of the carotid baroreflex (CBR) such that the operating point of the CBR is shifted to a pressure below the threshold of the reflex rendering it ineffectual in correcting the downward drift in MAP. In order to test this hypothesis, experiments have been designed to uncouple the global hemodynamic response to prolonged exercise from the central command mediated response via: (i) continuous maintenance of cardiac filling volume by intravenous infusion of a dextran solution; and (ii) whole body surface cooling to counteract thermoregulatory cutaneous vasodilation. As the type of work (exercise) performed by astronauts is inherently arm and upper body dependent, we will also examine the physiologic responses to prolonged leg cycling and arm ergometry exercise in the supine positions with and without level lower body negative pressure (-10 torr) to mimic spaceflight-related decreases in cardiac filling volumes.

Revised Work Tasks for Grant #NAG4668

Title: "Carotid Baroreflex Function during Prolonged Exercise"

Specific Aim 1. Eight volunteer subjects will perform four 1-hour bouts of 65% VO_{2peak} arm or leg exercise in a thermoneutral environment.

Experiment 1

- a. One hour of leg exercise with carotid baroreflex function determined at rest; at 10 min and 50 minutes of exercise.
- b. Three hours of rest after (1a) followed by another one hour of leg exercises while central venous pressure is maintained constant by dextran infusion. Carotid baroreflex function determined at rest, at 10 min and 50 minutes of exercise.

Experiment 2

Arm and leg exercise used to increase the active muscle mass from rest to 50%, 75%, and 100% of VO_{2peak} . Carotid baroreflex function determined at each steady state work load.

Experiment 3

- a. One hour of arm exercise with carotid baroreflex function determined at rest, 10 min and 50 minutes of exercise.
- b. Three hours of rest after (2a) followed by another one-hour arm exercise with reduced CVP by applying -10 torr LBNP with carotid baroreflex function determined at rest, at 10 minutes and 50 minutes of exercise.

Results:

Experiment 1.

CAROTID BAROREFLEX FUNCTION DURING PROLONGED EXERCISE.

K.H. NORTON, K.M. GALLAGHER, S.A. SMITH, R.G. QUERRY, R.M. WELCH-O'CONNOR AND P.B. RAVEN.

The present investigation was designed to uncouple the hemodynamic physiologic effects of thermoregulation from the effects of a progressively increasing central command activation during prolonged exercise. Subjects performed two one hour bouts of leg cycling exercise with a) no intervention and b) continuous infusion of a dextran solution to maintain central venous pressure constant at the 10 minute pressure. Volume infusion resulted in a significant reduction in the decrement in mean arterial pressure (MAP) seen in the control exercise bout, 6.7 ± 1.8 vs. 11.6 ± 1.3 mmHg, respectively. However, indices of central command such as heart rate and ratings of perceived exertion rose to a similar extent during both exercise conditions. In addition, the carotid-cardiac baroreflex (CBR) stimulus-response relationship as measured using the neck pressure neck suction technique was reset from rest to 10 minutes of exercise and was further reset from 10 to 50 minutes of exercise in both exercise conditions with the operating point being shifted toward the reflex threshold. We conclude that the progressive resetting of the carotid baroreflex and the operating point renders the carotid-cardiac reflex ineffectual in counteracting the continued decrement in MAP that occurs during the prolonged exercise.

Manuscript (in press) J. Appl. Physiol. 1999

Experiment 2.

RESETTING OF THE CAROTID ARTERIAL BAROREFLEX DURING DYNAMIC EXERCISE IN HUMANS. K.H. NORTON, R. BOUSHEL, S. STRANGE, B. SALTIN AND P.B. RAVEN.

Recent investigations have demonstrated that at the onset of low to moderate intensity leg cycling exercise the carotid baroreflex (CBR) was classically in direct relation to the intensity of exercise. Based on this data, we proposed that the CBR would also be classically reset at the onset of moderate to maximal intensity leg cycling exercise. Therefore, CBR stimulus-response relationships were compared in seven volunteer humans using the neck pressure/neck suction technique during dynamic exercise ranging in intensity from 50% to 100% of maximal oxygen uptake ($\dot{V}O_{2max}$). Leg exercise alone (L) was performed at 50% and 75% $\dot{V}O_{2max}$ and leg exercise combined with arm (L+A) exercise was performed at 75% and 100% $\dot{V}O_{2max}$. $\dot{V}O_2$ and heart rate (HR) increased in direct relation with the increases in exercise intensity. The

threshold and saturation pressures of the carotid-cardiac reflex at 100% $\dot{V}O_{2max}$ were $>75\% \dot{V}O_{2max}$ which were in turn $>50\% \dot{V}O_{2max}$ ($p<0.05$), without a change in the maximal reflex gain (G_{max}). In addition, the HR response value at threshold and saturation at 75% $\dot{V}O_{2max}$ was $>50\% \dot{V}O_{2max}$ ($p<0.05$) and 100% $\dot{V}O_{2max}$ was $>75\% \dot{V}O_{2max}$ ($p<0.07$). Similar changes were observed for the carotid-vasomotor reflex. In addition, as exercise intensity increased, the operating point (the pre-stimulus blood pressure) of the CBR was significantly relocated further from the centering point (G_{max}) of the stimulus-response curve and was at threshold during 100% $\dot{V}O_{2max}$. These findings identify the continuous classical rightward and upward resetting of the CBR, without a change in G_{max} , during increases in dynamic exercise intensity to maximal effort.

Manuscript (in revision) J. Appl. Physiol.

Plans for future investigations.

Experiment 3. Prolonged arm exercise (one hour) in the supine position with and without lower body negative pressure (-10 torr) and model carotid baroreflex function.

EVALUATION OF THERMOREGULATION AFTER SPACEFLIGHT

S.M. Schneider¹, W.J. Williams², J.E. Greenleaf³, S.M.C. Lee², and R. Gonzalez⁴

¹NASA Johnson Space Center, ²Wyle Laboratories, ³NASA Ames Research Center, ⁴U.S. Army Research Institute of Environmental Medicine

INTRODUCTION

Altered thermoregulation has been reported following spaceflight simulations such as water immersion and bedrest but it has never been evaluated immediately after actual spaceflight. Impaired thermoregulation may have significant impact during various spaceflight activities such as countermeasure exercise, extravehicular activity (EVA), landing, and egress. It would be manifested as an increased body temperature and heart rate and decreased work capacity and endurance. In this study we evaluated the exercise responses of two crewmembers following a long duration spaceflight and measured their changes in body temperatures, skin blood flow, sweating and heat production during a mild submaximal exercise stress.

METHODS

The results from two male crewmembers from the 115 day Mir-18 space mission are presented. Each crewmember volunteered to participate in this protocol which was approved by the JSC Institutional Review Board. Preflight comparisons were performed in duplicate 145 or 146 days before launch. Postflight comparisons were performed five days after landing. The supine, cycle exercise protocol consisted of 30 minutes of quiet rest, immediately followed by 20 minutes of exercise at 40% and 20 minutes at 65% of each crewmember's preflight maximal oxygen consumption. During each exercise test, continuous measurement of heart rate (Polar Heart Watch), core temperature (telemetry pill system), skin temperatures (thermistors on the chest, arm, thigh, and calf), local chest sweating rate (dew point hygrometry), and change in forearm blood flow (Laser Doppler flowmeter) were obtained. Metabolic heat production (by indirect calorimetry) was obtained during the final 5 minutes of each exercise level. Total body sweat loss was calculated from the pre to post-exercise change in body weight.

RESULTS

Preflight both crewmembers easily completed the submaximal exercise protocol. Postflight neither crewmember completed the 65% $\dot{V}O_{2\max}$ stage. Both tests were terminated upon direction from the flight surgeon in response to subject leg fatigue during pedaling. Final heart rates and core temperatures were similar to the preflight tests.

Heat production as calculated from the oxygen consumption data was not markedly different after flight but this data was incomplete in one of the crewmembers who had difficulty tolerating the mouthpiece after flight.

There were no consistent differences in skin temperatures at rest or during exercise at any measurement site following spaceflight. Core temperature was similar at rest following spaceflight but rose at a faster rate such that the final core temperature during exercise postflight was similar to the preflight value, despite the shorter postflight exercise time (11 and 12 min of exercise postflight vs. 20 min preflight for both subjects).

The total body sweat loss postflight was reduced in both crewmembers compared to preflight; 636g preflight vs. 272g for subject 1 and 455 g preflight vs. 45 g postflight for subject #2.

The skin blood flow and sweating responses of both crewmembers were greatly altered during the postflight tests as shown below:

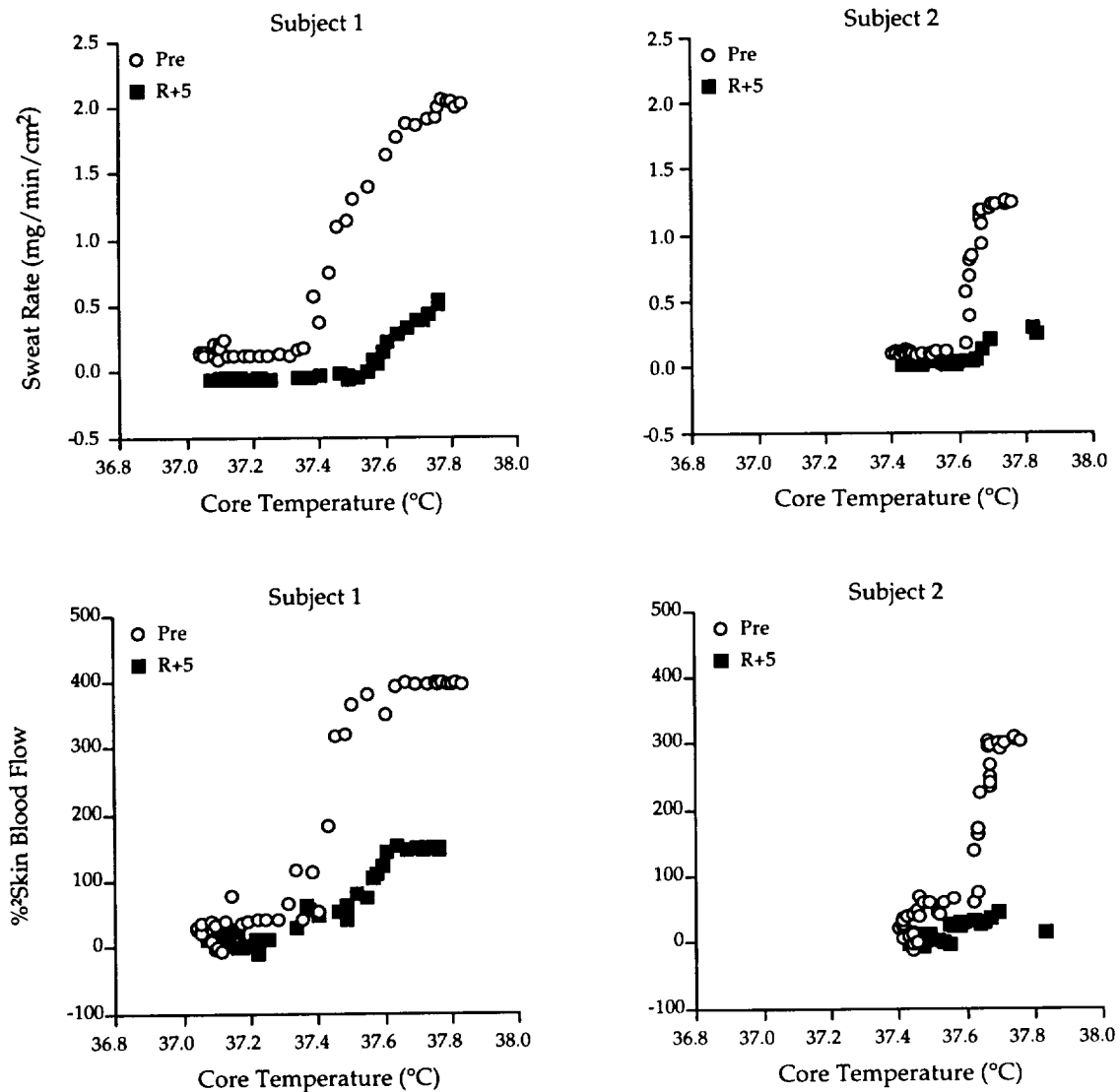


FIGURE 1

CONCLUSION

These preliminary results suggest alteration of heat loss responses in crewmembers following 115-days of spaceflight. An impaired ability to sweat and to redirect blood flow to the skin may result in greater heat storage, thus limiting work performance especially in a warm environment or during conditions where crewmembers must wear impermeable clothing such as the launch and entry suit. The mechanism for such changes in autonomic control of thermoregulatory responses is not evident without further measurements. Whether this effect is also present during flight has yet to be determined.

HYDRAULIC AND COMPUTER MODELING OF CARDIOVASCULAR RESPONSE TO WEIGHTLESSNESS

M. K. Sharp, G. M. Pantalos, K. J. Gillars and K. Peterson
Biofluid Mechanics Laboratory, University of Utah, Salt Lake City, UT 84112

INTRODUCTION

Hydraulic and computer models of the systemic and pulmonary circulation have been developed for studying the acute effects of gravity on the cardiovascular system, including regional fluid shifting and the influence of hydrostatic pressure within the ventricle on diastolic ventricular filling, cardiac output and vascular pressures.

METHODS

Hydraulic model - The hydraulic model incorporated left and right ventricles of a pneumatic artificial heart, left and right atria, a peripheral venous pool, three systemic vascular sections (cephalic, central and caudal) and a pulmonary section. Each vascular section comprised four elements - proximal resistor, proximal compliance, peripheral resistor and peripheral compliance - a Westkessel configuration with an additional downstream compliance to represent the compliance of the regional veins. A small amount of inertance was also introduced in connecting tubing. The resistors were made from open-cell foam compressed by a motorized piston. Each compliance unit incorporated a coil spring-loaded piston moving inside a cylinder sealed with an elastomeric diaphragm [Woodruff, *et al.* 1997]. Non-linear compliance was provided by both high pressure and low pressure limits on the displacement of the piston and diaphragm. The peripheral venous pool (PVP) consisted of a spring-loaded bellows designed to mimic the human blood vessel pressure-volume relationship measured by Katz [1969] corresponding to vessel cross sectional shapes of 1) collapsed, 2) partially filled elliptical, and 3) inflated circular and the blood volume displacements due to gravity measured by [Smith 1990] and Wolthuis [1975]. An extensive computer model, which incorporated over 1000 elements (lumped resistance, compliance and inertance), was used to choose values of the elements in the regional mock circulation units most closely approximating the input impedance of the human system. Tests were performed to find and adjust the hydrostatic indifference level (HIL) of the hydraulic model to be just below the ventricles. The hydraulic model was flown in simulated 0-G aboard the NASA KC-135, with a different posture being tested each flight day and a different cardiac output for each set of ten parabolas.

Computer model - The computer model consisted of a distributed parameter systemic arterial system with 28 tapered elastic segments representing the large arteries and lumped parameter terminal Windkessel elements representing the small arteries, along with resistive elements representing minor artery branches off the main systemic tree. Also included were a three-region lumped parameter systemic venous system with non-linear compliance, lumped parameter pulmonary circulation, Windkessel left and right atria and ventricles modeled with time-dependent elastance. Energy losses were included in the unsteady Bernoulli equations describing flow from parent to daughter branches across systemic arterial bifurcations and the influence of hydrostatic pressure was included in the ventricular response, as well as in the systemic venous volume calculations. The quasi-one-dimensional unsteady equations of momentum and continuity modeled the flow in each artery segment. A third equation, the tube law relating

pressure and cross-sectional area of the tube was used to describe arterial wall behavior, including wall viscoelasticity. The three equations were solved for state variables of pressure, cross-sectional average velocity, and cross-sectional area. The MacCormack finite difference predictor-corrector scheme was used to solve the non-linear partial differential equations.

RESULTS AND DISCUSSION

Hydraulic model - Heart function curves depicting cardiac output (AOQ) versus left atrial pressure (LAP) are shown in Fig.1 for data collected on KC-135 flights in the upright posture. Cardiac operating conditions begin on the right of each plot near the Starling limited cardiac output value, where cardiac performance for all gravitational conditions converges. For the left side of Fig. 1, a shift to the left of the cardiac performance curve is evident with increasing gravity, as previously noted by the investigators [Pantalos, *et al.* 1998]. Linear least squares fits are included on Fig. 1 to demonstrate the reduced rate of decrease of cardiac output as the cardiac filling pressure is reduced for increased gravity. This improvement in cardiac performance at low LAP is attributed to the augmentation of cardiac filling by the hydrostatic pressure within the ventricle. Note that in the recumbent positions (launch and supine), the intraventricular hydrostatic pressure difference is smaller (along the anterior-posterior axis) than in the upright position, but does not disappear. Augmented filling was seen in the supine posture, though less than in the upright posture. Fig. 2 demonstrates the expected convergence of cardiac performance for all postures in 0-G.

Because of the large compliance of the PVP when elevated to model the launch posture, LAP, aortic pressure (AOP) and AOQ dropped sharply from 1-G to 0-G. This phenomenon did not occur in the supine posture, because the PVP in the supine posture was located at the same level as the heart and, therefore, significant fluid shifting did not occur among G levels. The smaller compliance of the PVP for further volume reduction was clearly reflected in the limited increases (AOQ actually decreased slightly) in LAP, AOP and AOQ between 1-G and 1.8-G in the launch posture. With the HIL slightly below the heart in the upright posture, increases in LAP, AOP and AOQ would be expected upon entry into weightlessness from 1-G. These changes, however, were moderated by the elimination of the beneficial effects of the intraventricular hydrostatic pressure. In these results, it appeared that the intraventricular hydrostatic pressure was the more important factor, since only AOP rose with entry into weightlessness, while LAP and AOQ decreased slightly.

The change in right atrial pressure (RAP) in the model from 10.1 mmHg in 1-G to 4.1 mmHg in 0-G at the nominal 6.0 l/min set point in the launch posture compared favorably with measurements by Buckey, *et al.* [1996], who found that central venous pressure (CVP) dropped in three astronauts from 11 mmHg in 1-G to 1.8 mmHg in 0-G. The lower CVP in 0-G in humans has been attributed to decreased intrathoracic pressure due to unweighting of the thorax and abdomen, which acts to augment diastolic filling by maintaining ventricular transmural pressure.

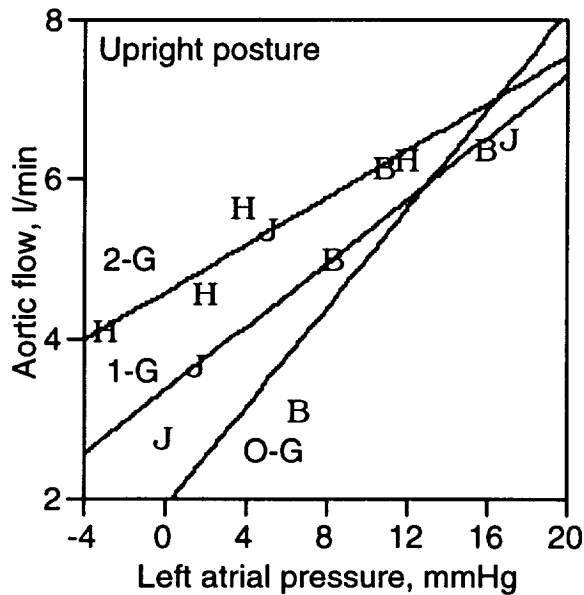


Fig. 1. Upright position cardiac function.

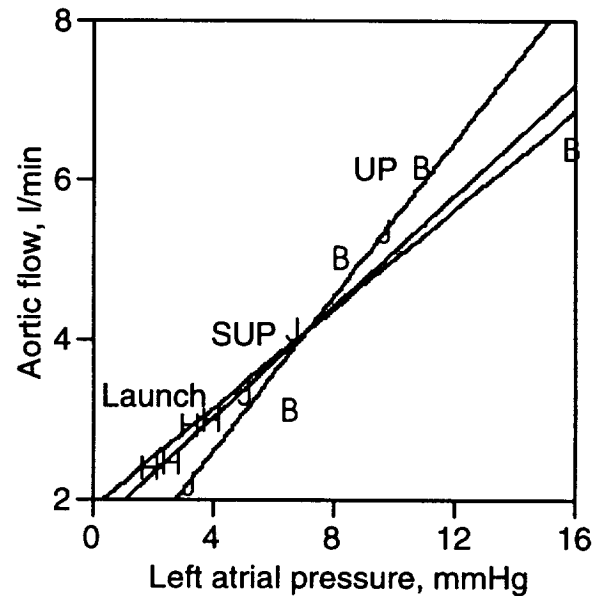


Fig. 2. Cardiac function in 0-G.

Computer model – Simulated arterial pressure and flow waveforms resembled those of the human, including the dicrotic notch in the aortic pressure waveform due to the closure of the aortic valve. Because the model included hydrostatic gradients only in the headward/footward direction, supine results for all G levels and 0-G results in all postures were computationally equivalent. Dramatic changes were seen in the numerical model output for the 1-G standing posture as compared to 0-G. Peak systolic pressure, peak left ventricular volume, and peak aortic pressure were all increased. The output appeared more dependent on the increased cardiac output in the standing 1-G posture rather than the effects of fluid shifting. In comparison, the results of left ventricular pressure and aortic pressure for the hydraulic model decreased in the 1-G standing posture as compared to 0-G supine due to the shifting of blood footward even though cardiac output increased. In both the numerical and hydraulic models, however, aortic outflow and pulmonary arterial pressure increased, both due to increases in stroke volume of the ventricles. Systemic venous volume shifts in the computer model followed expected trends in the 1-G standing posture as compared to 0-G. Caudal venous volume increased 373 ml supine (0-G) to standing (1-G), with 241 ml shifting from the central venous region and the remaining 132 ml from the cephalic region. Small changes were seen in the 1-G launch posture versus 0-G as well. Most notably, caudal venous volume decreased in the launch position as compared to supine and was shifted into both the cephalic and central regions. Stroke volume and left ventricular end-diastolic pressure increased in the 1-G standing posture as compared to 0-G, due to the absence of hydrostatic augmentation of diastolic filling. Central venous pressure (right atrial pressure) decreased in the 1-G standing position as compared to 0-G, consistent with the hydraulic model. Since both models neglect at this stage body structural interactions [Buckey, *et al.* 1996], this increase was expected. Fluid shifts headward increase volume and therefore pressure at the level of the right atrium [Watenpaugh and Hargens 1995].

CONCLUSIONS

A striking phenomenon evident in the flow and pressure data from both models was the dependence of the results on the state of each compliance relative to its pressure-volume relationship. The compliances in both models are adjustable and may be designed to a wide variety of compliance curves, however, there is a general lack of data in humans for matching, as well as potential variations among humans and between rest and exercise conditions. The results showed that hydromechanical mechanisms are important in determining cardiovascular responses and, therefore, must be considered in developing countermeasures. Improvements are planned in both models for monitoring cranial arterial pressure and flow so that postflight orthostatic intolerance can be predicted and candidate countermeasures evaluated.

REFERENCES

- Buckey JC, Gaffney FA, Lane LD, Levine BD, Watenpaugh DE, Wright SJ, Yancy CW, Meyer D & Blomqvist CG. Central venous pressure in space. *J Appl Physiol*, 81(1):19-25, 1996.
- Katz et al, *Biophysics Journal*, 9:1261-1271, 1969.
- Pantalos GM, Sharp MK, Woodruff SJ, O'Leary DJ, Lorange R, Everett SD, Bennett TE & Schurfranz T, "The influence of gravity on cardiac performance," *Ann Biomed Eng*, 26:1-13, 1998.
- Smith JJ, Circulatory Response to the Upright Posture, CRC Press, Boca Raton, Florida, 1990, p. 10.
- Watenpaugh DE. Upper Body Venous Compliance Exceeds Lower Body Venous Compliance in Humans. *NASA Technical Memorandum 110409*, 1969, p. 9.
- Wolthuis RA, LeBlanc A, Carpenter WA, et al, Response of Local Vascular Volumes to LBNP Stress. *Aviation Space Environmental Medicine* 46:697, 1975.
- Woodruff SJ, Sharp MK & Pantalos GM, "Compact compliance chamber design for the study of cardiac performance in microgravity," *ASAIO J* 43:4:316-320, 1997.

SYMPATHETIC CONTRIBUTIONS TO ORTHOSTATIC TOLERANCE AND VASCULAR TONE FOLLOWING BED REST

J. Kevin Shoemaker and Lawrence I. Sinoway

Penn State College of Medicine, The Milton S. Hershey Medical Center, Hershey, PA 17033

BACKGROUND

Augmentation of total peripheral resistance is critical for brain blood flow when cerebral perfusion pressure is diminished as one moves from the supine to the upright posture. Under these conditions increased total peripheral resistance is a function of changes in both stroke volume and peripheral vascular tone. In turn, vascular resistance is highly dependent upon a functioning sympathetic nervous system that can produce vasoconstriction in skeletal muscle and abdominal vascular beds. Current evidence suggests that blood vessel regulation may be altered by space flight, and its ground based analog of head-down tilt bed rest (HDBR), possibly contributing to the diminished orthostatic tolerance observed in many individuals following these interventions. We report on two studies that have examined the effects of 14 days HDBR on the relationship between sympathetic outflow and vascular resistance in humans.

EXPERIMENT #1:

INTRODUCTION

We have used a model whereby continuous measures of both stroke volume and muscle sympathetic nerve activity are obtained during supine and upright postures to examine the temporal contributions of both stroke volume and sympathetic activation to OI following bed rest. In this experiment we tested the hypothesis that altered orthostatic tolerance following 14 days of HDBR was related to either inadequate sympathetic outflow or to excessive reductions in stroke volume during a 10-15 min head-up tilt (HUT) test.

METHODS

Continuous measures of heart rate, blood pressure (Finapres), muscle sympathetic nerve activity (MSNA; microneurography) and stroke volume blood velocity (SVV; Doppler ultrasound) were assessed during supine, 30° (5 min) and 60° (5-10 min) HUT positions in 15 individuals who successfully completed the pre HDBR test without incidence of presyncope or hypotension. The average MSNA burst frequency was assessed for baseline and for each min of HUT. Corresponding values of SVV, heart rate diastolic and systolic blood pressure were determined over 1-2 min in the supine position and over 10-20 consecutive cardiac cycles at the end of each min of tilt. Following HDBR these individuals were classified as being orthostatically tolerant (OT, n=9) or intolerant (OI, n=6).

RESULTS

For the OT group supine MSNA burst frequency was unchanged following HDBR and increased similarly in the pre and post HDBR HUT tilts. The relative increase in total MSNA (% Δ MSNA) with HUT was also unchanged in the OT group following HDBR (Figure 1). The heart rate and SVV responses to HUT increased and decreased, respectively, after HDBR ($P < 0.0002$). However, a greater increase in systolic and diastolic blood pressure during HUT was observed following HDBR ($P < 0.05$). Importantly, baseline MSNA was increased in the OI group following HDBR ($P < 0.05$). Also, MSNA increased normally for the OI group throughout the

majority of the tilt period in both HUT tests until end tilt (marked by presyncope and early termination in 4 of the 6 OI subjects) where attenuated MSNA and blood pressure responses were observed in the post, compared with the pre, HDBR test. This is demonstrated in Figure 1 where the % Δ MSNA for the OI group increased normally during 30° HUT but was diminished during 60° HUT ($P < 0.05$) (60° HUT measures of MSNA were obtained two minutes prior to the onset of presyncope). Also, a notable reduction in systolic blood pressure was observed early in the 30° HUT phase following HDBR for the OI group (Figure 2); however, MSNA responses at this time were similar to pre HDBR (Figures 1 and 2). The diminished blood pressure during the 30° HUT phase was only partially explained by concurrent reductions in SVV.

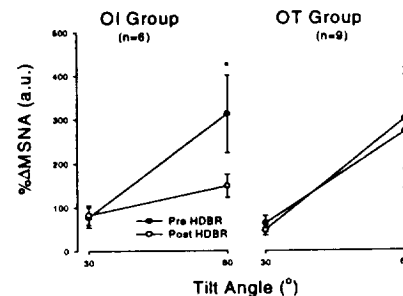


Figure 1: (see text for details); MSNA, muscle sympathetic nerve activity; HDBR, head-down tilt bed rest; OI, orthostatically intolerant; OT, orthostatically tolerant.

CONCLUSIONS

The elevated blood pressure response but unchanged MSNA in the post HDBR test for the OT group suggest augmented vascular responses to sympathetic constrictor outflow. Presyncope in the OI group was associated with diminished sympathetic discharge. However, the early and progressive hypotension in the post HDBR test for the OI group during mild orthostatic stress (i.e., 30° HUT), despite an augmented MSNA response, suggests diminished vascular responses. It was concluded that the diminished orthostatic tolerance following prolonged bed rest in susceptible individuals was associated with a blunted peripheral vasoconstrictor response. The diminished vascular response led to orthostatic intolerance and presyncope when sympathetic discharge was not adequate.

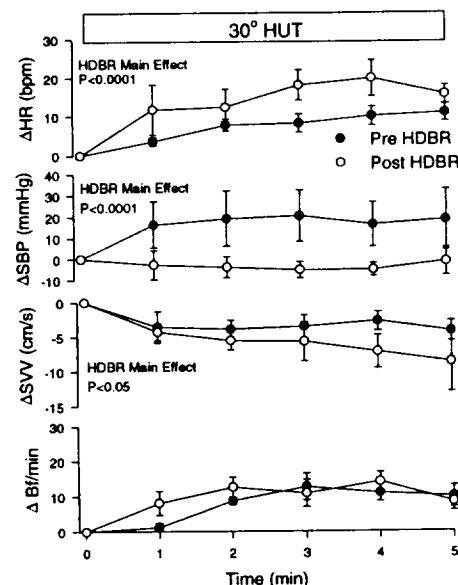


Figure 2: Changes in heart rate (HR), systolic blood pressure (SBP), stroke volume velocity (SVV) and muscle sympathetic nerve burst frequency (Bf) from supine to 30° head-up tilt (HUT) in four subjects who demonstrated orthostatic hypotension and presyncope during a subsequent period of 60° HUT.

EXPERIMENT #2:
INTRODUCTION

In a separate group of study participants we examined more closely the role of altered control over vascular tone by testing the hypothesis that HDBR for 14 days alters vascular reactivity to vasodilatory and vasoconstrictor stimuli in humans.

METHODS

Vasodilatory capacity was examined by measuring the reactive hyperemia blood flow (RHBF; venous occlusion plethysmography) and arterial blood pressure response after 10 min of circulatory arrest both before and following 14 days of HDBR. Values were obtained at 5 sec following release of the circulatory arrest and every 15 sec thereafter for 3 min. These tests were performed in a control trial (n=20) and when sympathetic discharge was increased by a cold pressor test (n=10).

RESULTS

In the control trial at 5 s after circulatory arrest peak RHBF and vascular conductance were reduced in the post- compared with the pre-HDBR test ($P < 0.05$; Figure 2). Total excess flow over 3 min was diminished in the post-compared with the pre-HDBR trial (84.8 vs. 117 ml/100ml, $P < 0.002$). The ability of the cold pressor test to lower forearm blood flow during the RHBF period was less in the post than in the pre-HDBR tests (Figure 3; $P < 0.05$), despite similar increases in arterial pressure.

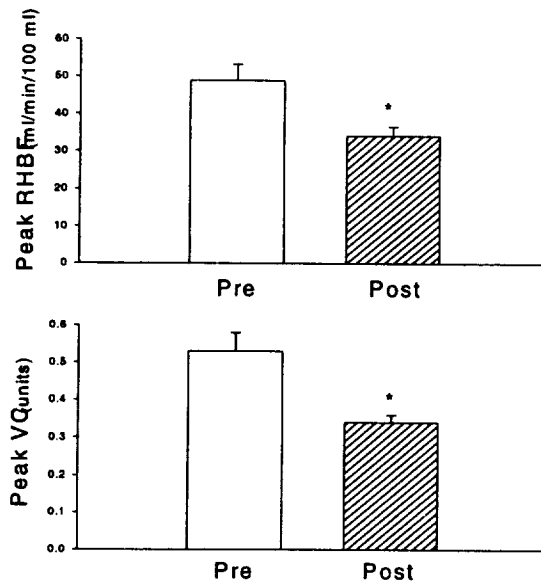


Figure 3: Peak reactive hyperemia blood flow (RHBF; top panel) and vascular conductance (VC; bottom panel) following 10 min of forearm circulatory arrest were attenuated following 14 days of head-down tilt bed rest. *, Significantly different from Pre bed rest ($P < 0.05$).

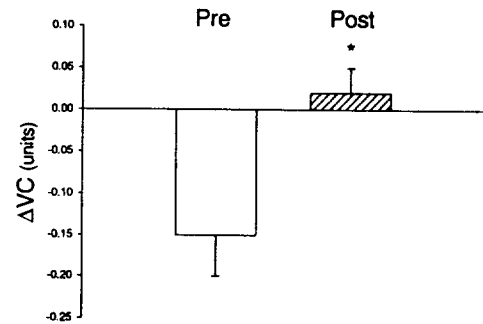


Figure 4: Ability of cold pressor test to lower the peak reactive hyperemia vascular conductance (VC) at 5 sec following 10 min of ischemia was reduced following 14 days of head-down tilt bed rest. *, Significantly different from Pre bed rest ($P < 0.05$).

CONCLUSIONS

These data demonstrated a reduced forearm vasodilatory capacity following bed rest. In addition, these observations indicate that the ability to evoke sympathetic vasoconstriction in a dilated vascular bed was diminished in the same individuals. Therefore, regulation of vascular dilation and the interaction between dilatory and constrictor influences were altered with bed rest.

RENAL AND CARDIO-ENDOCRINE RESPONSES IN HUMANS TO SIMULATED MICROGRAVITY

Gordon H. Williams, M.D, Thomas Mullen, Ph.D. and Craig Ramsdell, M.D.

INTRODUCTION

The volume-regulating systems are integrated to produce an appropriate response to both acute and chronic volume changes. Their responses include changing the levels of the hormones and neural inputs of the involved systems and/or changing the responsiveness of their target tissues. Weightlessness produces a volume challenge which is unfamiliar to the organism. Thus, it is likely that the volume regulatory mechanisms may respond inappropriately, e.g., an inappropriate decrease in total body volume in space and abnormal responses to upright posture and stress on return to earth. A similar "inappropriateness" also can occur in disease states, e.g., congestive heart failure. While it is clear that weightlessness produces profound changes in sodium and volume homeostasis, the mechanisms responsible for these changes are incompletely understood. Confounding this analysis is sleep deprivation, common in space travel, which can also modify volume homeostatic mechanisms.

There are two overarching hypotheses:

- Simulated micro-gravity disrupts the renal and cardio-endocrine systems responses to steady state and acute stress, with these disruptions being more profound in the salt-loaded than the salt -depleted state.
- Sleep deprivation has an additive adverse effect to microgravity on the responsiveness and regulation of the renal and cardio-endocrine homeostatic systems.

CURRENT STATUS OF RESEARCH

METHODS

Thirteen healthy volunteers have been recruited for the study. After completion of the screening procedures subjects begin the first of four phases of their study. Phase I lasted three days and took place in the Ambulatory GCRC where the volunteers began a calculated isocaloric diet consisting of 200 mEq sodium, 100 mEq potassium, 2500 ml fluid. Twenty-four hour urines were collected at the end of the four day period. During Phase II the subjects continued the diet, and 24 hour urines were collected for the duration of the hospital stay. During this phase renal hemodynamics were measured by PAH clearance, and hormonal responses to upright posture were assessed. Plasma renin activity (PRA), aldosterone, cortisol, and atrial natriuretic peptide were assessed during the posture test.

RESULTS

Ten subjects have completed two pilot projects. PRA levels were assessed during the upright posture study before and following supine bed rest. The levels across time and the levels in the pattern across the two synchrony conditions were not significantly different ($P > 0.4$). In the upright analysis, PRA significantly increased over time ($P=0.001$). A different pattern was shown for aldosterone across time. In the baseline supine analysis the effective time shift in

interaction were not significant ($P>0.15$). In the upright analysis aldosterone significantly increased across time ($P=0.0013$). Aldosterone was slightly higher for the unshifted condition than for the shifted condition overall ($P=0.088$), however the change across time was significantly greater for the unshifted than the shifted condition ($P=0.001$). Overall, levels of cortisol were similar for each shifted condition. In the subjects who had sleep disruption a similar pattern was observed. Finally, circadian rhythms for PRA did not vary across a 40-hour period, whether the individuals had been supine for five days or had had normal activity.

CONCLUSIONS

These results suggest that prolonged bed rest (a surrogate marker for microgravity), and particularly sleep deprivation, substantially disrupts the normal relationship between the renin-angiotensin system and aldosterone secretion. Renin-angiotensin levels in response to upright posture remain unchanged after either of these perturbations. However, aldosterone response to the increase in renin was significantly delayed in the sleep-deprived subjects, with a suggestive but smaller delay in subjects who remained in the supine position for five days. In contrast, the circadian rhythm of renin was not disrupted. Thus, these results provide entree to a better understanding of the potential role of changes in volume homeostatic mechanisms in space flight that could account, in part, for the cardiovascular instability upon return to one G. Either or both sleep deprivation and microgravity may contribute to this.

PLANS FOR FUTURE INVESTIGATIONS

Future studies will include an extension of the bed rest studies employed in our pilot project. Bed rest will be continued for 14 days, and the individuals will have cardiovascular monitoring performed throughout the study. In addition, studies involving infusion of angiotensin II and norepinephrine will assess hormonal and vascular responses. The final phase of studies will be to combine the 14-day simulated microgravity study with sleep deprivation to determine the effect of the combine experimental conditions on acute cardiovascular perturbations.

Immunology, Infectious Disease, and Hematology

Chair

William Shearer, M.D., Ph.D.

Co-Chair

Gerald Sonnenfeld, Ph.D.

IMMUNOLOGY, INFECTIOUS DISEASE, AND HEMATOLOGY SESSION SUMMARY

Overview

The presentations of the Immunology, Infectious Disease, and Hematology Scientific Session are divided into four groups of common theme: immune responses in space travel, virus infections in space travel, biological effects of space travel, and health hazards and bacterial containment in space travel. It was clear from the extent of the discussion following each presentation that the general themes of immunology, infection, and toxicity and bacterial containment in long-term space travel have a particularly relevant importance for human survival and quality of life, based upon preliminary evidence of the participating researchers. Each presentation touched upon the possible risks of long-term space travel due to alteration in immune responses, reactivation of previously controlled infections, biological alterations in cell membrane function and gene activation, and toxic chemical and bacterial contamination.

Immune Responses

The investigations described in this group of presentations used animal models flown in space and earth-bound human and animal equivalent models. In the first instance, the direct effects of space travel itself were used to test a hypothesis; whereas, in the other instances, certain conditions that are thought to mimic some of those in space travel were used.

Sonnenfeld et al. presented research findings on 10 pregnant rats and their fetuses and newborn pups exposed to an 11-day space flight. The hypothesis of the experiment was that stress, microgravity, re-entry to Earth's atmosphere, and other factors associated with space travel would reduce immune responses of young animals exposed *in utero*. With appropriate earth-bound control animals as a baseline, it was discovered that the pregnant rat dams had diminished cellular mediated immunity ($p < 0.05$) and decreased response of bone marrow progenitor cells to colony stimulating factor ($p < 0.05$). However, using this model, it was not possible to discern these same differences in the rat fetuses and rat newborn animals, although the small number of study animals may have limited the statistical power to determine important differences. Similar experiments with longer-term space travel will be necessary to completely address the hypothesis.

Shearer et al. presented a study design to test the hypothesis that long-term space travel harms the human immune response and creates a secondary state of immunodeficiency, possibly leading to chronic microbial infection and malignancy. Because of the limitations of performing sophisticated human immune studies in space travel, three earth-bound equivalent human models will be utilized. First, in collaboration with **Lugg**, volunteer subjects will be studied during an 8-9 month winter-over in the Antarctic continent. Second, space center technical personnel enclosed in a survival capsule for 6 months at NASA's Johnson Space Center (and possibly Russian counterparts at the Moscow Institute for Biomedical Problems) will be studied. Finally, in studies already underway with **Dinges** and **Mullington**, the effects of sleep deprivation and cytokine regulation will be studied in human subjects.

The focus of investigation in these three earth-bound, space-equivalent model systems will be on the specific humoral immune response, since previous space research has not adequately explored this aspect of immunity. In collaboration with **Ochs**, immune responses to the neoantigen, bacteriophage Phi-X 174, will be assessed: primary antibody (IgM), secondary antibody (IgG), IgM to IgG class switching, affinity of antibodies for antigen, and antigen clearance. Sophisticated cell phenotyping will be performed on peripheral blood mononuclear cells, including determining the release of the important naive (CD45RA) T-cell subpopulation from the thymus gland. Lymphoproliferative responses to Epstein-Barr virus (EBV) antigen will be assessed in subjects experiencing reactivation of EBV infection, which is known to produce B-cell tumors in immunosuppressed humans. These EBV studies will be performed in collaboration with **Butel**. The sleep deprivation research has proceeded to a point where it has been possible to quantitate interleukin (IL)-6, the soluble high affinity (IL-2R1), IL-2 receptor, and the soluble low affinity IL-2 receptor (sIL-2R2), and IL-2R2 in the plasma of seven study subjects. With this preliminary data in hand, other cytotoxic and inflammatory regulatory cytokines and their soluble receptors will be measured, as well as certain aspects of cellular-mediated immunity.

Kanwar described the statistically significant ($p < 0.05$) effects of anti-orthostatic suspension on murine delayed-type hypersensitivity *in vivo* skin reactions and spleen mononuclear cell *in vitro* IL-2 production in mice sensitized to a T-cell antigen, oxazalone. This new research fills the void in quantitatively studying inflammatory reactions, either non-specific or specific, in space travel in earth-bound equivalent models. Animals suspended in the anti-orthostatic position for 8 days had an increased reaction to specific antigen, indicating that the lack of normal position orientation deregulates normal T-cell responses to antigen and creates a state of hyperresponsiveness. IL-2 production in the spleen assay appeared to be increased in this model, indicating that the anti-orthostatic suspension created an immune imbalance and a state of hypersensitivity.

In the future, experiments involving real-time intravital microscopy will be performed, which will enable investigators to visualize leukocyte passage through blood vessels and tissue spaces during specific and non-specific hypersensitivity reactions.

Virus infections

This series of presentations addressed the possibility that viral infections may pose a risk to long-duration space flight. Alterations in the immune system associated with space flight may allow latent viruses endogenous in the human population to reactivate and shed to higher levels than normal, which in turn could affect the health of crew members.

Conner used a ground-based rodent model (hind-limb suspended mice) to examine the mucosal immune response to an intestinal virus infection (rotavirus), known to cause disease in both humans and animals. This project represents the first important test of the effects of space flight on the mucosal immune system, important because the mucosal immune system represents the first line of defense against most human pathogens. The rotavirus model was chosen because it is known that the systemic response is not important in either clearance of infection or establishment of immunity. Dr. Conner reported that suspension of CD-1 mice for 4 days prior

to virus inoculation resulted in significantly longer mean duration of virus shedding than in orthostatically-suspended or non-suspended control animals (8.0 days vs. 6.0 days vs. 6.3 days, $p = 0.003$). However, when challenged 6 weeks later, all groups of mice showed equal protective mucosal memory immune responses. These preliminary results suggest that some alterations in mucosal immune responses occur under simulated space flight conditions. Future studies will model longer times of anti-orthostatic suspension prior to virus inoculation and testing of gene knock-out mice to determine if delay in virus clearance is due to $CD8^+$ T-cells or antibody responses.

The next three presentations addressed the potential for reactivation and spread of latent viruses during long-duration space flight. Contributing factors may include altered host immune systems, crowded conditions, closed loop environment, and limited disinfection capabilities. Finally, radiation exposure may predispose a host to carcinogenesis by reactivated tumor viruses. Two types of viruses known to establish latent infections and to be human pathogens, as well as tumor viruses (herpesviruses, polyomaviruses), are being studied initially.

Pierson et al. summarized results of herpesvirus EBV shedding in saliva samples collected from flight crew members and individuals in several ground-based models of space flight. Polymerase chain reaction (PCR) assays for viral DNA were performed; some were qualitative assays and some were quantitative. Models examined were astronauts on shuttle-Mir flights, Antarctic winter-over subjects, and closed environmental chamber studies. A total of 37 subjects and 1659 saliva samples were analyzed. Of these, 356 samples (21%) were positive for EBV, with individual groups ranging from 17-42% positive samples. Of 14 controls (609 samples), 22 (4%) were positive, suggesting increased EBV reactivation and shedding under space flight conditions. Interestingly, quantitative PCR on some samples indicated that higher copy numbers of EBV DNA were present in samples from crew members in flight, as compared to preflight and postflight. **Lugg**, collaborator on the Antarctica studies, had performed cell-mediated immunity (CMI) tests, and several of those subjects that shed EBV were judged to be anergic or immune suppressed. **Pierson** also presented preliminary data on detection of cytomegalovirus (CMV; another herpesvirus) shedding in the urine of space shuttle astronauts. Of 46 subjects seropositive for CMV, 13 (29%) shed virus in one or more urine samples. Taken together, these data suggest that latent herpesviruses may be reactivated under space flight conditions.

Ling et al. described the development of a reproducible quantitative competitive (QC) PCR assay for EBV, which will be a powerful way to quantitate viral genome copies in different biological samples. A single-copy human gene is used as an internal control for the QC-PCR assays to control for different amounts of sample. **Ling** described initiation of a longitudinal study of virus reactivation in normal volunteers ($n = 30$), in which herpesvirus and polyomavirus shedding in saliva, blood, and urine will be quantitated in 7 collections over one year. This study will establish normal baseline patterns of virus reactivation in healthy adults and will facilitate interpretation of data from individuals in space flight or space flight analogs. Finally, he reported quantitative EBV DNA data using the QC-PCR assay from blood samples from HIV-immunocompromised individuals, who represent the extreme end of the spectrum of altered immune systems, as well as preliminary detection of polyomaviruses BKV and JCV DNA by PCR in urine samples from two normal volunteers.

Future plans are to complete the baseline data from normal volunteers, to analyze samples from a sleep deprivation study in collaboration with **Mullington** and **Dinges**, and to extend the quantitative studies to samples from Antarctica and a closed chamber study.

Stowe et al. described a serological study that showed changes in EBV-specific antibodies associated with space flight. The data were obtained from astronauts on 5 shuttle flights (9 or 16 days long). The geometric mean titer (GMT) for antibody to EBV viral capsid antigen was significantly elevated ($p < 0.05$) ten days before launch (L-10), compared to titers present in blood taken at annual medical exams (29 subjects). Interestingly, there was no change in the GMT for measles antibody in some of the same subjects ($n = 10$). He proposed that stress develops pre-flight and may lead to virus reactivation. In certain individuals, large (≥ 10 -fold) increases in antibody titers to EBV early antigen occurred the first 3 days after return to Earth. This was observed in 25% of male and 80% of female astronauts. The mechanism underlying this sharp increase in antibody titers is unclear. IL-10 levels were observed to be elevated after space flight in some individuals. This study also indicated that herpesvirus EBV may be reactivated during space flight.

Biological effects

It is suspected that the effects of long-term space travel will have diverse biological effects in humans, including alteration of gene function and protein production. Four presentations were given:

Alfrey et al. reported on "Neocytolysis: Mechanisms of Monitoring Neocytes". There is a consistent decrease in red blood cell mass (RBCM) seen in space flight that lasts longer than 24 hours — usually between 10 - 12.5%. The investigators have proposed a hypothesis that young red cells (neocytes) are predominately removed by the reticuloendothelial (RE) system under conditions of low erythropoietin (EPO) seen in space flight. Plasma volume decreases rapidly ($\approx 25\%$) during space flight, leading to an effective increase in hematocrit and a decrease in the secretion of EPO by the kidney. The new postulate is that low EPO leads to a different interaction of neocytes and RE cells, resulting in neocyte catabolism. This hypothesis is supported by studies done by these investigators on a population in Peru at 14,500 ft. Upon descent to sea level, they lose EPO production and RBCM. This decrease in RBCM can be blocked by injection of EPO. EPO also blocks the increase in iron stores, consistent with blocking RE catabolism. Further work to test this hypothesis will involve inducing a large number of neocytes by giving EPO to volunteers, then stopping EPO. The hypothesis is that there will be increased neocytolysis. Also, investigations will begin on the molecular mechanism of regulating RE-neocyte interactions by EPO.

Sytkowski and Davis presented studies of "Inhibition of Erythropoiesis by Simulated Microgravity". The studies on regulation of erythropoietin (EPO) were reviewed. EPO downregulated *Cmyb* expression in Rauscher murine erythroleukemia cells in a phosphatase signaling pathway. EPO upregulated *Cmyc* via a protein kinase C signaling pathway. Interplay between *Cmyb* and *Cmyc* activation is important in regulating differentiation and growth in the cell line. Using a rotating wall vessel (RWV), they found both retarded growth of the Rauscher cells and also less hemoglobin production in the presence of EPO, compared to standard flask

controls. There was no difference in glucose consumption between cultures. If Rauscher cells were grown for 24 hours in the RWV before addition of EPO, differentiation was inhibited virtually completely. Future work will look at the details of the signaling process induced by EPO and how this is altered by exposure to the RWV environment, as a ground-based model for microgravity.

McIntire presented his research on “Gene Regulation by Mechanical Forces in Vascular Cells”. He discussed a model protein important in human smooth muscle cell (hSMC) functional response, including proliferation, protein activated receptor-1 (PAR-1). Transmembrane flows across a vessel wall can expose hSMC to stresses in the range of 1-20 dynes/cm². Altered pressure distribution in the vascular system, as seen during space flight, will dramatically alter transmembrane flows, perhaps leading to vessel remodeling. A parallel plate flow chamber was employed to expose hSMC to controlled wall shear stresses. PAR-1 was strongly downregulated. Other genes were differently regulated by hSMC shear stress exposure, including tissue plasminogen activation and nitric oxide synthesis. Promoter deletion experiments indicated that a unique promoter sequence was responsible for the shear stress response of PAR-1, not the stress sensitive response element. Future work will study the signal transduction pathways involved in this mechanochemical signal transduction process, particularly the role of cytoskeletal elements.

Durban discussed “Regulation of Epidermal Growth Factor (EGF) by Gravity”. A brief review of EGF and its tissue distribution was presented. The rodent submandibular gland was chosen for study, since it expresses high levels of EGF. Studies in hypergravity using a centrifuge at 2.9 g and 3.5 g demonstrated virtually no EGF in this gland after 2 weeks and only 40% of control after five weeks of study. Tissue from rats flown on space flight STS-54 demonstrated 2-fold higher EGF levels 3 hours after return from space (a six-day mission).

Cell cultures from primary cultures of gland cells enriched from expression of EGF production and grown in a NASA rotating wall bioreactor showed no differences from those grown in collagen gels under static conditions.

Future work will involve looking at other tissues known to express EGF. Also, the 3D collagen gel cultures should be exposed to hypergravity to see if the *in vivo* mouse studies could be reproduced in culture (or was that response due to an *in vivo* hormonal change).

Health hazards and bacterial contamination

Microbiological issues can potentially impact long duration missions in a number of ways. These include water quality, human disease conditions, system integrity (e.g., corrosion), air quality, and possible damage to food crops. It is believed that ensuring low levels of bacteria in the water supply is an especially important preventive step in avoiding microbial problems. It is of particular interest to detect increasing microbial levels at an early stage. Characterizing and monitoring water quality was therefore a central theme in this group of talks.

Pierre et al. described the performance of the water reclamation hardware on the Mir Space Station from a chemical perspective. Although the water typically met performance and

potability standards, transient exceptions occurred in both the ground supplied water and recycled water. The only long-term problem was with total organic carbon and turbidity in the recycled water, which consistently exceeded NASA standards and sometimes the less stringent Russian standards, as well. The raw condensate exhibited increasing levels of ethylene glycol following incidents involving cooling system leaks, and monitoring the presence of this compound in the raw condensate may provide early evidence of such leaks.

A number of techniques were described for detecting and monitoring bacteria in water. **Elayan et al.** (presented by Suleiman) described a pizeoelectric biosensor that, in conjunction with an organism specific antibody, can sensitively measure bacterial numbers in the 10-100/ml range. **Fox et al.** outlined the potential of ribosomal RNA targeted DNA probes to identify bacteria in a species or group specific way using fluorescence or chemiluminescence. Assays targeting rRNA might be done by either *in situ* hybridization, in which single cells can be detected, or by DNA hybridization arrays. The latter format would allow simultaneous monitoring of several bacteria and appears to be compatible with miniaturization requirements.

Although steadily increasing bacterial numbers in the water system is qualitatively a good indicator of a pending problem, it would be ideal to measure actual bacterial metabolic activity. Physiological activity might be very different in two samples with similar numbers of bacteria. Although ribosomal RNA levels correlate with actual cell activity, RNA is only an indicator of one aspect of such activity. **Lisle et al.** described an approach that examines the metabolic condition of individual cells of *E. coli* for membrane potential, membrane integrity, respiratory activity, and intracellular esterase activity using a suite of fluorescent stains that allow cells to be visualized *in situ*. Typically, such an approach would be problematic due to the necessity of examining prohibitive numbers of microscope fields. This problem has been overcome by using solid phase cytometry, which is able to scan entire 25mm filters in 10-15 minute intervals. The result is that anywhere from 1 to 1×10^6 stained cells can be counted. It is likely that a mission version of this instrument can be made. It is, moreover, entirely feasible that assessments of metabolic activity can be integrated with organism identification by ribosomal RNA stains using this instrumentation.

Pyle et al. described recent results from the Biofilm flight experiment that was flown for six days on STS-81. It was found that biofilms of *Burkholderia cepacia* form as readily in space as on Earth. The organism was in fact able to grow in water alone and, to a limited extent, in water treated with Iodine as a disinfectant. It was also found that acceleration and vibration associated with mission launch appears to stimulate bacterial growth. **Pyle** also described a novel method for concentrating bacteria in a species-specific way using magnetic beads in combination with fluorescent antibodies and solid phase cytometry.

Implications for future research

Existing human models of acquired and genetic diseases (such as chronic viral infection and malignancy) in which humans are exposed to external stresses of immunosuppression, infection, physical and mental stress, and chemical/microbial contamination suggest the possibility of developing iatrogenic diseases in space travel. This possibility needs to be explored at an increased tempo and with the highest priority. With the potential launch of an exploration class

mission 15 years hence, it is not yet too late to redouble our efforts to assess the possibility of severe adverse outcomes to astronauts and to develop appropriate countermeasures.

William Shearer and Gerald Sonnenfeld

NEOCYTOLYSIS: MECHANISMS OF MONITORING NEOCYTES

C.P. Alfrey¹, L Rice¹, J. Trial², P. D. Kessler³ and B.J. Byrne⁴

¹Baylor College of Medicine, Houston TX, ²VA Medical Center, Houston, TX, ³ Johns Hopkins University School of Medicine, Baltimore, MD, ⁴ University of Florida, Gainesville, FL

INTRODUCTION

A decrease in red cell mass (RBCM) has been an invariable occurrence following spaceflight that lasts more than 24 hours. Previous studies have indicated this decrease begins within the first day in microgravity because of the elimination of young circulating red cells or neocytolysis. This process of RBCM modulation had not been previously recognized and its exact mechanism has not been thoroughly investigated.

Initially, to more clearly define this process, we have developed methods to separate red cells of various ages and have defined suitable markers to monitor the presence, absence or quantitative variation within this population of red cells. This is the first phase of the overall project to study a ground based model of neocytolysis.

METHODS

Age specific red cells were separated by phthalate ester density gradients as described by Danon et al (1964) and Wallas et al (1980). After removal of plasma, unseparated red cells as well as cells from the top and bottom of each gradient (least versus most dense red cell populations) were resuspended in RPMI 1640 plus 10% fetal bovine serum as 10^7 /ml and 10^6 red cells were placed into polypropylene tubes. Some samples were allowed to take up CellTrackerTM Green (Molecular Probes, Eugene, OR), a supravital dye converted to a green fluorescent product inside living cells. Exposure to the dye was at 37°C for 15 minutes. Other samples were reacted with fluorescein-conjugated wheat germ lectin (Sigma, St. Louis, MO) for 30 minutes at 4°C. All of these samples plus unlabeled cells were immediately analyzed for fluorescent intensity by flow cytometry after washing and placing in hypotonic buffer to induce spherocytosis.

In order to evaluate sequestration, red cells were opsonized by a 1:20 dilution of IgG anti-Rh₀(D) antiserum and labeled with CellTrackerTM Green. These cells were allowed to interact with adherent 14 day monocyte-derived macrophages at a 10:1 (erythrocyte:macrophage) ratio. The adherent cells were scraped from the plate and any red cells still external to the macrophages (i.e. free or adherent) were lysed by exposure for one minute to 2/5X PBS and then normalization of tonicity. The macrophages were then analyzed for green fluorescence by flow cytometry.

RESULTS

Similar difference in fluorescence intensity between samples were seen for CellTrackerTM Green uptake and wheat germ lectin binding. That is, compared to the unseparated population, the less dense cells exhibit more fluorescence and the denser cells exhibit less fluorescence. Furthermore, the green fluorescence due to CellTrackerTM Green persisted inside macrophages that had been allowed to phagocytose opsonized cells.

CONCLUSIONS

It has been argued by van der Vegt et al (1985) and Clark (1988) that cell volume is a better discriminator of red cell age than density. To account for this opinion we have developed two

methods to separate and identify the youngest population of red cells. We have shown that the uptake of a supravital dye, CellTracker™ Green (which is dependent upon the volume of cells) correlates closely with differences in cell density and with the binding of wheat germ lectin, a known marker of sialic acid which decreases with red cell age. CellTracker™ Green, which does not alter cell functions and remains fluorescent after internalization of the red cells by phagocytes, should provide several advantages over previously-reported methods for separation of red cell subpopulations for study of age-related phenomena. The first is that red cells can be separated by fluorescence-activated cell sorting without exposure to a chemical gradient that might alter their membranes. The second is that the separation can be based on cell volume, which has been reported to be the most reliable measurement of red cell age. The third is that the fluorescence label inside the red cells persists inside cells that have internalized them. This novel method will allow definitive studies of the preferential destruction of young red cells in an in vitro model of neocytolysis.

Having developed the necessary techniques to selectively separate and identify young red cells, we are presently confirming reproducibility and normal variability of selected surface or adhesion molecules amongst healthy controls. Additionally we have initiated the next phase of our project; volunteers will be administered erythropoietin while simultaneously monitored for changes in RBCM, changes in the quantity of young red cells in circulation and changes in the selected surface markers. These same techniques will be applied to a hypoxic animal model under controlled conditions.

DETERMINATION OF WHETHER IMMUNE CLEARANCE AND PROTECTION FROM MUCOSAL VIRUS INFECTION ARE ALTERED IN GROUND-BASED MOUSE MODELS OF SPACE FLIGHT

M.E. Conner

Division of Molecular Virology, Baylor College of Medicine and Veterans Affairs Medical Center, Houston, TX 77030

INTRODUCTION

We are using anti-orthostatic suspension of mice to determine whether the mucosal immune system is adversely affected in this ground-based model of space flight. Although this model does not simulate all aspects of space flight, it is an accepted ground-based model for studies on a number of parameters including alterations of the immune system. We will utilize rotavirus and the well-characterized immune response to rotavirus in different mouse strains. The effect of space flight or anti-orthostatic suspension on the immune system has been established by examining isolated aspects of the immune system by the use of soluble protein antigens or mitogens or by using viruses or bacteria that establish systemic infections. In all studies, systemic but not mucosal immune responses were evaluated. It is important to evaluate the mucosal response, as ~80% of all pathogens invade across mucosal surfaces, so it is the first line of an immunological defense. Many important pathogens, including viruses that cause respiratory and gastrointestinal diseases, produce localized infections at mucosal surfaces.

METHODS

Primary rotavirus clearance is being assessed in mice housed under three conditions: standard housing, orthostatic (no tilt), and anti-orthostatic. Since it was previously observed that the duration of the anti-orthostatic suspension at the time of primary infection altered the kinetics of clearance of primary infection and development of a memory immune response to *Listeria*, groups of orthostatic and anti-orthostatic mice are being inoculated either on the day of suspension or 4 or 7 days following suspension. One group of control mice has been mock-inoculated with phosphate-buffered saline (PBS). Mice were inoculated orally with 10^5 infectious dose 50 (ID_{50}) of EC murine rotavirus.

Following virus inoculation, rotavirus clearance is being evaluated by daily collection of fecal samples (0–14 dpi) from individual mice and tested for virus shedding by ELISA. Serum and fecal samples will be collected prior to infection and at 2-week intervals thereafter. The amount and duration of virus shedding will be compared between groups to determine if anti-orthostatic suspension altered the ability of the mucosal immune response to clear rotavirus infection. To determine whether suspension alters the ability of mice to mount a primary immune response, serum and intestinal antibody responses will be measured by isotype-specific ELISAs and neutralizing assays. To determine whether the type of T helper (TH) cell response induced is different in anti-orthostatic mice, we will measure specific IgG subtypes by ELISAs.

The memory immune response is being evaluated by assessing protection from rotavirus challenge 6 weeks post-primary infection in each of the groups of mice used in the clearance experiments. To determine whether anti-orthostatic suspension alters the expression of the memory immune response, thereby altering protection from virus challenge, virus challenges

will be performed on mice under normal conditions or orthostatic or anti-orthostatic suspension. Mice are being challenged with 10^5 ID₅₀ of EC murine rotavirus 4 days post-suspension. Protection from rotavirus challenge will be compared between groups by the duration and level of virus shedding post-challenge. Fecal samples are being collected 0–14 days post-challenge (dpc) and tested for virus excretion by ELISA.

RESULTS

The initial experiment is currently being performed. Mice were suspended for 4 days prior to inoculation with 10^5 SD₅₀ of murine rotavirus. Preliminary analysis of virus shedding 3-10 days post primary inoculation has been performed. Mock-immunized mice did not shed rotavirus. The mean duration of rotavirus shedding was 5.5 and 4.8 days in mice that were orthostatically suspended or housed under normal conditions, respectively. The mean duration of virus shedding was 7.2 days in the anti-orthostatically suspended mice. Additional samples need to be analyzed, but the preliminary results indicate that virus clearance is delayed in the anti-orthostatic mice. Further analysis based both on the amplitude and duration of virus shedding will allow comparison of the total amount of virus shedding between the groups. The challenge portion of the experiment has just been initiated. Mice will be suspended for 4 days and then challenged, which is 7 weeks post-primary infection. Immune responses to primary and challenge infection with rotavirus will be evaluated after the experiment has been completed.

CONCLUSION

The effects of suspension on clearance of a primary rotavirus infection will provide information on whether immune mechanisms important in virus clearance are altered, as well as provide data on the establishment of primary and memory antibody immune responses. The preliminary virus clearance results indicate that the primary mucosal immune response may be impaired in anti-orthostatically suspended mice. Following primary rotavirus infection of normal mice, antibody responses and resistance to rotavirus challenge are long-lived (≥ 1 year). The existence of a memory immune response and the ability of that response to protect mice from rotavirus challenge is being evaluated by assessing protection from rotavirus challenge 6 weeks post-primary infection in each of the groups of mice used in the clearance experiments. The results from this portion of the experiment will indicate whether mucosal immune responses, established either on the ground or in space, are likely to be altered under flight conditions, rendering astronauts more susceptible to mucosal virus infections that may be encountered in space.

REGULATION OF EPIDERMAL GROWTH FACTOR BY GRAVITY

Elisa M. Durban, Ph.D., University of Texas-Houston, Dental Branch

INTRODUCTION

Background and Rationale

Epidermal growth factor (EGF) is synthesized in a variety of tissues as a large membrane-bound precursor protein (approximately 130 kDa) from which mature EGF (6 kDa) and other EGF-like polypeptides are produced by proteolytic cleavage. Measurable levels of EGF are also found in many body fluids including plasma, saliva, urine, prostatic and seminal fluid, sweat, tears, gastric juice, and amniotic fluid. EGF is a principal regulator of proliferation and differentiation in development and throughout life.

Documented *in vivo* functions of EGF include a role in maintaining gastric and oral mucosal integrity and cytoprotection, stimulating epidermal wound healing and renal tissue repair, regulating local bone formation by stimulating bone resorption, and modulating fluid balance and nervous system functions. Additionally EGF influences reproduction by stimulating the meiotic phase of spermatogenesis, enhancing maturation of oocytes, and participating in pregnancy-induced mammary gland development and lactation. This broad range of physiological functions is induced by binding of EGF to the EGF receptor, an integral membrane glycoprotein (170 kDa) with tyrosine kinase activity that is stimulated by EGF binding. The physiological role of EGF in normal cell function is strengthened by the presence of EGF receptors in virtually every cell in the body. The importance of EGF in human physiology also is highlighted by successful EGF therapy in patients requiring skin grafting, wound management or gastroduodenal ulcer treatment. Conceivably, subtle alterations in the regulation of the EGF biosynthetic/secretory pathway in various tissues could affect a variety of physiological processes, therefore the effects of gravitational changes on EGF production were examined.

Effects of Excess Gravity on EGF Production

The rodent submandibular salivary gland (SSG) was chosen as indicator organ for EGF production as it synthesizes, stores, and secretes vast amounts of this growth factor, and does not exhibit circadian changes in EGF concentration. Three groups of BALB/c mice (6 males, 6 females/group) /experiment defined by gravitational forces of 2.9 and 3.5 g were maintained in a small animal centrifuge for either 2 or 5 weeks. The third group, control mice (1g), were housed in the same room. All mice were weighed weekly beginning 1 week prior to centrifugation to determine adaptation. EGF production was evaluated by immunocytochemistry followed by quantification by image analysis. Already by 2 weeks of exposure to hypergravity, and after the period of adaptation had taken place, intracellular EGF content decreased to negligible levels in both female and male mice compared to 1g controls. As summarized below, reductions in intracellular EGF levels were found to be statistically significant:

TIME	1g	3.5g	SIGNIFICANCE	
2 weeks		6.6 ± 1.1	<0.01	p < 0.001
4 weeks		7.4 ± 0.9	0.06 ± 0.02	p < 0.001
5 weeks		5.6 ± 0.7	2.6 ± 0.4	p = 0.001

Means ± standard errors

Effects of Spaceflight on EGF Production

The Biospecimen Sharing provided the opportunity to obtain SSGs from 6 flight rats and 6 control rats from the STS-54, 6 day-mission. Three hours after recovery, SSGs were dissected from flight animals over a period of 5-7 hours and fixed in Bouin's. SSGs from 6 control rats housed at a ground animal enclosure module at Kennedy Space Center were obtained with a 24 hr delay. EGF production was evaluated again by immunocytochemistry and image analysis. In contrast to the results observed in excess gravity, intracellular EGF levels were found to be at least two-fold higher in flight animals compared to levels observed in 1g controls. A concomitant reduction in EGF immunoreactivity within the luminal space of ductal cells was apparent, suggestive of impaired secretion. The effects of microgravity on EGF production appeared to be specific as the levels of another growth factor, transforming growth factor- α , were not affected.

CURRENT STATUS OF RESEARCH

The observations described above with hypergravity and microgravity suggest that the EGF biosynthetic/secretory pathway is gravity-sensitive. Intensive discussion has focused on whether cells sense gravity directly. Thus, recent studies in this laboratory have addressed the question of whether the effects of microgravity on EGF production are the result of a direct cellular response.

METHODS

The mouse SSG was again used as indicator organ as it produces vast amounts of EGF under the regulation of testosterone (Dtt) and triiodothyronine (T3). Additionally, we have shown in previous studies that 3-D collagen gel cultures of SSG epithelial cells can be modulated by hormones to produce EGF. Thus, advantage was taken of our knowledge with this culture system to examine whether EGF production is altered under simulated microgravity conditions in the absence of systemic influences on mediator molecules (e.g., hormones).

SSG cells were prepared for primary culture following our published procedures. Cells were cultured either at 1g within a collagen matrix or under simulated microgravity in a NASA-designed Rotating Wall Vessel (RWV). Cultures without and with hormones (Dtt: 1.7×10^{-7} M; T3: 1.5×10^{-8} M) were sampled at time intervals and monitored for growth and intracellular levels of EGF.

RESULTS

Although there is much evidence that epithelial cells (primarily cell lines) exhibit enhanced growth potential under simulated microgravity conditions, SSG epithelial cells in primary culture grew slower than 1g controls under these conditions. Substantial growth was only obtained in the presence of 20% defined horse serum, and the addition of collagen matrices as support did not enhance the growth and survival of simulated microgravity cultures (although an essential component of 1g cultures). Unlike 1g SSG cultures which generate within 1 week ductal-type structures with lumens, simulated microgravity grown cells only rarely generated structures with lumens in the time period of our experiments (2-3 weeks). As summarized below, despite the slower growth of the simulated microgravity cultures, no statistically significant difference in intracellular EGF content was detectable regarding either the quantity or quality of the EGF immune reaction.

CULTURE CONDITIONS	% OF EGF POSITIVE CELLS	INTENSITY OF EGF IMMUNOREACTIVITY (% of cells)	
		+	++
1g	50	65	22
simulated microgravity	58	73	26

CONCLUSIONS

With the caveat that the Bioreactor conditions may not completely mimick the spaceflight environment, these results suggest that in the absence of systemic influences that may alter hormone levels, microgravity does not directly affect the ability of EGF-synthesizing cells to produce and store this growth factor.

PLANS FOR FUTURE INVESTIGATIONS

Studies are ongoing regarding the potential relationship between the levels of EGF, transforming growth factor- α , and EGF-receptors as a function of gravity. Additionally, to differentiate between a potential experimental problem and a real growth effect of microgravity on SSG epithelial cells, we continue to address the unexpected observation that this cell system in primary culture grows rather poorly and with little morphological differentiation in simulated microgravity. Studies have been initiated as well to determine whether multi-organ effects on EGF content are operative as a function of gravitational changes. The mammary gland, which also produces EGF in response to hormones, is being examined first in this context as we have extensive experience in manipulating this organ in culture and *in vivo*.

NEW STRATEGIES FOR THE DETECTION OF E.COLI

N. Elayan, Y. Xu, C. Theegala, and A. Suleiman

Department of Chemistry, Southern University, Baton Rouge, LA 70813.

INTRODUCTION

Conventional methods for the detection and determination of bacteria involve incubation and culturing techniques, which are tedious and time consuming. Methodologies were or are being evaluated utilizing antibodies in conjunction with piezoelectric, electro-chemical, fiberoptic, and membrane-based sensors.

METHODS

The piezoelectric sensors involve immobilizing the antibody on the gold electrodes of a quartz crystal. The crystal is then exposed to various concentrations of E.coli, then the changes in the frequency is noted and correlated to the number of bacteria attached to the crystal. The electrochemical sensor involves co-immobilizing the enzyme horseradish peroxidase and the antibody on an activated membrane, which is mounted over the tip of an oxygen electrode. In the presence of bacteria, the activity of the enzyme decreases due to the formation of an immuno-complex. The changes in current response to peroxidase are monitored and related to the concentration of bacteria.

In another approach, an antibody-FITC conjugate is immobilized on a microporous membrane, which is mounted over the tip of an optical fiber bundle. The formation of an antigen/antibody complex shields the fluorescence label, resulting in a decrease in fluorescence intensity that is proportional to antigen concentration. In addition, a rapid confirmatory technique will be described. A horseradish peroxidase labeled antibody is added to the sample to be tested, then the solution is filtered utilizing a special porous membrane, where the conjugate-antigen complex will be strained. Finally, an enzymatic reaction is triggered to indicate the presence of bacteria.

CONCLUSION

The construction, variables affecting performance of the proposed sensors will be described. Preliminary studies indicate that 10 cells of E.coli/ml of water can be detected utilizing the above mentioned techniques.

MICROBIAL MONITORING TECHNOLOGY FOR LONG DURATION SPACE FLIGHTS

George E. Fox, Jamie Wibbenmeyer¹, Maia Larios-Sanz¹, Katerina Kourentzi², Jason C. Murphy², and Richard C. Willson²

¹Department of Biology and Biochemistry, University of Houston, Houston, TX 77204-5934;

²Department of Chemical Engineering, University of Houston, Houston, TX 77204-4792

INTRODUCTION

Crew health is a dominant issue in space flight. As mission duration and resupply intervals increase it is essential to be able to effectively monitor air and water supplies for gradual or acute buildup of microorganisms. We are developing methods that will allow simultaneous monitoring for multiple bacterial types in space environments.

METHODS

Nucleic acid hybridization technology is being used to target characteristic sequences in ribosomal RNA (rRNA). There are thousands of copies of the rRNAs in each cell. This natural amplification may allow development of suitable detection methodology without a PCR step. Such a detection system would be compatible with emerging DNA chip hybridization technology. We are initially targeting water samples and have developed preliminary probe designs for the purpose of monitoring water quality. The initial probe designs are being evaluated with standard dot blot hybridizations and fluorescence detection. In addition, we are evaluating molecular beacons as an approach to improved signal detection and studying the use of compaction agents such as spermine and spermidine for use in rapid purification of nucleic acid samples.

RESULTS

Probes have been designed for the detection of total bacteria, faecal coliforms, *Escherichia coli*, *Pseudomonas aeruginosa*, *Enterococcus* and *Burkholderia*. A sampling of these probes were tested in a hybridization array format in collaboration with Genometrix Inc. Although many of the probes did not have the desired specificity, there was no significant difficulty in terms of unwanted interactions between the probes. Separately, it was found that compaction agents are very effective in purifying nucleic acids. Initial work with molecular beacons indicates that they are very effective when used in conjunction with rRNA targets.

CONCLUSIONS

The results to date indicate that rRNA targeted hybridization as the basis of a spacecraft compatible microbial monitoring system is very promising. Work is now focused on improving probe design, evaluating approaches to improved signal detection and methods for sample preparation.

THE EFFECT OF ANTI-ORTHOSTATIC SUSPENSION ON DELAYED-TYPE HYPERSENSITIVITY REACTIONS

Samina Kanwar, James E. Smolen and C. Wayne Smith
Baylor College of Medicine, Houston, Texas

INTRODUCTION

The anti-orthostatic rodent model is an established ground-based model of simulated space flight. It has been reported that this model induces many physiological changes consistent with those observed in humans and animals during actual space flight. These include changes in stress hormone levels, over-use of upper and under-use of lower extremities and a cephalad fluid shift. To date there is limited evidence to suggest that these physiological changes affect the process of inflammation. Therefore, we propose to systematically study whether anti-orthostatic suspension (AOS) and the associated physiological changes directly influence basic inflammatory mechanisms. We will determine whether AOS induces tissue dysfunction and alters leukocyte infiltration, which is a hallmark feature of inflammation, during acute, non-specific inflammation and/or chronic, antigen-specific inflammation. We anticipate that any changes in leukocyte recruitment induced by AOS will significantly contribute to the development and/or resolution of inflammation.

CURRENT STATUS OF RESEARCH

Objective

Our initial studies will directly examine the effect of AOS on the development of antigen-specific inflammation, during a delayed-type hypersensitivity (DTH) reaction.

Methods

Male C57Bl/6 mice (20-40 g) will be anti-orthostatically suspended for 14 days. Control mice will have all suspension apparatus attached, but will not be suspended. A DTH reaction will be elicited in suspended and control mice by topical sensitization (abdominal skin) and local challenge (ear skin) with dinitrofluorobenzene. Animals will be sensitized on day 7 or 8 and challenged on day 12 or 13 of suspension. A DTH response in the ear will be measured 24 or 48 hours following challenge. Specifically, we will assess tissue dysfunction and leukocyte recruitment, by measuring ear swelling and thickness, and histological analysis of ear sections, respectively.

PLANS FOR FUTURE

The studies proposed above will allow for the quantitative and systematic assessment of the effects of AOS on inflammation associated with DTH. If a defect in the development of a DTH reaction is observed, it will be important to ask at what stage the defect appeared, ie. sensitization or challenge phase. To answer this question, in another series of experiments, we will sensitize animals prior to AOS, and subsequently measure the DTH response. Leukocyte recruitment is a key feature of inflammation, and involves a series of distinct interactions between circulating leukocytes and vascular endothelial cells. Furthermore, leukocyte recruitment depends almost entirely on the expression of and interactions between surface adhesion molecules. It is conceivable that AOS and the associated physiological changes (eg. cephalad fluid shifts) directly affect leukocyte-endothelial cell interactions, thereby influencing

total leukocyte infiltration. Therefore, in future studies, we propose to directly examine leukocyte-endothelial cell interactions (using intravital microscopy) and cell surface adhesion molecule expression in control and anti-orthostatically suspended mice. These measurements will be made in untreated (non-inflamed) mice, and following acute, non-specific (ischemia/reperfusion) or chronic, antigen-specific (allergic) inflammation. The studies and techniques proposed here will allow definition of steps in the inflammatory cascade that may be altered by simulated conditions of space flight and enhance our understanding of the potential cellular and molecular dysfunctions likely to be experienced by astronauts.

LATENT VIRUSES-A SPACE TRAVEL HAZARD??

P. D. Ling¹, R. S. Peng¹, D. Pierson², J. Lednicky¹, and J. S. Butel¹.

¹Division of Molecular Virology, Baylor College of Medicine, Houston, Texas 77030, ²NASA Johnson Space Center, Houston, Texas 77058.

A major issue associated with long-duration space flight is the possibility of infectious disease causing an unacceptable medical risk to crew members. Our proposal is designed to gain information that addresses several issues outlined in the Immunology/Infectious disease critical path. The major hypothesis addressed is that space flight causes alterations in the immune system that may allow latent viruses which are endogenous in the human population to reactivate and shed to higher levels than normal which can affect the health of crew members during a long term space-flight mission. We will initially focus our studies on the human herpesviruses and human polyomaviruses which are important pathogens known to establish latent infections in the human population. Both primary infection and reactivation from latent infection with this group of viruses can cause a variety of illnesses that result in morbidity and occasionally mortality of infected individuals. Effective vaccines exist for only one of the eight known human herpesviruses and the vaccine itself can still reactivate from latent infection. Available antivirals are of limited use and are effective against only a few of the human herpesviruses. Although most individuals display little if any clinical consequences from latent infection, events which alter immune function such as immunosuppressive therapy following solid organ transplantation are known to increase the risk of developing complications as a result of latent virus reactivation.

This proposal will measure both the frequency and magnitude of viral shedding and genome loads in the blood from humans participating in activities that serve as ground based models of space flight conditions. Our initial goal is to develop sensitive quantitative competitive PCR-based assays (QC-PCR) to detect the herpesvirus Epstein-Barr virus (EBV), and the polyomaviruses SV40, BKV, and JCV. Using these assays we will establish baseline patterns of viral genome load in the blood and viral shedding from normal volunteers in a longitudinal study over 1 year in length. As a comparison, we will measure patterns of viral genome loads and shedding from individuals who are severely immunosuppressed, in whom herpesvirus reactivation or primary infection with a herpesvirus is known to cause complications. In addition, we will proceed to testing ground based analogs in collaboration with Dr. Duane Pierson (Lyndon B. Johnson Space Center). This will include measuring samples obtained from individuals living and working in the extreme environment of Antarctica.

We expect to detect viral shedding or reactivation from most of the test groups, although the magnitude of shedding or reactivation cannot be predicted. The data accumulated from studies in this proposal should allow us to evaluate whether events that simulate certain aspects of space flight reactivate viral infections severe enough in nature that they may compromise the success of long-term space flight missions. These studies will also provide a foundation to monitor viral reactivation and shedding from crew members participating in actual space flight missions.

We will present data showing the establishment of our QC-PCR assay for detection of EBV. We will also present preliminary data obtained from a patient cohort study performed in collaboration with Dr. Cathal O'Sullivan (University of Alabama, Birmingham) to analyze blood

samples from AIDS patients both before and after antiviral (HAART) therapy for EBV genome load in the blood. The overall aim of this study is to use the levels of EBV genome load in the blood as a marker of immune competence. This study will indicate the range of EBV genome load during extreme immunosuppression and the possible value of using detection of EBV as a marker of immune competence.

RAPID ASSESSMENT OF BACTERIAL ACTIVITY IN SPACECRAFT WATER SYSTEMS

John T. Lisle, B.H. Pyle, S.C. Broadaway, and G.A. McFeters
Montana State University, Department of Microbiology, Bozeman, MT 59717

Maintaining and monitoring the microbiological quality water supplies on the shuttle and space station is imperative for crew health. To achieve these goals, rapid methods for the detection of bacteria that may indicate the presence of a health threat or deterioration of water quality are needed. We have used fluorescent antibodies, in conjunction with a suite of intracellular fluorescent stains, to identify the drinking water quality indicator and pathogen *Escherichia coli* and assess its physiological activity at the level of a single cell. This approach was used to assess the influence of starvation on physiological activity based upon membrane potential (Rh123), membrane integrity (LIVE/DEAD BacLight kit), respiratory activity (CTC) and intracellular esterase activity (Scan RDI). Each assay was performed in less than one hour. Growth dependent assays were also used to assess substrate responsiveness (DVC), ATP activity (MicroStar) and culturability (R2A agar). This study demonstrates this suite of stains can rapidly assess multiple indices of physiological activity allowing decisions to be made concerning the microbiological quality of spacecraft water in a more timely fashion relative to traditional culture-based methods.

GENE REGULATION BY MECHANICAL FORCES IN VASCULAR CELLS

Larry V. McIntire, Ph.D., Institute of Biosciences and Bioengineering, Rice University, Houston, Texas 77005-1892

INTRODUCTION

Exposure of endothelial cells to shear stress *in vitro* produces marked alteration in cell morphology, consistent with the proposed *in vivo* role of shear stress. Moreover, shear stress-mediated regulation of endothelial gene expression has been demonstrated for proteins with key roles in maintaining homeostasis, cell migration, and in cell growth.

It has been recently suggested that vascular smooth muscle cells (VSMC) may also be responsive to shear stress. *In vivo* studies of VSMC growth rates after balloon catheter injury have demonstrated an inverse correlation between growth rates and calculated shear stress forces. *In vitro* studies have confirmed the *in vivo* observations and demonstrated that the synthesis of transforming growth factor- β 1 (TGF- β 1), tissue plasminogen activator (tPA), heme oxygenase-1, nitric oxide, and prostaglandins increased under shear stress. Consistent with these observations, modeling studies supported the concept that VSMC in the normal vasculature are exposed to significant shear stresses, in the order of 1-10 dyn/cm², due to interstitial fluid flow driven by transmural pressure gradients.

On the basis of these findings, the present study was designed to determine whether shear stress also mediates gene expression in VSMC, ultimately leading to the pathologic proliferation of VSMC at sites of disturbed blood flow in the vasculature and perhaps control of vessel wall homeostasis under normal physiological conditions. The human protease activated receptor-1 (PAR-1) gene was chosen because: 1) PAR-1 expression is known to be increased dramatically after experimental injury in animal models, after percutaneous transluminal coronary angioplasty in patients and in human atherosclerosis and 2) the known roles of thrombin on VSMC function and proliferation state can be modulated by regulation of PAR-1 expression.

RESEARCH

The objective of this study was to investigate the effect of mechanical hemodynamics such as shear stress and cyclic strain on the expression of thrombin receptor: protease activated receptor-1 (PAR-1) in human aortic smooth muscle cells (HASMC).

Cultured HASMC were exposed to different levels of shear stress using the parallel plate flow chamber system. Northern blot and flow cytometric analysis indicated that PAR-1 mRNA and protein levels were reduced 3 fold by high wall shear stress (25 dyn/cm²), while low shear stress (5 dyn/cm²) actually increased PAR-1 expression at short times of exposure. mRNA half-life studies showed that the decreased mRNA level was not due to changes in the stability of PAR-1 mRNA. In order to see if shear stress would change cell responsiveness to thrombin, Ca²⁺ mobilization and proliferation were measured in presheared cells. Ca²⁺ rise after thrombin stimulation in sheared cells was 50% less than in control cells using digital imaging microscopy of Fura-2 fluorescence on individual HASMC (n>20 cells). Proliferation of HASMC after thrombin treatment was also reduced in HASMC exposure to shear stress (11931 \pm 1473) versus control (15887 \pm 677 cpm) using 3H-thymidine incorporation.

In contrast to shear stress, PAR-1 mRNA level was upregulated 2 fold by high level of cyclic strain, 20% strain at 60 cycles/min. Further studies will be developed to explore the effect of cyclic strain on PAR-1 protein and alterations in HASMC function to explore the effects of shear stress on regulation of other MASMC gene expression important for vascular wall homeostasis.

These results indicate that hemodynamic forces, shear stress and cyclic strain, can significantly modulate PAR-1 expression in HASMC and alter HASMC function such as attenuation in Ca²⁺ rise and proliferation in response to thrombin. They also support an important role of hemodynamic forces on gene regulation of PAR-1 in vascular diseases and a possible role in vascular remodeling after changes in transmural flux, as would occur with altered pressure distribution during space flight.

REFERENCES

Papadaki, M., Tilton, R.G., Eskin, S.G., and McIntire, L.V., "Effects of Shear Stress on Nitric Oxide Production by Human Aortic Smooth Muscle Cells" *Amer J. Physiol.* **273**, H616-H626 (1998).

Papadaki, M., Ruef, J., Nguyen, K.T., Patterson, C., Eskin, S.G., McIntire, L.V., and Runge, M.S., "Differential Regulation of Protein Activated Receptor-1 and Tissue Plasminogen Activator Expression by Shear Stress in Vascular Smooth Muscle Cells" *Circulation Resch.* **83**, 1027-1034 (1998).

McIntire, L.V., Wagner, J.E., Papadaki, M., Whitson, P.A. and Eskin, S.G., "Effect of Flow on Gene Regulation in Smooth Muscle Cells and Macromolecular Transport Across Endothelial Cell Monolayers" *Biol. Bull.* **194**, 103-109 (1998).

HEALTH HAZARDS IN CLOSED ENVIRONMENTS: THERMODEGRADATION OF WIRE INSULATION

G. Oberdörster¹, J.N. Finkelstein², R. Gelein¹, P. Mercer¹, N. Corson¹, **C.J. Johnston²**, and B. Weiss¹

University of Rochester, Depts. of ¹Environmental Medicine and ²Pediatrics, New York 14642

INTRODUCTION

Thermodegradation events during manned space missions can give rise to fumes originating from overheating of wire insulation. The high toxicity of such fumes is well known from accidental exposures resulting in symptoms summarized under the term "polymer fume fever." We have studied the composition and toxicity of fumes generated by heating of polytetrafluoroethylene (Teflon[®]), which is a frequently used component of insulation material. We have characterized the particulate phase of the fumes as consisting of extremely fine particles with count median diameters of ~15-25 nm (ultrafine particles). We hypothesize that these ultrafine particles are the major cause for the extremely high toxicity of PTFE fumes since particles in this range have a very high deposition efficiency throughout the lower respiratory tract, higher than for any other particle size, and they also penetrate rapidly across the epithelium to interstitial and vascular compartments. The objectives of our studies were to determine (i) the role of the ultrafine Teflon[®] fume particles for causing toxicity; (ii) the impact of Teflon[®] fume exposure on work performance; (iii) the effect of repeated exposures.

METHODS

For evaluating ultrafine particle involvement in toxicity, 4 groups of male Fischer-344 rats were used (n=5/group). Group 1: sham-exposed control; group 2: exposure to total fume (particle and gas phase); group 3: gas phase only; group 4: particle phase only. Particle number concentration and gas phase fluoride content (F) were measured during the 25-min. whole-body exposure to a particle concentration of ~50 µg/m³. At 4 hrs. post-exposure, or at the time of death, animals were lavaged and cellular and biochemical parameters of lung injury were measured. For work performance, male Long Evans rats were trained to run in a running wheel and their performance was measured over a period of 1 hr. Their work performance immediately after a 10-min. PTFE fume exposure and 24 hrs. and 48 hrs. later was compared to the pre-exposure values. For the repeat exposure studies male Fischer-344 rats were exposed in 3 groups (n=6/group) as follows: Group 1: 5-min sham-exposure for 3 days, followed by a 15-min. sham-exposure on day 4; group 2: 5-min. sham-exposure for 3 days, followed by a 15-min. exposure to PTFE fumes at 50 µg/m³ (non-adapted rats); group 3: 5-min. PTFE fume (50 µg/m³) for 3 days followed on day 4 by a 15-min. PTFE fume exposure (adapted rats). Lung lavage parameters were evaluated at 4 hrs. after exposure, or at the time of death if before 4 hrs.

RESULTS

Lung lavage parameters after exposure to the particle and gas phase alone and together showed the expected highly inflammatory response in the rats exposed to the combined particle + gas phase. Gas phase exposure alone and particle phase exposure alone did not show significant

changes of inflammatory parameters compared to sham-exposed controls. Measurement of gas phase F revealed about 4 $\mu\text{g}/\text{l}$ in the air of groups exposed to gas phase alone and to the combined particle + gas phase, whereas sham-exposed and ultrafine particle only exposed had background F. Results of the work performance study showed a significant decrease in the 1hr. running wheel performance after Teflon[®] fume exposure which lasted for more than 48 hrs. Short-term pre-exposures for 3 days prevented this decline in work performance. The result of the adaptation study was that 3-day short-term pre-exposure led to the development of tolerance so that the 15-min. exposure to PTFE fumes did not result in significant changes of cellular and biochemical lung lavage parameters compared to controls. All of the non-adapted rats died within 4 hrs. after exposure with severe acute hemorrhagic pulmonary edema.

CONCLUSION

We conclude from these studies that the ultrafine particles in Teflon[®] fumes are essential but not sufficient for causing the acute pulmonary effects after inhalation exposure. It appears that gas phase F may be involved, potentially adsorbed to the large particle surface or forming reactive groups on the particle surface with the ultrafine particles acting as efficient carriers for deep lung delivery. We conclude further that pre-exposure to Teflon[®] fumes can lead to the development of tolerance to subsequent lethal exposures to the fumes. This is similar to the development of tolerance in metal-fume fever, or tolerance to oxidant gases. Potential mechanisms may include upregulation of antioxidants in the lung. The adaptive response extends also to physical performance protection. The potential risks of exposures to toxic fumes from thermodegradation events during manned spaceflight need to be recognized. We are presently studying the influence of color additives to Teflon[®] which may have a profound effect on the toxicity of insulating material. Future studies will also include studying secondary systemic effects based on acute pulmonary inflammation, involving acute phase responses and subsequent effects on the cardiovascular system. Effective preventive measures include the installation of ultrafine particle monitors such as condensation nuclei counters.

ANALYSIS OF MIR CONDENSATE AND POTABLE WATER

L. M. Pierre¹, L. Bobe², N. N. Protasov³, R. L. Sauer⁴, J. R. Schultz¹, Y. E. Sinyak⁵, and V. M. Skuratov⁵

¹Wyle Laboratories, Houston, TX 77058, ²NIICHIMMASH, ³RSC Energia, ⁴NASA-Johnson Space Center, ⁵Institute of Biomedical Problems.

INTRODUCTION

Approximately fifty percent of the potable water supplied to the Russian cosmonauts, American astronauts, and other occupants of the current Russian Mir Space Station is produced by the direct recycle of water from humidity condensate. The remainder comes from ground supplied potable water that is delivered on a Progress resupply spacecraft, or processed fuel cell water transferred from the Shuttle. Reclamation of water for potable and hygiene purposes is considered essential for extended duration missions in order to avoid massive costs associated with resupplying water from the ground.

The Joint U.S./Russian Phase 1 program provided the U.S. the first opportunity to evaluate the performance of water reclamation hardware in microgravity. During the Phase 1 program, the U.S. collected recycled water, stored water, and humidity condensate samples for chemical and microbial evaluation. This experiment was conducted to determine the potability of the water supplied on Mir, to assess the reliability of the water reclamation and distribution systems, and to aid in developing water quality monitoring standards for International Space Station.

METHODS

During inflight water sampling sessions, a Water Experiment Kit (WEK) was used to collect water samples onboard Mir. The WEK contained disinfectant wipes, potable water samplers, waste bags, chemical sample bags, and storage bags needed for water sampling. Prepackaged benzalkonium chloride disinfectant wipes were used to disinfect the Mir galley-hot, galley-cold, or SVO-ZV (ground supplied) stored water port prior to sample collection. The wipes were discarded after use. Next, a specially designed, presterilized hot or cold potable water sampler was connected to the Mir water port. The sampler, which mates the Mir water dispenser port and the sample bag, consisted of an adapter connected to a stainless steel luer lock that interfaced with the sample bag. After the sampler was attached, a small wastewater bag was then connected to the potable water sampler and used to purge approximately 50 mL of water from the port. This bag was then discarded. Next, 700 ml of water were collected into the chemical sample bag. The sample bag was placed in a self sealing storage bag and stowed for return on the Shuttle. These procedures were used to collect galley-hot, galley-cold, and SVO-ZV stored water for postflight chemical analysis. Following the collection of the chemical samples, microbiological samples were obtained for the related microbial quality. During the Phase 1 program, 27 galley- hot, 8 galley-cold, and 8 stored water samples were collected.

Humidity condensate samples were collected during several missions using hardware provided by the Russian Space Agency. This hardware, known as an "atmospheric condensate sampler" was used to collect 27 samples of "raw" humidity condensate at the inlet of the condensate processing system after filtering and removal of the initial phase excess entrained air, and before any processing of the condensate occurred. In addition, the U.S. developed humidity condensate

sampling hardware (first used on STS-84) so that larger volumes of condensate could be collected for more comprehensive postflight analysis. The U.S. condensate sampler collected humidity condensate that had been partially processed. Four of these samples were collected during the later portion of the NASA/Mir program.

During the Phase 1 program, operational problems onboard the Mir necessitated the collection of unscheduled samples. Samples were collected because of coolant leaks and as a result of a February 1997 fire in the Mir Core Module. Because of thermal control system coolant leaks onboard Mir, the U.S. condensate sampler was used to collect samples of partially processed condensate. These data were used to determine the amount of contaminants present. Several samples of surface fluid (condensate) which had accumulated on walls and floors because of humidity control problems were also collected. Samples of raw humidity condensate and partially processed condensate were collected immediately after a fire which occurred in the Mir Core Module. These data were used to determine the effect of combustion byproducts in the atmosphere on the condensate.

Once returned to Earth, water samples were divided between the Johnson Space Center Water and Food Analytical Laboratory (WAFAL) and the Institute for Biomedical Problems (IBMP) Water Laboratory for analysis. The IBMP lab analyzed the samples for conductivity, pH, color, odor, chemical oxygen demand (COD), total solids, calcium, magnesium, and silver. Parameters tested at JSC included total carbon (total inorganic carbon, purgeable organic carbon, nonpurgeable organic carbon and total organic carbon), and specific organic compounds (alcohols, organic acids, semivolatile organic compounds, volatile organic compounds, nonvolatile organic compounds, formaldehyde, glycols, anions, cations, and metals).

RESULTS

In general, the recycled and stored water supplied to the Mir Space Station met US, Russian, and/or EPA standards. Exceptions were found, to include:

1. Chloroform in the ground supplied (stored) water ranged from nondetected to 205.5 $\mu\text{g/L}$. The EPA standard is 100 $\mu\text{g/L}$. Total organic carbon (TOC) in the stored water exceeded NASA/Russian Space Agency (RSA) standards, primarily due to the presence of ethanol and formate in U.S. supplied stored water. Ethanol is used in the servicing of the Shuttle Water System, while formates are present in the U.S. processed water for use on the Mir. These violations were transient.
2. Total organic carbon and turbidity in the recycled water routinely exceeded NASA standards. The TOC, in some cases, exceeded Russian standards as well. Barium and nickel occasionally exceeded NASA/RSA standards. All but the TOC violations were transient. None of these contaminants, in the levels found, were considered to have health consequences.
3. Dioctyl phthalate in the recycled water occasionally exceeded the EPA Health Advisory of 6 $\mu\text{g/L}$.

Raw condensate exhibited steadily increasing levels of ethylene glycol throughout Phase 1. This is believed to reflect the increased levels of ethylene glycol in the Mir atmosphere following coolant loop leaks and maintenance activities. In one case, the presence of ethylene glycol in a

condensate sample alerted the ground and crew to the presence of a previously undetected coolant loop leak.

CONCLUSION

The chemical quality of the recycled and stored water, as determined through postflight analysis, met performance and potability requirements. The analysis of samples has provided important data for assessing the potability of recycled water. In addition, these data will be instrumental in developing appropriate water quality monitoring standards for ISS.

REACTIVATION OF LATENT VIRUSES IN SPACE

D. L. Pierson¹, S. K. Mehta², S. K. Tying³, and D. J. Lugg⁴

¹Life Sciences Research Laboratories, Lyndon B. Johnson Space Center, Houston, Texas, ²Enterprise Advisory Services Inc., Houston, Texas, ³University of Texas Medical Branch, Galveston, Texas, and ⁴Australian Antarctic Division, Hobart, Tasmania, Australia.

INTRODUCTION

Reactivation of latent viruses is an important health risk for people working and living in physically isolated extreme environments such as Antarctica and space. Preflight quarantine does not significantly reduce the risk associated with latent viruses, however, pharmaceutical countermeasures are available for some viruses. The molecular basis of latency is not fully understood, but physical and psychosocial stresses are known to initiate the reactivation of latent viruses. Presumably, stress induced changes in selected hormones lead to alterations in the cell-mediated immune (CMI) response resulting in increased shedding of latent viruses. Limited access to space makes the use of ground-based analogs essential. The Australian Antarctic stations serve as a good stress model and simulate many aspects of space flight. Closed environmental chambers have been used to simulate space flight since the Skylab missions and have also proven to be a valuable analog of selected aspects of space flight.

METHODS

Saliva was collected at specific intervals from Space Shuttle and Mir crewmembers, Antarctic winter-over expeditioners, and crewmembers of the closed environmental chamber tests. All saliva samples were analyzed for Epstein-Barr Virus (EBV). Urine specimens were collected from Shuttle crewmembers before and after flight and analyzed for cytomegalovirus (CMV). Viral DNA was extracted from the saliva and urine specimens using Qiagen's extraction system, amplified by PCR, and detected by the Digene SHARP Signal detection system. Quantitation of EBV DNA was completed for Space Shuttle studies using the BioSource Viral Quant EBV (PCR) procedure. CMI response was evaluated in the Antarctic expeditioners using the Multitest CMI skin test.

RESULTS

EBV DNA was detected in 13% of the saliva specimens from the Space Shuttle crewmembers, 18% from the Mir crewmembers, and 17% from the Antarctic expeditioners and 17% from the closed environmental chamber crewmembers. EBV DNA was detected more frequently prior to Space Shuttle flights than during or after the mission; however, the number of EBV DNA copies was highest during the flight. In the Antarctic and environmental chamber studies, EBV DNA was found more frequently during the isolation phase. The CMI was determined in Antarctic expeditioners, and 80% of the subjects had a reduced CMI response at all 5 measurement periods. Similar decreased CMI responses have been observed with space flight and chamber data. CMV was detected in 28% of the Space Shuttle crewmembers compared to 0% in control group.

CONCLUSIONS

Decreased CMI response results in reactivation and increased shedding of EBV and CMV. The presence of large numbers of EBV DNA in saliva during space flight increases the risk of infection. CMV shedding incidence in crewmembers indicates a potential role for this virus as a sensitive indicator of space flight associated stress. Results indicate that Antarctic winter-over expeditions and closed environmental chambers are valuable ground-based analogs of space flight.

BACTERIAL BIOFILMS IN MICROGRAVITY

Barry H. Pyle, S.C. Broadaway, C.K. Johnsrud, R.T. Storfa, and G.A. McFeters.
Montana State University, Department of Microbiology, Bozeman, MT 59717

Human life support systems planned for future long-term space flight missions will require high quality water to minimize the risk of infectious disease and system deterioration. It has been demonstrated that some bacteria may grow more rapidly and can become less susceptible to antimicrobial agents under conditions of microgravity. Also, humans suffer immunosuppression with prolonged space flight. This study was planned to determine the effect of spaceflight and microgravity on biofilm formation by waterborne bacteria and the efficacy of iodine in preventing biofouling. A strain of *Burkholderia cepacia*, which had been isolated from a NASA Shuttle Orbiter water system, was used to represent oligotrophic bacteria which are likely to be found in water treatment and distribution systems on spacecraft. The results indicated that *B. cepacia* can form biofilms in a weightless environment. Thus, disinfection and management of spacecraft water systems must take into account the well-known difficulties of controlling attached bacteria.

STUDY DESIGN TO TEST THE HYPOTHESIS THAT LONG-TERM SPACE TRAVEL HARMS THE HUMAN AND ANIMAL IMMUNE SYSTEMS

William T. Shearer¹, Desmond J. Lugg², HD Ochs³, Duane L. Pierson⁴, James M. Reuben⁵, Howard M. Rosenblatt¹, Clarence Sams⁴, C. Wayne Smith¹, E. Obrian Smith¹, James E. Smolen¹, David F. Dinges⁶, Janet L. Mullington⁷

INTRODUCTION

The potential threat of immunosuppression and abnormal inflammatory responses in long-term space travel, leading to unusual predilection for opportunistic infections, malignancy, and death, is of major concern to the National Aeronautics and Space Administration (NASA) Program. This application has been devised to seek answers to questions of altered immunity in space travel raised by previous investigations spanning 30-plus years. We propose to do this with the help of knowledge gained by the discovery of the molecular basis of many primary and secondary immunodeficiency diseases and by application of molecular and genetic technology not previously available. Two areas of immunity that previously received little attention in space travel research will be emphasized: specific antibody responses and non-specific inflammation and adhesion. Both of these areas of research will not only add to the growing body of information on the potential effects of space travel on the immune system, but be able to delineate any functional alterations in systems important for antigen presentation, specific immune memory, and cell:cell and cell:endothelium interactions. By more precisely defining molecular dysfunction of components of the immune system, it is hoped that targeted methods of prevention of immune damage in space could be devised.

CURRENT STATUS OF RESEARCH

We plan to use ground-based human and animal models of space travel existence in making measurements of immune function. Human studies will include neo-antigen (• X 174 bacteriophage) challenge of research subjects before and after subjection to eight-month Antarctic isolation with the Australian National Antarctic Research Expedition (ANARE) with Dr. Desmond Lugg, Head of Polar Medicine, and six-month closed chamber isolation at the NASA/Johnson Space Center in Houston, in collaboration with Dr. Duane L. Pierson, Director of Microbiology and Dr. Clarence F. Sams, Director of Immunology. Also, as a supplementary project to the original plans, we will be collaborating in a sleep-deprivation mode with Dr. David F. Dinges, Chief of the Division of Sleep and Chronobiology and Director of the Unit for Experimental Psychiatry at the University of Pennsylvania Medical School in Philadelphia, and Dr. Janet L. Mullington, Director of the Sleep Laboratory at Harvard Medical School in Boston. Assessments of specific antibody production (IgM or primary and IgG or secondary), IgM to IgG class switching, and antigen clearance will be useful in assessing antibody responses, antigen clearance, and T-cell helper effects. In addition, using 3-color flow cytometry with new monoclonal reagents, we will be able to detect differences in memory and naive T-cells and in

¹ Baylor College of Medicine,

² Australian Antarctic Division

³ University of Washington School of Medicine

⁴ National Aeronautics & Space Administration

⁵ M.D. Anderson Cancer Center

⁶ University of Pennsylvania School of Medicine

⁷ Harvard Medical School

activated and cytotoxic T-cells. These new measurements will more carefully define the subpopulations of T-cells that carry out specific effector function. Also, by studying lymphocyte responsiveness to recall antigens, we will be able to detect harmful effects upon cellular-initiated immunity. By assessment of T-lymphocyte helper type 1 (TH1) and TH2 cytokine secretion, we will be able to discern a loss of cytotoxic T-lymphocyte control and a shift to inflammatory cytokine control. By determination of the chemokine secretion patterns of human peripheral blood mononuclear cells, we will be able to discern the likelihood of viral infection in subjects, since several viruses compete with chemokines for chemokine receptor occupancy and cell entry. We will determine nonspecific natural killer (NK) cell activity in subjects under space flight conditions to assess potential damage to this primal protective cellular immune system. Lymphocyte apoptosis studies will enable us to recognize whether space flight conditions accelerate the natural process of planned cell death. Finally, with determination of proto-oncogene, oncogene, and transcription factors in subjects under space flight conditions, we will be able to assess the possibility of abnormal gene regulation. Since Dr. Janet Butel will be studying reactivation of latent viruses in these same subjects in a research project of the Immunology, Infection, and Hematology Research Team, currently funded by the National Space Biomedical Research Institute (NSBRI), we will be able to correlate immune suppression with reactivation of latent virus infections.

Animal model studies by Dr. Wayne Smith will concern the stress and shear forces experienced by cellular membrane adhesion molecules. Specifically, the model (anti-orthostatic suspension) system is already being utilized by Dr. Janet Butel and Dr. Margaret Connor in the funded study on latent viruses and immune function. This is an established model that induces many physiological changes consistent with those observed in humans and animals returning from actual space flight. In an effort to establish whether basic inflammatory mechanisms are influenced by simulated space flight, we will elicit both non-specific, acute inflammation (ischemia/reperfusion), and relatively delayed, antigen-induced specific inflammation (late phase allergic and delayed type hypersensitivity responses) in anti-orthostatically suspended and control mice. Specifically, we will directly determine if anti-orthostatic suspension affects various stages of leukocyte recruitment, which is a key feature of inflammation. We anticipate that any changes in leukocyte recruitment induced by the experimental conditions will significantly contribute to the development and/or resolution of inflammation. In addition, since leukocyte recruitment is almost entirely dependent upon the expression of and interactions between adhesion molecules, we will systematically measure adhesion molecule expression on the surface of both endothelial cells and leukocytes. These assays will be conducted in anti-orthostatically suspended and control mice, under non-inflamed and inflamed conditions. It is likely that any observed changes in adhesion molecule expression will contribute significantly to leukocyte recruitment and the overall inflammatory process. Finally, we will systematically examine whether anti-orthostatic suspension affects the ability of inflammatory leukocytes (neutrophils and macrophages) to perform basic functions, including oxidative burst, phagocytic, bactericidal and candidacidal activity. Insight into these mechanisms in animals models of anti-orthostatic suspension will enhance our understanding of the potentially increased infectious susceptibility associated with long term space travel. The knowledge gained on the importance of phagocytic and endothelial cellular adhesion recognition pathways will be shared with the other NSBRI-funded research project on "Neocytolysis", headed by Dr. Clarence Alfrey, which concerns cellular adhesion pathways on erythrocytes as part of its goals.

PLANS FOR FUTURE INVESTIGATIONS

By exploring perturbations of specific and non-specific immunity in space models in humans and animals, we expect to be able to make definitive statements concerning the types of cellular and molecular dysfunction likely to be experienced by space travelers on long journeys. With better definition of space-induced defects in immunity, it might be possible to avoid these changes with specific immune intervention. Since immune reconstitution has now become the primary goal of several human diseases, e.g. HIV-infected patients given highly active antiretroviral therapy, it may be possible to prescribe specific immune prophylaxis or early treatment of space flight immunodeficiency. Examples of such prophylaxis and treatment regimens would include potential drugs, such as pentoxiphylline, which inhibits the inflammatory cytokine profile and boosts the cytotoxic cytokine profile, and intravenous immunoglobulin, which contains a panoply of specific antibodies to infectious agents.

UPDATE ON THE EFFECTS OF SPACE FLIGHT ON DEVELOPMENT OF IMMUNE RESPONSES

G. Sonnenfeld^{1,2}, M. Foster², D. Morton², F. Bailliard², N.A. Fowler², A.M. Hakenwewerth², R. Bates³, and E.S. Miller².

¹Department of Microbiology and Immunology, Morehouse School of Medicine, Atlanta, GA 30310-1495, ²Department of General Surgery Research, Carolinas Medical Center, Charlotte, NC 28232 2861, ³Department of Pharmaceutical Sciences, School of Pharmacy, Texas Tech University Health Sciences Center, Amarillo, TX 79106

INTRODUCTION

This study has been completed, and the following is an update of the results as published. Pregnant rats were flown on the Space Shuttle in the NIH.R1 mission for 11 days, and pregnant control rats were maintained in animal enclosure modules in a ground-based chamber under conditions approximating those in flight. Additional controls were in standard housing. The effects of the flight on immunological parameters (including blastogenesis, interferon-gamma production, response to colony stimulating factor and total immunoglobulin levels) of dams, fetuses, and pups was determined.

METHODS

On the eighth day of gestation, ten pregnant rats were placed into NASA animal enclosure modules (AEM) (five rats per cage) and loaded on to the mid-deck of the Space Shuttle. On the ninth day the Space Shuttle was launched for an 11 day flight. After landing, flight animals were recovered, anesthetized, and subjected to unilateral hysterectomy. The dams were then allowed to recover and deliver vaginally. Three additional groups of rats were kept at the Kennedy Space Center. A synchronous control group that received the same surgeries as the flight group and was housed five animals per cage in AEMs and was exposed, as closely as possible, to all flight conditions except microgravity. Vivarium control group 1 was housed in standard rat cages without any surgery. The second vivarium control received a unilateral hysterectomy on day 20 of gestation, but was housed in standard rat caging. Spleens were removed from all animals and individual spleen cells were prepared to carry out a blastogenesis assay. Cells were washed in RPMI-1640 medium, counted and resuspended in RPMI-1640 medium. Cells were distributed in 96-flat-bottom-well plates at 2×10^5 cells/well and cultivated in the presence of supplemented RPMI-1640 medium with or without concanavalin-A. After 30 hours of incubation tritiated thymidine was added to each well. After additional incubation, the cells were harvested onto glass filter paper and the level of thymidine uptake was determined using a liquid scintillation counter. Titers of interferon-gamma were determined in supernatant fluids of spleen cells placed in 96 well culture dishes at a concentration of 3×10^6 cells/ml, and then exposed to $5 \mu\text{g/ml}$ of concanavalin A. Supernatant fluids were harvested 48 hr later, and interferon-gamma titers were determined using rat interferon-gamma ELISA kits. 1×10^5 bone marrow cells/ml from the humerus of dams were resuspended in a 2% methylcellulose solution prepared in supplemented McCoy's 5-A medium containing 30% fetal bovine serum. 1×10^5 individual liver cells of fetuses and pups were placed in the medium. Medium for experimental group cultures contained a concentration of 40 ng/ml recombinant murine granulocyte-macrophage colony stimulating factor. Cell suspensions were placed in 35 mm tissue culture dishes. Following 7 days of incubation, 10 different microscope fields from each culture were evaluated for the number of

colonies formed. An ELISA procedure was used to determine concentrations of IgG in the serum. The sera from dams and pups were thawed rapidly at 37°C and diluted 1:10, 1:100, and 1:1,000 in PBS.

RESULTS

Compared to rats that were used as AEM controls leukocyte blastogenesis, interferon-gamma production, and the ability to form colonies in response to granulocyte-macrophage colony stimulating factor were all inhibited in the dams after space flight. Not all differences were statistically significant, which could have been accounted for by the relatively small sample size. None of the pups nor fetuses (analyzed where possible) showed significant changes or a trend towards changes of any of the observed immunological parameters after space flight.

CONCLUSION

Leukocyte blastogenesis, interferon-gamma production, the response to colony stimulating factor and serum IgG levels of offspring of rats that had been exposed to space flight while pregnant were not changes significantly compared to controls. The results of the current study do not necessarily demonstrate that space flight had no effect on the development of immunological parameters in rats beyond the parameters examined during the present study. Beginning space flight prior to conception or earlier in gestation could have resulted in marked changes in the development of immunological responses. Additionally, longer-term space flights could also have effects not observed during the present study. Additional experimentation will, be necessary before a complete answer can be obtained on the effects of space flight on the development of the immune system.

This study was funded by NASA agreement NCC2-859. These data have been recently published: Sonnenfeld, G., Foster, M., Morton, D., Bailliard, F., Fowler, N.A., Hakenwerth, A.M., Bates, R., and Miller, E.S. Spaceflight and development of immune responses. *J. Appl. Physiol*, 85: 1429-1433, 1998.

LYTIC REPLICATION OF EPSTEIN-BARR VIRUS DURING SPACE FLIGHT

R. P. Stowe¹, D. L. Pierson², and A. D. T. Barrett¹

¹Department of Pathology, The University of Texas Medical Branch, Galveston, 77555, ²Life Science Research Laboratories, Johnson Space Center, Houston, 77058

INTRODUCTION

Reactivation of latent Epstein-Barr virus (EBV) may be an important threat to crew health during extended space missions. Cellular immunity, which is decreased during and after space flight, is responsible for controlling EBV replication *in vivo*. In this study, we investigated the effects of short-term space flight on latent EBV reactivation.

METHODS

Peripheral blood and urine samples were collected from 29 astronauts (three 9-day and two 16-day missions) ten days before launch (L-10), at landing (R+0), and three days after landing (R+3). The samples were analyzed for white blood cell (WBC) counts and differentials, EBV antibodies to structural (viral capsid antigen-VCA) and nonstructural (early antigen-EA) proteins, human (h) and/or viral (v) interleukin (IL)-10, stress hormones (IL-6, cortisol, etc.), and percent B-cells.

RESULTS

WBC counts were significantly increased ($p < 0.05$) at landing (primarily due to elevated neutrophil numbers) while monocytes and lymphocytes were significantly decreased at landing. No change was observed in plasma cortisol; however, urinary cortisol was significantly elevated at landing as compared to preflight ($p < 0.05$; 98 ± 9.5 vs. $68.6 \pm 6 \cdot \text{g}/24\text{h}$). IL-6 was significantly elevated at landing indicating an acute stress response to atmospheric entry. The VCA geometric mean titer was significantly increased at L-10 as compared to baseline (annual physical) samples. In several astronauts, 4-fold decreases in VCA titers were observed at R+0 followed by a 4-fold increase at R+3. Plasma levels of hIL-10/vIL-10 were generally elevated at R+0, and percent B-cells were elevated at R+0 in some subjects and R+3 in the majority of the subjects. Three astronauts exhibited high hIL-10/vIL-10 levels ($>10 \text{ pg/ml}$) which positively correlated with either 4-fold increases in EA titers or high VCA/EA titers.

CONCLUSIONS

These results indicate that lytic replication of EBV, as reflected by rising EA/high VCA antibodies, occurs during short-term space flights. These stress-induced shifts in leukocyte subpopulations may reduce the ability of the immune system to respond to immunologic challenge and pose a significant health risk on longer Lunar/Mars expeditions.

INHIBITION OF ERYTHROPOIESIS IN SIMULATED MICROGRAVITY

A.J. Sytkowski and K.L. Davis, Laboratory for Cell and Molecular Biology,
Beth Israel Deaconess Medical Center, Harvard Medical School, Boston, MA

INTRODUCTION

The microgravity conditions experienced in space flight have been shown to have adverse effects on hematopoietic cells leading to anemia and reduced immune responsiveness. The cellular basis for these effects is unknown. We have now begun to investigate potential mechanisms responsible for the reduced erythropoiesis encountered in microgravity.

METHODS

We used the erythropoietin responsive Rauscher murine erythroleukemia cell line. We compared the growth and hormone responsiveness of these cells at unit gravity with growth in the unique simulated microgravity environment of the NASA rotating wall vessel (RWV) bioreactor. Cells were inoculated into tissue culture flasks at 1xg or into the RWV in the absence or presence of erythropoietin. At specified times thereafter ranging over a 4 day period, cell densities were determined and erythroid differentiation was quantified by measuring the number of hemoglobin containing cells.

RESULTS

We found a profound inhibitory effect of simulated microgravity on erythroid cell growth and differentiation. At both 1xg and in the simulated microgravity of the RWV, the cells grew at log phase for 72 hours. However, the growth rate in the RWV was significantly less than that at 1xg. The cells were equally viable under both conditions, and no increase in apoptotic cells in the RWV was detected. Erythropoietin induced differentiation under both culture conditions. However, the number of hemoglobin containing cells in the RWV was only half that observed at 1xg. Importantly, when cells were grown in simulated microgravity for 24 hours before addition of erythropoietin, differentiation was inhibited virtually completely.

CONCLUSION

Our results suggest a profound effect of microgravity on erythropoiesis at the cellular level. This effect may be responsible in part for the anemia of space flight. We propose that one or more aspects of erythropoietin receptor binding and/or signal transduction are inhibited under conditions of reduced gravity.

Muscle

Chair

Kenneth Baldwin, Ph.D.

Co-Chair

Daniel Feedback, Ph.D.

MUSCLE SESSION SUMMARY

Presentations from the assembled group of investigators involved in specific research projects related to skeletal muscle in space flight can be categorized into five thematic subtopics. A brief synopsis of each of the presentations grouped by appropriate thematic subtopic follows:

Regulation of contractile protein phenotypes

Epstein et al.: Protein machines are either proteins that actually perform mechanical work such as protein motors or complexes of proteins that act as a system of intricate machinery which performs specific biological functions. The sarcomeric myosin molecule is the classical paradigm for the concept. It performs work and also functions as a part of the larger complexes such as the thick filament and the myofibril. New findings suggest the assembly of myosin requires cross-linking proteins and a novel protein machine which selects proper myosin isoforms for assembly. Myotonic dystrophy protein kinase, itself a key signaling molecule, functions in a dynamic complex with other protein kinases, protein phosphatases, molecular chaperones, and 21 K Da GTPase proteins. These studies raise the possibility that successful pharmacological interventions for microgravity-induced muscle atrophy may block the specific protein-protein interactions required for the activities of protein machines in myofibril assembly and molecular signaling with skeletal muscle.

Baldwin et al.: Ground-based and flight-based studies involving neonatal animals in the presence and absence of an intact nerve and intact thyroid state suggest the following: 1) muscles used for normal weight bearing and locomotor activities are undifferentiated during early post natal development with regard to contractile protein phenotype; 2) weight bearing activity, in opposing gravity, is essential for normal body and muscle growth and for normal expression of the slow myosin heavy chain (MHC) gene, but not for the fast motor MHC genes; 3) the differentiation process for fast MHC gene expression (especially IIb) is dependent on thyroid hormone while not gravity dependent; 4) an intact nerve is essential for establishing the normal expression of both the slow and fast type IIb MHC genes.

Neville et al.: The nodal role of the E protein transcription factor family in modulating fiber-specific gene expression has been demonstrated in both gain and loss of function experiments. The gene products of at least two of the three loci encoding E proteins are regulated at the post-transcriptional level. Loss of muscle strength due to microgravity involves both atrophy and fiber type conversion. The role of E proteins in these processes will be determined in HU experiments.

Muscle growth and atrophy

Draghia-Akli et al. (presented by Schwartz): These investigators showed that gene therapy regimens using a muscle vector system with substituted growth hormone releasing hormone (GHRH) injected into muscles of large animals (pigs) was sufficient to elicit long term (at least two months) growth (25-50% increases) involving mass which is associated with three to six-fold increases in IGF-1 levels in blood. These investigators are making GHRH vectors that can be regulated under gene switch technology for human applications. Also, over expression of IGF-1 alone does not prevent tail-suspension-induced muscle atrophy. More experiments in this

regard are underway to determine if there is synergy between exercise and GH/IGF-1 in preventing unloading-induced muscle atrophy.

Vandenburgh et al.: Tissue cultured muscle cells can directly "sense" changes in gravitational forces and provide a model to study pharmacological countermeasures. Muscle cell protein synthesis rates are decreased in microgravity, leading to myofiber atrophy. Growth hormone and/or insulin-like growth factor I stimulate muscle protein synthesis and are therefore attractive potential therapeutics. New methods for long-term delivery of physiological doses of these proteins are under development.

Goldberg et al.: The activation of muscle protein breakdown seen with weightlessness and in many disease states is due to activation of the ubiquitin-proteasome pathway. Inhibitors of the proteasome have therapeutic potential in reducing excessive proteolysis, but their use is seriously complicated by problems of pharmacodynamics and potentially toxic effects (if proteolysis is inhibited more than partially). However, the possibility of inhibiting ubiquitin-conjugation seems promising, because recent finding in this laboratory that one pair of ubiquitination enzymes (E214K and E3 α , the components of the "N-end ubiquitination system") are particularly important in atrophying muscles.

Fitts et al.: In humans, after a 17-day space flight, both the slow type I and fast type IIa fibers showed significant declines in fiber diameter (8%), force (16-21%) and force per cross-sectional area (4%). In both fiber types, the V_o increased by 27%, such that, peak power showed only a small decline. The data suggests that the increased V_o was caused by a selective loss of the actin filament, which in turn, increased lattice spacing and reduced the internal drag thus elevating V_o . In rats, high intensity isometric exercise was more effective than isotonic weight lifting in protecting the type I fiber from HU-induced declines in fiber diameter, force and power.

Muscle structure: injury, recovery, and regeneration

Mosier et al.: To determine whether alterations in neuromuscular junction structure and function accompany muscle atrophy induced by hindlimb suspension, a combination of ultrastructural and electrophysiological tests were performed in mice after 3 weeks of HU. Increased spontaneous release was noted at NJMs of plantaris muscles after HU, as well as simplification of the post-synaptic folds in the soleus NMJs. Stimulated single-fiber EMG, which was adapted and validated for mouse studies, demonstrated increased jitter and occasional blocking of neuromuscular transmission after HU suggesting that neuromuscular transmission may be susceptible to failure under certain conditions following HU. The amelioration of these alterations in NMJ function by countermeasures is under investigation.

Ingalls et al.: In the mouse soleus muscle, cytosolic free Ca^{2+} concentration ($[Ca^{2+}]_i$) at rest increased within three days of HU and remains elevated through 14 days. Myofibrillar protein and maximal isometric force (P_o) gradually decline during this time. Tetanic ($[Ca^{2+}]_i$) is unaffected by 14 days of unloading but is reduced after one day of physiological reloading.

Tidball: Our data support a model of muscle injury during reloading after periods of unloading in which initial injury to the muscle is caused by mechanical loading which then induces an

inflammatory response. Further muscle damage is then caused by superoxide released by neutrophils and nitric oxide released by macrophages that invade the reloaded muscle.

Schultz and Mozdziak: Weightlessness reduces skeletal muscle growth and regeneration. A critical step in each process is the formation and accumulation of myonuclei, through mitotic division and subsequent fusion of satellite cells. In anti-gravity muscles, unweighting suppresses satellite cell mitotic activity to the extent that a deficit in myonuclear content continues to accumulate for as long as the muscle remains unladen. Preliminary results suggest that simply returning to weight-bearing is not sufficient to induce a sustained compensatory increase in satellite cell mitotic activity that makes up the myonuclear deficit in a timely manner.

Metabolism and fatigue

Lujan and Bertocci (presented by Bertocci): **RESULTS:** Resting rat muscle preferentially oxidizes endogenous (glycogen or triglycerides) fuels. With contraction, oxidation of vascular lactate and pyruvate increases. In contrast, hindlimb-suspended muscle oxidizes more exogenous lactate and pyruvate during rest but does not increase with contraction. **FUTURE:** Use longer perfusions to increase fractional enrichment and measure anaplerosis.

Murthy et al.: The goal was to develop an objective tool to study the role of decreased muscle oxygenation on muscle force production, and to evaluate muscle fatigue during prolonged glove box work. Our results indicate that near infrared spectroscopy is an effective technique to measure changes in oxygenation at or greater than 10% MVC. Furthermore, muscle force production is reduced significantly with only a ~7% muscle oxygenation reduction. Reduction in muscle force is strongly associated with a reduction in muscle oxygenation. Our research has important implications in the study of muscle fatigue in any sustained task. Muscle may be a problem for musculoskeletal disorders and muscle injury.

Fotedar et al.: Fatigue of forearm and intrinsic hand musculature is a limiting factor which affects efficiency of EVA by crew members. *In vivo* noninvasive analysis of tissue level metabolism and fluid exchange dynamics can be monitored in exercised forearm muscles by the combined use of proton MRI and ³¹P-MRS. Simulation of EVA-related tasks can be used to provide noninvasive, objective identification and analysis of forearm muscle function and fatigue resistance in EVA-trained crew members using MRI/MRS. Such an approach, once well-defined and characterized, can be used to provide a useful and reliable longitudinal dynamic assessment with applications to the evaluation of EVA-related task performance, fatigability, countermeasure efficacy and glove/tool ergonomic design.

Greenisen et al.: Space Shuttle astronauts have been required to wear the launch and entry suit (LES) since 1988. Previous work demonstrating that CO₂ accumulation in the LES non-conformal helmet occurs during locomotion was an impetus to characterize inspired CO₂%, metabolic requirements, and egress performance in healthy subjects by use of an unaided egress simulation on a treadmill while wearing the LES. Specific protocols tested egress performance at 4 different G-suit pressures ranging from 0.0 to 1.5 psi. Failure to complete the unaided egress occurred in 75% of 12 subjects at G-suit pressures of 1.0 and 1.5 psi. At these G-suit pressures, elevation of CO₂ (>4%) in the LES helmet along with the increased metabolic cost of walking

clearly can negatively impact the capability of returning space flight crews to complete an unaided emergency egress.

Motor control and loading factors

Edgerton et al.: Seventeen days of bed rest or 17 days of space flight induces multiple adaptations in the sensorimotor system. The accuracy of controlling the position and torque of the elbow and ankle is distorted when there is a transition from 1g to 0g and from 0g to 1g. Further, the regulation of the release of a bioassayable form of growth hormone in response to exercise is completely suppressed by prolonged absence of weight-bearing. In summary, proprioceptive processing is modified significantly by exposure to 0g and to prolonged bed rest.

Hargens et al. presented "Space Physiology Studies," which consisted of two projects:

1. Countermeasures for microgravity should be approached from a mechanistic and integrative standpoint. LBNP exercise on a treadmill provides comfortable, yet high, loads on the musculoskeletal and cardiovascular systems. Both aerobic and high resistive exercises are possible. A series of 5 and 15 day HDT bed rest studies at JSC and ARC demonstrate that LBNP running produces similar MS and DV loads as upright running in 1 g and also maintains many physiologic systems at their 1 g levels.
2. Ultrasound can be used to measure small pulsations of intracranial diameter and follow ICP changes in space and in patients on Earth.

Davis et al.: The calcaneus is a weight-bearing bone that can lose up to 20% of its bone mineral density (BMD) following long-duration missions. In 1 g activities, this bone experiences high impact forces during walking and running. Our research has shown that impact forces generated during jumping exercises can cause global strains in the calcaneus of up to 0.4%. A significant portion of this strain is likely caused by *triceps surae* muscle contractions. The combination of muscle activity and direct compression due to impact can cause tensile stresses to occur in certain regions of the calcaneus. It is hypothesized that bone strains and strain distribution induced during jumping will be osteogenic in nature.

Kenneth Baldwin and Daniel Feedback

MYOSIN HEAVY CHAIN GENE EXPRESSION IN DEVELOPING NEONATAL SKELETAL MUSCLE: INVOLVEMENT OF THE NERVE, GRAVITY, AND THYROID STATE

K. M. Baldwin, G. Adams, F. Haddad, M. Zeng, A. Qin, L. Qin, S. McCue, and P. Bodell.
Department of Physiology and Biophysics, University of California, Irvine 92697.

INTRODUCTION

The myosin heavy chain (MHC) gene family encodes at least six MHC proteins (herein designated as neonatal, embryonic, slow type I (β), and fast IIa, IIx, and IIb) that are expressed in skeletal muscle in a muscle-specific and developmentally-regulated fashion. At birth, both antigravity (e.g. soleus) and locomotor (e.g., plantaris) skeletal muscles are undifferentiated relative to the adult MHC phenotype such that the neonatal and embryonic MHC isoforms account for 80-90% of the MHC pool in a fast locomotor muscle; whereas, the embryonic and slow, type I isoforms account for ~ 90% of the pool in a typical antigravity muscle. The goal of this study was to investigate the role of an intact nerve, gravity and thyroid hormone (T3), as well as certain interactions of these interventions, on MHC gene expression in developing neonatal skeletal muscles of rodents.

METHODS

The study was conducted into two phases designated as Ground-based and Flight-based experiments. For each phase of experiments, pregnant Sprague Dawley rats, with timed-birthing windows, were used as subjects. Pups derived from these Dams were randomly allocated into litters of matched number (~10 pups per litter). In ground-based experiments, selected litters were designated as: a) Normal-Control (NC); b) Unilateral Denervated (Den); and c) Thyroid Deficient (TD). Animals designated as TD were treated with propylthiouracil (PTU; 12m/ kg). Denervation was performed on the left leg at 12-15 days of age, at a time when the muscles are still in an undifferentiated state.

In the flight-based experiments litters were designated as a) Ground-Control-Normal; b) Ground-Control-TD; c) Normal-Flight (NF); and d) TD-flight. In these latter experiments, the nursing Dams were implanted with osmotic pumps to deliver the PTU drug, which was passed to the neonates via the Dam's milk (verified in pilot experiments). NC and TD Litters exposed to microgravity were launched on the shuttle at ~seven days of age and were returned at ~ 23 days of age, at which time the muscles were analyzed for MHC gene expression at both the protein and mRNA level of analyses. These analyses involved gel electrophoresis and RT-PCR technology.

RESULTS

The ground based studies revealed the following. At seven days of age both the slow soleus and fast plantaris muscles are in an undifferentiated state with regard to MHC expression. In the soleus, both the slow type I and embryonic/neonatal MHCs are expressed in ~ equivalent proportions, and by 20-28 days of age the embryonic/neonatal isoforms are repressed and replaced by augmented expression of type I MHC along with small proportions of the IIa MHC. In the plantaris, the pattern seen at seven days consists almost exclusively of the neonatal and embryonic isoforms, and by 28 days of age these isoforms are repressed while that of the IIb, IIx,

and IIa isoforms are dramatically upregulated with the IIb and IIx isoforms accounting for ~ 85% of the MHC pool. Interestingly, the stoichiometry of this transformation suggests a relationship between the loss of neonatal and an increase in type IIb MHC expression. Whereas, the repression in embryonic MHC expression appears to be more associated with the up regulation of the IIa and IIx MHCs. TD dramatically blunts the neonatal to IIb MHC transitions in the plantaris muscle; whereas, it enhances expression of the type I MHC in the soleus muscle. Further, in these ground based experiments it is obvious that thyroid hormone is essential for both body and muscle growth, because in its absence the muscles fail to grow and remain in an infantile state. Also, denervation prevents the optimal expression of the IIb MHC in the plantaris, while reducing type I MHC expression in the soleus.

The flight-based experiments revealed the following. Both body weight and relative muscle weights were dramatically reduced in both the NC-flight and TD-flight groups relative to their respective ground-based controls. Growth of the antigravity muscles such as the soleus and vastus intermedius were retarded to a greater extent than the locomotor muscles such as the plantaris and the medial gastrocnemius muscles. In the soleus muscle of the NF group, the normal transition to slow MHC predominance that is seen in ground-based animals, was markedly reduced such that the type IIa and IIx pools comprised ~ 50% of the MHC pool. In contrast, in the TD groups type I MHC predominates independently of gravity state. These findings suggest that in the absence of gravity, the soleus muscle appears to become more sensitive to thyroid hormone; and this sensitivity is manifest in the repression of type I MHC gene expression. Such a repression in response to microgravity is lost in the absence of thyroid hormone. Since the mRNA data paralleled the protein data, these findings further suggest that the processes regulating the development of MHC expression operate at a pretranslational level of control. In the plantaris, microgravity had relatively little effect on the differentiation process with the exception that it enhanced IIb MHC expression relative to the other isoforms.

CONCLUSIONS

Collectively, these findings suggest the following: 1) muscles used for normal weight bearing and locomotor activity are undifferentiated during early post natal development with regard to contractile protein phenotype; 2) weight bearing activity, in opposing gravity, is essential for normal muscle growth and the normal expression of slow MHC genes but not for the fast motor genes; 3) The differentiation process for fast MHC gene expression (especially IIb) is dependent on both thyroid hormone; whereas, an intact nerve is essential for establishing the normal adult MHC phenotype in both slow and fast types of muscle. Supported by NASA NAG2-942 and NIH NS 33483.

QUANTIFYING BIOMECHANICAL CHARACTERISTICS OF JUMPING EXERCISES IN 1G AND IN SIMULATED AND TRUE MICROGRAVITY.

B.L. Davis, S.E. D'Andrea*, G. Perusek**, T. Orlando

Department of Biomedical Engineering, Cleveland Clinic Foundation, OH 44195

*Barry University, Miami FL, and **NASA Lewis Research Center, Cleveland OH.

INTRODUCTION

Exercise in microgravity is one of the most promising countermeasures to the dual problems of space flight-induced bone loss and muscle atrophy. Although exercise in microgravity has been studied extensively from a metabolic standpoint, little research has focused on the efficacy of different forms of exercise for maintaining musculoskeletal integrity. Exercise protocols have not been effective in preventing muscle atrophy and bone loss during space flight, especially in the lower extremities. In 1-G, however, animal experiments have clearly indicated that (i) certain bone strains and strain rates do stimulate bone deposition, and (ii) repetitive loading of the lower extremity can increase osteonal bone formation even as proximally as the vertebral column. Such studies have also indicated that a relatively small number of appropriate loading cycles may lead to bone deposition. This suggests that an optimal exercise regimen might be able to maintain bone and muscle integrity during space flight.

Since there is evidence that the bones and muscles of the lower limbs are particularly affected by space flight, the present study addressed two major aims: (1) quantify externally applied impact loads and rates of loading under the feet during tethered jumping exercises, and (2) determine the amount of eccentric and concentric whole-muscle activity during these jumping exercises in true and in simulated zero-gravity

METHODS

Experiments were carried out in a standard 1G environment, in NASA's microgravity aircraft (KC-135), and in a zero gravity simulator (ZGS). The ZGS (Figure 1) was constructed using latex cords to suspend subjects from the ceiling in a supine position.

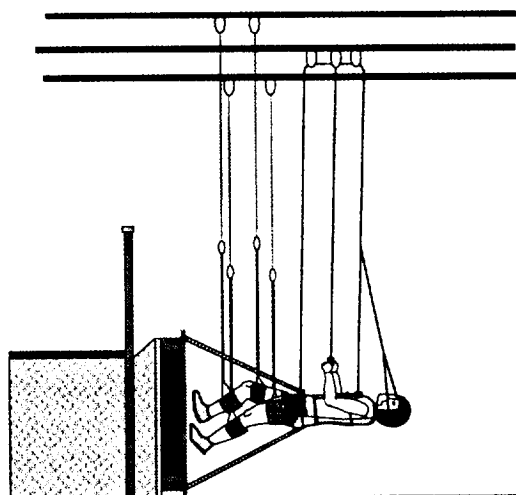


Figure 4.1: Side view of the zero gravity simulator (ZGS) (D'Andrea 1997).

A gravity replacement system consisting of two steel springs, attached at the waist in front and back, was used to tether the subject to the wall (in the ZGS) or to the floor (in the KC-135). The springs were tensioned in order to provide forces equal to 60 and 75% of the subject's body weight. Twelve subjects performed jumping exercises and each subject performed three types of landing: 1) two-feet, with first the toes and then the heel making contact with the support surface; 2) two-feet, flat-footed; and 3) one-foot, toe first then heel contact. Electromyographic data, ground reaction forces, loading rates and 3-D kinematic data were measured in all subjects. In four of the twelve subjects, bone strain in the right calcaneus was measured in four of the twelve using "Capacitex" sensors to measure the time-varying distance between two pins that were orthopedically inserted into the calcaneus. These four subjects also performed jumping exercises in the KC-135 where only EMG and ground reaction forces were measured. Kinematic data were recorded at 60 Hz using four cameras in the 1G and ZGS conditions and two cameras in the KC-135. EMG activity was recorded at 2400 Hz using bipolar electrodes spaced 1.5 cm apart and placed on the belly of the vastus lateralis and gastrocnemius.

RESULTS

All of the subjects could elicit loads under the calcaneus which is important given the fact that there is an absence of heel loading in many exercises currently used during extended orbital missions. Average peak strain in the calcaneus ranged from 0.38% to 0.57%. The strain from the flat-footed landing was significantly greater ($p < 0.0001$) than either of the toe-heel landings. There was not a significant effect of tension level on calcaneal strain.

Data from the KC-135 showed that ground reaction forces were remarkably similar to the ZGS data across all three types of landing. For Type 1 landings, peak force values (Figure 2) were 1700N (KC135) and 1800N (ZGS); Type 2 values were 2600N (KC135) and 2590N (ZGS); and for Type 3 the mean values were 2250N and 2300N, respectively. Additionally, loading rates (Figure 3) were found to be similar with regard to the KC135 and ZGS testing environments. Type 1: 275 kN/s (KC135), 250kN/s (ZGS); Type 2: 375kN/s, 410kN/s; and Type 3: 255kN/s, 275 kN/s, respectively.

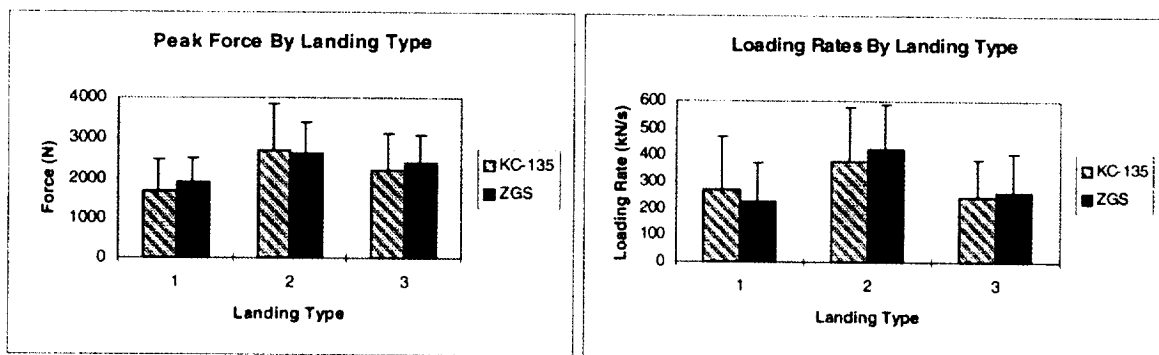


Figure 2: Peak force by landing type for KC-135 and ZGS experiments. Landing type 1 = Two Foot Toe-Heel, type 2 = Two-Foot Flat-Footed, and type 3 = One-Foot Toe-Heel.

Figure 3: Loading rates by landing type for KC-135 and ZGS experiments. Landing type 1 = Two Foot Toe-Heel, type 2 = Two-Foot Flat-Footed, and type 3 = One-Foot Toe-Heel.

Electromyographic results showed that during the push off phase, the duration of concentric activity exhibited by vastus lateralis was significantly higher ($p < 0.001$) for jumping exercises performed in the ZGS (mean 0.15 s, s.d. 0.004 s) compared to the 1G situation (mean 0.12 s, s.d. 0.004 s). The differences caused by the various spring tensions in the ZGS were minimal (duration of concentric activity at a tension of 100% BW was only 0.01 s higher than at the 45% BW setting). Gastrocnemius concentric activity was similar across both spring tensions and gravity situation (mean 0.11 s, s.d., 0.004 s). Duration of eccentric activity during the landing phase was significantly higher for jumping in 1G for both gastrocnemius and vastus lateralis (Gastrocnemius in 1G: mean 0.1 s, s.d., 0.004; in ZGS, mean 0.06 s, s.d. 0.004 s; vastus lateralis in 1G: 0.14 s, s.d. 0.003 s; in ZGS, mean 0.11, s.d., 0.003 s).

CONCLUSIONS

There are difficulties encountered in measuring bone strain during dynamic activities. Firstly, the calcaneus likely experiences bending in both the sagittal and (because of a pronounced concavity on the medial aspect) frontal planes. It is thus possible to measure either compression or tension with sensors that are placed either above or below the neutral axis. Secondly, in an impact situation it is possible for the sensors we used to "overshoot", particularly in the case of tension estimates. Despite these technical difficulties, the results suggest that the calcaneal strain elicited in normal 1G jumping can be obtained in simulated microgravity. Additionally, and more importantly, the results show that the calcaneal strain has a magnitude that, based on animal experiments (Rubin and Lanyon, 1987) is likely to be osteogenic in nature.

The finding that both ground reaction forces and eccentric activity were significantly reduced during ZGS exercises, even at the highest spring tension levels, indicates that it is difficult to design exercises that exactly mimic the biomechanics jumping in 1G. Possible reasons for the decreased eccentric activity include (i) impact landing forces that are higher in 1G, and (ii) differences between a uniform gravitational force in 1G and a simulated force caused by springs which is dependent on their length, and thus highly affected by knee angle at landing.

In terms of the performance of the ZGS, the results showed little discrepancy between the ZGS and KC-135 data (<5% for force magnitudes and <10% for loading rates). This lends support to the notion that a suspension-type simulator can be used to study certain exercise countermeasures for long-duration missions.

D'Andrea, S., Davis, B.L., Courtney, A.C., and Perusek, G.P. "External impact loads on the lower extremity during jumping in simulated microgravity and the relationship to internal bone strain." The 12th Man in Space Symposium: The Future of Humans in Space, Washington, DC (June 8 - 13, 1997).

Rubin, C.T., & Lanyon, L.E. "Osteoregulatory nature of mechanical stimuli: Function as a determinant for adaptive remodelling in bone." *Journal of Orthopedic Research*, 5, 300-310.

ACKNOWLEDGEMENTS

The authors would like to thank Julie Perry for her technical assistance and Dr. Jim Sferra for inserting the calcaneal pins. This project was funded by NASA, grant NAG5-4086.

ECTOPIC EXPRESSION OF PORCINE HV-GHRH BY A SYNTHETIC MYOGENIC VECTOR ELICITS ENHANCED GH AND IGF-1 SECRETION AND ANIMAL GROWTH

Ruxandra Draghia-Akli¹, Daniel R. Deaver³, Marta L. Fiorotto^{1,2}, **Robert J. Schwartz¹**

¹ Baylor College of Medicine, Houston, Texas

² Children Nutrition Research Center, Department of Pediatrics and USDA-ARS, Houston, Texas

³ The Pennsylvania State University, University Park, Pennsylvania

INTRODUCTION

The tremendous importance of growth hormone stimulating therapies for growth, geriatric associated pathology, or to prevent muscle atrophy in microgravity environments provides a strong incentive to develop myogenic vector systems to drive the expression of peptides like growth hormone releasing hormone (GHRH), strong upstream stimulator of GH.

METHODS

3 week old piglets (commercially bred) were used in the study: 4 pigs injected with GHRH-HV, pigs injected with wild-type porcine GHRH and 4 controls. The pigs were injected with 10 mg specific plasmid in the quadriceps muscle, followed by electroporation. We monitored serum GH, IGF-1, urea, creatinine, glucose and total proteins, total body weight, lean/fat body mass, feed efficiency and total feed intake.

RESULTS

Ectopic expression of a truncated and mutated porcine GHRH from muscle tissues by a novel growth promoting myogenic plasmid DNA vector directed by a synthetic promoter, pSPc5-12-GHRH-HV, causes profound growth hormone (GH) secretion. A single intramuscular injection of 10mg pSPc5-12-GHRH-HV DNA, followed by electroporation in adult pigs was sufficient to elevate serum GH levels, to enhance serum IGF-1 to 3-6 times the control levels and to increase body weight approximately 25%, up to 49 days, the last time-point of the experiment.

CONCLUSION

pSPc5-12-GHRH-HV can serve as a potent GH secretagogue gene therapeutic reagent, useful in long duration space missions.

EFFECTS OF MICROGRAVITY ON THE ACCURACY OF ELBOW AND ANKLE FLEXOR AND EXTENSOR MOTOR POOLS IN MAINTAINING A TARGET TORQUE

V. R. Edgerton^{1,2}, G.E. McCall¹, K.O. Fleischman¹, G.I. Boorman¹, C. Goulet¹, and R.R.Roy²

¹Department of Physiological Science and ²Brain Research Institute, University of California, Los Angeles, Los Angeles, CA 90095

INTRODUCTION

The microgravity environment significantly alters proprioceptive inputs to the spinal cord motor pools. However, the means for accommodating those changes so that movements can be controlled in microgravity, and further adapt to this new environment, has received little attention. We hypothesized that the neural control to the motor pools of antigravity (primary extensor) muscles would be affected more by alterations of sensory systems influenced by gravitational forces than the motor pools of non-antigravity (primary flexor) muscles. To test this hypothesis, the effects of a 17-day spaceflight on the ability to maintain constant torque output at the elbow or ankle joint were studied.

METHODS

Using a torque-velocity dynamometer, four male astronauts from the NASA STS-78 mission were requested to maintain a torque of 10% or 50% of a maximal voluntary contraction (MVC) during 10 degree peak to peak sinusoidal movements at 0.5 and 1 Hz with and without visual feedback of torque output. This testing protocol was conducted for both the elbow and the ankle joints three time pre-flight, three or four times during flight and four or five times after flight. Electromyographic (EMG) activity was monitored using bipolar skin surface electrodes.

RESULTS

From the first flight day to day eight post-flight, the elbow flexion torques at 10% MVC, without visual feedback, were underestimated relative to pre-flight. No changes in the accuracy of maintaining a requested torque during flight were observed in the elbow extensor motor pools. Additionally, agonist EMG activity was elevated on the second day post-flight. The estimated plantarflexor torques were elevated on the second and third days of flight compared to the estimates at mid-flight and at the end of the flight. These elevated estimates occurred when the target torque was either 10% or 50% MVC. The opposite effect occurred during ankle dorsiflexion, i.e. the torque estimates at both 10% and 50% MVC were lower for the middle and later tests than for the early tests during flight. Elbow extensor tests at 50% MVC matched the results of ankle dorsiflexion, whereas elbow flexion tests were qualitatively similar to the results from the ankle plantarflexion tests. Compared to both pre- and post-flight tests, there was a marked decrease in antagonist muscle activity for most tasks during flight.

CONCLUSION

These results indicate that the ability to execute a targeted torque was altered differentially in extensor and flexor motor pools at both the elbow and ankle joints in response to changing gravitational environments. Therefore, these data suggest that the presence of gravity imposes a differential bias on motor pools relative to the gravitational vectors that they have been designed to accommodate on Earth.

MOLEUCLAR SIGNALING IN MUSCLE PLASTICITY

H.F. Epstein¹, S. Gordon², F.W. Booth², H. Rajadurai¹

¹Baylor College of Medicine; ²The University of Texas H.S.C.-Houston

BACKGROUND

Extended spaceflight under microgravity conditions leads to significant atrophy of weight-bearing muscles. Atrophy and hypertrophy are the extreme outcomes of the high degree of plasticity exhibited by skeletal muscle. Stimuli which control muscle plasticity include neuronal, hormonal, nutritional, and mechanical inputs. The mechanical stimulus for muscle is directly related to the work or exercise against a load performed. Little or no work is performed by weight-bearing muscles under microgravity conditions. A major hypothesis is that focal adhesion kinase (FAK) which is associated with integrin at the *adherens* junctions and costameres of all skeletal muscles is an integral part of the major mechanism for molecular signaling upon mechanical stimulation in all muscle fibers. Additionally, we propose that myotonic protein kinase (DMPK) and dystrophin (DYSTR) also participate in distinct mechanically-stimulated molecular signaling pathways that are most critical in type I and type II muscle fibers, respectively. To test these hypotheses, we will use the paradigms of hindlimb unloading and overloading in mice as models for microgravity conditions and a potential exercise countermeasure, respectively, in mice. We expect that FAK loss-of-function will impair hypertrophy and enhance atrophy in all skeletal muscle fibers whereas DYSTR and DMPK loss-of-function will have similar but more selective effects on Type II and Type I fibers, respectively. Gene expression will be monitored by muscle-specific creatine kinase M promoter-reporter construct activity and specific mRNA and protein accumulation in the soleus (type I primarily) and plantaris (type II primarily) muscles. With these paradigms and assays, the following Specific Project Aims will be tested in genetically altered mice: 1) identify the roles of DYSTR and its pathway; 2) evaluate the roles of the DMPK and its pathway; 3) characterize the roles of FAK and its pathway and 4) genetically analyze the mechanisms and interactions between the FAK, DYSTR, and DMPK-associated pathways in single and specific combinations of mutants. The identification of potential signaling mechanisms may permit future development of pharmacological countermeasures for amelioration and prevention of the microgravity-induced atrophy in extended spaceflight, and the analysis of both overloading and unloading paradigms may provide further support for development of exercise-based countermeasures. Understanding the basic mechanisms of molecular signaling in muscle plasticity may aid our understanding and treatment of skeletal muscle atrophy not only in spaceflight but in similar problems of the aging population, in prolonged bed rest, and in cachexia associated with chronic disease.

PRELIMINARY RESULTS

Preliminary experiments suggest that mice with DMPK knocked out genetically respond differently to unloading than normal mice. Normal or wild-type C57 mice show significant changes in myosin heavy chain composition in soleus muscle. Type I myosin heavy chain is decreased, and Type II myosin heavy chain is increased. However in the DMPK knockout mice these changes in myosin appeared markedly reduced or absent. Further experiments are in progress to verify these initial observations.

ALTERATIONS IN SKELETAL MUSCLE FUNCTION WITH MICROGRAVITY, AND THE PROTECTIVE EFFECTS OF HIGH RESISTANCE ISOMETRIC AND ISOTONIC EXERCISE

R.H. Fitts, J.E. Hurst, K.M. Norenberg, J.J. Widrick, D.A. Riley, J.L.W. Bain, S.W. Trappe, T.A. Trappe, and D.L. Costill.

Introduction. Exposure to microgravity or models designed to mimic the unloaded condition, such as bed rest in humans and hindlimb unloading (HU) in rats leads to skeletal muscle atrophy, a loss in peak force and power, and an increased susceptibility to fatigue (1-4). The posterior compartment muscles of the lower leg (calf muscle group) appear to be particularly susceptible. Following only 1 wk in space or HU, rat soleus muscle showed a 30 to 40 % loss in wet weight (2,5). After 3 wk of HU, almost all of the atrophied soleus fibers showed a significant increase in maximal shortening velocity (V_o), while only 25 to 30 % actually transitioned to fast fibers (3,6). The increased V_o was protective in that it reduced the decline in peak power associated with the reduced peak force (3).

When the soleus is stimulated in situ following HU or zero-g one observes an increased rate and extent of fatigue (7,8), and in the former the increased fatigue is associated with a more rapid depletion of muscle glycogen and lactate production. Our working hypothesis is that following HU or spaceflight in rats and bed rest or spaceflight in humans limb skeletal muscles during contractile activity depend more on carbohydrates and less on fatty acids for their substrate supply. Baldwin et al. (9) found 9 days of spaceflight to reduce by 37% the ability of both the high and low oxidative regions of the vastus muscle to oxidize long-chain fatty acids. This decline was not associated with any change in the enzymes of the tricarboxylic acid cycle or β -oxidation pathway.

The purpose of the current research was to establish the extent of functional change in the slow type I and fast type II fibers of the human calf muscle following 17 days of spaceflight, and determine the cellular mechanisms of the observed changes. A second goal was to study the effectiveness of high resistance isotonic and isometric exercise in preventing the deleterious functional changes associated with unloading.

Methods. Biopsies were obtained from the soleus and gastrocnemius muscles of humans before and after a 17-day spaceflight (Life and Microgravity Spacelab, Space Shuttle Mission STS-78), and from rats in the following groups: control, HU, HU plus isotonic weight lifting (HU+ISO), and HU plus isometric (HU+ISM) exercise. The biopsy was cut in half longitudinally, and one section immediately aligned on a small index card, quick frozen in liquid nitrogen, freeze-dried at -35°C , and stored at -80°C until used for biochemical analysis (see below). The other section of the muscle biopsy was stored (-20°C) in a glycerol skinning solution for up to 4 wk. The HU groups were suspended by a tail harness for a period of 14 days, and the HU+ISO and HU+ISM exercise groups were removed from unweighting to perform exercise 2 and 3 times/day, respectively. The HU+ISO group averaged 35 lifts/day at an average load of 140% of body weight, while the HU+ISM group performed 30, 5 s contractions with loads up to 400% of body weight. In the rat experiments, in situ whole muscle contractile properties were determined on the soleus muscle, and then the muscles were removed, weighed, and bundles of fibers prepared

from the soleus, and red and white regions of the gastrocnemius. In both the human and rat experiments, single fibers were isolated from the glycerol skinned muscle bundles and placed between a motor arm and a force transducer, and fiber diameter, peak force (N and kN/m^2), and V_o measured. Additionally, the fibers were subjected to 12-15 isotonic load clamps to construct a force-velocity and force-power curve. From the latter peak power was determined.

Single fibers were isolated from the freeze-dried samples and selected substrates and enzymes measured using published techniques (10).

Results and Discussion. Unlike rat, where the slow fibers appear to be selectively effected by weightlessness, in humans, the slow type I fibers of the soleus and fast type IIa fibers of the gastrocnemius showed essentially identical changes in function following the 17-day spaceflight. The slow type I fibers showed a 8, 21, and 4 % decline in diameter, force (N), and force per cross-sectional area (kN/m^2) post-flight, compared to a 7, 16, and 3 % decline in these variables in the fast type IIa fiber. In both fiber types, the V_o increased by 27 %. The increased V_o was not caused by an increased expression of fast myosin as the fibers identified as type I contained only the slow myosin isozyme. The increased V_o countered the decline in force such that peak power showed only a small decrease in both fiber types. The reduced force per cross-sectional area can be attributed to a decline in contractile protein, and our results showed a selective loss of actin. This filament rearrangement may have caused both the decline in force and the increased V_o .

In rats, the 14-day HU caused a decline in the type I fiber diameter from 70.0 to 51.5, and this decline was completely prevented by the isometric exercise, and partially prevented by isotonic exercise where the fiber diameter averaged 60.8. Peak force was also partially and completely protected by the isotonic and isometric exercise, respectively. Compared to the control, HU induced a 51% drop in peak force, while the HU+ISO group showed a 25% decline, and the force of the HU+ISM group was not significantly different from the control group. HU increased V_o by ~ 15% and this parameter was unaffected by the isotonic exercise. In contrast, isometric exercise completely prevented the HU-induced change in V_o . Thus fiber V_o averaged 1.1 and 1.08 FL/s in the control and HU+ISM groups, respectively. HU depressed absolute peak power ($\mu\text{N}\cdot\text{FL/s}$) by 45%, and both exercise countermeasures prevented 30% of the loss. When corrected for cross-sectional area (CSA), both isotonic and isometric exercise increased the peak power relative to the HU and control groups. Relative to the controls, the HU group showed a 11% decline, while the peak power ($\text{kN}\cdot\text{m}^2\cdot\text{FL}\cdot\text{s}^{-1}$) of the HU+ISO and HU+ISM groups averaged 14 and 20 % higher than the control group, respectively.

HU-induced significant changes in the whole muscle contractile properties of the soleus. For example, contraction and one-half relaxation times decreased from 58 and 78 ms to 35 and 55 ms, respectively. Both countermeasures prevented the majority of the change in twitch duration. Peak tetanic force (P_o) fell by 38% with HU, while the P_o of the HU+ISO group was only 6% below and the HU+ISM group P_o not significantly different from the control group.

The reduced ability to oxidize fatty acids following spaceflight might result from a microgravity-induced decline in CoA-carnitine acyl transferase (CAT) activity as this enzyme has been reported to be rate limiting. However, following the 17-day spaceflight the CAT activity of the human slow type I fibers of the soleus and the gastrocnemius was increased rather than

decreased. Additionally, selected enzymes of β -oxidation and the tricarboxylic acid cycle were also increased post-flight. These data are consistent with the hypothesis that mitochondrial proteins showed less loss with microgravity than contractile protein, and thus mitochondrial enzyme activity per cell dry wt increased. Consistent with the hypothesis that microgravity increases the need to metabolize carbohydrates, the soleus type I fibers showed a 17% increase in cell glycogen. Previous studies have demonstrated an increased glucose transport protein (GLUT-4) and muscle glycogen in rats following unloading (11), but this is the first study to document an increased cell glycogen in humans.

In summary, spaceflight and models of unloading in humans and animals have demonstrated significant muscle atrophy, loss of peak force and power, and an increased susceptibility to fatigue. The decline in force (N) is due to a selective loss in contractile protein, while the loss in force/CSA and the increased fiber V_0 maybe caused by an increased spacing between the thin and thick filament. High resistance exercise proved to be an effective countermeasure, and isometric exercise was more effective than isotonic exercise in preventing the cell atrophy and functional changes associated with HU in rats.

(Supported by NASA grants NAS9-18768 and NAG5-6058 to R.H. Fitts)

REFERENCES

1. Convertino, V.A. Physiological adaptations to weightlessness: Effects on exercise and work performance. *Exerc. Sport Sci. Rev.* 18: 119-166, 1990.
2. Fitts, R.H., J.M. Metzger, D.A. Riley, and B.R. Unsworth. Models of disuse: a comparison of hindlimb suspension and immobilization. *J. Appl. Physiol.*, 60(6): 1946-53, 1986.
3. McDonald, K.S., C.A. Blaser, and R.H. Fitts. Force-velocity and power characteristics of rat soleus muscle fibers after hindlimb suspension. *J. Appl. Physiol.*, 77(4): 1609-16, 1994.
4. Riley, D.A., S. Ellis, J.F. Giometti, Y. Hoh, E. Ilyina-Kakueva, V.S. Oganov, G.R. Slocum, J.W.L. Bain, and F.R. Sedlak. Muscle sarcomere lesions and thrombosis after spaceflight and suspension unloading. *J. Appl. Physiol.*, 73(2), suppl.: 33S-43S, 1992.
5. Riley, D.A., S. Ellis, G.R. Slocum, F.R. Sedlak, J.L.W. Bain, B.B. Krippendorf, C.T. Lehman, M.Y. Macias, J.L. Thompson et al. In-flight and postflight changes in skeletal muscles of SLS-1 and SLS-2 spaceflown rats. *Am. J. Physiol.*, 81(1): 133-144, 1996.
6. McDonald, K.S. and R.H. Fitts. Effect of hindlimb unweighting on single soleus fiber maximal shortening velocity and ATPase activity. *J. Appl. Physiol.*, 74(6): 2949-2957, 1993.
7. McDonald, K.S., M.D. Delp, and R.H. Fitts. Fatigability and blood flow in the rat gastrocnemius-plantaris-soleus after hindlimb unweighting. *J. Appl. Physiol.*, 73(3): 1135-40, 1992.
8. Caiozzo, V.J., M.J. Baker, R.E. Herrick, M. Tao, and K.M. Baldwin. Effect of spaceflight on skeletal muscle: mechanical properties and myosin isoform content of a slow muscle. *J. Appl. Physiol.*, 76(4): 1764-1773, 1994.
9. Baldwin, K.M., R.E. Herrick, and S.A. McCue. Substrate oxidation capacity in rodent skeletal muscle: effects of exposure to zero gravity. *J. Appl. Physiol.*, 75(6): 2466-2470, 1993.
10. Fitts, R.H., C.J. Brimmer, A. Heywood-Cooksey, and R.J. Timmerman. Single muscle fiber enzyme shifts with hindlimb suspension and immobilization. *Am. J. Physiol.*, 256(5 Pt 1): C1082-91, 1989.
11. Henriksen, E.J. and L.S. Ritter. Effect of insulin-like factors on glucose transport activity in unweighted rat skeletal muscle. *J. Appl. Physiol.*, 75(2): 820-824, 1993.

IN VIVO NONINVASIVE ANALYSIS OF HUMAN FOREARM MUSCLE FUNCTION AND FATIGUE: APPLICATIONS TO EVA OPERATIONS AND TRAINING MANEUVERS

L.K. Fotedar, Ph.D.¹, T. Marshburn, M.D.², M. J. Quast, Ph.D.³, and **D. L. Feedback**, Ph.D.⁴
¹NRC/NASA-Johnson Space Center, SD3, Houston, Texas 77058; ²NASA-JSC, SD2;
³University of Texas Medical Branch, Department of Neuroscience/MBI, Galveston, Texas, 77555; ⁴NASA-JSC, SD3.

INTRODUCTION

Forearm muscle fatigue is one of the major limiting factors affecting endurance during performance of deep-space extravehicular activity (EVA) by crew members. Magnetic resonance (MR) provides *in vivo* noninvasive analysis of tissue level metabolism and fluid exchange dynamics in exercised forearm muscles through the monitoring of proton magnetic resonance imaging (MRI) and phosphorus magnetic resonance spectroscopy (³¹P-MRS) parameter variations. Using a space glove box and EVA simulation protocols, we conducted a preliminary MRS/MRI study in a small group of human test subjects during submaximal exercise and recovery and following exhaustive exercise. In assessing simulated EVA-related muscle fatigue and function, this pilot study revealed substantial changes in the MR image longitudinal relaxation times (T₂) as an indicator of specific muscle activation and proton flux as well as changes in spectral phosphocreatine-to-phosphate (PCr/Pi) levels as a function of tissue bioenergetic potential.

METHODS

Subjects were imaged prior to start of exercise, at an estimated 20% of maximum voluntary effort, following exhaustion protocol, and after 30 minutes of exercise recovery. Throughout the fatigue-generating protocol, subjects were periodically asked to generate an 80% maximal contraction (according to the individual's capabilities). Exhaustion was defined by the subject's inability to generate 80% of their previous maximal effort. Using a rapid "snapshot" imaging sequence, T₂-weighted MR images were collected and analyzed in 5 male volunteers. Based on signal intensity (SI) changes, average T₂ values were then calculated and compared over the experimental time course.

In a preliminary study of 4 volunteers, phosphorus spectra were collected at rest, with submaximal exercise (estimated 20% effort) and 8-9 minutes of post-exercise recovery. The subject then performed exhaustive exercise, and ³¹P spectra were collected approximately 30 min after the fatigue protocol was completed (total acquisition time of 1 min). A typical resting state phosphorus spectrum from one of the test subject forearms is shown in Figure 1. *In vivo* muscle tissue resonances from inorganic phosphate, phosphocreatine, and ATP (γ -, α -, and β - forms) are clearly observed. Spectral PCr/Pi peak height ratios were then calculated and compared over time.

RESULTS AND CONCLUSION

From MR images shown in Figure 2, we observed increased signal correlating with the appearance of edema in the forearm muscle extensors. As shown in Figure 3, average T₂ pre-exercise values, estimated at 19 ± 1 ms, increased significantly following exhaustive exercise to

25 ± 1 ms and then approached resting levels after 30 minutes of recovery ($p < 0.05$). Our preliminary data suggested that exercise-induced image signal intensity changes help in identifying affected forearm muscle, and that MRI T2 variations are objective quantitative indicators of the dynamic characteristics of fatigue-related edema/proton flux.

As illustrated in Figure 4, average spectral PCr/Pi peak height ratios reveal a significant decline of approximately 68% after 2 min of submaximal exercise ($p < 0.05$ with paired t-test), indicative of increased metabolic turnover. Following 20% effort, there appears to be a “compensatory” increase in phosphocreatine levels, resulting in PCr/Pi levels up to 68% above baseline/resting values at 8 minutes of recovery. Thirty minutes after exhaustive exercise protocol is stopped, there is a significant decrease in PCr/Pi of 75% from the baseline, which increases slightly to within 28% of the baseline/resting values after 40 min ($p < 0.05$), possibly indicative of a shift in bioenergetic potential towards anaerobic metabolism.

In conclusion, we found MRI/MRS provided noninvasive, objective identification and analysis of EVA-induced muscle function and fatigue. Thus, these preliminary results support our plan of further defined testing and reliable, longitudinal dynamic assessment - with clear applications in the evaluation of EVA-related task performance, fatigue, training/countermeasures effects, and glove/tool technology feedback.

ACTIVATION OF THE UBIQUITIN-PROTEASOME PATHWAY IN ATROPHYING MUSCLES AND POTENTIAL INHIBITORS

A.L. Goldberg, D. H. Lee, V. Solomon, and S. Lecker

Dept. of Cell Biology, Harvard Medical School, Boston, MA 02115.

Many observations indicate that the rapid loss of muscle mass with denervation atrophy, hind-limb suspension, cancer cachexia, sepsis, and hyperthyroidism is primarily due to enhanced protein breakdown via the ubiquitin-proteasome pathway. This proteolytic system is responsible for most protein degradation in extracts of skeletal muscle. Also, inhibitors of the proteasome, such as MG132, can selectively reduce the enhanced proteolysis in atrophying muscles during *in vitro* incubation. While such inhibitors have potential in the prevention of muscle wasting, the "therapeutic window" is narrow, and they can induce apoptosis at high concentrations. Interestingly, our recent studies of the effects of proteasome inhibitors indicate that concentrations that inhibit protein breakdown also cause induction of heat-shock proteins and thus enhance cell resistance to high temperatures and free radical damage.

We have also attempted to identify more selective sites in this pathway for inhibition. One property of a protein which leads to its rapid ubiquitination is the presence of a bulky hydrophobic or charged N-terminal residue, but natural substrates of this "N-end rule" pathway have not been identified. Surprisingly, we found that this pathway, which involves E2-14K and E3 α , catalyzes degradation of most soluble proteins in muscle extracts. Moreover, we showed that in many catabolic states, where muscle proteolysis rises, rates of protein ubiquitination increase, due mainly to activation of the "N-end rule" pathway. In extracts of atrophying rat leg muscles from tumor-bearing, hyperthyroid and hind-limb suspended animals, ubiquitin conjugation to soluble proteins increases, and inhibitors of the E3 α suppress most of the enhanced ubiquitination. Furthermore, ubiquitination of lysozyme, a typical "N-end rule" substrate, increases in these atrophying muscles. Thus, overall rates of ubiquitination vary under different conditions, and activation of the "N-end rule" pathway is a major contributor to the accelerated proteolysis in atrophying muscles.

CO₂ ACCUMULATION IN THE NON-CONFORMAL HELMET OF THE NASA LAUNCH AND ENTRY SUIT DURING SIMULATED UNAIDED EGRESS

Greenisen M.C., Bishop P.A.* , Lee S.M.C.** , Moore, A.** , Williams J.**

NASA Johnson Space Center, Houston, TX

*University of Alabama, Tuscaloosa, AL

**Wyle Laboratories, Houston, TX

The Launch and Entry Suit (LES) has been worn by astronauts since 1988 for Space Shuttle launch and landing. Previous work indicated that carbon dioxide (CO₂) accumulation in the LES non-conformal helmet might be high during locomotion while wearing the LES. The purpose of this study was to characterize the inspired CO₂%, metabolic requirements, and egress performance during a simulation of an unaided egress from the Space Shuttle in healthy male subjects wearing the LES and walking on a treadmill. With the helmet visor closed, 12 male subjects completed a 6-min seated prebreathe with 100% O₂ followed by a 2-min stand and 5 min of walking at 1.56 m/sec (5.6 km/h, 3.5 mph) as a simulation of unaided egress. All subjects walked with four different G-suit pressures (0.0, 0.5, 1.0, 1.5 psi). After a 10-min recovery, subjects walked 5 min with the same G-suit pressure and helmet visor open for the measurement of metabolic rate (VO₂). When G-suit inflation levels were 1.0 or 1.5 psi, only 4 of our 12 healthy, non-micro-gravity exposed subjects completed the unaided egress. Inspired CO₂ levels > 4% were routinely observed during walking. The metabolic cost at the 1.5 psi G-suit inflation was over 135% of the metabolic cost at 0.0 psi inflation. During unaided egress, G-suit inflation pressures of 1.0 (required inflation for missions > 11 days) and 1.5 psi resulted in elevated CO₂ in the LES helmet and increased metabolic cost of walking, either of which could impact unaided egress by returning space flight crews.

SPACE PHYSIOLOGY STUDIES

1. EXERCISE WITHIN LBNP TO PRODUCE ARTIFICIAL GRAVITY

A. R. Hargens¹, Ballard, R. E.², Boda, W. L.³, Ertl, A. C.⁴, Schneider, S. M.⁵, Hutchinson, K. J.², Lee, S. M.⁵, Murthy, G.², Putcha, L.⁵, and Watenpaugh, D. E.⁶

¹Gravitational Research Branch, Mail Stop 239-11, NASA Ames Research Center, Moffett Field, CA 94035-1000, ²University of California, San Diego, ³Sonoma State University, ⁴Vanderbilt University, ⁵NASA Johnson Space Center, ⁶University of North Texas

INTRODUCTION

Calculations suggest that exercise in space to date has lacked sufficient loads to maintain musculoskeletal mass. Lower body negative pressure (LBNP) produces a force at the feet equal to the product of the LBNP and body cross-sectional area at the waist. Supine exercise within 50-60 mm Hg LBNP improves tolerance to LBNP and produces forces similar to those occurring during upright posture on Earth. Thus, exercise within LBNP may help prevent deconditioning of astronauts by stressing tissues of the lower body in a manner similar to gravity and also, may provide a safe and effective alternative to centrifugation in terms of cost, mass, volume, and power usage. We hypothesize that supine treadmill exercise during LBNP at one body weight (50-60 mm Hg LBNP) will provide cardiovascular and musculoskeletal loads similar to those experienced while upright in 1g. Also, daily supine treadmill running in a LBNP chamber will maintain aerobic fitness, orthostatic tolerance, and musculoskeletal structure and function during bed rest (simulated microgravity).

RECENT PROGRESS

The overall goal of this research project is to determine whether treadmill exercise within lower body negative pressure (LBNP) can simulate cardiovascular and musculoskeletal effects of gravity, and in doing so help prevent the physiologic deconditioning normally associated with bed rest and space flight.

Self-generated LBNP exercise permits aerobic *and* resistance training with no external power.

Allowing the legs themselves to generate the negative pressure against which they work is a simple, inexpensive, and compact way to accomplish LBNP exercise without an external power source. A self-generated LBNP device consists of a flexible cylinder, sealed around the lower body, which expands and collapses longitudinally, but not radially. As the legs push footward, the cylinder expands, decreasing internal air pressure, and increasing the generated footward force. Negative pressure is limited by an adjustable valve to control air flow into the chamber. Force depends on air inflow rate, cylinder volume, and rate of expansion. We hypothesized that this device could be used to generate substantial footward forces and provide simultaneous cardiovascular stress. Seven healthy subjects performed supine knee bend exercise in the self-generated LBNP device for 5 to 6 min. Exercise rate was maintained at 20 cycles/min and the inflow valve was adjusted so footward force during cylinder expansion peaked at approximately 150% of body weight. Maximum footward force at the peak of the exercise cycle averaged 1116 ± 87 N (114 ± 9 kg), and pressure within the cylinder concomitantly decreased 26 ± 3 mm Hg below ambient. Heart rate and oxygen consumption increased 75 ± 4 beats/min and 26.3 ± 14 ml

O₂/kg/min from supine resting values, respectively. In addition, two supine subjects performed maximal efforts with the inflow valve completely closed, and achieved 332% and 337% of body weight equivalent force and concomitant pressure decreases of 63 mm Hg and 62 mm Hg, respectively. Depending on the setting of the inflow valve, this device can emphasize cardiovascular (rapid, low resistance) or musculoskeletal (slow, high resistance) conditioning. Exercise with self-generated LBNP may provide a low cost, low mass countermeasure to musculoskeletal and cardiovascular deconditioning in space while minimizing exercise time and payload disturbance.

LBNP vs. centrifugation to simulate cardiovascular effects of gravity.

Gravity creates blood pressure gradients which redistribute body fluids towards the feet and elicit lower body vasoconstriction. We hypothesized that artificial orthostatic stresses such as G_z centrifugation and LBNP differ from whole-body tilting (normal gravitational stress) in terms of the distribution of microvascular blood flow. Cutaneous microvascular flows were measured by laser Doppler flowmetry at the neck, thigh, and leg of 15 normal subjects. Volunteers underwent stepwise head-up tilt (HUT) and short- and long-arm centrifugation protocols from supine control (0 G_z) to 0.2, 0.4, 0.6, 0.8, 1.0, 0.8, 0.6, 0.4, 0.2, and 0 G_z at the feet, for 30 s periods with 10 s transitions between levels. The same subjects underwent a corresponding supine LBNP protocol, up to 100 mm Hg (in 20 mm Hg increments) and back to zero pressure, which produced transmural pressure across blood vessels in the foot approximately equal to the HUT protocol. In general, application of all orthostatic stresses produced significant flow reductions in the lower body. At low levels of each stress (0.4 G_z, 40 mm Hg), LBNP generated the greatest relative reduction in flow in the lower body (-66.9 ± 5.7%, thigh; -60.6 ± 5.7%, leg, mean ± SE). HUT caused a less severe flow reduction than LBNP at the thigh and leg (-39.9 ± 8.1% and -55.9 ± 4.8%), while the effects induced by both forms of centrifugation were the least profound (e.g. -13.0 ± 7.5%, leg, long-arm centrifugation @ 0.4 G_z). Higher levels of each stress generally resulted in similar relative responses. Therefore, in terms of lower body vasoconstrictor responses, LBNP produces more cardiovascular stress than normal gravity, whereas centrifugation produces less. The regional disparity of blood flows, and a strong relationship we observed across treatments between changes in local blood flow and local arterial pressure, each suggest that local reflexes play a significant role in determining microvascular perfusion during orthostatic stress. The above results taken together strongly support continued development of LBNP exercise as a cost-effective alternative to centrifugation for periodic simulation of gravity and preservation of 1g function during long-term existence in microgravity.

DISCUSSION

Our finding of the magnitude and mechanism of force production by LBNP has important implications for simulating gravity in space and increasing weightbearing on Earth without the use of a centrifuge. The use of a different air pressure separating the upper and lower body, such as proposed in this project, distributes the net force uniformly over the entire upper surface of the body. This concept thereby avoids the discomfort of localized high pressures typical of bungee cord harness systems. Variations of blood pressures due to inertial loads with normal gait have been documented in humans and other animals and such variations are important for maintenance of normal vascular structure and function in dependent tissues. LBNP simulates

gravitational blood pressures in the lower body circulation, and permits the simultaneous additional impact loading of lower body tissues and blood vessels during exercise.

EARTH BENEFITS

Our results will help determine exercise regimens and exercise devices needed to maintain crew health during long-duration flight as well as improve our understanding of how exercise can be optimized to maintain cardiovascular and musculoskeletal function in people on Earth.

Presently, Mir crew members exercise for 2-3 hours per day at about 50% body weight. Our apparatus allows comfortable loading of lower body tissues at one or more body weights. Thus, we expect that the exercise time required for astronauts and Earth-bound people to maintain musculoskeletal strength can be substantially reduced by optimally-increased levels of exercise loads. For example, a recent study of aged subjects found that muscle strength can be regained through an increased level of exercise loads. Thus, our bed rest results will have direct benefits to improve exercise for astronauts in space, and on Earth for bedridden or inactive aged citizens as well as the public at large.

BIBLIOGRAPHY

Abstracts

Sánchez ER, JM William, T Ueno, RE Ballard, and AR Hargens. Arterial pressure gradients during upright posture and 30° head down tilt. *Gravitational and Space Biology Bulletin* 11(1):8(15), 1997.

Boda WL, JA Campbell, C Yang, and AR Hargens. Comparison of upright gait with supine bungee-cord gait. *Experimental Biology '98*, San Francisco, CA, 18-22 April 1998.

Campbell JA, E Sánchez, C Yang, I Mitsui, G Murthy, D Schwandt, KP Fechner, R Ballard, DE Watenpaugh, and AR Hargens. MRI evaluation of spinal length and vertebral body angle during loading with a spinal compression harness. *Experimental Biology '98*, San Francisco, CA, 18-22 April 1998.

Hsieh ST, HB Lillywhite, RE Ballard, and AR Hargens. Cardiovascular responses of snakes to gravitational gradients. *Experimental Biology '98*, San Francisco, CA, 18-22 April 1998.

Pantalos G, J Buckey, D Watenpaugh, MK Sharp, S Parnis, and AR Hargens. Cutaneous tissue perfusion in humans with posture and acceleration alterations. *Aerospace Medical Association Annual Meeting*, Seattle, WA, 17-21 May, 1998.

Murthy G, JA Campbell, I Mitsui, KP Fechner, DE Watenpaugh, and AR Hargens. Spine length decreases and curvature increases with axial loading in the horizontal supine posture. *19th Annual International Gravitational Physiology Meeting*, Rome, Italy, 31 May - 5 June, 1998.

Murthy G, A Hargens, S Lehman, and D Rempel. Work-related fatigue may be caused by muscle deoxygenation. *PREMUS-ISEOH 1998 Conference*, Helsinki, Finland, 21-25 September 1998.

Articles in peer reviewed journals

Hsieh ST, RE Ballard, G Murthy, AR Hargens, and VA Convertino. Plasma colloid pressure increases in humans during simulated microgravity. *Aviation, Space, and Environmental Medicine* 69:23-26, 1998.

Ballard RE, DE Watenpaugh, GA Breit, G Murthy, DC Holley, and AR Hargens. Leg intramuscular pressures during locomotion in humans. *Journal of Applied Physiology* 84:1976-1981, 1998.

Hargens AR and SJ Mubarak. Current concepts in the pathophysiology, evaluation, and diagnosis of compartment syndrome. *Hand Clinics* 17:371-383, 1998.

Mack GW, R Yang, AR Hargens, K Nagashima, and A Haskell. Influence of hydrostatic pressure gradients on regulation of plasma volume after exercise. *Journal of Applied Physiology* 85:667-675, 1998.

Ballard RE. Leg intramuscular pressures during locomotion in humans. M.S. Thesis in Biology from San Jose State University, 1998.

Books or book chapters

Hargens AR, KJ Hutchinson, RE Ballard, and G Murthy. "Intervertebral Disc: Loaded on Earth and Unloaded in Space." In: *Connective Tissue Biology: Integration and Reductionism*, edited by R Reed and K Rubin. London: Portland Press, Ltd, pp. 125-133, 1998.

Hargens AR. "Pressure and Time Thresholds for Acute Compartment Syndromes." In: *Das Kompartiment-Syndrome*, edited by C Willy, J Sterk, and H Gerngroß. Berlin: Springer-Verlag, 154-163, 1998.

Hargens AR, RA Pedowitz, LR Mohler, and GA Breit. "Noninvasive Diagnosis of Exertional, Anterior Compartment Syndrome using Near-Infrared Spectroscopy." In: *Das Kompartiment-Syndrome*, edited by C Willy, J Sterk, and H Gerngroß. Berlin: Springer-Verlag, 296-303, 1998.

2. NONINVASIVE INTRACRANIAL DIAMETER AND PRESSURE MEASUREMENT USING ULTRASOUND

A.R. Hargens¹, Matsuyama, M², Ueno, T³, Yost, W. T.⁴, Pedowitz R.², Ballard, R. E.², Cantrell, J. H.⁴, Shuer, L. M.⁵, Marshall, L², Macias, B², Murthy, G² and Cutuk, A.²

¹Gravitational Research Branch, Mail Stop 239-11, NASA Ames Research Center, Moffett Field, CA 94035-1000, ²University of California, San Diego, ³National Research Council Associate, ⁴NASA Langley Research Center, ⁵Stanford University

INTRODUCTION

NASA and the National Institutes of Health identified intracranial pressure (ICP) as one of the most important parameters to investigate problems of astronauts in space and head trauma of patients on Earth. Current clinical techniques for measuring pressure in the head, however,

require surgery to implant a pressure sensor. The primary objectives of the proposed research are to: 1) refine and validate a noninvasive ultrasound technique for monitoring changes in ICP; 2) examine the effects of simulated and actual microgravity on ICP and cerebrovascular hemodynamics; and 3) facilitate transfer of the technology for Space Station and clinical use. The device, which was originally developed and patented by co-investigators Yost and Cantrell in 1993 and later modified by Hargens and co-workers in 1996, uses an ultrasonic phase comparison method to measure slight changes in cranial diameter which occur with changes in ICP. The proposed research will be conducted over three years. Year one will involve correlation with ICP in cadavera and optimization of the ultrasound measurement technique in healthy humans. Years two and three will include measurement of cranial diameter and pulsatility in patients with elevated ICP and in healthy individuals during parabolic flight. The proposed research will help refine and validate the noninvasive ultrasound device for future space flight investigations and for clinical use. A noninvasive method for monitoring ICP may aid our understanding of the pathophysiology of space adaptation syndrome and post-flight orthostatic intolerance, and may provide a valuable clinical tool for early diagnosis and treatment of patients with elevated ICP.

RECENT PROGRESS

During this past year we progressed significantly to validate our new ultrasonic technique for the noninvasive measurement of intracranial pressure. This technique will be valuable for monitoring headward fluid shifts in microgravity and separately, for monitoring neurosurgery patients on Earth.

Hardware Development

The ultrasound technique we utilized to detect skull pulsation is based upon a modification of the pulsed phase-lock loop (PPLL) design, making it possible to measure slight changes in distance between an ultrasonic transducer and a reflecting target. In the typical operation of the PPLL, the instrument transmits a 500 kHz ultrasonic tone burst through the cranium via a transducer placed on the head. The ultrasonic wave passes through the cranial cavity, reflects off the inner surface of the opposite side of the skull, and is received by the same transducer. The instrument compares the phase of emitted and received waves and alters the frequency of the next stimulus to maintain a 90° phase difference between the output of the device and the received signal. This repetition takes place at intervals of approximately 0.5 to 20 msec.

Correlation of Intracranial Diameter with Dynamic Changes of ICP

We evaluated the correlation of PPLL output and directly-measured ICP in several fresh cadavara. In supine position, a catheter was inserted into the frontal horn of the right lateral ventricle through a burr hole, and the other end of the catheter was connected to pressure tubing and a plastic syringe. To correlate the PPLL output with ICP directly, a fiber-optic, transducer-tipped catheter was placed in the epidural space through another burr hole. The ultrasonic transducer was placed on the temporal area above the ear and fixed with pressure cuff around the head to increase the external pressure. Pulsatile changes of ICP were generated by infusing saline into the lateral ventricle. We recorded the PPLL output while generating ICP pulsations at a frequency of 0.5, 1, and 2 Hz. Thereafter, we increased external pressure around the head in steps of 10 mmHg (0-40 mmHg) by inflating the pressure cuff at 1 Hz of ICP pulsation. We also

recorded the pulsatile PPLL output by infusing saline of different temperatures into the ventricle (4°C and 20°C) at 1 Hz of ICP pulsation.

The PPLL output correlated linearly with pulsatile components of ICP at each frequency of ICP pulsation. Interestingly, slopes of PPLL output amplitudes over ICP amplitudes depended on the frequency of ICP pulsations. Although data are not shown here, the ratio of pulsation amplitudes for PPLL output over ICP significantly decreased with increased external compression around the head ($R^2=0.87$, $p=0.020$). Also, the correlation between the PPLL and ICP amplitudes was expressed as the same equation at both saline temperatures: $PPLL = 3.0 \times 10^{-4} ICP + 0.0011$.

Effects of Whole-Body Tilting on Cranial Distance Pulsations

For the purpose of evaluating the feasibility of our device to future space flight experiments, we measured changes in cranial distance pulsations during whole-body tilting in six healthy volunteers. The subjects were positioned randomly up or down at 60°, 30° head-up tilt, supine, and 15° head-down tilt positions for one minute at each angle.

The ratio of pulsation amplitudes for PPLL output over arterial blood pressure significantly decreased ($p < 0.05$) as the angle of tilt was increased ($y = -0.105x + 13.5$).

DISCUSSION

Our external compression study strongly indicates that the PPLL technique measures skull movement, not just changes in sound velocity. As shown in the results of our whole-body tilting study, we detected significant effects of tilt angle on pulsatile amplitudes of ICP, which represent intracranial compliance. Compliance is defined as a ratio of change in volume over the corresponding change in pressure. Because the brain is surrounded with relatively-rigid skull, intracranial compliance is inversely related to static intracranial pressure. Therefore, reduced intracranial compliance indicates increased ICP in head-down position. At this point, we cannot extrapolate our results directly to microgravity exposure. However, we do conclude that postural changes significantly alter intracranial compliance and pressure. Taken together, our ultrasonic technique is sensitive enough to detect slight skull movement associated with dynamic ICP pulsation. Furthermore, head-down tilt decreases intracranial compliance and increases intracranial pressure in normal volunteers.

EARTH BENEFITS

Considerable Earth benefit is derived from our research. Previously ICP has been measured using invasive techniques by inserting a catheter or probe into the intracranial or intraspinal space. Invasive procedures are time and personnel consuming and represent significant risk to patients. Early noninvasive measurements of ICP will help reduce both the mortality and morbidity associated with head trauma, tumors, and cerebrovascular diseases.

BIBLIOGRAPHY

Abstracts

Ueno T, RE Ballard, WT Yost, and AR Hargens. Noninvasive measurement of intracranial pressure pulsation using ultrasound. *Aviation, Space and Environmental Medicine* 68:646, 1997.

Kuriyama K, T Ueno, RE Ballard, DE Watenpaugh, and AR Hargens. Cerebrovascular responses during lower body negative pressure-induced presyncope. *Aviation, Space and Environmental Medicine* 68:(7) 646(196), 1997.

Ueno T, RE Ballard, LM Shuer, JH Cantrell, WT Yost, and AR Hargens. Non-invasive measurement of pulsatile intracranial pressures using ultrasound. Tenth International Symposium on Intracranial Pressure and Neuromonitoring in Brain Injury, Williamsburg, VA, 25-29 May 1997.

Hargens AR. Gravity and living systems: May the force be with you. International Symposium of Adaptive Medicine, Framingham, MA, 7-10 September 1997.

Sánchez ER, JM William, T Ueno, RE Ballard, and AR Hargens. Arterial pressure gradients during upright posture and 30° head down tilt. *Gravitational and Space Biology Bulletin* 11(1):8(15), 1997.

Ueno T, RE Ballard, LM Shuer, JH Cantrell, WT Yost, and AR Hargens. Postural effects on intracranial pressure as assessed noninvasively. *Experimental Biology '98*, San Francisco, CA, 18-22 April 1998.

Articles in peer reviewed journals

Watenpaugh DE, GA Breit, RE Ballard, and AR Hargens. Monitoring acute whole-body fluid redistribution by changes in leg and neck volumes. *Aviation, Space, and Environmental Medicine* 68:858-862, 1997.

Hsieh ST, RE Ballard, G Murthy, AR Hargens, and VA Convertino. Plasma colloid pressure increases in humans during simulated microgravity. *Aviation, Space, and Environmental Medicine* 69:23-26, 1998.

Ueno T, RE Ballard, LM Shuer, JH, Cantrell, WT Yost, AR Hargens. Noninvasive measurement of pulsatile intracranial pressure using ultrasound. *Acta Neurochirurgica (Suppl)* 71: 66-69, 1998.

Zippel KC, HB Lillywhite, CRJ Mladinich. Contribution of the vertebral artery to cerebral circulation in the rat snake *Elaphe obsoleta*. *Journal of Morphology* 238:39-51, 1998.

INTRACELLULAR CALCIUM TRANSIENTS IN MOUSE SOLEUS MUSCLE AFTER HINDLIMB UNLOADING AND RELOADING

C.P. Ingalls, G.L. Warren, and R.B. Armstrong. Muscle Biology Laboratory, Dept. of Health and Kinesiology, Texas A&M University, College Station, Texas 77843

INTRODUCTION

Unloading of the antigravity skeletal muscles by space flight or hindlimb suspension initiates a rapid and significant loss of skeletal muscle mass and strength. Furthermore, skeletal muscles atrophied by unloading have an increased susceptibility to contraction-induced muscle injury, so reloading of these muscles may compound existing mass and strength deficits. The mechanisms responsible for the reductions in skeletal muscle mass and strength following unloading and subsequent reloading are not fully understood. The objective of this study was to determine if altered intracellular Ca^{2+} handling contributes to the force loss in the soleus muscle after unloading and/or subsequent reloading of mouse hindlimbs.

METHODS

Three groups of female ICR mice were studied: 1) unloaded mice (n=11) that were hindlimb suspended for 14 days; 2) reloaded mice (n=10) that were returned to their cages for 1 day after being hindlimb suspended; and 3) control mice (n=10) that had normal cage activity. Maximum isometric tetanic force (P_o) and specific force (P_o /cross-sectional area) were measured in the soleus muscle from the left hindlimb, whereas resting free cytosolic calcium concentration ($[\text{Ca}^{2+}]_i$), tetanic $[\text{Ca}^{2+}]_i$, and 4-chloro-*m*-cresol-induced $[\text{Ca}^{2+}]_i$ were measured in the contralateral soleus muscle using confocal laser scanning microscopy. 4-chloro-*m*-cresol is thought to be a specific activator of the sarcoplasmic reticulum Ca^{2+} release channel.

RESULTS

Two weeks of hindlimb unloading resulted in marked decreases in soleus muscle mass and strength. The soleus muscle wet weight, P_o , and specific force were 45%, 58%, and 24% less than that of the control mice, respectively. Unloading of the soleus muscle disturbed intracellular Ca^{2+} handling. Compared to control mice, resting $[\text{Ca}^{2+}]_i$ was increased by 36% and 4-chloro-*m*-cresol-induced $[\text{Ca}^{2+}]_i$ was reduced by 50% in the unloaded soleus muscles. However, tetanic $[\text{Ca}^{2+}]_i$ was not significantly altered (-12%) in the unloaded soleus muscle. Twenty-four hours of physiological reloading did not exacerbate the unloading-induced deficits in soleus muscle mass or strength. The soleus muscle wet weight, P_o , and specific force were 43%, 58%, and 23% less than that of the control mice, respectively. Resting $[\text{Ca}^{2+}]_i$ was increased by 24% while 4-chloro-*m*-cresol-induced $[\text{Ca}^{2+}]_i$ was unchanged when compared to control mice. Finally, tetanic $[\text{Ca}^{2+}]_i$ was not different between unloaded and reloaded mice but was reduced 23% when compared to control mice.

CONCLUSION

These data indicate that although hindlimb unloading results in disturbed intracellular Ca^{2+} homeostasis, changes in tetanic $[\text{Ca}^{2+}]_i$ do not contribute to the force deficits. Compared with unloading, 24 hours of physiological reloading in the mouse does not result in further changes in maximal strength or tetanic $[\text{Ca}^{2+}]_i$.

IMPAIRED UTILIZATION OF EXOGENOUS SUBSTRATES BY RAT SKELETAL MUSCLE AFTER HINDLIMB SUSPENSION.

B.F. Lujan and L.A. Bertocci. Institute for Exercise and Environmental Medicine, Presbyterian Hospital of Dallas and the Department of Radiology, UT Southwestern Medical Center, Dallas, TX.

INTRODUCTION

Chronic exposure to the microgravity of spaceflight causes severe skeletal muscle atrophy. Although much is known about the structural consequences of this atrophy, the metabolic effects of this atrophy are much more ambiguous: literature reports of the effects of disuse atrophy on the activities of many of the enzymes involved in exercise metabolism, and the linkage of these changes to indices of the patterns of substrate utilization, are quite contradictory. We speculated that this was due in part to methodological limitations. To address this, we used a combination of ^1H and ^{13}C nuclear magnetic resonance (NMR) spectroscopy plus a carefully controlled animal model to assess the effect of severe disuse atrophy on the relative utilization of exogenous and endogenous oxidizable substrate in resting versus contracting rat hindlimb muscle.

METHODS

We compared the muscle of normal, caged rats with muscle from rats after a 28-day period of tail-supported hindlimb suspension. For each animal studied ($n=16$ in each group), the hindquarter circulation was completely isolated between the descending aorta and ascending vena cava. Through this isolated circulation, we provided a non-recirculating perfusate of warmed, oxygenated Krebs-Henseleit buffer, containing a 40% hematocrit of washed porcine erythrocytes, and a mixture of the following oxidizable substrates: of 5 mM [$3\text{-}^{13}\text{C}$]lactate, 0.5 mM pyruvate, 1 mM [$1,3\text{-}^{13}\text{C}$]acetoacetate, 2.5 mM α -hydroxybutyrate and 2 mM [$\text{U-}^{13}\text{C}$]fatty acids (in a mixture of chain lengths and saturation patterns). After peak hindquarter flow was reached, the muscles of one hindlimb were contracted (100msec trains of pulses, at 100Hz, each for 0.2msec duration, with no delay, at a train rate of 2 Hz, for 30 minutes). The contralateral hindlimb muscles were the rested control. At the end of the contraction period, the soleus (Type I fibers) and gastrocnemius+plantaris (mostly Type II fibers) muscles were rapidly freeze-clamped. The soluble fraction of the muscle samples were extracted in perchloric acid plus potassium hydroxide. After lyophilization, the solutes were resuspended in D_2O and analyzed by ^1H and ^{13}C NMR. The individual peaks in the resultant NMR spectra were Lorentzian-curve fitted and the results analyzed by isotopomer analysis.

RESULTS

In general, the relative intensity of most peaks arising from incorporation of the exogenously-supplied oxidizable substrates was greater in contracted versus rested muscle, and in control versus suspended muscle. Of particular interest is that in control muscle, the doublet 34 (D34) was not visible in spectra from rested muscle (Table 1), and contraction increased (* $p<0.05$ vs rested control) the relative area of the D34. This is the pair of peaks that reflect the relative incorporation of label from lactate+pyruvate that has been scrambled by one or more turns of the citric acid cycle. In suspended muscle, the relative size of this peak was larger than in control muscle during rest, but did not increase during contraction.

Table 1 Relative areas of the peaks of the glutamate C3 and C4 multiplets.

GLUTAMATE PEAK	CONTROL		HINDLIMB SUSPENDED	
	RESTED	CONTRACTED	RESTED	CONTRACTED
C4S	0.575±0.091	0.614±0.076	0.724±0.118	0.657±0.136
C4D34	0.000±0.000	0.172±0.051 ¹	0.026±0.025 ¹	0.042±0.041 ^{1,2}
C4D45	0.424±0.091	0.213±0.115	0.246±0.106	0.297±0.132
C4DQ	0.001±0.000	0.001±0.000	0.003±0.001	0.003±0.001
C3S	0.583±0.033	0.546±0.031	0.677±0.122	0.527±0.098
C3D	0.415±0.033	0.453±0.031	0.317±0.124	0.408±0.123
C3T	0.001±0.000	0.000±0.000	0.006±0.004	0.002±0.001

These peak areas were used for the calculation of the relative contribution of the different possible forms of acetyl-CoA that enter the citric acid cycle (Table 2). The dominant form of acetyl-CoA that entered these muscles was unlabeled ([1,2-¹²C]acetyl-CoA, or Fc0). In control muscle, contraction increased greatly the relative uptake of exogenous ([3-¹³C]lactate+pyruvate). In contrast, in suspended muscle, there was no increase in the relative uptake of exogenous ([3-¹³C]lactate+pyruvate). Neither contraction nor suspension had any detectable effect on the relative incorporation of [¹³C]ketones or [¹³C]fatty acids.

Table 2 Relative contribution to the citric acid cycle of the different acetyl-CoA sources

		CONTROL		HINDLIMB SUSPENDED	
		RESTED	CONTRACTED	RESTED	CONTRACTED
Fc0	[U- ¹² C]acetyl-CoA	0.99±0.00	0.80±0.06 ¹	0.95±0.03	0.93±0.06
Fc2	[2- ¹³ C]acetyl-CoA	0.00±0.00	0.20±0.06 ¹	0.04±0.03	0.06±0.06
Fc3	[1,2- ¹³ C]acetyl-CoA	0.00±0.00	0.00±0.00	0.01±0.00	0.01±0.00

CONCLUSIONS

We conclude that the disuse atrophy that results from a 28-day period of hindlimb suspension attenuates the relative oxidation of exogenous versus endogenous substrates and prevents the normal increase in oxidation of exogenous lactate+pyruvate induced by muscle contraction. We suspect that this is due to the effects of chronic disuse atrophy on reducing the overall mitochondrial volume and thus the overall oxidative capacity of muscle as well as on reducing the capacity for transport of exogenous monocarboxylic acids, ketones, and fatty acids. This results in a preferential dependence on oxidation of endogenous substrates, most likely glycogen and triglycerides. If this is so, it would mean that the exercise capacity of muscle after the disuse atrophy of spaceflight would be limited in part by its relative dependence on the finite stores of endogenous fuels and its relative inability to utilize the more limitless supply of exogenous fuels.

ALTERATIONS IN NEUROMUSCULAR JUNCTIONS ASSOCIATED WITH MUSCLE ATROPHY INDUCED BY HINDLIMB UNLOADING

D.R. Mosier,¹ L. Siklós,^{1,2} C.L. Gooch,¹ S. Gordon,³ and F.W. Booth³

¹Department of Neurology, Baylor College of Medicine, Houston, TX 77030; ²Institute of Biophysics, Szeged, Hungary; ³Department of Integrative Biology, University of Texas Health Science Center, Houston, TX 77030

INTRODUCTION

Many alterations in motor unit structure and function occur with exposure to microgravity during spaceflight, and could lead to impairment of motor performance. In particular, morphologic changes suggestive of denervation and remodeling have been reported at neuromuscular junctions in atrophying muscle, both in space-flown animals (D'Amelio and Daunton, *J Neuro-pathol Exp Neurol* 1992, 51:415) and in rodent models of limb immobilization. However, the anatomic extent and physiologic significance of these alterations is unclear. To begin to address these questions, we assayed neuromuscular junctions electrophysiologically using intracellular micropipette recordings and stimulated single-fiber electromyography, in parallel with electron microscopic studies of end-plates, in hindlimb muscles of ICR mice following a 3-week period of unloading by tail suspension.

METHODS

1. *Hindlimb unloading.* ICR mice aged 5-7 weeks underwent hindlimb unloading for an additional 3 weeks using a modification of a protocol reported for rats (Babij and Booth, *Am J Physiol* 1988; 254:C651). Tail-suspended mice were allowed ad lib access to water and food during the protocol, as were age-matched control mice.
2. *Intracellular recordings.* Under deep anesthesia, soleus (SOL) or plantaris (PLT) muscles were dissected and pinned on Sylgard discs in a chamber perfused with oxygenated saline. In some experiments, a 2nd muscle was dissected and placed on mesh in a vial containing oxygenated saline for later use. Miniature end-plate potentials (MEPPs) were detected with KCl-filled glass micropipettes inserted into randomly selected muscle fibers, amplified (Axoclamp-2A, Axon), displayed (Hitachi VC-6020 oscilloscope), and stored for analysis (pClamp, Axon).
3. *Ultrastructural studies.* Mice were perfused with Karnofsky's fixative and muscles in the contralateral hindlimb dissected for electron microscopy. Systematic random sampling techniques were used to avoid bias in determining the fields for analysis. Sections were examined using a Zeiss CEM 902 electron microscope, and the following parameters measured at all sampled end-plates: surface ratio of postsynaptic membrane to presynaptic membrane portion not covered by Schwann cells, percent terminal surface enveloped by Schwann cells, synaptic vesicle density, and mitochondrial volume fraction.
4. *Single-fiber EMG recordings.* Stimulated single-fiber electromyography (S-SFEMG) was performed in the medial gastrocnemius (MG) muscle of anesthetized mice, while directly stimulating the sciatic nerve with hook electrodes at a rate of 2/sec. Signals were filtered (low cutoff, 500 Hz; high cut-off, 10 kHz), displayed, and analyzed online with an Advantage-SE EMG system.

RESULTS

A 3 week period of hindlimb unloading (HU) produced atrophy of 47% in the soleus (SOL) and 17% in the plantaris (PLT) muscles of ICR mice, consistent with previous reports of differential atrophy between these muscles induced by hindlimb unloading in rat models. MEPP frequency, measured in randomly sampled fibers, did not differ significantly between control and HU soleus muscles. In contrast, there was an approximate doubling of MEPP frequency in the plantaris muscles with HU ($p < 0.005$). These findings were consistent with a presynaptic locus of effect in the PLT. Parallel electron microscopic studies of end-plate boutons demonstrated a decrease in the surface ratio of postsynaptic membrane to presynaptic membrane in the SOL following HU ($p = 0.012$), whereas a trend toward an opposite effect in the PLT was not statistically significant. These changes were most consistent with an additional postsynaptic change at the neuromuscular junction. In a second series of experiments, S-SFEMG recordings of the medial gastrocnemius showed a significant increase in jitter in HU mice ($p = 0.007$), suggesting a reduction in the overall safety factor for neuromuscular transmission. Further studies to validate the S-SFEMG technique in mice will be available at presentation.

CONCLUSIONS

These studies demonstrate structural alterations and abnormal function of the neuromuscular junction associated with muscle atrophy induced by hindlimb unloading. It is possible that the presynaptic changes observed in this model could result from an activity-dependent, retrogradely acting signal from muscle, a hypothesis which requires further study. Whether the changes seen are of adaptive or detrimental significance (or both) is unclear, although the finding of increased jitter on stimulated SFEMG suggests a heightened vulnerability to failure of neuromuscular transmission in atrophied muscle. Future studies will need to determine the effects of countermeasures to muscle atrophy in this paradigm, as well as to extend the approaches used in this model to testing of human subjects for alterations in neuromuscular transmission.

MUSCLE DEOXYGENATION CAUSES MUSCLE FATIGUE

G. Murthy¹, A.R. Hargens^{2,3}, S. Lehman¹, and D. Rempel¹

¹University of California, Berkeley, California, ²University of California, San Diego, California

³NASA Ames Research Center, Moffett Field, California

INTRODUCTION

Muscle fatigue is a common musculoskeletal disorder in the work place, and may be a harbinger for more disabling cumulative trauma disorders. Although the cause of fatigue is multifactorial, reduced blood flow and muscle oxygenation may be the primary factor in causing muscle fatigue during low intensity muscle exertion. Muscle fatigue is defined as a reduction in muscle force production, and also occurs among astronauts who are subjected to postural constraints while performing lengthy, repetitive tasks. The objectives of this research are to 1) develop an objective tool to study the role of decreased muscle oxygenation on muscle force production, and 2) to evaluate muscle fatigue during prolonged glovebox work.

METHODS

Near infrared spectroscopy (NIRS) has been used to study muscle oxygenation noninvasively in the brain and large muscle groups such as the quadriceps and the tibialis anterior of the thigh and leg. NIRS is based on the differences in absorption characteristics of oxygenated and deoxygenated hemoglobin and myoglobin at 760 nm and 850 nm wavelengths. The NIRS instrument was designed to measure muscle oxygenation at 2-3 cm below the skin surface. The distance between the light sources and the detectors determine the depth of photon penetration. We used ultrasonography to determine that the forearm extensor carpi radialis (ECR) muscle was only 1.2 ± 0.2 cm (SD) beneath the skin. Therefore, we adjusted the distance between the light source and the detectors to 2 cm (as opposed to 4 cm) to provide the necessary penetration depth (Fig. 1). Numerous pilot studies ensured that the correct forearm extensor muscle was studied and that reproducible data were generated (Murthy & Hargens, 1995). Furthermore, we documented that NIRS was sensitive enough to detect alterations in muscle oxygenation (TO_2) at levels below 20% maximum voluntary contraction (Murthy et al., 1997).

To determine the role of decreased muscle oxygenation in the reduction of muscle force production, we applied a tourniquet compression cuff on the upper arm to reduce blood flow and TO_2 , and measured twitch force in the ECR muscle. We hypothesized that decreased TO_2 during tourniquet compression will decrease muscle force production. Eight healthy (ages 20-53) were seated with shoulder abducted to 45° and flexed to 35°. The pronated forearm and wrist were maintained in neutral posture throughout the protocol. Ischemia to the ECR muscle was induced by tourniquet compression of the upper-arm. Altered TO_2 of the ECR muscle was measured noninvasively using NIRS. ECR twitch force was generated by continuous 1Hz electrical stimulation. ECR TO_2 and twitch force were measured continuously during the following conditions: Five minutes of baseline control (0 mmHg cuff pressure), followed by upper-arm compression of 20, 40, 60 mmHg, diastolic and systolic blood pressure levels applied in random order. A recovery period (2-7 min) followed each level of compression and lasted until twitch force reached baseline value (Murthy et al., 1998).

To study the effects of prolonged glovebox work on muscle oxygenation, we hypothesized that working in a constrained posture in the glovebox will cause a reduction in muscle oxygenation and hence, muscle fatigue as compared to working in a free-floating arm posture. Three subjects worked in a constrained posture (shoulder abduction was 35° and flexion was 45°) for 20 minutes in the Life Sciences Glovebox designed for the Space Station. Subjects worked as fast as possible to debone thawed chicken thighs. Muscle oxygenation was measured noninvasively using NIRS both in the supraspinatus muscle and the forearm ECR muscle.

RESULTS

Mean TO₂ decreased from resting baseline (100% TO₂) to 99 ± 1.2% (SE), 96 ± 1.9%, 93 ± 2.8%, 90 ± 2.5%, and 86 ± 2.7% at 20, 40, 60 mmHg, diastolic, and systolic cuff pressures, respectively. Similarly, mean twitch force decreased from resting baseline (100% TO₂) to 99 ± 0.7% (SE), 96 ± 2.7%, 93 ± 3.1%, 88 ± 3.2%, and 86 ± 2.6% at 20, 40, 60 mmHg, diastolic, and systolic cuff pressures, respectively. TO₂ and twitch force at and above 60 mmHg were significantly lower ($p < 0.05$) than baseline value. Reduced twitch force was strongly associated with reduced TO₂ ($r^2 = 0.99$).

Preliminary results for muscle oxygenation during glovebox work indicate that there was no reduction in oxygenation in the forearm ECR muscle. However, there was a reduction in muscle oxygenation in the supraspinatus muscle of the shoulder compared to baseline relaxed posture following 20 minutes of glovebox work.

DISCUSSION AND CONCLUSIONS

Our results from the tourniquet study indicate that TO₂ and muscle twitch force are closely associated and therefore, offer a likely mechanism for localized muscle fatigue. An adequate recovery period during any task is required to maintain blood flow and TO₂ to prevent localized loss of force production. Our findings from the Life Sciences Glovebox study may be exacerbated during microgravity exposure because of the cephalad fluid shifts which occur in space. Cephalad fluid shifts and higher than normal blood pressure in the upper body may increase tissue fluid pressure and decrease blood flow and oxygenation to the shoulder muscle. Consequently, under microgravity conditions, muscle fatigue may result sooner than it does on Earth. Although studies need to be conducted in the microgravity environment to test this hypothesis, additional ground based studies are warranted.

(Supported by NASA Headquarters Graduate Student Research Fellowship to GM)

REFERENCES

Murthy G and AR Hargens. Near infrared spectroscopy: A noninvasive technique for diagnosing exertional compartment syndrome. *Operative Techniques in Sports Medicine* 3(4):256-258, 1995.

Murthy G, NJ Kahan, AR Hargens, and DM Rempel. Forearm muscle oxygenation decreases with low levels of voluntary contraction. *Journal of Orthopaedic Research* 15:507-511, 1997.

Murthy G, A Hargens, S Lehman, D Rempel. Work-related fatigue may be caused by muscle deoxygenation. 3rd International Scientific Conference on Prevention of Work-Related Musculoskeletal Disorders, Helsinki, Finland, September 1998.

E PROTEINS CONTROL SKELETAL MUSCLE FIBER TYPE

¹Craig Neville, ¹Donald Gonzales, ¹Joy Purdy, ²Yuan Zuang, and ¹Nadia Rosenthal
¹Cardiovascular Research Center, Massachusetts General Hospital, Harvard Medical School, Charlestown MA 02129, ²Department of Immunology, Duke University, Durham NC.

INTRODUCTION

Vertebrate skeletal muscle development involves the fusion of undifferentiated mononucleated myoblasts to form multinucleated myofibers, with a concomitant activation of muscle-specific genes encoding proteins that form the contractile apparatus. The regulatory circuit controlling skeletal muscle gene expression has been well studied in a number of vertebrate animal systems, and has resulted in a rather extensive understanding regarding muscle formation during embryonic development. In contrast, the molecular mechanisms underlying the further specification of muscle cells into different fiber types is poorly understood. We have investigated the role of a family of transcriptional proteins, known as E proteins, as the genetic basis of fiber specificity. The aims of this project are to define the mechanisms, and the potential importance of E proteins, responsible for the shifts in fiber type under conditions of microgravity.

METHODS

The role of E proteins in defining fiber type was determined by both loss- and gain-of-function experiments. Expression of specific myosin heavy chain (MyHC) isoforms in mice carrying homozygous targeted disruptions of each of the E protein loci (E2A, E2-2, and HEB) was detected by immunohistochemistry. Ectopic expression of the HEB protein in Type IIB fibers was achieved by utilizing a transgene containing the Myosin Light Chain 1 regulatory elements. Activation of the Type IIX gene expression program was detected with the Type IIX-specific skeletal alpha-actin/CAT ($sk\alpha$ /CAT) transgene. The role of the ubiquitin-proteasome pathway in determining E protein stability was determined by IP injection of the proteasome inhibitor MG132 at a final concentration of 10 micromolar and examining HEB and $sk\alpha$ /CAT expression after 24 hrs.

RESULTS

Immunohistochemistry of cross-sections of the crural muscles and measurement of HEB mRNA and protein levels indicate that the E protein is restricted to Type IIX fibers by a post-transcriptional mechanism. Application of the proteasome inhibitor MG132 causes a stabilization of HEB in all fast fiber types, with a concomitant activation of the Type IIX – specific transgene $sk\alpha$ /CAT. Transgenic expression of HEB induces the transactivation of $sk\alpha$ /CAT in Type IIB fibers. Mice homozygous null for the E protein E2-2 lack MyHC IIB-expression fibers; mice without E2A have only a few remaining IIA-expressing cells. Compound heterozygotes displayed loss of multiple fast fiber types.

CONCLUSION

E proteins play a pivotal and non-redundant role in the determination of myosin isoform expression. Loss of expression of a specific E protein results in the loss of a skeletal muscle fiber type, indicating the unique and necessary roles that individual members of the transcription factor family play. The E protein HEB is restricted to Type IIX myofibers by ubiquitin-directed

degradation in non-permissive fiber types. Forcing transgenic expression of HEB alone in Type IIB myofibers is sufficient to activate the Type IIX program of gene expression. Future investigations will determine if the E proteins comprise upstream targets for the effects of weightlessness upon muscle atrophy.

WEIGHTLESSNESS REDUCES SKELETAL MUSCLE GROWTH AND REGENERATION POTENTIAL

Schultz, E and P.E. Mozdziak, Department of Anatomy, University of Wisconsin Medical School, Madison, WI 53706

INTRODUCTION

Myonuclear increase is required for myofiber enlargement during skeletal muscle growth and is solely dependent upon the proliferation of satellite cells and the fusion of their progeny with the enlarging myofibers. Likewise, regeneration of injured skeletal muscles is dependent upon the proliferation of satellite cells to produce a sufficient supply of myogenic cells for the formation of replacement myofibers and for the subsequent growth of these myofibers.

METHODS

The effect of unweighting on myonuclear accretion during skeletal muscle growth was studied using immature rats placed in hindlimb suspension. Bromodeoxyuridine (BrdU) was administered using an Alzet miniosmotic pump to obtain a history of the mitotic activity of satellite cells during a growth period in hindlimb suspension. Soleus muscles of experimental and weightbearing animals were removed, individual myofiber segments were enzymatically isolated and the BrdU labeled nuclei were immunocytochemically visualized and quantitated. Similarly, the relationship between satellite cells and DNA unit size during muscle growth was studied after mitotic activity of satellite cells was inhibited by irradiation. Pectoralis muscles of immature turkeys were irradiated with a 6MeV electron beam at a dosage of 25Gy. Irradiated and control animals were infused with BrdU using Alzet miniosmotic pumps to obtain a mitotic history of satellite cells during a growth period following irradiation. Labeled nuclei were assayed on enzymatically isolated myofiber segments using immunocytochemistry. Finally, regeneration of the soleus was studied after injection of myotoxic snake venom Notexin. After Notexin injection, rats were placed in hindlimb suspension. BrdU was administered to experimental and weightbearing control animals to obtain a history of mitotic activity during the regeneration period.

RESULTS

Soleus muscles from immature animals, placed in hindlimb suspension, exhibited a transient cessation of satellite cell mitotic activity, followed by a reduction in satellite cell mitotic activity that persisted throughout the duration of suspension. The unweighted muscles were significantly growth retarded. Similarly, irradiation was used to reduce satellite cell mitotic activity in immature muscles. Irradiation resulted in reduced myonuclear accretion. There was no increase in the size of the DNA unit to compensate for the decreased accumulation of myonuclei. Muscles were significantly growth retarded, and they did not achieve control size 15 weeks after irradiation.

Muscle regeneration is also dependent on satellite cell proliferation, and can be broken down into two phases. During the initial phase of regeneration, satellite cells are activated to divide, and they produce a population of myogenic cells that will fuse to form new myofibers. The newly formed myofibers increase in size during the second phase of regeneration. Satellite cell mitotic activity during the initial phase of regeneration was not altered by unweighting, however growth

of the newly formed myofibers was retarded. Therefore the primary effect of unweighting appears to be on the myofiber, and the satellite cell mitotic activity appears to be regulated through a myofiber pathway.

CONCLUSIONS

Unweighting and irradiation reduced the number of myonuclei in immature growing myofibers and unweighting reduced the number of myonuclei following myofiber regeneration. The regeneration studies suggest that the primary effect of unweighting is on the myofiber because the initial phase of regeneration was not influenced by unweighting, yet cells in the contralateral undamaged muscles that were associated with myofibers had reduced mitotic activity. These results suggest that satellite cell mitotic activity is regulated through a pathway that includes the myofiber.

Myofibers did not compensate for the reduced myonuclear accretion by increasing the size of each DNA unit. Therefore, any deficit in myonuclei within a myofiber results in a reduced growth potential, because each myonucleus governs a finite volume of cytoplasm. Consequently, recovery after a growth period in an unloaded or weightless environment will take place only if the missing myonuclei are acquired. Taken together these findings lead to the conclusion that muscles placed in an unweighted environment during their growth period or during a regeneration period, will not develop to their full potential size. Current studies are focused on the hypothesis that muscle development in an unweighted environment during a critical period will result in a permanent growth deficit even if weightbearing is reinstated.

MECHANICAL AND INFLAMMATORY COMPONENTS OF MUSCLE INJURY FOLLOWING MODIFIED MUSCLE LOADING.

J. G. Tidball

Department of Physiological Science, University of California, Los Angeles 90095

INTRODUCTION

The ability of personnel to function following space flight is limited by debilitating muscle weakness, pain, and inflammation that develop following return to gravitational loading. It has been proposed previously that muscle injury that occurs during muscle loading following periods of reduced loading can result from direct mechanical damage to the muscle or through the actions of inflammatory cells that invade the muscle during the reloading period, but these possibilities have not been tested experimentally. In this investigation, we are examining the contribution of inflammatory cells to muscle injury that occurs following modified muscle use and determining the mechanisms through which inflammatory cells induce muscle injury. We have used the rat hindlimb suspension model followed by muscle reloading by normal weight-bearing activity to examine muscle inflammation *in vivo* and employed co-cultures of specific inflammatory cell populations with rat muscle cells to perform further studies of the mechanisms of muscle cell injury. The goal of these studies is to characterize the specific inflammatory cell derived mediators of muscle injury during loading following periods of reduced loading, so that therapeutic approaches can be designed to reduce muscle injury following return to gravitational loading after space flight.

METHODS

1. Muscle unloading and reloading.

Rat hindlimb muscles were unloaded for 10 days by hindlimb suspension using a tail harness. Rats experiencing reloading were removed from the suspension apparatus for designated periods of reloading until sacrificed for collection of the soleus muscle for analysis.

2. Quantification of timecourse of muscle inflammation and necrosis.

Tissue sections from soleus muscles collected from animals at 0, 2, 6, 12, 24 and 48 hours of reloading and from ambulatory controls were analyzed using quantitative immunohistochemical techniques for neutrophils, phagocytic macrophages (ED1+ macrophages) and non-phagocytic macrophages (ED2+ macrophages). In addition, the frequency of occurrence of muscle fiber necrosis was assessed by determining the percentage of total muscle fibers shown in cross-sections that contained invading populations of macrophages.

3. Quantification of timecourse of muscle fiber injury.

Soleus muscle of rats receiving intraperitoneal injections of Evans blue prior to muscle reloading were analyzed after 0, 2, 6, 12 and 24 hours of reloading by quantitative analysis of the presence of Evans blue within muscle fibers. Evans blue enters cells through membrane lesions and serves as a marker of cell injury.

4. Assessment of muscle injury and inflammation following brief periods of reloading followed by return to unloading.

Rats were subjected to hindlimb unloading followed 2 hours reloading and then return to unloading for 22 hours. Soleus inflammation, fiber necrosis and injury in these animals was compared to that occurring in animals continuously reloaded for 24 hours. This manipulation was shown to prevent the invasion of phagocytic macrophages into the reloaded muscle without affecting the invasion of neutrophils, and thereby enabled us to assess the contribution of macrophage populations to muscle fiber injury during reloading.

5. Complement activation during muscle reloading.

Changes in the concentrations of Factor B and complement C4 in serum during the course of muscle reloading were assessed to test whether activation of either the alternative or classical pathway of the complement system were activated. Complement activation was also inhibited by functionally blocking C3b and C4b, and the effects of complement activation on muscle inflammation and necrosis were assessed by quantitative immunohistochemical techniques.

6. In vitro analysis of inflammatory cell mediated injury of muscle cells.

Cytotoxicity assays using measurement of chromium release from target muscle cells loaded with radiolabeled chromium were performed on cocultures with neutrophils or ED1+ macrophages. Cytotoxicity was measured in the presence of nitric oxide synthase (NOS) inhibitors, to assess the contribution of NO or its derivatives to cytotoxicity, in the presence of superoxide dismutase (SOD), to assess superoxide or its derivatives, or in the presence of catalase, to assess peroxide. In addition, the possibility that NO production during muscle reloading and inflammation could act as a negative regulator of inflammation by the induction of apoptosis was assessed by quantification of inflammatory cell apoptosis in the presence and absence of NOS inhibitors during reloading.

7. In vivo analysis of free radical mediated damage to muscles during reloading.

Soleus muscles from rats that were subjected to hindlimb loading and reloading in the presence of NOS inhibitors, SOD and catalase were assayed for neutrophil invasion, macrophage invasion and muscle fiber necrosis to test for a contribution of NO, SO, peroxynitrite and peroxides to muscle pathology during reloading.

RESULTS

We tested mechanical and inflammatory components of muscle membrane damage by assaying the time course of membrane lesions and inflammatory cell invasion during modified loading. Rat hindlimbs were unloaded for 10 days followed by reloading by normal ambulation, and the resulting membrane injury was measured by assaying Evans blue-bound serum protein influx through membrane lesions. Approximately half of the muscle membrane damage during 24 hours of reloading occurred between 2 and 24 hours of reloading. However, removal of loading from the hindlimbs from hours 2 to 24 resulted in significantly more muscle membrane damage than in muscles that were reloaded from hours 0 to 24. Thus, membrane injury during that period was not primarily attributable to mechanical factors. Immunohistochemical analysis showed that neutrophils increased in concentration in muscle by a factor of 3.4-times during the first 6 hours of reloading when most membrane damage occurred, but there was no significant change in the concentration of macrophages during that period. Muscle reloading for 2 hours followed by 22 hours unloading produced similar increases in neutrophil concentration as measured in muscles reloaded for 24 hours. However, muscle reloaded for 2 hours followed by

22 hours unloading showed no increase in ED1 macrophages compared to controls. Thus, the presence of neutrophils in the tissue, and not the presence of mechanical loading or macrophages, is associated with most muscle membrane injury that occurs in reloading.

We have found that muscle loading following periods of unloading activates the complement system through the classical pathway. Complement activation contributes to the early recruitment of neutrophils to the reloaded muscle, and inhibition of complement activation decreases muscle inflammation and injury. We have further examined the mechanisms of inflammatory cell mediated injury of skeletal muscle during modified muscle use by testing whether free radicals contribute to injury. By performing muscle reloading in the presence of nitric oxide synthase inhibitors, we have found that nitric oxide (NO) or one of its intermediates promotes muscle inflammation and fiber necrosis during modified muscle use. We have also shown that NO plays no more than a minor role in the resolution of muscle inflammation by inducing apoptosis of inflammatory cells. Parallel studies conducted *in vitro* have shown that neutrophil killing of muscle cells *in vitro* occurs by NO mediated events, but macrophage killing of muscle cells occurs via NO independent events.

CONCLUSION

Together, these data support a model for inflammatory cell contribution to muscle fiber injury in which muscle reloading results in activation of the complement system through the classical pathway, thereby causing neutrophil invasion of muscle where they contribute to muscle fiber injury through NO mediated cytotoxicity. Continuing work is employing more specific perturbations of neutrophil function to further test this model of muscle injury during modified muscle use and assessing potential therapeutic approaches for reducing muscle fiber injury during modified reloading by controlling inflammatory cell contribution to the injuries.

TISSUE ENGINEERING ORGANS FOR SPACE BIOLOGY RESEARCH

H.H. Vandenburg, J. Shansky, M. Del Tatto, P. Lee, and J. Meir

Department of Pathology, Brown University School of Medicine and The Miriam Hospital, Providence RI 02906.

INTRODUCTION

Long-term manned space flight requires a better understanding of skeletal muscle atrophy resulting from microgravity. Atrophy most likely results from changes at both the systemic level (e.g. decreased circulating growth hormone, increased circulating glucocorticoids) and locally (e.g. decreased myofiber resting tension). Differentiated skeletal myofibers in tissue culture have provided a model system over the last decade for gaining a better understanding of the interactions of exogenous growth factors, endogenous growth factors, and muscle fiber tension in regulating protein turnover rates and muscle cell growth. Tissue engineering these cells into three dimensional bioartificial muscle (BAM) constructs has allowed us to extend their use to Space flight studies for the potential future development of countermeasures.

METHODS

Embryonic avian muscle cells were isolated and BAMs tissue engineered as described previously (Vandenburg *et al.*, 1998b; Shansky *et al.*, 1997). The myoblasts proliferate and fuse into aligned postmitotic myofibers after ten to fourteen days *in vitro*. A cylindrical muscle-like structure containing several thousand myofibers is formed which is approximately 30 mm in length, 2-3 mm in diameter, and attached at each end. For the Space Shuttle experiments, the BAMs were transferred to 55 mL bioreactor cartridges (6 BAMs/cartridge, **Figure 1**). At Kennedy Space Center, the cartridges were mounted in two Space Tissue Loss (STL) Modules (three to four cartridges per Module) and either maintained as ground controls or loaded in a Mid-Deck locker of the Space Shuttle. The BAM cartridges were continuously perfused during the experiment at 1.5 mL/min with tissue culture medium. Eighteen BAMs were flown for nine days on Mission STS66 while eighteen BAMs served as ground controls. The complete experiment was repeated on Mission STS77 with twenty four BAMs in each group.

RESULTS

BAMs could be maintained in a healthy state for at least 30 days in the perfusion bioreactor cartridges (Chromiak *et al.*, 1998). The BAM muscle fibers directly detected both the loss of gravity and the reloading effects of 1 x g. While total cellular metabolism and total protein degradation rates were not altered during 9 to 10 days in Space, protein synthesis rates were significantly reduced and resulted in significant myofiber atrophy compared to ground controls. One g reloading of the flight muscle cells post-flight significantly increased protein synthesis rates and the synthesis rates of myosin heavy chain, fibronectin, and collagen.

CONCLUSIONS

Tissue cultured muscle cells can directly "sense" changes in gravity and provide a valid model to begin the study of countermeasures. Based on our ground-based experiments (Vandenburg *et al.*, 1998a), and the experiments of others, growth hormone and/or insulin-like growth factors are attractive protein therapeutics which may assist in attenuating skeletal muscle wasting in Space.

Our laboratory is developing a new cell-based delivery system for this and other potential therapeutic factors for attenuating muscle and bone wasting.

(Supported by NASA Grants NAG2-914 and NAG2-1205)

Reference List

- CHROMIAK J., SHANSKY J., PERRONE C.E. & VANDENBURGH H.H. (1998) Bioreactor perfusion system for the long term maintenance of tissue-engineered skeletal muscle organoids. *In Vitro Cell Dev. Biol.* 34, 694-703.
- SHANSKY J., DEL TATTO M., CHROMIAK J. & VANDENBURGH H. (1997) A simplified method for tissue engineering skeletal muscle organoids *in vitro*. *In Vitro Cell. Dev. Biol. Anim.* 33, 659-661.
- VANDENBURGH H.H., DEL TATTO M., SHANSKY J., GOLDSTEIN L. & RUSSELL K., GENES, N., CHROMIAK, J. and YAMADA, S. (1998a) Attenuation of skeletal muscle wasting with recombinant human growth hormone secreted from a tissue engineered bioartificial muscle. *Hum. Gene Therapy* (In Press)
- VANDENBURGH H.H., SHANSKY J., DEL TATTO M. & CHROMIAK J. (1998b) Organogenesis of skeletal muscle in tissue culture. In *Methods in Molecular Medicine: Tissue Engineering*. Eds J. Morgan & M. Yarmush. Totowa, NJ: Humana Press. pp. 205-217.

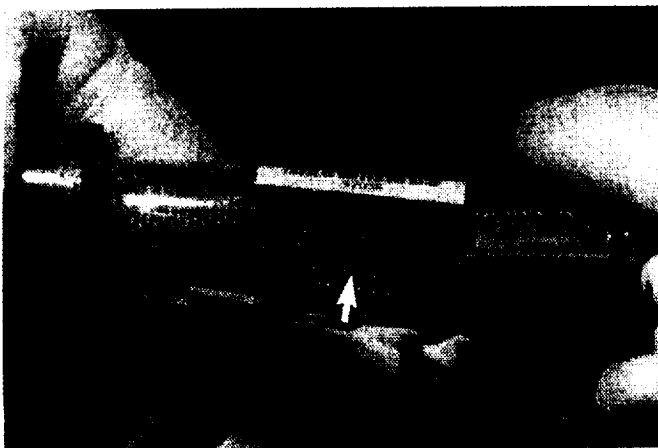


Figure 1. Bioartificial muscle in bioreactor cartridge

Neurovestibular

Chair

Charles Oman, Ph.D.

Co-Chair

Malcolm Cohen, Ph.D.

NEUROVESTIBULAR SESSION SUMMARY

Introduction

Oman - The early mission operational problems caused by space motion sickness have been largely resolved in recent years. This has been achieved by appropriate timeline adjustments, voluntary head movement restriction, and judicious use of promethazine. Crew members now simply accept that some symptoms "come with the job," and usually last only a few days. But as more people have flown longer flights, we've seen cases of space sickness and inversion illusion that take several weeks to resolve. Visual reorientation illusions continue throughout long flights, and occasionally cause difficulties. EVA astronauts sometimes suddenly fear they will fall out of the payload bay or off of the RMS or Strella arms. Orientation and navigation in three dimensions in the MIR station reportedly does not come naturally, because modules have different visual verticals. It is clear that the neurovestibular problems of spaceflight have not disappeared. After return to Earth, many crew members are disoriented and ataxic in the first hour after return, and require assistance leaving the vehicle. Flight surgeons say that the longer the mission, the stronger the aftereffects, certain of which last for weeks. We do not yet know how to predict who will be afflicted. Looking ahead to 3-4 month long voyages to Mars, it seems obvious that if cruise is in 0-G, the crew may encounter neurovestibular problems on arrival. Artificial G may be broadly effective as a countermeasure for many of the physiological changes of spaceflight, but from the neurovestibular perspective, it is a double-edged sword. We know that the Coriolis stimulus resulting from rotation is potentially disorienting and nauseogenic. But we don't yet know how much artificial G will be enough, nor how successfully people can adapt to a specific angular velocity and hypo G level. Development of countermeasures remains a big challenge for our neurovestibular community. Maintaining an interdisciplinary perspective is important. Three examples were presented at this meeting: 1) Transgenic animal experiments suggest that in addition to the light illumination cycle, vestibular inputs may also serve as an important input to the circadian system. 2) Radiation can cause important CNS effects in animals, including loss of spatial memory. 3) As described in our session, otolith inputs may contribute to cardiovascular regulation of orthostatic tolerance.

Over the past three days, we've all enjoyed catching up with old friends, and making many new ones. On behalf of my colleagues, I want to thank Al Coats and the USRA DSLS staff for the great job they did in running this meeting. And keeping the emphasis on fun. And also my Co-Chair, Mal Cohen, who had more stamina than many of us, despite major surgery only three weeks ago. Mal and I have written a few lines describing each of the seventeen papers in our session, to give you a quick overview, and as a guide to the full abstracts. We have grouped them under five themes:

Preflight and Inflight Countermeasures

Markham and Diamond reviewed evidence that space motion sickness is caused by decompensation of otolith asymmetry. The hypothesis is that on earth, the nervous system compensates for asymmetries in otolith responses. However, in 0-G, this compensation produces inappropriate disconjugate movements of the eye. Presented data from 1-6 month spaceflights, and showed that eye torsion was disconjugate and offset by several degrees compared to

preflight. This persisted several weeks to months after return. Persistent torsional offsets have also been seen in parabolic flight. Their origin is uncertain, and mechanisms were discussed.

Moore et al. (presented by Cohen) reported that promethazine had effects on rapid changes in monkey optokinetic nystagmus eye velocity but not VOR or ocular counterrolling.

Oman et al. discussed preflight and inflight visual orientation training to enhance orientation and 3D spatial memory. Oman described tumbling room experiments showing that static tilt illusions - even inversion - can be created in 1-G using a strongly polarized visual scene. Illusions were not strongly dependent on head position, but positively correlated with age and putative visual experience. Performance in a task analogous to orientation in an ISS node showed 3D spatial learning was independent of head position. Rat head direction cells tested in parabolic flight continued to respond in 0-G, in ways corresponding to human visual reorientation illusions when rats were placed on the ceiling of the test chamber.

McDonald and Riccio discussed methods for measuring postural stability of EVA astronauts performing mass handling tasks. Using this information to enable crew members to avoid unstable limb configurations was also described. This method is currently being applied to test and evaluate new space suit designs at JSC.

Layne et al. reported that during stereotyped 90° arm movements in 0-G, muscle activation synergies, as revealed by correlations between EMG recordings, were largely unchanged in the lower extremity as compared to preflight. However, applying pressure to the sole of the foot using a modified Cuban boot increased lower limb activation. Use of the technique to increase muscle activation was discussed.

Postlanding posture and locomotion deficits: assessment and prediction

Bloomberg et al. discussed locomotion in NASA MIR astronauts. Head, eye, trunk and lower limb kinematics is altered. Dynamic visual acuity is impaired. Vertical integration of multiple sensory motor subsystems is degraded by spaceflight. Integrative approaches to postflight locomotor dysfunction are required.

Peterka presented a heuristic mathematical model for human postural control, discussed the role of different sensory modalities, and described the responses expected during exposure to terrestrial and altered gravitational conditions. He demonstrated that subjects exposed to sudden changes in environmental conditions rapidly change their position feedback gain in response to altered sensory feedback. Gain modification allows modification of response to altered environmental conditions.

Wall and Krebs demonstrated how nonlinear Floquet stability analysis techniques may be applied to distinguish the stability of repeated stepping movements made by normals and vestibular patients. The techniques may be useful in assessing postflight changes in astronauts.

Adaptive processes

Shelhamer et al. showed that the human linear vestibulo-ocular reflex and saccades may be conditioned so that the phase of the response depends on vertical eye position. There was discussion of how to optimize such dual adaptation, e.g., the role of trial spacing, duration, stimulus magnitude increments, the role of context cues, and whether or not motor output is required to switch adaptations.

Angelaki and Hess described otolith ocular reflex experiments with normal and canal plugged animals exposed to conflicting visual and rotational stimuli. With this stimulus, both canal and otolith response components adapted. Adaptation of the otolith component could be demonstrated at frequencies other than that of the adapting head movement.

Reschke et al. reviewed evidence for changes in gaze control after long duration space flight. Head velocity was reduced and eyes moved in multiple saccades. Gaze holding in the dark showed an involuntary return to starting position, suggestive of an increased leak rate in the final oculomotor integrator. Mechanisms responsible for these changes and their functional significance were the subject of extensive discussion.

DiZio and Lackner quantified non-vestibular effects of rotating environments on head, arm and leg movements due to coriolis forces. Changes in trajectory and endpoints were noted, and could be manipulated independently. Endpoint adaptation showed intermanual transfer, while trajectory curvature did not.

Relationships among physical stimuli, perceptions, and eye movements

Moore et al. (presented by Cohen) questioned if, after adaptation to 0-G, otolith signals are reinterpreted to code only linear acceleration, as suggested by other evidence supporting Otolith Tilt Translation Reinterpretation (OTTR). Neurolab oculomotor and perceptual data suggest not. Ocular counterrolling on the off axis rotator inflight showed no significant change from preflight response to this sustained linear acceleration stimulus. However, sensation was of 90° tilt, rather than continuous acceleration. Subjects felt no translation. In the first days after return to earth, subjects overestimated head tilt.

Parker reported that subjects described their motion illusions after making coriolis head movements in a rotating chair, using a mannequin head connected to a computer animation system. Mannequin trajectories were highly repeatable, but often not in the same direction as concurrently measured compensatory VOR eye movement. Possible explanations, and the advantages and limitations of the animation technique were discussed.

Welch reported that in a pitched room, adaptive changes in adjustments to visually perceived eye level in a tilted room can be created by exploring the physical environment. Changes are independent of visually perceived orientation of objects, suggesting a cognitive rather than perceptual basis for the adaptation.

Paloski et al. noted that human perceptual responses during and after short radius centrifugation are of interest, since this stimulus is being considered as a 0-G countermeasure. Subjects exposed to prolonged 45° body tilt or 1.4 G centrifugation (producing the same 45° tilt of the gravitoinertial force vector) indicated the subjective horizontal and vertical by making voluntary eye movements. Responses differed. Postural stability was decreased following centrifugation, but not following body tilt. Possible reasons for the difference were discussed.

Black et al. reported on tests with normals and vestibular patients in a tilt chair. Using a handlebar to indicate the subjective horizontal is probably more accurate and less variable than having subjects set a visual line display, as the latter is influenced by unperceived changes in ocular torsion. Handlebar indicator responses were linear, and veridical (no Aubert effect) for tilt angles up to 60°.

Vestibular contribution to human autonomic responses

Kaufman et al. showed evidence that autonomic responses, including heart rate, RR interval, and muscle sympathetic nerve activity are modulated during off vertical axis body rotation. The component of gravity along the body's long axis – which presumably drives the baroreflex – is unchanged. However, the stimulus to the otolith organs is sinusoidal and may be the cause of the sympathetic efferent activity, which peaks in the face-up position, supporting the view that vestibular information contributes to orthostatic tolerance.

Implications and recommendations

- Semicircular canals appear to function normally in space; most 0-G problems appear to be related to interpretation of otolith information. Some postflight changes can be long lasting.
- Coriolis stimulation of the semicircular canals is an important factor to consider in the use of artificial gravity as a countermeasure.
- Vestibular stimulation can affect multiple systems, including cardiovascular and musculoskeletal.
- Simultaneous adaptation to multiple environments (dual adaptation) is an important potential preflight and inflight countermeasure.
- The following are important points for consideration:
 - Training that addresses both nominal and off nominal situations.
 - Emphasis on operational relevance of research.
 - Integration of research across multiple disciplines and national boundaries.
 - Utilization of Russian data on long duration flight.

Charles Oman and Malcolm Cohen

VISUALLY-INDUCED ADAPTATION IN GRAVITY-SENSITIVE PROPERTIES OF PRIMATE VESTIBULO-OCULAR REFLEX

Dora E. Angelaki¹ and B. J. M. Hess²

¹Dept. of Surgery (Otolaryngology), University of Mississippi Medical Center, Jackson MS

²Dept. of Neurology, University Hospital Zürich, CH-8091, Switzerland

INTRODUCTION

Most natural head movements, particularly those including pitch and roll movements, involve dynamic changes in the orientation relative to gravity. In addition to the semicircular canals, these head movements also activate the otolith system. Even though the adaptive ability of the semicircular canal-activated aspects of the vestibulo-ocular reflex (VOR) have been repeatedly demonstrated, very little is currently known about the adaptive processes underlying the gravity-related aspects of the VOR. The present studies aimed at addressing this issue.

METHODS

The adaptive plasticity of the spatial organization of the VOR has been investigated in intact and lesioned primates using two- or three-hour exposures to conflicting visual (optokinetic, OKN) and vestibular rotational stimuli about mutually orthogonal axes (generating torsional VOR + vertical OKN, torsional VOR + horizontal OKN, vertical VOR + horizontal OKN and horizontal VOR + vertical OKN). Monkeys were subjected to simultaneous vestibular and optokinetic oscillations at each of two frequencies: 0.5 Hz ($\pm 18^\circ$ for both vestibular and optokinetic stimuli) or 0.05 Hz ($\pm 60^\circ$ for vestibular and $\pm 180^\circ$ for optokinetic stimuli). During adaptation, and approximately every 15 min during each adapting session, the lights were turned off, animals were given a period of rest for approximately 1 min and the VOR in the dark was tested at the adapting frequency, amplitude and axis orientation (i.e., earth-vertical for EVA or earth-horizontal for OVAR adaptation protocols) in order to monitor the time course of adaptation. After completion of the two (or three) hours of adaptation, the VOR was tested in the dark using sinusoidal oscillations at 0.01 ($\pm 90^\circ$), 0.02 ($\pm 45^\circ$), 0.05 ($\pm 90^\circ$ and $\pm 180^\circ$), 0.1 ($\pm 90^\circ$), 0.2 ($\pm 45^\circ$), 0.5 ($\pm 18^\circ$) and 1 Hz ($\pm 5^\circ$). For each EVA and OVAR adapting condition, the VOR was tested with the axis of rotation both earth-vertical and earth-horizontal. Since the changes in VOR observed with adapting protocols where the axis of rotation was earth-horizontal also reflected the adaptive states of the otolith signals, these protocols were optimized to address specifically the role of otolith system changes in the adapted VOR. Thus, in addition to the main protocol described above, the VOR after 0.05 Hz OVAR adaptation was also studied in selected animals with the following stimuli: (a) Sinusoidal oscillations where peak amplitude was kept constant at 60° while frequency varied. (b) Sinusoidal oscillations at the adapting frequency with different peak amplitudes (10° , 20° , 30° , 60° , 90° and 180°).

RESULTS

Adaptation protocols with 0.5 Hz ($\pm 18^\circ$) head movements about either an earth-vertical or an earth-horizontal axis induced orthogonal response components as high as 40-70% of those required for ideal adaptation. Orthogonal response gains were highest at the adapting frequency with phase leads present at lower and phase lags present at higher frequencies. Furthermore, the time course of adaptation, as well as orthogonal response dynamics were similar and independent of the particular visual/vestibular stimulus combination.

Low frequency (0.05 Hz, vestibular stimulus: $\pm 60^\circ$; optokinetic stimulus: $\pm 180^\circ$) adaptation protocols with head movements about an earth-vertical axis induced smaller orthogonal response components which did not exceed 20-40% of the head velocity stimulus (i.e., approximately 10% of that required for ideal adaptation). At the same frequency, adaptation with head movements about an earth-horizontal axis generated large orthogonal responses that reached values as high as 100-120% of head velocity after two hours of adaptation (i.e., approximately 40% of ideal adaptation gains). The particular spatial and temporal response characteristics after low frequency, earth-horizontal axis adaptations in both intact and canal-plugged animals strongly suggests that the orienting (and perhaps translational) but not inertial (velocity storage) components of the primate otolith-ocular system exhibit spatial adaptability.

Due to the particular nested arrangement of the visual and vestibular stimuli, the optic flow pattern exhibited a significant component about the third spatial axis (i.e., orthogonal to the axes of rotation of the head and visual surround) at twice the oscillation frequency. Accordingly, the adapted VOR was consistently characterized by a third response component (orthogonal to both the axes of head and optokinetic drum rotation) at twice the oscillation frequency after earth-horizontal but not after earth-vertical axis 0.05 Hz adaptation.

Surgical ablation of the cerebellar nodulus and ventral uvula did not prevent adaptive changes in the spatial organization of the primate VOR. From this, we conclude that the cerebellar nodulus and ventral uvula might not be as critical for inducing visually adaptive changes in the spatial organization of the VOR despite the fact that these cerebellar areas have been shown to control the three-dimensional spatial and temporal organization of the low frequency inertial VOR responses.

CONCLUSION

The results show that not only semicircular canal-activated but also otolith-activated components of the VOR exhibit adaptability to altered visual environments. In fact, the otolith-ocular (but not the semicircular canal-ocular) system can adaptively change its spatial organization at optic flow frequencies that are different from that of the head movement. Among the different aspects of the otolith-ocular system, it is the orienting components (i.e., counter-rolling and counter-pitching) and not the inertial system (i.e., velocity storage) that are responsible for these adaptive changes.

ROLL-TILT PERCEPTION USING A SOMATSENSORY BAR TASK

F.O. Black, S.W. Wade, and A. Arshi

Neurotology Research, Legacy Holladay Park Clinical Research and Technology Center, Portland, Oregon, 97232

INTRODUCTION

Visual estimates of roll-tilt perception during static roll-tilt are confounded by an offset due to the ocular counterroll that simultaneously occurs (Wade and Curthoys, 1997). An alternative, non-visual ('somatosensory') measure of roll-tilt perception was developed which is not contaminated by this offset. The aims of this study were to determine: 1) inter-subject variability of somatosensory settings across test session in normal subjects and patients with unilateral or bilateral vestibular loss and 2) intra-subject variability of settings across test session in normal subjects.

METHODS

Normals: eight subjects ages 17 - 39 years. Patient groups: 1) five with complete unilateral loss following vestibular neurectomy or labyrinthectomy (time since operation ranged from 8 weeks to 15 years), 2) one patient with complete unilateral vestibular loss (4 months after head injury, and 3) one patient with complete bilateral vestibular loss (13 years prior). All patients had clinically compensated. Subjects were blindfolded, seated in a tilt chair and tilted about their naso-occipital axis at 1°/s to roll-tilt stimulus angles of $\pm 15, 30, 45$ and 60° . After one minute at the desired angle, measurements of roll-tilt were made by asking subjects to set a small bar with two hands so that it was aligned with the perceived horizontal (perpendicular to earth vertical). Four settings were made at each angle; the experimenter off-set the bar after each setting. Settings at each angle were referenced against the subjective horizontal measured in an upright position. After each of the four settings were made, subjects were returned to an upright position for one minute, after which the next angle was tested. The blind fold was removed during this one minute period. Normal subjects were tested within one week of the initial test.

RESULTS

For the inter-subject variability series in normals, there were no systematic errors in the settings across the group at any of the angles tested. Intra-subject variability was slightly higher than reported for visual measures. The average standard deviation for all subjects was 2.1 on the initial test and 2.2 on the retest. There were no systematic changes in the SDs as the roll-tilt stimulus angle increased. The settings were extremely reliable in normals ($r^2=0.9091$, $p<0.001$) across test sessions. All patients with unilateral vestibular loss had reduced sensitivity to roll-tilt when tilted towards the lesioned ear. Because the five subjects also showed reduced sensitivity to roll-tilt when tilted towards the intact side, there was no statistically significant asymmetry in the settings across the group between settings to tilt towards the intact side versus the lesioned side (tobs < 1.6 for all angles, $p > 0.1$). The bilateral patient underestimated the degree of roll-tilt at all angles.

CONCLUSION

Normal subjects were able to accurately align the bar with the earth horizontal at all roll-tilt stimulus angles. This replicates previous results using a similar somatosensory task (Wade & Curthoys, 1997). Patients with vestibular deficits showed an underestimation of earth horizontal relative to normal subjects. This result is consistent with findings of Dai, et al., 1989 for visual angle estimates for small

angles. These results confirm that somatosensory bar settings to perceived earth horizontal in response to static tilt constitute a valid measure of roll-tilt perception. Test-retest reliability is very high.

This study supported in part by NASA grant NAGW-3799 and NIH (NIDCD) R01 DC00205.

THE EFFECTS OF LONG-DURATION SPACEFLIGHT ON POSTFLIGHT TERRESTRIAL LOCOMOTION

J.J. Bloomberg¹, A.P. Mulavara², P.V. McDonald², C.S. Layne³, L.A. Merkle¹, H.S. Cohen⁴, I.B. Kozlovskaya⁵

¹NASA Johnson Space Center, Houston, TX, ²Wyle Life Sciences Inc., Houston, TX, ³University of Houston, Houston, TX, ⁴Bobby R. Alford Department of Otorhinolaryngology and Communicative Sciences, Baylor College of Medicine, Houston, TX, ⁵Institute for Biomedical Problems, Moscow, Russia

INTRODUCTION

Locomotion is a complex task requiring the coordinated integration of multiple sensorimotor subsystems. This coordination is exemplified by the precise control of segmental kinematics that allows smooth progression of movement in the face of changing environmental constraints. Exposure to the microgravity environment encountered during space flight induces adaptive modification in the central processing of sensory input to produce motor responses appropriate for the prevailing environment. This inflight adaptive change in sensorimotor function is inappropriate for movement control in 1-g and leads to postflight disturbances in terrestrial locomotor function. We have previously explored the effects of short-duration (7-16 days) space flight on the control of locomotion (Glasauer, et al., 1995; Bloomberg, et al., 1997; McDonald, et al., 1996; Layne, et al., 1997; Newman, et al., 1997). The goal of the present set of studies was to investigate the effects of long-duration spaceflight (3-6 months) on the control of locomotion with particular emphasis on understanding how the multiple interacting systems are adaptively modified by prolonged microgravity exposure.

METHODS

Six astro/cosmonaut subjects were tested before and after 3-6 months aboard the Mir Space Station. Subjects were tested before launch and 1, 3-6 and 7-9 days after their return to Earth. Subjects performed two protocols: 1) walking on a motorized treadmill while performing different gaze fixation tasks; 2) overground locomotion on a 6.0 m walkway. In the treadmill task, subjects walked at 6.4 km/h while performing three distinct gaze fixation tasks: i) visual fixation of a target at 2m from the eyes, ii) visual fixation of a target at 30 cm from the eyes and, iii) a number recognition task. In the number recognition task subjects identified strings of numbers presented on a laptop computer located 2m from the eyes. In the overground locomotion task subjects walked at a preferred pace while visually fixating on a centrally placed target on a far wall in front of them. Segmental kinematic data were collected with a motion analysis system. During the overground locomotion task, head acceleration was measured with a triaxial accelerometer mounted onto a Plexiglas bitebar which was held firmly between the subject's teeth.

RESULTS

Segmental kinematic data obtained during treadmill locomotion revealed postflight alterations in both head movement control and lower limb coordination. Analysis of the Fourier spectra of roll, pitch and yaw head movement during treadmill walking revealed postflight alterations in head movement control in all three planes of motion. Change in lower limb coordination was

exemplified by modification in control of thigh, knee and ankle angular displacement, particularly during the heel-strike event of the gait cycle. Subjects also experienced oscillopsia during walking which led to impairment in performance of the number recognition task. Analysis of the spectra of head movement during overground locomotion showed postflight changes in the X, Y and Z planes of motion.

CONCLUSION

Taken together these data indicate that exposure to long-duration space flight causes alteration in head movement control, lower limb coordination and dynamic visual acuity during locomotion. Thus, after spaceflight there is a loss of integration of the multiple full-body cascade of sensorimotor events required for efficient terrestrial locomotion. These results emphasize the need for integrative approaches to elucidate the emergent adaptive properties responsible for postflight locomotor dysfunction.

REFERENCES

- Glasauer, S., Amorim M.A., Bloomberg, J. J., Reschke, M.F., Peters, B.T., Smith, S.L., Berthoz. A. Spatial orientation during locomotion following space flight. Acta Astronautica 36: 423-431, 1995.
- Bloomberg, J.J., Reschke, M.F., Huebner, W.P., Peters, B.T., Smith, S.L. Locomotor head-trunk coordination strategies following space flight, Journal of Vestibular Research, 7: 161-177, 1997.
- Layne, C.S., McDonald, P.V., Bloomberg, J.J. Neuromuscular activation patterns during locomotion after space flight. Experimental Brain Research, 113: 104-116, 1997.
- McDonald, P.V., Basdogan, C., Bloomberg, J.J., Layne, C.S. Lower limb kinematics during treadmill walking after space flight: Implications for gaze stabilization. Experimental Brain Research, 112: 325-334, 1996.
- Newman, D.J., Jackson, D.K., Bloomberg, J. J. Altered astronaut lower-limb and mass center kinematics in downward jumping following space flight. Experimental Brain Research, 117: 30-42, 1997.

MOTOR CONTROL AND ADAPTATION IN A ROTATING ARTIFICIAL GRAVITY ENVIRONMENT

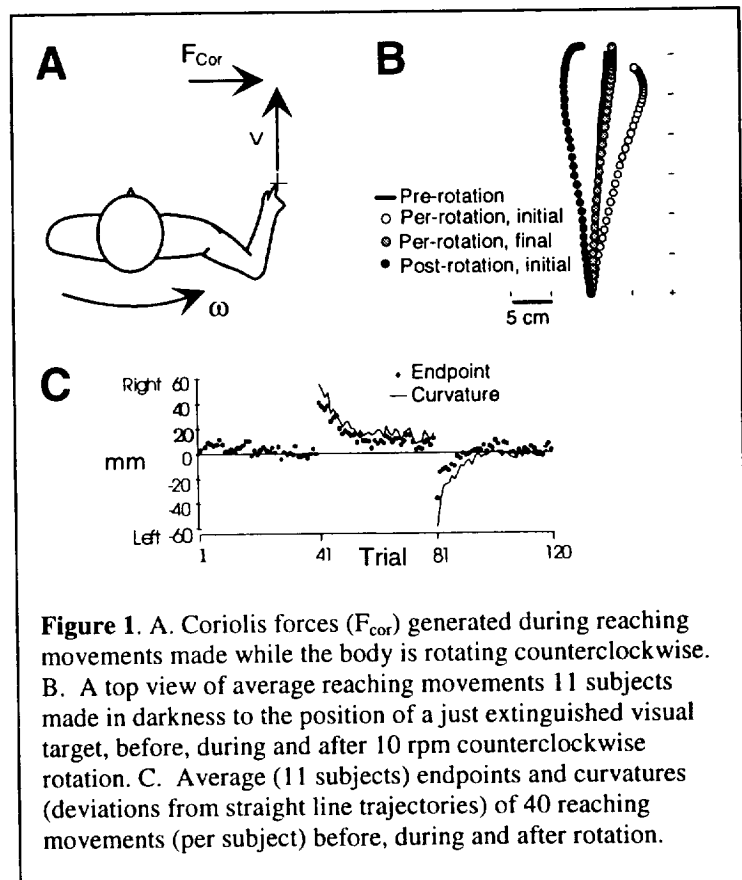
P.DiZio, J.R. Lackner. Ashton Graybiel Spatial Orientation Laboratory and Volen Center for Complex Systems, Brandeis University MS033, Waltham, MA 02254-9110.

INTRODUCTION

One obstacle to the idea of rotating a space vehicle to generate artificial gravity is concern about the side effects of rotation on human sensorimotor control. The most conspicuous side effects in a rotating room are the severely disorienting and nauseogenic consequences of head movements at high room speeds. In early experiments, adapting people to tolerate head movements at rotation rates greater than 3 rpm required great effort and resulted in powerful aftereffects upon return to a non-rotating environment (Guedry, et al., 1964). Generating 1 g of artificial gravity at 3 rpm requires a radius of about 100 meters, which is technically and financially unrealistic (Nicogosian & McCormack, 1987). Approaches to adapting humans to tolerate higher rates of rotation have focussed on vestibular mechanisms. We have investigated the effects of linear Coriolis forces generated in a rotating environment on voluntary arm and leg movements as well as on head movements and posture. The results indicate that adaptation up to 10 rpm can be achieved if exposure history is appropriately controlled.

ARM MOVEMENTS

We have studied subjects making reaching movements before during and after constant velocity 10 rpm counterclockwise (CCW) rotation, in the center of a rotating room. They reached to a light that shone through a translucent table and went off at movement onset, leaving them in total darkness. During rotation, moving the arm or any other appendage generates Coriolis forces proportional to limb velocity, $\vec{F}_{Cor} = -2m(\vec{\omega} \times \vec{v})$, where m is the mass of the moving appendage, \vec{v} its linear velocity and $\vec{\omega}$ the angular velocity of the rotating environment in radians/sec. This means there is not a Coriolis force acting at the very beginning nor at the very end of a movement, but while the arm is extending forward a Coriolis force acts on it, rightward during CCW rotation. (See Figure 1A.) Neither sensory signals about rotation nor significant centrifugal forces are present during constant velocity rotation on subjects in the center of the room, so they feel like they are stationary in a 1 g environment



before reaching.

We found that subjects' first movements during rotation were abnormally curved and missed the target in the direction of the Coriolis force. Even without sight of their arm subjects adapted completely in 10-20 reaches so that their movements again went straight to the target location. At first they felt they were fighting an external force but when adapted they no longer felt the existence of the Coriolis force acting on their arm. Adaptation was more rapid and complete if at the end of each reach subjects touched down on the table although its surface did not demarcate the target. When rotation ceased, subjects again made reaching errors with the adapted arm, mirror-image to the trajectory and endpoint errors that had originally occurred during rotation. Re-adaptation restored straight accurate reaches at the same rate as adaptation to rotation had. See Figures 1B and 1C, from DiZio & Lackner, 1995.

Perturbations of arm movements were present at rotation speeds of 2.5 to 20 rpm, and there was rapid, complete adaptation at all speeds. If sight of the arm was permitted, Coriolis forces still caused initial errors and aftereffects, but adaptation was more rapid than in darkness. Subjects without vestibular function showed similar patterns of Coriolis force perturbation to normals but adapted less fully. Adaptation of one arm during rotation transferred partially to the arm that was immobile during rotation.

These experiments prove that earlier experiments in rotating artificial gravity environments greatly underestimated the capacity for limb movement adaptation. Cutaneous cues from the finger landing on a surface are crucial for adaptation of movement endpoint. Subjects can adapt reaching movements rapidly to rotation rates much faster than any that would be considered for generating artificial gravity in a spacecraft. Recent experiments on subjects in parabolic flight and at the periphery of the rotating room have validated the original results for predicting effects of rotation in non-1g force backgrounds (Lackner and DiZio, 1998).

LEG MOVEMENTS

We have also studied leg movement control and adaptation in a similar paradigm. Subjects holding hand rails stood on one leg at the center of the rotating room and pointed with the other foot to a visual target on the floor that was extinguished at movement onset. When the room was rotating 10 rpm CCW, rightward Coriolis forces were generated and the movement path and endpoint were deviated right. Adaptation occurred within 20 movements during rotation, followed by symmetric aftereffects and re-adaptation when rotation stopped.

HEAD MOVEMENTS

Previous studies of head-eye coordination and spatial disorientation in a rotating room emphasized vestibular effects and neglected the Coriolis force actions on the head/neck system. We have made the first kinematic measurements of unconstrained pitch head movements during constant velocity rotation, showing perturbations and rapid adaptation. The perturbations involved lateral translatory deviations of path and endpoint as well as deviations in roll in the direction of Coriolis forces on the head. The lateral translations adapted often within 8 movements but the roll component of adaptation was incomplete after 24 movements. These results suggest there are dual adaptation processes involving rapid motor adjustments analogous to arm and leg adaptation to Coriolis forces on the head/neck system and a slower adaptation to

vestibular cross-coupled stimulation. Overall functional adaptation may be hastened with controlled exposures that sequentially engage each sub-system.

POSTURE CONTROL

In the rotating room, standing quietly is difficult because of vestibular cross-coupling stimulation and Coriolis forces on the body generated by small random sway movements. We have tested subjects in the center of the rotating room attempting to stand "as stable as possible" with eyes closed and feet placed in tandem. They alternated using light touch (less than 40 grams) of the finger on a stable surface or no touch. Touch approximately halved the normal pre-rotation sway. During 10 rpm rotation subjects without touch swayed to the limits of stability and had to grab the safety rails for support. With touch, rotation did not increase sway over the baseline period. Even patients lacking vestibular function could stand with light touch in darkness during rotation. After only eight 25 sec rotation trials without touch, postural sway post-rotation without touch was significantly greater than baseline. Light touch suppressed this aftereffect. These results show that a highly integrative task like stance adapts quickly to rotation if the proper sensory cues are provided.

CONCLUSIONS

All the movements studied adapt rapidly to 10 rpm rotation. Even head movements and posture may be fully compensated for rotation up to 10 rpm if the proper adaptation schedules and sensory cues are provided. Light, precision contact is effective for suppressing the effects of making transitions between rotating and non-rotating environments as well as hastening adaptation. Context-specific adaptation is also possible to facilitate transitions between force environments without any adjustment period (Cohn, DiZio & Lackner, forthcoming). Thus, human sensorimotor control is not an obstacle to a relatively short radius space vehicle (20-40 meters) spinning fast enough to provide the benefits of artificial gravity.

REFERENCES

- Cohn, J., DiZio, P., Lackner, J.R. Reaching during virtual rotation: context-specific motor compensations for apparent self-displacement. Submitted to *J Neurophysiol*.
- DiZio P., Lackner, J.R.. Motor adaptation to Coriolis force perturbations of reaching movements: endpoint but not trajectory adaptation transfers to the non-exposed arm. *J. Neurophysiol.*, 72:299-313, 1994.
- Guedry, F.E., Kennedy, R.S., Harris, C.S., Graybiel, A.. Human performance during two weeks in a room rotating at 3 rpm. *Aerospace Med.*, 35:1071-1082, 1964.
- Lackner J., DiZio, P. Gravitoinertial force background level affects adaptation to Coriolis force perturbations of reaching movements. *J Neurophysiol.*, 80: 546-553, 1998.
- Nicogossian, A.E., McCormack, P.D.. Artificial gravity - a countermeasure for zero-gravity. IAF/IAA-87-533, Proceedings of the 38th Congress of the International Astronautical Federation, 1987.

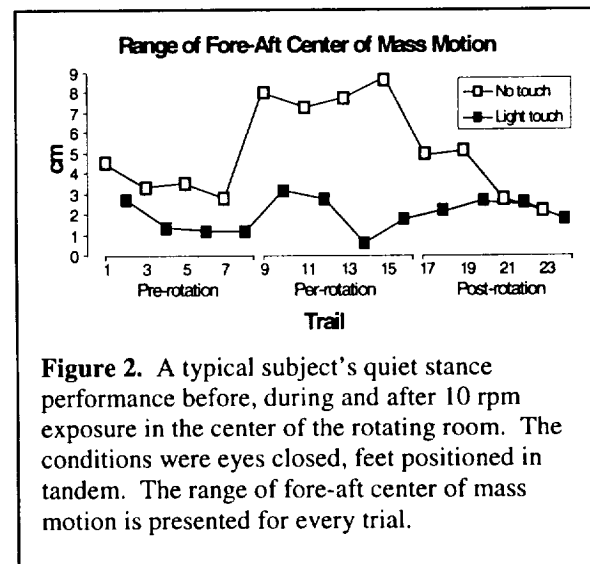


Figure 2. A typical subject's quiet stance performance before, during and after 10 rpm exposure in the center of the rotating room. The conditions were eyes closed, feet positioned in tandem. The range of fore-aft center of mass motion is presented for every trial.

SYMPATHETIC EFFERENT ACTIVITY IS DRIVEN BY OTOLITH STIMULATION

H. Kaufmann¹, I. Biaggioni², A. Voustaniuk¹, A. Diedrich², F. Costa², R. Clark³, M. Gizzi³, and B. Cohen¹

¹Mount Sinai School of Medicine, NY, NY; ²Vanderbilt University, Nashville, TN; ³JFK Neuroscience Institute, Edison, NJ

INTRODUCTION

This study was designed to test the hypothesis that stimulation of vestibular otolith organs in humans activates sympathetic outflow. A vestibular-autonomic reflex triggered by changes in posture or gravity has been postulated. This reflex produces changes in heart rate and vascular tone that are important in the maintenance of blood flow to the brain, particularly during orthostatic stress. In the vestibular apparatus, semicircular canals sense angular acceleration and otolith organs, sense translation and tilt of the head with regard to gravity, i.e., they are gravireceptors. Thus, otolith organs are the ones likely to trigger a reflex mechanism that maintains cerebral blood flow against gravity during orthostasis. Accordingly, in this study we investigated whether selective stimulation of the otolith organs activates sympathetic efferents.

METHODS

To stimulate the otolith organs selectively we used off-vertical axis rotation (OVAR) at constant velocity. Otolith receptors were sinusoidally activated by rotating subjects, in yaw, about an axis tilted 15 degrees from the vertical. At the onset of OVAR, semicircular canals are also activated but when constant velocity is achieved, all canal influences disappear, and only otolith receptors are activated. Rotation around a vertical axis at constant velocity produces no vestibular activity and was used as a control condition. We monitored blood pressure (Portapress), ECG from precordial leads, respiration (Respirace), and muscle sympathetic nerve activity (MSNA) in the right peroneal nerve, using a miniaturized microneurography device, in eight normal subjects. Eye movements were recorded to determine periods of constant velocity (no semicircular canal induced nystagmus). Experimental conditions, each lasting six minutes, were on-axis and OVAR tilted 15° clockwise rotations at 60°/s. Three subjects were also tested at lower (24°/s) and higher (110°/s) angular velocities. Acceleration and deceleration were 240°/s². Data were processed according to the Berger algorithm and treated with lowpass filter at 40 Hz. R-R, systolic and diastolic blood pressure and respiratory frequency were analyzed for their mean values and power spectral density (Blackman Tukey with linear detrending, 4 Hz resolution). Frequency bands were set at: 0-0.07 Hz (very low frequency), 0.07-0.148 Hz (low frequency), and 0.148-0.301 Hz (high frequency).

RESULTS

As compared to control, during OVAR, RR intervals were significantly shorter (916 ± 46 vs. 840 ± 46 ms, $p < 0.02$), heart rate was higher ($p < 0.02$), rate of respiration was lower ($p < 0.01$) and peak power spectral density in the low frequency band was higher ($t(7) = 2.52$, $p < 0.05$). There were no significant changes in systolic or diastolic blood pressure or their associated spectra during OVAR. A new RR spectral peak at 0.16 Hz (the speed of chair rotation) occurred during OVAR, but not during on-axis rotation. OVAR triggered sinusoidal bursts of MSNA synchronous with the head-up position during each chair rotation. In the subjects tested at lower and higher chair angular velocities, bursts of MSNA also occurred synchronous with the head-up position during OVAR.

CONCLUSION

A higher heart rate and RR interval spectral power in the low frequency band during OVAR suggest that stimulation of the otolith organs increase sympathetic efferent activity to the heart. Further, the appearances of a new RR interval spectral peak at the frequency of otolith stimulation suggest otolith-driven modulation of autonomic outflow to the heart. Finally, microneurography showed sinusoidal increases of MSNA synchronous with pitch up position during OVAR, indicating that sympathetic efferent activity to the legs is also driven by otolith receptors sensitive to linear acceleration along specific axes.

ANTICIPATORY POSTURAL ACTIVITY DURING LONG-DURATION SPACE FLIGHT

C. S. Layne¹, A.P. Mulavara², P.V. McDonald³, C.J. Pruett⁴, B. Koslovskaya⁵, J.J. Bloomberg⁶

¹Department of Health and Human Performance, University of Houston, Houston TX, 77204,

²Wyle Life Sciences, ³Nascent Technologies, ⁴TECMATH, ⁵Institute of Biomedical Problems,

⁶Life Sciences Research Laboratories, NASA-JSC

INTRODUCTION

Somatosensory input has been used to modify motor output in many contexts (Sabbahi et al, 1981, Rogers et al., 1996, Shumway-Cook et al, 1997). During space flight, the use of the lower limb musculature is much less than during activities in 1g. Consequently the neuromuscular activity of the legs is also reduced during space flight. This decrease in muscle activity contributes to muscle atrophy. Furthermore, adaptations to weightlessness contribute to posture and locomotion problems upon the return to Earth. Providing techniques to counter the negative effects of weightlessness on the neuromuscular system is an important goal, particularly during a long-duration mission. Previous work by our group has shown that lower limb neuromuscular activation that normally precedes arm movements in 1g is absent or greatly reduced during similar movements made while freefloating (Layne and Spooner, 1990). However, preliminary evidence indicates that applying pressure to the feet results in enhanced neuromuscular activation during rapid arm movements performed while freefloating (Layne et al., 1998). This finding suggests that sensory input can be used to "drive" the motor system to increase neuromuscular functioning throughout a mission. The purpose of this investigation was to quantify the increase in neuromuscular activation resulting from the application of pressure to the feet.

METHODS

The subjects for this study were 6 crewmembers who flew aboard the Mir space station for 3-6 months. The subjects performed rapid right shoulder flexions during two freefloating conditions. During one condition the subjects wore specially constructed "boots" that contained pneumatic bladders and sole inserts. During the "with pressure" condition the boots were inflated to provide pressure to the feet during the arm movement. The other condition consisted of arm movements made "without pressure". Surface electromyography (EMG) was collected from the right anterior deltoid, biceps femoris, gastrocnemius, rectus femoris, tibialis anterior and the left paraspinals and biceps femoris. An accelerometer, secured to a wrist splint on the right arm, was used to obtain arm movement metrics. During the flight, data were stored on cassette tapes and A/D converted upon return to Earth. Prior to the missions, baseline data was collected during arm movements performed while standing.

The raw data were digitally sampled at 500 Hz, filtered and full-wave rectified prior to storage. The onset of arm acceleration was used to separate the data into trials consisting of data 300 ms prior to movement initiation and 50 ms after the cessation of arm movement. To facilitate statistical analysis, the individual data trials were reduced to files containing 50 samples. Each sample represented the average of approximately 16 ms of data. Group mean waveforms and standard deviations for all muscles and arm acceleration were computed. To determine if foot pressure resulted in enhanced neuromuscular activation, the mean muscle waveforms obtained from each condition were compared using Student's t tests. Pearson r correlation coefficients

were used to compare the phasic features of the "with" and "without" pressure waveforms and the "baseline" waveforms collected in the laboratory prior to flight.

RESULTS

All lower limb musculature, with the exception of the rectus femoris, displayed increased neuromuscular activation during the "with pressure" arm movements. There were no changes in the mean amplitude of the anterior deltoid and paraspinals. The phasic features of muscle activation were very similar across all three conditions, as indicated by high correlation coefficients.

DISCUSSION

The results of this investigation verify that foot pressure increases lower limb neuromuscular activation during arm movements made while freefloating. During ground-based testing, neuromuscular activity is positively correlated with arm acceleration. The increases in muscle activity observed in this study were present despite the fact that arm acceleration remained unchanged with the addition of foot pressure. Thus, the enhancement of muscle activity during the "with pressure" condition suggests it is the increase in sensory input associated with foot pressure that "drives" the additional motoneuronal activation. The high correlations across the conditions indicate that the neuromuscular synergies that support coordinated arm movements in 1g are sustained in weightlessness. However, without foot pressure, there is minimal muscle activation, that is greatly enhanced with the addition of pressure. These results suggest that in the future, a device that provides enhanced sensory input could be used to increase muscle activation throughout a long-duration mission.

REFERENCES

- Layne, C.S. and B.S. Spooner. EMG Analysis Of Human Postural Responses During Parabolic Flight Microgravity Episodes. *Aviation, Space and Environmental Medicine* 60: 994-998, 1990.
- Layne, C.S., Mulavara, A.P., Pruett, C.J., McDonald, P.V., Kozlovskaya, I.B., Bloomberg, J.J. The Use Of Inflight Foot Pressure As A Countermeasure To Neuromuscular Degradation. *Acta Astronautica* 42(1-8) 231-246, 1998.
- Rogers, M.W., Cain, T.D., Hanke, T.A. Enhancement of Anticipatory Postural Adjustments Due To An Electrocutaneous Reaction Stimulus For Step Initiation Among Elderly Human Subjects. *Society for Neuroscience Abstracts* 726.9, 1997.
- Sabbahi, M.A., DeLuca, C.J., Powers, W.R. (1981) Topical anesthesia: A Possible Treatment For Spasticity. *Archives of Physical Medicine and Rehabilitation* 62: 310-314.
- Shumway-Cook, A., Woollacott, M. Attentional Demands Of Posture Control: The Effect of Sensory Context and Cognitive Demand. *Society for Neuroscience Abstracts* 610:10., 1997.

OTOLITH-OCULAR TORSION IS MODIFIED IN NOVEL G STATES

Charles H. Markham and Shirley G. Diamond
University of California, Santa Barbara, Santa Barbara, CA

The inner ear otolith system responds to linear acceleration including gravity. Its main motor control function is stabilizing the neck, axial musculature and limbs to maintain posture. It also modulates ocular torsion, giving a window to view the otolith system in ways not possible in viewing the spinal reflexes.

Otolith-ocular torsion, when examined binocularly, is especially sensitive to novel changes in G as observed during parabolic flight and in spaceflight. Under these conditions, life-long compensation to possible asymmetries in this bilateral system may become decompensated and at least four unusual responses may be seen.

- (1) Ocular torsional disconjugacy, increasing over increasing parabolas has allowed prediction of who has or has not had previous motion sickness. Use of this test by NASA could lead to better prophylactic treatment (an exclusionary test) since it is known that most of the 60-70% who develop space motion sickness nevertheless perform well after the first 3-4 days of flight.
- (2) Changes in binocular ocular torsion in the 0 G and 1.8 G portions of parabolic flight reveal in most subjects a systematic reversal of direction. The reversal is consistent within subjects, but not across subjects. We suggest this phenomenon is due to the responsible hair cells being deflected first in one direction and then in the opposite direction. We do not know the location of the critical hair cells but plan appropriate experiments.
- (3) Parabolic flights in the Ilyushin and Caravelle aircraft have 3-5 minutes of level 1 G between each parabola. Binocular torsion in most subjects becomes disconjugate and offset from pre-parabola values in the first parabola and this persists for the remainder of the flight. It is best seen in the intervals between parabolas. We suggest the abrupt G changes experienced in the first parabola causes otoconial displacement or other end organ instability.
- (4) In one and six months spaceflights in three cosmonauts, ocular torsion was dis-conjugate and offset by several degrees compared to preflight reference values. On return to earth, torsional disconjugacy and offset persisted for weeks to months. Such long duration changes in the otolith-ocular reflex have unknown impact in humans during and after long-duration spaceflight.

A METHODOLOGY FOR INVESTIGATING ADAPTIVE POSTURAL CONTROL

P. V. McDonald, G. E. Riccio, Nascent Technologies, Houston, TX.

INTRODUCTION

Our research on postural control and human-environment interactions [1-6] provides an appropriate scientific foundation for understanding the skill of mass handling by astronauts in weightless conditions (e.g., extravehicular activity or EVA) [7]. We conducted an investigation of such skills in NASA's principal mass-handling simulator, the Precision Air-Bearing Floor, at the Johnson Space Center. We have studied skilled movement-body within a multidisciplinary context that draws on concepts and methods from biological and behavioral sciences (e.g., psychology, kinesiology and neurophysiology) as well as bioengineering. Our multidisciplinary research has led to the development of measures, for manual interactions between individuals and the substantial environment, that plausibly are observable by human sensory systems [8-10]. We consider these methods to be the most important general contribution of our EVA investigation.

We describe our perspective as control theoretic because it draws more on fundamental concepts about control systems in engineering than it does on working constructs from the subdisciplines of biomechanics and motor control in the bio-behavioral sciences. At the same time, we have attempted to identify the theoretical underpinnings of control-systems engineering that are most relevant to control by human beings [11]. We believe that these underpinnings are implicit in the assumptions that cut across diverse methods in control-systems engineering, especially the various methods associated with "nonlinear control," "fuzzy control," and "adaptive control" in engineering. Our methods are based on these theoretical foundations rather than on the mathematical formalisms that are associated with particular methods in control-systems engineering.

The most important aspects of the human-environment interaction in our investigation of mass handling are the functional consequences that body configuration and stability have for the pick up of information or the achievement of overt goals. It follows that an essential characteristic of postural behavior is the effective maintenance of the orientation and stability of the sensory and motor "platforms" (e.g., head or shoulders) over variations in the human, the environment and the task [1]. This general skill suggests that individuals should be sensitive to the functional consequences of body configuration and stability. In other words, individuals should perceive the relation between configuration, stability, and performance so that they can adaptively control their interaction with the surroundings [4].

Human-environment interactions constitute robust systems in that individuals can maintain the stability of such interactions over uncertainty about and variations in the dynamics of the interaction. Robust interactions allow individuals to adopt orientations and configurations that are not optimal with respect to purely energetic criteria. Individuals can tolerate variation in postural states, and such variation can serve an important function in adaptive systems. Postural variability generates stimulation which is "textured" by the dynamics of the human-environment system [1, 5, 10]. The texture or structure in stimulation provides information about variation in

dynamics, and such information can be sufficient to guide adaptation in control strategies. Our methods were designed to measure informative patterns of movement variability.

METHODS

In prior research, we demonstrated that informative patterns of movement variability can be observed with videography [1] and accelerometry [3]. In our EVA investigation, we measured the position and motion of various body segments with both videography and accelerometry. We also measured forces and torques on the support surface and at the manipulandum [9]. We have developed methods for analysis of such kinematic and kinetic data that are grounded in psychophysics and neurophysiology. Sampling rates were based on the bandwidth of various sensory systems (e.g., cutaneous, vestibular) or the bandwidth for specific dimensions of sensitivity within each sensory system (e.g., at least up to 50 Hz, and as high as 500 Hz, for proprioception and kinesthesia). Activity within dimensions of stimulation was summarized or reduced to (temporally) global parameters for data distributions (e.g., location, spread, asymmetry) that are robust to noise or fuzzy observation. These global parameters were "updated" at rates that are based on the bandwidth of the task-relevant action systems (e.g., 2 Hz for postural control).

Data reduction that leads to global parameters for action-relevant update intervals is the most novel aspect of our methodology [1, 9]. The standard deviation (SD) of acceleration (anterior-posterior and yaw) was the key measure of shoulder stability for each 0.5 s update interval [2-5]. The within-update SD of sagittal torque at the support surface was the key measure of overall postural stability. The within-update SD of corner position was the key measure of stability of the manipulandum [1]. The within-update skewness of acceleration was the key measure of departure from equilibrium [3-6]. These parameters could be compared, across update intervals, to postural configuration which was measured in terms of upper-body and lower-body angles [1, 4]. These parameters could be the basis of an evaluation function for robust and adaptive control of posture [4].

Quadratic response-surface regression was used to summarize the topological patterns in the relationships between postural configuration and either postural stability, postural equilibrium, or manual stability. We consider the topological landmarks (e.g., attractors and separatrices) that emerge in these configuration spaces to be fundamental to observability and controllability in the postural control system because they would tend to be invariant over adaptation and fatigue in the perception and action systems [1, 4]. Distance-weighted-least-squares (DWLS) regression was used to characterize "noise" that could obscure the topological (i.e., quadratic) patterns.

RESULTS

The quadratic fits in the EVA investigation, while relatively weak (e.g., multiple-R only as high as 0.28), indicate that topological patterns of movement variability are observable over systematic changes in body configuration and during interactions with the substantial environment [9]. The regression fits also allow us to characterize the relative amount of variance accounted for as "signal-to-noise" (S/N) ratios for observation of the topological patterns. In general the results reveal S/N in the range from -20 to -10 dB. By way of analogy, these S/N are comparable to thresholds for detection and recognition, respectively, of patterns in noise by the auditory and visual systems. This seems appropriate because we consider the conditions of the

EVA investigation to be at the limits of proprioception and kinesthesia. The quadratic relationships that we have seen under less constrained conditions of observation [4] have been considerably stronger (e.g., multiple-R as high as 0.81).

CONCLUSION

We believe that the resulting methods of data analysis and representation, along with the associated measurement system, provide an anthropomorphically valid approach to the qualitative analysis of human movement and skill. As with human skill, this approach is adaptable to a wide range of situations including those that approach the limits of observability (e.g., measurement and evaluation in noisy or impoverished conditions).

Operationally this investigation promoted a better understanding of the whole-body skill of extravehicular mass-handling and, thus, it can help crewmembers convey their knowledge and experience about EVA for the purposes of training and planning for future missions. The investigation also promoted a better understanding of simulator fidelity with respect to mass-handling and, thus, it can lead to improvements or developments in simulators used to train and plan for future missions. Finally, the investigation expedited the development of measurement techniques that will be utilized in the evaluation and rapid prototyping of advanced space suits.

REFERENCES

1. Riccio, G. (1993). Information in movement variability about the qualitative dynamics of posture and orientation. In K. Newell (Ed.), Variability and Motor Control, pp. 317-357, Champaign, IL: Human Kinetics.
2. Riccio, G.E., Martin, E.J., & Stoffregen, T.A. (1992). The role of balance dynamics in the active perception of orientation. Journal of Experimental Psychology: Human Perception and Performance, 18, pp. 624-644.
3. Riccio, G., Lee, D., & Martin, E. (1993). Task constraints on postural control. In S.S. Valenti (Ed.), VIIth International Conference on Event Perception and Action, pp. 306-310. Vancouver Canada: Erlbaum.
4. Riccio, G. & Stoffregen, T. (1988). Affordances as constraints on the control of stance. Human Movement Science, 7, pp. 265-300.
5. Riccio, G.E., & Stoffregen, T.A. (1991). An ecological theory of motion sickness and postural instability. Ecological Psychology, 3, pp. 195-240.
6. Stoffregen, T. & Riccio, G. (1988). An ecological theory of orientation and the vestibular system. Psychological Review, 96, pp. 1-12.
7. Riccio, G.E. McDonald, P.V., Peters, B.T., Layne, C.S., & Bloomberg, J.J. (1997) Understanding Skill in EVA Mass Handling: Part I: Theoretical & Operational Foundations. NASA Technical Paper 3684. Johnson Space Center, Houston, TX.
8. McDonald, P.V., Riccio, G.E., Peters, B.T., Layne, C.S., & Bloomberg, J.J. (1997) Understanding Skill in EVA Mass Handling: Part II: Empirical Investigation. NASA Technical Paper 3684. Johnson Space Center, Houston TX.
9. McDonald, P.V. & Riccio, G.E. (1998). Evaluating postural control with movement variability. Society for Neuroscience Abstracts, V24.
10. Riccio, G.E. & McDonald, P.V. (1998). Understanding Skill in EVA Mass Handling: Part III: Empirical Developments and Conclusions. NASA Technical Paper 3684. Johnson Space Center, Houston TX.

11. Riccio, G.E. & McDonald, P.V. (1998). Multimodal Perception and Multicriterion Control of Nested Systems: I. Coordination of Postural Control and Vehicular Control. NASA Technical Paper 3703. Johnson Space Center, Houston TX.

This work was supported by NASA grant 199-16-11-48 and the NSBRI.

LOW-FREQUENCY OTOLITH FUNCTION IN MICROGRAVITY: A RE-EVALUATION OF THE OTOLITH TILT-TRANSLATION REINTERPRETATION (OTTR) HYPOTHESIS

Steven T. Moore¹, Bernard Cohen¹, Gilles Clement² and Theodore Raphan³

¹Mt Sinai School of Medicine, NY NY, ²CNRS, Toulouse, France, ³Brooklyn College, CUNY.

INTRODUCTION

On Earth, the low-frequency afferent signal from the otoliths encodes head tilt with respect to the gravitational vertical, and the higher frequency components reflect both tilt and linear acceleration of the head. In microgravity, static tilt of the head does not influence otolith output, and the relationship between sensory input from the vestibular organs, and the visual, proprioceptive and somatosensory systems, would be disrupted. Several researchers have proposed that in 0-g this conflict may induce a reinterpretation of all otolith signals by the brain to encode only linear translation (otolith tilt-translation reinterpretation or OTTR) [1, 2]. Ocular counter-rolling (OCR) is a low-frequency otolith-mediated reflex, which generates compensatory torsional eye movements (rotation about the visual axis) towards the spatial vertical during static roll tilt with a gain of approximately 10%. Transient linear acceleration and off-axis centrifugation at a constant angular velocity can also generate OCR. According to the OTTR hypothesis, OCR should be reduced in microgravity, and immediately upon return from a 0-g environment. Results to date have been inconclusive. OCR was reduced following the 10 day Spacelab-1 mission in response to leftward roll tilts (28-56% in 3 subjects and unchanged in one subject), and sinusoidal linear oscillations at 0.4 and 0.8 Hz [3, 4]. OCR gain declined 70% in four monkeys following a 14 day COSMOS mission [5]. Following a 30 day MIR mission OCR gain decreased in one astronaut, but increased in two others following a 180 day mission [6]. We have studied the affect of microgravity on low-frequency otolith function as part of a larger study of the interaction of vision and the vestibular system. This experiment (E-047) involved off-axis centrifugation of payload crewmembers and flew aboard the recent Neurolab mission (STS 90). Presented below are preliminary results focusing on perception and the OCR response during both centrifugation and static tilt.

METHODS

Six subjects, consisting of the payload crew for the Neurolab mission plus the two alternate payload specialists, participated in this study. Subjects were rotated in a short-arm centrifuge in one of three configurations: left-ear-out (LEO), right-ear-out (REO) and lying-on-back (LOB). The chair was positioned such that the subject's head was 0.5 m from the center of rotation in LEO/REO, and 0.65 m in LOB. The chair was accelerated at $26^\circ/\text{s}^2$ over a period of approximately 10 seconds, reaching a constant angular velocity of $253^\circ/\text{s}$ (LEO/REO) and $222^\circ/\text{s}$ (LOB). This resulted in a 1-g centripetal acceleration directed along either the inter-aural (LEO/REO configuration) or dorso-ventral (LOB configuration) axes. A second paradigm utilized a lower constant angular velocity to generate a centripetal acceleration of 0.5-g. On Earth, this centripetal acceleration sums with gravity to tilt the gravito-inertial acceleration (GIA) 45° with respect to the subject's head at 1-g, and 27° at 0.5-g. In microgravity, the GIA is equivalent to the centripetal acceleration. The subject's perception of tilt was obtained from verbal reports approximately 30 seconds after reaching constant angular velocity. Subjects were maintained at constant angular velocity for periods of up to 6 minutes. Binocular eye images

were recorded on videotape and post-processed to obtain three-dimensional eye position in Fick coordinates. The flight centrifuge, eye movement monitor and visual display were developed by the European Space Agency. Centrifugation was carried out pre-flight on all 6 subjects, and in-flight and post-flight on the payload crew. A static tilt chair was used to obtain perceptual and eye movement data in response to static roll tilt two days prior to launch and 2-4 hours after landing.

RESULTS

During 1-g centrifugation, the mean pre-flight perception of static tilt was 35° roll left or right in the LEO/REO position and a pitch backwards of 39° in LOB (Fig. 1A). On flight day (FD) 2 the crew reported that centrifugation felt much the same as on Earth, but with a slightly larger sensation of tilt in LEO/REO (45°), and the LOB orientation felt as if they were close to “upside-down” (70°). By FD 5, the perceived tilt was close to lying-on-side during LEO/REO centrifugation (70°), and upside-down during LOB (75°). Perception of static tilt during 0.5-g centrifugation was also increased in-flight (Fig. 1A). Post-flight, astronauts tended to over-estimate roll (LEO/REO) and pitch (LOB) tilt during centrifugation (Fig. 1A) and static roll tilt (left ear down) in a tilt chair (Fig. 1B). Nine days after landing (R+9) the astronauts' perception of tilt during centrifugation was close to pre-flight values.

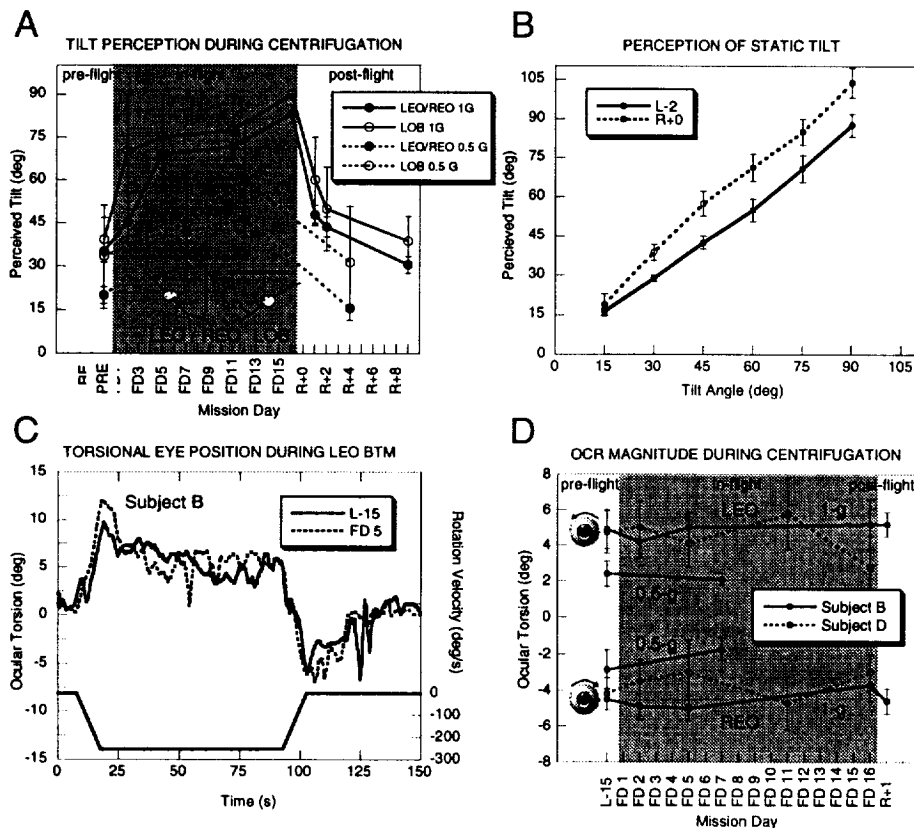


Figure 1. A) Tilt perception (mean ± SE of payload crew) during 1-g and 0.5-g centrifugation in LEO/REO (roll tilt to the left or right) and LOB (pitch backwards). All subjects perceived the

centripetal acceleration stimulus as a tilt. B) Tilt perception (mean \pm SE of payload crew) during static tilt (left ear down) on L-2 and R+0. Subjects consistently overestimated tilt angle after landing. C) Comparison of torsional eye position for subject B during centrifugation in the LEO position back to motion (CCW) on L-15 and FD 5. There was no significant change in the torsional eye position response after 5 days in microgravity. D) Static torsional eye position (mean and SD of a 5 second interval) for subject B and D, acquired 75 seconds into LEO and REO centrifugation runs with 1-g or 0.5-g centripetal acceleration. The magnitude of the OCR response was not significantly affected by exposure to microgravity.

Preliminary right eye movement data from two crewmembers (designated subjects B and D) was consistent with perceptual reports. A comparison of torsional eye position data from subject B during an LEO back-to-motion (CCW) 1-g rotation profile 15 days prior to launch (L-15) and on FD 5 shows little difference between the eye movement response on Earth and in microgravity (Fig. 1C). During constant velocity centrifugation, static ocular torsion is generated by the low-frequency otolith "tilt" response, i.e. OCR. Pre-, in- and post-flight torsional eye position for subject B and pre- and in-flight ocular torsion for subject D was sampled from a 5 s interval approximately 75 s into the LEO and REO rotation profiles (Fig. 1D). No significant change was seen in the magnitude of the OCR response in microgravity compared to pre- and post-flight results. OCR magnitude during 0.5-g centrifugation obtained from a single subject exhibited a similar tendency (Fig. 1D). Although the perception of roll tilt was considerably greater in microgravity than on Earth, the magnitude of the OCR response did not increase.

CONCLUSION

In microgravity, the GIA has the same magnitude and direction as the centripetal acceleration, and "tilt" has no meaning. The 1-g centripetal acceleration, however, is orientated along the inter-aural axis in LEO/REO, which on Earth would be equivalent to 90° "tilt" (i.e. lying on one's side), and along the dorso-ventral axis in LOB, which is equivalent to being upside-down. By FD 5 all crewmembers perceived the centripetal acceleration stimulus in this manner. At no point did the crew perceive this linear acceleration stimulus as a translation. The fact that astronauts perceived the LOB stimulus as -1-g (i.e. they felt as if they were standing on their heads) suggests that central adaptation of the dorso-ventral otolith (primarily saccular) afferent activity in microgravity had resulted in re-calibration to a 0-g bias.

In-flight torsional eye measurements show the existence of a strong OCR response that was similar in magnitude to that measured on Earth. This is consistent with crew perceptual reports of tilt and indicates that the centripetal acceleration was not reinterpreted as a translation, as predicted by the OTTR hypothesis. The inter-aural 1-g centripetal acceleration stimulus applied to the otoliths during centrifugation was constant throughout the mission, on Earth and in microgravity. The OCR magnitude was unchanged in 0-g despite the fact that there was effectively a 90° "tilt" sensed by the otoliths. In-flight OCR magnitude was also proportional to the magnitude of the applied centripetal acceleration in much the same manner as on Earth, which suggests that this result does not represent a saturation of the response. This implies that OCR is largely generated by the utricles, and that utricular function is not affected by microgravity.

These results, although preliminary, indicate that the OTTR hypothesis is incorrect, and that a combination of linear acceleration stimuli applied to the otoliths is sensed as a tilt in microgravity, in much the same manner as on Earth. There appears to be a time course for adaptation of the bias of the portion of the otoliths which sense dorso-ventral acceleration (primarily the saccules) to 0-g in the first few days of space-flight, and a subsequent re-adaptation phase on return to Earth. During this phase, the astronaut's ability to perceive tilts is compromised. This may play a role in post-flight postural and locomotor instability.

1. Parker, D.E., *et al.*, *Aviat Space Environ Med*, 1985. **56**: 601-607.
2. Young, L.R., *et al.*, *Exp Brain Res*, 1986. **64**: 291-298.
3. Vogel, H. and J.R. Kass, *Exp Brain Res*, 1986. **64**: 284-290.
4. Arrott, A.P. and L.R. Young, *Exp Brain Res*, 1986. **64**: 347-357.
5. Dai, M., *et al.*, *Otolaryngol Head Neck Surg*, 1998. **119**: 65-77.
6. Diamond, S.G. and C.H. Markham, *J Vest Res*, 1998. **8**(3): 217-231.
- 7.

This project was supported by NASA Neurolab Contract NAS 9-19441.

HUMAN VISUAL ORIENTATION IN UNFAMILIAR GRAVITO-INTERTIAL ENVIRONMENTS

C. Oman¹, I. Howard², W. Shebilske³, J. Taube⁴, and A. Beall¹

¹Man Vehicle Laboratory, MIT, Cambridge, Massachusetts

²Human Performance Laboratory, York University, Toronto, Canada

³Department of Psychology, Texas A&M University, College Station, Texas

⁴Department of Psychology, Dartmouth College, Hanover, New Hampshire

INTRODUCTION

The vestibular, visual, tactile, and proprioceptive senses provide the essential cues necessary for spatial orientation and sensory-motor coordination both on Earth and in weightlessness. Space motion sickness associated with neurovestibular adaptation affects early in-flight performance of astronauts arguably more than any other physiological change. Post-flight neurovestibular problems, including earth sickness, disorientation and locomotor ataxia increase in severity with flight duration. In the fall of 1997, the National Space Biomedical Institute Neurovestibular Adaptation Team initiated three projects to help define the mechanisms, and to develop improved neurovestibular countermeasures for use in NASA's Space Station and future Planetary exploration programs. These include the present multi-investigator, inter-institutional project on human visual orientation, and also two other projects presented at this meeting (Shelhamer, et al's study of context-specific adaptation of gravity-dependent reflex responses; Wall, et al's investigation of locomotor ataxia, spatial orientation, and gaze stability).

The objective of the Visual Orientation project is to better understand the process of spatial orientation and navigation in unfamiliar gravito-inertial environments, and to use this information to develop effective countermeasures against the orientation and navigation problems experienced by astronauts. Our intrinsic sense of location and direction is ultimately visually determined. On Earth, the gravitational stimulus to our otolith organs, and proprioceptors in skin, muscles and joints strongly influence our sense of "down". In space, the gravitational "down" reference is absent, so our sense of self-orientation is labile. When astronauts work in unpracticed orientations relative to the visual environment, they sometimes misinterpret visual cues from surrounding objects. They experience striking "visual reorientation illusions" (VRIs), and misperceive their own orientation with respect to the environment, usually because the walls, ceiling, and floors of the spacecraft have exchanged subjective identities. VRIs occur because of scene symmetries, and the subconscious assumption that the floor is beneath their feet. Fluid shift and gravireceptor bias also contribute, and make certain astronauts feel continuously inverted. VRIs cause disorientation, reaching errors, trigger attacks of space motion sickness, and potentially complicate emergency escape. MIR astronauts say that at least several weeks of experience in 0-G are required before orientation and navigation become natural, particularly when traversing modules. Crew members learn routes, but most do not develop 3D "survey" knowledge of the station. Are humans more facile at 2-D navigation in the well practiced, gravitationally horizontal plane? Anecdotally, experience in mockups, parabolic flight, neutral buoyancy and virtual reality (VR) simulators helps astronauts orient in 0-g. However, no techniques have been developed to quantify individual differences in orientation and navigation abilities, or the effectiveness of spacecraft-specific or generic preflight visual

orientation training in simulators or virtual reality devices. Our understanding of the underlying physiology of orientation and navigation in 0-g is incomplete. Studies show that animals construct an internal spatial representation of their environment and use this for spatial orientation and navigation. Some of this neural circuitry involves the limbic system. "Head direction" (HD) cells have been found which discharge as a function of the animal's head direction in an earth-horizontal plane. The direction of maximum response ("preferred direction") lies in a fixed direction and varies from cell to cell. It is an important question whether and how HD cells respond in 0-G, in the context of understanding the physiologic basis of 0-G spatial orientation illusions.

METHODS

Spatial orientation in 30 human subjects is being studied in an 8 foot cubic tumbling room at York University, and also in similar virtual environments created using a NASA Virtual Environment Generator (VEG) at MIT. Perceived orientation of the York subjects is also being studied when they lie supine, and view the world through a mirror mounted at 45 degrees above their head. Human 3 dimensional spatial memory and learning performance are being investigated at TAMU using a 4 foot cubic test environment, analagous to a node on the MIR space station, and - to validate the use of VR techniques in astronaut training - also in an equivalent virtual environment at MIT. To study the physiologic basis of 3 dimensional orientation, responses of head direction cells in the anterior thalamic nucleus of unrestrained Long-Evans rats are being quantified as they climb on the floor, walls, and ceiling of a gridded test chamber, both in 1-g, and in 0-g parabolic flight.

RESULTS

Principal results from first year of this project are: 1) Human subjects viewing either a real or virtual room which has strongly polarized visual verticals aligned with the head to foot axis often report feeling subjectively upright, even though they are actually supine or prone. Tests in a real environment confirm this is true for some prone and inverted subjects as well. Supine subjects who extend their arms describe them as feeling weightless. 2) Subjects in the York mirror apparatus describe their head as upright, with their torso subjectively inclined to the horizontal. 3) Subjects learned to correctly predict the relative direction of all 6 targets in an 3 dimensional array which was rotated around the subject into a different orientation after each trial. Learning did not depend on the gravitational orientation of the subject's head. Subjects used a variety of cognitive strategies (e.g. inside out vs. outside in). Results in real (TAMU) and virtual (MIT) environments were comparable. 4) In 0-g parabolic flight, rat head direction cells continue to exhibit directional tuning in the plane of the "floor" of the test chamber. When the animal is placed on the ceiling in 0-g, responses sometimes reversed direction, as would be expected if the animal - like an astronaut - experienced a VRI. To quantify the 3-D tuning of HD cells in our 1-G Dartmouth laboratory, we have successfully trained animals to crawl successively on the gridded ceiling, wall, and floor of a special test enclosure.

CONCLUSIONS

Appropriate real or virtual visual cues can create compelling illusions of static orientation which may prove useful in simulation. 3D spatial learning depends on the cognitive strategy used by the subject, and appears to transfer across gravitational head orientation. VR techniques may be useful for astronaut preflight orientation and navigation training, and in some situations more

practical. Our finding of “ceiling” reversal in preferred direction of some HD cells in parabolic flight represents the first use of an animal model to define the limbic basis of a 0-G orientation illusion.

Supported by the National Space Biomedical Research Institute

MECHANISMS OF SENSORIMOTOR ADAPTATION TO CENTRIFUGATION

W. H. Paloski¹, S. J. Wood², and G. D. Kaufman³

¹Life Sciences Research Laboratories, NASA/Johnson Space Center, Houston, TX, USA 77058,

²National Space Biomedical Research Institute, ³National Research Council

INTRODUCTION

We postulate that centripetal acceleration induced by centrifugation can be used as an inflight sensorimotor countermeasure to retain and/or promote appropriate crewmember responses to sustained changes in gravito-inertial force conditions. Active voluntary motion is required to promote vestibular system conditioning, and both visual and graviceptor sensory feedback are critical for evaluating internal representations of spatial orientation. The goal of our investigation is to use centrifugation to develop an analog to the conflicting visual/gravito-inertial force environment experienced during space flight, and to use voluntary head movements during centrifugation to study mechanisms of adaptation to altered gravity environments. We address the following two hypotheses:

- (1) Discordant canal-otolith feedback during head movements in a hypergravity tilted environment will cause a reorganization of the spatial processing required for multisensory integration and motor control, resulting in decreased postural stability upon return to normal gravity environment.
- (2) Adaptation to this "gravito-inertial tilt distortion" will result in a negative after-effect, and readaptation will be expressed by return of postural stability to baseline conditions.

During the third year of our grant we concentrated on examining changes in balance control following 90–180 min of centrifugation at 1.4 g. We also began a control study in which we exposed subjects to 90 min of sustained roll tilt in a static (non-rotating) chair. This allowed us to examine adaptation to roll tilt without the hypergravity induced by centrifugation. To these ends, we addressed the question: Is gravity an internal calibration reference for postural control? The remainder of this report is limited to presenting preliminary findings from this study.

METHODS

Eighteen healthy adult subjects of both genders were exposed to interaural centripetal acceleration of 1.4 g (resulting in 45° roll tilt) while seated upright on a 0.8 m radius centrifuge for periods of 90 min in the dark. Each subject's head was fixed upright, except when instructed to make head movements (every 4 of 10 min) to track randomly illuminated point-targets (red light emitting diodes) located at $\leq \pm 30$ deg in the Earth horizontal plane. Postural sway and multisegment body kinematics were measured before and ~10 min after the centrifugation using a modified dynamic posturography system (NeuroCom EquiTest) and a three-dimensional video analysis system (Optotrak 3020). Subjects were kept in darkness until after the completion of the post-centrifuge posture tests. Postural data were gathered during six successive twenty second trials throughout which the subject attempted to maintain upright stance while making sequential active pitch and roll head movements with arms-folded, eyes-closed, and support surface sway-referenced (Figure 1). To control for the effect of gravito-inertial force magnitude,

eight of the subjects repeated the protocol during and after static (non-rotating) 45° roll tilt for periods of 90 min in the dark.

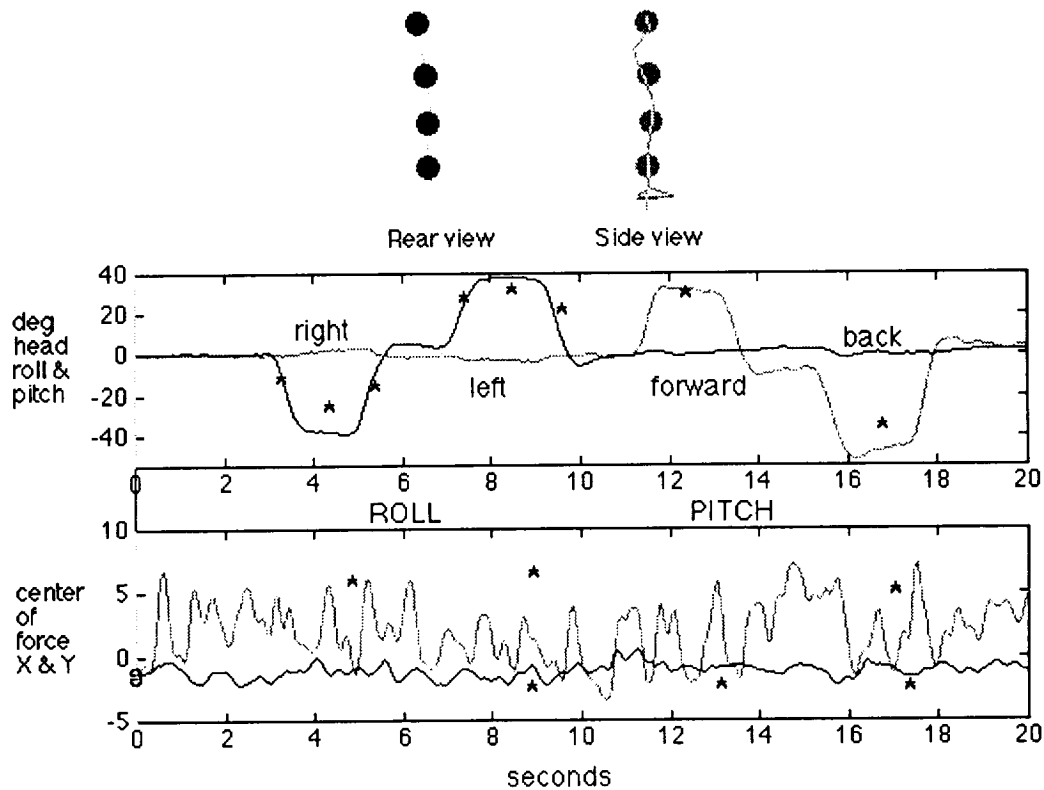


Figure 1. A typical head movement and center of force sway trace of subject motion during the postural test. Asterisks indicate portions of the test where postcentrifuge measures were significantly ($p < 0.05$) lower than pre-test values. Above are rear and side view stick-figures showing multi-segment kinematics.

RESULTS

Ninety minutes of 1.4 g dynamic (centrifuge) roll tilt stimulation in the dark with head movements in the plane of rotation resulted in a transient degradation of postural stability (Figure 2) in the 15 subjects completing the centrifugation protocol. (Three adaptation sessions were aborted after 30 minutes due to motion sickness symptoms—one of these subjects had protracted nausea and was unable to participate in the post-centrifuge posture testing.) The peak antero-posterior sway (p-p sway), sway variance in both antero-posterior (X) and medio-lateral (Y) directions, and the pathlength of the sway during the 20 sec balance test conditions were all significantly increased ($p < 0.05$) following centrifugation. In contrast to these dynamic roll tilt data, ninety minutes of 1.0 g static (non-rotating) roll tilt stimulation in the dark with head movements in the yaw plane resulted in no significant degradation of postural stability in 8 subjects tested (Figure 2).

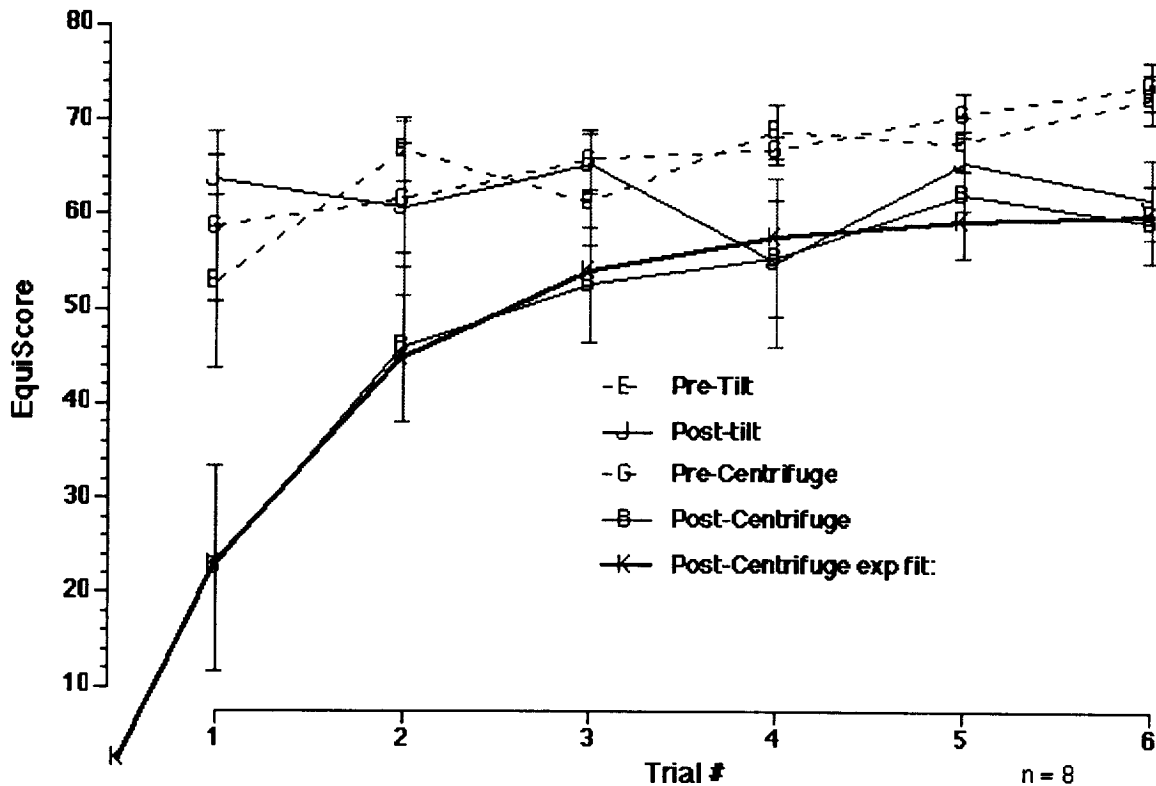


Figure 2. Equilibrium scores($mean \pm sem$; $EquiScore = (1 - p - p \text{ sway} / 12.5) * 100$) before (Pre) and after (Post) the dynamic (Centrifuge) and static (Tilt) roll tilt conditions. The heavy line represents an exponential curve fit to the Post-Centrifuge data.

DISCUSSION

Our preliminary results demonstrate that there was a transient decrease in postural stability immediately following our centrifugation protocol. This is consistent with our hypothesis that discordant canal-otolith feedback during head movements in a hypergravity tilted environment will result in a negative after-effect. In our static roll tilt control condition, the canal-otolith information was not discordant (i.e., the otoliths continued to signal changes in head position relative to a 1g gravitational vector, just as when the subjects were upright). In the hypergravity-tilted environment, however, the otolith afferent input was modified due to the increased shearing force. There is also a possibility that Coriolis effects could have played a role in the dynamic roll tilt adaptation; however these effects were presumably minimal since the head movements during centrifugation were made primarily in the plane of rotation.

We conclude that short arm centrifugation can provide useful environments for studying the mechanisms underlying the central adaptive processes during sustained alterations in gravito-inertial force. Further experiments are needed to verify whether the negative after-effects to the *familiar* gravito-inertial environment could be prolonged by adding discordant visual information to the dynamic roll tilt paradigm and whether subjects can be dual-adapted to different gravito-inertial environments.

SELF-MOTION PERCEPTION: ASSESSMENT BY REAL-TIME COMPUTER-GENERATED ANIMATIONS

Donald E. Parker

Department of Otolaryngology - HNS and Human Interface Technology Laboratory
University of Washington, Seattle, WA 98195

INTRODUCTION

Our overall goal is to develop materials and procedures for assessing vestibular contributions to spatial cognition. The specific objective of the research described in this paper is to evaluate computer-generated animations as potential tools for studying self-orientation and self-motion perception. Specific questions addressed in this study included the following. First, does a *non-verbal* perceptual reporting procedure using real-time animations improve assessment of spatial orientation? Are reports reliable? Second, do reports confirm expectations based on stimuli to vestibular apparatus? Third, can reliable reports be obtained when self-motion description vocabulary training is omitted?

CURRENT STATUS OF RESEARCH

METHODS

18 subjects reported illusory self-motion by generating animations. Subjects seated on chair rotated clockwise or counter-clockwise around their yaw axis at 50 deg/s. While rotating, subjects rolled the head from left to right or vice versa. "Cross-coupling" produced illusory motion. The chair was then stopped and the subjects moved a doll head in which a magnetic field tracker (Polhemus) was embedded so that motion of the virtual head displayed on monitor corresponded to their own perceived head motion. "Real-time" virtual head motion was generated by a PC using WORLD UP (Sense 8) at 24 frames/s. Virtual head-movement data were saved for later analyses by the WORLD UP virtual VCR. *Experiment 1.* 8 subjects performed 3 head motions (upright to roll left, upright to roll right and upright to pitch forward) while rotating either clockwise (CW) or counter-clockwise (CCW). Each of the 6 conditions was replicated once for a total of 12 trials. *Experiment 2.* 10 subjects performed 2 head motions (roll left to roll right and roll right to roll left) while rotating either CW or CCW. Each of the 4 conditions was replicated once for a total of 8 trials.

RESULTS

Two raters summarized the animations for each trial using the pitch, roll, yaw, x-axis, y-axis, z-axis translation nomenclature. Test-retest reliability was 0.50 for Experiment 1 and 0.94 for Experiment 2. Subsequent analysis focused on the illusory pitch component of reported self-motion. Analysis of recorded animations indicated that, contrary to previous reports, illusory self-motion did not corresponded to semicircular canal stimulation.

CONCLUSIONS

The results of this study suggest that a *non-verbal* perceptual reporting procedure using animations may produce reliable data if the set of stimuli is limited and large (90 deg) head motions are used. Perceptual reports did not correspond to expectations based on mechanical stimuli to vestibular apparatus described by Groen (The problems of the spinning top applied to the semicircular canals. *Confinia Neurologica* (Basel). 1961;21:454-5). Guedry reported that

perceptual responses elicited by cross-coupling did correspond to expectations (Psychophysics of vestibular sensation. In HH Kornhuber, *Vestibular System Part 2: Psychophysics, Applied Aspects and General Interpretations, Handbook of Sensory Physiology*, Vol. 6/2. New York: Springer Verlag, 1974. Pp. 3-154). The use of real-time computer-generated animations permits use of naive subjects who lack a motion perception reporting vocabulary; this may partially account for the discrepancy between the findings from the present study and previous ones. The fact that the author always reports illusory pitch in the expected direction supports this suggestion.

PLANS FOR FUTURE INVESTIGATIONS.

We are currently studying the relationship between vertical eye-movement direction and perceptual reports following cross-coupling. We anticipate that eye movements will reflect that mechanical stimulus more accurately than perceptual reports. Numerous reports suggest discrepancies between perceptual reports and vestibular stimulation. This suggests that exploration of perceptual responses with patients might be fruitful. However, development of real-time animations as a clinically useful procedure requires identification of stimuli that evoke in normal subjects consistent responses which differ from those evoked in vestibular disordered patients.

Supported by NASA Grants NAG5-4074 and 9-958

EVIDENCE FOR A RAPID GAIN CHANGE MECHANISM THAT REGULATES HUMAN POSTURAL CONTROL DYNAMICS

R. J. Peterka, Neurological Sciences Institute, Oregon Health Sciences University, Portland, OR

INTRODUCTION

An upright stance position is inherently unstable. A small body sway deviation from a perfect upright position results in a torque due to gravity that accelerates the body farther away from the upright position. To maintain upright stance, the destabilizing torque due to gravity must be countered by corrective torque exerted by the feet against the support surface. This corrective torque is most likely generated through the action of a feedback control system. That is, body motion away from upright is detected by sensory systems, the motion information is processed by the CNS, and the processed signals are used to generate corrective torques that move the body back toward the upright position.

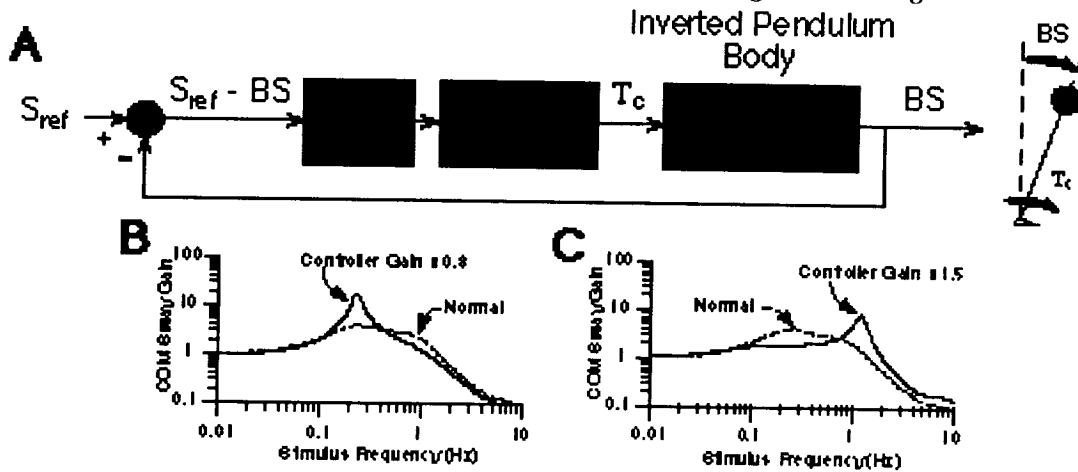
The visual, proprioceptive, and vestibular systems are the primary sensory systems contributing to postural control. However, altered environmental conditions can eliminate or compromise the accuracy of sensory information. Examples include: (1) eye closure or darkness that eliminates visual orientation cues, (2) soft or compliant surfaces that alter proprioceptive information related to the feet and ankle joint motion, and (3) altered vestibular cues due to space-flight induced adaptive changes in the interpretation of vestibular sensory information.

Simulation results from a simple feedback control model of the postural control system (Fig. 1A) suggest that the dynamic properties of body sway can be particularly sensitive to conditions that change body dynamics or change the available sensory information. In this model, the body is represented as an inverted pendulum. A deviation of the body's center-of-mass (COM) position in space, BS , away from upright is detected by sensory systems and a corrective torque, T_c , is generated by a "neural controller." In this representation, the controller includes both the CNS processing of sensory information and the generation of torque by the muscles. The overall postural control dynamics can be represented by a "transfer function" which characterizes the relative amplitude of body sway (COM sway gain) evoked by motion stimuli at varying frequencies. If the gain of the neural controller is reduced to 80% of its "normal" value, the postural system's transfer function shows a resonant peak at about 0.2 Hz (Fig. 1B). If the neural controller gain is increased by 50%, the postural system's transfer function shows a resonant peak at about 1 Hz (Fig. 1C). In general, the presence of a sharp resonant peak indicates that the system is close to instability.

These modeling results suggest that it would be advantageous for the nervous system to be able to rapidly alter its effective controller gain to adjust to changing environmental conditions..

Experimental evidence for such a gain alteration has recently been obtained.

Fig. 1A. Simple feedback model of postural control. **B.** Predicted COM sway gain as a function of stimulus frequency showing the effect of lowering the neural controller gain. **C.** Predicted COM sway gain showing the effect of increasing controller gain.



METHODS

Five normal subjects were tested under changing environmental conditions that potentially required adjustment in their postural system's gain in order to maintain stability. Each subject was constrained to sway as a single-link inverted pendulum by a lightweight backboard support frame. The backboard was attached to the subject by shoulder straps, waist belt, and head rest. The backboard frame rotated about an axis aligned with the subject's ankle joint axis and, therefore, only allowed body sway in the anterior/posterior (AP) direction. The backboard's rotational motion, measured by a potentiometer, provided a measure of the subject's AP COM rotational motion. The subject stood on an instrumented support surface that measured changes in the AP center-of-pressure (COP) associated with body sway.

During portions of a test trial, the support surface was rotated by a servo motor about an axis aligned with the subject's ankle joints. The rotational position command to the servo motor was obtained from the instantaneous position signal from the backboard potentiometer. Therefore the support surface was "sway-referenced" to the subject's body orientation in space. This greatly reduces the proprioceptive cues associated with ankle joint motion that normally are present with body sway on a fixed support surface. In addition, all tests were performed with eyes closed to eliminate visual orientation cues. Therefore during sway-referenced conditions, vestibular orientation cues were providing the major sensory input required for postural control.

Each subject performed a minimum of three test trials. Each trial began and ended with a 60 s period of quiet stance with eyes closed on a fixed support surface. The support surface was sway-referenced during the middle portion of each trial. The duration of the sway-referencing was either 30 s, 120 s, or 300 s. Body sway data were analyzed to determine if oscillatory behavior was present that was consistent with alterations in control system gain as shown in Fig. 1.

RESULTS

Based on the Fig. 1A model, we speculated that when subjects stand on a sway-referenced support surface with eyes closed, the absence of accurate visual and proprioceptive cues effectively reduces the amplitude of the error signal (S_{ref-BS}), causing decreased postural stability. We hypothesized that the nervous system could compensate for this decreased error signal by increasing the gain of the neural controller. A transition from a sway-referenced to a fixed support surface condition would restore accurate proprioceptive cues and, therefore, would increase the error signal amplitude. An increased error signal amplitude coupled with an increased controller gain would result in a control system whose gain was too high, leading to the development of 1 Hz resonant behavior (Fig. 1C). Therefore, experimental evidence showing 1 Hz oscillatory behavior following the end of sway-referencing will support the hypothesis that neural controller gain was increased to compensate for reduced sensory input due to support surface sway-referencing.

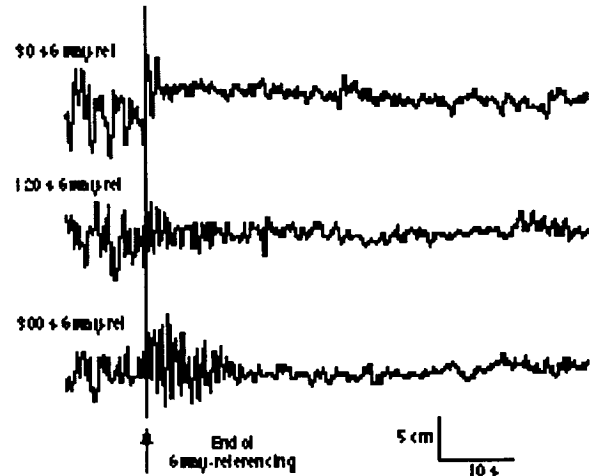


Fig. 2. AP COP data showing 1 Hz oscillations following the end of a test period where the support surface was sway-referenced for varying lengths of time. Eyes were closed throughout all trials to eliminate visual cues.

Fig. 2 shows AP COP recordings from one subject following 30, 120, and 300 s exposures to support surface sway-referencing. The top trace shows about 1 1/2 cycles of an approximately 1 Hz oscillation occurring immediately after the end of 30 s of sway-referencing. This rapid oscillation was quickly replaced by lower amplitude COP signals, consistent with eyes closed quiet stance. This result suggests that the postural control system had increased its gain during sway-referencing and then rapidly decreased its gain (1-2 s response time) back to a value suitable for maintaining quiet, non-resonant stance on a fixed support surface.

Fig. 2 also illustrates that, for this subject, the time required to complete a gain change depended upon the duration of the previous test condition. The lower two traces in Fig. 2 show COP data following exposure to 120 s and 300 s of the eyes closed, sway-referenced surface condition. The duration of ~1 Hz oscillation increased the longer the subject remained in the prior sway-referenced condition. That is, the postural control system became more resistant to switching back to the lower gain necessary to provide good, non-resonant control behavior in the fixed-support surface condition.

All subjects showed ~1 Hz oscillatory responses similar to those seen in Fig. 2 on most trials, although on some individual trials no oscillation was evident or was only weakly present. In addition, one of the subjects showed a gradual increase in oscillatory behavior over the course of testing such that by the end of testing, a sustained oscillation was present throughout the 60 s fixed-surface test periods that preceded and followed the sway-referenced portion of the trial. This sustained oscillation is consistent with an increased controller gain that was slow to return

to lower values required for non-resonant balance control under conditions where both vestibular and proprioceptive cues provide accurate orientation information.

CONCLUSIONS

The results suggest that the human postural control system is capable of rapidly adjusting its gain. This gain modification allows the postural system to alter its dynamic behavior to adapt to changing environmental conditions. The existence of this gain control system implies that the CNS is able to monitor some feature(s) of postural behavior to determine if gain should be increased or decreased. We speculate that detection of the resonant conditions illustrated in Fig. 1 B&C may play a role in determining the direction of gain adjustment. Sensory information indicating excessive 1-2 Hz body sway might trigger a gain reduction, while excessive body sway in the 0.1-0.2 Hz region might trigger a gain increase.

Future experiments will focus on characterizing the properties of this gain control mechanism and on conditions which initiate gain changes. In addition to altered sensory environments, changes in body mass and moment of inertia, and changes in the effective force due to gravity could also be compensated for by altering neural controller gain. Therefore, factors which influence this gain control mechanism could either favorably or adversely affect a subject's ability to adapt to changing environmental conditions.

VISUAL-VESTIBULAR RESPONSES DURING SPACE FLIGHT

M.F. Reschke¹; I.B. Kozlovskaya², and W.H. Paloski¹

¹Nasa Johnson Space Center, Medical Research Branch (SD3), Houston, TX 77058, ²Institute for Biomedical Problems, Moscow, Russia,

INTRODUCTION

Given the documented disruptions that occur in spatial orientation during space flight and the putative sensory-motor information underlying eye and head spatial coding, the primary purpose of this paper is to examine components of the target acquisition system in subjects free to make head and eye movements in three dimensional space both during and following adaptation to long duration space flight. It is also our intention to suggest a simple model of adaptation that has components in common with cerebellar disorders whose neurobiological substrate has been identified.

METHODS

Approximately 30 American astronauts and 6 Russian cosmonauts participated in a series of experiments that investigated head and eye movement responses to spatially and temporally predictable targets. The relevant experiments for this paper included (1) target acquisition, (2) pursuit tracking with eyes alone or with both the head and eyes together, and (3) ocular compensation or gaze stabilization. Horizontal and vertical eye movements were recorded with conventional DC electro-oculographic techniques, and three dimensional head movements were obtained with a triaxial rate sensor system mounted firmly to the head. All inflight measurements were made on U.S. Shuttle flights lasting • 16 days, while pre- and postflight measurements were obtained on both U.S. and Russian Mir flights lasting • 176 days.

RESULTS

Typically an orienting gaze movement initiated to bring a selected part of the visual world onto the fovea consists of an eye movement saccade and a head movement followed by a reflexive compensatory eye movement driven by the VOR and visual fixation responses (VVOR). Unlike the majority of the preflight observations which used a normal sequence of head and eye movements to assist in acquisition of a target, and in spite of evidence for common driver signals to the head and eye, different strategies were used inflight and postflight to bring gaze onto a target. Preflight the responses, even to those targets beyond the EOM were normal. Inflight during the shuttle missions and postflight following the Mir flights target acquisition was accompanied by multiple saccades that could not be interpreted as simple VOR or VVOR responses. These saccades had slow phase slopes with gains that were often greater than 4 or 5. This same phenomena was observed with head and eye smooth pursuit of a predictable 0.33 Hz target, and during smooth pursuit with the eyes alone. During the gaze stabilization measurements end-point nystagmus was observed during the dark phase of the measurement. Taken together, these results suggest that the common path brainstem neural integrator (in conjunction with the appropriate cerebellar structures) may be responsible for what appears to be high gain slow phase eye movements observed in these separate measurements of visual-vestibular interactions. This hypothesis was tested by performing eccentric gaze-holding experiments on those subjects participating in the long duration Mir flights. The results of the eccentric gaze-holding tests clearly showed that when gaze is offset from the primary position centripetal drifts of the eyes with corrective quick phases develops. These results have been

supported by Russian research conducted postflight showing centripetal eye drifts and the effect of gravity on the neural mechanisms responsible for eccentric gaze-holding.

CONCLUSIONS

Clear vision and accurate localization of objects in the environment are prerequisites for reliable performance of motor tasks. Space flight confronts the crew member with a stimulus rearrangement that requires adaptation to function effectively with altered spatial orientation and motor coordination. Adaptation and motor learning driven by the effects of cerebellar disorders may share some of the same demands that face our space travelers. Below is a simple learning model containing components necessary for adaptation to unique inertial environments.

CONTEXT-SPECIFIC ADAPTATION OF GRAVITY-DEPENDENT VESTIBULAR REFLEX RESPONSES (NSBRI NEUROVESTIBULAR PROJECT 1)

Mark Shelhamer¹, Jefim Goldberg², Lloyd B. Minor¹, William H. Paloski³, Laurence R. Young⁴, and David S. Zee¹

¹Johns Hopkins University School of Medicine, Baltimore MD, ²Baylor College of Medicine, Houston TX, ³NASA Johnson Space Center, Houston TX, ⁴MIT, Cambridge MA

INTRODUCTION

Impairment of gaze and head stabilization reflexes can lead to disorientation and reduced performance in sensorimotor tasks such as piloting of spacecraft. Transitions between different gravito-inertial force (gif) environments – as during different phases of space flight – provide an extreme test of the adaptive capabilities of these mechanisms. We wish to determine to what extent the sensorimotor skills acquired in one gravity environment will transfer to others, and to what extent gravity serves as a context cue for inhibiting such transfer.

We use the general approach of adapting a response (saccades, vestibuloocular reflex: VOR, or vestibulocollic reflex: VCR) to a particular change in gain or phase in one gif condition, adapting to a different gain or phase in a second gif condition, and then seeing if gif itself – the context cue – can recall the previously-learned adapted responses. Previous evidence indicates that unless there is specific training to induce context-specificity, reflex adaptation is sequential rather than simultaneous.

Various experiments in this project investigate the behavioral properties, neurophysiological basis, and anatomical substrate of context-specific learning, using otolith (gravity) signals as a context cue. In the following, we outline the methods for all experiments in this project, and provide details and results on selected experiments.

METHODS

1. **Context-specific Adaptation in Parabolic Flight.** This experiment studies the ability of human subjects to switch between two adapted oculomotor behaviors (either the VOR or saccades to visual targets) based on gif, using parabolic flight in NASA's KC-135 aircraft to provide alternating hypo- and hyper-gravity. Saccadic gain, for example, will be adaptively increased, using a standard double-step paradigm, during the 0 g segment of flight, and decreased during the 1.8 g segment. Near the end of the flight, saccades will be tested under the different g conditions to determine if the change in g level can serve as a context cue for the adapted responses. Adaptation and testing on consecutive days will examine the rate of acquisition of context-specificity, and its possible loss during intervening 1 g experience.
2. **Context-specific Adaptation of the Human LVOR.** This experiment studies the ability of subjects to switch between two adapted LVORs based on a context cue. Eventually this cue will be the orientation of gravity with respect to the head (induced by head tilt). We first used vertical eye position as a context cue, since it correlates directly with some of our earlier work. We previously found significant LVOR phase changes with 20 min adaptation (lateral accelerations, 0.5 Hz, 0.3 g), asking for 53 deg phase lead or lag. In the present study, we asked for a lag of 45

deg for 3 min, while the subject looked 20 deg up, alternating with a phase lead of 45 deg, while the subject looked down 20 deg. This was repeated for 30 min (5 intervals up, 5 down). A computer-generated visual display presented an image of a moving wall at a virtual distance of 1 m, with vertical markers at 20 deg up and down. Before and after adaptation, the LVOR was measured in the dark with the eyes up and down 20 deg, and centered. The subject was told to track the remembered location of a target at each vertical position. For the initial analysis, saccades were not removed from the (EOG) eye movement records, because tracking was clean (catch-up saccades were common). For each stimulus segment (four contiguous cycles, omitting the first in each segment), a sine was fit to the horizontal eye motion.

3. **Context-specific Adaptation of Oculomotor Responses to Centrifugation.** This experiment studies the acquisition of context-specific adaptation in human subjects during repeated exposure to short-radius centrifugation. Subjects will lie on their sides while rotated at 23 rpm, creating a 1g gradient from head to feet. During rotation, head movements will initially provoke disorientation and noncompensatory eye movements (due to Coriolis forces). Repeated head movements in this situation will reduce (adapt out) the noncompensatory eye movements. Subjects will be exposed alternately to the rotating and non-rotating situations, making yaw head movements in each setting. We propose that after sufficient training the context cue of the gravity gradient and the cross-coupled forces will be sufficient to switch between two different adaptation states (so that the correct compensatory horizontal eye movements are made in response to head yaw, while stationary and while rotating, even though the canal stimuli are different in each case).

4. **Properties and Context-specificity of Vestibulocollic Reflex.** This experiment quantifies and models the contributions of canal and otolith feedback to head movements induced by trunk rotations and translations in 3 dimensions. The head/neck system is inherently unstable in 1 g and requires tonic neck activity, mediated via the vestibular system, for upright posture. We propose that damping of the head/neck is controlled by VCR (vestibulo-collic reflex) feedback and depends on gif. Rotations (centered and eccentric) will be applied to human subjects while upright or supine, to assess the contributions of gravity and tangential acceleration. We will also quantify short-term adaptation of this system to artificial gif contexts. The major goal so far has been to characterize roll and pitch head/neck dynamics in upright posture through parallel experimental and modeling approaches. We hope to quantify the effects of gif contexts on adaptation in terms of a few model parameters which are easily interpreted.

We have completed a series of experiments on closed-loop (unrestrained) 3-D head/neck responses. A short-arm centrifuge applied translational and rotational sum-of-sines accelerations to the trunk. Head and trunk rotations were recorded in 3 dimensions in 17 subjects. Subjects were seated upright in a chair at the end or the center of a 0.8 m centrifuge arm. The eccentric chair was pivoted to apply the primary translational acceleration along the fore-aft or lateral trunk axis. The center chair was positioned to minimize translational accelerations and to apply angular acceleration along the longitudinal (yaw) axis.

5. **Cerebellar Contribution to Context-specific Adaptation in Monkeys.** These experiments will determine the role of the vestibulocerebellum in the LVOR at high and low frequencies, and its

role in ocular counterroll and in LVOR adaptation. Using these as supporting studies, we will determine the role of the vestibulocerebellum in context-driven VOR adaptation.

The interaural and naso-occipital LVORs will be studied over a range of sinusoidal translation profiles (0.01-4.0 Hz and 0.2-0.6 g). For rotations <0.1 Hz, the properties of the rotation-translation apparatus are exploited to increase effective sled length by rotating the base axis at constant velocity while oscillating the primate chair linearly back and forth across its axis. Responses to earth-horizontal axis (tilt) rotations at 0.1-2.0 Hz (10-25°/sec) are measured in addition to eye movements evoked by static positioning in the 45° and 90° right and left ear down positions. Horizontal, vertical, and vergence pursuit will be studied with sinusoidal stimuli over a frequency range of 0.1-1.0 Hz. Associated studies characterize nonlinearities in the VOR. To induce LVOR adaptation, interaural translation will be applied with relative motion of a visual scene to require gain increase or decrease, or phase lead or lag. Animals will be exposed to one of these stimulus conditions during a given test session, and transfer of the adapted gain or phase to tilt responses and AVOR will be assessed. Animals will then undergo either flocculectomy or nodulectomy followed by repetition of the same testing.

Finally, context-specific adaptation will be attempted. The animal will be placed at the end of the rotator arm, facing motion or back to motion. With a constant velocity of rotation (constant interaural centripetal acceleration), a sinusoidal modulation will be superimposed to generate a sinusoidal LVOR. The two different contexts will be facing motion and back to motion, with the direction of the inter-aural component of gif opposite in the two situations. An associated visual display will be used to ask for different LVOR gains in each direction of motion.

RESULTS

1. Context-specific Adaptation of the Human LVOR. Although not as robust as conventional phase adaptation, there was after the adaptation session a tendency for phase changes to be associated with vertical eye position. These changes were small and dissipated quickly, but provide evidence for context-specific capability in adapted LVOR responses. Not all subjects showed significant or reliable context-specific adaptive changes. One subject gave results that are statistically significant if the later testing segments are omitted (Wilcoxon $p=0.025$), reflecting the fact that with this short adaptation period, adaptation may decay even during the course of the post-adaptation testing (approximately 2 min). Another final subject showed significant context-specific adaptation ($p=0.025$) with all stimulus segments. A third subject gave disappointing results; all phase changes, with gaze up or down, were positive (adaptation in the leading direction). This subject differed from the others in that his pre-adaptation phases were always lagging, which is unusual, and in later testing he had almost purely saccadic LVOR in the dark, indicating inability to track smoothly and consistently a remembered target. These factors suggest that this subject does not resemble the "normal" majority of subjects we have tested who have natural phase leads and reliable smooth tracking in the dark. A third subject produced mixed results; if the first segment of each type (up/down) is used, or only those segments with good smooth tracking are used, then this subject shows some degree of context-specific adaptation.

2. Properties and Context-specificity of Vestibulocollic Reflex. As expected, yaw head rotation is the largest response component to on-axis yaw trunk rotation, and roll and pitch head rotations

are the largest response components to lateral and fore-aft trunk translations, respectively. We are approximately half done with full data analysis on our 17 subjects, fitting parameters to multiple-input models of the head stabilization system. This work is confirming that our second-order models of this system are sufficient to characterize changes due to adaptation that will be found in subsequent experiments.

3. Cerebellar Contribution to Context-specific Adaptation in Monkeys. So far we have been performing supporting studies of the horizontal AVOR with sines (2-20 Hz) and steps ($3000^\circ/s^2$). There is an interesting and significant nonlinearity in the response to such rotations. This nonlinearity is important in boosting the AVOR gain at higher frequencies and accelerations to keep the reflex compensatory. Deficits in the nonlinear pathway were induced by unilateral lesions and create response asymmetries between inhibition and excitation. The origin of the nonlinear pathway remains to be discerned; we hypothesize that a group of less-regularly discharging vestibular-nerve afferents may provide the sensory inputs for this pathway and that inhibitory cutoff of these afferents at high frequencies and velocities may be responsible for asymmetries observed after unilateral lesions. These issues will be explored before going on to context adaptation experiments.

CONCLUSIONS

During extended space flight crew members may live in artificial gravity and will make transitions to and from weightlessness for planetary exploration and return to Earth. If they learn sensorimotor skills such as piloting in the normal gravity of Earth, will they be able to perform them adequately in the weightless or the artificial gravity environment? In our work to date, we have found small but promising evidence for context-specificity in the human LVOR in response to translation, which we hope to extend to the VCR and to animal responses.

APPLICATION OF FLOQUET STABILITY ANALYSIS TO REPEATED STEPPING IN LD AND NORMAL SUBJECTS.

Conrad Wall, III & David E. Krebs

INTRODUCTION

One aim of this work is to characterize the dynamics of locomotion stability in response to perturbations of the Body Segment Variables. This report concerns the application of Floquet multipliers to analyze the stability of normal and labyrinthine deficient (LD) subjects. At the Massachusetts General Hospital Biomotion Laboratory, a preliminary analysis of a stair stepping experiments done on 24 subjects.

METHODS

Subjects stepped repeatedly up and down a single step at 120 steps per min., while the infrared selpot system recorded the movement of their body parts for further analysis. Half of the subjects had vestibulopathies as documented by vestibular function testing (LD subjects), while the other half had normal vestibular function. Floquet multipliers were used to estimate the stability of phase planes produced by the upper trunk in pitch and by the lower trunk in yaw.

RESULTS

Based upon a preliminary analysis of these data, the average value, for upper trunk pitch, of the multipliers for the patients with uni- and bilateral vestibulopathy is significantly larger ($p < 0.05$) than the average for the "normal" group. A larger value of Floquet multipliers mean less stable system. The actual numbers are 0.85 ± 0.06 for LD subjects and 0.62 ± 0.08 for normals, where the error limits are one standard error. The motion of the lower trunk in yaw was also analyzed to estimate the timing of the four pace sequence that makes up one cycle in the phase plane. The Floquet multiplier estimates for yaw were 0.62 ± 0.06 for LD's and 0.78 ± 0.07 for normals. The difference between these means is not significant.

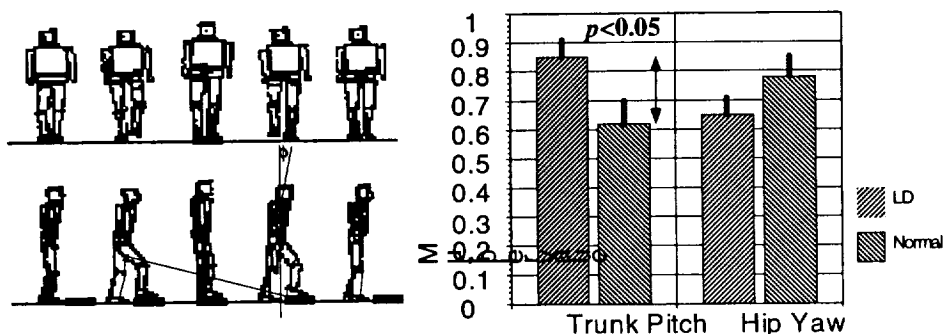


Figure. Repeated single stair stepping produces complex phase plane trajectories which are difficult to analyze. Here we show a Floquet analysis for two groups: Normals and Labyrinthine Defective [LD] subjects. The Floquet Multipliers for trunk pitch is significantly larger for the LD group compared to the Normal group. This suggests that the LD group is less stable during repeated stair stepping.

CONCLUSIONS

These results suggest that Floquet analysis looks promising for Neurovestibular applications, since it can distinguish between normal and LD groups during repeated stepping. Repeated stepping may not be as efficient as looking at the responses to a single perturbation of gait. We are in the process of developing a simple "impulse-like" perturbation.

PLANS FOR FUTURE INVESTIGATIONS

Floquet analysis is currently being compared with other methods of gait assessment during repeated stepping. We are in the process of developing a simple "impulse-like" perturbation.

VISION AND VISUAL-MOTOR COORDINATION IN PITCHED VISUAL ENVIRONMENTS

Robert B. Welch

NASA-Ames Research Center

The everyday perception of one's bodily orientation is determined by two classes of sensory cues: Vision and gravity. Because these cues typically agree, as when one is standing in a lighted room, it is difficult if not impossible to determine the degree to which each contributes to spatial perception. Therefore, in order to make this judgment it is necessary to introduce a *conflict* between vision and gravity and note the resulting perceptual experience. One simple way to do this is to expose the observer to a visual framework that has been rolled or pitched relative to the gravitational vector. The underlying assumption is that the separate contributions of vision and gravity to the perception of bodily orientation that are measured in such a situation of intersensory conflict are the same as those that operate under normal (i.e., non-conflicting) circumstances.

In a common example of this kind of research, subjects stand facing a room that has been pitched either 20 degrees top-toward them or 20 degrees top-away (e.g., Stoper & Cohen, 1989). They are then instructed to indicate where on the far wall of the room they perceive their eye level to be located by directing a beam of light at it, a measure referred to as "visually perceived eye level" (VPEL). The typical outcome is that VPEL is shifted in the direction of the pitch of the room by approximately 50% of that pitch (e.g., Matin & Fox, 1989). According to the logic outlined above, this result indicates that, under normal circumstances, vision and gravity contribute about equally to the perception of bodily orientation. Surprisingly, when asked to point (open-loop) at targets that have been placed at true eye level, subject's err much less than would be predicted by their VPEL shifts (e.g., Welch & Post, 1996). Other effects of pitchrooms include the misperception of the height and orientation of objects located near the back wall. For example, in a room that has been pitched top-toward the observer, a physically vertical rod appears shorter than it actually is and pitched top-away.

A commonsense explanation of these visual effects is that they result from observers' underestimation of the pitch of the room. Thus, according to this argument, the fact that the pitchroom causes about a 50% shift in VPEL means that observers must be underestimating its pitch by 50%, since if they were correctly perceiving its real pitch they should be able to compensate for it and thus correctly perceive their bodily orientation. However, several forms of evidence contradict this notion. For example, Hudson, Li, and Matin (1996) reported that the correlation coefficients calculated between perceived orientation of a pitched display and its effects on VPEL were not statistically significant. Furthermore, it was shown very recently by Welch, Post, Lum, Kang, Napoli, and Cohen (1998) that becoming familiar with the true pitch of the room by walking around in it did not lead to a reduction in the effect of the room on either VPEL or the perceived orientation of a vertical rod.

An alternative explanation for the visual effects of a pitchroom is that the observer's eyes are caused to turn involuntarily in a direction more orthogonal to the pitched display. Cohen, Ebenholtz, and Linder (1995) measured such unconscious eye turning (which they referred to as

the “optostatic response”) and found it to be almost perfectly correlated with measured VPEL shifts.

The relevance of these and other similar observations for the NASA space mission is that they demonstrate and clarify the role played in the perception of spatial orientation by the visual surround, which in space is the only cue available to astronauts to tell them what is up and down.

REFERENCES

- Cohen, M. M., Ebenholtz, S. M., & Linder, B. J. (1995). Effects of optical pitch on oculomotor control and the perception of target elevation. *Perception & Psychophysics*, **57**, 433-440.
- Hudson, T., Li, W., & Matin, L. (1996). Independence of visually perceived eye level and perceived pitch. Psychonomic Society Meeting, Chicago.
- Matin, L., & Fox, C. R. (1989). Visually perceived eye level and perceived elevation of objects: Linearly additive influences from visual field pitch and from gravity. *Vision Research*, **29**, 315-324.
- Stoper, A. E., & Cohen, M. M. (1989). Effect of structured visual environments on apparent eye level. *Perception & Psychophysics*, **46**, 469-475.
- Welch, R. B. & Post, R. B. (1996). Accuracy and adaptation of reaching and pointing in pitched visual environments. *Perception & Psychophysics*, **58**, 383-389.
- Welch, R. B., Post, R. B., Lum, W., Kang, M., Napoli, C., & Cohen, M. (1998, Nov.). *Adapting to a pitchroom*. Paper presented at the 39th meetings of the Psychonomic Society, Dallas, TX.

Nutrition

Chair
Helen Lane, Ph.D.

Co-Chair
T.P. Stein, Ph.D.

NUTRITION SESSION SUMMARY

Overview

Nutrition deficiencies affect multiple systems including muscle, bone, cardiovascular, renal, and gastrointestinal. Humans require many nutrients, ranging from the macronutrients (water, protein, energy sources) to micronutrients (minerals, vitamins). The ability to withstand shortfalls in intake of individual nutrients ranges from one or two days (e.g., water) to weeks (energy, protein, potassium) and months (some vitamins, minerals). In addition to putting humans at risk for nutrition deficiencies, space flight may also change the absorption, hence the pharmacodynamics, of several important medications. Papers given in this session dealt with all of these nutritional and pharmacological factors related to space flight.

Protein metabolism and muscle formation

Muscle proteins are continually being broken down and resynthesized (protein turnover). The half-life of human muscle protein is about 18 days. An important part of maintaining good muscle status is the ability to synthesize muscle proteins. For muscle protein synthesis to proceed normally both an adequate amount of amino acids and the energy to support protein synthesis must be available. **Stein** summarized research with Mir astronauts and several U.S. missions that demonstrated a tendency towards negative energy balances in space flight caused both by decreased energy intake from food and increased energy expenditures. These energy deficits were of sufficient magnitude to depress protein synthesis.

On the U.S. missions, the elevated energy expenditures were due to on orbit aerobic exercises. For the International Space Station, aerobic exercise is a requirement. However, the data presently available suggest that the additional exercise might be self-defeating, because it will create a negative energy balance that will depress protein synthesis. Another potential problem is the finding of **Ferrando et al.** that the loss of muscle mass and skeletal muscle protein catabolism due to the inactivity associated with bedrest is increased by a cortisol challenge. Thus inactivity exacerbates the catabolic effects of cortisol on skeletal muscle protein.

Because changes in lean body mass often reflect metabolic derangements, there is a need to monitor lean body mass during long duration missions. Methods for determining body composition suitable for use on orbit must be light, compact, and easy to use and must require minimum crew time and electrical power. Ground studies have shown that bioelectric impedance methods, which measure conductivity between selectively placed electrodes on the body, have these characteristics. However, the problem with applying this method to space flight is that it is susceptible to fluid shifts. **Schoeller** reported experiments in progress designed to validate this bioelectric impedance-measuring hardware under conditions of fluid shifts. His preliminary data suggest that the bioelectric impedance approach has the potential for excellent precision, reliability, and accuracy under space flight conditions.

Pharmacodynamics

Space flight perturbs metabolism and gastric absorption, and these metabolic changes impact how drugs are absorbed and distributed within the body, as well as the time course of their

metabolism. There is little data available on drug absorption and pharmacokinetics during space flight.

Putchal et al. reported a study demonstrating that promethazine, a drug widely used to treat space motion sickness, produced significant drowsiness and salivary flow rate suppression with time courses that correlated closely with the drug's elimination half life. This study clearly demonstrates the need for pharmacodynamics studies in space.

Welage et al. have developed a noninvasive gastric emptying/intestinal absorption test based on enteric-coated particles that release their contents on entering the small intestine. They reported a study validating this test by demonstrating that, as expected, in gravity larger particles enter the small intestine earlier than smaller particles. Further, they demonstrated that measurements of salivary concentrations of the pellets' contents (acetaminophen and caffeine) correlated with plasma concentration, thus indicating that this procedure can be used in space for noninvasive monitoring of both gastric emptying and drug absorption.

Calcium metabolism and bone formation/resorption

Bone loss is one of the major problems created by long duration space flight. **Smith et al.** presented measurements of calcium kinetics and bone loss markers showing that, during space flight, bone resorption increased to a mean of 250mg/day. Concurrently, gastrointestinal absorption of calcium and vitamin D status decreased. Also, of great significance is the observation that replacement of the lost calcium from bone took about four times longer than the time required for loss. These investigators reported plans to continue these studies on the International Space Station.

Loss of gravitational tension is not the only factor that can lead to calcium loss from bone. Non-nutritive compounds in foods can affect bone status. For example, **Holmes et al.** reported that dietary oxalate (a component of many fruits and vegetables, particularly spinach) interferes with calcium absorption from the diet and at the same time, by complexing with the enhanced release of calcium from bone, increases the chances of renal stone formation.

Fluid and electrolytes

Lane et al. summarized space flight data demonstrating that, concurrent with the evidence for poor energy and protein status, fluid and potassium intakes were below recommended levels, while sodium intakes were generally above recommendations. These findings have cardiovascular implications since fluid and electrolyte balance plays an important role in the low blood volume that leads to orthostatic intolerance at landing.

Summary

Malnutrition impacts many systems. Prevention requires knowing the nutrition requirements of crew members during space flight; hence these requirements need to be studied. The limited data available so far suggests that the main cause of nutritional deficiency in space is a poor dietary intake in either quantity (energy, water, potassium) or quality (excess sodium, oxalate).

The mechanisms that lead to this depressed intake need to be determined. Space flight also leads to metabolic alterations – for example, the efflux of amino acids from muscle, loss of calcium from bone and increased susceptibility to renal stone formation; these tendencies can be exacerbated by an inappropriate diet. Another consequence of altered metabolism, to which little attention has been paid, is a different response to drugs, of importance because of the use of medications for space motion sickness, sleep, and pain. The effectiveness of medications under the conditions of space flight also needs to be investigated. Finally, exploration class missions will not be possible unless a food system that can be used for long-duration flights that do not offer re-supply opportunities is developed.

Nutrition engineering

While detailed investigations of absorption, metabolism, and elimination of nutrients both in space and on earth provide the data necessary for determining nutritional requirements during space flight, the engineering challenges of providing foods that meet these requirements, yet are varied and palatable, must still be met. These challenges are particularly daunting for long duration space flights that must rely on bioregenerative life support systems. **Hunter** reported progress on an extensive project designed to develop a database of nutritious and appealing dishes that can be prepared from the output of bioregenerative life support systems. The project's goals include development of preparation methods, estimation of labor and equipment requirements, and determination of food manufacturing costs. Around 120 recipes have been tested, with another 120 to be developed. The project promises to play a key role in meeting nutritional challenges presented by exploration class missions.

Helen Lane and T.P. Stein

THE COMBINED EFFECTS OF INACTIVITY AND CORTISOL ON MUSCLE PROTEIN METABOLISM

Arny A. Ferrando¹, Charles S. Stuart², and Robert R. Wolfe¹

¹Departments of Surgery and ²Internal Medicine, Endocrinology, University of Texas Medical Branch, Galveston, Texas 77550

INTRODUCTION

We have previously noted that inactivity results in a loss of lean body mass (LBM) due to reduced protein synthesis. We have also shown that severely burned patients lose lean body mass due to an increase in net protein breakdown. Severe burn injury is also associated with an increased cortisol secretion, whereas inactivity does not alter this hormonal profile. Thus, we tested the hypothesis that inactivity exacerbates the catabolic effects of cortisol on skeletal muscle protein.

METHODS

Four male subjects (25.8 ± 7.6 yrs, 59.1 ± 0.2 kg LBM) were admitted to the GCRC for 5d of diet stabilization followed by 14d of strict bed rest (BR). Dual energy x-ray absorptiometry (DEXA) was performed 2d prior and 1d after BR for the determination of LBM. Skeletal muscle protein metabolism was studied coincident with a 12 hr infusion of cortisol ($120\mu\text{g}\cdot\text{kg}^{-1}\cdot\text{hr}^{-1}$) the day prior (BR-1) and again after 14d (BR14) of inactivity. The methodology involved the use of stable isotopic tracers of amino acids, arterio-venous catheterization of the femoral vessels, and biopsy of the vastus lateralis muscle.

RESULTS

After 14d of inactivity, DEXA revealed that subjects lost an average of 140g of leg LBM ($P<0.05$), while whole-body LBM remain unchanged. Net amino acid balance across the leg became significantly more negative on BR14 ($P<0.05$). Net protein breakdown tended to increase at BR14, as did outward amino acid transport and de novo synthesis of the gluconeogenic precursors, alanine and glutamine. The ratio of intracellular amino acid appearance to outward transport also decreased, indicating that a greater proportion of amino acids were not re-utilized for protein synthesis.

CONCLUSION

We conclude that a cortisol challenge after prolonged inactivity results in greater skeletal muscle protein catabolism.

DIETARY OXALATE AND ITS INFLUENCE ON URINARY OXALATE EXCRETION

Ross P. Holmes, Ph.D. and **Dean G. Assimos, M.D.**, Department of Urology, Wake Forest University School of Medicine, Winston-Salem NC.

INTRODUCTION

One in eight white Caucasian males will form a calcium oxalate kidney stone at some point in their lifetime and up to one in three may be genetically susceptible to forming one. As physiological changes during space flight increase stone risk factors the formation of a kidney stone during extended space flight becomes a distinct possibility. Effective countermeasures are required to offset this stone risk. We have investigated the contribution of dietary oxalate to stone risk as gauged by changes in urinary oxalate excretion as this risk factor has the potential to be modified.

CURRENT STATUS OF RESEARCH

METHODS

Two direct methods for estimating the oxalate content of foods were compared; ion chromatography and capillary electrophoresis. Both these techniques were found to be accurate and precise. Ion chromatography was superior to capillary electrophoresis but the electrophoresis technique was more rapid and less costly. Both the ion exchange column used for the ion chromatography and the capillary tubing used in the electrophoresis tended to poison rapidly and this was the main reason causing the cost differential. Using capillary electrophoresis we analyzed food items for inclusion in diets to assess the effects of dietary oxalate consumption on urinary oxalate excretion.

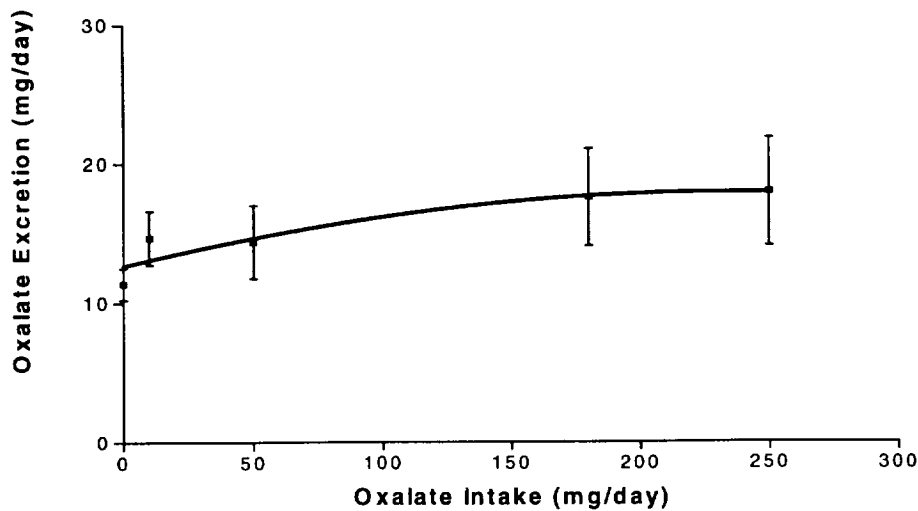
Twelve normal healthy individuals (6 males and 6 females, mean age 28 years) were recruited for these studies. Diets were designed to contain controlled amounts of calories, carbohydrates, fat, protein, calcium, sodium, potassium and phosphorus as well as oxalate. Two levels of dietary oxalate were evaluated, 50 and 250 mg/2500 kcal. The diets were constructed so that constant ratios of calcium:oxalate were consumed at every meal. Diets were consumed for 10 days with complete 24 hr urine collections obtained on the last 4 days of the diet. A wash-out period of at least 2 weeks occurred between each diet. The concentrations of oxalate and other ions that affect the interaction of calcium and oxalate were measured in urine samples.

RESULTS

Mean oxalate excretion increased significantly from 14.6 ± 3.9 mg/g creatinine on the 50 mg oxalate diet to 18.1 ± 4.6 mg/g creatinine on the 250 mg oxalate diet ($P < 0.005$). The response to different oxalate levels was variable with 2 individuals showing no increase in oxalate excretion. The increase in oxalate excretion in the other 10 individuals ranged 10-fold from 8.0 to 80.6%, with a mean increase of 35.4%. This variability in the absorption of dietary oxalate supports other evidence from our laboratory that this absorption process has a significant genetic component. Despite the significant increase in oxalate excretion on the high oxalate diet observed in most individuals a significant increase in the supersaturation of urine with either calcium oxalate monohydrate (COM) or dihydrate (COD) was not generally observed. In one individual COM significantly increased and in another both COM and COD significantly increased, but no change was observed in the other 10 individuals. It was noteworthy that in the

individual with the greatest increase in oxalate absorption that calcium absorption was significantly suppressed with the result that the increase in urinary oxalate excretion was offset by a decrease in urinary calcium excretion.

Six of the twelve individuals have also consumed 3 diets with other oxalate levels in prior studies in our laboratory. Two of these diets, 0 mg and 180 mg, were formula diets. The urinary oxalate excretion of these individuals ingesting this range of oxalate intakes is shown in the figure below. The response is hyperbolic with the oxalate values declining sharply on a zero oxalate diet. With intakes of oxalate between 50 and 250 mg per day an average 4% of the dietary oxalate was absorbed.



CONCLUSIONS

The following conclusions can be drawn from our studies:

1. In most individuals, but not all, the amount of oxalate excreted in urine increases as the intake of dietary oxalate increases.
2. The response is variable possibly due to inherent genetic differences in the absorption process.
3. The increase in urinary oxalate excretion on the high oxalate diet increased the relative supersaturation of urine with calcium oxalate salts in only 2 out of 12 individuals.

In determining the significance of these results for stone formation it must be borne in mind that this study was conducted in normal individuals and stone formers may respond differently. Furthermore, the ratio of calcium to oxalate was constant with every meal and this may not reflect the pattern of nutrient ingestion by most individuals.

PLANS FOR FUTURE INVESTIGATIONS

The development of an accurate and precise method for oxalate determination will permit more accurate determinations of the oxalate content of foods and will provide an important tool for assessing the bioavailability of oxalate in these foods. These methods will also permit the estimation of the range of oxalate intakes in various populations and will permit more definitive assessment of whether the amount of oxalate ingested is truly a risk factor for stone disease. Further lines of investigation that are warranted are to determine whether the amount of calcium ingested influences oxalate absorption and whether the discordant consumption of calcium and oxalate during the day enhances oxalate absorption. The development of a test that identifies those individuals most at risk for absorbing an excessive amount of dietary oxalate will also be investigated.

FOOD SYSTEM CHALLENGES FOR LONG-DURATION SPACE MISSIONS

Jean B. Hunter, Associate Professor, Department of Agricultural and Biological Engineering, Cornell University, Ithaca, NY 14853

On long-duration manned space missions food is at once a key habitability issue, a biomedical issue, and an issue of engineering and systems design. As mission duration increases, a bioregenerative life support system becomes more cost-effective than the physico-chemical regeneration systems now used on Shuttle and ISS; however, bioregenerative life support requires growing and processing of in-situ grown crops, treatment of food wastes, and preparation of daily meals, all within severe labor constraints. Though plant production for space missions has been extensively studied, space-compatible technologies for processing crops and preparing ready to eat foods have yet to be developed. These processing and preparation problems constitute a major engineering challenge for food systems in space.

The goal of our project is to develop an expandable database of food processing information and a user-friendly optimization system to support informed decisions regarding food processing and preparation for long-duration space missions. We are developing a "bioregenerative cuisine" of 200+ nutritious and appealing dishes that an astronaut crew can prepare and eat during a long-duration mission. This large number is required to provide future crews with a range of dietary choices, and to allow mission management to optimize the menu for closure, labor costs, or other constraints. The dishes include both familiar and novel menu items. Each food is evaluated for palatability, nutrient content and preparation cost in terms of equivalent system mass. The project includes the following components:

Development and testing of foods (recipes) intended for a bioregenerative life support system with around 90% food closure. Currently, at the halfway point of the project, around 120 recipes have been tested, with another 120 to be developed.

Estimation of labor and equipment costs of food ingredient manufacture from CELSS crops and of food preparation from these ingredients. Our current spreadsheet models predict the portion of food costs traceable to energy, cooling, processing equipment, and non-renewable resources. Labor costs, the most challenging to predict and to scale, are now under study.

Evaluation of the acceptability of a chiefly plant-based diet to an omnivorous population, through a 30-day closed feeding study near the end of the project

Nutritional analysis of individual foods and ingredients, ongoing with their development

Linear programming optimization of the diet to arrive at low-cost diets satisfying given constraints on nutrient content, labor requirements and acceptability of the overall menu. To date we have performed "proof of concept" optimizations and are now working on larger scale runs and sensitivity analyses to predict the marginal cost of food quality, variety, and other habitability criteria for the menu.

Development of a spreadsheet model to estimate the cost of food production, processing and

preparation given reasonable assumptions on crew size, mission duration, and resource costs in terms of equivalent system mass (payload mass equivalents) . Component models have been developed and are now being linked together and updated to reflect interactions between the food system and other components of bioregenerative life support.

FLUID AND ELECTROLYTE NUTRITION

Helen W. Lane¹, Scott M. Smith¹, Carolyn S. Leach¹, Barbara L. Rice²

¹ NASA Johnson Space Center, Houston, TX 77058

² Enterprise Advisory Services, Inc., Houston, TX 77058

Studies of fluid and electrolyte homeostasis have been completed since the early human space flight programs, with comprehensive research completed on the Spacelab Life Sciences missions SLS-1 and SLS-2 flights, and more recently on the Mir 18 mission. This work documented the known shifts in fluids, the decrease in total blood volume, and indications of reduced thirst. Data from these flights was used to evaluate the nutritional needs for water, sodium, and potassium. Interpretations of the data are confounded by the inadequate energy intakes routinely observed during space flight. This in turn results in reduced fluid intake, as food provides approximately 70% water intake. Subsequently, body weight, lean body mass, total body water, and total body potassium may decrease. Given these issues, there is evidence to support a minimum required water intake of 2 L per day. Data from previous Shuttle flights indicated that water intake is 2285 ± 715 ml/day (mean \pm SD, n=26). There are no indications that sodium intake or homeostasis is compromised during space flight. The normal or low aldosterone and urinary sodium levels suggest adequate sodium intake (4047 ± 902 mg/day, n=26). Because excessive sodium intake is associated with hypercalciuria, the recommended maximum amount of sodium intake during flight is 3500 mg/day (i.e., similar to the Recommended Dietary Allowance, RDA). Potassium metabolism appears to be more complex. Data indicate loss of body potassium related to muscle atrophy and low dietary intake (2407 ± 548 mg/day, n=26). Although possibly related to measurement error, the elevations in blood potassium suggest alterations in potassium homeostasis. The space RDA for minimum potassium intake is 3500 mg/day. With the documented inadequate intakes, efforts are being made to increase dietary consumption of potassium.

SALIVARY PHARMACODYNAMICS AND BIOAVAILABILITY OF PROMETHAZINE IN HUMAN SUBJECTS

Lakshmi Putcha¹, Deborah L. Harm¹, Ram Nimmagudda², Kurt L. Berens², and David W. A. Bourne³

¹NASA Johnson Space Center, Houston, TX, ²Wyle Laboratories, Houston, TX, and ³University of Oklahoma, Oklahoma City, OK

INTRODUCTION

The acute effects of exposure to microgravity include the development of space motion sickness which usually requires therapeutic intervention. The current drug of choice, promethazine (PMZ), has side effects which include nausea, drowsiness, dizziness, sedation and impaired psychomotor performance. In a ground-based study with commercial airline pilots and shuttle simulator trainers, we measured sleep and psychomotor performance variables, and physiological variables such as blood pressure and heart rate, as a function of circulating drug concentrations in the body. We evaluated a non-invasive sampling method (saliva) as a means of assessing pharmacodynamics following a single intramuscular (IM) dose of PMZ.

METHODS

In a placebo-controlled, randomized double-blind crossover study, nine subjects received a single IM injection of 50 mg PMZ. The subjects collected saliva samples at pre-determined time intervals and PRN urine voids for 48 h. after dosing. Subjects also completed a subjective drowsiness log, Stanford Sleepiness Scale (SSS) and performed 6 simulated shuttle landings using the Portable Inflight Landing Operations Trainer at the same times as those of saliva collections. Blood pressure and heart rate measurements were recorded for the first 8 h and a medication side effects check list was completed by each subject. Salivary flow rate and pH were measured and PMZ concentrations in saliva were determined using a high performance liquid chromatographic assay. Drug concentration - time profiles were analyzed using conventional data analysis methods (RSTRIP, BOOMER) to estimate pharmacokinetic variables. Percent suppression of saliva flow rate and SSS scores were used for the pharmacodynamic assessment of the drug.

RESULTS

A mean peak salivary drug concentration of 6.5 ng was reached at 8 h after dosing. The mean biological half-life of PMZ was 11.9 h. Area Under Plasma Concentration - time curve (AUC), a measure of bioavailability, was low and variable among subjects. A single dose of 50 mg induced a statistically significant increase in perceived drowsiness for 8 h after administration of PMZ compared to placebo controls. Similarly, SSS were significantly higher at corresponding time periods after PMZ administration compared to placebo controls. No significant changes in blood pressure and heart rate were noticed after PMZ administration. Maximum suppression of salivary flow rate occurred at the same time as that of salivary peak concentration of PMZ and the half-life of this effect was similar to that of the elimination half-life of PMZ.

CONCLUSION

Results of this study demonstrate that a single IM dose of 50 mg PMZ can induce significant pharmacodynamic effects of sleepiness and salivary suppression. Duration

of both these effects was similar to that of the drug's biological half-life. Results of this study emphasize the need for similar investigations in space to ensure safety of current pharmacologic treatment for space motion sickness.

MEASUREMENT OF BODY COMPOSITION FOR NUTRITIONAL ASSESSMENT IN SPACE FLIGHT

Dale A. Schoeller, Department of Nutritional Sciences, University of Wisconsin, Madison, WI 53706

INTRODUCTION

Long term space flight increases the risk of reduced human performance due to the loss of body cell mass from the combined effects of weightlessness and energy imbalance. Loss of body mass can now be measured during space flight, but this cannot be assumed to equal body cell mass as loss in mass can also result from decreases in body water or loss of body fat. In order to determine whether the loss of body mass results from loss of body cell mass or other components of body mass, it is necessary to measure body composition. At this time, no methods have been validated for the measurement of body composition during space flight. To address this limitation, we will validate the use of bioelectrical impedance analysis to measure the change in body composition in simulated microgravity.

CURRENT STATUS OF RESEARCH

We have validated the use of multifrequency bioelectrical impedance analysis to measure changes in intracellular and extracellular water volume in humans at 1G. Changes in total body water, intracellular water, and extracellular water were induced by infusing 2L of Lactated Ringer's solution or administering a diuretic agent. Bioelectrical impedance was measured at 49 frequencies between 5 and 500 kHz using a Xitron 4000. Results were compared with dilution using deuterium oxide and bromide combined with short term changes of body weight. Bioelectrical spectroscopy analysis, using proximal, tetrapolar electrodes, was performed from 5kHz to 500kHz, including 50kHz. Single frequency, 50 kHz models did not accurately predict change in total body water, but the 50kHz parallel model did accurately measure changes in ICW. The only model that accurately predicted change in extracellular, intracellular and total body water was the Cole-Cole multifrequency model. Use of the Hanai correction for mixing was less accurate. We conclude that the multifrequency Cole-Cole model is superior under conditions in which body water compartmentalization is altered from the normal state.

PLANS FOR FUTURE INVESTIGATIONS

Although valid, the Xitron 4000 had limited precision at high frequencies and these limited the precision of the assessment of intracellular water to between 500 and 1000mL. This limited the precision of the assessment of body cell mass. We are therefore testing the reproducibility of the Xitron Hydra bioelectrical impedance analyzer. This instrument has superior high frequency performance compared to the Xitron 4000.

After completion of the reproducibility study, we will begin a validation of bioelectrical impedance spectroscopy using 6 degree head-down tilt to simulate microgravity. Two studies will be performed which alter body composition. In the first, we will place participants at head down tilt while providing normal nutrition. Previous studies indicate that this will induce a loss in total body water, which is anticipated to be mainly due to loss of extracellular fluid. The second intervention will add a protein and energy deficient diet to head down tilt to induce a loss of intracellular water in addition to extracellular water. Bioelectrical spectroscopy will be

performed and compared against total body water measured by deuterium dilution and extracellular water measured by bromide dilution. Intracellular water will be estimated by difference. In addition, we will measure nitrogen balance and fluid balance. Finally, we will test the ability of bioelectrical impedance analysis to measure the muscle mass of the calf and upper arm by comparison with MRI. These studies will test the accuracy and provide a measure of the precision of bioelectrical spectroscopy for the measurement of body composition during simulated microgravity.

CALCIUM KINETICS DURING SPACE FLIGHT

Scott M. Smith¹, Meryl E. Wastney², Kimberly O. O'Brien³, Helen W. Lane⁴

¹Life Sciences Research Laboratories, NASA Johnson Space Center; ²Department of Pediatrics, Georgetown University Medical Center; ³Johns Hopkins University; ⁴Space and Life Sciences Directorate, NASA Johnson Space Center

Bone loss is one of the most detrimental effects of space flight, threatening to limit the duration of human space missions. The ability to understand and counteract this loss will be critical for crew health and safety during and after extended-duration missions. The hypotheses to be tested in this project are that space flight alters calcium homeostasis and bone mineral metabolism, and that calcium homeostasis and bone mineral metabolism will return to baseline within days to weeks of return to Earth. These hypotheses will be evidenced by elevated rates of bone mineral resorption and decreased bone mineral deposition, decreased absorption of dietary calcium, altered calcitropic endocrine profiles, elevated excretion of calcium in urine and feces, and elevated excretion of markers of bone resorption. The second hypothesis will be evidenced by return of indices of calcium homeostasis and bone metabolism to preflight levels within days to weeks of return to Earth. Studies will be conducted on International Space Station astronauts before, during, and after extended-duration flights. Measurements of calcium kinetics, bone mass, and endocrine/biochemical markers of bone and calcium homeostasis will be conducted. Kinetic studies utilizing dual isotope tracer kinetic studies and mathematical modeling techniques will allow for determination of bone calcium deposition, bone calcium resorption, dietary calcium absorption and calcium excretion (both urinary and endogenous fecal excretion). These studies will build upon preliminary work conducted on the Russian Mir space station. The results from this project will be critical for clarifying how microgravity affects bone and calcium homeostasis, and will provide an important control point for assessment of countermeasure efficacy. These results are expected to aid in developing countermeasures for bone loss, both for space crews and for individuals on Earth who have metabolic bone diseases.

PROTEIN-ENERGY RELATIONSHIPS DURING SPACE FLIGHT

T.P. Stein, Department of Surgery Science Center, University of Medicine and Dentistry of New Jersey, Stratford, New Jersey

Protein metabolism has been investigated on five missions, three short term (Shuttle missions SLS1, SLS2 and D2) and two long term missions (Skylab and NASA/MIR). Measurements made have included nitrogen balance (four missions), whole body protein kinetics with ^{15}N glycine as the tracer (four missions) and 3-methyl histidine (four missions). Also available for comparison are bed rest studies with and without exercise. The following conclusions can be drawn: (i) No two missions are alike, (ii) Entry into orbit is associated with a metabolic stress response. (iii) Comparison of energy intake (5 missions) and energy balance (four missions) suggests that for at least three of the missions an energy deficit was a major factor in the protein loss. (iv) Serious energy deficits occur on mission with high mandatory exercise requirements. (v) Fidelity with the bed rest models is poor.

A NONINVASIVE TEST FOR GASTRIC EMPTYING AND INTESTINAL ABSORPTION

Lynda S. Welage¹, Gordon L. Amidon¹, Julie Rhie², Brien L. Neudeck¹ and Sally Choe¹

¹College of Pharmacy, The University of Michigan, Ann Arbor, Michigan, 48109-1065,

²National Cancer Institute, Rockville, MD 20852.

INTRODUCTION

Gastric emptying depends on the size and densities of ingested particles including nondigestible food. In the low gravity environment in space, gastric emptying is expected to be altered due to the low gravitational force constant. Thus, gastrointestinal adaptation may occur in a microgravity environment. We have developed a pellet gastric emptying test composed of enteric coated particles of caffeine and acetaminophen of 0.7 and 3.6 mm in diameter. The enteric coat prevents dissolution in the stomach but allows for rapid dissolution in the small intestinal environment. In a gravity environment, it is expected that the large particles will empty slower than the small particles and will appear at a later time in the plasma, while particles of the same size would be expected to empty at the same rate.

METHODS

In order to validate the pellet gastric emptying test, two prospective clinical trials were conducted. In trial 1, using a randomized three way crossover design, the relationship between the absorption of the drug markers, caffeine and acetaminophen, and gastric emptying was explored at three viscosity levels (i.e., 4000, 6000, 8000 cPs) in 12 healthy volunteers. Both plasma and salivary concentrations of the drug markers were evaluated in relation to gastric motility which was determined manometrically. Trial 2 was designed to validate that the emptying of the pellets was in fact the result of pellet size and gastric environment. Specifically, in a randomized four way crossover trial the absorption of the drug markers were evaluated when both drug markers were administered as 0.7 mm enteric coated pellets (Phase A), or as 0.7 mm enteric coated caffeine pellets plus 3.6 mm acetaminophen enteric coated pellets administered with a viscous solution (Phase B), in the fasted state (Phase C) and following the ingestion of a high fat meal (Phase D).

RESULTS

We have validated that the large particles do indeed empty behind the small particles in the gravity environment and this correlated with gastric motility measured by manometric techniques. Specifically, when the pellets were administered with a 4000cPs viscous meal, the appearance of caffeine (0.7 mm pellets) in the plasma occurred an average 49.5 ± 11.4 minutes before the appearance of acetaminophen (3.6 mm pellets). In a separate study, it has been validated that particles of equivalent size empty at the same rate. The average corresponding time between the appearance of caffeine and acetaminophen (i.e. • t_{initial}) was -0.17 ± 0.22 minutes during Phase A as compared with 0.59 ± 0.42 minutes during Phase B. Finally, salivary concentrations of acetaminophen and caffeine correlated with plasma concentrations, thus allowing for noninvasive monitoring of gastric emptying.

CONCLUSION

Overall, these studies demonstrate that in a gravity environment, size differentiated gastric emptying occurs. In a microgravity environment size discrimination would be expected to be much less. The noninvasive pellet gastric emptying test may be a useful means to evaluate the magnitude of changes in gastric emptying and drug absorption as well as their adaptation over time in a microgravity environment.

Radiation

Chair

Amy Kronenberg, Ph.D.

Co-Chair

Jack Miller, Ph.D.

Co-Chair

David L. Huso, DVM, Ph.D.

RADIATION SESSION SUMMARY

Introduction

The National Academy of Sciences (NAS) has identified radiation hazards as one of the potential “show stoppers” for long term human exploration of space. NASA supports a multi-disciplinary research effort encompassing diverse fields including radiation physics and transport, basic research in radiation carcinogenesis and research on behavioral effects. To supplement the current research effort, the National Council on Radiation Protection and Measurements (NCRP) has assembled Scientific Committee 1-7 (SC 1-7) to provide recommendations on further information that is required to develop radiation protection guidelines for manned missions beyond low earth orbit. **Townsend** presented an update on the recent activities of NCRP SC 1-7, and reviewed the knowledge base that will be required to accurately assess the risks to humans from exposure to the radiation environment of space.

The presentations in the Radiation Session addressed the critical research needs identified by the NAS and the NCRP. These included: (1) characterization of the space radiation environment, (2) modeling and ground-based measurement of the fragmentation properties of heavy charged particles as they interact with shielding and tissue equivalent materials, (3) biodosimetry in astronauts, (4) ground- and flight-based studies to elucidate the mechanisms of biological response to space radiation (and potential interactions with microgravity), and (5) ground-based studies to quantify the risks of carcinogenesis and other damage to normal tissues that may ensue after exposure to different components of the space radiation environment.

Characterization of the space radiation environment

The two types of radiation in space that present the most serious potential hazards to humans during long duration spaceflight in low earth orbit and on exploration class missions are solar particle events (SPE) and the galactic cosmic radiation (GCR). **Turner** reviewed the physics and characteristics of SPE, which consist of high fluxes of charged particles, primarily protons, ejected from the Sun, either during solar flares or coronal mass ejections (CME). (Although “SPE” and “solar flares” are often used synonymously, CME are not necessarily associated with flares.) Very large SPE could be life threatening under certain conditions, for example during extravehicular activity. The relatively simple nature of this type of radiation (mostly protons in a well-defined energy range) and their relatively short duration (on the order of tens of hours) makes for straightforward countermeasures, such as restrictions on astronaut activities and provision for small, heavily shielded “storm shelters” within spacecraft and planetary habitats. For such countermeasures to be effective, it is important to be able to predict SPE both accurately and precisely. This is not yet possible, but Turner reviewed the state of the art in solar monitoring and SPE prediction, concluding that better predictive tools are needed.

The GCR originates from outside the solar system and is isotropic, but is modulated by solar wind-generated magnetic fields. The particles of greatest biological concern are the atomic nuclei. Ions of all the naturally occurring elements are found in the GCR, but the most important are those with charges between 1 (hydrogen) and 26 (iron), after which the abundance drops off drastically. The energy deposited by charged particles in matter, including the human body, is

roughly proportional to the square of the charge; therefore the heavier ions, while relatively small in numbers compared to hydrogen, are highly ionizing and can produce significant biological effects. Iron ions are of special concern due to their high charge and their abundance relative to other heavy nuclei.

Perhaps the simplest countermeasure is for exploration class missions to take place during "solar minimum," the part of the 11 year solar cycle when the sun is relatively quiescent and SPE are least likely to occur. In contrast, solar minimum is when the GCR flux is greatest, making remediation of GCR effects all the more important.

Fragmentation properties of heavy charged particles

The design of effective shielding is complicated by nuclear and electromagnetic interactions of heavy charged particles in matter that modify the ambient space radiation field. It is impractical to verify the radiation transmission properties of many proposed spacecraft and planetary habitat shielding materials and configurations in space. **Wilson et al.** investigated several physical and biophysical models that address this need. Modeling is cost effective, but the uncertainties in model predictions of transmitted flux and dose dictate increased shielding, and consequently increased mission cost. Thus, efforts are continuing to make the models more accurate and more precise. To improve the models it is necessary to improve the physics that goes into them, primarily the nuclear interaction probabilities, or cross sections. The models must also be validated in the laboratory, by testing their predictions of the radiation transport properties of various materials.

Miller et al. reviewed ground-based radiation transport measurements. Two types of measurements are needed: *cross sections*, which are the probabilities for a given projectile and target nucleus to interact, and *fluences*, which are measurements of particle production in thick targets, such as shielding or tissue equivalent materials. Cross sections are required for input to transport models; fluences are used for transport model validation, evaluation of biological data and detector calibration. The experimental techniques in the two cases are similar. NASA-supported experiments are being done at three particle accelerators: the Alternating Gradient Synchrotron at Brookhaven National Laboratory, the Heavy Ion Medical Accelerator at Chiba, Japan and the Loma Linda University proton synchrotron. Construction will start during 1999 on the Booster Applications Facility at Brookhaven, a NASA-funded facility dedicated to space radiobiological and biophysics research with high energy heavy ions.

Dosimetry

Physical measurements are integral to space biomedicine in the characterization of the radiation field at the sample location in ground-based accelerator radiobiology experiments, and in the calibration and intercomparison of radiation detectors and dosimeters used in human space flight. A wide variety of such detectors are being used now on the Space Shuttle and the Mir space station, and many more are planned for use on the International Space Station.

Badhwar and Benton et al. discussed dosimetric measurements made on board the Mir space station, which is at an orbital inclination close to that of the International Space Station.

Badhwar highlighted the challenge of reconciling measurements made at different times, with different detectors and at different locations on Mir; however a great deal has been learned which will be of use as we move into the ISS era. One particularly interesting finding is the correlation between the absorbed dose rate from trapped particles and atmospheric density recorded more than one year before the dose measurement. This is attributed to the dynamics of particle gyrations in the atmosphere. **Benton et al.** presented data from passive radiation detectors exposed both inside and outside Mir. The external detectors provided data on the low energy radiation incident on the space station wall. Similar detectors have been exposed to 70-250 MeV protons at Loma Linda University, and the results suggest that proton-induced target fragmentation in bone and tissue makes a significant contribution to dose equivalent, both in space and in charged particle radiotherapy.

The fragmentation of charged particles as they interact with matter also leads to the production of secondary neutrons. **Maurer et al.** reviewed the status of the development of a portable neutron spectrometer to measure neutron fluences and the characteristics of the neutron spectrum from 10 keV to 500 MeV. The instrument under construction will be a compound detector in which neutrons from 10 keV to several MeV will be captured in ^3He gas, while higher energy neutrons will be measured using a silicon solid state detector, which is under development.

NASA compliments the physical dosimetry obtained during spaceflight with biodosimetry based on the quantitation and classification of different types of chromosome aberrations in peripheral blood lymphocytes from astronauts. **Wu et al.** reviewed improvements in the classification and quantitation of these aberrations, involving the detection of telomeres on individual chromosomes. The proportion of true incomplete exchanges between chromosomes now appears significantly lower than previously reported. Advances have also been made in the quantitation of initial chromatin breaks in a high proportion of cells. These studies will lead to improved biodosimetry for spaceflight.

Biological response to radiation

The basic research presented in radiation biology addresses the risks of exposure to protons, alpha particles, and ions with higher charges and mass states (often called heavy ions) across a wide variety of endpoints. These range from studies of DNA damage and repair to the response of normal tissues and the assessment of carcinogenesis *in vivo*. Access to spaceflight has been limited, but **Nelson et al.** reviewed results from STS-76 in which mutations and chromosomal aberrations were measured in *C. elegans*. The goal was to test whether the absence of gravity modified the mutagenic or clastogenic response to an exogenously added isotope, ^{45}Ca . Mutations were recovered at the *fem-3* locus but not at the *unc-22* locus. The radioisotope exposure led to anaphase bridge formation, an indication of chromosomal damage, but the frequency of bridge formation was not affected by the gravitational load.

Protons are the most abundant ion for both SPE and GCR. A cooperative research program on the effects of proton radiation has been established at Loma Linda University and is comprised of scientists working in medical and accelerator physics and radiation biology. A new beam line has been configured for research use and a new suite of labs has been constructed and outfitted for use by NASA investigators. The Loma Linda University program, described by **Nelson et**

al., focuses on tumorigenesis in the C57BL6 mouse and addresses the impact of proton dose-rate on tumor incidence in several different organ systems and immune system performance in the same animals. Related studies include an assessment of differential gene expression in *C. elegans*, a study of tissue integration and its effects on radiation response in the rat thyroid gland, and an assessment of changes in the microvasculature of the rat retina.

Rabin et al. discussed the neurophysiological and behavioral effects of heavy ion exposures. Using three approaches, one that measures conditioned taste aversion (CTA) learning, a second that evaluates conditioned place preference (CPP), and the Morris water maze test to evaluate radiation-induced deficits in spatial learning and memory, his team finds that exposing rats to low fluences of Fe ions can affect the performance of a range of behavioral tasks. The impact on the dopaminergic system was highlighted by the CTA and CPP tests, while the Morris water maze test showed a clear deficit in spatial learning and memory. These studies are the first to suggest that space radiation exposures may affect the capability of astronauts to utilize spatial cues and change their behavior in response to their environment.

Risks of carcinogenesis

Studies on DNA damage and repair are intimately linked with the assessment of the toxicity of charged particle radiations and their potential mutagenic and carcinogenic effects. **Chatterjee et al.** demonstrated that a heavy ion interaction fragments DNA into patterns inconsistent with the previously accepted solenoidal model of DNA. Modeling and experimental studies showed that a zig-zag model of DNA structure is more likely to be correct.

Further work confirms that linear energy transfer is not an adequate predictor of the proportion of non-rejoined DNA fragments. **Rydberg and Cooper** and **Muhlmann-Diaz et al.** (presented by Bedford) showed that the ability to rejoin DNA molecules following exposure to sparsely ionizing x-rays was dose-dependent, with proper rejoining more likely after low doses than after higher doses. In contrast, the ability to carry out proper rejoining following exposure to densely ionizing radiations was less dependent upon dose, suggesting an explanation for the increased toxicity of these radiations at low fluences. Chromatin structure and/or recombinational repair also influence the amount of residual damage left in specific DNA structures within human cells.

The mutagenic effectiveness of protons and densely ionizing radiations has been addressed using three different model systems: A_L human x hamster hybrid cells, human lymphoid cells, and in a transgenic mouse model. The A_L cell model allows the quantitation of mutations at the CD59 locus on a single copy of human chromosome 11. Both small and very large chromosomal scale mutations can be detected. **Lenarczyk et al.** (presented by Waldren) summarized work showing that densely ionizing Fe ions were more toxic than gamma rays, and that they were also more mutagenic per unit dose. However, Fe ions were slightly less mutagenic than gamma rays when equitoxic doses of the two radiations were compared. Most radiation-induced CD59 mutants had chromosomal scale deletions. A notable difference, however, was the 7x greater frequency of complex mutations among the Fe treated clones. Complex mutations have been associated with genomic instability. Present studies are focused on testing two aminothiols, WR-1065 and RibCys, to evaluate their potential to mitigate against Fe-induced mutations.

The genetic background of the cell at risk can influence susceptibility to mutation. **Kronenberg et al.** used 2 human lymphoblastoid cell lines from the same donor and showed that a homozygous mutation in the *TP53* gene was associated with a marked elevation in the risk of mutation at the *TK1* locus. This was true for both proton and Fe ion exposures. Fe ions were substantially (up to 100x) more mutagenic than protons as a function of fluence. Analysis of *TK1*-deficient mutants showed that loss of heterozygosity (LOH) was the predominant mechanism of mutagenesis after Fe ion exposure. LOH arose predominantly by deletion in cells with normal *TP53*, while recombination-mediated LOH occurred more frequently in cells with only mutant *TP53*. The extent of LOH along chromosome 17 was substantially larger in cells with mutant *TP53*. Thus, both the frequencies and the mechanisms of mutagenesis differed as a function of the genetic background of the cell at risk.

Mutations are important in cells that proliferate, as they are thought to contribute to carcinogenesis, but mutations may also be important in non-dividing cells if they affect the function of those cells *in situ*. **Chang et al.** presented results obtained with a transgenic mouse model in which the *lacZ* mutation target is integrated in the germline, and where mutations can be quantified in proliferative and non-proliferative tissues. Fe ion exposures led to elevated *lacZ* mutation frequencies in three different tissues, but not to the same extent. The genetic background of the animal was also important. Mice nullizygous for *Mmp53* were at increased risk for Fe-ion-induced mutations. Micronucleus induction was measured in erythrocytes, and the observed frequencies also depended on the genetic background of the animal at risk.

Alterations in gene and protein expression are indicators of radiation response and may guide tissue repair, remodelling, and the development of late effects, including cancer and cataract. **Balcer-Kubiczek et al.** identified two trefoil peptide genes with altered response profiles at late times after Fe ion exposures. The response patterns of these genes were tissue specific. They are likely to be involved in the remodelling of the gut and mammary gland.

Several investigations focused on changes in protein localization and expression following exposure to Fe ions and protons. Two proteins of importance in the response(s) to DNA damage were studied: Ku86 and p53. **Metting** used confocal microscopy to quantify the appearance of Ku86 protein in the nuclei of human cells, and found a rapid change in the immunoreactivity of Ku86 and a time and dose-dependence for the altered reactivity. The Ku86 protein expression was localized to the nucleus, and staining patterns were dependent on cell type. **Warters et al.** discussed the movement and expression of the tumor suppressor and cell cycle regulator p53, seeking to define the mechanistic basis for the action of aminothiols that are candidate antimutagens. Immunofluorescence microscopy suggests that the immunoreactivity of p53 increases in response to radiation exposure and aminothiol exposure, but Western analysis suggests epitope unmasking.

Changes in gene and protein expression direct progression of early radiation damage to late tissue effects. One of the best known late effects of radiation exposure is cataractogenesis. **Blakely et al.** have used normal human lens epithelium to examine proton-induced alterations in the expression of FGF-2, a cytokine thought to regulate lens proliferation and differentiation. They saw cyclical increases in the expression of FGF-2 following proton exposure, and

hypothesize that altered expression of FGF-2 promotes dysregulated differentiation of lens epithelium leading to cataract formation. **Barcellos-Hoff et al.** discussed radiation-induced remodelling of the extracellular matrix (ECM) in mouse tissues. In the mammary gland, some changes in the stromal ECM were specific to Fe ions. The predominant effect was increased immunoreactivity of collagen type III in the adipose stroma. ECM remodelling was also observed in the liver, but different components of the ECM were affected: reduced immunoreactivity of collagen type I and type III in the perisinusoidal space, along with reduced reactivity for laminin. Tissue specific alterations in the ECM may regulate the progression of preneoplastic cells.

The Radiation Effects Team of the NSBRI (**Dicello et al., Sinden et al., Williams et al.**) described a series of projects that support and extend the core project, which seeks to define the risk of mammary carcinogenesis of protons and Fe ions in the Sprague-Dawley rat. These are long term studies that were initiated last year. Early results show that Fe ion exposures produce mammary nodules, as do γ -rays. To date, most excised tumors are carcinomas. This program will use tamoxifen to test the hypothesis that low dose radiation carcinogenesis can be mitigated by pharmaceutical countermeasures. Mechanistic questions will be addressed, including the types of recombination events that ensue in repeated DNA sequences, and quantitation of chromosome aberrations in rat and human mammary epithelial cells. Aberrations will be measured after high and low dose-rate exposures to γ -rays, protons, and Fe ions.

Summary

The presentations in this session dealt with the characterization of the space radiation environment, radiation physics and transport, basic and applied radiation biology, and both physical and biodosimetry for spaceflight. The research in these diverse areas will contribute to a more accurate determination of the risks to human health from space radiation and to the development of physical and pharmacological countermeasures to use in future long-duration orbital and exploration class missions.

Amy Kronenberg, Jack Miller, and David Huso

RADIATION MEASUREMENTS ON THE RUSSIAN MIR ORBITAL STATION

Gautam D. Badhwar, NASA Johnson Space Center, Houston, Texas 77058-3696

The Russian *Mir* orbital station was launched into an orbit with a 51.65° inclination in March 1986. It has operated continuously in the altitude range of 380 to 460 km. Almost immediately, cosmonauts began to carry out missions to the station. To date, there have been some 25 Russian missions. As part of the NASA Mir Program, a comprehensive set of radiation measurements were made to map the radiation in all of the *Mir* module.

Numerous radiation measurements have been made on the *Mir* station throughout its lifetime. However, the comparison of these measurements have been difficult because of different sensitivities of detectors, some active and some passive, differing self shielding and in most cases unknown location shielding. In spite of these complications, very significant progress in the knowledge of the radiation environment onboard the *Mir* station has been made. These results are directly applicable to expected radiation environment on the *International Space Station*.

In this paper, we describe the combined results from all seven NASA Mir missions. We show: (1) the absorbed dose rate from trapped particles is well correlated with the atmospheric density computed nearly 400 days earlier than the time of observation, (2) developed a relationship between the absorbed dose rate from galactic cosmic rays to the deceleration potential derived using the Climax neutron monitor rate, giving a tool to predict GCR dose rates to $\pm 15\%$ nearly 90 days prior to observations, (3) describe the drift of the South Atlantic Anomaly (SAA) with time, (4) compare the predictions of the dose rates as a function of time from the November 6-8, 1998 solar particle event with observations, (5) compare measurements made with NASA Tissue Equivalent Proportional Counter (TEPC) with the ESA DOSTEL device, the Hungarian Pille system, and the Russian R-16 dosimeter. Implications of these measurements for the *ISS* will be discussed.

CHARACTERIZATION OF TREFOIL PEPTIDE GENES IN IRON-ION OR X-IRRADIATED HUMAN CELLS

E.K. Balcer-Kubiczek, G.H. Harrison, J.F. Xu and X.F. Zhou

Department of Radiation Oncology, Division of Radiation Research, University of Maryland School of Medicine, Baltimore, Maryland 21201.

INTRODUCTION

The gastrointestinal (GI) tract is especially sensitive to ionizing radiation, probably because of its high rate of cell turn over. Most of the data in the literature concerns the histological/anatomical description of damage rather than functional studies. In fact, previous reports in humans have shown that, at doses of 2 Gy or more, functional abnormalities appear indicating that in radiation sensitive tissues the effects of radiation are not limited to cell death. GI functions are controlled in particular by GI peptides. One hypothesis is that ionizing radiation may modulate the synthesis and release of these peptides and consequently may contribute largely to abnormalities in GI function. However, no previous studies have been concerned with GI-specific gene expression in irradiated GI tissues. The family of human trefoil peptides comprises three members thus far, all of which are expressed in specific regions of the GI tract. In addition, two trefoil peptides, pS2 (TFF1) and hITF (TFF2) are expressed in breast tissue. Their exact function in GI and breast tissues is unclear but mucosal integrity, repair, mucin secretion and responsiveness to hormones have been shown. We recently isolated and characterized pS2 as a novel p53- and estrogen receptor-independent gene whose mRNA expression in several cells lines was found to be delayed 4 to 7 days after irradiation with X-rays, fission neutrons or 1 GeV/n Fe-ions. The aim of the present study was to determine whether pS2 and hITF have a similar induction kinetics in irradiated gastric and breast cell lines, and whether they have the phorbol ester (TPA) responsive element (TRE).

METHODS

hITF and pS2 mRNA distributions were investigated in normalized multi-tissue mRNA arrays, leading to the selection of MCF7 (breast) and four colon cell lines: HCT-15, HCT116, LoVo and LS180. Except for HCT15 homozygous for the wild type p53, all the other cells have two wild type p53 alleles. Each colon cell lines has a different mutator gene, however LoVo and HCT116 cells have mutated hMSH2 and hMLH1 genes, respectively. HCT-15 cells have mutated hMLH1 and are null for hMSH6. LoVo cells are wild-type for these genes and also for hPMS1 and hPMS2 mismatch repair genes. The effect of X-irradiation on cell survival was determined by the standard colony formation assay. The effect of X- or Fe-ion irradiation on transcription of pS2 and hITF was determined by Northern blot analysis of samples obtained at 0, 3, 5 h as well as 1,4, 7 or 14 d following 5 Gy X-irradiation or 1.2Gy Fe-ions. pS2 cDNA was previously isolated in our laboratory by differential screening of the MCF7 cell library in Fe-ion irradiated *versus* control MCF7 cells at 7-day RNA samples. A 0.4-kb probe against 0.6-kb hITF mRNA was obtained by RT-PCR using gene-specific primers designed based on the corresponding cDNA sequence data in the GenBank library (accession no. L08044).

RESULTS

We observed no difference in radiation sensitivity among the four colon cell lines. Kinetics studies revealed similar patterns of expression for pS2 and hITF in MCF7 cells following X- or

Fe-ion irradiation as well as inducibility by TPA. Analysis of RNA from X-irradiated colon cell lines showed the induction of trefoil peptide mRNAs in LoVo and LS180 cells, beginning on the day 4 after irradiation. Therefore, both pS2 and hITF were found to be new tissue-specific radiation- and TPA-responsive which in addition are the first reported examples of genes having a delayed induction following ionizing radiation and early response following TPA exposure.

CONCLUSION

We have identified two novel radiation responsive genes each of which demonstrates tissue specificity and p53-and mismatch gene status independence. The important finding is that pS2 and hITF exhibit delayed expression after irradiation which may be indicative of late phenotypic alterations in irradiated breast or GI tissues. These results also suggest that the induction of trefoil peptide genes in tumor cells of the microsatellite mutator phenotype may have diagnostic applications to discriminate among the diverse underlying mutator genes. (Supported in part by NASA grant NAGW-4392).

COMPARISON OF GAMMA AND IRON PARTICLE IRRADIATION INDUCED REMODELING OF EXTRACELLULAR MATRIX IN MURINE LIVER

M.H. Barcellos-Hoff, C. Wang, and S.A. Ravani

Life Sciences Division, Lawrence Berkeley National Laboratory, Berkeley, CA 94720

INTRODUCTION

Cells in tissues exist in complex microenvironments that mediate phenotype and cell interactions. Microenvironments, which includes the insoluble extracellular matrix (ECM) and soluble cytokines, also modulate cellular response to stimuli, which in turn may modify the microenvironment. Our studies have demonstrated rapid and global remodeling of the microenvironment in irradiated murine mammary gland and have identified characteristics of the HZE-irradiated remodeling that are distinct from those following sparsely ionizing radiation (Ehrhart, et al., 1996). The hypothesis is that certain effects of HZE particles cause specific modifications of tissue microenvironment as compared to reference gamma-radiation. This in turn is postulated to contribute to the functional and carcinogenic cellular effects of HZE exposure. Identification of HZE-induced changes in the microenvironment will provide insight into how fundamental cellular effects are integrated into multicellular tissue responses.

The goal of this study was to evaluate early (1 hr - 7 day) temporal and spatial changes in the composition of the irradiated liver microenvironment as a function of radiation quality and dose or particle fluence. Comparison of liver to mammary gland in terms of microenvironment remodeling may provide insight into mechanisms. Tissue-dependent changes are most likely to be the result of particular cellular response to radiation and may reveal specific mechanisms that underlie tissue sensitivity to radiation of various qualities important to the environment in space.

METHODS

Liver from Balb/c mice that were irradiated whole body with 1 GeV Fe particles or ^{60}Co gamma-radiation were evaluated. The extracellular matrix (ECM) was qualitatively assessed using immunofluorescence to localize the basement membrane proteins, laminin and collagen type IV, and the interstitial proteins, collagen type I, collagen type III and fibronectin, in cryosections of mouse liver. Duplicate sections from 2-3 animals were assessed. Immunofluorescence images were obtained using a 40x (0.75 numerical aperture) objective on a Zeiss Axiovert equipped with epifluorescence. A multiband pass dichroic mirror, barrier filter and differential wavelength filter wheel combinations was used to selectively excite fluorochromes in sequence. Images were captured using a scientific-grade 12-bit charged coupled device (KAF-1400, 1317 x 1035 6.8 μm square pixels) camera (Xillix, Vancouver, Canada). This camera has a linear response (pixel intensity range= 1-4000) suitable for quantitative imaging using exposures for which the intensities for a given experiment fall within the 12-bit linear range. Relative intensity of images were maintained when constructing figures by scaling the 12-bit data set to a common 8-bit scale using Scilimage (TNO Institute of Applied Physics, Delft, The Netherlands) using the data set minimum and maximum. Selected images were saved in TIFF format and composite figures were constructed using Adobe Photoshop. Internal standardization was achieved by comparing only images stained with the same antibodies in the same experiment, captured with identical parameters and scaled and displayed identically. Selected changes were quantified using image analysis to assess dose response relationships.

RESULTS

The ECM of liver tissue collected between 1 hr to 7 days after 5 Gy whole body gamma-irradiation was evaluated. Liver perivascular collagen type I and III showed a persistent loss that was evident by 24 hr. Fibronectin rapidly decreased in hepatic sinuses but began to recover at 7 days post-irradiation. Collagen type IV showed an initial rise between 1 and 24 hr followed by loss at 3 and 7 days. The dose dependence of perisinusoidal remodeling was evaluated using image analysis following gamma-irradiation with doses from 0.1-5Gy at 3 days post-irradiation. Fibronectin immunoreactivity decreased at doses of ≥ 1 Gy and collagen type IV decreased following doses ≥ 0.5 Gy.

In contrast, tissue collected from 3 hr to 96 hr following 0.8 Gy (~ 3 particles / $10 \mu\text{m}^2$) whole body 1 GeV Fe-particle irradiation showed increased perisinusoidal fibronectin, collagen type IV and laminin immunoreactivity as early as 24 hr. In addition, the localization of these proteins became more distinctly sinusoidal and continuous following Fe-particle irradiation. No changes in perivascular collagen type I or III were noted.

CONCLUSIONS

Following ionizing radiation remodeling of the liver ECM is rapid and global, as we have shown in the mammary gland, but the character and composition is distinct. Whereas in mammary gland there is modest decrease in collagen III in the periepipithelial stroma, the predominant effect is increased collagen type III in the adipose stroma, while laminin or collagen IV were unaffected (Barcellos-Hoff, 1993). In contrast, collagen type I and III are rapidly (>1 d) and persistently (> 7 d) decreased in liver. Collagen type IV is induced in the perisinusoidal space and laminin is decreased. These data suggest that cell type and tissue interactions play a prominent role in determining the character and composition of radiation-induced ECM remodeling. These preliminary data suggest a possible radiation quality dependence for ECM remodeling in liver. Increased perisinusoidal staining of fibronectin and collagen type IV was observed in tissue following 0.8 Gy Fe-particle exposures while they were decreased following doses as low as 1 Gy gamma-radiation.

The character of the irradiated tissue microenvironment is postulated to be important during radiogenic carcinogenesis for the following reasons:

- (1) *Normal microenvironments inhibit the expression and characteristics of neoplastic cell.*
- (2) *Abnormal regulation of the microenvironment may result from the action of the carcinogen itself, particularly in the case of external radiation which democratically damages all cells of a tissue.*
- (3) *Radiation-induced perturbations in the microenvironment may mediate the process of carcinogenesis by promoting genomic instability.*
- (4) *Changes in non-target cells (e.g. stroma) that contribute to the microenvironment may promote progression of the preneoplastic cell.*

Our studies show that HZE-irradiation elicits distinct microenvironment changes when compared to sparsely ionizing radiation. We previously reported that laminin, an important mediator of epithelial integrity, is altered in Fe-particle irradiated mammary gland (Ehrhart, et al., 1996). Normally the basement membrane serves as a barrier to invasive growth, but one hallmark of cancer is the ability to destroy and traverse the basement membrane. Furthermore disruption of

basement membrane integrity by either chemically-mediated and transgenic means promotes the expression of mammary tumors (Lewko, et al., 1981, Sympson, et al., 1995). Radiation induced changes in basement membrane integrity might thus promote neoplastic progression.

REFERENCES

Barcellos-Hoff, M.H. (1993) Radiation-induced transforming growth factor and subsequent extracellular matrix reorganization in murine mammary gland. *Cancer Res.*, 53:3880-3886.

Ehrhart, E.J., E.L. Gillette and M.H. Barcellos-Hoff (1996) Immunohistochemical evidence of rapid extracellular matrix remodeling after iron-particle irradiation of mouse mammary gland. *Rad. Res.*, 145:157-162.

Lewko, W., L.A. Liotta, M.S. Wicha, B.K. Vonderhaar and W.R. Kidwell (1981) Sensitivity of N-nitrosomethylurea-induced rat mammary tumors to cis-hydroxyproline, an inhibitor of collagen production. *Cancer Res.*, 41:2855-2862.

Sympson, C.J., M.J. Bissell and Z. Werb (1995) Mammary gland tumor formation in transgenic mice overexpressing stromelysin-1. *Sem. Cancer Biol.*, 6:159-163.

RADIATION DOSIMETRY ON MANNED SPACE MISSIONS AND AT GROUND-BASED ACCELERATORS

E.V. Benton¹, E.R. Benton², A.L. Frank¹, and M.M. Moyers³

¹University of San Francisco, Physics Dept., 2130 Fulton St. San Francisco 94117

²Eril Research, Inc., ³Loma Linda University Medical Center

INTRODUCTION

Exposure to ionizing radiation of space crews engaged in long-term space missions such as on space stations, Lunar bases and trips to Mars, poses a set of complex scientific and technological problems which are being resolved on the road toward achieving adequate radiation protection. At the same time, both space and ground-based radiobiological experiments, and radiation sensitive biomedical experiments require adequate dosimetric support. In both areas, passive radiation detectors have in the past and are now playing an important role. Recently we have been conducting two separate but related experiments involving environmental radiation measurements aboard the Russian Mir Space Station and ground-based accelerators aimed at clarifying the role of proton-induced target fragmentation.

METHODS

Sets of passive radiation detectors were deployed throughout the interior of the Mir Space Station on several NASA/Mir missions. On one mission, an additional set of detectors was exposed outside the Mir under extremely low shielding conditions. At the same time high energy proton beams available at the Loma Linda University Medical Center have been used in conjunction with tissue equivalent passive detectors to measure the dose equivalent fraction resulting from high LET particles produced in target fragmentation of nuclei in tissue.

RESULTS

Inside the Mir Space Station data on the dose and dose equivalent as measured by passive detectors has been obtained and compared with other detector systems. An external detector array exposed outside the Mir has been analyzed to yield information on the low energy component incident on Mir under conditions of very low shielding. Several sets of fragmentation experiments performed with 70–250 MeV proton beams at the Loma Linda University Medical Center have been analyzed.

CONCLUSIONS

In addition to the dosimetric information gathered, the results strongly suggest that proton-induced, high LET target fragments in tissue contribute significantly to the dose equivalent on the Mir and therefore need to be taken into account on the ISS. Preliminary results also suggest that further investigations are needed to clarify the role of target fragments in the tissue/bone interface for cancer proton therapy.

PROTON IRRADIATION ALTERS EXPRESSION OF FGF-2 IN HUMAN LENS EPITHELIAL CELLS

E. A. Blakely, K. A. Bjornstad, P. Y. Chang, M. P. McNamara, and E. Chang
Life Sciences Division, Berkeley National Laboratory, Berkeley, CA 94720

INTRODUCTION

We are investigating a role for proton radiation-induced changes in FGF-2 gene expression as part of the mechanism(s) underlying lens cell injury. Radiation injury to the human lens is associated with the induction of cataract following exposure to protons.

METHODS

Normal human lens epithelial (HLE) cells are maintained on extracellular matrix (ECM) derived from bovine corneal endothelial cells. The HLE cultures express protein markers for differentiation during growth. In addition, we are growing human lens cells immortalized by viral transformation (HLE-B3) that can be maintained without ECM *in vitro*. Comparisons have been made between exponentially growing and confluent cell cultures. Cultures with low passage numbers (<8) are used for HLE experiments, while the HLE-B3 cultures have higher passage numbers (>13). Total RNA and proteins were isolated from unirradiated controls and from cultures irradiated with 4 Gy of 55 MeV protons and processed immediately for RT/PCR, Northern or Western analyses of FGF-2 expression, or over a time course up to 24 hours of incubation at 37° C. Cultures of each cell type and growth status were fixed and prepared for FGF-2 immunofluorescence to study the intracellular localization of the protein. Recombinant FGF-2 protein, and RNA and protein isolated from the FGF-2 producing human hepatoma (SK-Hep1) cells were used as positive controls.

RESULTS

We observed differences in the expression of the three isoforms of FGF-2 in transformed HLE-B3 cells compared to the normal HLE cells. We also demonstrated differences in FGF-2 expression that are dependent on cell culture conditions. After irradiation with 4 Gy of 55 MeV protons, we observe alterations in FGF-2 transcription levels in both the normal and transformed cells. In confluent HLE cells, FGF-2 transcripts are in very low copy number and are barely detectable using Northern analysis, but fluorescence immunostaining reveals evidence for enhanced FGF-2 expression in exponentially growing HLE cells within hours after irradiation.

CONCLUSION

FGF-2 expression changed during cell proliferation and as a function of the differentiation of normal HLE cells *in vitro*. Immortalized HLE-B3 cells showed a modified expression of FGF-2 that may be important to their successful growth without ECM. We will report on the time course of the transcriptional and translational expression of FGF-2 after proton irradiation of both immortalized and differentiating normal lens cells, and discuss the role of FGF-2 in the radiation response.

Supported by NASA Award #W-18758.

HEAVY ION INDUCED GENETIC DAMAGE IN TRANSGENIC ANIMALS

P. Y. Chang¹, L. Lutze-Mann², V. Walker³, D. Torous⁴, and R. A. Winegar¹

¹SRI International, Menlo Park, CA 94025; ²University of New South Wales, Sydney, Australia

³Wadsworth Center, NY State Dept. of Health, NY; ⁴Litron Laboratories, Rochester, NY.

INTRODUCTION

The radiation environment in space is complex in that it contains a variety of densely ionizing particles that are capable of producing DNA damage. The long-term radiation risks are dependent on the types of molecular injuries and the subsequent processing of these lesions. We are using transgenic mice containing *lacZ* reporter genes in every cell to evaluate the tissuespecific responses at the molecular level after heavy particle radiation. The *lacZ* target gene has also been introduced into p53 knockout transgenic mice to obtain animals that are either hemizygous (*p53+/-lacZ*) or nullizygous (*p53-/-lacZ*) with regard to their p53 status. The use of these animals allows us to evaluate the influence of p53 genetic background on radiation-induced genetic damage. We evaluated the induced *lacZ* mutation frequency (MF) in three tissues: liver, brain and spleen. Using the same animals, we also measured *hprt* in splenic lymphocytes and cytogenetic damage in erythrocytes.

CURRENT STATUS OF RESEARCH

METHODS

We exposed *lacZ* animals with different p53 genetic status to a single acute dose of 1 Gy 1 GeV/amu iron ions at the Alternating Gradient Synchrotron (AGS), Brookhaven National Laboratory (BNL). At various times after irradiation, mice were euthanized and blood and tissue samples collected. For evaluation of *lacZ* MF, DNA was isolated from frozen tissues, and *lacZ* plasmid was purified using magnetic bead particle separation. Purified plasmid DNA was then electroporated into *E. coli*, and colonies containing mutant *lacZ* were screened using selective plating. Mutational spectra were evaluated using restriction digest and Southern hybridization analysis.

To measure *hprt* mutant frequencies, splenic lymphocytes were stimulated and cultured in selective media. For the micronucleus assay, small volumes of peripheral blood were fixed in methanol, and stained with an FITC-conjugated anti-transferrin receptor and propidium iodide. Flow cytometry was then used to quantitate mature normochromatic erythrocytes (NCE), immature polychromatic erythrocytes (PCE), micronucleated NCE (MN-NCE), and MN-PCE.

RESULTS

Iron particle radiation increased *lacZ* MFs in the liver, brain and spleen in each of the three strains, regardless of p53 status. There were also tissue-specific differences in the pattern of *lacZ* MF as a function of time after particle radiation. The overall radiation-induced *lacZ* MF in p53-/- animals was higher than in the p53+/+ and the p53+/- animals. The spectrum of harvested *lacZ* mutants from irradiated mice indicates irradiation induced mainly deletions rather than point mutations.

Mutant frequencies in the endogenous *hprt* locus were measured at 2, 4, and 8 wk after irradiation. The pattern of elevation of *hprt* MF as a function of time post-radiation was the same

regardless of p53 status. MF was increased at 2 wk post-radiation, peaked at 4 wk post-radiation, and declined at 8 wk post-radiation. However, the magnitude of the induced *hprt* MF was dependent on the p53 gene dosage, with a 20-fold increase in MF in the *p53*^{+/-} animals and a 40-fold increase in the *p53*^{-/-} animals at 4 wk post-irradiation. Additionally, the *hprt* MF at 8 wk post-radiation remained elevated in the p53-deficient mice.

Micronuclei in circulating PCEs were elevated 2.3- to 2.6-fold at 72 hours post-irradiation in the *p53*^{+/+} *lacZ* and the *p53*^{+/-} *lacZ* animals. A greater (4.3-fold) induction was seen in the *p53*^{-/-} *lacZ* animals. The kinetics of recovery from chromosomal damage as measured by the frequency of micronuclei in PCEs differed with p53 genetic background. In the *p53*^{+/+} *lacZ* and *p53*^{+/-} *lacZ* animals, micronucleus levels returned to control values within 9 days after irradiation. In the *p53*^{-/-} *lacZ* animals, micronucleus levels remained elevated (2-fold greater than the controls) at 13 wk post-irradiation. Since PCE have a lifespan of only a few days, this persistent elevation indicates the continual production of micronuclei in bone marrow. This may indicate that loss of p53 influences radiation-induced genomic instability.

CONCLUSIONS

We have shown that the *lacZ* transgenic model is a powerful system that allows multiple types of genetic damage to be measured in each animal. In the present study, we have measured high LET radiation effects (1) at the gene level using a surrogate non-transcribed transgene, (2) at the gene level using the endogenous transcribed *hprt* locus, and (3) at the chromosomal level by measuring the kinetics of micronuclei induction in circulating PCEs.

Our results indicate that iron particle radiation induces *lacZ* transgene mutations and that the magnitude of this induction is dependent on the tissue assayed. We have also demonstrated that exposure to 1 Gy of iron beam results in time-dependent elevation of MF in the endogenous *hprt* locus and dramatic immediate response in the hematopoietic system, as indicated by a large induction of micronuclei in circulating PCEs. For all endpoints, the magnitude of the initial response and the subsequent recovery from genetic damage are dependent on the p53 status of the animal.

PLANS FOR FUTURE INVESTIGATIONS

This research is directed towards an understanding, at the molecular level, of genetic damage induced by space radiation. Our results indicate that radiation-induced genetic damage is tissue specific, and highly dependent on the genetic background of the animal.

We would like to extend our research by using *lacZ* mice with different p53 status to compare the mutagenic and clastogenic potential of protons and other HZE radiation that are prevalent in the space environment. The results from these studies will allow us to characterize the mutagenic and cytogenetic damage induced by known doses and qualities of HZE radiation. Our present results suggest that particle induced cytogenetic damage may have long-term consequences in animals. We plan to study the long-term consequences of radiation-induced DNA damage, including genetic instability, which might result in persistent elevated mutation rates. Finally, we are interested in examining the effects of cytokines as radioprotective agents to mitigate the DNA damaging effects of particle radiation. An understanding at the molecular level of cellular

responses to ionizing radiation-induced damage should increase the ability to estimate the risks to humans exposed to the space radiation environment.

SIMULATION OF CLUSTERS OF DNA DAMAGE INDUCED BY IONIZING RADIATION ENCOUNTERED IN SPACEFLIGHT

A. Chatterjee, W.R. Holley and I.S. Mian, Lawrence Berkeley National Laboratory, Life Sciences Division, Berkeley, CA 94720

INTRODUCTION

Energetic Protons and Heavy Charged particles are present in the Galactic Cosmic Rays (GCR). Thus, an assessment of their possible harmful health effects to astronauts in long duration space flights above the earth's magnetic field is of high priority in NASA supported research. The research presented here is from our efforts in the NASA Specialized Center of Research and Training related to Radiation Health. Theoretical modeling of radiobiological effects of charged particles found in the GCR can provide very useful information which may not be obtainable through experiments alone. One such example is the production of clusters of damage by tracks of charged particles interacting with cellular DNA. Based on our general theory of radiation damage to DNA, it has been demonstrated that several damaged sites (base damage, single strand breaks and double strand breaks) can be produced in close proximity, generally within twenty base pairs. The severity of the clustering can vary greatly based on the quality of radiation. One recurring theme in our studies and a feature which distinguishes radiation damage from most other types of insult to DNA is the strong spatial correlations in the damage.

The next obvious question is what are the biological consequences of such clustering? Furthermore, since clustering of damaged sites cannot be measured directly, is it possible to correlate theoretical estimates of the frequencies with which certain types of clusters are generated by particle tracks with selected biological end points? In this presentation, we demonstrate our initial efforts in correlating clusters of damage with experimentally measured unrejoined double strand breaks.

METHODS

Our theory includes direct and indirect effects and is based on general features of track structure and stopping power theory in conjunction with a variety of detailed DNA models. Charged particle tracks are modeled by partitioning the energy deposition between primary track glancing collisions (energy transfer < 100 eV) and production of delta-rays (energy transfer > 100 eV). Monte Carlo simulation techniques are used which incorporate damage due to the following molecular mechanisms: (1) ionization of water molecules forming .OH, .H, eaq, etc.; (2) OH radical attack on sugar molecules leading to formation of DNA strand breaks; (3) radical attack on bases; (4) direct ionization of sugar molecules leading to strand breaks; (5) direct ionization of bases. We can calculate, in detail, the damage sites for essentially any charged particle and energy interacting with any of several DNA models ranging from simple linear DNA, to 30 nm chromatin fibers in various solenoidal or ribbon configurations.

The calculations are performed on Unix workstations and typically take from a few hours to a few days of CPU time to generate a few thousand double strand break (DSB) events. To obtain these numbers of DSB's usually requires approximately 10^4 - 10^7 incident tracks.

We concentrate here on the short range correlated damage, i.e., DSB's and local clusters of DSB's. Our general definition of a "cluster of damage" is a group of nearby damaged sites, usually caused by a single incident particle, separated by some undamaged DNA on each side. In particular, for the results discussed here, a cluster, refers to a group (one or more) of damaged sites with no internal undamaged regions of 20 base pairs or more separated by at least 20 undamaged base pairs on each side from other damaged regions. Most of the time we refer to clusters which contain at least one DSB.

RESULTS

We have examined some general properties and characteristics of damage clusters as a function of LET. Most clusters, even for high LET, are less than 30 base pairs wide; that is clusters usually extend less than +/- 15 base pairs from the cluster center near where double strand breaks are located. In fact, the typical (or most frequent) cluster is contained within about 10 base pairs.

A useful method for summarizing general properties is by looking at average values. We have calculated average properties of DSB clusters for various categories of damage for several particles over a wide range of energies. At low LET, a general characteristic of clusters is that they mostly contain a single DSB and a couple of damaged bases and half the time an extra strand break. In the LET range of 100-200 ev/nm, the energy deposition becomes high enough in the core of the track to produce on average more damage than needed for a minimal DSB cluster and these averages start to increase. It is reasonable that, as the LET increases beyond a value of 100 ev/nm and the local energy deposition exceeds the order of 100-200 eV, more and more sites in a typical local cluster will be damaged. At an LET of ~100 ev/nm the average number of bases and sugars damaged per cluster (and even the number of DSB's per cluster) starts to rise. At a few hundred ev/nm there may be 5-10 extra base and several sugar damages in a typical local cluster.

As an example of the potential utility of such considerations we will relate a particular damage severity index, that is, the number of DSB's in a cluster to the ability of the cell to rejoin within a reasonable time (24 hours) the DSB's in the cluster. The general experimental result is that after low LET radiation, only few percent of the DSB's or clusters of DSB's remain unrejoined but this unrejoined fraction rises with increasing LET. This fraction left unrejoined has an LET dependence similar to some of the average cluster properties, i.e., flat up to about 100 ev/nm and then increasing rapidly, to a value of 30% or higher. A comparison with experimental data will be presented.

NSBRI RADIATION EFFECTS: CARCINOGENESIS IN SPRAGUE-DAWLEY RATS IRRADIATED WITH IRON IONS, PROTONS, OR PHOTONS

J. F. Dicello,¹ F. A. Cucinotta,² D. S. Gridley,³ S. P. Howard,⁴ G. R. Novak,¹ R. Ricart-Arbona¹, J. D. Strandberg,¹ M. E. Vazquez,⁵ J. R. Williams,¹ Y. Zhang,¹ H. Zhou,¹ and D. L. Huso.¹
¹Johns Hopkins University, Baltimore, MD 21287; ²NASA Johnson Space Center, Houston, TX 77058; ³Loma Linda University, Loma Linda, CA 92354; ⁴University of Wisconsin, Madison, WI 53792; ⁵Brookhaven National Laboratory, Upton, NY 11973

INTRODUCTION

Our ability to confidently develop appropriate countermeasures for radiations in space in terms of shielding and design of a spacecraft, the mission scenario, or chemoprevention is severely limited by the uncertainties in both the risk itself and the change in that risk with intervention. Despite the fact that the risk of carcinogenesis from exposures of personnel to radiations on long-term missions is considered one of the worst hazards in space,^{1,2} only a limited amount of *in-vivo* data exist for tumor induction from exposures to protons or energetic heavy ions (HZEs) at lower doses. The most extensive work remains the landmark study of Alpen et al.³ for tumor development in the harderian gland of the mouse. The objective of this study is to characterize the level of risk for tumor induction in another relevant animal model. Subsequent experiments are designed to test the hypothesis that the level of risk can be reduced by pharmaceutical intervention in the promoting and progressing stages of the disease rather than in the initiating stage.

The work presented here results from a cooperative effort on the part of investigators from two projects of the Radiation-Effects Team (J. F. Dicello, Leader) of the National Space Biomedical Research Institute (NSBRI). The collaborating projects are the Core Project (J. F. Dicello, Principal Investigator) which is investigating the risk of carcinogenesis in Sprague-Dawley rats and the Chemoprevention Project (David Huso, Principal Investigator) which is investigating the ability of Tamoxifen to reduce the number of malignant tumors in the irradiated animals. Research at the cellular and subcellular levels is being conducted in two other projects of the Radiation-Effects Team, Cytogenetics with J. R. Williams as Principal Investigator and Mutations from Repeated DNA Sequences with R. R. Sinden as Principal Investigator. Results for these other projects also are being presented at this Workshop.

BACKGROUND

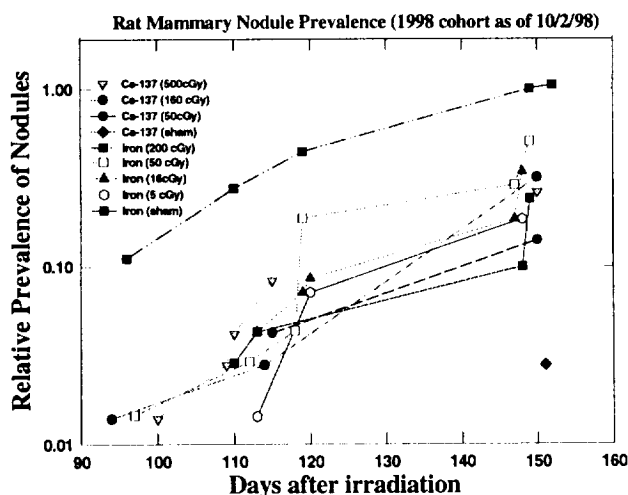
In the 1996 report of the National Research Council, the Task Group on the Biological Effects of Space Radiation¹ listed carcinogenic risks by protons and HZE particles as the first question needed to be addressed. The group also listed as one of its priorities the question of whether drugs might be used to protect against acute or carcinogenic effects from space radiations, particularly in the case of acute exposures from solar particle events (SPEs). At the same time they conveyed a degree of pessimism that specific types of agents could modify risks from daily exposures to cosmic radiation because of the relatively low level of risk associated with such protracted exposures.

To address the question concerning the carcinogenic risk from protons and HZEs and the degree to which it could be modified through pharmaceutical intervention, we are investigating tumor

induction in the Sprague-Dawley rat. This animal is one of the best characterized models, having been used extensively to study the effects of both gamma radiation and drugs, so there exists one of the best data bases the present objectives. This animal is hypersensitive to the formation of mammary tumors from both photon radiation and drugs, so measurable responses at low dose levels are possible. Data are available for tumor induction from exposures to high-LET particles, albeit neutrons,^{4, 5, 6} so there is less uncertainty, in comparison with most other animal models, in designing the HZE experiments for which beam time is both rare and expensive. Likewise, this animal model has been used for studies of Tamoxifen as a chemopreventive agent⁷ leading to successful clinical trials, thus providing us some confidence in extrapolating our results to humans.

METHODS

Female Sprague-Dawley rats at approximately 60-65 days of age are receiving total-body irradiations with energetic iron ions, protons, or photons. A Lucite holder was designed to allow the animals to be irradiated in a fixed position and at a specified depth. The lateral uniformity of the particle beams was about $\pm 5\%$. The HZE irradiations were performed at the Brookhaven National laboratory with an incident iron energy of 1 GeV/nucleon. A second series of irradiations was done with a degraded iron beam at a depth corresponding to a mean energy of approximately 600 MeV/nucleon at the proximal surface of the rat. The proton irradiations were performed at the Loma Linda University with an initial energy of 250 MeV. Photon irradiations were done with either cesium-137 (Brookhaven) or cobalt-60 (Loma Linda) with concurrent cesium-137 irradiations carried out at Johns Hopkins. One group of animals have been irradiated with 500 cGy of cesium-137 gamma rays with half of the animals being administered Tamoxifen according to the protocol developed by Welsch et al.⁷ The animal colony is housed in barrier cages in a controlled and monitored environment at Johns Hopkins University. The animals are palpated periodically, tumors are removed surgically, and histology is performed to classify the specimen as fibroadenoma, adenoma, or carcinoma with subtypes of carcinomas designated.



RESULTS

For the first series of experiments, 36 animals were irradiated at each dose of 0, 5, 15, and 50 cGy of iron ions and 0, 50, 160, and 500 cGy of protons or photons. One additional group of 18

animals was irradiated at a dose of 200 cGy of iron. The initial prevalence of nodules as a function of time is shown the figure.

CONCLUSIONS

Mammary nodules are developing in the Sprague-Dawley rats irradiated with iron ions and photons with increased prevalence roughly correlating with increased dose and higher atomic number, as would be expected. The higher level of tumor induction from iron for equal doses is also about what was anticipated as evidenced by the overlapping of the data from the two groups, with the exception of the small number of rats irradiated at 200 cGy. The proton irradiations took place about three months later than the iron studies, and nodules are just beginning to appear. Although the number of tumors remains small at this point, most of the tumors at higher doses of both iron and photons are carcinomas. No bone-marrow toxicity, gut complications, or CNS damage has been observed in the animals to date even at the highest dose levels.

REFERENCES

1. National Research Council, "Radiation Hazards to Crews of Interplanetary Missions: Biological Issues and Research Strategies." National Academy Press, Washington, D.C., 1996.
 2. National Research Council, "A Strategy for Research in Space Biology and Medicine in the New Century." National Academy Press, Washington, D.C., 1998.
 3. E. L. Alpen, P. Powers-Risius, J. D. Chapman, S. B. Curtis, and R. DeGuzman, "Tumorigenic Potential of High-Z, High-LET Charged-Particle Radiations." *Radiat. Res.* 136, 382-391 (1993).
 4. C. J. Shellabarger, D. Chmelevsky, and A. M. Kellerer, "Induction of Mammary Neoplasms in the Sprague-Dawley Rat by 430-keV Neutrons and x-Rays." *J. NCI* 64, 821-833 (1980)
- J. J. Broerse , L. A. Hennen, M. J. vanZwieten, C. F. Hollander: Mammary carcinogenesis in different rat strains after single and fractionated irradiations. In J. J. Broerse & G. B. Gerber, eds, Neutron Carcinogenesis, Brussels, Commission of European Communities. pp 155-168, 1982.
- J. J. Broerse, L. A. Hennen, H. A. Solleveld: Actuarial analysis of the hazard for mammary carcinogenesis in different rat strains after X- and neutron irradiation. *Leuk. Res.* 10, 749-754, (1986).
7. C. W. Welsch, M. Goodrich-Smith, C. K. Brown, N. Miglorie, and K. H. Clifton, "Effect of an Estrogen Antagonist (Tamoxifen) on the Initiation and Progression of g-Irradiation-Induced Mammary Tumors in Female Sprague-Dawley Rats." *Eur. J. Cancer Clin. Oncol.* 17, 1255-1258 (1981).

GENETIC REGULATION OF CHARGED PARTICLE MUTAGENESIS IN HUMAN CELLS

A. Kronenberg¹, S. Gauny¹, C. Cherbonnel-Lasserre², W. Liu¹, C. Wiese¹

¹Lawrence Berkeley National Laboratory, Life Sciences Division, 1 Cyclotron Road Bldg. 70A-1118, Berkeley, CA 94720, and ²CEA, Fontenay-aux-Roses, FRANCE

INTRODUCTION

Our studies use a series of syngeneic, and where possible, isogenic human B-lymphoblastoid cell lines to assess the genetic factors that modulate susceptibility apoptosis and their impact on the mutagenic risks of low fluence exposures to 1 GeV Fe ions and 55 MeV protons. These ions are representative of the types of charged particle radiation that are of particular significance for human health in the space radiation environment.

The model system employs cell lines derived from the male donor WIL-2 (Levy, Virolainen and Defendi, 1968). These cells have a single X chromosome and they are hemizygous for one mutation marker, hypoxanthine phosphoribosyltransferase (HPRT). TK6 and WTK1 cells were each derived from descendants of WIL-2 and were each selected as heterozygotes for a second mutation marker, the thymidine kinase (TK) gene located on chromosome 17q (Liber and Thilly, 1982; Amundson and Liber, 1991). The HPRT and TK loci can detect many different types of mutations, from single basepair substitutions up to large scale loss of heterozygosity (LOH). The single expressing copy of TK in the TK6 and WTK1 cell lines is found on the same copy of chromosome 17, and this allele can be identified by a restriction fragment length polymorphism (RFLP) identified when high molecular weight DNA is digested by the SacI restriction endonuclease and hybridized against the cDNA probe for TK (Yandell, Dryja and Little, 1986). A large series of polymorphic linked markers has been identified that span more than 60 cM of DNA (~60 megabasepairs) and distinguish the copy of chromosome 17 bearing the initially active TK allele from the copy of chromosome 17 bearing the silent TK allele in both TK6 and WTK1 cells (Kronenberg and Little, 1989; Chaudhry, et al, 1996; Giver, 1997). TK6 cells express normal p53 protein while WTK1 cells express homozygous mutant p53. Expression of mutant p53 can increase susceptibility to x-ray-induced mutations (Xia and Liber, 1997). It's been suggested that the increased mutagenesis in p53 mutant cells might be due to reduced apoptosis (Xia, et al, 1995).

RESULTS

Our ongoing studies are designed to test the hypothesis that programmed cell death (PCD) removes the most heavily damaged cells from the population following low fluence exposures to Fe ions and to similar doses of protons, thereby reducing the mutagenic load. Our initial studies were performed using the TK6 and WTK1 cell lines. PCD was induced by low fluence exposure (3 particles/cell, dose = 94.5 cGy) to densely ionizing Fe ions in TK6 cells (normal p53), as measured with a histone-DNA ELISA that detects the release of oligonucleosomal DNA fragments. The maximum amount of apoptosis in the TK6 cells was observed 48 hours post-exposure, similar to what we had observed for sparsely ionizing radiation (Cherbonnel-Lasserre, Gauny, and Kronenberg, 1996). The WTK1 cell line was much less susceptible to PCD following both densely ionizing Fe ions and sparsely ionizing radiation, and the release of

oligonucleosomes was also delayed in time. These data support the hypothesis that mutant p53 dysregulates the apoptotic response to charged particle radiations in WTK1 cells.

Our studies with 55 MeV protons were performed at the 88 inch cyclotron at LBNL. The average LET in the sample volume = 1.46 keV/ μ m. The results obtained for modulation of mutagenesis in response to protons are summarized below (Table I). The failure to undergo apoptosis was associated with a slight increase (2-3x) in mutagenesis at the X-linked, hemizygous HPRT locus in the WTK1 cells with mutant p53. By contrast, the susceptibility to proton-induced mutation at the autosomal TK locus is elevated by ~100-fold in the cells that express only mutant p53. Studies are underway to determine whether the vast increase in the levels of mutation at the autosomal TK locus in the WTK1 cells are attributable to an increased yield of a particular type of mutation (e.g., LOH by deletion or recombination).

TABLE I
Susceptibility of Syngeneic Lymphoblasts Differing in p53 Status to Mutagenesis After Exposure to 55 MeV protons

<u>Locus</u>	<u>Cell Line</u>	<u>Induced Mutant Fraction/ cGy</u>
HPRT	TK6	$4.9 \times 10^{-8}/\text{cGy}$, $r^2 = .811$
	WTK1	$13.6 \times 10^{-8}/\text{cGy}$, $r^2 = .752$
TK	TK6	$21.1 \times 10^{-8}/\text{cGy}$, $r^2 = .950$
	WTK1	$1340 \times 10^{-8}/\text{cGy}$, $r^2 = .803$

We used TK6 and WTK1 cells to quantitate the susceptibility to mutation following low fluence exposures to 1 GeV Fe ions (1-6 particles/cell, 0-189 cGy, LET=146 keV/ μ m) obtained at the AGS at Brookhaven National Laboratory. The results are summarized in Table II.

TABLE II
Susceptibility of Syngeneic Lymphoblasts Differing in p53 Status to Mutagenesis After Exposure to 1 GeV Fe ions

<u>Locus</u>	<u>Cell Line</u>	<u>Induced Mutant Fraction/ cGy</u>
HPRT	TK6	$11.6 \times 10^{-8}/\text{cGy}$, $r^2 = .953$
	WTK1	$22.8 \times 10^{-8}/\text{cGy}$, $r^2 = .901$
TK	TK6	$50.2 \times 10^{-8}/\text{cGy}$, $r^2 = .937$
	WTK1	$1435 \times 10^{-8}/\text{cGy}$, $r^2 = .955$

Fe ions were more mutagenic than protons, per unit dose, for both loci in TK6 cells, and for the HPRT locus in WTK1 cells. There does not appear to be a difference in susceptibility to TK mutation in the WTK1 cells for the two types of particles when the results are considered in terms of absorbed dose. In terms of fluence, the Fe ions were substantially more mutagenic than the protons (factors ranging from ~ 100 fold more mutagenic for the TK locus in WTK1 cells, to ~250 fold for the TK locus in TK6 cells).

We have used molecular biological techniques to evaluate the types of TK mutations arising after low fluence Fe ion exposures (94.5 cGy, average of 3 particles/cell) to both TK6 and WTK1 cells. We were interested to know whether the increased mutagenesis observed in the WTK1 cells might reveal a shift in the mutation spectrum associated with the expression of mutant p53 and the failure to execute a normal apoptotic response. We hybridized DNA from each TK-deficient mutant with the cDNA probe for human TK to classify the mutants as follows: LOH - loss of the wild-type allele, partial deletion or rearrangement - appearance of a new size band, no detectable alteration - below our limit of detection (100-200bp). To determine whether LOH occurred by recombination or by deletion, we quantitated the signal from the silent TK allele and compared it with a similar size band revealed when the filters were stripped and reprobated with the cDNA for BCL-2, located on a different chromosome. The results are summarized below (Table III).

The mutation spectrum for the TK locus in WTK1 cells is clearly different than in TK6 cells. Recombinational mutagenesis is significantly greater in early arising TK mutants of WTK1 cells (\bullet 2, 2 d.f.=31.06, $p<0.001$), and also for late arising TK mutants in WTK1 cells (\bullet 2, 2 d.f.=9.09, $p<0.025$). An ongoing linkage analysis suggests that LOH tracts are larger in the WTK1 cells. For these studies, we use 14 polymorphic microsatellite markers that span > 60 cM of DNA inclusive of the TK locus.

TABLE III

<u>WTK1 cells (mutant p53)</u>		<u>TK6 cells (wtp53)</u>	
Early arising mutants		Early arising mutants	
LOH by recombination	26	LOH by recombination	2
LOH by deletion	<u>21</u>	LOH by deletion	<u>48</u>
TOTAL	47	TOTAL	50
Late arising mutants		Late arising mutants	
LOH by recombination	20	LOH by recombination	6
LOH by deletion	<u>24</u>	LOH by deletion	<u>34</u>
TOTAL	44	TOTAL	40

Our latest studies focus on the dissecting the importance of altered susceptibility to apoptosis in the mutagenic process. To carry out these studies, we are using isogenic human B-lymphoblastoid cell lines developed by us that have normal p53, and where susceptibility to PCD is inhibited by ectopic expression of either BCL-2 or BCL-X_L. We have previously shown that x-ray-induced TK mutagenesis is elevated in the cell lines that overexpress either of the anti-apoptotic proteins, but to a lesser extent than in the WTK1 cells that express only mutant p53 (Cherbonnel-Lasserre, Gauny, and Kronenberg, 1996). Recently, we measured PCD following low fluence exposure to 1 GeV Fe ions in these cell lines, and Fe-ion-induced PCD was suppressed by overexpression of either BCL-2 or BCL-X_L. Preliminary studies using the 1 GeV Fe beam suggest that susceptibility to TK mutation is also elevated in the subclones that overexpress BCL-X_L. Taken together, our studies demonstrate that susceptibility to charged particle mutagenesis is dependent on the genotype of the cell at risk, and that apoptosis plays an important role in modulating both the frequency and the types of mutagenic changes that follow even low fluence exposures to the types of radiations of importance in the space radiation environment. As part of our ongoing studies, we are also measuring the fidelity of DNA double

strand break rejoining and mutation in synchronized human lymphoblastoid cells to determine how well we can predict the mutagenic yield in defined DNA segments following exposures to different types of ionizing radiations.

Supported by NASA grant T-864W to A. Kronenberg and the NASA NSCORT in Radiation Health.

LITERATURE CITED

- Amundson S.A . and Liber H.L. *Mutat Res.* 247:19-27, 1991.
- Chaudry, M. A., Jiang, Q., Ricanati, M., Horng, M. F. & Evans, H. H. *Radiat. Res.* 145:31-38, 1996.
- Cherbonnel-Lasserre, C., Gauny, S. & Kronenberg, A. *Oncogene* 13:1489-1497, 1996.
- Giver, C. Mutagenesis and recombination at a model heterozygous locus in human cells. Ph.D. Thesis. University of California, Riverside, CA, 1997.
- Kronenberg, A., and Little, J.B. *Mutat. Res.* 211:215-224, 1989.
- Levy, J.A., Virolainen, M. and Defendi, V. *Cancer* 22: 517-524, 1968.
- Liber, H. L. & Thilly, W. G. *Mutat. Res.*94:467-85, 1982.
- Nelson, S. L., Jones, I. M., Fuscoe, J. C., Burkhart-Schultz, K. & Grosovsky, A. J. *Radiat. Res.* 141:2-10, 1995.
- Xia, F., Wang, X., Wang, Y. H., Tsang, N. M., Yandell, D. W., Kelsey, K. T. & Liber, H. L. *Cancer Res.* 55:12-15, 1995.
- Xia, F. & Liber, H. L. *Mutat. Res.* 373:87-97, 1997.

MUTAGENIC EFFECTS OF ⁵⁶FE RADIATION ON CULTURED MAMMALIAN CELLS

M. Lenarczyk¹, A. Ueno¹, D. Vannais¹, R. Wartners², J. Roberts², A. Kronenberg³, T. Hei⁴, C. Waldren¹

¹Dept of Radiological Health Sciences, Colo. State. Univ., Ft. Collins, CO 80523, ²Univ. of Utah HSC, Salt Lake City, UT 84132, ³Dept of Life Sciences, LBL, Berkeley, CA 94720, ⁴Ctr for Rad. Res., Columbia Univ, NY, NY 10032

INTRODUCTION

Travelers in space will almost certainly be exposed to various kinds of ionizing radiation especially high linear energy transfer (LET) particles such as HZE Fe. Such exposures can cause mutations in somatic cells that can increase the risk of developing such genetic diseases as cancer. We have, therefore, measured the mutagenic potency of HZE Fe in culture mammalian cells and begun experiments to determine if mutagenicity can be reduced by radioprotective chemicals like WR-1065 and RibCys, a prodrug of L-cysteine.

METHODS

Irradiations with ⁵⁶Fe beams were carried out with the (BEVALAC) Lawrence Berkeley and (AGS) Brookhaven, 190 keV/μm and 145 keV/μM, respectively (1). Mutation was measured at the *CD59* locus (formerly known as *MIC1*) of human-hamster hybrid CHO-A_L cells (2-9) This hybrid contains a standard set of CHO chromosomes plus a single, normal human chromosome 11 in which mutations ranging in size from a single base pair to deletions >144 million base pairs can be detected. The *CD59* gene encodes a surface antigen (CD59) (10). Cells expressing this antigen are killed by rabbit serum complement in the presence of a particular monoclonal antibody directed against CD59. Cells not expressing this antigen by virtue of mutations in the *CD59* gene grow into colonies. Mutant yields (M_Y) are obtained by plotting the number of mutants obtained vs. the dose of irradiation administered. M_Y = no. of mutant colonies/number of cells at risk x 1/P.E. in the presence of complement without antiserum. (P.E. = plating efficiency). M_Y are expressed for convenience as per 10⁵ cells. The kinds of mutations (mutational spectra) obtained are determined by molecular analysis of individual CD59⁻ mutant colonies using Southern and polymerase chain reaction (PCR) analysis with a series of genes on human chromosome 11 (3-9).

RESULTS

Killing: Dose response curves were constructed to determine the lethality of the Fe beams. The mean lethal dose (D₀ = dose required to reduce survival by 1/e in the log linear portion of the dose response curve) was 0.6 Gy (compared to 1.5 Gy for ¹³⁷Cs-γ rays. The values were about the same for both Fe beams.

Mutagenicity: The mutant yield (M_Y) per unit dose (Gy) of ⁵⁶Fe radiation was 200 compared to a value of 100 for ¹³⁷Cs- γ rays. By this parameter, the former is more mutagenic than the latter. But, there are sound theoretical reasons to believe that comparing mutant yields per equitoxic dose (11) is more relevant to carcinogenesis than mutants per unit dose. When M_Y were compared per equitoxic dose (D₀) the value for Fe was 120 vs. 150 for γ rays so that the

latter are more mutagenic than the former. This same relationship holds for mutations measured at the hypoxanthine guanine phosphoribosyl transferase (HPRT) locus. A reasonable explanation for these results is that the lesions caused by Fe are more lethal, and therefore less mutagenic, than those induced by ^{137}Cs - γ rays e.g. (12). Preliminary experiments with the radio protectors WR-1065 (4 mM) and RibCys (10 mM) indicate that when present during irradiation they can provide a significant reduction in the mutagenicity of Fe.

But the carcinogenic potential of an agent depends on both the number of mutants produced and the kinds of mutations they contain. Mutational spectra obtained by Southern and PCR analysis of individual CD59⁻ clones induced by 2 Gy of Fe revealed that, contrary to expectation, the mutations induced by Fe were not much different than those induced by an equitoxic dose (3 Gy) of ^{137}Cs - γ rays, with one notable exception in the proportion of mutations of the class termed 'complex' and unstable. Only 3% of the mutations induced by ^{137}Cs - γ rays were complex compared to 21% for Fe. Complex mutations display genic instability and may, therefore, represent a greater risk of carcinogenesis than simple, stable mutations (5,6,13).

CONCLUSION

Fe is more lethal and more mutagenic per unit dose than ^{137}Cs - γ rays to cultured cells. dose. But these two radiations are about equally mutagenic when mutation is expressed in terms of equitoxic dose, a measure more relevant to carcinogenesis. The radioprotectors WR-1065 and RibCys appear to reduce the mutagenicity of Fe. The mutations induced by the two radiations are not strikingly different in quality with the important exception of mutations that are complex and unstable which are 7-fold more prevalent in cells irradiated with Fe than with ^{137}Cs - γ rays. So exposure to Fe may not create more mutant cells than exposure to ^{137}Cs - γ rays but certain kinds of mutations induced by the former may pose a greater risk in terms of their carcinogenic potential than those induced by the latter.

REFERENCES

1. L. Zeitlin, L. Heilbronn, J. Miller, *Radiat.Res.* 149, 560 (1998).
2. C.A. Waldren, *Chemical Mutagens: Principles and Methods for Their Detection*, Vol. 8., F.J. de Serres, Ed. (Plenum Publ Corp, New York, 1983), p. 235.
3. T.K. Hei, L.X. Zhu, D. Vannais, C. Waldren, *Adv.Space Res.* 14, 355 (1994).
4. A. Kronenberg, *et al*, *Molecular Mechanisms in Radiation Mutagenesis and Carcinogenesis*, K.H. Chadwick, R. Cox, H.P. Leenhouts and J. Thacker, Eds. (European Commission, Luxembourg, 1994), p. 191.
5. S. McGuinness, M. Shibuya, A. Ueno, D. Vannais, C. Waldren, *Radiat.Res.* 142, 247 (1995).
6. A.M. Ueno, D.B. Vannais, D.L. Gustafson, J.C. Wong, C.A. Waldren, *Mutat.Res.* 358, 161 (1996).
7. L.X. Zhu, C.A. Waldren, D. Vannais, T.K. Hei, *Radiat.Res.* 145, 251 (1996).
8. S. Kraemer, C. Waldren, *Mutat.Res.* 379, 151 (1997).
9. T.K. Hei, *et al*, *Proc.Natl.Acad.Sci.USA* 94, 3765 (1997).
10. A. Davies, *et al*, *J.Exp.Med.* 170, 637 (1989).
11. T.T. Puck, C.A. Waldren, *Somat.Cell Mol.Genet.* 13, 405 (1987).
12. J.F. Ward, *Radiat.Res.* 104, S103 (1995).

13. W.F. Morgan, J.P. Day, M.I. Kaplan, E.M. McGhee, C.L. Limoli, *Radiat. Res.* 146, 247 (1996).

PORTABLE REAL TIME NEUTRON SPECTROMETRY

R.H. Maurer¹, D.R. Roth¹, R. Fainchtein¹, J.O. Goldsten¹, J.D. Kinnison¹ and A.K. Thompson²
¹The Johns Hopkins Applied Physics Laboratory, 11100 Johns Hopkins Road, Laurel, MD 20723-6099 ²NIST, Orchard Rd., Gaithersburg, MD 20899

INTRODUCTION

High energy charged particles of extra-galactic, galactic and solar origin collide with spacecraft structures in Earth orbit outside the atmosphere and in interplanetary travel beyond the Earth's magnetosphere. These primaries create a number of secondary particles inside the structures that can produce a significant ionizing radiation environment. This radiation is a threat to long term inhabitants or travelers for space missions and produces an increased risk of cancer and DNA damage. The primary high energy cosmic rays and trapped protons collide with common spacecraft materials such as aluminum and silicon and create secondary particles inside structures that are mostly protons and neutrons. Charged protons and heavy ions are readily detected and instruments are already in existence with new versions in development for this task. Neutrons are electrically neutral and therefore much more difficult to detect and measure. These neutrons have been hypothesized to contribute 30-35% of the dose inside space structures and cannot be ignored. A recent measurement of low energy neutrons on a shuttle flight and suggest a contribution of 36% inside a shuttle locker (Badhwar 1997). Currently there is no compact, portable and real-time neutron detector instrumentation available for use inside spacecraft or on planetary surfaces where astronauts will live and work.

OBJECTIVES

Given the lack of a portable, real time neutron monitor and the need to know the neutron energy spectrum for accurate risk assessment of the possible radiation effects on astronauts, we have developed the following objectives.

1. Measure the energy spectrum of secondary neutrons generated by nuclear spallation reactions from particle radiation hitting the shell of space structures or planetary atmospheres.
2. Determine whether neutrons contribute 30-35% of the equivalent dose to spacecraft inhabitants.
3. Determine the characteristics, shape and slope of neutron spectra inside spacecraft or on planetary surfaces from 10 KeV to 500 MeV with an energy resolution of at least 10% for the various bins.
4. Design the instrument to be portable (brief case size) with a mass less than 10 kilograms so that it can monitor locations with variable shielding within spacecraft and be transported onto planetary surfaces.
5. Actively record and process data and produce readouts of the desired parameter (neutron flux, dose or dose equivalent).
6. Include an alarm system to warn astronauts of high fluxes so that countermeasures such as seeking shelter or using an appropriate drug may be taken.

In addition, we are to support the National Space Biomedical research Institute (NSBRI) Radiation Effects Research Team (John Dicello, Team Leader) by measuring and supplying the needed information on the neutron environment so that, combined with the work on damage to

living organs, an accurate assessment of the increased risk of cancer or other radiation damage to astronauts could be made. The five energy intervals specified in Table 1 make it important to obtain a spectrum that contains the number of neutrons in each interval rather than just making a total count. This table also shows that neutrons have damage equivalence or weighting factors of 5-20 when compared to x-rays or electrons. Over the neutron energy range of 100 KeV to 2 MeV the damage factor is a maximum of 20.

DESIGN DEVELOPMENT APPROACH

We are designing and building a portable, low power and robust neutron spectrometer that will measure the neutron spectrum from 10 KeV to 500 MeV with at least 10% energy resolution in the various energy intervals. The instrument uses highly efficient proportional counter Helium 3 tubes at the lowest energy intervals where equivalent damage factors for tissue are the highest. It also uses thick silicon solid state detectors with more dynamic range at the higher energy intervals where equivalent damage factors are lower but hits from one or a small number of neutrons may prove to be important.

The low energy tubes and the higher energy solid state systems are combined to get the best possible efficiencies across the energy ranges shown in the table. The International Conference on Radiation Protection (ICRP) and the National Conference on Radiation Protection (NCRP) have agreed upon weighting factors shown in the Table 1. The weighting factors represent the equivalent tissue damage of various radiation sources and energies. The italic notes represent the type of detector that will be employed in the various energy bins.

Radiation Component	Weighting factor ICRP	Weighting Factor NCRP
X-rays, gamma rays, electrons, positrons, muons	1	1
Neutrons with energy of < 10 KeV <i>tube</i>	5	5
10-100 KeV <i>tube</i>	10	10
> 100 KeV → 2 MeV <i>tube/solid state</i>	20	20
> 2 MeV → 20 MeV <i>solid state</i>	10	10
> 20 MeV <i>solid state</i>	5	5
Protons with energy of > 2 MeV	5	2
Alpha particles, fission fragments and nonrelativistic heavy nuclei	20	20

Table 1. Recently recommended radiation weighting factors (Wilson 1995).

The final instrument, an engineering model, will consist of the two detector systems with associated electronics, read-outs and alarm packaged in a brief case size configuration. It will be rack mountable or able to be transported to monitor the neutron environment inside space structures or on planetary surfaces. Using the proportional counter tube it will count neutrons less than 10 KeV in the region where thermal and epithermal neutrons are available and where the damage factor is constant. Between 10 KeV and several MeV it will utilize the neutron capture reaction of the Helium 3 gas to produce charged secondary protons and tritons (H 3) which are easily detected (Knoll 1989). The cross section for the capture reaction falls sharply

as MeV energies are approached decreasing the efficiency of neutron detection significantly. At this point in the energy spectrum a solid state silicon detector is as or more efficient and will be responsible for monitoring the higher energy neutrons. The silicon solid state detector depends on its function upon both the elastic and inelastic collisions of neutrons with the silicon nuclei. Secondary charged particles in the form of protons, alpha particles, spallation products or recoil nuclei are readily detected since an electron hole pair is produced by ionization for each 3.64 eV of deposited energy. A moderator that converts neutrons to protons and/or a degrader to reduce secondary proton energy to a reasonable capture length may be necessary to boost the efficiency of the silicon detector.

The details of the requirements of the design with respect to detection efficiency and energy resolution were addressed during the first year of the research. While the Helium 3 detector was quickly chosen for the lowest energy intervals, the three—below 10 KeV, 10-100 KeV and 100 KeV- 2MeV— which include those with the largest damage weighting factors of 10 and 20, the appropriate silicon detector to be used in the higher energy intervals was undetermined due to concerns about efficiency. Sentiment existed for both change in energy (also known as delta E detectors) as well as for larger bulk total energy detectors. Opinions were also divided between using a single large area detector or an array of smaller detection sites such as exist in commercially available static and dynamic memories (SRAMs and DRAMs). The SRAMs and DRAMs serve to represent the delta E detectors while commercially available PIN diodes and surface barrier detectors were chosen as the best possible total energy detectors. Both radioactive alpha particle and neutron source experiments were executed to compare and evaluate these detector elements.

Our concept emphasizes compactness, robustness, low weight and low power in comparison to other present techniques. We can sacrifice some energy resolution since the energy bins for equivalent neutron damage are broad. We may need to sacrifice some efficiency to cover the large range in energy so that we can determine how many neutrons are present at tens to hundreds of MeV to begin to quantify a component of the environment previously poorly known and possibly important for DNA damage.

Results of several rounds of experiments will be presented and the present status of the instrument development will be summarized.

DNA REPAIR-PROTEIN RELOCALIZATION AFTER HEAVY ION EXPOSURE

N.F. Metting

Pacific Northwest National Laboratory

INTRODUCTION

Ionizing radiation is good at making DNA double strand breaks, and high linear energy transfer (LET) radiations such as heavy ion particles are particularly efficient. For this reason, the proteins belonging to repair systems that deal with double strand breaks are of particular interest.

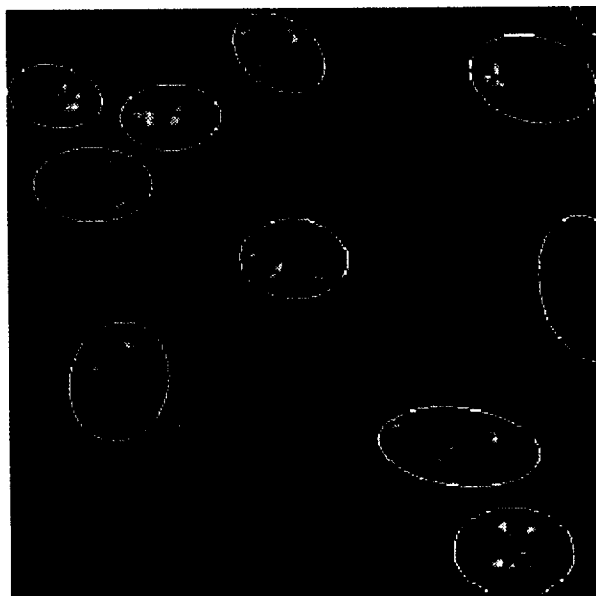
One such protein is Ku, a component in the non-homologous recombination repair system. The Ku protein is an abundant, heterodimeric DNA end-binding complex, composed of one 70 and one 86 kDa subunit. Ku protein binds to DNA ends, nicks, gaps, and regions of transition between single and double-stranded structure. These binding properties suggest an important role in DNA repair. The Ku antigen is important in this study because it is present in relatively large copy numbers and it is part of a double-strand-break repair system. More importantly, we consistently measure an apparent upregulation *in situ* that is *not* verified by whole-cell-lysate immunoblot measurements. This apparent upregulation is triggered by very low doses of radiation, thus showing a potentially useful high sensitivity. However, elucidation of the mechanism underlying this phenomenon is still to be done.

CURRENT STATUS OF RESEARCH

METHODS

The visualization of heavy particle traversal through individual human cell nuclei has been studied extensively for the last few years. Two *in situ* assays have been used: a DNA end-labeling assay, to look for strand breaks, and an immunoassay to look for the recruitment of a DNA repair protein, Ku-86, to the sites of particle traversal. Four types of human cells have been studied: the HeLa cervical carcinoma cell line, the NFF neonatal foreskin fibroblast cell strain, the HMEC normal mammary epithelial cell strain, and the HNEK skin epithelial keratinocyte strain. The doses of 1 GeV/amu Fe ion were calculated to give very low particle fluences to the cell nuclear cross-section, based on a track-averaged LET of 120 keV/• m and cell nuclear cross-section measurements.

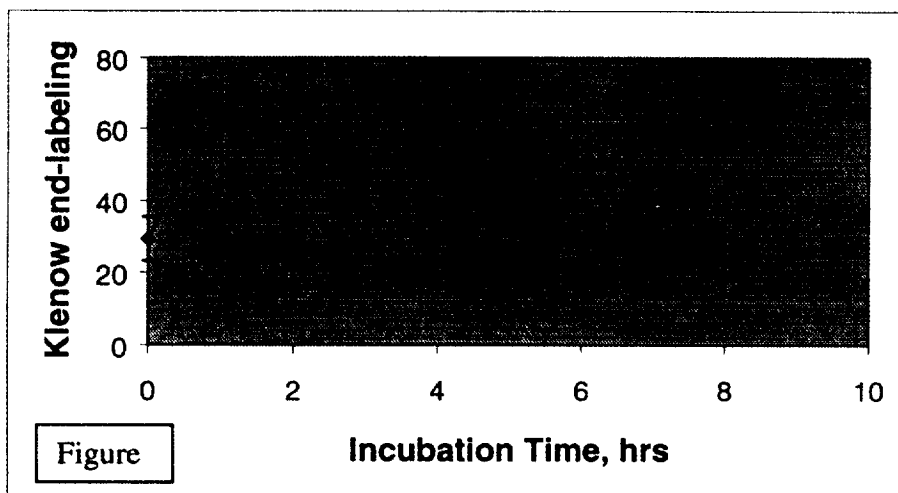
Three nominal fluences, plus the sham control, were used: 0, 1, 2, or 4 particles per cell nuclear area. Cobalt-60 gamma rays used in parallel experiments for a low LET comparison. After irradiation, cells were incubated for varying lengths of time, then fixed and stored at 4°C. In subsequent assays, the cellular DNA was probed by enzymatic addition of labeled dNTP's to 3'-OH ends, or probed for the repair protein, Ku-86, by immunocytochemical methods. The cells were then assayed by flow cytometry or confocal laser scanning microscopy, to



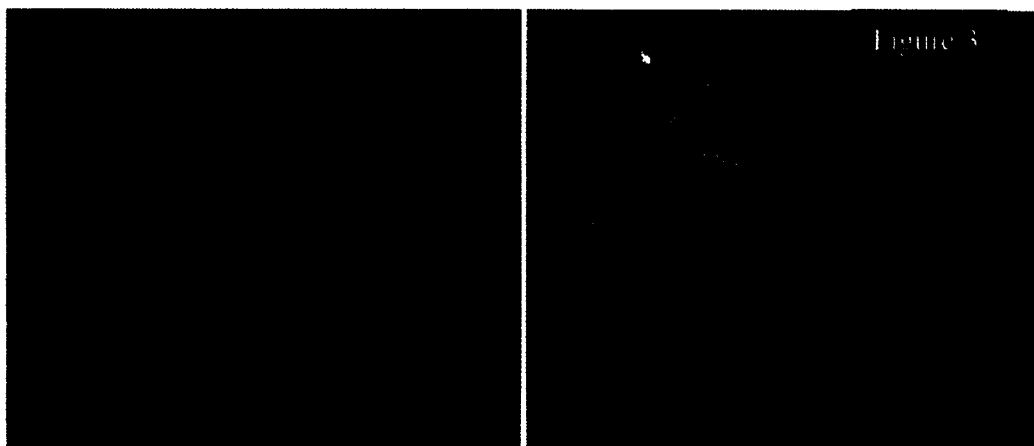
quantify and/or locate within the cell the fluoresceinated probes.

RESULTS

Enzyme labeling of strand breaks. In cells exposed to 1 GeV/amu iron ions the irradiated cells labeled in discrete foci, when viewed in horizontal and vertical section. In contrast, labeling in the control cells was diffuse and spread across most of the cell nucleus. Figure 1 shows a horizontal section through HMEC cells exposed to 20 cGy, fixed almost immediately (4 minutes), and then end-labeled for strand breaks. This figure also shows the elliptical shapes, which were drawn around each of the cell nuclei during the quantification of the fluorescein label by the analysis program of the confocal microscope. Figure 2 shows a time course of up-regulation greater than two-fold by 30 minutes, holding through at least 60 minutes, and returning to at or below control levels by 2 hours. The error bars represent standard deviation for at least 50 cell nuclei. Dose responses and time courses for both enzyme labeling and Ku86 antibody staining will be shown for this particle exposure, and will also be compared to low LET results.



Ku-86 immunolabeling. The DNA repair protein, Ku-86, was studied in • -ray irradiated human neo-natal foreskin fibroblasts using immunocytochemistry. After irradiation, the cells were incubated for various times

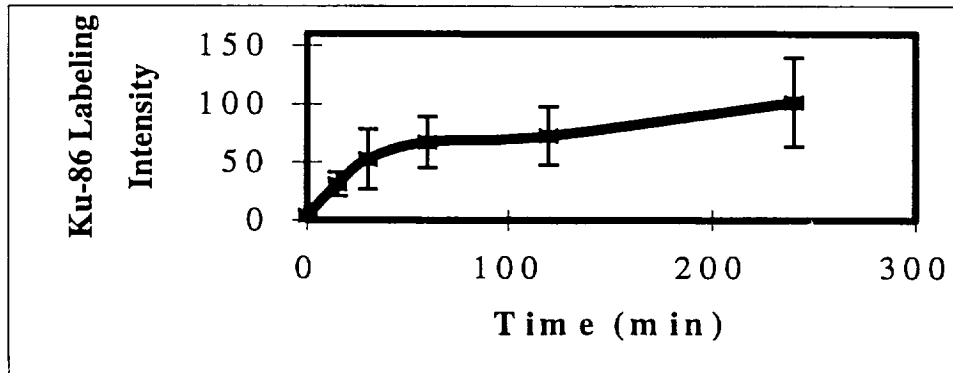


before fixation, immunostaining, and quantification of cell nuclear staining by confocal microscopy. Figure 3a shows control-unexposed

cells

immunostained with the Ku-86 antibody, and Figure 3b shows the cells one hour after irradiation by 10 cGy. These data plotted in three dimensions, with the intensity of Ku

labeling on the Z axis. The DNA was not stained in either sample. Each of these pictures represents a horizontal section, $0.19 \cdot \mu\text{m}$ thick, through the cells in a plane parallel to the



attachment surface. Notice that in the controls the Ku protein is seen more or less throughout the cell, and in relatively small amounts. The irradiated cells, in contrast, are highly labeled, and mainly in the cell nucleus.

A time course experiment of cells exposed to 50 cGy of gamma rays, Figure 4, showed a steep up-regulation of Ku-86 in cell nuclei. The amount of Ku labeling rose about 8-fold higher than unirradiated cells by 15 minutes, 17-fold higher in 1 hour, with a more gradual climb to a high of 25-fold at 4 hours. This may be interpreted as either a slowing down or a plateauing of the up-regulation after about 3 hr. In this figure, the error bars represent the standard deviation for at least 25 individual cells. In a similar experiment, cells were assayed by flow cytometry for both Ku-86 and DNA content, and protein up-regulation was found to occur in all phases of the cell cycle (data not shown).

Figure 5 shows the DNA repair enzyme, Ku-86, relocated to the sites of damage induced by high energy iron ions traversing human HeLa cells. The 1 GeV/a.m.u. Fe ions approximate cosmic ray particles that will be encountered on deep space missions. In this 3D picture, the protein staining intensity is plotted on the z axis, and each island of peaks is a single cell. Cells were exposed to ~ 4 ions per cell nucleus, then incubated for three hrs. The inset picture shows control cells.

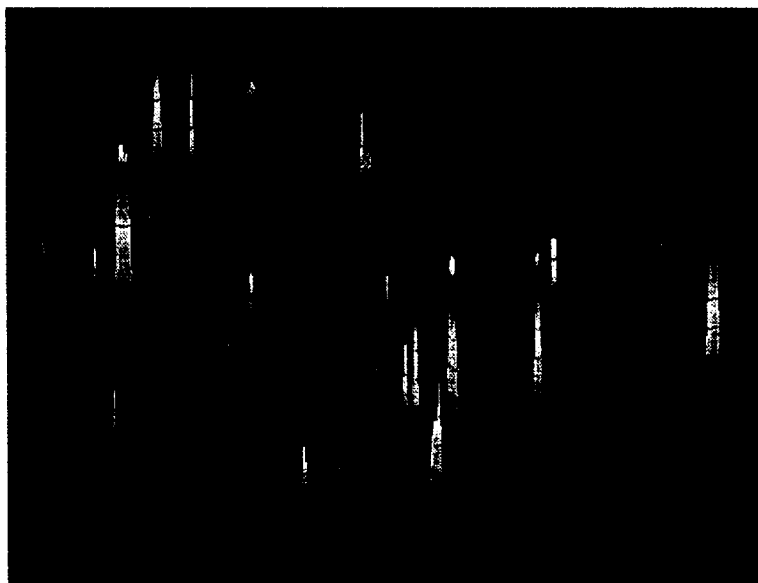


Figure 5

CONCLUSIONS

Analysis and comparison of these experiments is presently ongoing, but several tentative conclusions will be offered.

1. A differential response is shown for both DNA end-labeling and Ku-86 upregulation for different human cell types, and for different radiations.
2. The number of DNA end-labeling foci per irradiated HMEC cell is much higher than the calculated number of particles traversing the cell nucleus. These higher numbers probably reflect the sites of DNA synthesis, which in the unirradiated cells are masked by the more homogeneous distribution of endonuclease (repair) proteins. The recruitment of this activity to sites of both damage and normal synthetic activity is triggered within minutes of irradiation.
3. There is an up-regulation of Ku-86 protein in the nuclei of gamma-irradiated cells at low- but not higher doses that we are now studying for high LET irradiated cells. Preliminary data are not clear cut, and this may be due to the uncertainty in the number of particles traversing the cell, and the lower limit on dose imposed by the impossibility of delivering a fraction of a particle to the cell.

PLANS FOR FUTURE INVESTIGATIONS

Upcoming experiments are planned to help prove a new hypothesis that part of the apparent up-regulation of Ku protein is due to a protein conformational change that sensitively occurs in response to irradiation.

Supported by the National Aeronautics and Space Administration (NASA) Space Radiation Health Program under DOE contract DE-AC06-76RLO 1830.

ACCELERATOR-BASED STUDIES OF HEAVY ION INTERACTIONS RELEVANT TO SPACE BIOMEDICINE

J. Miller, L. Heilbronn, C. Zeitlin

Lawrence Berkeley National Laboratory, Berkeley, California, USA

INTRODUCTION

Evaluation of the effects of space radiation on the crews of long duration space missions must take into account the interactions of high energy atomic nuclei in spacecraft and planetary habitat shielding and in the bodies of the astronauts. These heavy ions (*i.e.* heavier than hydrogen), while relatively small in number compared to the total galactic cosmic ray (GCR) charged particle flux, can produce disproportionately large effects by virtue of their high local energy deposition: a single traversal by a heavy charged particle can kill or, what may be worse, severely damage a cell. Research into the pertinent physics and biology of heavy ion interactions has consequently been assigned a high priority in a recent report by a task group of the National Research Council (1).

Fragmentation of the incident heavy ions in shielding or in the human body will modify an initially well known radiation field and thereby complicate both spacecraft shielding design and the evaluation of potential radiation hazards. Since it is impractical to empirically test the radiation transport properties of each possible shielding material and configuration, a great deal of effort is going into the development of models of charged particle fragmentation and transport. Accurate nuclear fragmentation cross sections (probabilities), either in the form of measurements with thin targets or theoretical calculations, are needed for input to the transport models, and fluence measurements (numbers of fragments produced by interactions in thick targets) are needed both to validate the models and to test specific shielding materials and designs. Fluence data are also needed to characterize the incident radiation field in accelerator radiobiology experiments (2).

For a number of years, nuclear fragmentation measurements at GCR-like energies have been carried out at heavy ion accelerators including the LBL Bevalac, Saturne (France), the Synchrophasotron and Nuklotron (Dubna, Russia), SIS-18 (GSI, Germany), the Alternating Gradient Synchrotron at Brookhaven National Laboratory (BNL AGS) and the Heavy Ion Medical Accelerator (HIMAC) in Chiba, Japan. Until fairly recently most of these experiments were done to investigate fundamental problems in nuclear physics, but with the increasing interest in heavy charged particles on the part of the space flight, radiobiology and radiotherapy communities, an increasing number of experiments are being directed at these areas. Some of these measurements are discussed in Refs. (3-5) and references therein.

Over the past several years, our group has taken cross section and fluence data at the AGS and HIMAC for several incident beams with nuclear charge, Z , between 6 and 26 at energies between 290 and 1050 MeV/nucleon. Iron ($Z=26$) has been studied most extensively, since it is the heaviest ion present in significant numbers in the GCR. Targets have included tissue-equivalent and proposed shielding materials, as well as a variety of elemental targets for cross section measurements. Most of the data were taken along the beam axis, but measurements have been made off-axis, as well. Here we present selected data and briefly discuss some implications for spacecraft and planetary habitat design.

EXPERIMENTAL METHODS

The same basic detection system is used at both accelerators. It consists of a stack of silicon detectors of varying thickness, some of which are position-sensitive, augmented at HIMAC by plastic scintillation counters for time of flight measurements and a thick sodium iodide detector to measure total fragment energy. Charged fragments are identified primarily through their differential energy loss in one or more of the detectors. A typical configuration is described in Ref. (6).

RESULTS AND DISCUSSION

Townsend, Cucinotta and Wilson have discussed (7) the sensitivity of the calculated absorbed dose behind shielding to the uncertainties in transport model calculations. These in turn reflect uncertainties in the source terms, *i.e.* in the nuclear fragmentation cross sections. This is a critical issue for spacecraft design because, as Townsend and Wilson have pointed out, uncertainty in the radiation dose behind shielding can translate into very large uncertainties in mission cost. We have compared measured charge changing cross sections to fragmentation model calculations for 1.05 GeV/nucleon ^{56}Fe incident on several different targets at the AGS (3). We have found that while some models perform better than others, at present no model accurately reproduces the measured cross sections over the full range of beam energies and target masses studied.

Also at the AGS, we have measured the fragment fluence spectra produced by interactions of ^{56}Fe ions in shielding material. Figure 1 shows a fluence spectrum produced by iron ions incident on borated polyethylene. The surviving primary iron ions comprise the highest peak at the far right, and smaller peaks representing lighter fragments can be clearly seen. These secondary fragments have greater penetrating power, albeit lower dose, than the primary iron ions. Both of these factors must be taken into account when evaluating the biological implications of fragmentation.

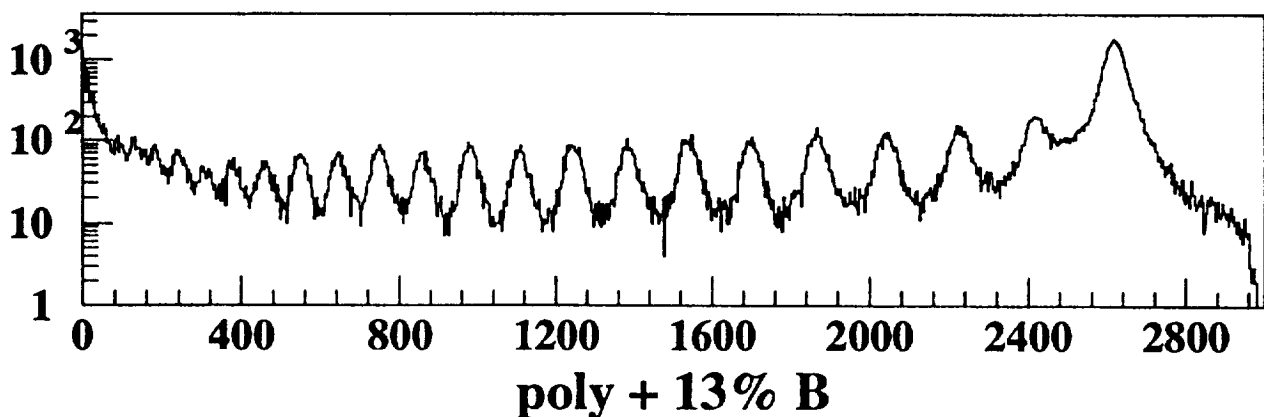


Figure 1. Measured fluence spectra for 1.05 GeV/nucleon ^{56}Fe ions incident on borated polyethylene. The units are number of fragments vs. energy (arbitrary units).

Data are still needed for light ions at lower energies, to extend the nuclear data base and to study the behavior of light nuclei, which are prominent in both the primary GCR and the secondary radiation produced by interactions of the primaries in matter. In 1997 we began a series of measurements at HIMAC, where light ions of the appropriate energies are available. Thus far we have measured the fragmentation of 290 and 400 MeV/nucleon ^{12}C and 600 MeV/nucleon ^{20}Ne and ^{28}Si . One thing that stands out in these data is the complexity of the charged particle spectra, with many interactions producing multiple light charged fragments in the forward direction.

It is also important to know how the absorbed dose behind shielding varies with angle relative to the incident ion, and to this end we took data as a function of fragment charge, Z , and angle at 0° , 5° and 10° , for 400 MeV/nucleon ^{12}C ions in polyethylene. With the exception of protons, we find that the absorbed dose is dominated at each Z by the fragments near the beam axis, indicating that at least in this case it is reasonable to assume that the bulk of the dose, even after fragmentation, will be concentrated in the forward direction.

For completeness, we should also mention the importance of neutrons, which are produced in copious numbers in fragmentation reactions, are very difficult to shield against, and can produce serious biological effects. While outside the scope of this paper, neutron production in heavy ion interactions is a critical area of concern for space biomedicine. (See, *e.g.*, Ref. (5), pp. 249-259.)

ACKNOWLEDGEMENTS

We thank the AGS and HIMAC staffs for their outstanding work in support of the experiments. We are especially grateful to D. Lazarus (BNL) and T. Murakami (NIRS). This work was supported primarily by the NASA Space Radiation Health Program under Contract No. L14230C through the U.S. Department of Energy under Contract No. DE-AC03076SF00098. Additional support for work at HIMAC was provided by the National Institute of Radiological Sciences, Chiba, Japan and the Japan Society for the Promotion of Science.

REFERENCES

1. National Research Council, Task Group on the Biological Effects of Space Radiation. *Radiation Hazards to Crews of Interplanetary Missions - Biological Issues and Research Strategies*. National Academy Press, Washington, DC, 1996.
2. C. Zeitlin, L. Heilbronn and J. Miller, Detailed characterization of the 1087 MeV/nucleon ^{56}Fe beam used for radiobiology at the AGS. *Radiat. Res.*, 149, 560 (1998).
3. C. Zeitlin, L. Heilbronn, J. Miller, S. E. Rademacher, T. Borak, T. R. Carter, K. A. Frankel, W. Schimmerling and C. E. Stronach, Heavy fragment production cross sections from 1.05 GeV/nucleon ^{56}Fe in C, Al, Cu, Pb and CH_2 targets. *Phys. Rev. C* 56, 388 (1997).
4. I. Schall, D. Schardt, H. Geissel, H. Irnich, E. Kankaleit, G. Kraft, A. Magel, M. F. Mohar, G. Münzenberg, F. Nickel, C. Scheidenberger and W. Schwab, Charge-changing nuclear reactions of relativistic light-ion beams ($5 \leq Z \leq 10$) passing through thick absorbers. *Nucl. Instr. and Meth. B* 117, 221 (1996).

5. *Shielding Strategies for Human Space Exploration*, Proceedings of a workshop sponsored by NASA, Johnson Space Center, Houston, Texas, December 6-8, 1995, Eds. J. W. Wilson, J. Miller, A. Konradi and F. A. Cucinotta, NASA Conference Publication 3360 (1997).
6. C. Zeitlin, K. A. Frankel, W. Gong, L. Heilbronn, E. J. Lampo, R. Leres, J. Miller and W. Schimmerling, A Modular Solid State Detector for Measuring High Energy Heavy Ion Fragmentation Near the Beam Axis. *Rad. Meas.* 23, 65 (1994).
7. L. W. Townsend, F. A. Cucinotta and J. W. Wilson, HZE Reactions and Database Development, in *Biological Effects and Physics of Solar and Galactic Cosmic Radiation*, proceedings of a NATO Advanced Study Institute, Algarve, Portugal, Oct. 13-23, 1991, Eds. C. E. Swenberg, G. Horneck and E. G. Stassinopoulos, pp. 787-809, Plenum Press, New York, NY (1993).

MOLECULAR AND CHROMOSOMAL DAMAGE AND MIS-REPAIR IN HUMAN X CHROMOSOMES

M.C. Muhlmann-Diaz¹, M. Loebrich², B. Rydberg², P.K. Cooper², and J.S. Bedford¹

¹Dept. Radiological Health Sciences, Colorado State University, Fort Collins, CO 80523, ²Dept. of Radiation Biology, Lawrence Berkeley Laboratory, Berkeley, CA 94720

INTRODUCTION

The structure and/or activity of chromatin is known to influence substantially the damage and damage processing in cells after exposure to both ionizing and non-ionizing radiations as well as other genotoxic agents. There is virtually no information, however, on the comparison of ionizing radiation damage and its processing at the DNA and chromosome levels in relation to the influence of chromatin structure/activity. To study this question, we compared initial ionizing radiation damage in terms of DNA double strand breaks and breaks in prematurely condensed chromatin as well as the end product of mis-repair in DNA and the development of chromosomal aberrations in human X chromosomes of cells from normal males, females with an active and an inactive X, and individuals with supernumerary X chromosomes which are particularly inactive. The object was to determine whether the total initial and mis-repaired damage per cell simply increased in proportion to the number of X chromosomes, or whether one or the other (or both) damage end-points varied depending (presumably) on the known differences in structure/activity of the X chromosomes in these cells.

METHODS

Contact-inhibited human fibroblast cells in culture derived from either males (XY), females (XX), or individuals with supernumerary X chromosomes, XXX, XXXX or XXXXX were irradiated and then either processed immediately to determine "initial" damage, or were incubated a sufficient time to allow for full damage processing to occur before assaying to measure the product of mis-repair in either DNA or at the level of chromosomal aberrations viewed at the first post-irradiation mitosis. For DNA damage, double strand breaks were assayed by pulsed field gel electrophoresis in a megabase-sized X-specific restriction fragment either immediately after irradiation or after damage processing. Shifts in DNA size away from the well-defined restriction fragment band were taken on an index of both breakage, and later, mis-rejoining. Interphase chromatin damage was measured by inducing premature chromosome condensation by fusion with mitotic HeLa cells. Processed damage in chromosomes was measured in the first post-irradiation mitosis. X-chromosome damage was measured after fluorescence in situ hybridization (FISH) with whole X chromosome painting probes.

RESULTS

The initial breakage in the X chromosomes of both DNA and interphase chromatin increased in direct proportion to the number of X chromosomes per cell, i.e., the fact that one or more X chromosomes were inactive did not protect them from initial breakage in either case. In terms of mis-rejoining vs. correct rejoining, with time after irradiation, however, we found that increasing the number of X chromosomes beyond two did not further increase either the amount of X chromosome specific restriction fragment mis-rejoining or the frequency of chromosomal aberrations involving the X chromosome.

CONCLUSION

Our data strongly suggest that the structure and/or activity of supernumerary X chromosomes greatly favor correct rejoining (as opposed to mis-rejoining) after breakage by ionizing radiation. Such DNA or chromatin is not more resistant or refractory to initial breakage.

COOPERATIVE RESEARCH IN PROTON SPACE RADIATION

G.A. Nelson¹, J.M. Slater¹, J.O. Archambeau¹, L.M. Green¹, D.S. Gridley¹, G.A. Abell¹, M.M. Moyers², G.A. Coutrakon²

¹Radiobiology Program, Loma Linda University and ²Department of Radiation Medicine, Loma Linda University Medical Center, 11175 Campus Street, Room A1010, Loma Linda, CA. 92354.

INTRODUCTION

Loma Linda University and NASA Code UL are participating in a cooperative research agreement whose focus is on the effects of proton radiation on biological systems. Principal elements of this agreement are: 1) development of physics and biology facilities for controlled irradiation of subjects with protons in the energy and dose ranges found in space, 2) facility and personnel support for visiting investigators, and 3) conduct of radiobiology and physics research emphasizing the unique properties of protons. Loma Linda has upgraded its Proton Treatment Center by designing and installing a dedicated beam line that can provide high energy protons for biological investigations. Supporting biological laboratories have been outfitted for investigations with subjects ranging from microorganisms and cultured cells to rodents. A visitors' laboratory is maintained exclusively for visiting scientists and radiobiological investigations with protons are now underway.

FACILITY DEVELOPMENT

The Chan Shun Pavilion was opened in May of 1997 and configured for biological research over the subsequent 12 months. The Radiobiology Program currently operates a 7000 square foot laboratory suite, core laboratories and a 1400 square foot visitors' laboratory. These laboratories are primarily used for cell and molecular biology studies. Major capital equipment items include: a flow cytometer, laser scanning cytometer, ultracentrifuges, capillary electrophoresis system, phosphor imager, scintillation counter, microinjection system, walk-in cold room, cryogenic storage systems, laminar hoods, incubators, microscopes and a confocal microscope. New laboratories intended to enhance capabilities for rodent-based investigations are under development with emphasis on enabling neuroscience investigations.

The research beamline was designed in response to scientific requirements reviewed by investigators of the NASA Space Radiation Health Program. It was installed in March 1998 in the "calibration room" of the Proton Treatment Facility. The beamline consists of an optical bench fitted with a series of precision-aligned collimators, scattering foils, transmission ion chambers, segmented ion chambers, secondary emission monitor, modulator wheels, mounting fixtures and alignment lasers designed to provide a flexible configuration of components for experiments. Beams of protons of energies from 40 MeV to 250 MeV are delivered to the target position at rates of the order 1 Gy/min and a typical field size of 15 cm diameter. The beam line is supported by a local control console with customized software and provides power and data acquisition for dosimetric devices. A set of customized incubators which mount directly to the target location are available to provide 4 to 40°C environments for cultured cells and other samples during radiation exposures. A Cobalt-60 gamma irradiator is operated by the program and access to linear accelerators for high energy electrons and photons can be arranged.

RESEARCH ACTIVITIES

Four research groups are currently operating in the radiobiology laboratories and are conducting research with accelerated protons and gamma rays. Dr. John Archambeau and collaborators are investigating the radiation responses of retinal vasculature in the rat. This work is directed at establishing the treatment dose of the eye for macular degeneration and understanding the role of the microcirculation in determining the radiation response of the nervous system. Dr. Daila Gridley is investigating the role of tissue necrosis factor alpha in modifying tumor regression in conjunction with radiation treatment; human glioma and mouse lung tumor cells are used in these studies. Dr. Gridley is also characterizing changes in the immune system following irradiation utilizing flow cytometric techniques. Dr. Lora Green is using the rat thyroid and thyroid cell line FRTL-5 in studies aimed at determining how the differentiated state and organization of cells into tissues controls their response to radiation-induced stress. These studies emphasize the role of gap junctions and extracellular matrix in regulating social interactions amongst cells. Dr. Gregory Nelson is using the nematode, *C. elegans* to investigate genetic damage caused by charged particles, including protons. Mutant strains of nematodes which are defective in programmed cell death pathways and in managing reactive oxygen species are being used to address the roles of these processes in the expression of genetic damage. Drs. Green and Nelson are jointly using the differential display technique for identifying changes in patterns of gene expression following gamma ray and proton irradiation of nematodes and thyroid cells. All of the investigators are collaborating on a radiation-induced tumorigenesis study with C57Bl mice which will investigate tumor formation at several organ sites in response to protons and gamma rays at high and low dose rates.

The medical and accelerator physics groups are continuing to improve the beam delivery system and have been able to generate proton beams of 40 to 250 MeV on the research beamline with field sizes up to 30 cm. Modulated beams have also been produced for spread out Bragg peak applications. Dose rates have been controlled over two orders of magnitude and work continues on describing the composition of the proton beams.

MODULATION OF RADIOGENIC DAMAGE BY MICROGRAVITY: RESULTS FROM STS-76

Gregory Nelson¹, Gayane Kazarians¹, Wayne Schubert², Roger Kern², David Schranck², Philip Hartman³, Anthony Hlavacek³, Honor Wilde³, Dan Lewicki³, Eugene Benton⁴, and Eric Benton⁴

1 Radiobiology Program, Loma Linda University; Loma Linda, CA.

2 Jet Propulsion Laboratory, Pasadena, CA

3 Texas Christian University, Fort Worth, TX

4 University of San Francisco, San Francisco, CA

INTRODUCTION

The STS-76 (Shuttle-Mir 3) spaceflight provided an opportunity to test two questions about radiation responses in *C. elegans*. First, does the absence of gravity modify the dose-response relation for mutation and chromosome aberration and second, what are the features of the mutation spectrum resulting from exposure to cosmic rays? These questions were put to the test in space using the ESA "Biorack" facility which was housed in the Spacehab module aboard shuttle Atlantis. The mission flew in March, 1996 and was a shuttle rendezvous with the Russian space station Mir.

RESULTS AND METHODS

To address the first question, worms of translocation balancer strain JP10 (*dpy-18/3T1(III)III; unc-46/eT1(V) V*) were launched as dauer larvae in phosphate buffered saline (S medium). Dauer larvae are an estivating phase which corresponds to an alternate third larval stage and require no food for several weeks to months. On orbit the dauer larvae were injected into a series of lexan tubes containing a cylindrical shell of agarose-gelled S medium with a central airspace. The surface of the agarose cylinders were pre-loaded with metabolically inactive *E. coli* (food supply) and subjected to a controlled drying step to allow uptake of buffer during the dauer injection step. The agarose media also contained 0 to 1.3 mCi of ⁴⁵CaCl₂ (a Beta particle emitter) such that a dose vs. response curve would be generated from each series of tubes. One series of tubes was incubated at 22°C at 0 gravity while a matched set was placed on a 1 x g centrifuge. Matched ground controls at 1 x g and 1.4 x g were also performed. Worms were washed and plated onto *E. coli*-seeded plates immediately after landing to recover the dauers and processed for autosomal recessive lethal mutation. The results showed that viability and fertility of worms were not significantly altered by gravity and that the mutation dose-response from 0 to 100 Gy yielding 0 to 7% mutants was not significantly affected by gravitational acceleration level.

For chromosome aberration determination first larval stage animals of wild type and two radiation sensitive mutations (*rad-2* and *nuc-1*) were launched in S medium and injected into culture tubes with ⁴⁵CaCl₂ as described above. After three days the exposed worms (now young adults) were frozen at -20°C for return to earth. They were washed free of radioactivity, fixed and stained as whole mounts with the DNA-specific dye DAPI. Binucleated intestine cells were scored for the presence of anaphase bridges using fluorescence. The yield of worms was lower than expected for this experimental endpoint but results were consistent with a radiation-induced

aberration rate unaffected by gravity levels.

To answer the second question, *fem-3(q20gf)* and wild type dauer larvae (suspended in S buffer) were placed in lexan tubes and transferred on orbit from a storage locker to the Biorack where they were incubated for the duration of the mission at 22°C. The cosmic ray environment for these worms was measured using a combination of thermoluminescent detectors and plastic nuclear track detectors included in the tube-holding container. Upon landing these animals were recovered and screened for mutants by a temperature shift to 25°C (Fem-3) or challenge by the drug levamisole. No *unc-22* mutants were recovered but twenty-five independent *fem-3* mutants were recovered, giving a mutation frequency of 2×10^{-5} . This is approximately three times that for ground controls. Each strain was analyzed by Southern hybridization. Only one polymorphism was detected. This spectrum will be compared to those obtained using several ground-based radiation sources and to those obtained on a previous spaceflight where *unc-22* mutants were recovered (STS-42, IML-1).

SOME BEHAVIORAL EFFECTS OF EXPOSURE TO LOW DOSES OF ^{56}Fe PARTICLES

Bernard M. Rabin¹, James A. Joseph², and Barbara Shukitt-Hale²

¹Department of Psychology, University of Maryland Baltimore County, Baltimore, MD 21250;

²Human Nutrition Research Center on Aging, USDA-ARS, Tufts University, Boston, MA 02111

INTRODUCTION

Future missions in space (such as a mission to Mars) will involve long-term travel beyond the magnetic field of the Earth. As a result, astronauts will be exposed to radiation qualities and doses that differ from those experienced in low earth orbit, including exposure to heavy particles, such as ^{56}Fe , which are a component of cosmic rays. Although the hazards of exposure to heavy particles are often minimized, they can affect neural functioning, and as a consequence, behavior. Unless the effects of exposure to cosmic rays can somehow be reduced, their effects on the brain throughout long duration flights could be disastrous. In the extreme case, it is possible that the effects of cosmic rays on space travelers could result in symptomatology resembling that of Alzheimer's or Parkinson's diseases or of advancing age, including significant cognitive and/or motor impairments. Because successful operations in space depend in part on the performance capabilities of astronauts, such impairments could jeopardize their ability to satisfy mission requirements, as well as have long-term consequences on the health of astronauts. As such, understanding the nature and extent of this risk may be vital to the effective performance and possibly the survival of astronauts during future missions in space.

METHODS

Rats were exposed to 1-1.5 Gy of 1 GeV/n ^{56}Fe particles using the AGS at Brookhaven National Laboratory (BNL). The behavioral testing that was conducted 3-5 days following irradiation was performed at BNL. The remaining rats were returned to the labs at either UMBC or HNRCA for testing. The behavioral tests that were utilized were:

Conditioned Taste Aversion (CTA): A CTA is produced by placing rats on a 23.5-hr water deprivation schedule for 7 days. On the conditioning day, they are presented with a calibrated drinking tube containing 10% sucrose solution instead of water, and intake recorded. Immediately following the drinking period, the rats are presented with the unconditioned stimulus, amphetamine (3 mg/kg, ip) or lithium chloride (LiCl, 2.2 mEq/kg, ip). On the test day the rats are again given the 10% sucrose solution for 30 min. The acquisition of a CTA is shown by reduced sucrose intake on the test day compared to the conditioning day. The effects of exposure to ^{56}Fe particles on both amphetamine- and LiCl-induced CTA learning were tested either three days or four months following irradiation. Because exposure to heavy particles affects the dopaminergic system, exposure to ^{56}Fe particles should disrupt the acquisition of an amphetamine-induced CTA, which depends upon the integrity of the dopaminergic system, but have no effect on LiCl-induced CTA learning, which is independent of the dopaminergic system. Also, because neurons are post-mitotic, the behavioral effects of exposure to ^{56}Fe should be similar at both conditioning intervals.

Conditioned Place Preference (CPP): This procedure, which is used to evaluate the reinforcing qualities of a specific stimulus, utilizes an apparatus with three distinct compartments (black and white compartments which are separated by a gray compartment). The rat is given a reinforcing stimulus (e.g., amphetamine, 2 mg/kg) in one compartment and, on alternate days, a neutral stimulus (e.g., isotonic saline) in the other. After three pairings of each compound with a specific compartment, the rat is allowed to move freely about the apparatus and the amount of time spent in each compartment is measured. A CPP is shown when the organism spends significantly more time in the compartment paired with the presumptive reinforcing stimulus (amphetamine) than in the compartment paired with the neutral stimulus. To the extent that exposure to ^{56}Fe particles disrupts the neural mechanisms that mediate reinforcement, irradiated rats should show no preference for either compartment, in contrast to control animals who show a preference for the amphetamine compartment.

Morris Water Maze: This procedure is a standard one used to evaluate changes in cognitive performance, specifically in spatial learning and memory. Performance on this task is decreased by damage to the hippocampus and in aged organisms. The maze consists of a circular black fiberglass pool (134 cm in diameter x 50 cm in height), filled to a depth of 30 cm with water maintained at 23°C. The pool is divided into four equal-size quadrants. A black circular escape platform (10 cm in diameter) is hidden from sight by submerging it 2 cm below the surface of the water in the center of one of the quadrants. The location of the platform is changed to a different quadrant for each session of testing. The task requires an animal to use spatial cues to find the submerged platform, and to remember its location from the previous trial. Accurate navigation is rewarded by escape from the pool. Several experimental procedures have been developed to measure different aspects of cognitive performance, including reference (long-term) and working (short-term) memory. If exposure to ^{56}Fe particles affects the organism's cognitive ability, then the irradiated should show poorer performance than control rats.

RESULTS

Taste Aversion Learning: When conditioning occurs three days following irradiation, exposing rats to 1 Gy of 1 GeV/n ^{56}Fe particles disrupts the acquisition of a CTA produced by the dopamine agonist amphetamine but not the CTA produced by lithium chloride, which is not mediated by the dopaminergic system. This effect is characterized by a threshold: no effect is observed until a specific threshold dose is achieved, and further increases in the dose do not produce corresponding increases in the behavioral effect. Compared to rats tested 3 days following exposure, who failed to acquire an amphetamine-induced CTA, the rats conditioned 4 months following exposure to 1 Gy of ^{56}Fe particles showed an enhanced aversion to treatment with amphetamine. This observation suggests that there is enhanced dopaminergic responsiveness to an agonist which may result from an upregulation of dopamine receptors.

Conditioned Place Preference: Preliminary results show that compared to unirradiated controls, rats exposed to 1 Gy of ^{56}Fe particles fail to acquire a preference for the side of the maze paired with dopamine agonist amphetamine. Control rats spent significantly more time on the side of the maze that was paired with the amphetamine (785±30 sec.) than on the side of the maze in which they were given a saline injection (69±28 sec.). In contrast, the irradiated rats failed to

show a significant difference in the amount of time spend in the amphetamine- or saline-paired compartments (403 ± 66 sec. compared to 361 ± 64 sec., respectively).

Morris Water Maze: The initial experiments using the Morris water maze to evaluate the possibility of ^{56}Fe -induced deficits in spatial learning and memory showed that rats exposed to 1 Gy of 1 GeV/n ^{56}Fe particles initially make fewer crossings of the previous platform position while locating the new platform position than the control rats. This difference in performance may occur because the irradiated rats cannot recall the location of the platform between a trial in the morning and a trial in the afternoon and, unlike the non-irradiated rats, do not explore the quadrant of the maze where the platform had been located previously. On subsequent trials, the performance of the control rats improves, while that of the irradiated rats declines.

CONCLUSIONS

The results obtained thus far indicate that exposing rats to low doses of ^{56}Fe particles can affect performance on a range of behavioral tasks. Although these results must be considered suggestive at the present time, they do indicate that exposure to heavy particles has the potential to produce permanent alterations in behavior. During a long duration mission outside the magnetosphere, astronauts will be expected to perform tasks that depend upon their ability to utilize spatial cues and to change their behavior in response to changes in reinforcement contingencies. As such, the observation of changes in these endpoints following exposure to low doses of ^{56}Fe particles, suggests the possibility that exposure to cosmic rays may affect the capability of astronauts to successfully complete mission requirements.

Supported in part by N.A.S.A. Grants NAGW-4394 and NAG5-6093.

NON-REJOINED DNA DOUBLE-STRAND BREAKS IN HUMAN CELLS. A SHIFT IN RBE vs LET FOR HZE IRON PARTICLES IN COMPARISON WITH LOW ENERGY HELIUM PARTICLES

B. Rydberg and P. K. Cooper

Life Sciences Division, Lawrence Berkeley National Laboratory, One Cyclotron Road, Berkeley, CA 94720.

INTRODUCTION

DNA double-strand breaks (dsbs) are likely to be the most important lesions produced by ionizing radiation. Among the dsbs, those that are either misrejoined or remain unrejoined a long time after induction are probably the most relevant for a variety of biological endpoints. We present here results of unrejoined dsbs in human fibroblasts 16 hrs after irradiation with HZE Fe particles with LETs of 190 and 150 keV/ μ m and compare this with similar results with He particles in the LET range of 65-160 keV/ μ m.

METHODS

Irradiations were performed using the Alternating Gradient Synchrotron at Brookhaven National Laboratory and the 88 inch cyclotron at Lawrence Berkeley National Laboratory. Normal human fibroblasts at the G0 stage of the cell cycle were irradiated with 80 Gy, incubated for various times at 37 °C, trypsinized, and embedded in agarose plugs. After lysis, the DNA was separated with pulsed field gel electrophoresis and unrejoined dsbs determined by the fraction of DNA that was released from the plug. Cells irradiated with doses in the range 0 - 80 Gy without repair incubation served as calibration of the method. The percentage of dsbs that remained unrepaired after 16 hrs was determined for each particle energy.

RESULTS

Normal human fibroblast cells were irradiated with two energies of Fe ions (950 MeV/n, LET=150 keV/ μ m and 470 MeV/n, LET=190 keV/ μ m) and several energies of He ions (0.5-2 MeV/n, LET 60-140 keV/ μ m). Both Fe and He particles induced in human fibroblasts an increasing percentage of unrejoined dsbs with increasing LET as measured by pulsed-field gel electrophoresis (FAR assay). However, when non-rejoined breaks after 16 hours repair incubation are plotted as a function of LET, the data for the Fe ions and He ions fall on two distinct curves with the Fe ion data shifted towards higher LET. This result probably reflects different track structures for the two particles. An important factor could be that the Fe particles have a low-LET component from energetic delta rays that may correspond to as much as half of the dose. The LET for the Fe track on a local scale is therefore considerably lower than the total stopping power for the Fe ions.

CONCLUSION

It can be argued that the shift in RBE - LET relationship observed for unrejoined dsbs is a general feature for biological effects of HZE particles in comparison with particles of low energy (when the total stopping power (LET.) is used as equivalent for LET). This will have implications for risk estimations.

QUANTITATION OF RADIATION INDUCED DELETION AND RECOMBINATION EVENTS ASSOCIATED WITH REPEATED DNA SEQUENCES

Richard R. Sinden¹, John R. Ford², and Leslie A. Braby²

¹Center for Genome Research, Institute of Biosciences and Technology, Texas A & M University, 2121 W. Holcombe Blvd., Houston, TX 77030-3303

²Department of Nuclear Engineering, 129 Zachry Engineering Center, Texas A&M University, College Station, Texas 77843-3133

INTRODUCTION

Manned exploration of space exposes the explorers to a complex and novel radiation environment. The galactic cosmic ray component of this environment is relatively constant, and the variations with the solar cycle are well understood and predictable. However, a significant fraction of the dose may be delivered by solar particle events which vary dramatically in dose rate and incident particle spectrum. When these radiations interact with spacecraft materials and added shielding they produce a spectrum of secondary particles which depends on the spectrum of the incident particles as well as the shielding material. The different particle types and energies result in different patterns of energy deposition at the molecular and cellular level. Differences in these energy deposition patterns significantly alter the ability of cellular systems to repair the resulting damage. It is likely that these differences also effect the spatial distribution of damage within the DNA of the interphase cell nucleus and produce corresponding differences in endpoints related to health effects.

Nearly one-third of the human genome is composed of DNA repeats, which include simple mono-, di-, tri-, and tetranucleotide repeats; widely separated small and large repeats; and inverted repeats. Mutations associated with repetitive DNA are a source of many genetic diseases and cancer. In fact, the vast majority of mutations leading to human disease likely result from replication errors involving misalignment between repeated DNAs. Therefore, understanding how the various kinds of repeats contribute to the disease burden and understanding the impact of DNA damage on repeat-associated genomic instability is important for human health. DNA damage from ionizing radiation induces DNA structures and DNA repair events that can promote errors associated with repeated DNA sequences. Such repeated DNA sequences are likely to be very prone to mutation following exposure to high-Z high-energy (HZE) particles during space flight. Cells in the direct line of the HZE particle sustain a high dose of energy while cells surrounding the primary tract sustain a lower dose of energy from the energetic delta rays (electrons) produced by HZE particles. Therefore, the nature and pattern DNA damage to cells in tissue upon irradiation with HZE particles is particularly complex. It is important to understand the types of mutational changes induced by both the HZE particles as well as the delta rays.

CURRENT STATUS OF RESEARCH METHODS

Preliminary experiments involving X-rays:

To ensure that our systems for analysis are operational before analyzing cells treated with Fe particles, we performed preliminary experiments of cells treated with x-rays. We have now measured X-ray survival for the four cell lines described below, and measured and G-418 reversion frequencies for 122-2 and F14C following X-ray treatment. In addition, to the analysis

of the repeated DNAs in these four cell lines in my lab, Drs. Braby and Ford have begun analyzing several features of these cells in the new tissue culture lab at the microbeam facility. Procedures being used include sister chromatid exchanges (SCE's) using a fluorescence plus Giemsa technique and using a micronucleus assay measuring in binucleated cells after cytochalasin B treatment. Procedures to determine these endpoints are now working smoothly and they will begin analyzing iron ion-irradiated F14C-23 and 122-2 cell lines that are currently under G-418 selection.

A. Experiments involving 1000 MeV/n Fe

Four different cell lines were irradiated during the BNL-4 run with between 0 and 100 cGy 1000 MeV/n Fe:

Cell lines F14C-23 and 122-2 are human fibrosarcoma lines with either a 122 bp inverted repeat or 122 bp non palindromic sequence, both flanked by direct repeats, in a neo reporter gene that is integrated into the chromosome. Upon precise deletion of the inverted repeat the cells become resistant to the antibiotic G-418. The spontaneous deletion frequency for F14C-23 is 1×10^{-8} , and the deletion frequency after 4 Gy X-rays is about 3×10^{-8} . The spontaneous deletion frequency for 122-2 is $<3 \times 10^{-9}$, and as high as 8.3×10^{-6} after 4 Gy X-rays.

We have recently begun selection on the F14C-23 and 122-2 cell lines since it has taken quite some time to reestablish the optimum antibiotic concentration for selection. Too little antibiotic and all cells grow, too much, and all are killed, including "revertants". It was imperative that this be done with the current lot of antibiotics and cells or there would be a chance that the cells exposed at Brookhaven would have been wasted. F14C-23 and 122-2 cells exposed to iron during BNL-4 are now under G-418 selection to measure the frequency of deletions associated with direct and inverted repeats.

Mouse lymphoblast cell line (7#7-7) contains a 30.6 kb inverted repeat, which shows instability in culture. Both my lab and that of Dr. Susanna Lewis (Toronto) will begin analysis of clonal lines from BNL-4 irradiated cells shortly. Genomic instability, as indicated by a delayed asymmetric deletion within the inverted repeat, will be assessed by use of Southern hybridization.

Cell line 3134 is a mouse mammary cancer cell line containing a 1.8 mb direct repeated region comprised of 200 tandem direct repeats of a 9 kb hormone inducible gene (MMTV driven ras gene) integrated near the centromeric end of chromosome 4. We plan a collaborative investigation of genomic instability in this region using FISH analysis for genome rearrangement involving the 1.8 mb region.

RESULTS

G-418 reversion frequencies are being measured for cell lines F14C-23 and 122-2 treated with Fe. Survival data and initial analyses of the frequency of deletions between direct repeats associated with inverted repeats and non palindromic DNA should be completed by the time of the meeting.

PLANS FOR FUTURE INVESTIGATIONS

By the time of BNL-5 we will have initial data for F14C-23 and 122-2 from the 0, 25, 50, and 100 cGy irradiations. If needed we can adjust the dose for repetitions of this experiment. If not, we will repeat the experiments at the same doses in order to reduce statical uncertainty. We expect that very low doses may be needed for 7#7-7 cells given their high frequency of spontaneous mutations, these irradiations will be performed, if necessary. Better characterized sub clones of the 3134 cells are available (from FISH analysis) and these will be irradiated at BNL-5.

We are developing additional cell lines that contain other reporters of genome instability, including deletion, recombination, and gene conversion. Planned constructs involve 600 bp inverted repeats cloned into rat mammary cells.

INFORMATION NEEDED TO MAKE RADIATION PROTECTION RECOMMENDATIONS FOR TRAVEL BEYOND LOW-EARTH ORBIT

Lawrence W. Townsend, Ph.D, Department of Nuclear Engineering , The University of Tennessee, Knoxville, Tennessee 37996-2300

Scientific Committee 1-7 (SC 1-7) of the National Council on Radiation Protection and Measurements (NCRP) has been assembled for the purpose of providing recommendations to NASA concerning the information needed to make radiation protection guidelines for manned space missions beyond low-Earth orbit. Current space radiation limits pertain only to missions in low-Earth orbit and are not considered relevant for future deep space missions. SC 1-7 has met numerous times over the past three years to review the current status of scientific knowledge relevant to this task. The committee is currently formulating a set of recommendations for additional research needed to provide the data necessary to establish astronaut radiation limits for exomagnetospheric missions, such as a Lunar base or mission to Mars.

In this presentation, the procedures followed by the NCRP for making recommendations are briefly discussed. The composition of SC 1-7 and the scope of its efforts and activities are presented. Brief overviews of the current status and shortcomings of scientific knowledge of the space radiation environment, radiation physics and transport, radiation biology, dosimetry and radiation risk are presented. However, formal recommendations of research necessary to establish radiation limits for deep space missions will not be presented since they have not been developed by the committee or approved by the Council.

RISK MANAGEMENT STRATEGIES DURING SOLAR EVENTS

Dr. Ron Turner

ANSER, Suite 800, 1215 Jefferson Davis Hwy, Arlington VA 22202

The natural radiation from galactic cosmic rays (GCR) and solar particle events (SPEs) will pose a serious health risk to humans during missions to Mars or the Moon. The opportunities and limitations of astronauts on these missions will be constrained by the radiation environment and NASA's response to it.

NASA recognizes both an ethical and legal responsibility to minimize the acute and long-term risks to astronauts during space flight. There is an extensive program underway to collect statistically meaningful data to understand the fundamental biological impacts of the radiation environment. These data can be directly related to the well-characterized incident, slowly varying, galactic cosmic ray flux. There is greater uncertainty in predicting and characterizing the rapidly changing solar particle radiation which, over time periods of hours to days, can produce particle fluences comparable to mission-long GCR fluence.

Work by this investigator in an earlier grant (NAGW-4166) systematically identified the types of solar particle events (SPEs), the stages of a human Lunar or Mars mission when the events may occur, and the methods used to detect and forecast these events. Alternative scenarios were identified that represented the range of architectures that could be employed to mitigate SPE risk. The advantages and disadvantages of each scenario were discussed.

Based on the earlier results, we initiated a program to continue this research through a sequence of additional phases that will progressively add to NASA's ability to develop a comprehensive SPE risk management strategy. These subsequent phases examine in more detail the science, engineering, and operational requirements. The focus in each phase is to identify the key issues and general approaches to address these issues, rather than to attempt to specify a particular solution. This presentation will include a short review of the physics of SPEs and the current ability to forecast SPEs. It will then cover techniques to observe SPEs and the solar precursors to SPEs.

AMINOTHIOL INDUCED MODULATION OF P53 PROTEIN ACTIVITY IN HUMAN CELLS

Raymond L. Warters¹, David K. Thai¹, Jeanette C. Roberts¹, David K. Gaffney¹ and Anne E. Cress², ¹University of Utah Health Sciences Center, Salt Lake City, UT 84132 and ²University of Arizona Cancer Center, Tucson, AZ 85724.

INTRODUCTION

The aminothiols (S-2-(3-aminopropylamino)ethylphosphorothioic acid (WR1065) and the thiazolidine prodrug Ribose Cysteine (RibCys) have been reported to be antimutagenic in mammalian cells when present either during irradiation, or more significantly when present only after irradiation. The antimutagenesis effect mediated by these agents when present during irradiation may be attributable to their ability to reduce radiation-induced DNA damage. The antimutagenesis effect observed when these agents are added well after irradiation must be due to some modification of the cell's response to DNA damage. In an attempt to better understand this modulation of the cellular response to radiation, we are investigating the intracellular changes in cells exposed either to ionizing radiation or aminothiols.

METHODS

Modification of intracellular physiology by either ionizing radiation or aminothiols was assessed by measuring changes in the activity of the p53 transcription factor in two p53^{+/+} human cell lines: the SK-N-SH neuroblastoma and the HCT116 colon carcinoma. Intracellular p53 protein mass and distribution were examined either by confocal immunofluorescence microscopy of methanol fixed cells, or by western analysis of SDS-PAGE separated proteins with p53 specific antibodies. The biological activity of the p53 protein was examined by quantifying down stream p53-induced responses (e.g., upregulation of the p21/WAF1 target gene). The biochemical activity of the p53 protein was examined by assessing the binding of the p53 protein to a synthetic oligonucleotide containing the p53 consensus binding sequence.

RESULTS

Using immunofluorescence microscopy, increasing amounts of the PAb421 p53 antibody epitope (amino acids 372-381) were detected in nuclei of irradiated cells or cells exposed to WR1065, cysteine or RibCys. Reactive nuclear PAb421 epitopes increased to a maximum by 1-2 hours either after irradiation or after a 60 minute exposure to aminothiols. A 4-fold increase in nuclear PAb421 epitope was observed in either 5 Gy irradiated or 4 mM WR1065 exposed cells. Nuclear p53 expression increased as a function of increasing aminothiol concentration or exposure time. Increased nuclear expression of PAb421 epitope could be detected in cells exposed to WR1065 concentrations as low as 100 μ M.

Western analysis of p53 protein from irradiated or aminothiol exposed cells using the PAb421 antibody indicated no detectable change in p53 protein mass in irradiated or aminothiol exposed cells. In contrast, western analysis of p53 protein with the PAb1801 antibody (p53 amino acids 46-55) indicated a substantial increase in p53 protein mass beginning by 1 hour after cell irradiation, with maximum expression by 2 hours after cell irradiation. Western analysis detected no PAb1801 epitope expression in aminothiol exposed cells.

By western analysis WAF1/p21 protein mass increased substantially by 2 hours in irradiated cells, with maximum expression occurring by 3-4 hours which remained elevated for at least 6 hours after irradiation. Western analysis detected no increase in WAF1/p21 protein in aminothiols exposed cells.

CONCLUSIONS

Immunofluorescence microscopy of fixed cells indicates an increase in the total amount of nuclear p53 PAb421 epitope in irradiated or aminothiol exposed human cells. This apparent increase in p53 protein mass was not confirmed by western analysis, which detected no change in the cellular content of the Pab421 epitope. The combined results indicate that the PAb421 epitope is masked in the unstressed cell, either by p53 association with another protein or by p53 protein folding upon itself. Cell irradiation or aminothiol exposure results in a p53 structural change that unmasks the PAb421 epitope, thus allowing its detection in fixed cells. In irradiated cells this unmasking of the PAb421 epitope likely results in activation of the protein as a transcription factor and its subsequent binding to and transactivation of the WAF1/p21 gene. In contrast, in aminothiol exposed cells the p53 structural change does not result in its activation as a transcription factor.

Our results indicate that both cell irradiation and exposure to aminothiols alter the structure of the p53 protein and/or its association with other cellular proteins. The relationship of these changes in intracellular proteins to radiation-induced mutagenesis remains to be fully understood.

CYTOGENETIC DAMAGE FROM PHOTONS, FE-IONS AND PROTONS: MODULATION BY DOSE-RATE AND CELL TYPE.

J.R. Williams, Z. Houming, F.E. Dicello, and Y. Zhang
Johns Hopkins Oncology Center, Baltimore Md, 21287-5001

INTRODUCTION

We examined the induction of chromosome damage in multiple cell types irradiated with graded acutely-delivered doses of photons, Fe-ions and protons. Further we have compared the effects of photons delivered at ~50 Gy/hr to effects when irradiation is delivered at 0.25 Gy/hr.

METHODS

Cells (human lymphocytes, human mammary epithelial cells, rat mammary cells and human colorectal tumor cells) were irradiated for doses of 0.5, 1.0, 2.5 and 5.0 Gy of Cs-137 gamma rays delivered acutely at high dose rate (50 Gy/hr) or low dose-rate (0.25 Gy/hr). These cells were also irradiated with protons (250 Kev) at the same doses or with 0.1, 0.25, 0.5 and 1.0 Gy of Fe-ions (1 Gev). The number of chromosome aberrations were scored at the first post-irradiation mitosis. Results were analyzed using the alpha-omega model.

RESULTS

There was no significant differences in the induction of complex chromosome aberrations induced by photons and protons. There was up to a n 18 fold difference in the rate of induction of complex aberrations between Fe-ions and photons irradiated at low dose-rate and an approximately 3 fold difference in aberrations induced by Fe-ions and high dose-rate photons. There was a 7 fold difference in the induction of chromosome aberrations by Fe-ions in different cell types.

CONCLUSION

Three factors are observed to modulate induction of chromosome aberrations by radiations of different quality: 1) intrinsic cellular radiosensitivity, 2) dose-rate and 3) an unknown factor probably associated with differences in repair of induced DNA lesions. The relative magnitude of these effects are 7:6:3. Strategies to mitigate carcinogenicity of space radiations must be developed through these modulating factors.

IMPACT OF TRACK STRUCTURE EFFECTS ON SHIELDING AND DOSIMETRY

J. W. Wilson¹, F. A. Cucinotta², W. Schimmerling³, and M. Y. Kim¹

¹NASA Langley Research Center, ²NASA Johnson Space Center, ³NASA Headquarters

INTRODUCTION

Galactic cosmic rays (GCR) consisting of nuclei of all the known elements with kinetic energies extending from tens to millions of MeV pose a significant health hazard to future deep space operations. Even half of the radiation exposures expected in ISS will result from GCR components. The biological actions of these radiations are known to depend on the details of the energy deposition (not just linear energy transfer, LET, but the lateral dispersion of energy deposition about the particle track). Energy deposits in tissues are dominated by the transfer of tens to hundreds of eV to the tissue's atomic electrons. In the case of low LET radiations, the collisions are separated by large dimensions compared to the size of important biomolecular structures. If such events are also separated in time, then the radiation adds little to the background of radicals occurring from ordinary metabolic processes and causes little or no biological injury. Hence, dose rate is a strong determinant of the action of low LET exposures. The GCR exposures are dominated by ions of high charge and energy (HZE) characterized by many collisions with atomic electrons over biomolecular dimensions, resulting in high radical-density events associated with a few isolated ion paths through the cell and minimal dose rate dependence at ordinary exposure levels. The HZE energy deposit declines quickly laterally and merges with the background radical density in the track periphery for which the exact lateral distribution of the energy deposit is the determinant of the biological injury. Although little data exists on human exposures from HZE radiations, limited studies in mice and mammalian cell cultures allow evaluation of the effects of track structure on shield attenuation properties and evaluation of implications for dosimetry.

The most complete mammalian cell HZE exposure data sets have been modeled including the C3H10T1/2 survival and transformation data of Yang et al.¹, the V79 survival and mutation data of various groups², and the Harderian gland tumor data of Alpen et al.³ Model results for the Harderian gland tumor data are shown in figure 1 in comparison with data from Alpen et al.³ The Harderian target cell initiation cross section is shown in figure 2 and compares closely with the transformation cross section found for the C3H10T1/2 cell transformation data of Yang et al. The most notable feature of the cross sections in figure 2 are the multivalued cross sections for a given LET which implies the corresponding relative biological effectiveness (RBE) is dependent not only on the LET but also the ion type. This fact is at variance with the latest ICRP recommended quality factor⁴ which is a defined function of only the LET.

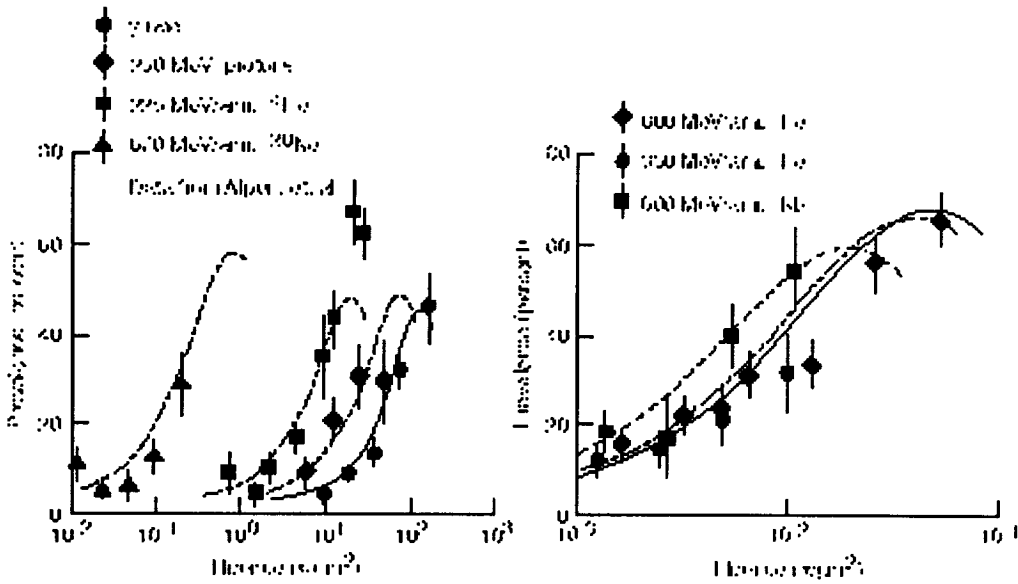


Fig. 1. Fluence response for Harderian gland tumors for several radiation types.

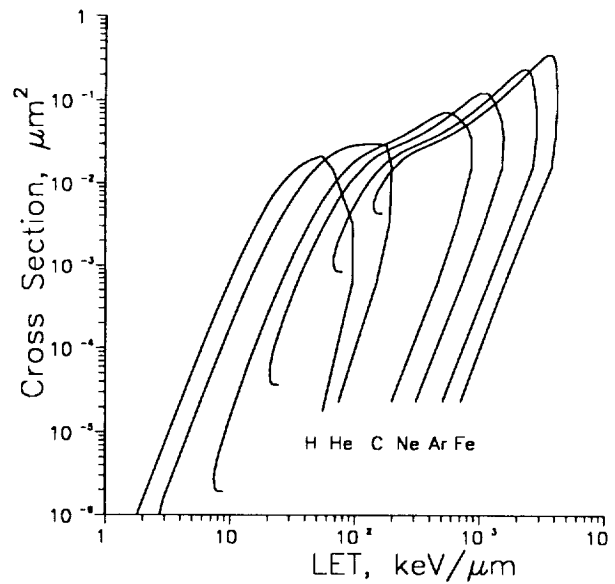


Fig. 2. Harderian gland cell initiation cross section obtained from fits to the Alpen *et al.* data.

Track structure related events are difficult to study in whole animals since the local environment within an animal varies across the organ under study and is modified by the surrounding tissues. Cell cultures can be used to control the local environment and provide an improved system for track structure studies. Among the best studied cell systems is V79 for survival and mutation end points. The model of the V79 system is shown in comparison with data from various groups in figure 3². As we shall see, these features have important implications for attenuation of biological effects within spacecraft materials.

IMPACT ON SHIELDING

We have used these models and the LET dependent quality factor⁴ to investigate the attenuation of biologically damaging radiation within shield materials in the space environment⁵ using the HZETRN code. In terms of dose equivalent, we find that aluminum structures attenuate radiation effects over most of the range of depths used in human rated vehicles (2-10 g/cm²) as shown in figure 4. In contrast, track structure models show markedly different attenuation characteristics and, in fact, show that a transformed cell is more likely to result by increasing the aluminum shielding in spite of the decreasing dose equivalent. Such findings may have important implications for deep space exploration⁶ but also for ISS which receives half its exposure from GCR ions.

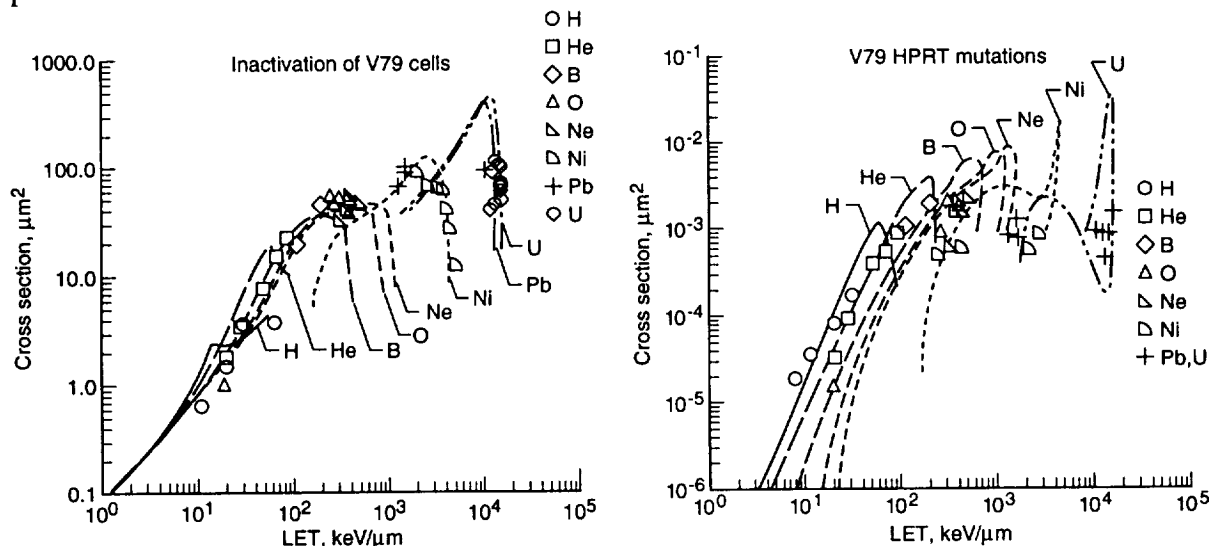


Fig. 3. Track structure effects in the V79 cross sections for (a) inactivation and (b) HPRT mutation.

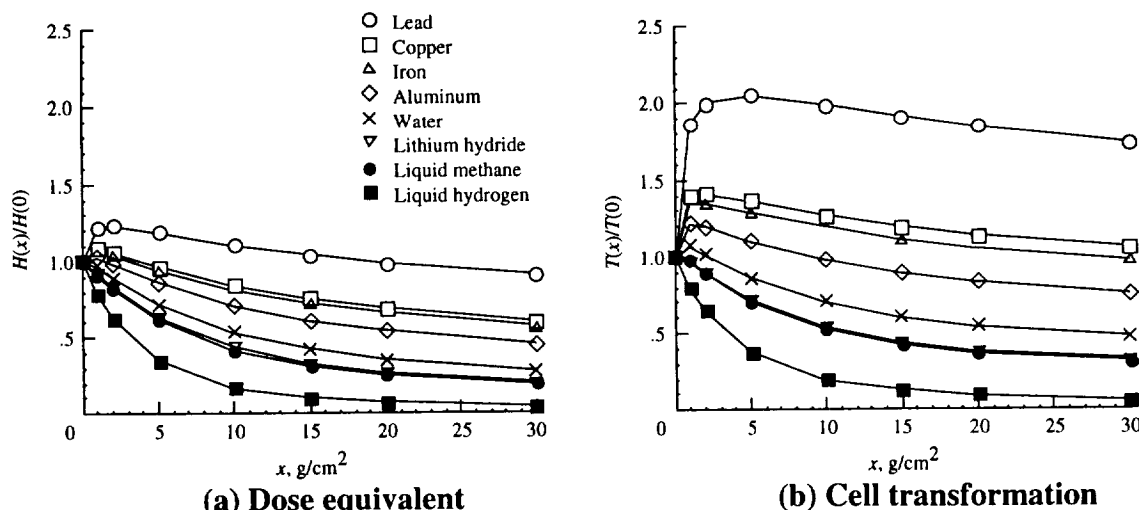


Fig. 4. Attenuation of dose equivalent and cell transformation for a one-year GCR exposure at solar minimum behind various shield materials.

DISCUSSION

The biologically based models show complex dependence on radiation quality which is expressed in terms related to the details of the particle track as distinct from the simple LET dependence of the quality factor used in conventional radiation practice. Even the cancer risk attenuation characteristics of spacecraft shield materials are found to be vastly different for the track structure dependent and LET dependent models⁵ leading one to conclude that any useful dosimetric technique must reflect these differences as well. Most important in this respect is that LET dependent quality factors overestimate the effectiveness of most shielding materials and would falsely indicate reduced cancer risk. Clearly, the dosimetric quantities used to monitor risk must be carefully chosen to ensure adequate representation of track structure effects.

Sufficient knowledge of the radiation components at specific tissue sites must be the aim of the dosimetric system. Aside from LET as an indicator of radiation quality, the lateral spread of the track (which is related to ion speed and the fluctuations along the track length related to the effective charge) needs to be adequately taken into account. Although microdosimetry could possibly provide some details, the current site sizes are limited by current technological capability and are probably too large to adequately represent the details available in some current biological data (fig. 3). The representation of such details is presently available in a fluence based model (used herein) requiring the specification of the particle spectral environment and is the only method known that can adequately represent biological risks.

CONCLUSIONS

Just as the estimation of shield attenuation characteristics of various materials depends on the details of the biological response model, the impact of the requirements for dosimetric characterization of the radiation fields depends on the biological model used in risk assessment. In that the experimental biological evidence displays clear dependence on other parameters in addition to LET, the adequate estimation of risk in future deep space missions needs to reflect this dependence on these other factors. One test of an adequate dosimetry system would be to assure that the track structure dependent data already derived from heavy ion experiments can in fact be represented (e.g., the data in figure 3). Failure to do so could be an indication of the inadequacy of the dosimetric system. The only method known to date to pass such a test is a fluence based risk assessment method as used in the present paper.

¹ J. W. Wilson, F. A. Cucinotta, J. L. Shinn, Cell Kinetics and Track Structure, *Biological Effects and Physics of Solar and Galactic Cosmic Radiation*, Part A, eds. C. E. Swenberg et al., Plenum Press 1993, pp. 295-338.

² F. A. Cucinotta, et al., Effects of track structure and cell inactivation on the calculation of heavy ion mutation rates in mammalian cells. *Int. J. Radiat. Biol.* 69:593-600; 1995.

³ F. A. Cucinotta, J. W. Wilson, An initiation promotion model of tumor prevalence from high charge and energy radiations. *Phys. Med. Biol.* 39:1811-1831; 1994.

⁴ ICRP, *1990 Recommendations of the International Commission on Radiological Protection*. ICRP Publication 60, Pergamon Press, 1991.

⁵ J. W. Wilson et al., Issues in space radiation protection: Galactic cosmic rays. *Health Physics* 68:50-58; 1995.

⁶ NRC/NAS, *Radiation Hazards to Crews of Interplanetary Missions: Biological Issues and Research Strategies*. NAS, 1996.

ANALYSIS OF INCOMPLETE CHROMOSOMAL EXCHANGES USING FLUORESCENCE *IN SITU* HYBRIDIZATION WITH TELOMERE PROBES

H. Wu^{1,2}, K. George^{1,3} and T. C. Yang^{1,*}

¹NASA Johnson Space Center, Radiation Biophysics Laboratory, Houston, Texas 77058,

²Kelsey-Seybold Clinic, NASA Johnson Space Center, Mail Code SD23, Houston, Texas 77058,

³WYLE Life Sciences, 1290 Hercules Drive, Houston, Texas 77058; *Deceased

INTRODUCTION

To determine the frequency of true incomplete exchanges induced by both low- and high-LET radiation.

METHODS

Human lymphocytes were exposed *in vitro* to 2 and 5 Gy of γ rays, and to 1 and 3 Gy of 1 GeV Fe ions. Chromosome aberrations were analyzed by fluorescence *in situ* hybridization technique using a combination of whole chromosome specific probes and human telomere probes. Chromosomes #2 and #4 were examined in the study of low-LET radiation and chromosomes #1, #3 and #4 were investigated for high-LET radiation.

RESULTS

For γ -irradiation, the percentage of incomplete exchanges was found to be 27% when telomere signals were not considered. After excluding false incomplete exchanges identified by the presence of telomere signals, the percentage of incomplete exchanges decreased to 11%. Since telomere signals appear on about 82% of the telomeres, the percentage of true incomplete exchanges should be even lower and was estimated to be 3%. This percentage was found to be similar for chromosomes #2 and #4 and for doses of both 2 and 5 Gy. For Fe ion-irradiation, the percentage of incomplete exchanges was found to be between 23 and 29% if telomere signals were not considered. The percentage decreased to around 10% after ruling out false incomplete exchanges containing telomere signals. The final estimation of true incomplete exchanges was found to be below 10%.

CONCLUSION

The frequency of true incomplete exchanges in human lymphocytes was significantly lower than the frequencies reported in the literature. Within a degree of uncertainty and with complete exchanges properly defined, the percentage of true incomplete exchanges for 1 GeV Fe ion-irradiation was similar to those induced by low-LET radiation.

Sleep/Circadian Rhythm

Chair

David Dinges, Ph.D.

Co-Chair

Charles Czeisler, Ph.D.

SLEEP/CIRCADIAN RHYTHM SESSION SUMMARY

Background

Sleep and circadian rhythm systems are fundamental regulatory processes of the nervous system, and the most ubiquitous endogenous controls of human biobehavioral functions—everyone is internally programmed to sleep every night. The need for sleep is a homeostatic drive that occurs regardless of time of day, but it is also modulated by the endogenous circadian pacemaker. Conversely, the endogenous circadian pacemaker oscillates regardless of the need for sleep, although its promotion of wakefulness can be overwhelmed by elevated homeostatic sleep drive. These two powerful neurobiological systems interact continuously to control brain state (i.e., waking vs. sleep) and the intensity of state (e.g., alert vs. sleepy). Sleep and circadian rhythmicity also temporally modulate a wide range of physiological functions (e.g., body temperature, cardiovascular activity, respiration, immune responses), hormonal functions (e.g., growth hormone, melatonin, cortisol, thyroid hormones), behavioral functions (e.g., movement, posture, reaction time), and cognitive functions (e.g., fatigue, alertness, vigilance, memory, cognitive throughput). No astronaut—no matter how much training, preparation, nutrition, psychosocial support, or environmental protection is provided—is immune from the daily control of physiology and performance by the homeostatic drive for sleep and the endogenous circadian timing system. Failure to take these two interactive neurobiological imperatives into account when planning human activities in space will have catastrophic consequences.

The need for sleep and the circadian pacemaker have a sustained influence over many biomedical systems essential for maintaining astronaut physical condition, mental health, and performance capability. Dysfunction of sleep and circadian systems can adversely affect an organism's ability to respond to environmental challenges and has been linked to physiological and psychological disorders. This area therefore has a high degree of relevance to a number of other space life science technical areas including research on muscle and bone loss, cardiovascular and immune changes, neurovestibular alterations and nutritional needs, and behavioral and psychological health in space flight.

Acute gravitational changes and space flight disrupt circadian rhythms and reduce sleep.

Separate lines of evidence presented by **Fuller**, and **Barger and Fuller**, confirmed that space flight and acute gravitational changes disrupt circadian rhythms and reduce sleep homeostasis in a wide range of organisms including *Neurospora*, insects, rodents, and primates. Some of the basic mechanisms by which space flight and acute gravitational changes may alter circadian rhythms and sleep homeostasis are coming to be known through use of animal models. **Murakami et al.** presented evidence from the BRN 3.1 knockout mouse, which lacks a neurovestibular system, that the vestibular system mediates some of the disruptive effects of gravitational changes (2G) on circadian rhythmicity in body temperature and activity.

There is now mounting evidence that space flight is associated with adverse effects on both circadian and sleep regulatory systems. Data presented by **Monk et al.** from three astronauts/cosmonauts aboard NASA 4/Mir 23 and NASA 5/Mir 24 missions, and preliminary data from **Czeisler et al.** from recent STS-90 and STS-95 shuttle missions, confirmed that during shuttle flights physiological sleep is chronically altered, reduced in duration, and less deep. In this study, strenuous efforts (much stricter than NASA's Appendix K) were made to avoid circadian disruptions. These appeared to be effective, preventing disruption of the phase and

amplitude of circadian rhythms during this 17-day mission. In contrast, preliminary data from shuttle mission STS-90, reported by **Czeisler et al.**, showed chronic disruption of the circadian system due to the mission's 20-minute daily phase advance in work-rest schedules (i.e., 23.67-hr day) and the very low light levels on the space craft. As reported by **Wright et al.**, problems ensue when light levels are too low on the space craft (e.g., STS-90 mid-deck light < 10 lux) or the light/dark cycle is outside the entrainment capacity of the circadian pacemaker (e.g., Mars 24.6 hr day). In such instances, circadian desynchrony occurs, which results in neurobehavioral and physiological disturbances during space flight, especially when endogenous circadian rhythms are not entrained to a light/dark cycle, and/or when they are misaligned relative to work-rest schedules on spacecraft and orbital dynamics of other planets, such as Mars. For example, the research with astronauts reported by **Monk et al.** showed that phase shifts of the time for sleep led to the highest ratings of end-of-shift tiredness.

Data were also presented by **Monk et al.** and by **Czeisler et al.** documenting that sleep is shorter and less deep during space flight. In fact, evidence has been accumulating during the past 25 years, culminating with the data on actual sleep physiology reported by the **Czeisler et al.** and **Monk et al.** research teams, that sleep duration during space flight is rarely 8 hours, and most often averages around 6 hours—occasionally reducing to well below 5 hours. There appear to be multiple causes for the sleep loss in space flight including microgravity, circadian disruption, environmental disturbances, operational demands, and insomnia from other causes. The pervasiveness of the insomnia problem during space flight is perhaps best illustrated by the results from a recent study by **Putchala et al.** at Johnson Space Center that categorized pharmacological countermeasures by indication. Out of 11 indications, sleeping medications accounted for the largest category of use by astronauts, comprising 32% of unit doses administered in space. But hypnotics have not solved the problem of sleep loss during space flight, which remains common.

Sleep loss and circadian disruptions result in physiological and performance deficits.

There are definite physiological and neurobehavioral consequences for the chronic restriction of sleep in space flight, regardless of the cause. **Smith et al.** presented data showing that sleep restriction to 4 hours/night for 4 nights produced subtle changes in cardiovascular responses to simulated orthostasis. **Mullington et al.** presented data that sleep restriction results in elevated cortisol levels during the circadian nadir of cortisol. This group is currently evaluating additional neuroendocrine and neuroimmune responses to sleep loss at levels experienced in space flight. **Dinges et al.** found that the chronic reduction of sleep duration to the level most often experienced by astronauts (i.e., an average of 6 hours per day) results in measurable deficits in neurobehavioral performance that accumulate to very debilitated levels of vigilance and cognitive functioning. It is especially noteworthy that these cognitive performance deficits accumulate in a dose-response manner, yet subjects' self-estimates of their alertness are only minimally altered. This results in a dangerous profile of high impairment without subjective awareness. Thus, circadian disturbance and sleep loss in space flight can result in neurobehavioral and physiological dysfunction as a result of acute and/or chronic cumulative, but astronauts may not be aware of the effects until an error actually occurs.

Countermeasure research on sleep/circadian disruptions of physiology and performance.

The focus of countermeasure research presented by scientists supported by NASA through the National Space Biomedical Research Institute (NSBRI) was in three areas: (1) preventing the adverse effects of sleep loss; (2) enhancing circadian adjustment; and (3) monitoring and enhancing performance during prolonged space flight.

As part of investigations of entrainment of the human circadian pacemaker to dim light-dark cycles, and to the 24.6 hr Martian day, underway in Charles Czeisler's laboratory, **Wright et al.** reported on the effects of varying light schedules on circadian entrainment, to prevent impaired daytime performance and reduced growth hormone secretion. From the standpoint of circadian synchronization, light intensity and timing are among the most critical factors. In related NASA projects from this laboratory, **Khalsa and Dijk** reported double-blind placebo-controlled experiments underway to determine whether oral administration of the pineal hormone melatonin could synchronize the human circadian pacemaker to a shortened sleep-wake schedule typical of those encountered on space shuttle missions. In complementary experiments, **Czeisler et al.** reported testing the effectiveness of orally administered melatonin as a sleeping medication (hypnotic), independent of its effects on circadian timing. This group has also studied the efficacy of melatonin as a hypnotic during the STS-90 and STS-95 shuttle missions, focusing on its effects on sleep physiology and waking performance.

Dinges et al. reported on experiments underway to prevent performance impairments and reduced growth hormone secretion during the chronic reduction of sleep duration typical of space flight. These studies focus on evaluating the cumulative benefits of a broad range of sleep-wake periods using combinations of anchor sleep and nap sleep. There is also an emphasis on identifying the factors that promote individual vulnerability to impairment from sleep loss. Research reported by **Dijk and Cajochen** is focused on finding ways to reliably track moment-to-moment performance vulnerability in sleep-deprived subjects, using sophisticated electroencephalographic (EEG) and electrooculographic (EOG) markers of performance. This research holds promise for the development of unobtrusive objective monitors that can reliably track performance capability. Related to the issue of predicting human performance on-line during prolonged space flight is the biomathematical modeling work presented by **Brown et al.** These investigators are developing a mathematical model that can predict performance and alertness as a function of the state of the circadian system and recent sleep-wake history. The model is being tested and improved using data from related NSBRI projects by Czeisler, Dinges, Dijk, and colleagues.

The vulnerability of human performance during prolonged space flight also involves the remote isolation that limits Earth-bound support for problem solving. **Callini et al.** (presented by Young) reported both successful shuttle mission and ground-based studies of the "Principal Investigator in a Box [PI]," which is an expert problem solving system designed to enhance astronaut performance. This device, and all of the research presented on countermeasures to performance failures during space flight, also has potential usefulness for helping millions of people working on Earth.

David F. Dinges and Charles A. Czeisler

GENDER DIFFERENCES IN THE RESPONSES OF RHESUS MONKEYS TO 2G

L.K. Barger and C.A. Fuller. Section of Neurobiology, Physiology and Behavior
University of California, Davis.

INTRODUCTION

Organisms exposed to alterations in the gravitational environment demonstrate several physiological and behavioral responses. Among the affected physiological systems is the Circadian Timing System (CTS). The CTS coordinates an animal's physiology and behavior, ensuring that the body is in the proper state for anticipated activities. We know from previous research that exposure to spaceflight affects the circadian rhythms of organisms ranging from unicells to primates. Different rhythms do not respond in the same fashion, producing an internal desynchronization between the various circadian rhythms. Desynchronization between internal rhythms may be linked to reduced capabilities in the performance of simple tasks and to psychological abnormalities.

There is a preponderance of women among those treated for psychological disorders, including those linked to circadian dysfunction. This has been attributed to various physiological, psychological and sociological differences, but no innate underlying cause has yet been proved. Moreover, women now form a substantial part of the space research program and are frequent space travelers. Therefore, it is important to characterize the responses of females to an altered force environment.

We undertook this study to elucidate the response of multiple physiological and behavioral circadian rhythms of a non-human primate to an altered force environment. Male and female responses to chronic centrifugation were characterized and examined for gender differences. Additionally, when studying the circadian rhythms of females, menstrual cyclicity may play a major role. It has been shown that reproductive cyclicity has a significant influence on the regulation of circadian rhythms in rodents. An extensive study had not been undertaken using a menstrual animal such as the Rhesus monkey (*Macaca mulatta*) as a biomedical model. It was important to define the cycling status of our female subjects and examine the effects of menstrual cyclicity on physiological and behavioral circadian rhythms in female Rhesus monkeys before beginning the chronic centrifugation study.

CURRENT STATUS OF RESEARCH

METHODS

A battery operated biotelemetry unit (Koningsberg Instruments) was surgically implanted in eight male and eight female Rhesus monkeys. These units measure body temperature and heart rate. The signals are received by an antenna and sent to a microcomputer based data hard disk. Software was developed to translate body temperature and heart rate telemetry files into a form that could be analyzed for circadian rhythmicity. Performance measures were made using the psychomotor test system (PTS), developed at the University of Georgia Language Research Center. The PTS is a computer-based video task system that enables us to test short term memory, hand-eye coordination, and other performance parameters. Successful completion of a video task is rewarded with a food pellet. Animals were fully trained so that in most cases all caloric needs could be met through PTS. When pellet intake was below caloric requirement,

supplemental monkey chow biscuits (Purina) were provided. PTS was available during light hours. Water was available *ad lib* through a lixit. Drinking was measured via an electronic contact circuit attached to the lixit. Number of contacts was collected and summed in ten minutes bins. Urine samples were collected daily. Estrone conjugate (E₁C) and pregnanediol-3-glucuronide (PdG) were assayed and quantified by enzyme immunoassay. Lighting schedule was LD 16:8. Daily husbandry was performed on a non-24 hour schedule so as not to introduce circadian time cues.

Eight females and seven males were housed at the California Regional Primate Research Center for 30-day baseline studies. Six males and then six females were individually housed on a 6-meter centrifuge at the Chronic Acceleration Research Unit for the hyperdynamic study. Data were collected for: 2 weeks (1G), 2 weeks (2G), then 2 weeks (1G).

Circadian analysis was completed using in-house software to calculate an average phase, amplitude, and mean. Factorial ANOVA with repeated measures ($p \leq 0.05$) was used to examine differences in environmental conditions and gender.

RESULTS

Baseline Studies. Circadian rhythms of body temperature, heart rate, activity, and drinking were characterized for males and females. Based on estrone and progesterone patterns, follicular and luteal phases were defined for each female. Body temperature changes throughout the menstrual cycle appeared to be different than observed in humans. There were no significant differences between follicular and luteal phases in activity or drinking. Mean body temperature was significantly ($p < 0.05$) increased during the follicular phase. There was a delay in heart rate acrophase during the luteal phase.

Gender Differences in the Responses of Rhesus to 2G. There were several physiological alterations associated with the onset of 2G. We investigated the circadian changes in body temperature and heart rate. Mean female body temperature was significantly ($p < 0.05$) higher than male mean body temperature. During 2G, female body temperature increased while male body temperature decreased. Body temperature showed a marked decrease in circadian amplitude during the first week at 2G. At 2G onset, females showed a phase advance while males showed a phase delay. Mean heart rate was significantly higher in females ($p < 0.05$) than males. On day 1 of 2G, female heart rate increased an average of 20 beats/min, while male heart rate increased an average of 2 beats/min. This was a significantly different ($p < 0.01$) response. There were no significant changes in heart rate amplitude or phase. There was a significant decrease in urine volume for both male and female subjects throughout 2G and recovery. Mean drink counts did not show any significant change between 1G and 2G conditions. PTS utilization reflects the general pattern of mean daily food intake. Both genders showed a similar response to 2G: a significant ($p < 0.05$) decrease on the first day of 2G followed by a gradual 7-day increase back to baseline. Rhesus complete PTS tasks with a high degree of accuracy and speed. There was a significant ($p < 0.05$) increase in response time on psychomotor tasks at 2G onset, but percent correct on matching tasks remained unchanged. Males performed matching tasks with a significantly ($p < 0.05$) greater accuracy.

CONCLUSIONS

Both male and female Rhesus monkeys are able to adapt and perform in a chronic 2G environment. Physiologically and behaviorally, both genders respond similarly to a hyperdynamic environment. Responses to 2G did not appear dependent on menstrual phase in female Rhesus. There are robust changes in circadian rhythmicity at 2G onset. Amplitude of the body temperature rhythm is significantly decreased at 2G onset in both genders. Past studies with rodents show a significant drop in body temperature, while the Rhesus did not show any change in mean body temperature. Interestingly male body temperature did show a slight decline, while female body temperature rose. Differences in responses or the magnitude of responses between genders could possibly be due to weight differences, vestibular sensitivity, or differences in fluid shifts. At 2G, primates perceive a hypovolemia due to fluid shifts. Decreased urine output appears to be the dominant physiological compensation, as mean drink counts remained unchanged. This was true for both males and females. Performance changes at 2G are task dependent, with psychomotor tasks showing a decrement at 2G. Memory-based tasks appear unaffected by hypergravity.

PLANS FOR FUTURE INVESTIGATIONS

Current experiments are examining the sensitivity of the circadian system of the rhesus monkey to a phase shift in the light-dark cycle during chronic hypergravity. Advances and delays to the light cycle are being examined at both 1 and 2G.

DYNAMIC ASSESSEMENT OF CIRCADIAN PHASE AND AMPLITUDE UNDER THE SIMULATED LIGHTING CONDITIONS OF LONG-DURATION SPACE MISSIONS

E.N. Brown¹, H.H. Luithardt¹, K.P. Wright Jr. ² and C.A. Czeisler²

¹Statistics Research Laboratory, Department of Anesthesia and Critical Care, Massachusetts General Hospital, Harvard Medical School, Boston, MA 02114, ²Center for Circadian and Sleep Disorders Medicine, Brigham and Women's Hospital, Harvard Medical School

INTRODUCTION

Maintenance of physiologic and neurobehavioral homeostasis during long-duration space missions is crucial for ensuring optimal crew performance. Alterations in the circadian system will occur due to loss of contact with the normal geophysical light-dark cycles. Assessing the status of the circadian system is an especially challenging task because this normally requires special protocols such as the constant routine, free-run and forced desynchrony. We are developing statistical methods to make dynamic assessments of circadian phase and amplitude from core-temperature measurements collected under the simulated lighting conditions of long-duration space missions.

METHODS

The simulated lighting conditions were tested in a protocol whose principal parts consisted of 3 consecutive segments: 25 days of 24 hour rest-activity cycles; a 60 hour constant routine; and 12 28 hour days of forced desynchrony. Ambient light levels during the activity and constant routine segments of the protocol were maintained less than 50 lux. We assessed the status of each subject's circadian system by representing the core-temperature rhythm as a signal plus correlated noise model with 4 terms: an endogenous circadian component, a rest-activity component, thermoregulatory fluctuations and measurement noise. The circadian component was modeled as the solution to a modified van der Pol differential equation, the rest-activity component as either a harmonic or Walsh function regression, and the thermoregulatory component together with the measurement noise were modeled as a first-order Gaussian autoregressive process. A separate analysis was performed on the data from each of the 3 segments of the protocol. Beginning on day 3 of the 25 24 hour day segment, the signal plus noise model was fit to each subject's core-temperature data by maximum likelihood, and circadian phase and amplitude were assessed. Each day an additional 24 hours of data were added to the analysis and the estimates of phase and amplitude were updated. The sequence of phase assessments was used to predict the phase of the subject's circadian pacemaker on day 26, the time of the constant routine. The constant routine estimate of phase was compared with the prediction from the analysis of the 25 24 hour days for each subject. Period estimates of each subject's circadian pacemaker were computed from the forced desynchrony segment of the protocol. To date the data from 4 subjects studied under this protocol have been analyzed.

RESULTS

The dynamic assessments of circadian phase gave very accurate predictions of the phase of the circadian pacemaker for each subject as determined by the constant routine analyses. The estimates of circadian amplitude were less accurate due to the apparent lack of separation between the estimated circadian process and the rest-activity cycle from this part of the cycle. Modeling the rest-activity cycle with Walsh functions gave a better separation of the rest-activity

and circadian components in the data than that obtained when the former was represented as a harmonic regression. Period estimates from the 25 24 hour day segment were all statistically indistinguishable from 24 hours whereas each subject had a non-24 hour period based on the forced desynchrony analysis. This finding suggests that all of the subjects were entrained during the 24 hour protocol despite the light levels being less than 50 lux.

CONCLUSION

Our analysis suggests that it is possible make dynamic assessments of circadian phase under the simulated lighting conditions of long-duration space missions. Accurate dynamic assessment of circadian amplitude requires techniques to separate circadian and non-circadian processes with nearly identical periods but different functional forms. The dynamic assessments of phase and amplitude will be inputs to a model we are currently constructing to predict performance as a function of circadian phase and recent sleep-wake history. The latter model will serve as a basis for the design of countermeasures appropriate for correcting alterations in circadian physiology. Our finding that all 4 subjects were entrained during the 24 hour protocol points to the possibility of a yet to be defined non-photic mechanism of entrainment.

EFFECTIVENESS OF AN EXPERT SYSTEM FOR ASTRONAUT ASSISTANCE ON A SLEEP EXPERIMENT

G. Callini*, M.S., S. M. Essig*, M.S., D. Heher, M.S.[‡], L. R. Young, Sc.D.*

*Man-Vehicle Laboratory, Massachusetts Institute of Technology, 77 Massachusetts Avenue, Room 37-219, Cambridge, MA 02139, [‡]Caelum Research Corporation - NASA Ames Research Center, Mail Stop 269-2 (Building 269, Room 235), Moffett Field, CA 94035

INTRODUCTION

Principal Investigator-in-a-Box ([PI]) is an expert system designed to train and assist astronauts with the performance of an experiment outside their field of expertise, particularly when contact with the Principal Investigators on the ground is limited or impossible. In the current case, [PI] was designed to assist with the calibration and troubleshooting procedures of the Neurolab Sleep and Respiration Experiment during the pre-sleep period of no ground contact. It displays physiological signals in real time during the pre-sleep instrumentation period, and alerts the astronauts when a poor signal quality is detected.

METHODS

The first (ground based) study presented in this paper required twelve subjects to monitor a set of pre-recorded physiological signals and identify any signal artifacts appearing on the computer screen. Every subject performed the experiment twice, once with the assistance of [PI] and once without. The second part of this study focuses on the post-flight analysis of the data gathered from the Neurolab Mission. After re-playing the physiological signals on the ground, the frequency of correct alerts and false alarms (i.e. incorrect diagnoses by the expert system) was determined in order to assess the robustness and accuracy of the rules.

RESULTS

Results of the first study indicated a beneficial effect of [PI] and training in reducing anomaly detection time and the number of undetected anomalies. For the in-flight performance, excluding the saturated signals, the expert system had an 84.2% detection accuracy, and the questionnaires filled out by the astronauts showed positive crew reactions to the expert system.

**AMBIENT LIGHT INTENSITY, ACTIGRAPHY, SLEEP AND RESPIRATION,
CIRCADIAN TEMPERATURE AND MELATONIN RHYTHMS AND DAYTIME
PERFORMANCE OF CREW MEMBERS DURING SPACE FLIGHT ON STS-90 AND
STS-95 MISSIONS**

C.A. Czeisler¹, D-J. Dijk¹, D.F. Neri², R.J. Hughes¹, J.M. Ronda¹, J.K. Wyatt¹, J.B. West³, G.K. Prisk³, A.R. Elliott³, L.R. Young⁴

¹Brigham and Women's Hospital and Harvard Medical School, ²NASA Ames Research Center, ³University of California, San Diego, ⁴Massachusetts Institute of Technology

INTRODUCTION

Sleep disruption and associated waking sleepiness and fatigue are common during space flight. A survey of 58 crew members from nine space shuttle missions revealed that most suffered from sleep disruption, and reportedly slept an average of only 6.1 hours per day of flight as compared to an average of 7.9 hours per day on the ground. Nineteen percent of crewmembers on single shift missions and 50 percent of the crewmembers in dual shift operations reported sleeping pill usage (benzodiazepines) during their missions. Benzodiazepines are effective as hypnotics, however, not without adverse side effects including carryover sedation and performance impairment, anterograde amnesia, and alterations in sleep EEG.

Our preliminary ground-based data suggest that pre-sleep administration of 0.3 mg of the pineal hormone melatonin may have the acute hypnotic properties needed for treating the sleep disruption of space flight without producing the adverse side effects associated with benzodiazepines. We hypothesize that pre-sleep administration of melatonin will result in decreased sleep latency, reduced nocturnal sleep disruption, improved sleep efficiency, and enhanced next-day alertness and cognitive performance both in ground-based simulations and during the space shuttle missions.

Specifically, we have carried out experiments in which:

- (1) ambient light intensity aboard the space shuttle is assessed during flight;
- (2) the impact of space flight on sleep (assessed polysomnographically and actigraphically), respiration during sleep, circadian temperature and melatonin rhythms, waking neurobehavioral alertness and performance is assessed in crew members of the Neurolab and STS-95 missions;
- (3) the effectiveness of melatonin as a hypnotic is assessed independently of its effects on the phase of the endogenous circadian pacemaker in ground-based studies, using a powerful experimental model of the dyssomnia of space flight;
- (4) the effectiveness of melatonin as a hypnotic is assessed during the STS-90 (Neurolab) and STS-95 missions in a double-blind placebo-controlled trial. In both flight-based experiments, the effects of melatonin on sleep stages and spectral composition of the EEG during sleep will be determined as well as its effects on daytime alertness and performance;
- (5) the impact of space flight on sleep and waking neurobehavioral alertness and performance in 30-45-year-old astronauts is compared with its impact in a 77-year-old astronaut. This case study is the first to assess the effects of space flight on an older individual.

Because the investigators are still blind to the treatment in this double-blind, placebo-controlled trial, preliminary results will be presented independent of the drug condition.

RESULTS

LIGHT LEVELS ABOARD THE SPACE SHUTTLE:

We recorded light levels in the mid-deck, the flight deck as well as in the Spacelab (STS-90) or Spacehab (STS-95). Actillumes were placed in these three compartments on FD-1 until the end of the mission. Preliminary results are presented for the Neurolab mission. On the flight deck, the recorded ambient light levels reflect the 90 minute orbital cycle (day and night) as well as the slightly shorter than 24 h rest-activity cycle. During the rest phase, even though the window shades on the flight deck were shut, the recurring orbital dawn can be observed in the recordings, with light levels reaching 10 lux. During the activity phase of the near 24-h days, ambient light varied with the orbital day and night such that during the orbital day light levels reached 10,000 lux. Very high light levels were sometimes observed during the late evening, just before the scheduled time of lights out. During the scheduled activity part of the day, the light levels recorded on the mid-deck were relatively constant (1-10 lux) and lower than in the Spacelab. In the Spacelab, light levels were constant and low (approximately 10-100 lux) during the working day. The approximately 20 min advance per day of the rest-activity cycle is visible in the recordings of light levels in the mid-deck. These data demonstrate that light levels vary between the different compartments of the spacecraft, are low in those compartments in which most of the crew spends most of the working day, and are variable and high on the flight deck. This variability indicates that light exposure (intensity and temporal distribution) depends strongly on the location within the spacecraft. However, no data on light exposure of individual astronauts are available. Therefore no prediction on the impact of these light levels on synchronization of the circadian system to the 23 h 40 min rest-activity cycle can be made. However, if some crew members were exposed to the high light levels present on the flight deck, especially during their time off in the evening, this evening light exposure in combination with the low levels during the day in the Spacelab would be expected to compromise circadian synchronization in those individuals. Routine recording light exposure in the spacecraft compartment together with ambulatory recording of light exposure of individual astronauts would provide the necessary information.

ACTIGRAPHY:

Actigraphic assessments of rest-activity cycles were successfully obtained in 4 crew members during the L-90, L-60, L-30 and L-7 pre-flight baseline data collection segments, during the in-flight segment, and during the post-flight segment of the Neurolab mission. The activity data reflect the approximately 20 minute advance of wake time during the 17 day mission as well as deviations from this schedule on 04/25/98 and 04/28/98. The data also illustrate that, on average, bedtimes advanced in the course of flight. Interestingly, the night to night variability in bedtimes appeared much greater than the variability in wake times. The data demonstrate that actigraphic assessments reliably represent the timing of the non-24-h rest-activity cycle that is dictated by operational constraints, and adherence to as well as deviations from this schedule. Preliminary assessment of total sleep time on the basis of these actigraphic recordings indicate that the four crew members slept on average 6.6 hours per day on this mission.

NEUROBEHAVIORAL PERFORMANCE:

We successfully obtained 62 neurobehavioral performance assessments (each approximately 25 minutes in duration) in four crew members during the pre-flight, in-flight and post-flight segments of the Neurolab mission. An additional 30 assessments were made in two crew members during the STS-95 mission. These data are currently being analyzed.

CORE BODY TEMPERATURE RECORDING:

Core body temperature was recorded with the Body Core Temperature Monitoring System (BCTM-3, PED, Inc., Wellesley, MA) in four STS-90 crew members and in two STS-95 crew members during the pre-flight, in-flight and post-flight segments of the mission. A total of 32 BCTMS sessions of approximately 32 hours each were acquired during the Neurolab and STS-95 missions. These data are currently being analyzed.

SLEEP LOGS:

Sleep logs were successfully obtained in 6 crew members during the L-90, L-60, L-30 and L-7 pre-flight baseline data collection segments as well as during the flight and post-flight segments of the Neurolab mission. These data are currently being analyzed.

POLYSOMNOGRAPHIC RECORDING OF SLEEP:

We obtained 64 recordings of the daily sleep episode in four Neurolab crew members during the pre-flight, in-flight and post-flight segments of the Neurolab mission and 30 nocturnal sleep opportunities in the two STS-95 crew members. Variables included EEG, EOG, and EMG. These signals were recorded on the digital sleep recorder (DSR, Temec Instruments, The Netherlands) and flash RAM cards. Application of bio-sensors to the skull and skin was achieved by an E-net (Physiometrix, Billerica, MA). The quality of physiological signals was monitored and evaluated by an artificial intelligence system called "PI-in-a-Box". It alerted the flight crew to possible anomalies and suggested procedures for correcting the problems. All sleep recordings were scored according to standard criteria by a registered polysomnographic technologist. For the Neurolab mission, total sleep time (TST) averaged 445 (SEM 7), 452 (SEM 5) and 446 (SEM 8) minutes during the L-60, L-30 and L-7 segments respectively. During flight, TST was reduced to 423 (SEM 16) minutes per flight day, whereas during the post-flight segment total sleep time increased to 459 (SEM 11) minutes. These changes in TST were accompanied by changes in sleep efficiency (SE) ($SE = TST$ divided by the duration of the interval time between lights out and lights on) such that lowest sleep efficiencies were observed during the in-flight segment and highest sleep efficiencies were observed during the post-flight segment. The data indicate that total sleep time during the mission is reduced compared to the pre-flight segments and that after the flight this sleep loss is recovered by increased TST as well as increased sleep efficiency. The apparent discrepancies between TST as assessed by actigraphy and polysomnography may be explained by the observation that on nights during which crew-members recorded sleep polysomnographically, they selected to go to sleep at the scheduled clock time, whereas on the nights during which sleep was not recorded polysomnographically, sleep was often postponed.

PRELIMINARY CONCLUSIONS

While aboard the shuttle, astronauts live in an environment characterized by highly variable ambient light intensities. The associated pattern of retinal light exposure may jeopardize entrainment of the circadian timing system to the imposed rest-activity cycle that is required by operational constraints, which typically requires a rest-activity schedule that is, on average, shorter than 24 h. Total sleep time is reduced and sleep is disrupted in space. Whether or not this disruption can be successfully treated by melatonin administration will be assessed after the data are unblinded and analyzed by drug condition.

ELECTROENCEPHALOGRAPHIC AND OCULAR CORRELATES OF NEUROBEHAVIORAL PERFORMANCE DECREMENTS

Derk-Jan Dijk and Christian Cajochen

Harvard Medical School, Brigham and Women's Hospital, Boston, MA 02115

INTRODUCTION

Neurobehavioral performance of astronauts during long duration space flight may be compromised by sleep loss, non-24 h rest-activity cycles, desynchrony of the sleep-wake cycle and endogenous circadian rhythms as well as micro-gravity itself. Ground-based research has demonstrated that all of these factors contribute significantly to neurobehavioral performance decrements and interact in a complex non-additive manner (1-3). In particular, it has been shown that prolonged partial sleep loss, i.e., loss of 3-4 hours of sleep per night, results in a progressive deterioration of neurobehavioral performance (4). Furthermore, it has been demonstrated that stable levels of alertness and cognitive throughput during a 16-18 h wake episode are critically dependent on the maintenance of an appropriate phase relationship between the sleep-wake cycle and the circadian timing system. When this appropriate phase relationship is not maintained neurobehavioral performance deteriorates even within an episode of wakefulness of 16 h in duration (1) (5). Finally, posture has been shown to interact with the effects of the hormone melatonin on subjective alertness as well as the spectral composition of the electroencephalogram (EEG), such that it appears that humans are more susceptible to the effects of melatonin when in a supine position (6). Previous research has indicated that sleep loss and circadian phase affect the EEG during sleep (7-9) as well as during wakefulness (10;11). EEG and ocular (EOG) parameters recorded during wakefulness are associated with neurobehavioral performance decrements in the laboratory (12) as well as in real life situations (13). However, this association of EEG and EOG parameters with neurobehavioral performance has not been investigated under conditions in which a wide variety of combinations of sleep pressure (i.e., wake duration) and circadian phase has been realized. Furthermore, the interaction between these independent variables and posture has not been investigated in detail.

The aim of the present research is to investigate the robustness of the associations between EEG/EOG parameters and neurobehavioral performance and to identify new associations under conditions in which circadian phase, circadian amplitude, sleep pressure and posture are manipulated. Identification of EEG and EOG parameters that are highly correlated with neurobehavioral performance under these conditions could lead to the development of algorithms and devices that allow on-line and non-invasive monitoring, as well as prediction, of neurobehavioral performance during long duration space flight.

CURRENT STATUS OF RESEARCH

METHODS/GENERAL METHODOLOGY

We report and review results from experiments in which the duration of wakefulness, circadian phase and circadian amplitude were manipulated. Some details of these experiments have in part been reported elsewhere (14;15). The duration of wakefulness was manipulated by sleep deprivation in a constant routine protocol in which subjects were in a supine posture and had no knowledge of clock-time (16). The phase relationship between the circadian pacemaker and the sleep-wake cycle was manipulated in a forced desynchrony protocol (1,3) and circadian

amplitude was manipulated by scheduled light exposure as first described by Jewett and co-workers (17). Subjects in these experiments were healthy young men or women without sleep complaints. Neurobehavioral performance was assessed with a computerized test battery that includes the Psychomotor Vigilance Test (PVT), which is a simple visual reaction time task, the Karolinska Sleepiness Scale (KSS), for the assessment of subjective sleepiness, a Digit Symbol Substitution Test (DSST), and a Addition Test (ADD) (18,19). All of these tests were previously used to assess neurobehavioral performance in crew members aboard STS90.

EEG activity was recorded from scalp electrodes placed along the mid-line or from a full 10-20 montage. EEGs were recorded on an ambulatory digital recorder (Vitaport-2, Temec, The Netherlands). This recorder was previously used to record polysomnograms from crew-members aboard STS90. Signals were digitized at a sampling rate of 256 and stored at 128 Hz on Flash RAM cards. High pass filters were set at either 0.3 or 1 s. Low pass filter settings were 35 or 60 Hz (24 dB/Oct). All results on EEG activity reported here were derived from scheduled sessions (4 minutes in duration) during which subjects, with eyes open, fixated a point on the wall. EOG activity was recorded from the outer canthi, digitized at 64 Hz and also stored on the Flash RAM cards.

RESULTS

Our preliminary analyses of these ongoing experiments indicate that EEG activity in the low frequency range (approximately 1-7 Hz), and in particular EEG activity recorded from frontal areas of the brain, increased with the duration of wakefulness. Higher frequency activity was modulated by circadian phase. Slow eye-movements were modulated by the duration of wakefulness, circadian phase and circadian amplitude. Neurobehavioral performance (PVT) and subjective sleepiness were correlated with changes in EOG and EEG parameters.

CONCLUSIONS

It appears from these preliminary analyses that low frequency EEG activity during wakefulness is exquisitely sensitive to the duration of wakefulness in particular when recorded from frontal areas of the brain and that the time course of EOG activity parallels the time course of neurobehavioral performance. The data imply that under conditions in which the duration of wakefulness, circadian phase and circadian amplitude are modulated, EEG and EOG parameters may be used to online monitor neurobehavioral performance capability.

PLANS FOR FUTURE INVESTIGATIONS

In these experiments the association between neurobehavioral performance and EEG and EOG parameters was investigated under conditions in which subjects were exposed to acute total sleep deprivation. However, in many real life situations, neurobehavioral performance is compromised by chronic partial sleep deprivation. We therefore plan to study the association between neurobehavioral performance and EEG and EOG parameters under conditions of chronic partial sleep deprivation. In addition we plan to implement new EEG analysis methods such as instantaneous frequency analyses.

Supported by the National Space Biomedical Research Institute

REFERENCES

1. Dijk, D.-J., J.F. Duffy, and C.A. Czeisler. Circadian and sleep/wake dependent aspects of subjective alertness and cognitive performance. *J.Sleep Res.* 1: 112-117, 1992.
2. Kronauer, R.E., M.E. Jewett, D.-J. Dijk, and C.A. Czeisler. A model for reduced circadian modulation of alertness at extremes of homeostatic influence. *J.Sleep Res.* 5: 113-113, 1996.
3. Wyatt, J.K., D.-J. Dijk, J.M. Ronda, M.E. Jewett, J.W. Powell, D.F. Dinges, and C.A. Czeisler. Interaction of circadian and sleep/wake homeostatic-processes modulate psychomotor vigilance test (PVT) performance. *Sleep Res.* 26: 759, 1997.
4. Dinges, D.F., F. Pack, K. Williams, K.A. Gillen, J.W. Powell, G.E. Ott, C. Aptowicz, and A.I. Pack. Cumulative sleepiness, mood disturbance, and psychomotor vigilance performance decrements during a week of sleep restricted to 4-5 hours per night. *Sleep* 20: 267-277, 1997.
5. Czeisler, C.A., D.-J. Dijk, and J.F. Duffy. Entrained phase of the circadian pacemaker serves to stabilize alertness and performance throughout the habitual waking day. In: *Sleep Onset: Normal and Abnormal Processes*, edited by R.D. Ogilvie and J.R. Harsh. Washington, D.C.: American Psychological Association, 1994, p. 89-110.
6. Cajochen, C., K. Kräuchi, and A. Wirz-Justice. The acute soporific action of daytime melatonin administration: Effects on the EEG during wakefulness and subjective alertness. *J.Biol.Rhythms* 12: 636-643, 1997.
7. Dijk, D.-J., D.G.M. Beersma, and S. Daan. EEG power density during nap sleep: reflection of an hourglass measuring the duration of prior wakefulness. *J.Biol.Rhythms* 2: 207-219, 1987.
8. Dijk, D.-J., D.P. Brunner, D.G.M. Beersma, and A.A. Borbély. Electroencephalogram power density and slow wave sleep as a function of prior waking and circadian phase. *Sleep* 13: 430-440, 1990.
9. Dijk, D.-J., T.L. Shanahan, J.F. Duffy, J.M. Ronda, and C.A. Czeisler. Variation of electroencephalographic activity during nonREM and REM sleep with phase circadian melatonin rhythm in humans. *J.Physiol.(Lond.)* 505.3: 851-858, 1997.
10. Brunner, D.P., D.-J. Dijk, and A.A. Borbély. Repeated partial sleep deprivation progressively changes the EEG during sleep and wakefulness. *Sleep* 16: 100-113, 1993.
11. Cajochen, C., D.P. Brunner, K. Krauchi, P. Graw, and A. Wirz-Justice. Power density in theta/alpha frequencies of the waking EEG progressively increases during sustained wakefulness. *Sleep* 18: 890-894, 1995.
12. Makeig, S. and T.P. Jung. Tonic, phasic, and transient EEG correlates of auditory awareness in drowsiness. *Cognitive Brain Research* 4: 15-25, 1996.
13. Åkerstedt, T., L. Torsvall, and M. Gillberg. Sleepiness in shiftwork. A review with emphasis on continuous monitoring of EEG and EOG. *Chronobiol.Int.* 4: 129-140, 1987.
14. Cajochen, C., S.B.S. Khalsa, C.A. Czeisler, and D.-J. Dijk. Circadian variation of slow eye movements during sustained wakefulness. *Soc.Res.Biol.Rhythms* 6: 33, 1998.
15. Cajochen, C., S.B.S. Khalsa, C.A. Czeisler, and D.-J. Dijk. Time course of EEG power density during wakefulness and subjective sleepiness during a 24-H constant routine. *Sleep* 21 suppl.: 243, 1998.

16. Czeisler, C.A., E.N. Brown, J.M. Ronda, R.E. Kronauer, G.S. Richardson, and W.O. Freitag. A clinical method to assess the endogenous circadian phase (ECP) of the deep circadian oscillator in man. *Sleep Res.* 14: 295-295, 1985.
17. Jewett, M.E., R.E. Kronauer, and C.A. Czeisler. Light-induced suppression of endogenous circadian amplitude in humans. *Nature* 350: 59-62, 1991.
18. Dinges, D.F. and J.W. Powell. Microcomputer analyses of performance on a portable, simple visual RT task during sustained operations. *Behavior Research Methods, Instruments & Computers* 17: 652-655, 1985.
19. Gillberg, M., G. Kecklund, and T. Åkerstedt. Relations between performance and subjective ratings of sleepiness during a night awake. *Sleep* 17: 236-241, 1994.

COUNTERMEASURES TO NEUROBEHAVIORAL DEFICITS FROM CUMULATIVE PARTIAL SLEEP DEPRIVATION DURING SPACE FLIGHT

D. F. Dinges, Ph.D. & H. P. A. Van Dongen, Ph.D.

INTRODUCTION

The performance capability of astronauts during extended-duration space flight depends heavily on achieving recovery through adequate sleep. Even with appropriate circadian alignment, sleep loss will erode fundamental elements of human neurobehavioral performance capability including vigilance, cognitive speed and accuracy, working memory, reaction time, and physiological alertness. Our preliminary experiments have revealed that these deficits occur reliably when sleep is limited to 6 hr per day. Such chronic sleep restriction has been a common experience during manned space flight, occurring in response to endogenous disturbances of sleep (motion sickness, stress, circadian rhythms), environmental disruptions of sleep (noise, temperature, light), and curtailment of sleep due to the work demands that accompany extended space flight operations.

In order to prevent cumulative waking deficits resulting from sleep restriction, research suggests that the sleep drive must be met through increased duration of the major (anchor) sleep period, and/or through the strategic use of a single pre-planned (preemptive) nap each day. The implementation of a brief nap may be an important way in which cumulative sleep loss and waking performance deficits could be reversed or prevented. However, nap strategies have not been systematically tested as countermeasures to performance impairment from cumulative anchor sleep restriction. Thus, there is a critical deficiency in knowledge of which combinations of anchor sleep and nap durations yield the most efficient return of performance per unit time invested in sleep. The primary aim of this project is to meet this critical deficiency through utilization of a response surface model design, testing in a dose-response manner varying combinations of anchor sleep and nap sleep durations for the purpose of establishing how to most effectively and efficiently limit the cumulative effects of chronic sleep restriction in space operations. A search algorithm involving two-stage regression analyses is being used to test the hypothesis that the addition of a relatively brief preemptive nap to restricted sleep each day markedly attenuates the cumulative performance deficits developing across days. This approach is also being used to explore the possibility that the addition of a nap to anchor sleeps increases sleep-related secretion of growth hormone, which may be a countermeasure for the effects of microgravity on muscle and loss in prolonged space flight.

CURRENT STATUS OF RESEARCH

Methods

To develop a response surface model, 90 healthy men and women are being tested in a 14-day ground-based isolated-laboratory protocol involving random assignment to one of 18 sleep-ration cells, each with the same sleep ration for 10 consecutive days. The goal of our approach is to evaluate daily sleep times that vary in duration around the mean of 6 hr reported for astronauts during space flight. Therefore, the sleep-ration assignments involve 4 anchor sleep durations (4.2, 5.2, 6.2, 8.2 hr) and 6 nap sleep durations (0.4, 0.8, 1.2, 1.6, 2.0, 2.4 hr), crossed to yield a total of 4 anchor-sleep-only conditions and 14 anchor-plus-nap-sleep conditions, and spanning a dynamic range of cumulative sleep debts from approximately 0 to 40 hr in a 10-day period. Anchor sleep times are being centered on 0200 hr and nap times on 1400 hr to maintain relatively stable circadian rhythms. While awake, subjects undergo a wide range of quasi-continuous neurobehavioral performance tests and continuous physiological monitoring of waking EEG, sleep PSG, behavioral motility, and core body temperature. The neurobehavioral performance tests, and in particular the psychomotor vigilance test (PVT), serve to quantify the cumulative performance decrements associated with the sleep rations of the experiments.

To estimate the performance decrements associated with cumulative exposure to the various sleep rations, performance degradation slopes are calculated with stage-one linear regression on key performance variables such as PVT or vigilance lapses. By plotting the slope values versus the anchor sleep durations and the nap sleep durations, a response surface map is created, as simulated in figure 1 for psychomotor vigilance lapses. Statistically, the response surface model is handled by means of stage-two multiple regression analyses. The search for the optimal sleep condition then no longer depends on the number of subjects studied for each condition, but rather on the total number of subjects in the whole experiment.

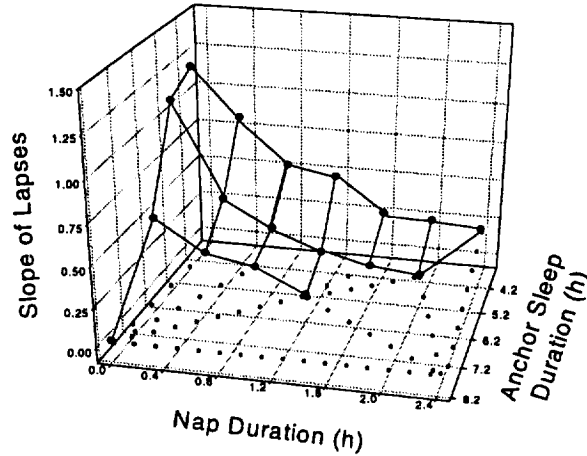


Figure 1: Simulated response surface map.

Results

In the first year of investigation, n = 30 subjects have been enrolled in the protocol. Table 1 shows the sleep-ration cells filled to date, as well as those that have yet to be studied.

Table 1: Overview of sleep-ration cells. N =30 subjects have been studied in 6 sleep-ration cells (n=5/cell) with varying anchor + nap sleep durations.

Time in bed	Anchor sleep	Nap sleep	Cell filled
4.2 hr	4.2 hr	0.0 hr	No
4.6 hr	4.2 hr	0.4 hr	Yes
5.0 hr	4.2 hr	0.8 hr	No
5.2 hr	5.2 hr	0.0 hr	No
5.4 hr	4.2 hr	1.2 hr	No
5.6 hr	5.2 hr	0.4 hr	Yes
5.8 hr	4.2 hr	1.6 hr	No
6.0 hr	5.2 hr	0.8 hr	No
6.2 hr	4.2 hr	2.0 hr	No
6.2 hr	6.2 hr	0.0 hr	No
6.4 hr	5.2 hr	1.2 hr	No
6.6 hr	4.2 hr	2.4 hr	Yes
6.6 hr	6.2 hr	0.4 hr	Yes
6.8 hr	5.2 hr	1.6 hr	No
7.0 hr	6.2 hr	0.8 hr	No
7.2 hr	5.2 hr	2.0 hr	No
7.4 hr	6.2 hr	1.2 hr	Yes
8.2 hr	8.2 hr	0.0 hr	Yes

Conclusions

Analysis of neurobehavioral outcomes in the 4.6 hr time-in-bed condition demonstrated that the restriction to 4.2 hr anchor sleep at night and 0.4 hr nap sleep during the daytime did not prevent the cumulative buildup of performance deficits. Furthermore, figure 2 shows that for the PVT and DSST performances, results are very similar to those obtained in an NIH investigation we conducted earlier. However, for full conclusions to be drawn from the surface response model, the majority of the 18 sleep-restriction cells must be filled. We expect to continue adding to the completed conditions in year 2 and present preliminary conclusions on the basis of a larger number of cells at the end of year 2.

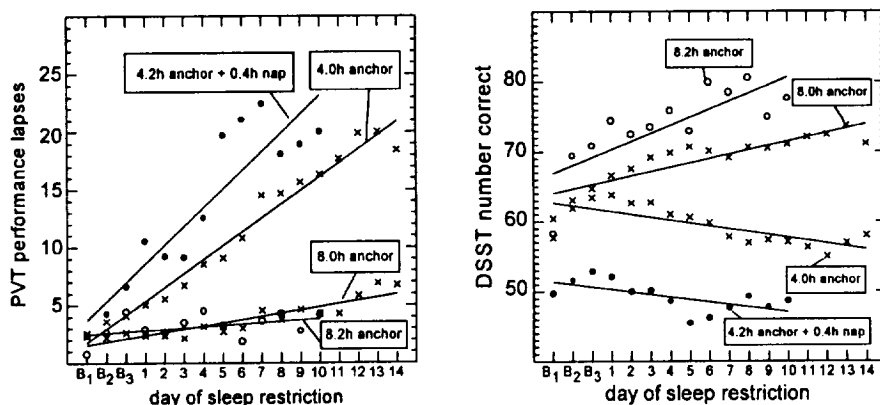


Figure 2: Average neurobehavioral performance as measured by psychomotor vigilance lapses (left panel; up is poorer performance) and number correct on the digit-symbol substitution test (right panel; down is poorer performance) across baseline days (B₁, B₂, B₃) and successive days of sleep restriction in the 4.2 hr anchor + 0.4 hr nap sleep condition (closed circles) and the 8.2 hr anchor + 0.0 hr nap sleep condition (open circles) of this project. For comparison, results from an earlier NIH 14-day sleep restriction study we conducted are shown (crosses) for 4.0 hr and 8.0 hr anchor sleep conditions. The performance degradation slopes as calculated with stage-one linear regression are indicated for each of the four conditions as well. Both studies revealed that less than 5 hr sleep is insufficient to prevent cumulative performance decrements from developing across days, whereas 8 hr sleep per day or more involves no significant increase in PVT lapses or decrease in DSST throughput performance.

PLANS FOR FUTURE INVESTIGATIONS

The development of a response surface model of the effects of cumulative sleep loss across days is an important step in the acquisition of critical knowledge on the most effective ways to plan sleep during long-duration manned space flight, in order to optimize the return on waking performance for time invested in sleep. Such a model will afford a countermeasure strategy for planning schedules to maximize astronaut performance in the face of limited sleep time during extended-duration space flight. If we can document that the addition of a nap to anchor sleep limits cumulative functional decline from restricted sleep across days, especially for anchor sleep times of less than 6.2 hr, then an approach will be available to prevent cumulative performance deficits in long-duration space flight, without adding markedly to typical daily total sleep time. Once effective sleep-wake regimes are identified in this study, optimizing neurobehavioral output and possibly growth hormone release as well, the next phase of investigation will involve tests of these regimes during space flight. In addition, the data of this project will be used to test the hypothesis that a probed performance algorithm, to be derived retrospectively from our database of sleep-deprived subjects, can be used prospectively to predict individual vulnerability to cumulative sleep loss, thereby permitting more precise utilization of countermeasures for the prevention of performance impairment due to cumulative sleep loss during extended manned space flight.

THE EFFECTS OF GRAVITY ON THE CIRCADIAN TIMING SYSTEM

Charles A. Fuller, Section of NPB, University of California, Davis, CA, USA

All vertebrates have a physiological control system that regulates the timing of the rhythms of their daily life. Dysfunction of this system, the circadian timing system (CTS), adversely affects an organism's ability to respond to environmental challenges and has been linked to physiological and psychological disorders. Exposure to altered gravitational environments (the microgravity of space and hyperdynamic environments produced via centrifugation) produces changes in both the functioning of the CTS and the rhythmic variables it controls. The earliest record of primate rhythms in a spaceflight environment come from Biosatellite III. The subject, a pig-tailed macaque, showed a loss of synchronization of the body temperature rhythm and a fragmented sleep-wake cycle. Alterations in the rhythm of body temperature were also seen in rhesus macaques flown on COSMOS 1514. Squirrel monkeys exposed to chronic centrifugation showed an initial decrease in the amplitude and mean of their body temperature and activity rhythms. In a microgravity environment, Squirrel monkeys on Spacelab-3 showed a reduction in the mean and amplitude of their feeding rhythms. Since 1992 we have had the opportunity to participate on three US/Russian sponsored biosatellite missions on which a total of six juvenile male rhesus macaques were flown. These animals uniformly exhibited delays in the phasing of their temperature rhythms, but not their heart rate or activity rhythms during spaceflight. There was also a tendency for changes in waveform mean and amplitude. These data suggest that the spaceflight environment may have a differential effect on the different oscillators controlling different rhythmic variables. Ongoing studies are examining the effects of +G on the CTS. The long-term presence of humans in space highlights the need for effective countermeasures to gravitational effects on the CTS. (Supported in part by NASA Grants NAG2-840 and NAG5-4320.)

MELATONIN AS A COUNTERMEASURE FOR ENTRAINMENT TO THE SLEEP/WAKE SCHEDULES REQUIRED DURING SHUTTLE MISSIONS

Sat Bir S. Khalsa and Derk-Jan Dijk

Brigham and Women's Hospital, Harvard Medical School, Boston, MA

INTRODUCTION

Most if not all physiologic and behavioral variables in humans exhibit endogenous circadian rhythms with a period of about 24.2 hours. On earth, a stable phase relation between circadian rhythms and the 24-hr day is maintained by a process called entrainment, in which the daily alternation of light and darkness is the most important periodic environmental agent. Although bright light has been shown to be effective in synchronizing and resetting the human circadian pacemaker, the effects of dim levels of light have limited effectiveness in maintaining synchronization, especially when the imposed light/dark cycle is shifted with respect to the habitual sleep/wake cycle. This is the case for shuttle astronauts who are typically exposed to recurrent "sleep cycle shifting" due to mission-dependent orbital mechanics and mission duration requirements and is equivalent to imposition of a shorter-than-24 hour day. Power requirements on the shuttle necessitate a restricted level of ambient lighting. Together, these conditions are likely to result in misalignment of the endogenous circadian timing system with respect to the desired sleep/wake cycle, even among crew members who begin the mission with their sleep-wake cycle well adapted to mission elapsed time on the day of launch.

BACKGROUND

Melatonin is a hormone secreted at night by the pineal gland (4;7) and there is behavioral, anatomical, and physiological evidence in human and non-human mammals that melatonin is able to influence the activity of the circadian clock, the Suprachiasmatic Nucleus. Melatonin has become highly popular both in the general public and in the media and it is the subject of numerous scientific review articles. A significant portion of this popularity is due to its reported effect as a hypnotic, however it is also known for its potential role as a chronobiotic or synchronizing agent. The best quantification of the potential effectiveness of a synchronizing agent can be drawn from experiments which evaluate the magnitude of the phase shifts generated by a discrete pulse treatment. Employing such a protocol, Deacon et al. (3) and Krauchi et al. (1) observed phase advances to melatonin treatment applied 5 to 7 hours before scheduled sleep onset. The dose dependence of melatonin-induced phase shifting at this phase has also been reported by Deacon and Arendt (2) for singly applied doses of 0.05 mg, 0.5 mg or 5 mg.

However, the best characterization of the phase shifting characteristics of any agent is a phase response curve which reveals the magnitude of phase shifts as a function of circadian phase. This information is essential for the evaluation of the range of entrainment of melatonin treatment and for the informed design of effective entrainment protocols. To date, two studies have been completed which report phase response curves in human subjects to melatonin treatment. Lewy et al. (8), evaluated the phase shifts in the dim light melatonin onset to 4 consecutive daily treatments of 0.5 mg of melatonin delivered at phases throughout the circadian cycle, but predominantly in the range of time between 3 and 11 hr before scheduled sleep onset. It is this range of circadian time that represents the phase advance region for melatonin treatment in this study; the peak phase advance of approximately 1 hr occurs in the middle of this range at about 7

hr before scheduled sleep onset. The other study utilized an intravenous route of melatonin administration in a 3 hr single pulse treatment protocol (9). The resultant phase response curve showed peak phase advances of up to 2 hrs in magnitude at a circadian phase which is about 2 hr before scheduled sleep onset. Both studies confirm the existence of a similar phase response curve to melatonin with phase advances in the late subjective day before up to 7 hr before sleep onset, and a potential phase delay region in the early subjective day. Taken as a whole the studies described above suggest that melatonin administration should be capable of generating a daily phase advance of about 1 hr when applied in the afternoon/evening before sleep onset. This would imply a range of entrainment to shortened periods of up to 1 hr, e.g. for a subject with a free-running period of 24.2 hr, daily melatonin administration should be capable of entraining this subject to a sleep/wake cycle period of 23.2 hr.

Stable and high levels of alertness can only be maintained when the phase relation between the endogenous circadian timing system and the sleep/wake cycle is such that the circadian timing system opposes the wake dependent deterioration of alertness and performance (5;6). This is achieved most effectively when the waking day is initiated approximately 2 hours after the endogenous circadian minimum of the core body temperature rhythm. This implies that even modest changes in the phase relation between the circadian timing system and the sleep/wake cycle will result in a deterioration of alertness and performance during the waking day, especially under dim lighting conditions. Sleep initiation and sleep consolidation are also critically dependent on an appropriate phase relation between the endogenous circadian timing system and the sleep/wake-schedule.

HYPOTHESES

The purpose of the proposed studies is to test three specific hypotheses aimed at evaluating the ability of melatonin administration to entrain the human circadian pacemaker to a shortened sleep/wake schedule typical of those encountered on space shuttle missions. These hypotheses are based partly on the results of preliminary data which indicate that: (a) abnormal light-dark cycles such as those to which shuttle astronauts are exposed results in an inability of the endogenous circadian timing system to maintain the appropriate phase relationship to a 24-hour duty and sleep/wake schedule; and (b) the inappropriate relationship between the endogenous circadian timing system and the 24-hour sleep/wake cycle results in sleep disturbance and performance impairment. Furthermore, published data from other laboratories suggests that melatonin is capable of phase shifting the human circadian pacemaker. We have developed the following three hypotheses:

- (1) The human circadian pacemaker will be unable to maintain synchronization with a sleep-wake cycle of 23.5 hours in dim light conditions.
- (2) Such loss of synchronization will result in sleep onset insomnia, decreased sleep efficiency and decreased daytime alertness and performance resulting from imposition of the 23.5 hr day.
- (3) A daily dose of melatonin administered 30 minutes before bedtime, will be sufficient to entrain the circadian pacemaker to a 23.5 hour scheduled sleep-wake cycle.

METHODS

Subjects in this study (aged 20-60) will undergo a similar single-blind crossover design 50 day protocol which will address the hypotheses described above. Potential subjects will be required to maintain a regular sleep/wake schedule at home for at least two weeks prior to the start of

study, which will be supplemented in part by recordings of actigraphy and ambient lighting. During the in-lab experimental protocol subjects will be in a time-free environment but will maintain contact with staff members. Ambient illumination will be carefully controlled. Subjects' core body temperature (rectal), plasma cortisol and melatonin levels, salivary melatonin levels, urine volumes, and neurobehavioral performance (calculation performance task, tracking task, visual analogue scale (VAS), assessment of psychomotor vigilance, probe recall memory task) will be assayed continuously throughout the protocol. In investigating hypotheses 1 and 2, during the first half of the protocol we anticipate that subjects' endogenous circadian pacemaker will fail to synchronize to an imposed 23.5 hour sleep/wake cycle, and this will result in decrements in sleep quality and performance. In investigating hypothesis 3 during the second half of the protocol, we anticipate that a daily dose of 0.3 mg of melatonin will maintain entrainment of the endogenous circadian pacemaker to the imposed 23.5 hour sleep/wake cycle.

The in-lab experimental protocol is divided into 7 segments as follows: (1) Adaptation (days 1-4). Subjects sleep and wake at their habitual times under a waketime illumination of 150 lux. Thirty minutes prior to each sleep episode subjects will be given a placebo pill. (2) Constant Routine #1 (days 4-6). The accurate assessment of endogenous circadian phase and amplitude is an essential feature of all of the specific protocols for which we employ a constant routine which consists of a regimen of enforced semi-recumbent wakefulness in constant indoor light (10-15 lux), with nutritional intake divided into hourly aliquots, with activity restricted to prevent changes in body posture and activity level that could affect core body temperature. A technician will be present at all times during the constant routines to ensure wakefulness. The fitted minimum of the endogenous rhythm of core body temperature is determined in this 40 hour constant routine. Subjects will be in dim light (10-15 lux) conditions during the remainder of the protocol. Following the constant routine, subjects will have an 8 hour sleep episode. (3) 23.5 Hour Sleep/Wake Cycle - Placebo (days 6-24). A 23.5 hour sleep/wake cycle segment will continue for 19 consecutive sleep/wake cycles. Sleep episodes will be in darkness and will last 7 hours and 50 minutes each, and waking episodes will last 15 hours and 40 minutes each. Subjects will be given a placebo pill 30 minutes before the start of each sleep episode. (4) Constant Routine #2 (days 24-27). This segment is identical to Constant Routine #1 but will continue for a duration to be determined by the timing of the core body temperature minimum, mostly likely in the range of 40 to 55 hours. (5) 23.5 Hour Sleep/Wake Cycle - Melatonin (days 27-46). The timing of the first sleep episode of this segment will be adjusted so that the relationship between the time of the core body temperature minimum is identical to that determined on the Constant Routine #1. This segment is identical to that of first 23.5 hour cycle segment except that instead of a placebo pill, subjects will receive 0.3 mg of melatonin 30 minutes prior to each sleep episode. (6) Constant Routine #3 (days 46-48). This segment is identical to the constant routines above and with a range in duration of 40 to 55 hours. (7) Recovery (days 48-50). This segment allows for recovery sleep and re-entrainment to the habitual sleep/wake schedule.

CONCLUSION

If shown to be effective as a chronobiotic, melatonin would serve as a practical and efficient countermeasure to prevent internal desynchrony and circadian phase misalignment. It would complement investigations of the purported hypnotic or direct sleep-promoting action of melatonin, which we are evaluating using a very different protocol on the previous Neurolab

shuttle mission. Understanding the efficacy of melatonin not only as a hypnotic, but also as a chronobiotic could thus have a profound effect on the health, productivity and safety of astronauts during space shuttle missions. The proposed research is relevant for the round-the-clock work schedules on the International Space Station, the altered sleep/wake schedule on a Mars surface station (a period of 24.6 hr), or any other situation where the work-rest schedule must be shifted. It also has relevance for ground personnel monitoring orbiting crew members working round-the-clock schedules.

REFERENCES

1. Cajochen, C., K. Krauchi, D. Muzi, P. Graw, and A. Wirz-Justice. Melatonin and S-20098 increase REM sleep and wake-up propensity without modifying NREM sleep homeostasis. *Am.J.Physiol.* R1189-R1196, 1997.
2. Deacon, S. and J. Arendt. Melatonin-induced temperature suppression and its acute phase-shifting effects correlate in a dose-dependent manner in humans. *Brain Res.* 688: 77-85, 1995.
3. Deacon, S., J. English, and J. Arendt. Acute phase-shifting effects of melatonin associated with suppression of core body temperature in humans. *Neurosci.Lett.* 178: 32-34, 1994.
4. Dijk, D.-J. and C. Cajochen. Melatonin and the circadian regulation of sleep initiation, consolidation, structure, and the sleep EEG. *J.Biol.Rhythms* 12: 627-635, 1997.
5. Dijk, D.-J. and C.A. Czeisler. Paradoxical timing of the circadian rhythm of sleep propensity serves to consolidate sleep and wakefulness in humans. *Neurosci.Lett.* 166: 63-68, 1994.
6. Dijk, D.-J. and C.A. Czeisler. Contribution of the circadian pacemaker and the sleep homeostat to sleep propensity, sleep structure, electroencephalographic slow waves and sleep spindle activity in humans. *J.Neurosci.* 15: 3526-3538, 1995.
7. Dijk, D.-J., T.L. Shanahan, J.F. Duffy, J.M. Ronda, and C.A. Czeisler. Variation of electroencephalographic activity during nonREM and REM sleep with phase of circadian melatonin rhythm in humans. *J.Physiol.(Lond.)* 505.3: 851-858, 1997.
8. Lewy, A.J., S. Ahmed, J.M.L. Jackson, and R.L. Sack. Melatonin shifts human circadian rhythms according to a phase-response curve. *Chronobiol.Int.* 9(5): 380-392, 1992.
9. Zaidan, R., M. Geoffriau, J. Brun, J. Taillard, C. Bureau, G. Chazot, and B. Claustrat. Melatonin is able to influence its secretion in humans: description of a Phase-Response Curve. *Neuroendocrinology* 60: 105-112, 1994.

SLEEP AND CIRCADIAN RHYTHMS IN FOUR ORBITING ASTRONAUTS

Timothy H. Monk, Daniel J. Buysse, Bart D. Billy, Kathy S. Kennedy, Linda M. Willrich
 Sleep and Chronobiology Center, University of Pittsburgh Medical Center, Pittsburgh, PA 15213

INTRODUCTION

The study of human sleep and circadian rhythms in space has both operational and scientific significance. Operationally, U.S. Spaceflight is moving away from brief missions with durations of less than one week. Most space shuttle missions now last two weeks or more, and future plans involving space stations, lunar bases and interplanetary missions all presume that people will be living away from the gravity and time cues of earth for months at a time. Thus, missions are moving away from situations where astronauts can "tough it out" for comparatively brief durations, to situations where sleep and circadian disruptions are likely to become chronic, and thus resistant to short term pharmacological or behavioral manipulations. As well as the operational significance, there is a strong theoretical imperative for studying the sleep and circadian rhythms of people who are removed from the gravity and time cues of earth. Like other animals, in humans, the Circadian Timekeeping System (CTS) is entrained to the correct period (24h) and temporal orientation by various time cues ("zeitgebers"), the most powerful of which is the alternation of daylight and darkness. In leaving Earth, astronauts are removing themselves from the prime zeitgeber of their circadian system -- the 24h alternation of daylight and darkness.

METHODS

This experiment measured the sleep and circadian rhythms of four male astronauts (ages 38y - 47y) aboard a space shuttle (STS-78) orbiting the Earth for 17 days. The space mission was specially scheduled to minimize disruptions in circadian rhythms and sleep, so that the effects of

space flight and microgravity *per se* could be studied. Data were collected in 72h measurement blocks: one block 7d before launch, one early within the mission (3d after launch), one late in the mission (12d after launch), and one 18d after landing. Within each measurement block all sleeps were recorded both polysomnographically, and by sleep diary; core body temperature was sampled every 6 mins., Actillum[©] were worn continuously, all urine samples were collected separately, performance was assessed by a computerized test battery (3/day) and by end of shift questionnaires (1/day), mood and alertness was also measured by visual analogue scales (5/day).

RESULTS

As shown in Figure 1, body temperature circadian rhythms in orbit appeared to be very similar in phase and amplitude to those on the ground, and were

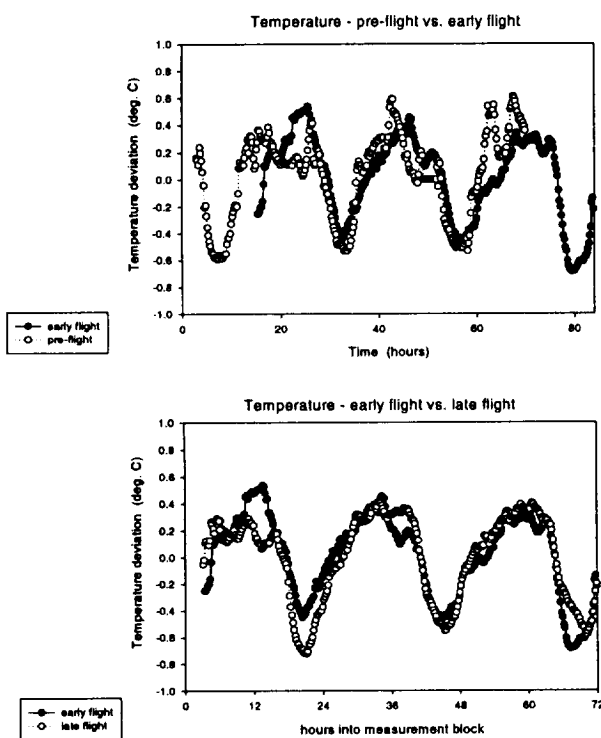


Figure 1

appropriately aligned for the required work/rest schedule. There was no change from early flight to late flight. This was also reflected in the circadian rhythms of urinary free cortisol and melatonin sulfate, which also showed no aberrant phases or deterioration in amplitude.

Mood, alertness and performance scores were satisfactory at both in-flight time points, showing no build-up in fatigue. However, in-flight sleep showed a decreased amount of sleep obtained (mean=6.1h), and all four astronauts showed a decrease in delta sleep. No further degradation in sleep was seen when early flight was compared to late flight, and no other sleep parameters showed reliable trends. For the 24 rated subject-nights of sleep in space (4 subjects x 2 blocks x 3 nights) reasons for sleep disruption (i.e. wake after sleep onset) during the "night" were as follows: ambient temperature (6/24), noise (3/24), need to void (3/24), vibration (1/24), mission circumstances (1/24) and general discomfort (1/24). On 4/24 subject-nights a sleep disruption was reported as "just woke" (i.e. of unknown etiology). For exactly half (12/24) of the subject-nights in space, the subject reported the final waking as "just woke" (i.e. endogenous), rather than being awakened by something or someone. The only systematic effect on mood and performance appeared to be an increase in alertness in the early flight measurement block. End of shift questionnaires revealed time line problems and equipment malfunction to be the major impacts on the astronauts' work.

CONCLUSION

When careful steps are taken to ensure that the astronauts' work/rest schedule does not lead to circadian desynchrony, there is no evidence that microgravity per se will disrupt the human circadian timekeeping system, or that such rhythms will degrade over a 17d mission. In particular, there was no evidence of amplitude reduction, phase lability or "free-running" behavior. Despite the astronauts' circadian rhythms being intact, there were some effects on sleep, notably a trend towards a reduction in sleep duration, and a suppression of the deepest stages of sleep (Stages 3 and 4). However, there were no other consistent effects of space flight in sleep architecture.

Work supported by NAS 9-18404, NAS 9-19407, MH 01235.

NEUROENDOCRINE & NEUROIMMUNE MODULATION BY SLEEP DEPRIVATION

J Mullington¹, M Carlin², S Kapoor², N Price², M Szuba², R Schwartz³, W Shearer³, J Butel³, D.F. Dinges²

¹Beth Israel Deaconess Medical Center, Boston, ²University of Pennsylvania Health System, Philadelphia and ³Baylor College of Medicine, Houston.

INTRODUCTION

Animal studies have shown that sleep deprivation impairs prognostic outcome during infectious disease in rabbits. We are analyzing blood sampled from subjects participating in a number of sleep deprivation conditions. We will present results of ongoing studies on the effects of total (TSD) and partial sleep deprivation (PSD) on neuroendocrine and neuroimmune parameters in humans.

METHODS

Healthy men and women who normally sleep between 7-9 hours per night (as verified through use of actigraphic recordings and sleep logs) and pass medical screening, have their sleep reduced under controlled and extensively monitored conditions. Subjects are randomly assigned to groups in which they are permitted 0, 4 or 8 (control condition) hours of sleep per 24 hour day. Depending on the protocol, subjects stay in the lab for 7-15 days. Total sleep deprivation does not exceed 88 hours. Blood is collected on selected days at frequent intervals, through indwelling forearm catheter. Blood samples are immediately centrifuged, and plasma separated into aliquots and frozen for later assay. Hormonal assays are performed using radioimmunoassay (RIA) methods, and cytokines using enzyme-linked immunoassay techniques (ELISAs). In addition, we are analyzing blood and urine for viral DNA, using polymerase chain reaction (PCR) techniques.

RESULTS

We have analyzed cortisol and melatonin profiles over 88 hours of total and partial sleep deprivation. The elevation of the circadian nadir of cortisol showed an increase over the testing period and returned to baseline levels during recovery sleep, significant for groups combined and when tested separately ($F(4,56)=5.76$, $p<0.001$ for TSD and $F(4,56)=6.54$, $p<0.001$ for PSD). In both sleep loss conditions, by the 4th night of PSD or TSD, the circadian nadirs were significantly elevated, and there was a significant drop in the nadir during the recovery night of sleep (all comparisons $p<0.01$). For changes in peak cortisol levels, an overall drop was seen through the sleep deprivation period, but unlike the changes in the nadir of cortisol, this effect did not immediately reverse on the first night of recovery sleep. Peak cortisol levels decreased significantly for PSD ($F(4,56)=3.57$, $p<0.05$), and showed a trend for the TSD group. In collaboration with investigators at Baylor College of Medicine, we are currently analyzing urine and blood for reactivation of latent viruses as a consequence of sleep loss.

CONCLUSION

The HPA axis is directly affected by both total and partial sleep deprivation. This effect is not likely to be attributable to the effects of caffeine, since all but one subject showed at least a small increase between the first and fourth nadirs, and all but one showed a subsequent immediate decrease in the nadir level during recovery sleep. Cortisol has previously been shown to be inhibited during sleep as compared to sleep deprivation (Weitzman et al, 1983, Mullington et al,

1996). A reduction in GH release resulting from TSD or PSD during the normal nocturnal phase might be a reasonable explanation for the rise in the cortisol nadir, since GH releasing hormone is thought to be reciprocally related to corticotropin releasing hormone (see Steiger & Holsboer 1997, for review). However, Spiegel et al., (1998), reported that nocturnal GH peak secretion was preserved during a partial sleep deprivation protocol of 4 hours per night. Since the nadir effect is also pronounced in our PSD condition, it is more likely that the effects are related to a physiological stress response, and may be related to the mechanism of altered host response seen during two nights of TSD (Mullington et. al., 1998). We are currently analyzing norepinephrine in plasma sampled from these subjects, four times per day, in order to further assess possible indicators of stress in these subjects.

REFERENCES

- Dinges et al, J Clin Invest 1994,93:1930-9
Mullington et al, Neuroendocrinol 1996,64:233-241
Mullington et al, Sleep 1998,21:s10.
Steiger & Holsboer, Sleep 1997,20:1038-52
Spiegel et al., Sleep 1998,21:s240
Weitzman et al, J Clin Endocrinol Metab 1986,56:352-8

BRN 3.1 KNOCKOUTS AFFECT THE VESTIBULAR, AUTONOMIC, AND CIRCADIAN RHYTHM RESPONSES TO 2G EXPOSURE.

D. M. Murakami¹, L. Erkman², M. G. Rosenfeld², and C. A. Fuller¹.

Section of NPB¹, University of CA at Davis, Davis, CA 95616; Howard Hughes Medical Institute², University of CA at San Diego, San Diego, CA 92093.

INTRODUCTION

Our previous studies have demonstrated that 2G exposure via centrifugation significantly attenuated the daily mean and circadian rhythm amplitude of rat body temperature (Tb), heart rate, and activity (Act). In addition, 2G exposure activates neural responses in several vestibular, autonomic, and circadian nuclei. Although we have characterized the effect of 2G on an animal's physiological, neuronal, and behavioral responses, it will be important to understand the underlying neural and physiological mechanisms that mediate those responses. For example, the vestibular responses, proprioceptive feedback, or fluid shifts may be the critical factors that mediate the responses to 2G. As a first step to understand the relative importance of these different response pathways to altered gravitational fields, this study examined the contribution of the vestibular system by utilizing an animal model from molecular biology. Brain 3.1 (Brn 3.1) is a POU domain homeobox gene involved in the normal development of the vestibular and auditory system. Brn 3.1 deletion results in a loss of hair cells in the otoliths, semicircular canals, and cochlea. As a result mice with a Brn 3.1 deletion do not have a functioning vestibular or auditory system. The BRN 3.1 knockout mouse could be a very useful animal model for isolating the role of the vestibular system in mediating the physiological responses to 2G exposure. Therefore, this study compared the effect of 2G exposure via centrifugation between Brn 3.1 knockout (KO) versus Wildtype (W) mice.

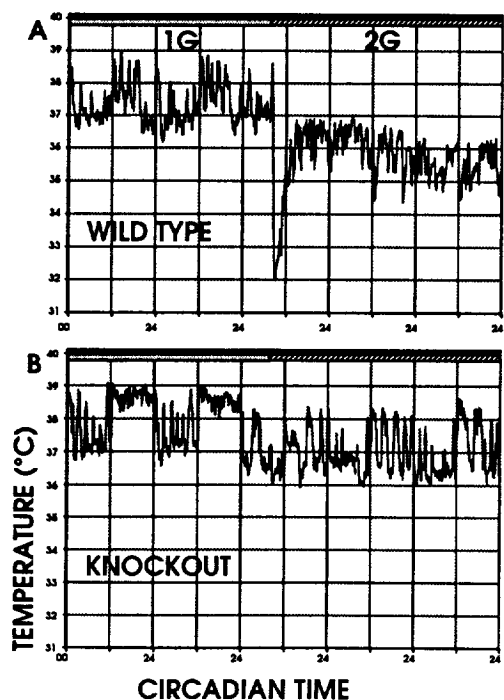
METHODS

Mice were implanted with a biotelemetry unit (Minimitter) to monitor the circadian rhythms of body temperature and activity. Mice were individually housed in isolated cages with food and water *ad libitum*. Mice were exposed to a LD 12:12 lighting condition and monitored for two weeks at 1G to establish a baseline. The mice were then exposed to chronic 2G for 3 weeks via centrifugation and then returned to 1G. Circadian rhythms were examined to compare the effects of 2G between wildtype and knockout mice. In addition, the c-Fos activity of neurons in KO and W were examined following an acute exposure to 2G to determine which CNS nuclei and pathways may mediate the vestibular effect on circadian function. Mice were exposed to a 2 hour 2G pulse at CT 9, sacrificed immediately, and immunohistochemically stained for c-Fos protein (Oncogene Sci.) using streptavidin complex (Vector) and True Blue (KPL) as the chromogen.

RESULTS

At 1G wildtype and knockout mice exhibited robust circadian rhythms of equal amplitude. As can be seen in the figure below, following exposure to 2G, wildtype mice exhibited a significant decrease in mean body temperature, mean activity, and attenuation of circadian rhythm amplitudes. However, the knockout mice exhibited a significantly different response compared to that of the wildtype mice. Knockout mice exhibited only very small changes in mean body temperature and circadian rhythm amplitude between 1G and 2G conditions. In addition, there were differences in the pattern of c-Fos reactivity within vestibular, autonomic, and hypothalamic associated nuclei. For example, exposure to 2G for 2 hours induced significant c-

Fos activity in the vestibular nucleus of wildtype mice. However, knockout mice did not exhibit any increase in c-Fos reactivity in the spinal vestibular nucleus. All wildtype mice exposed to 2G for 2 hours also exhibited an increase in c-Fos reactivity within the parabrachial nuclei, locus coeruleus, and raphe nuclei. This would suggest that 2G exposure activated several critical autonomic nuclei. By contrast, BRN 3.1 knockout mice that do not have a functioning vestibular system did not show increased c-Fos activity in the autonomic nuclei following 2G exposure. This would suggest that the vestibular system is a critical sensory system that mediates the autonomic responses following exposure to 2G.



CONCLUSION

These results suggest that the single gene deletion of BRN 3.1 significantly reduces the sensitivity of mean body temperature, mean activity, and circadian rhythms to 2G exposure. In addition, the autonomic and hypothalamic nuclei that are normally activated following 2G exposure, are not activated in the BRN 3.1 knockouts. These results suggest that the single gene deletion of BRN 3.1 significantly reduces the sensitivity of those neural structures that mediate autonomic function, homeostasis, and circadian rhythms to 2G exposure. Therefore, the physiological and neuronal responses to 2G exposure are primarily mediated through the vestibular system. (Supported by NASA Grant NAGW-4552 to DMM and NIH Grant to MGR).

SLEEP RESTRICTION EFFECTS ON CARDIOVASCULAR REGULATION

ML Smith, DE Watenpaugh, N Muentner, SL Wasmund, WL Wasmund, R Carter, III.
Department of Integrative Physiology, UNT Health Science Center, Ft Worth, TX 76107.

INTRODUCTION

It has been known for many years that spaceflight is associated with alterations of cardiovascular function, often referred to as "deconditioning". This deconditioning is manifested most prominently as decreased orthostatic tolerance and exercise capacity. Although recent investigations have improved the overall understanding of the cardiovascular adaptations to microgravity, the etiology of spaceflight-induced cardiovascular deconditioning remains unclear. Astronauts commonly are sleep deprived and complain of significant fatigue. Sleep restriction may affect cardiovascular regulation and exercise performance; however, the role sleep restriction plays in cardiovascular deconditioning is unknown. Thus, two specific aims of this research have focused on the effect of sleep restriction on cardiovascular regulation and orthostatic tolerance: **Aim 1**) to determine the effect of sleep restriction on cardiovascular responses to stress and **Aim 2**) to determine the effect of sleep restriction on orthostatic tolerance.

When astronauts perform the work of constructing the space station or any other physical activity in space, the work involves significant hand and forearm exercise accompanied by mental stress associated with environment. A third **Aim** of this research was to determine the nature of the physiologic interaction between static forearm exercise and mental tasking. Three studies have been performed to address these aims and are described below.

Study 1: Nine healthy subjects (3 females, 6 males) slept only 4 hours per night for 4 consecutive nights. Before and after sleep restriction, subjects performed static left handgrip endurance tests at 50% of presleep maximal grip strength. On the right (resting) arm, finger photoplethysmography measured arterial blood pressure and heart rate, and ultrasound measured brachial arterial blood flow. As an index of sympathoexcitation, we calculated right forearm vascular resistance (FVR) responses to left static handgrip as mean arterial pressure divided by brachial (forearm) blood flow. *Results:* Sleep restriction did not affect left handgrip endurance time, and heart rate and arterial pressure responses to handgrip endurance testing also remained unchanged after sleep restriction (all $P > 0.2$). However, the increase in FVR in the resting forearm during the handgrip endurance test doubled ($P = 0.04$) from the presleep restriction elevation of 10 ± 6 units (an 11% increase, $X \pm SE$) to 21 ± 4 after sleep restriction (a 23% increase). Also, the reduction in FVR over the first min following the handgrip endurance test equaled 14 ± 4 units (a 14% reduction) prior to sleep restriction, yet FVR decreased 27 ± 4 units (a 24% reduction) following the post-sleep restriction test.

Study 2: Ten healthy volunteers (4 females, 6 males) participated after giving written, informed consent. Subjects were tested in the morning or afternoon, but the time of study was consistent within each subject. On testing days, subjects were instrumented for recording of electrocardiogram, arterial blood pressure, brachial artery blood flow velocity and diameter (to calculate forearm blood flow and vascular resistance). Arterial baroreflex function was determined from heart rate and blood pressure responses to nitroprusside/phenylephrine

injections and orthostatic tolerance was tested via lower body negative pressure (LBNP), to simulate orthostasis. *Results:* No difference in baroreflex function (systolic blood pressure vs. heart rate) was observed with sleep restriction. LBNP tolerance (determined by pressure tolerated and duration of LBNP tolerated) was unaffected by sleep restriction. Sleep restriction was found to have a significant effect on systolic blood pressure and heart rate during LBNP. Systolic blood pressure tended to be greater for all post-sleep restriction measurements; this increase was statistically significant at -60 mmHg (pre= 110 ± 6 mmHg vs. post= 124 ± 3 mmHg, $P=0.038$). Diastolic and mean arterial blood pressure did not change significantly following sleep restriction, although each displayed a trend to be greater in comparison to pre-sleep restriction levels, especially at more stressful LBNP levels. Heart rate, on the other hand, tended to be lower post-sleep restriction; this decrease was statistically significant at LBNP of -60 mmHg (pre= 108 ± 8 bpm vs. post= 99 ± 8 bpm, $P=0.028$). Sleep restriction had no significant effect on forearm vascular resistance or blood flow. Heart rate variability (a generally accepted measure of vagal activity) significantly decreased with LBNP ($0.01 < p < 0.02$ for both pre- and post-sleep restriction) but was not affected by sleep restriction. Our data suggest that sleep restriction does not attenuate cardiovascular responses to LBNP as hypothesized. In fact, the ability to maintain blood pressure in the face of an LBNP challenge appears to be augmented slightly following sleep restriction, as LBNP-induced blood pressure reduction and heart rate elevation were less. Although sleep restriction had no overall effect on forearm vascular resistance, resistance fell sharply during -60 mmHg LBNP prior to sleep restriction while it continued to increase at this most extreme level of LBNP post-sleep restriction; this would help to explain the better maintenance of blood pressure post-sleep restriction, which was most apparent at -60 mmHg. The lower post-sleep restriction heart rates may simply be a baroreflex-mediated response to the higher blood pressures maintained post-sleep restriction. *Conclusion:* Sleep restriction to 4 hours/night for 4 nights does produce subtle changes in cardiovascular responses to simulated orthostasis, but these changes do not compromise orthostatic tolerance.

Study 3: The cardiovascular responses to 5 minutes of static left handgrip alone (25-35% of maximal grip strength), mental arithmetic alone, and combined stimuli were performed in 11 healthy volunteers in random order. Sympathetic nerve activity (SNA, microneurography), mean arterial blood pressure (MAP, Finapres), and heart rate (HR, ECG) were measured. *Results:* All 3 stressors significantly increased SNA, MAP, and HR (see table). SNA and MAP responses to handgrip and the combined stimuli each exceeded responses to mental arithmetic alone ($P < 0.03$), yet no significant difference existed between responses to handgrip alone and the combined stimuli ($P > 0.44$). The 3 stimuli increased heart rate similarly ($P > 0.19$). *Conclusion:* The data refuted our hypothesis: mental stimulation did not synergistically interact with or even add to the stress response elicited by handgrip exercise. In fact, a minor trend towards the opposite effect occurred: mean SNA, MAP, and HR were slightly lower when math accompanied the handgrip exercise vs. when handgrip was performed alone.

CIRCADIAN ENTRAINMENT, SLEEP-WAKE REGULATION AND NEUROBEHAVIORAL PERFORMANCE UNDER THE SIMULATED LIGHTING CONDITIONS OF LONG-DURATION SPACE MISSIONS

K.P. Wright, Jr., M.E. Jewett, E.B. Klerman, R.E. Kronauer, C.A. Czeisler
Circadian, Neuroendocrine and Sleep Disorders Section, Brigham and Women's Hospital,
Department of Medicine, Harvard Medical School, Boston, MA 02115

INTRODUCTION

Sustaining high levels of performance throughout extended duration space missions requires: 1) circadian entrainment of the intrinsic longer-than-24-hour period of the human circadian pacemaker to the 24-hour day; 2) maintenance of an appropriate phase relation of the human circadian pacemaker to the sleep-wake schedule. During space exploration, astronauts are likely to be exposed to light-dark cycles that are characterized by either an abnormal period different from the 24.0-hour duration of an Earth day, i.e., the 1.5-hour period of the light-dark cycle during earth orbit and the 24.6-hour period of the light-dark cycle on Mars, or by a light-dark cycle of reduced intensity, i.e., less than 50 lux in the angle of gaze, when the space craft is illuminated artificially and under power constraints. Such light-dark cycles maybe inadequate to maintain the appropriate phase-relation between the scheduled sleep-wake cycle and the circadian system, resulting in circadian misalignment. Such circadian misalignment can result in sleep disturbances, reduced growth hormone secretion, reduced attention, gastrointestinal disorders and impaired daytime alertness.

We have undertaken nine 55-day inpatient studies to evaluate: 1) whether entrainment of the human circadian pacemaker will be disturbed in humans when the strength of the environmental light-dark cycle is reduced, resulting in poor sleep and impaired daytime performance; and 2) whether abnormal entrainment to either the 24.0-hour Earth day or the 24.6 hour Mars day will result in disturbed sleep, impaired daytime performance, reduced growth hormone secretion during sleep and inappropriate secretion of the sleep-promoting hormone melatonin during the waking day. To do so, we have used a strict light-dark cycle comparable to that used in entrainment studies of plants and animals. The present report discusses preliminary results from these studies.

METHODS

Nine healthy male subjects (ages 20-38) were studied. All subjects were required to pass a rigorous health screening and also maintain a regular sleep/wake schedule for three weeks prior to the start of study. Subjects were scheduled to sleep for 8 hours at their habitual bedtime while living in the laboratory for six baseline days and nights. A constant routine protocol was used to assess circadian phase before the entrainment protocol. Following the circadian phase assessment, subjects were scheduled to either twenty-five 24.0 hour Earth days or to twenty-five 24.6 hour Mars days in dim ambient lighting (< 3 lux for 6 subjects and < 50 lux for 3 subjects). A second constant routine was then used to assess circadian phase after the entrainment protocol. This was followed by twelve 28-hour forced desynchrony days, and a third phase estimation, allowing quantification of the intrinsic period of the endogenous circadian temperature and melatonin rhythms. This will allow determination of the extent to which the subjects' entrained circadian phases were dependent upon the underlying period of their circadian pacemakers. Blood was sampled for melatonin, cortisol, and growth hormone during sampling windows and

core body temperature was collected every minute throughout the protocol. Sleep and actigraphy were recorded nightly and neurobehavioral performance and mood were assessed each day. Data are currently being collected and hormonal analyses are in progress. Once these initial studies are completed, a trial will be conducted to evaluate the efficacy of intermittent exposure to bright light as a countermeasure to maintain circadian entrainment under these conditions.

CONCLUSIONS

The results of the current research may have important implications for the treatment of circadian rhythm sleep disorders, such as delayed sleep phase syndrome and shift-work dyssomnia, which are anticipated to have a high incidence and prevalence during extended duration space flight such as planned for the International Space Station and manned missions to Mars.

Technology Development

USER FRIENDLY INSTRUMENTATION FOR NON-INVASIVE ASSESSMENT OF ALTERATIONS OF CARDIOVASCULAR REGULATION ASSOCIATED WITH SPACE FLIGHT

R.J. Cohen¹, N. Iyengar¹, T.J. Mullen², C.D. Ramsdell², G. Sundby¹

¹Massachusetts Institute of Technology, Cambridge, MA 02139, ²Harvard Medical School, Boston, MA 02115

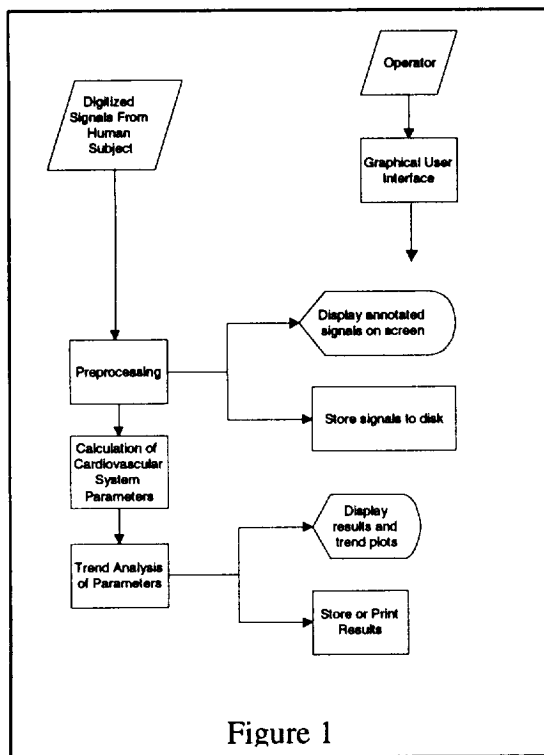
INTRODUCTION

It is critically important to be able to assess alterations in cardiovascular regulation during and after space flight. We are presently developing an instrument for the non-invasive assessment of such alterations that can be used on the ground and potentially during space flight. This instrumentation will be used by the Cardiovascular Alterations Team at multiple sites for the study of the effects of space flight on the cardiovascular system and the evaluation of countermeasures. In particular, the Cardiovascular Alterations Team will use this instrumentation in conjunction with ground-based human bed-rest studies and during application of acute stressors (*e.g.*, tilt, exercise) as well as in animal studies. In future studies, the Cardiovascular Alterations Team anticipates using this instrumentation to study astronauts before and after space flight and ultimately, during space flight. The instrumentation may also be used by the Bone Demineralization/Calcium Metabolism Team, the Neurovestibular Team and the Human Performance Factors, Sleep and Chronobiology Team to measure changes in autonomic nervous function.

The instrumentation is based on a powerful new technology – cardiovascular system identification (CSI) – which has been developed in our laboratory. CSI provides a non-invasive approach for the study of alterations in cardiovascular regulation. This approach involves the analysis of second-to-second fluctuations in physiologic signals such as heart rate and non-invasively measured arterial blood pressure in order to characterize quantitatively the physiologic mechanisms responsible for the couplings between these signals. Through the characterization of multiple physiologic mechanisms, CSI provides a closed-loop model of the cardiovascular regulatory state in an individual subject.

The application of CSI currently requires off-line computerized analysis of recorded physiologic signals by an expert user. The user operates in an iterative manner with the computer to preprocess the data, select data segments for analysis, run the CSI analyses, and to evaluate and interpret the results. Thus, the availability of this technology is currently limited to highly expert users located in Professor Cohen's laboratory. In this project, we are developing integrated instrumentation capable of acquiring the physiologic signals, performing the CSI analysis in a fully automated fashion, and displaying the results on-line. The design of this instrumentation will be such that users with minimal training (including astronauts and other NSBRI investigators) can perform CSI onsite, conveniently and effectively.

The availability of this instrumentation is essential for effectively studying the cardiovascular effects of space flight and for the subsequent development and evaluation of appropriate countermeasures. The development of such instrumentation may also have significant clinical



impact on Earth in the diagnosis and treatment of patients with a variety of cardiovascular and neurologic disorders.

METHODS

The instrument is being developed on a Pentium II platform with a 300MHz processor in a Windows NT 4.0 environment. This configuration was selected in part due to its widespread use and availability. All software is being developed in C++, which supports an object-oriented approach for rapid development of efficient software. Data acquisition is achieved through the use of a Keithley DAS-1701ST acquisition board. A simplified software block diagram is provided in Figure 1.

PROGRESS

A TIMELINE OF THE DEVELOPMENT AND ASSEMBLY PLAN IS GIVEN IN FIGURE 2.

The base skeleton system was completed and demonstrated in June 1998 at the NSBRI Conference. It includes basic acquisition, and display capabilities as well as advanced real-time preprocessing of the physiological signals. It also includes a system identification algorithm and interactive processing capabilities. We are currently re-implementing the system identification procedure to be more computationally efficient so that it can be carried out in real time with minimal delay. Specifically, for example, we are planning to use recursive estimation techniques so that when processing new data to determine ARX parameters for impulse responses, the previous calculations can be used as much as possible. We use this to our advantage and maximize computational efficiency with recursive algorithms taken from the system identification literature and developed in our laboratory. We also plan to implement advanced noise detection and correction algorithms and additional automation features in coming months.

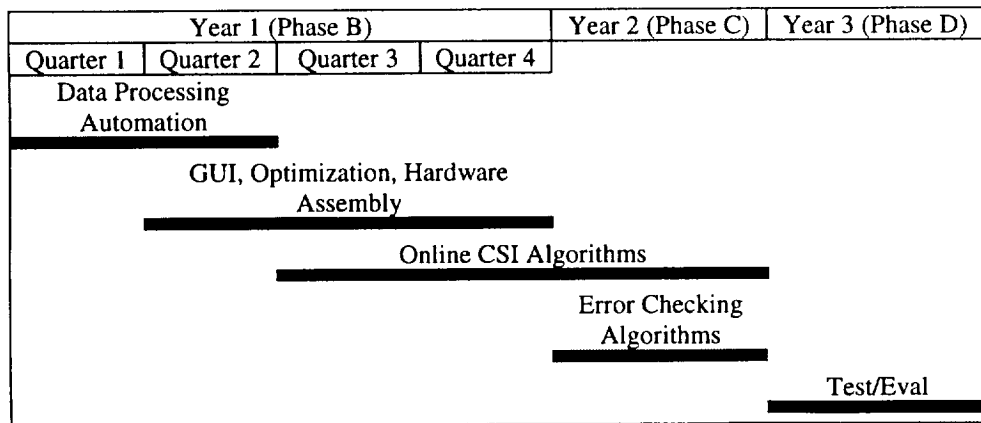


Figure 2

The system will be evaluated and tested by the Cardiovascular Alterations Team and other NSBRI Teams. An iterative debug, upgrade and re-release process will be used to improve the device's user-friendly interface.

WIRELESS AUGMENTED REALITY PROTOTYPE (WARP)

A.S Devereaux

Jet Propulsion Laboratory Caltech/NASA

Initiated in January, 1997, under NASA's Office of Life and Microgravity Sciences and Applications, the Wireless Augmented Reality Prototype (WARP) is a means to leverage recent advances in communications, displays, imaging sensors, biosensors, voice recognition and microelectronics to develop a hands-free, tetherless system capable of real-time personal display and control of computer system resources. Using WARP, an astronaut may efficiently operate and monitor any computer-controllable activity inside or outside the vehicle or station.



WARP Operational Concept

The WARP concept is a lightweight, unobtrusive heads-up display with a wireless wearable control unit. Connectivity to the external system is achieved through a high-rate radio link from the WARP personal unit to a base station unit installed into any system PC. The radio link has been specially engineered to operate within the high-interference, high-multipath environment of a space shuttle or space station module. Through this virtual terminal, the astronaut will be able to view and manipulate imagery, text or video, using voice commands to control the terminal operations. WARP's hands-free access to computer-based instruction texts,

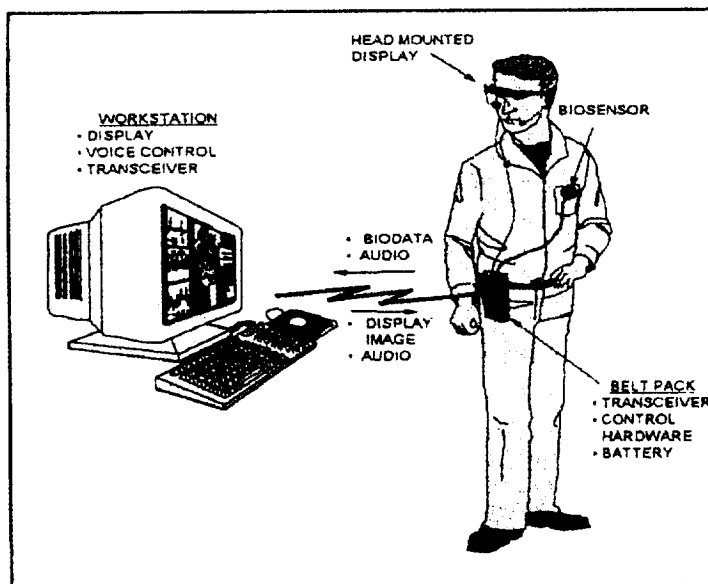
diagrams and checklists replaces juggling manuals and clipboards, and tetherless computer system access allows free motion throughout a cabin while monitoring and operating equipment.

Along with information provided to the astronaut, WARP also allows external observation of the astronaut's situation; personal biosensors can send back continuous telemetry through the WARP control unit and a miniature camera integrated into the headset provides real-time video of the wearer's field of view to remote observers. In this way, for example, a principal investigator located on Earth may consult with a payload specialist on the operation or troubleshooting of their equipment.

One of the major technology challenges with this concept is the ability to provide high-rate information wirelessly in the environment of a space module. Line-of-sight communications would be difficult to guarantee without greatly restricting an astronaut's movement through the tight quarters of a space module. RF links do not require visual line-of-sight to operate, but the metal walls and lack of RF absorbers, combined with moving human bodies, creates an enormous potential for destructive self-interference. Another strict constraint was the size, weight, and power draw which could be allowed for radio functions in a wearable device.

Substantial other technology development was also required in the areas of a lightweight heads-up display with sufficient resolution to read and operate a computer display, as well as the in development of a high-speed, compact audio/video coder/decoder (codec) to allow the high-resolution video to be shared between the base computer and remote wearable display in a constrained-bandwidth link.

The architecture of the system is two sided, consisting of a base station and a wearable unit. The base station computer serves as both a local computing resource as well as providing access into the facility computing system. The wearable unit, consisting of both a backpack controller and head-mounted display, allows monitor and control of the base station while sending back ancillary situational data (video, audio, and biological or environmental sensory). As shown in the diagram below, the base station is a PC, which may be networked into the facility backbone to provide access to remote information or allow control of remote devices or modules which have computer interfaces. The wearable unit displays computer video and audio from the base station and returns user situational awareness including real-time video from an integrated headset camera, audio from user microphone, and variable-bandwidth data from a biological or environmental sensor located on the person.



WARP System Architecture

To implement this system, a three-phase effort is underway to develop the concept demonstration unit and then improve this prototype to practical long-term use in EVA or IVA activities.

The WARP Phase I demonstration prototype is a wireless, portable (lunchbox-sized) control unit which connects via thin cable to a slim headset with video and 2-way audio. The Phase I headset is a custom unit developed by JPL and commercial partner to incorporate the highest resolution color display with ASIC drivers to produce the lightest-weight heads-up display available. The Phase I electronics

are composed of COTS elements for radio and codec, using a single-board PC as driver.

Development is underway on the Phase II system, which will feature improved visual performance and a backpack configuration. Substantial improvements in performance and form factor are achieved by the used of custom commercial parts which are not only more capable but also allow the deletion of the single-board PC controller of the Phase I portable unit. The Phase II wearable, single-user system will be available in early 1999.

To move from a prototype unit to a true production device suitable for long-term use and a increased base of customer applications, Phase III will incorporate the following : next-generation displays, full custom chips and layout, allowing even greater size and power reductions along with inherently greater flexibility for different applications, multiple access system supporting multiple users in one module, hand-off of connection when moving between space modules, full personal communications system capabilities, offering messaging, audio, etc. on-demand, incorporation of WARP capability in EVA helmet or biohazard suit, integration of other bio or environmental sensors such as Ames' Sensors 2000, JSC's Smart Suit or JPL's Electronic Nose, and integration of extremely compact, low power camera in headset, such as JPL's Active Pixel Sensor camera-on-a-chip.

Potential commercial applications of WARP are in any environment where heads-up, hands-free information retrieval improves efficiency, including tetherless operations/monitor consoles, remote consultations in medical or maintenance procedures, and hazardous or confined-space activities.

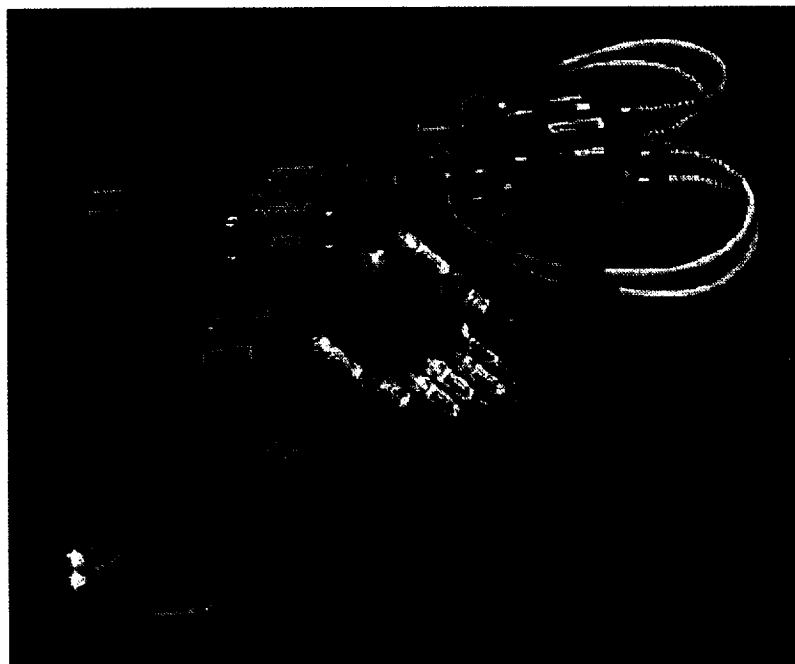
BIONA-C CELL CULTURE pH MONITORING SYSTEM

C. Friedericks

NASA Ames Research Center

Sensors 2000! is developing a system to demonstrate the ability to perform accurate, real-time measurements of pH and CO₂ in a cell culture media in Space. The BIONA-C Cell Culture pH Monitoring System consists of S2K! developed ion selective sensors and control electronics integrated with the fluidics of a cell culture system. The integrated system comprises a "rail" in the Cell Culture Module (CCM) of WRAIR (Space Biosciences of Walter Read Army Institute of Research). The CCM is a Space Shuttle mid-deck locker experiment payload.

The BIONA-C is displayed along with associated graphics and text explanations. The presentation will stimulate interest in development of sensor technology for real-time cell culture measurements. The transfer of this technology to other applications will also be of interest.



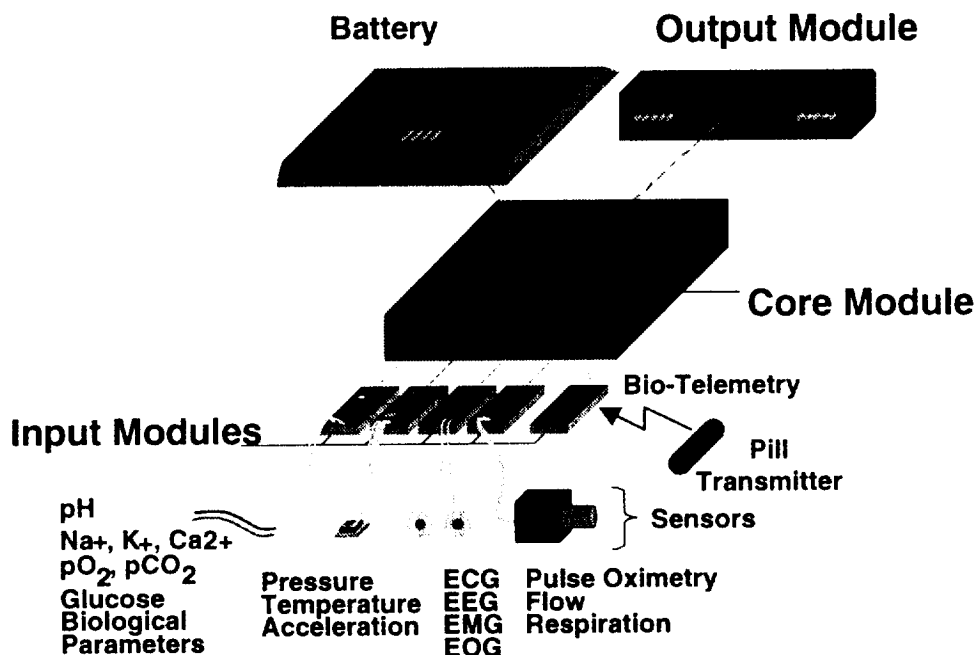
PHYSIOLOGICAL SIGNAL CONDITIONER

C. Friedericks

NASA Ames Research Center

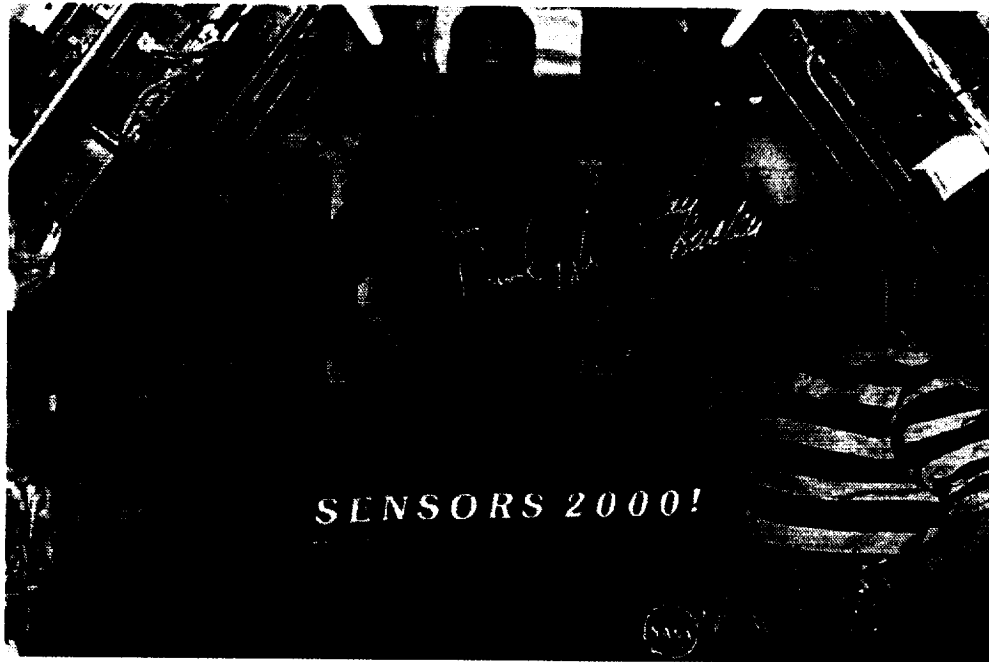
Sensors 2000! is developing a Physiological Signal Conditioner (PSC) for monitoring of astronauts in the ISS Human Research Facility. The PSC is battery powered and worn by the crew. The Engineering Development Unit (PSC EDU) and the form-and-fit PSC Tooling Model will be displayed along with associated graphics and text explanations. Results of a recent advanced PSC-2 feasibility study will be presented.

The presentation will stimulate discussion of the functional capabilities of a wireless, crew worn Physiological Signal Conditioner. Application of advanced technology to meet the conflicting demands of size, power, and functional capability will be of interest.



SENSORS 2000! PROGRAM: ADVANCED BIOSENSOR AND MEASUREMENT SYSTEMS TECHNOLOGIES FOR SPACEFLIGHT RESEARCH AND CONCURRENT, EARTH-BASED APPLICATIONS

J. Hines
NASA Ames Research Center



Sensors 2000! (S2K!) is a specialized, integrated projects team organized to provide focused, directed, advanced biosensor and bioinstrumentation systems technology support to NASA's spaceflight and ground-based research and development programs. Specific technology thrusts include telemetry-based sensor systems, chemical/ biological sensors, medical and physiological sensors, miniaturized instrumentation architectures, and data and signal processing systems. A concurrent objective is to promote the mutual use, application, and transition of developed technology by collaborating in academic-commercial-government leveraging, joint research, technology utilization and commercialization, and strategic partnering alliances.

Sensors 2000! is organized around three primary program elements: Technology and Product Development, Technology Infusion and Applications, and Collaborative Activities. Technology and Product Development involves development and demonstration of biosensor and biotelemetry systems for application to NASA Space Life Sciences Programs; production of fully certified spaceflight hardware and payload elements; and sensor/measurement systems development for NASA research and development activities. Technology Infusion and Applications provides technology and program agent support to identify available and applicable technologies from multiple sources for insertion into NASA's strategic enterprises and initiatives. Collaborative Activities involve leveraging of NASA technologies with those of other government agencies, academia, and industry to concurrently provide technology solutions and products of mutual benefit to participating members.

MINIATURE QUADRUPOLE MASS SPECTROMETER ARRAY

D. Karmon, M. Darrech, A. Chutjian, **D. Jan**
Jet Propulsion Laboratory, Pasadena, California

JPL is funded by Code U to develop a Miniature QMSA for an EVA flight test. The initial intent was to fly an experiment internal to the astronaut suit during a shuttle EVA. Following discussions with JSC the suit application was abandoned in favor of other more urgent needs. The JSC EVA office was particularly interested in hydrazine detection on the astronaut suit. While discussing and exploring the implementation of such an experiment, managers at JSC suggested combining the interests of *two* JSC groups. The Life Support and Thermal Systems Branch, Crew and Thermal Systems Division has a need for an ammonia detection instrument, while the EVA office has a need for hydrazine detection. The two groups were pursuing separate single-purpose solutions. Instead, the JPL QMSA offers a single instrument solution via a portable instrument to be used by an astronaut on an EVA. Such an instrument would serve *both* the ammonia leak detection and the hydrazine contamination needs.

The need for the QMSA was defined as urgent and targeted for a January 1999 flight. While the original JPL task (as funded by Code U) was for an experiment flight with JPL delivery in October 1998, this task was for a qualified flight instrument with a planned JPL delivery in August 1998. This schedule was very demanding and dictated a fast-track implementation.

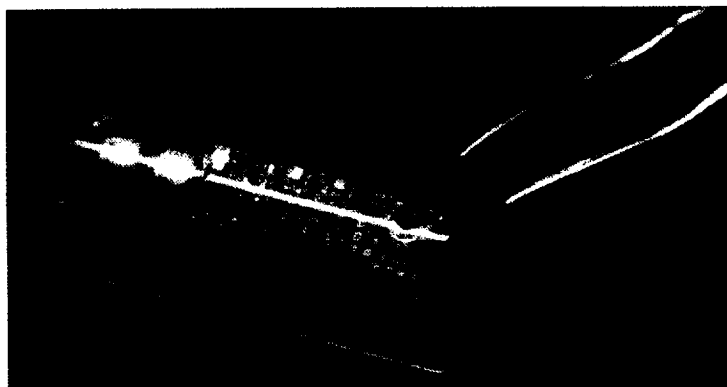
BIOTELEMETRY

C. Mundt

NASA Ames Research Center

Sensors 2000! is developing pill-shaped biotelemeters for measuring physiological parameters during space flight life sciences experiments using rodents aboard the ISS Gravitational Biology Facility, with the additional capability for monitoring the health of astronauts in the Human Research Facility. The first "pill transmitter" is capable of measuring pressure and temperature for up to 10 months. The NASA objective is to utilize these devices. The pill-transmitters can also be used by non-NASA users for medical applications. One application is fetal surgery. The "pill" is small enough to be endoscopically placed into the womb through a tube used during surgeries to correct fetal defects before birth. After surgery, the pill-transmitter will continue to monitor body temperature, pressure and other vital signs in the womb, radioing results to physicians. It will help them to detect preterm-labor, a serious problem after fetal surgery. The pill is about one-third-of-an-inch across and one-and-one-third-inches long.

Future pill-versions will include pH, heartrate, and ECG. A pH-pill prototype is currently being tested. Sensors 2000! has also designed and built a 2-channel biotelemetry receiver and has developed data acquisition software to display and record the measured physiological parameters. A DSP-base hand-held receiver (trispander) is currently under development.



Pressure/Temperature Pill



pH/Temperature Pill



Heartrate/Temperature Pill



ECG/Temperature Pill



**pH/Pressure/Temperature/
Heartrate Pill**

**NASA AMES RESEARCH CENTER R&D SERVICES DIRECTORATE
BIOMEDICAL SYSTEMS DEVELOPMENT**

J. Pollitt, K. Flynn
NASA Ames Research Center

The Ames Research Center R&D Services Directorate teams with NASA, other government agencies and/or industry investigators for the development, design, fabrication, manufacturing and qualification testing of space-flight and ground-based experiment hardware for biomedical and general aerospace applications. In recent years, biomedical research hardware and software has been developed to support space-flight and ground-based experiment needs including the E132 Biotelemetry system for the Research Animal Holding Facility (RAHF), E100 Neurolab neuro-vestibular investigation systems, the Autogenic Feedback Systems, and the Standard Interface Glove Box (SIGB) experiment workstation module. Centrifuges, motion simulators, habitat design, environmental control systems, and other unique experiment modules and fixtures have also been developed.

A discussion of engineered systems and capabilities will be provided to promote understanding of possibilities for future system designs in biomedical applications. In addition, an overview of existing engineered products will be shown. Examples of hardware and literature that demonstrate the organization's capabilities will be displayed.

The Ames Research Center R&D Services Directorate is available to support the development of new hardware and software systems or adaptation of existing systems to meet the needs of academic, commercial/industrial, and government research requirements.

The Ames R&D Services Directorate can provide specialized support for:

- System concept definition and feasibility
- Mathematical modeling and simulation of system performance
- Prototype hardware development
- Hardware and software design
- Data acquisition systems
- Graphical user interface development
- Motion control design
- Hardware fabrication and high-fidelity machining
- Composite materials development and application design
- Electronic/electrical system design and fabrication
- System performance verification testing and qualification.

Investigators are encouraged to contact the Ames R&D Services Directorate to discuss proposals or concepts.

MINIATURE TIME-OF-FLIGHT MASS SPECTROMETER

R.S. Potember, W.A. Bryden, M. Antoine, P. Scholl, H. Ko, V.L. Pisacane, M. Leonardo
Applied Physics Laboratory, The Johns Hopkins University, Laurel, MD 20723

R.J. Cotter, Middle Atlantic Mass Spectrometry Center, Department of Pharmacology, The Johns Hopkins Medical Institution, Baltimore, MD 21205

Major advances must occur to protect astronauts from prolonged periods in near-zero gravity and high radiation associated with extended space travel. The dangers of living in space must be thoroughly understood and methods developed to reverse those effects that cannot be avoided. Six of the seven research teams established by the National Space Biomedical Research Institute (NSBRI) are studying biomedical factors for prolonged space travel to deliver effective countermeasures. To develop effective countermeasures, each of these teams require identification of and quantification of complex pharmacological, hormonal, and growth factor compounds (biomarkers) in humans and in experimental animals to develop an in-depth knowledge of the physiological changes associated with space travel.

At present, identification of each biomarker requires a separate protocol. Many of these procedures are complicated and the identification of each biomarker requires a separate protocol and associated laboratory equipment. To carry all of this equipment and chemicals on a spacecraft would require a complex clinical laboratory; and it would occupy much of the astronauts' time. What is needed is a small, efficient, broadband medical diagnostic instrument to rapidly identify important biomarkers for human space exploration. The Miniature Time-Of-Flight Mass Spectrometer Project in the Technology Development Team is developing a small, high resolution, time-of-flight mass spectrometer (TOFMS) to quantitatively measure biomarkers for human space exploration.

The TOFMS will be used to identify and quantify biomarkers and support biomedical research and medical care. Several semi-quantitative miniature TOF mass spectrometers are presently under development at The Johns Hopkins University Applied Physics Laboratory (JHU/APL) for a DARPA program to analyzer to chemical and biological weapons with the sensitivity and mass range also required for human space exploration. A goal of this program is to develop a quantitative TOF mass spectrometer demonstration system from engineering model instruments available from the DARPA program. The virtue of the JHU/APL TOFMS technologies resides in the promise for a small (less than one cubic ft), lightweight (less than 5 kg), low power (less than 50 watts), rugged device that can be used continuously with advanced signal processing diagnostics. To date, the JHU/APL approach has demonstrated mass capability resolution from under 100 to beyond 10,000 atomic mass units (amu) in a very small, low power prototype for biological analysis. Further, the electronic nature of the TOFMS output makes it ideal for rapid telemetry to Earth for indepth analysis by ground support teams.

The TOFMS Team has completed initial laboratory studies with critical biomarkers identified by the Muscle Alterations and Atrophy Team. The TOFMS Team has recorded full spectrum mass spectral signature of key target biomarker analytes using the MALDI technique at physiological concentrations found in urine. Compounds under investigation in year one of this project include:

insulin like growth factors (IGF-I), Urinary 3-methylhistidine, and estradiol. IGF-I is a potent anabolic factor that mimics most of the growth promoting actions of GH in vivo. IGF-1 has also been identified by the Bone Demineralization / Calcium Metabolism Team as an important biomarker. Urinary 3-methylhistidine is a measure of myofibillar protein degradation. 3-methylhistidine cannot be re-utilized by the body. It is rapidly and quantitatively excreted in the urine.

Estradiol is a steroid hormone important for the maintenance of muscle mass and bone density. It is widely speculated that steroid hormones such as estradiol play a central role in the early stages of muscle atrophy and bone demineralization.

In addition to IGF-1 and estradiol, the TOFMS Team has also completed initial laboratory studies with biomarkers specific to the Bone Demineralization / Calcium Metabolism Team. These biomarkers include: trivalent hydroxypyridinium crosslinks and creatinine. Trivalent hydroxypyridinium crosslinks are released into the circulation during bone resorption and are excreted as both free pyridinolines. In bone and cartilage, the collagen is bound by pyridinoline or deoxypyridinoline, crosslinks. deoxypyridinoline is found exclusively in bone while pyridinoline is found in skin, joint and cartilage. Creatinine is used to extrapolate the status of bone remodeling activity in various metabolic bone conditions.

The TOFMS team has begun to identify non-invasive methods to extract important biomarkers from urine, blood, and breath.

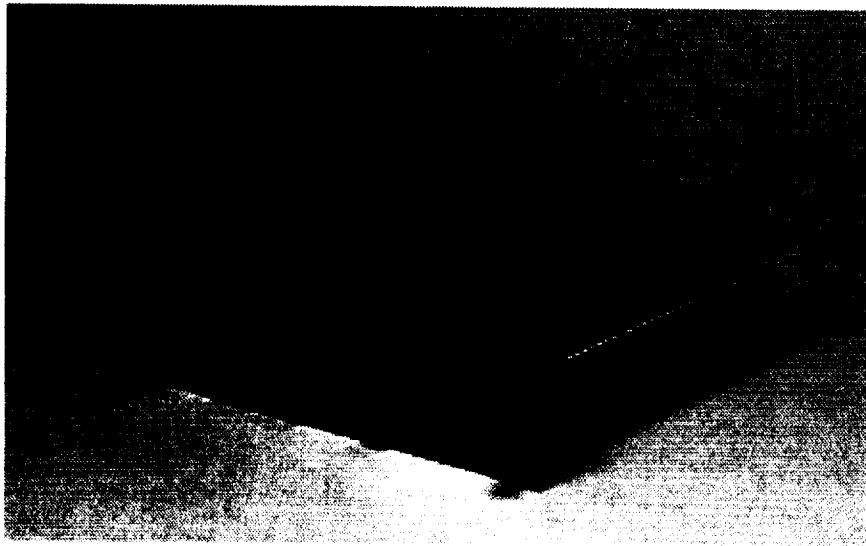
NEUROLAB BIOTELEMETRY SYSTEM (NBS)

J. Schonfeld

NASA Ames Research Center

This system was developed by the Sensors 2000! Program (S2K!) at Ames Research Center for the E132 STS-90 Neurolab Shuttle mission experiment to monitor 12 untethered adult male rats housed in the Research Animal Habitat Facility (RAHF). The system monitored the animals for body temperature, heart rate, and activity, and stored the data on board for up to 21 days for downloading after landing. The principal investigator's monitoring requirements were accomplished integrating a combination of both commercial and in-house developed hardware and software, including an off-the-shelf implantable telemetry transmitter and receiver system. In addition, a custom-developed antenna system was incorporated into the RAHF cages to perform the unique function of near-field radio-frequency (rf) measurement in the metal cages.

This system proved the ability to perform wireless physiological measurements in very non-ideal circumstances using existing habitats and cabling without interfering with other experiment or shuttle systems. S2K! is continuing development on a custom telemetry transmitter and receiver system which will expand measurement capabilities.



Neurolab Biotelemetry Chassis

NEW TECHNIQUES FOR THE NON-INVASIVE IMAGING OF TISSUE PERFUSION

D. A. Sherman, R. H. Rubin, and R. J. Cohen

Harvard-MIT Division of Health Sciences and Technology, Cambridge, MA 02139

INTRODUCTION

Non-invasively imaging and quantitating perfusion of tissue by blood is important for both space and civilian medicine. Changes in muscle perfusion may lead to atrophy and subsequent tissue loss. Changes in cerebral perfusion may be linked to motion sickness and altered brain function. Similarly, reduced perfusion of other organs may similarly compromise their function. Little is known about alterations in regional perfusion resulting from space flight because traditional methods for measuring perfusion have relied upon contrast agents injected into the blood stream. Because these agents have a limited half-life, they are not ideal for monitoring long-term changes in tissue perfusion. Alterations in perfusion may be more pronounced in older astronauts and astronauts with pre-existing disease. The development of non-invasive means of assessing regional tissue perfusion would also be of great benefit to diagnosing and treating patients on earth; it would be of particular value in managing patients in the intensive care unit.

METHODS

Traditional methods for measuring perfusion are based on detecting steady-state blood flow. Recent experiments have demonstrated that blood flow in the microvasculature is highly pulsatile.

We propose a new method of measuring tissue perfusion by using ultrasound to quantitate fluctuations in physical properties of tissue. Fluctuations which are temporally correlated with the heart beat and are spatially correlated over short (millimeter) length scales are proportional to tissue perfusion.

RESULTS

We have used phase fluctuations in B-mode ultrasound images to measure perfusion in skeletal muscle tissue. The images clearly show regions of high perfusion (muscle) and low perfusion (skin, fat). When a tourniquet is applied, the perfusion images show a dramatic drop in muscle perfusion.

CONCLUSION

We have shown that it is possible to non-invasively measure perfusion in muscle tissue. This is a promising new technology for non-invasively measuring the effect of space flight on alterations in regional tissue perfusion. This new technology may provide major benefits for maintaining astronaut health in space and civilian health on earth.

BION-11 SPACEFLIGHT MISSION

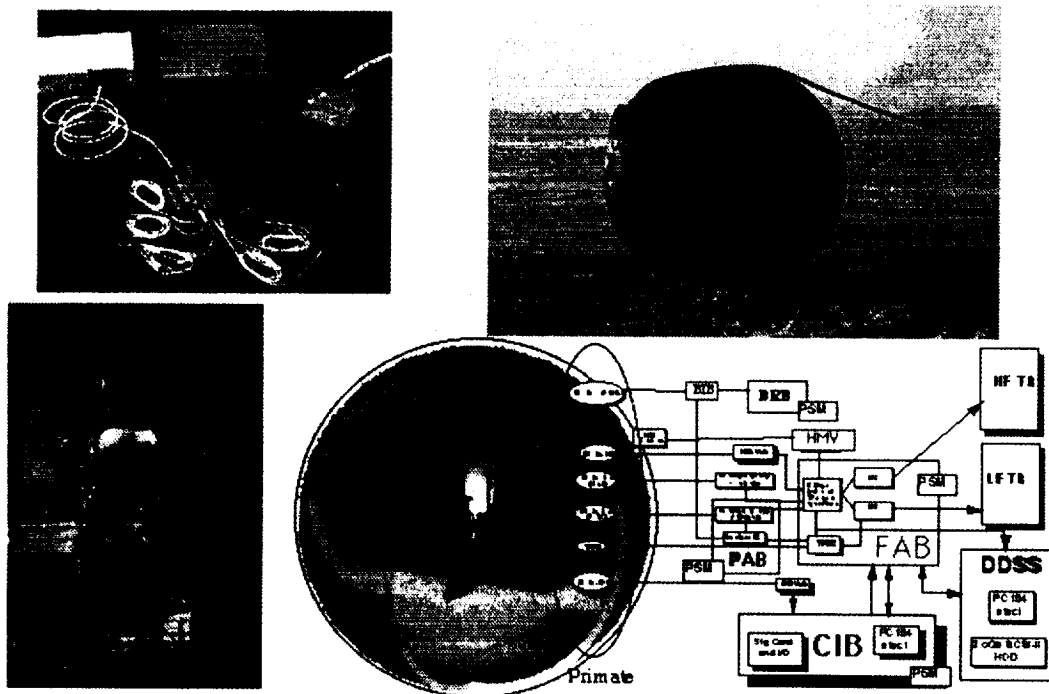
M. Skidmore

NASA Ames Research Center

The Sensors 2000! Program, in support of the Space Life Sciences Payloads Office at NASA Ames Research Center developed a suite of bioinstrumentation hardware for use on the Joint US/Russian Bion 11 Biosatellite Mission (December 24, 1996 - January 7, 1997). This spaceflight included 20 separate experiments that were organized into a complimentary and interrelated whole, and performed by teams of US, Russian, and French investigators. Over 40 separate parameters were recorded in-flight on both analog and digital recording media for later analysis. These parameters included; Electromyogram (7 ch), Electrogastrogram, Electrooculogram (2 ch), ECG/EKG, Electroencephlogram (2 ch), single fiber firing of Neurovestibular afferent nerves (7 ch), Tendon Force, Head Motion Velocity (pitch & yaw), pO₂ (in vivo & ambient), temperature (deep body, skin, & ambient), and multiple animal and spacecraft performance parameters for a total of 45 channels of recorded data.

Building on the close cooperation of previous missions, US and Russian engineers jointly developed, integrated, and tested the physiologic instrumentation and data recording system. For the first time US developed hardware replaced elements of the Russian systems resulting in a US/Russian hybrid instrumentation and data system that functioned flawlessly during the 14 day mission.

BION-11 SPACEFLIGHT MISSION



DIGITAL ECHOCARDIOGRAPHY ON THE INTERNATIONAL SPACE STATION: TECHNICAL PROGRESS AND EXPERIMENTAL PLANNING

J.D. Thomas, N.L. Greenberg, T. Shiota, L. Cardon, M.J. Garcia, Cardiovascular Imaging Center, Cleveland Clinic Foundation, Cleveland Ohio 44195

INTRODUCTION

To provide improved experimental data concerning the effects of microgravity on the cardiovascular system, NASA plans to place a commercial echocardiograph on the International Space Station (ISS), with launch tentatively scheduled for December 1999. Before this can occur, however, a great deal of background work has been necessary to specify the precise configuration for this unit and develop and validate the methodology for digital transfer of echocardiographic data from the ISS to the ground. Additionally, one of the key goals of this instrument is to assess changes in intrinsic ventricular systolic and diastolic function during prolonged space flight independent of known changes of cardiac preload. Extensive ground-based work has been needed to validate the load independence of novel echocardiographic modalities such as Doppler tissue imaging (measuring velocities within the myocardium, rather than the blood pool) and color M-mode flow propagation (measuring the diastolic propagation of blood from the atrium to the ventricle, shown to be highly sensitive to intraventricular pressure gradients). Finally, recognizing that two-dimensional echocardiography is difficult for the crew to perform on orbit, work has been necessary to investigate the potential for three-dimensional echocardiography on future space missions.

METHODS

Project 1 (specifying and flight readying of a commercial echocardiograph for the ISS): Working closely with engineers from Lockheed Martin (at JSC) and Advanced Technology Laboratories (ATL), an upgrade plan has been developed to place the HDI 5000 ultrasound machine on orbit. Human factors assessment has been made with input from the astronaut corps.

Project 2 (developing and validating a plan for digital transfer of echocardiographic data from the space station to the ground): Work has proceeded on several subprojects. At the Cleveland Clinic, we have tested transfer of looped echocardiographic data using the DICOM protocol and standard network infrastructure. To test telemedicine applications (both terrestrial and space-based), we have evaluated real-time digital transfer of echocardiographic data over the NASA Research and Education Network (NREN) between the Lewis Research Center (Cleveland) in the Ames Research Center (Mountain View, CA). Real-time echocardiographic data were encoded using MPEG-2 compression and transferred via ATM protocol at 2 to 5 Mbps. Interactive guidance of image acquisition was tested using an audio feedback loop, and image quality was evaluated at various levels of cell loss ratio and cell error ratios.

Project 3 (developing and validating new echocardiographic methods for assessing ventricular function in microgravity): Among many protocols for this project, we have specifically evaluated the load independence of Doppler tissue imaging and color M-mode flow propagation (v_p) in both invasive intraoperative studies and animal investigations. Specifically, in 14 patients and 4 dogs with Millar catheters in the left atrium and ventricle, we simultaneously acquired color M-mode flow propagation data across the mitral valve, storing it digitally and comparing it to the transmitral pressure data. Acquisitions were made before and after partial cardiopulmonary

bypass (patients) and with inferior vena cava (IVC) occlusion (dogs), causing a significant reduction in a left atrial pressure and left ventricular preload. Load independence of v_p was tested by paired t-testing before and after these interventions. Nonlinear regression was used to test the relationship between v_p and τ , the time constant of isovolumic relaxation.

Project 4 (real-time three-dimensional echocardiography): Since acquiring an instrument capable of the real-time 3-dimensional echocardiographic imaging in September 1997, we have examined a total of 289 patients with a variety of cardiac disorders, including hypertrophic, dilated, restrictive, and ischemic cardiomyopathy, aortic and mitral regurgitation, and aortic aneurysm. As one of many subprojects, we have compared ventricular volumes and ejection fractions with reference measurements from magnetic resonance imaging. Similar tests have been conducted in a sheep model of aortic insufficiency, using electromagnetic flow probes and conductance catheters as reference standards. LV volumes by three-dimensional echocardiography were compared with these references by paired t-testing and linear regression.

RESULTS

Project 1: After endorsement by the Science Working Group and a presentation to the Critical Design Review Board, the HRF ultrasound unit has been upgraded from the HDI 3000 to the HDI 5000 with a quadrupling of raw processing speed and a dramatic improvement in overall image quality. Board modification for placement in the HRF rack has been successfully completed, and the instrument has passed heat and vibration tests at Marshall Space Flight Center. Human factors evaluation by the astronaut corps has identified several minor recommendations, and consideration is being given to upgrading the system's software to the latest level of the commercial system. This upgrade would provide better digital output as well as output of velocities within the tissue and improved color Doppler velocity definition.

Project 2: At the Cleveland Clinic, we have successfully transmitted full studies (averaging 50 MB) between multiple vendors' instruments using the DICOM protocol over a TCP-IP network. For the initial NREN experiment between Lewis and Ames, echoes were transmitted with near-broadcast quality at a data rate of 5 Mbps and with quality superior to videotape (the current standard) at 2 Mbps. At cell loss and cell error ratios of 10^{-5} , performance was acceptable, but at 10^{-3} (an extreme degree of network noise), the system froze. Using a two-way audio link, a cardiologist in California was able to guide the acquisition of the echocardiogram in Cleveland, a model for future guidance of acquisition aboard the International Space Station.

Project 3: There was no significant change in v_p with preload reduction in both patients (37 ± 12 cm/sec) and dogs (35 ± 15 cm/sec), despite highly significant ($p < 0.001$) falls in LA pressure and peak E-wave velocity across the mitral valve. Both patients and dogs showed strong curvilinear relationships between v_p and τ . Interestingly, when canine and human data were combined there was still a very good correlation between v_p and τ ($\tau = 592.21(v_p)^{-0.68}$, $r = 0.78$, $p < 0.001$), with similar fit of animal and human data points around the regression line, indicating that the relationship between these indices was not species-specific. Similar data have been obtained pre- and post-hemodialysis for mitral annular velocities (Doppler tissue imaging), suggesting that both DTI and v_p are relatively load-independent measures of intrinsic ventricular function. Their utility in microgravity is being assessed in collaborative bed rest experiments sponsored by the National Space Biomedical Research Institute.

Project 4: Because of extensive parallel processing, the real time three-dimensional echocardiographic instrument is capable of acquiring 64 scan lines in 64 scan planes in as little as 25 milliseconds, leading to frame rates of 25-40 Hz. Because a single cardiac cycle contains all the volumetric information of the heart, examinations can be conducted much more rapidly than conventional two-dimensional examinations, which require sequential sector scans from multiple windows. Furthermore, precise image orientation is less important, as post processing and rendering will allow anatomically oriented sections to be viewed even if the original three-dimensional acquisition is nonstandard. This has important implications for improved echocardiographic ease of acquisition in space, critically important because of limited crew training. Among several quantitative evaluations of this new technology, we have demonstrated highly accurate ventricular volumes ($r > 0.95$) in comparison to magnetic resonance imaging data and have demonstrated the important utility of this methodology in reconstructing the complex movement of the mitral annulus following mitral valve repair.

DISCUSSION

The availability of a contemporary echocardiographic instrument aboard the International Space Station will enable investigators to examine the cardiovascular system with a degree of sophistication never before possible in space. Such investigations include accurate determination of changes in chamber volume, cardiac output, intraventricular pressure gradients (as assessed by applying the Euler equation to color Doppler M-mode velocity propagation), and intrinsic systolic and diastolic ventricular function (as assessed by Doppler tissue imaging). Real-time three-dimensional echocardiography is feasible today on earth, but will require considerable progress in miniaturization before this instrument can be placed in orbit. Significant advances in digital acquisition and transmission will enable tele-echocardiography both from space and on earth.

LASER-POLARIZED NOBLE GAS MAGNETIC RESONANCE

R.L. Walsworth¹, M.S. Albert², D.G. Cory³, F.W. Hersman⁴, D.P. Hinton⁵, D. Hoffmann¹, F.A. Jolesz², R.W. Mair¹, S. Patz², S. Peled², V. Pomeroy⁴, C.H. Tseng¹, G.P. Wong¹

¹Harvard-Smithsonian Center for Astrophysics, Cambridge, MA 02138

²Brigham and Women's Hospital, ³MIT, ⁴University of New Hampshire, ⁵Massachusetts General Hospital

INTRODUCTION

We are developing laser-polarized noble gas nuclear magnetic resonance (NMR) as a novel biomedical imaging tool for ground-based and eventually space-based application. This emerging multidisciplinary technology enables high-resolution gas-space magnetic resonance imaging (MRI)—e.g., of lung ventilation—as well as studies of tissue perfusion. In addition, laser-polarized noble gases (³He and ¹²⁹Xe) do not require a large magnetic field for sensitive detection, allowing practical MRI at very low magnetic fields with a lightweight, low-power device.

METHODS

Large nuclear spin polarizations (> 10%) were created in dense samples of the spin 1/2 noble gases (³He and ¹²⁹Xe) using the technique of spin-exchange laser optical pumping. Such large polarizations greatly enhanced the magnetic resonance detection sensitivity of the noble gases, enabling practical gas-space MRI, studies of gas diffusion in porous media, and investigations of fluids and tissues using the soluble ¹²⁹Xe species. Laser-polarized noble gas was imbibed in model porous media and benignly inhaled by rats and humans, with minimal loss of spin-polarization, and then detected using both high-field (1.5 T, 4.7 T) and low-field (0.002 T) magnetic resonance with a sensitivity comparable to that of water protons in biological tissue at high magnetic fields.

RESULTS

- We developed noble gas polarization and delivery systems using diode laser arrays that provide ~ 1 liter/hr of spin-polarized ¹²⁹Xe or ³He gas [U.S. Patent # 5,617,860, April 8, 1997].
- We developed a model of inhaled, laser-polarized ¹²⁹Xe uptake in distal tissues (e.g., the brain) and calculated the resultant ¹²⁹Xe NMR signal-to-noise-ratio as a function of time [S. Peled *et al.*, *Magn. Reson. Med.* **36**, 340 (1996)].
- We measured the spin polarization lifetime (T_1) of laser-polarized ¹²⁹Xe dissolved in fresh human blood in vitro. We found the ¹²⁹Xe T_1 \uparrow 5-10 s in arterial blood and 15-25 s in venous blood [C.H. Tseng *et al.*, *J. Magn. Reson.* **126**, 79 (1997)].
- We developed MRI pulse sequences optimized for the large but difficult-to-replenish magnetization of laser-polarized noble gas [L. Zhao *et al.*, *J. Magn. Reson., Series B* **113**, 179 (1996)].
- We acquired NMR spectra from laser-polarized ¹²⁹Xe dissolved in the thorax tissue of living rats breathing the gas (see Fig. 1), and obtained NMR images of laser-polarized ¹²⁹Xe gas inside rat lungs [K. Sakai *et al.*, *J. Magn. Reson., Series B* **111**, 300 (1996)]. We observed three well-resolved ¹²⁹Xe NMR tissue resonances, in addition to the gas resonance in the lung gas space. We tentatively identified these tissue resonances as ¹²⁹Xe in solution in pulmonary tissue, red blood cells, and plasma/adipose tissue. Once xenon inhalation was stopped, the

three ^{129}Xe tissue resonances were observed to decay with different time constants ranging from 11 to 50 seconds--i.e. longer than the blood circulation time in the animal. These results support our proposed NMR measurements of the exchange of laser-polarized ^{129}Xe between the gas and tissue phases to map the lung's surface area and perfusion.

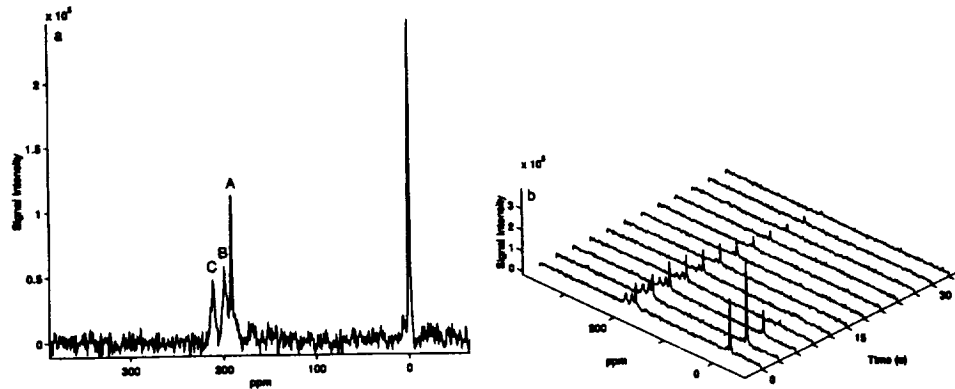


Fig. 1. ^{129}Xe NMR spectra from the thorax of a rat breathing the laser-polarized gas. Spectral peaks A, B, and C are ^{129}Xe in solution in plasma/adipose tissue, pulmonary tissue, and red blood cells, respectively. Polarization decay after cessation of breathing is shown at right.

- We demonstrated MRI of laser-polarized noble gas at low magnetic fields [C. H. Tseng *et al.*, Phys. Rev. Lett. **81**, 3785 (1998)]. We constructed a low-field MRI instrument that operates at 20 G (0.002 T) and can accommodate small samples: e.g., glass cells and excised rat lungs (see Fig. 2). With this demonstration, the door is opened to a wide variety of new MRI applications. Examples in biomedicine include portable noble gas systems for diagnostic lung imaging in humans, and inexpensive table-top lung imaging systems for the non-invasive characterization of lung disease models in animals. Furthermore, a low-field noble gas MRI system may be compatible with operation in restricted environments, such as onboard a space station, and may permit low-cost lung imaging in a simple, open magnet, as well as MRI of patients with artificial transplants such as pacemakers. We also demonstrated that low-field noble gas MRI is effective

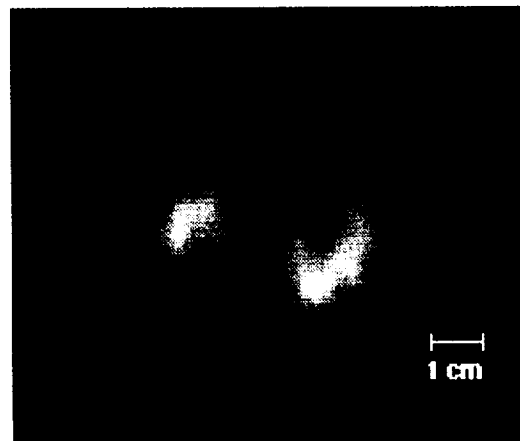
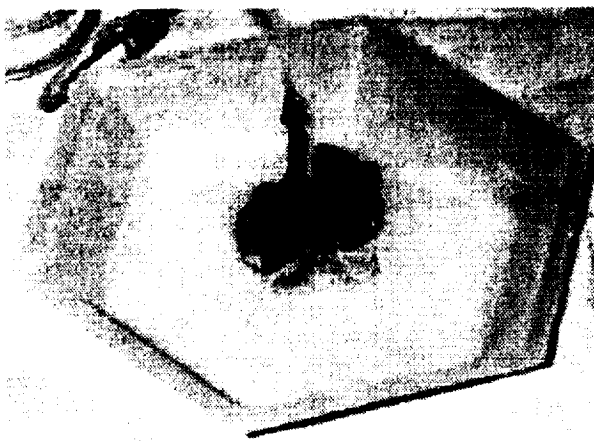


Fig. 2. Example of low-field noble gas MRI performed with prototype instrument. Excised rat lungs (photo on left) were filled with laser-polarized ^3He gas and imaged with NMR at 21 G (right). The two-dimensional spatial resolution is 1 mm^2 , with a 20 mm slice thickness, and the imaging time was ~ 25 seconds. Conventional, thermally-polarized proton (^1H) MRI is impractical at such low magnetic fields.

in imaging voids in two classes of materials that are problematic for high-field MRI: (i) heterogeneous systems, such as porous and granular media, which distort high-field MRI because of large, solid-gas magnetic susceptibility gradients; and (ii) electrical conductors, which prevent high-field MRI by Faraday (i.e., RF) shielding. These results support our proposed development of a low-field noble gas MRI system large enough for humans.

- We developed and tested pulsed-field-gradient NMR techniques to measure noble gas diffusion as a probe of the microstructure of heterogeneous porous media [R. W. Mair *et al.*, *J. Magn. Reson.*, (in press, 1998)]. We measured the time-dependent (i.e., restricted) diffusion of xenon gas in model porous media—randomly packed glass beads—with results that are consistent with numerical calculations. Free gas diffusion coefficients were measured for times much smaller than that required for xenon atoms to diffuse across pores in the restricted medium. For longer diffusion times, the measured diffusion coefficient decreased as the xenon atoms increasingly interacted with boundary restrictions. The initial decrease of the diffusion coefficient was found to be proportional to the average surface-area-to-volume-ratio (S/V) of pores in the bead pack; while the asymptotic (i.e., long time) value of the restricted diffusion coefficient provided a good measure of the system's tortuosity, which is related to the fluid permeability and porosity of the medium. These results support our proposed use of gas diffusion NMR as a probe of the microstructure of the lung.

CONCLUSION

Laser-polarized noble gas magnetic resonance is a powerful new tool for biomedical research and clinical imaging. Potential microgravity applications of this new diagnostic technology include determining the origins of: (i) perfusion heterogeneity in the lung; (ii) microgravity-induced changes in the pulmonary membrane component of the lung's diffusing capacity; and (iii) the cardiopulmonary interaction in microgravity that supports an increased cardiac output and stroke volume simultaneous with reduced central venous pressure and circulating blood volume. Potential ground-based applications of laser-polarized noble gas MRI include screening and surgical planning for lung disease, measurements of regional cerebral blood flow, and imaging white matter perfusion.

LIFE SCIENCES DIVISION SPACEFLIGHT HARDWARE

B. Yost

NASA Ames Research Center Life Sciences Division

The Ames Research Center (ARC) is responsible for the development, integration, and operation of non-human life sciences payloads in support of NASA's Gravitational Biology and Ecology (GB&E) program. To help stimulate discussion and interest in the development and application of novel technologies for incorporation within non-human life sciences experiment systems, three hardware system models will be displayed with associated graphics/text explanations. First, an Animal Enclosure Model (AEM) will be shown to communicate the nature and types of constraints physiological researchers must deal with during manned space flight experiments using rodent specimens. Second, a model of the Modular Cultivation System (MCS) under development by ESA will be presented to highlight technologies that may benefit cell-based research, including advanced imaging technologies. Finally, subsystems of the Cell Culture Unit (CCU) in development by ARC will also be shown.

A discussion will be provided on candidate technology requirements in the areas of specimen environmental control, biotelemetry, telescience and telerobotics, and *in situ* analytical techniques and imaging.

In addition, an overview of the Center for Gravitational Biology Research facilities will be provided. These NASA facilities are a National Resource available to qualified researchers throughout the world and may be used to characterize or help with the definition of the technologies mentioned above. In addition, basic research may also be performed using the facilities listed below:

Vestibular Research Facility

- Multi-axis Centrifuge
- 12' Linear Spring Sled
- 30' Human-rated Sled
- Programmable Linear Sled

Human-Rated Hypergravity Facilities

- 20-g Human-rated Centrifuge
- Human Powered Centrifuge
- Chronic Live aboard Exposure (52' dia) Centrifuge

Non-human Hypergravity Facilities

- Chronic Hyper-gravity Exposure (24' dia) Centrifuge
- International Space Station Test-bed (8' dia) Centrifuge

Biocomputation Center

Ground-based Bed Rest Facility

Investigators are encouraged to submit detailed proposals explaining how they would exploit the unique capabilities of the hardware available at the Center.

Space Biomedical Investigators' Workshop

Sunday, January 10

4:00 pm - 8:00 pm	Registration	Prefunction Area of Conference Center
6:00 pm - 8:00 pm	Session Chairs and Co-Chairs Meeting	Salon D

Monday, January 11

7:30 am - 8:30 am	Registration continues	Prefunction Area of Conference Center
8:30 am - 11:15 am	Plenary Session	Salon B/E
8:30 am - 8:40 am	Workshop Overview and Goals	Alfred Coats
8:40 am - 8:45 am	Welcome	George Abbey
8:45 am - 8:55 am	Welcome	Joan Vernikos
8:55 am - 9:25 am	Welcome	Arnaud Nicogossian
9:25 am - 9:45 am	JSC, NASA Lead Center	Charles Stegemoeller
9:45 am - 10:25 am	NASA Critical Path Plan	Charles Sawin
10:25 am - 10:35 am	Break	Prefunction Area of Conference Center
10:35 am - 11:00 am	NASA Biomedical Research Resources – JSC	William Paloski
11:00 am - 11:25 am	Hypergravity Facilities: Extending Knowledge over the Continuum of Gravity	Kenneth Souza
11:25 am - 12:45 pm	Lunch	Marina Plaza
	Space Biomedical Research Needs – A Clinical Perspective	Sam Pool
12:45 pm - 6:00 pm	Scientific Sessions (see following pages)	
6:00 pm – 7:00 pm	Reception	Harbour Club

Tuesday, January 12

8:15 am - 10:25 am	Plenary Session	Salon B/E
8:15 am - 8:30 am	Status of Countermeasures	Kenneth Baldwin
8:30 am - 9:00 am	Strategy for Research for Space Biology and Medicine in the New Century	Mary Jane Osborn
		John Charles
9:00 am - 9:25 am	Mars Mission Scenario	Laurence Young
9:25 am - 9:45 am	The National Space Biomedical Research Institute	
9:45 am - 10:05 am	Scientific Session Summary – Barophysiology	
10:05 am - 10:25 am	Scientific Session Summary – Nutrition	
10:25 am - 10:35 am	Break	Prefunction Area of Conference Center
10:35 am - 12:30 pm	Scientific Sessions (see following pages)	
12:30 pm - 1:30 pm	Lunch/Technology Development I	Marina Plaza
1:30 pm - 6:00 pm	Scientific Sessions (see following pages)	
6:00 pm - 9:30 pm	Kemah Waterfront Restaurant Area (transportation provided)	

Wednesday, January 13

8:30 am - 9:10 am	Plenary Session	Salon B/E
8:30 am - 8:45 am	Laboratory Radiobiology Facilities for Space Radiation Research	Frank Cucinotta
		Paul DiZio
8:45 am - 9:00 am	Rotating Room Facility	
9:00 am – 9:10 am	Break	Prefunction Area of Conference Center
9:10 am - 12:05 pm	Scientific Sessions (see following pages)	
12:00 pm - 1:30 pm	Lunch/Technology Development II	Marina Plaza
1:30 pm - 5:30 pm	Plenary Session	Salon B/E
1:30 pm - 1:55 pm	Scientific Session Summary – Behavior Performance & Human Factors	
1:55 pm - 2:20 pm	Scientific Session Summary – Bone	
2:20 pm - 2:45 pm	Scientific Session Summary – Cardiovascular	
2:45 pm - 3:10 pm		
3:10 pm - 3:35 pm	Scientific Session Summary – Immunology/Infectious Disease/Hematology	
3:35 pm - 3:50 pm	Break	Prefunction Area of Conference Center
3:50 pm - 4:15 pm	Scientific Session Summary – Muscle	
4:15 pm - 4:40 pm	Scientific Session Summary – Neurovestibular	
4:40 pm - 5:05 pm	Scientific Session Summary – Radiation	
5:05 pm - 5:30 pm	Scientific Session Summary – Sleep/Circadian Rhythm	
6:30 pm - 9:00 pm	Dinner Banquet	Salon B
	Space Exploration in the Next Millenium	Dave Williams

BAROPHYSIOLOGY SCIENTIFIC SESSION**BACCARAT/STEUBEN****CHAIR, MICHAEL POWELL****CO-CHAIR, RICHARD VANN****MONDAY, JANUARY 11, 1999**

Barophysiology and Biophysics	<i>M.R. Powell</i>	12:45
An Understanding of Decompression Physiology Leads to Safer and More Efficient Extravehicular Activity (EVA)	<i>R.D. Vann, W.A. Gerth</i>	13:10
Staged Decompression to a 3.5 psi EVA Suit Using an Argon-Oxygen (ARGOX) Breathing Mixture	<i>A.A. Pilmanis, K.M. Krause, J.T. Webb, L.J. Petropoulos, N. Kannan</i>	13:35
Break	PREFUNCTION AREA	14:00
Role of Inflammatory Response in Experimental Decompression Sickness	<i>B.D. Butler, T. Little</i>	14:15
Quantitative Prediction of Pulmonary Oxygen Poisoning Stress in Human Exposures to Changing Degrees of Inspiratory Hyperoxia	<i>C. J. Lambertsen, J. M. Clark, E. Hopkin</i>	14:40

MONDAY, JANUARY 11, 1999**BOARD ROOM**

Chair Writing		15:10
Group Session		16:05
End of Session		17:30

TUESDAY, JANUARY 12, 1999

Barophysiology Summary	SALON B/E	9:50
------------------------	------------------	------

**BEHAVIOR, PERFORMANCE, AND HUMAN FACTORS I
SCIENTIFIC SESSION**

BACCARAT/STEUBEN

CHAIR, NICK KANAS

CO-CHAIR, BARBARA WOOLFORD

MONDAY, JANUARY 11, 1999

Stability and Precision of Performance During Space Flight	<i>J.V.Brady, T.H. Kelly, R.D. Hienz</i>	15:10
Monitoring and Correcting Autonomic Function Aboard Mir: NASA Technology Used in Space and on Earth to Facilitate Adaptation	<i>P. Cowings, W. Toscano, B. Taylor, C. DeRoshia, L. Kornilova, I. Koslovskaya, N. Miller</i>	15:35
NASA Performance Assessment Workstation: A Tool for Astronaut Cognitive Performance Evaluation	<i>R.E. Schlegel, R.L. Shehab, S.G. Schiflett, and D.R. Eddy</i>	16:00
Cognitive Performance Assessment with a Bed Rest Analog for Microgravity	<i>R.L. Shehab, R.E. Schlegel, S.G. Schiflett, D.R. Eddy</i>	16:25
Cognitive Performance in Seven Shuttle Astronauts	<i>D. R. Eddy, S. G. Schiflett, R. E. Schlegel, R. L. Shehab</i>	16:50
Effects of Promethazine on Performance During Simulated Shuttle Landings	<i>D.L. Harm, L. Putcha, B. K. Sekula, K. L. Berens</i>	17:15
End of Session		17:40

TUESDAY, JANUARY 12, 1999

Interactions of Crewmembers and Mission Control Personnel During Shuttle/Mir Missions	<i>N. Kanas, V. Salnitskiy, E. Grund, V. Gushin, O. Kozerenko, C. Marmar, A. Sled, D. Weiss</i>	10:35
Predictors of Behavior and Performance During Long Duration Space Missions: The Antarctic – Space Analog Program (ASAP)	<i>L.A. Palinkas, E.K.E. Gunderson, J.C. Johnson, A.W. Holland, C. Miller</i>	11:00
Review and Analysis of Diaries Maintained by the Leaders and Physicians of French Remote Duty Stations	<i>J. Stuster, C. Bachelard, P. Suedfeld</i>	11:25
Psychological Adaptation to Extreme Environments: Effects of Team Composition on Individual Adaptation	<i>J. Wood, S.J. Hysong, D.L. Lugg, D.L. Harm</i>	11:50
Lunch	MARINA PLAZA	12:15

BEHAVIOR, PERFORMANCE, AND HUMAN FACTORS II
SCIENTIFIC SESSION
BACCARAT/STEUBEN

CHAIR, BARBARA WOOLFORD

CO-CHAIR, NICK KANAS

TUESDAY, JANUARY 12, 1999

Mission Control Information Flow Issues	<i>B.S. Caldwell</i>	13:30
Neurophysiological Indices of Sustained Focused Attention: Application to Monitoring Cognitive Load, Operational Fatigue, and Other Environmental Stressors	<i>A. Gevins, M.E. Smith, L. McEvoy, H. Brown</i>	13:55
An EVA Suit Fatigue, Strength, and Reach Model	<i>J.C. Maida</i>	14:20
Break	PREFUNCTION AREA	14:45
Noninvasive Motion Capture and Analysis	<i>D. Metaxas</i>	15:00
Measuring Astronaut Performance in Microgravity: Loads and Modeling	<i>D. Newman, S. Beck, A. Amir, G. Baroni, G. Ferrigno, A. Pedotti</i>	15:25
End of Session		15:50

WEDNESDAY, JANUARY 13, 1999

Microgravity Workstation and Restraint Evaluations	<i>C. Chmielewski, M. Whitmore, F. Mount</i>	9:10
Evaluations of Three Methods for Remote Training	<i>B. Woolford, C. Chmielewski, A. Pandya, J. Adolf, M. Whitmore, A. Berman, and J. Maida</i>	9:35
Chair Writing		10:00
Group Session		11:00
Lunch	MARINA PLAZA	12:00
Behavior, Performance and Human Factors I&II Summaries	SALON B/E	13:30

BONE SCIENTIFIC SESSION**SALON C****CHAIR, JAY SHAPIRO****CO-CHAIR, EDWARD BROWN****MONDAY, JANUARY 11, 1999**

Altered Bone Cell Metabolism During Spaceflight	<i>R. T. Turner</i>	12:45
Developmental Regulation of the Collagenase-3 Promoter in Osteoblasts	<i>N.C. Partridge, Y. Yang, R.C. D'Alonzo, and S.K. Winchester</i>	13:15
Effect of Spaceflight on Extracellular Matrix in Osteoblasts Growth Activated Under Microgravity Conditions	<i>M.Hughes-Fulford, V. Gilbertson</i>	13:45
The Role of Calcium in the Response of Osteoblasts to Mechanical Stimulation	<i>R.L. Duncan, M.C. Farach-Carson and F.M. Pavalko</i>	14:15
Break	PREFUNCTION AREA	14:45
Common Molecular Events by Hormones and Mechanical Strain Regulate Insulin-Like Growth Factor-I Expression in Osteoblasts	<i>T.L. McCarthy, Y. Chen, C. Ji, M. Centrella</i>	15:00
Novel Receptor-Based Countermeasures to Microgravity-Induced Bone Loss	<i>B.W. O'Malley, C.L. Smith, N.L. Weigel, E.M. Brown</i>	15:30
The Effect of Skeletal Unloading on Bone Formation: Role of IGF-I	<i>D.D. Bikle, P. Kostenuik, E.M. Holton, B.P. Halloran</i>	16:00
Expression of Novel Gene Products Upregulated by Disuse Is Normalized by an Osteogenic Mechanical Stimulus: Evidence for the Molecular Basis of a Low Level Biomechanical Countermeasure for Osteoporosis?	<i>C. Rubin, J. Zhi, G. Xu, M. Cote, K. McLeod, M. Hadjiargyrou</i>	16:30
Transgenic Markers of Lineage Progression in Mechanically Loaded Bones	<i>I. Kalajic, J. Terzic, K. Mack, D. Visnjic, A. Mapta, G. Gronowicz, S. Clark, J. Yeh, D. Rowe</i>	17:00
End of Session		17:30

BONE SCIENTIFIC SESSION**SALON C****CHAIR, JAY SHAPIRO****CO-CHAIR, EDWARD BROWN****TUESDAY, JANUARY 12, 1999**

Bone Proteoglycan Changes During Skeletal Unloading	<i>M. Yamauchi, K. Uzawa, S. Pornprasertsuk, S. Arnaud, R. Grindeland, W. Grzesik</i>	10:35
Skeletal Structural Consequences of Reduced Gravity Environments	<i>C.B. Ruff, T.J. Beck, D. Newman, M. Oden, G. Shaffner, A. LeBlanc, L. Shackelford, N. Rianon</i>	11:05
Effects of Spaceflight on the Attachment of Muscles to the Tibia, Fibula and Calcaneus	<i>R.B. Johnson, A.K. Tsao, K.R. St. John, R.A. Betcher, M.A. Tucci, D.E. Parsell, X. Dai, L.D. Zardiackas, H.A. Benghuzzi</i>	11:35
Lunch	MARINA PLAZA	12:05
Femoral Vein Ligation Increases Bone Mass in the Hindlimb Suspended Rat	<i>A.P. Bergula, W. Huang, J.A. Frangos</i>	13:30
Effects of Spaceflight on Bone: The Rat as an Animal Model for Human Bone Loss	<i>B. Halloran, T. Weider, E. Morey-Holton</i>	14:00
Alterations in pQCT-Derived Bone Geometry and Density Versus Mechanical Structural Properties of the Femoral Neck in Senescent Rats	<i>S.A. Bloomfield, H.A. Hogan, E.T. Dresser, J.A. Groves</i>	14:30
The Effects of Partial Mechanical Loading and Ibandronate on Skeletal Tissues in the Adult Rat Hindquarter Suspension Model of Microgravity	<i>L. Schultheis, J. Shapiro, S. Bloomfield, N. Fedarko, M. Thierry-Palmer, C. Ruff, J. Ruiz</i>	15:00
Break	PREFUNCTION AREA	15:30
Non-Invasive Investigation of Bone Adaptation in Humans to Mechanical Loading	<i>R. Whalen</i>	15:45
Bone Loss in Space: Shuttle/Mir Experience and Bed Rest Countermeasure Program	<i>L.C. Shackelford, A. LeBlanc, A. Feiveson, V. Oganov</i>	16:15
Exercise Countermeasures for Bone Loss During Space Flight: A Method for the Study of Ground Reaction Forces and Their Implications for Bone Strain	<i>M. Peterman, J.L. McCrory, N.A. Sharkey, S. Piazza, P.R. Cavanagh</i>	16:45

BONE SCIENTIFIC SESSION**SALON C****CHAIR, JAY SHAPIRO****CO-CHAIR, EDWARD BROWN****TUESDAY, JANUARY 12, 1999**

Compact, High Precision, Multiple Projection DEXA Scanner for Measurement of Bone and Muscle Loss During Prolonged Spaceflight	<i>H.K. Charles, Jr., T.J. Beck, H.S. Feldmesser, T C. Magee, V.L. Pisacane</i>	17:15
Renal Stone Risk During Space Flight	<i>P.A. Whitson, R.A. Pietrzyk, C.F. Sams, C.Y.C. Pak, J.A. Jones</i>	17:45
End of Session		18:15

WEDNESDAY, JANUARY 13 1999

The Effects of Twelve Weeks of Bedrest on Bone Histology, Biochemical Markers of Bone Turnover, and Calcium Homeostasis in Eleven Normal Subjects	<i>J.E. Zerwekh, L.A. Ruml, F. Gottschalk, C.Y.C. Pak</i>	9:10
Bone Density and High Salt Diets in a Space Flight Model	<i>S.B. Arnaud, M. Navidi, M.T.C. Liang, I. Wolinsky</i>	9:40
Chair Writing		10:10
Group Session		11:10
Lunch	MARINA PLAZA	12:10
Bone Summary	SALON B/E	13:55

CARDIOVASCULAR SCIENTIFIC SESSION**SALON E****CHAIR, PETER RAVEN****CO-CHAIR, SUZANNE SCHNEIDER****MONDAY, JANUARY 11, 1999**

Mechanisms for Load Control of Cardiac Mass: Cell Culture Studies in Adult Cardiomyocytes Using a 3-D Collagen Matrix 3-D Collagen Matrix	<i>C. F. Baicu, J. H. Turner, V. D. Young, M. Barnes, M. R. Zile</i>	12:45
Myocardial Performance and Metabolism in Mice with a Null Mutation in Cytochrome C Oxidase Subunit VIaH	<i>N. B. Radford, B. Wan, L. Szczepaniak, E. E. Babcock, A. Richman, C. S. Storey, J. L. Li, K. Li, R.W. Moreadith</i>	13:10
Influence of Gravity on Blood Volume and Flow Distribution	<i>D. Pendergast, A. Olszowka, E. Bednarczyk, B. Shyoff, L. Farhi</i>	13:35
Autonomic Consequences of Microgravity Exposure	<i>D.L. Eckberg</i>	14:00
Postural Regulation of Muscle Sympathetic Nerve Activity Before and After Simulated and Actual Microgravity Deconditioning	<i>J.A. Pawelczyk, B.D. Levine, Neurolab Autonomic Team</i>	14:25
Break	PREFUNCTION AREA	14:50
Head-Out Water Immersion in the Primate as a Model for the Cardiovascular/Renal Effects of Microgravity	<i>K.G. Cornish, K. Hughes</i>	15:05
Potential Mechanism Leading to Impaired Thermoregulation Following Microgravity Exposure	<i>C.G. Crandall, R.A. Etzel</i>	15:30
Heart Rate Dynamics During Microgravity: Bedrest and Spaceflight Studies	<i>A.L. Goldberger</i>	15:55
The Effect of Cardiac Mechanics on Orthostatic Intolerance Following Bed Rest	<i>B. D. Levine</i>	16:20
Peripheral Vascular Hyporesponsiveness and Elevated Cerebro-Vascular Myogenic Tone in Simulated Microgravity: Role of Nitric Oxide-Dependent and -Independent Mechanisms	<i>R. E. Purdy, Y. Ding, S. P. Duckles, G. G., Geary, D. N. Krause, N. D. Vaziri, and S. D. Sangha</i>	16:45
Gender-Related Differences in Cardiovascular Responses to Orthostatic Stress	<i>J.M. Fritsch-Yelle, D.S. D'Aunno, W.W. Waters, S. Freeman-Perez</i>	17:10
End of Session		17:35

CARDIOVASCULAR SCIENTIFIC SESSION**SALON E****CHAIR, PETER RAVEN****CO-CHAIR, SUZANNE SCHNEIDER****TUESDAY, JANUARY 12, 1999**

Sympathetic Contributions to Orthostatic Tolerance and Vascular Tone Following Bed Rest	<i>J. K. Shoemaker, L.I. Sinoway</i>	10:35
Mechanisms Underlying Altered Arterial Baroreflex Function in Hindlimb Unloaded Rats	<i>E.M. Hasser, J.A. Moffitt, J.T. Cunningham, C.M. Heesch</i>	11:00
Dietary Calcium, Blood Pressure and Vascular Function Following Space Flight	<i>D. Hatton, D. McCarron, Q. Yue, C. Roullet, H. Xue, K. Otsuka, J. Chapman, T. Phanouvong, J. Roullet, M. Watanabe, K. Nilan, V. Haight, J. Dierckx, J. Demeritt</i>	11:25
Hydraulic and Computer Modeling of Cardiovascular Response to Weightlessness	<i>M. K. Sharp, G. M. Pantalos, K. J. Gillars, K. Peterson</i>	11:50
Lunch	MARINA PLAZA	12:15
Renal and Cardio-Endocrine Responses in Humans to Simulated Microgravity	<i>G.H. Williams, T. Mullen, C. Ramsdell</i>	13:30
Cardiovascular System Identification of Alterations in Cardiovascular Regulation During Simulated Space Flight	<i>T.J. Mullen, C.D. Ramsdell, G. Sundby, G.H. Williams, R.J. Cohen</i>	14:10
Non-Invasive Assessment of Susceptibility to Ventricular Arrhythmias During Simulated Space Flight	<i>T.J. Mullen, C.D. Ramsdell, G. Sundby, G.H. Williams, R.J. Cohen</i>	14:35
Vascular Reactivity in a Rat Model of Microgravity	<i>D. Berkowitz, L. Marucci, E. asplund, B. winters, A. Szumski, D. Nyhan, A. Shoukas</i>	15:00
Break	PREFUNCTION AREA	15:25
Computational Models of the Cardiovascular System and Its Response to Microgravity	<i>T. Heldt, E.B. Shim, R.G. Mark, R.D. Kamm</i>	15:40
Direct Cloning of Genes Regulated by Mechanical Load	<i>M. Abdellatif, M.D. Schneider</i>	16:05

CARDIOVASCULAR SCIENTIFIC SESSION**SALON E****CHAIR, PETER RAVEN****CO-CHAIR, SUZANNE SCHNEIDER****TUESDAY, JANUARY 12, 1999**

Evaluation of Thermoregulation After Spaceflight	<i>S.M. Schneider, W.J. Williams, J.E. Greenleaf, S.M.C. Lee, R. Gonzalez</i>	16:30
Exercise Training During +Gz Acceleration	<i>J.E. Greenleaf, J.L. Chou, S.R. Simonson, C.G.R. Jackson, P.R. Barnes</i>	16:55
Application of Acute Maximal Exercise to Enhance Mechanisms Underlying Blood Pressure Regulation and Orthostatic Tolerance After Exposure to Simulated Microgravity	<i>V.A. Convertino, K.A. Engelke, F. Doerr</i>	17:20
End of Session		17:45

WEDNESDAY, JANUARY 13, 1999

Carotid Baroreflex Function During Prolonged Exercise	<i>P.B. Raven</i>	9:10
Renal Sodium Handling After Exercise Induced Plasma Volume Expansion	<i>G. W. Mack, S. A. Kavouras, K. Nagashima</i>	9:35
Chair Writing		10:00
Group Session		11:00
Lunch	MARINA PLAZA	12:00
Cardiovascular Summary	SALON B/E	14:20

**IMMUNOLOGY, INFECTIOUS DISEASE, AND HEMATOLOGY
SCIENTIFIC SESSION**

SALON F

CHAIR, WILLIAM SHEARER

CO-CHAIR, GERALD SONNENFELD

MONDAY, JANUARY 11, 1999

Update on the Effects of Space Flight on Development of Immune Responses	<i>G. Sonnenfeld, M. Foster, D. Morton, F. Bailliard, N.A. Fowler, A.M. Hakenwewerth, R. Bates, E.S. Miller</i>	12:45
Study Design to Test the Hypothesis That Long-Term Space Travel Harms the Human and Animal Immune Systems	<i>W.T. Shearer, D.J. Lugg, H.D. Ochs, D.L. Pierson, J.M. Reuben, H.M. Rosenblatt, C. Sams, C.W. Smith, E.O. Smith, J.E. Smolen, D.F. Dinges, J.L. Mullington</i>	13:20
The Effect of Anti-Orthostatic Suspension on Delayed-Type Hypersensitivity Reactions	<i>S. Kanwar, J.E. Smolen, C.W. Smith</i>	13:55
Break	PREFUNCTION AREA	14:30
Determination of Whether Immune Clearance and Protection from Mucosal Virus Infection Are Altered in Ground-Based Mouse Models of Space Flight	<i>M.E. Conner</i>	14:50
Reactivation of Latent Viruses in Space	<i>D. L. Pierson, S. K. Mehta, S. K. Tying, D. J. Lugg</i>	15:25
Latent Viruses -- A Space Travel Hazard??	<i>P. D. Ling, R. S. Peng, D. Pierson, J. Lednicky, J. S. Butel</i>	16:00
Lytic Replication of Epstein-Barr Virus During Space Flight	<i>R. P. Stowe, D. L. Pierson, A. D. T. Barrett</i>	16:35
End of Session		17:10

TUESDAY, JANUARY 12, 1999

Neocytolysis: Mechanisms of Monitoring Neocytes	<i>C.P. Alfrey, L Rice, J. Trial, P. D. Kessler, B.J. Byrne</i>	10:35
Health Hazards in Closed Environments: Thermodegradation of Wire Insulation	<i>G. Oberdörster, J.N. Finkelstein, R. Gelein, P. Mercer, N. Corson, C.J. Johnston, B Weiss</i>	11:10

**IMMUNOLOGY, INFECTIOUS DISEASE, AND HEMATOLOGY
SCIENTIFIC SESSION**

SALON F

CHAIR, WILLIAM SHEARER

CO-CHAIR, GERALD SONNENFELD

TUESDAY, JANUARY 12, 1999

Inhibition of Erythropoiesis in Simulated Microgravity	<i>A.J. Sytkowski, K.L. Davis</i>	11:45
Lunch	MARINA PLAZA	12:20
Gene Regulation by Mechanical Forces in Vascular Cells	<i>L.V. McIntire</i>	13:30
Regulation of Epidermal Growth Factor by Gravity	<i>E.M. Durban</i>	14:05
New Strategies for the Detection of E.coli	<i>N. Elayan, Y. Xu, C. Theegala, A. Suleiman</i>	14:40
Break	PREFUNCTION AREA	15:15
Bacterial Biofilms in Microgravity	<i>B.H. Pyle, S.C. Broadaway, C.K. Johnsrud, R.T. Storfa, G.A. McFeters</i>	15:35
Rapid Assessment of Bacterial Activity in Spacecraft Water Systems	<i>J.T. Lisle, B.H. Pyle, S.C. Broadaway, G.A. McFeters</i>	16:10
End of Session		16:45

WEDNESDAY, JANUARY 13, 1999

Analysis of Mir Condensate and Potable Water	<i>L. M. Pierre, L. Bobe, N. N. Protasov, R. L. Sauer, J. R. Schultz, Y. E. Sinyak, V. M. Skuratov</i>	9:10
Microbial Monitoring Technology for Long Duration Space Flights	<i>G.E. Fox, J. Wibbenmeyer, M. Larios-Sanz, K. Kourentzi, J.C. Murphy, R.C. Willson</i>	9:45
Chair Writing		10:20
Group Session		11:20
Lunch	MARINA PLAZA	12:20
Immunology, Infectious Disease, and Hematology Summary	SALON B/E	15:10

MUSCLE SCIENTIFIC SESSION**SALON A****CHAIR, KENNETH BALDWIN****CO-CHAIR, DANIEL FEEBACK****MONDAY, JANUARY 11, 1999**

Ectopic Expression of Porcine HV-GHRH by a Synthetic Myogenic Vector Elicits Enhanced GH and IGF-1 Secretion and Animal Growth	<i>R. Draghia-Akli, D.R. Deaver, M.L. Fiorotto, R.J. Schwartz</i>	12:45
Molecular Signaling in Muscle Plasticity	<i>H.F. Epstein, S. Gordon, F.W. Booth, H. Rajadurai</i>	13:15
Myosin Heavy Chain Gene Expression in Developing Neonatal Skeletal Muscle: Involvement of the Nerve, Gravity, and Thyroid State	<i>K.M. Baldwin, G. Adams, F. Haddad, M. Zeng, A. Qin, L. Qin, S. McCue, P. Bodell</i>	13:45
Intracellular Calcium Transients in Mouse Soleus Muscle After Hindlimb Unloading and Reloading	<i>C.P. Ingalls, G.L. Warren, R.B. Armstrong</i>	14:15
Break	PREFUNCTION AREA	14:45
E Proteins Control Skeletal Muscle Fiber Type	<i>C. Neville, D. Gonzales, J. Purdy, Y. Zuang, N. Rosenthal</i>	15:05
Tissue Engineering Organs for Space Biology Research	<i>H.H. Vandenburg, J. Shansky, M. Del Tatto, P. Lee, J. Meir</i>	15:35
Impaired Utilization of Exogenous Substrates by Rat Skeletal Muscle After Hindlimb Suspension	<i>B.F. Lujan, L.A. Bertocci</i>	16:05
Mechanical and Inflammatory Components of Muscle Injury Following Modified Muscle Loading	<i>J. G. Tidball</i>	16:35
End of Session		17:05

TUESDAY, JANUARY 12, 1999

Activation of the Ubiquitin-Proteasome Pathway in Atrophying Muscles and Potential Inhibitors	<i>A.L. Goldberg, D. H. Lee, V. Solomon, S. Lecker</i>	10:35
Muscle Deoxygenation Causes Muscle Fatigue	<i>G. Murthy, A.R. Hargens, S. Lehman, D. Rempel</i>	11:05
Effects of Microgravity on the Accuracy of Elbow and Ankle Flexor and Extensor Motor Pools in Maintaining a Target Torque	<i>V.R. Edgerton, G.E. McCall, K.O. Fleischman, G.I. Boorman, C. Goulet, R.R. Roy</i>	11:35

MUSCLE SCIENTIFIC SESSION**SALON A****CHAIR, KENNETH BALDWIN****CO-CHAIR, DANIEL FEEBACK****TUESDAY, JANUARY 12, 1999**

Lunch	MARINA PLAZA	12:05
Alterations in Neuromuscular Junctions Associated with Muscle Atrophy Induced by Hindlimb Unloading	<i>D.R. Mosier, L. Siklós, C.L. Gooch, S. Gordon, F.W. Booth</i>	13:30
Quantifying Biomechanical Characteristics of Jumping Exercises in 1G and in Simulated and True Microgravity	<i>B.L. Davis, S.E. D'Andrea, G. Perusek, T. Orlando</i>	14:00
Weightlessness Reduces Skeletal Muscle Growth and Regeneration Potential	<i>E. Schultz, P.E. Mozdziak</i>	14:30
Break	PREFUNCTION AREA	
Alterations in Skeletal Muscle Function with Microgravity, and the Protective Effects of High Resistance Isometric and Isotonic Exercise	<i>R.H. Fitts, J.E. Hurst, K.M. Norenberg, J.J. Widrick, D.A. Riley, J.L.W. Bain, S.W. Trappe, T.A. Trappe, D.L. Costill</i>	15:20
Space Physiology Studies	<i>A.R. Hargens, R. E. Ballard, W. L. Boda, A. C. Ertl, S. M. Schneider, K. J. Hutchinson, S. M. Lee, G. Murthy, L. Putcha, D. E. Watenpaugh</i>	15:50
End of Session		16:20

WEDNESDAY, JANUARY 13, 1999

CO ₂ Accumulation in the Non-Conformal Helmet of the NASA Launch and Entry Suit During Simulated Unaided Egress	<i>M.C. Greenisen, P.A. Bishop, S.M.C. Lee, A. Moore, J. Williams</i>	9:10
<i>In Vivo</i> Noninvasive Analysis of Human Forearm Muscle Function and Fatigue: Applications to EVA Operations and Training Maneuvers	<i>L.K. Fotedar, T. Marshburn, M. J. Quast, D. L. Feedback</i>	9:40
Chair Writing		10:10
Group Session		11:10
Lunch	MARINA PLAZA	12:10
Muscle Summary	SALON B/E	15:50

NEUROVESTIBULAR SCIENTIFIC SESSION**SALON D****CHAIR, CHARLES OMAN****CO-CHAIR, MALCOLM COHEN****MONDAY, JANUARY 11, 1999**

Visually-Induced Adaptation in Gravity-Sensitive Properties of Primate Vestibulo-Ocular Reflex	<i>D.E. Angelaki, B. J. M. Hess</i>	12:45
Low-Frequency Otolith Function in Microgravity: A Re-Evaluation of the Otolith Tilt-Translation Reinterpretation (OTTR) Hypothesis	<i>S.T. Moore, B. Cohen, G. Clement, T. Raphan</i>	13:20
Otolith-Ocular Torsion Is Modified in Novel G States	<i>C.H. Markham, S.G. Diamond</i>	13:55
Break	PREFUNCTION AREA	14:30
Context-Specific Adaptation of Gravity-Dependent Vestibular Reflex Responses (NSBRI Neurovestibular Project 1)	<i>M. Shelhamer, J. Goldberg, L.B. Minor, W.H. Paloski, L.R. Young, D.S. Zee</i>	14:50
Sympathetic Efferent Activity Is Driven by Otolith Stimulation	<i>H. Kaufmann, I. Biaggioni, A. Voustantiuk, A. Diedrich, F. Costa, R. Clark, M. Gizzi, B. Cohen</i>	15:25
Self-Motion Perception Assessment by Real-Time Computer Generated Animations	<i>D.E. Parker</i>	16:00
End of Session		16:35

TUESDAY, JANUARY 12, 1999

Human Visual Orientation in Unfamiliar Gravito-Inertial Environments	<i>C. Oman, I. Howard, W. Shebilske, J. Taube, A. Beall</i>	10:35
Vision and Visual-Motor Coordination in Pitched Visual Environments	<i>R.B. Welch</i>	11:10
Mechanisms of Sensorimotor Adaptation to Centrifugation	<i>W.H. Paloski, S.J. Wood, G.D. Kaufman</i>	11:45
Lunch	MARINA PLAZA	12:20
Evidence for a Rapid Gain Change Mechanism That Regulates Human Postural Control Dynamics	<i>R. J. Peterka</i>	13:30

NEUROVESTIBULAR SCIENTIFIC SESSION**SALON D****CHAIR, CHARLES OMAN****CO-CHAIR, MALCOLM COHEN****TUESDAY, JANUARY 12, 1999**

The Effects of Long-Duration Spaceflight on Postflight Terrestrial Locomotion	<i>J.J. Bloomberg, A.P. Mulavara, P.V. McDonald, C.S. Layne, L.A. Merkle, H.S. Cohen, I.B. Kozlovskaya</i>	14:05
Roll-Tilt Perception Using a Somatosensory Bar Task	<i>F.O. Black, S.W. Wade, A. Arshi</i>	14:40
Break	PREFUNCTION AREA	15:15
A Methodology for Investigating Adaptive Postural Control	<i>P.V. McDonald, G.E. Riccio</i>	15:35
Anticipatory Postural Activity During Long-Duration Space Flight	<i>C. S. Layne, A.P. Mulavara, P.V. McDonald, C.J. Pruett, I.B. Koslovskaya, J.J. Bloomberg</i>	16:10
Application of Floquet Stability Analysis to Repeated Stepping in LD and Normal Subjects	<i>C. Wall III, D.E. Krebs</i>	16:45
End of Session		17:20

WEDNESDAY, JANUARY 13, 1999

Visual-Vestibular Responses During Space Flight	<i>M.F. Reschke, I.B. Kozlovskaya, W.H. Paloski</i>	9:10
Motor Control and Adaptation in a Rotating Artificial Gravity Environment	<i>P. DiZio, J.R. Lackner</i>	9:45
Chair Writing		10:20
Group Session		11:20
Lunch	MARINA PLAZA	12:20
Neurovestibular Summary	SALON B/E	16:15

NUTRITION SCIENTIFIC SESSION**LALIQUE ROOM****CHAIR, HELEN LANE****CO-CHAIR, T. PETER STEIN****MONDAY, JANUARY 11, 1999**

Fluid and Electrolyte Nutrition	<i>H.W. Lane, S.M. Smith, C.S. Leach, B.L. Rice</i>	12:45
Measurement of Body Composition for Nutritional Assessment in Space Flight	<i>D.A. Schoeller</i>	13:10
Protein-Energy Relationships During Space Flight	<i>T.P. Stein</i>	13:35
The Combined Effects of Inactivity and Cortisol on Muscle Protein Metabolism	<i>A.A. Ferrando, C.S. Stuart, R.R. Wolfe</i>	14:00
Calcium Kinetics During Space Flight	<i>S.M. Smith, M.E. Wastney, K.O. O'Brien, H.W. Lane</i>	14:25
Break	PREFUNCTION AREA	14:50
Dietary Oxalate and Its Influence on Urinary Oxalate Excretion	<i>R.P. Holmes, D.G. Assimos</i>	15:05
A Noninvasive Test for Gastric Emptying and Intestinal Absorption	<i>L.S. Welage, G.L. Amidon, J. Rhie, B.L. Neudec, S. Choe</i>	15:30
Salivary Pharmacodynamics and Bioavailability of Promethazine in Human Subjects	<i>L. Putcha, D.L. Harm, R. Nimmagudda, K.L. Berens, D.W.A. Bourne</i>	15:55
Food System Challenges for Long-Duration Space Missions	<i>J.B. Hunter</i>	16:20
Chair Writing		16:45
Group Session		17:30
End of Session		18:00

TUESDAY, JANUARY 12, 1999

Nutrition Summary	SALON B/E	10:10
-------------------	------------------	-------

RADIATION SCIENTIFIC SESSION**SALON B****CHAIR, AMY KRONENBERG****CO-CHAIRS, JACK MILLER, DAVID HUSO****MONDAY, JANUARY 11, 1999**

Information Needed to Make Radiation Protection Recommendations for Travel Beyond Low-Earth Orbit	<i>L.W. Townsend</i>	12:45
Risk Management Strategies During Solar Events	<i>R. Turner</i>	13:10
Radiation Measurements on the Russian Mir Orbital Station	<i>G.D. Badhwar</i>	13:35
Radiation Dosimetry on Manned Space Missions and at Ground-Based Accelerators	<i>E.V. Benton, E.R. Benton, A.L. Frank, M.F. Moyers</i>	14:00
Modulation of Radiogenic Damage by Microgravity: Results from STS-76	<i>G. Nelson, G. Kazarians, W. Schubert, R. Kern, D. Schranck, P. Hartman, A. Hlavacek, H. Wilde, D. Lewicki, E.V. Benton, E.R. Benton</i>	14:25
Break	PREFUNCTION AREA	14:50
Impact of Track Structure Effects on Shielding and Dosimetry	<i>J.W. Wilson, F.A. Cucinotta, W. Schimmerling, M.Y. Kim</i>	15:05
Simulation of Clusters of DNA Damage Induced by Ionizing Radiation Encountered in Spaceflight	<i>A. Chatterjee, W.R. Holley, I.S. Mian</i>	15:30
Non-Rejoined DNA Double-Strand Breaks in Human Cells. A Shift in RBE vs LET for HZE Iron Particles in Comparison with Low Energy Helium Particles	<i>B. Rydberg, P. Cooper</i>	15:55
Molecular and Chromosomal Damage and Mis-Repair in Human X Chromosomes	<i>M.C. Muhlmann-Diaz, M. Loebrich, B. Rydberg, P.K. Cooper, J.S. Bedford</i>	16:20
Analysis of Incomplete Chromosomal Exchanges Using Fluorescence <i>in situ</i> Hybridization with Telomere Probes	<i>H. Wu, K. George, T.C. Yang</i>	16:45
Mutagenic Effects of ⁵⁶ Fe Radiation on Cultured Mammalian Cells	<i>M. Lenarczyk, A. Ueno, D. Vannais, R. Warters, J. Roberts, A. Kronenberg, T. Hei, C. Waldren</i>	17:10
End of Session		17:35

RADIATION SCIENTIFIC SESSION**SALON B****CHAIR, AMY KRONENBERG****CO-CHAIRS, JACK MILLER, DAVID HUSO****TUESDAY, JANUARY 12, 1999**

Genetic Regulation of Charged Particle Mutagenesis in Human Cells	<i>A. Kronenberg, S. Gauny, C. Cherbonnel-Lasserre, W. Liu, C. Wiese</i>	10:35
Heavy Ion Induced Genetic Damage in Transgenic Animals	<i>P. Y. Chang, L. Lutze-Mann, V. Walker, D. Torous, R. A. Winegar</i>	11:00
Characterization of Trefoil Peptide Genes in Iron-Ion or X-Irradiated Human Cells	<i>E.K. Balcer-Kubiczek, G.H. Harrison, J.F. Xu, X.F. Zhou</i>	11:25
DNA Repair-Protein Relocalization After Heavy Ion Exposure	<i>N.F. Metting</i>	11:50
Lunch	MARINA PLAZA	12:15
Comparison of Gamma and Iron Particle Irradiation Induced Remodeling of Extracellular Matrix in Murine Liver	<i>M.H. Barcellos-Hoff, C. Wang, S.A. Ravani</i>	13:30
NSBRI Radiation Effects: Carcinogenesis in Sprague-Dawley Rats Irradiated with Iron Ions, Protons, or Photons	<i>J.F. Dicello, F.A. Cucinotta, D.S. Gridley, S.P. Howard, G. R. Novak, R. Ricart-Arbona, J. D. Strandberg, M.E. Vazquez, J.R. Williams, Y. Zhang, H. Zhou, D.L. Huso</i>	13:55
Cytogenetic Damage From Photons, Fe-Ions and Protons: Modulation by Dose-Rate and Cell Type	<i>J.R. Williams, Z. Houming, J.F. Dicello, Y. Zhang</i>	14:20
Quantitation of Radiation Induced Deletion and Recombination Events Associated with Repeated DNA Sequences	<i>R.R. Sinden, J.R. Ford, L.A. Braby</i>	14:45
Break	PREFUNCTION AREA	15:10
Proton Irradiation Alters Expression of FGF-2 in Human Lens Epithelial Cells	<i>E.A. Blakely, K.A. Bjornstad, P.Y. Chang, M.P. McNamara, E. Chang</i>	15:25
Aminothiols Induced Modulation of P53 Protein Activity in Human Cells	<i>R.L. Warters, D.K. Thai, J.C. Roberts, D.K. Gaffney, A.E. Cress</i>	15:50

RADIATION SCIENTIFIC SESSION**SALON B****CHAIR, AMY KRONENBERG****CO-CHAIRS, JACK MILLER, DAVID HUSO****TUESDAY, JANUARY 12, 1999**

Some Behavioral Effects of Exposure to Low Doses of ^{56}Fe Particles	<i>B.M. Rabin, J.A. Joseph, B. Shukitt-Hale</i>	16:15
Cooperative Research in Proton Space Radiation	<i>G.A. Nelson, J.M. Slater, J.O. Archambeau, L.M. Green, D.S. Gridley, G.A. Abell, M.M. Moyers, G.A. Coutrakon</i>	16:40
End of Session		17:05

WEDNESDAY, JANUARY 13, 1999

Accelerator-Based Studies of Heavy Ion Interactions Relevant to Space Biomedicine	<i>J. Miller, L. Heilbronn, C. Zeitlin</i>	9:10
Portable Real Time Neutron Spectrometry	<i>R.H. Maurer, D.R. Roth, R. Fainchtein, J.O. Goldsten, J.D. Kinnison, A.K. Thompson</i>	9:35
Chair Writing		10:00
Group Session		11:00
Lunch	MARINA PLAZA	12:00
Radiation Summary	SALON B/E	16:40

SLEEP/CIRCADIAN RHYTHM SCIENTIFIC SESSION**LALIQUE ROOM****CHAIR, DAVID DINGES****CO-CHAIR, CHARLES CZEISLER****TUESDAY, JANUARY 12, 1999**

Introduction to Scientific Session Agenda	<i>D.F. Dinges</i>	10:35
The Effects of Gravity on the Circadian Timing System	<i>C.A. Fuller</i>	10:45
Gender Differences in the Responses of Rhesus Monkeys to 2G	<i>L.K. Barger, C.A. Fuller</i>	11:10
Brn 3.1 Knockouts Affect the Vestibular, Autonomic, and Circadian Rhythm Responses to 2G Exposure	<i>D.M. Murakami, L. Erkman, M.G. Rosenfeld, C.A. Fuller</i>	11:35
Lunch	MARINA PLAZA	12:00
Sleep and Circadian Rhythms in Four Orbiting Astronauts	<i>T.H. Monk, D.J. Buysse, B.D. Billy, K.S. Kennedy, L.M. Willrich</i>	13:10
Ambient Light Intensity, Actigraphy, Sleep and Respiration, Circadian Temperature and Melatonin Rhythms and Daytime Performance of Crew Members during Space Flight on STS-90 and STS-95 Missions	<i>C.A. Czeisler, D-J. Dijk, D.F. Neri, R.J. Hughes, J.M. Ronda, J.K. Wyatt, J.B. West, G.K. Prisk, A.R. Elliott, L.R. Young</i>	13:35
Break	PREFUNCTION AREA	14:00
Introduction to NSBRI Sleep and Chronobiology Team	<i>C.A. Czeisler</i>	14:15
Circadian Entrainment, Sleep-Wake Regulation and Neurobehavioral Performance Under the Simulated Lighting Conditions of Long-Duration Space Missions	<i>K.P. Wright Jr., M.E. Jewett, E.B. Klerman, R.E. Kronauer, C.A. Czeisler</i>	14:25
Countermeasures to Neurobehavioral Deficits from Cumulative Partial Sleep Deprivation During Space Flight	<i>D.F. Dinges, H.P.A. Van Dongen, G. Maislin, J. Mullington</i>	14:50
Electroencephalographic and Ocular Correlates of Neurobehavioral Performance Decrements	<i>D-J. Dijk, C. Cajochen</i>	15:15
Dynamic Assessment of Circadian Phase and Amplitude Under the Simulated Lighting Conditions of Long-Duration Space Missions	<i>E.N. Brown, H.H. Luithardt, K.P. Wright Jr., C.A. Czeisler</i>	15:40
Ground and Flight Evaluation of "Principal Investigator in a Box"	<i>G. Callini, S.M. Essig, D. Heher, L.R. Young</i>	16:05

SLEEP/CIRCADIAN RHYTHM SCIENTIFIC SESSION**LALIQUE ROOM****CHAIR, DAVID DINGES****CO-CHAIR, CHARLES CZEISLER****TUESDAY, JANUARY 12, 1999**

Neuroendocrine and Neuroimmune Modulation by Sleep Deprivation	<i>J. Mullington, M. Carlin, S. Kapoor, N. Price, M. Szuba, R. Schwartz, W. Shearer, J. Butel, D.F. Dinges</i>	16:30
Final Comments	<i>D.F. Dinges, C.A. Czeisler</i>	16:55
End of Session		17:30

WEDNESDAY, JANUARY 13, 1999

Introduction to Scientific Session Agenda	<i>C.A. Czeisler</i>	9:10
Sleep Restriction Effects on Cardiovascular Regulation	<i>M.L. Smith, D.E., Watenpaugh, N. Muentner, S.L. Wasmund, W.L. Wasmund, R. Carter, III</i>	9:15
Melatonin as a Countermeasure for Entrainment to the Sleep/Wake Schedules Required During Shuttle Missions	<i>B.S. S.Khalsa, D.-J. Dijk</i>	9:45
Chair Writing		10:25
Group Session		11:25
Lunch	MARINA PLAZA	12:05
Sleep/Circadian Rhythm Summary	SALON B/E	17:05

TECHNOLOGY DEVELOPMENT I**TUESDAY, JANUARY 12, 1999****MARINA PLAZA****12:00 - 13:30**

Sensors 2000! Program: Advanced BioSensor and
Measurement Systems Technologies for Spaceflight
Research and Concurrent, Earth-based Applications

J. Hines

BIONA-C Cell Culture pH Monitoring System

C. Friedericks

Physiological Signal Conditioner

C. Friedericks

BION-11 Spaceflight Mission

M. Skidmore

Neurolab Biotelemetry System (NBS)

J. Schonfeld

Biotelemetry

C. Mundt

NASA Ames Research Center R&D Services Directorate
Biomedical Systems Development

J. Pollitt, K. Flynn

Life Sciences Division Spaceflight Hardware

B. Yost

TECHNOLOGY DEVELOPMENT II**WEDNESDAY, JANUARY 13, 1999****MARINA PLAZA****12:00 - 13:30**

Miniature Time-of-Flight Mass Spectrometer

R.S. Potember, W.A. Bryden, M. Antoine, P. Scholl, H. Ko, V.L. Pisacane, M. Leonardo, R.J. Cotter

New Techniques for the Non-Invasive Imaging of Tissue Perfusion

D.A. Sherman, R.H. Rubin, R.J. Cohen

User Friendly Instrumentation for Non-Invasive Assessment of Alterations of Cardiovascular Regulation Associated with Space Flight

R.J. Cohen, N. Iyengar, T.J. Mullen, C.D. Ramsdell, G. Sundby

Digital Echocardiography on the International Space Station: Technical Progress and Experimental Planning

J.D. Thomas, N.L. Greenberg, T. Shiota, L. Cardon, M.J. Garcia

Laser-Polarized Noble Gas Magnetic Resonance

R.L. Walsworth, M.S. Albert, D.G. Cory, F.W. Hersman, D.P. Hinton, D. Hoffmann, F.A. Jolesz, R.W. Mair, S. Patz, S. Peled, V. Pomeroy, C.H. Tseng, G.P. Wong

Wireless Augmented Reality Prototype (WARP)

A.S. Devereaux

Miniature Quadrupole Mass Spectrometer Array

D. Karmon, M. Darrech, A. Chutjian, D. Jan

Attendees

Abdellatif, Maha, PhD
 Mail Code 506C
 Baylor College of Medicine
 One Baylor Plaza
 Houston TX 77030
 E-mail: mahaa@bcm.tmc.edu
 Work: 713-798-6683
 Fax: 713-798-7437

Alford, Bobby R., MD
 National Space Biomedical Research
 Institute
 NA 102
 One Baylor Plaza
 Houston TX 77030
 E-mail: balford@bcm.tmc.edu
 Work: 713-798-5906
 Fax: 713-798-3403

Alfrey, Clarence P. MDPH
 Professor of Medicine
 M902
 Baylor College of Medicine
 Department of Medicine
 Hematology/Oncology
 Methodist Hospital 930
 6565 Fannin
 Houston TX 77030
 E-mail: calfrey@bcm.tmc.edu
 Work: 713-790-2158
 Fax: 713-790-0828

Angelaki, Dora E. PhD
 Associate Professor
 University of Mississippi Medical
 Center
 Department of Surgery
 (Otolaryngology)
 2500 North State Street
 Jackson MS 39216
 E-mail: dea@umsmed.edu
 Work: 601-984-5090
 Fax: 601-984-5107

Arnaud, Sara B., MD
 MS 239-11

NASA Ames Research Center
 Moffett Field CA 94035-1000
 Work: 650-604-6561

Badhwar, Gautam D. PhD
 Senior Scientist
 SN
 Nasa Johnson Space Center
 2101 Nasa Road One
 Houston TX 77058
 E-mail: gbadhwar@ems.jsc.nasa.gov
 Work: 281-483-5065
 Fax: 281-483-5276

Baicu, Catalin F., PhD
 Postdoctoral Fellow
 Medical University of South
 Carolina
 Gazes Cardiac Research Institute
 114 Doughty Street
 Charleston SC 29403
 E-mail: baicuc@musc.edu
 Work: 843-577-5011, ex. 6826
 Fax: 843-953-6473

Balcer-Kubiczek, Elizabeth K. PhD
 Associate Professor
 University of Maryland School of
 Medicine
 Department of Radiation Oncology
 655 West Baltimore St.
 Bressler Research Building,
 BRB6-015
 Baltimore MD 21201
 E-mail: ekubicze@umaryland.edu
 Work: 410-706-7133
 Fax: 410-706-6138

Baldwin, Kenneth M. PhD
 Professor
 University of California Irvine
 College of Medicine
 Department of Physiology &
 Biophysics
 Cheney Hall, Room D-352
 Medical Science I
 Irvine CA 92697
 E-mail: kenbaldwi@uci.edu
 Work: 949-824-7192
 Fax: 949-824-8540

Barcellos-Hoff, Mary Helen PhD
Staff Scientist
MS 74-157
Lawrence Berkeley National
Laboratory
Department of Radiation Biology
One Cyclotron Road
Bldg. 74
Berkeley CA 94720
E-mail: mhbarcellos-hoff@lbl.gov
Work: 510-486-6371
Fax: 510-486-6746

E-mail: bedford@cvms.colostate.edu
Work: 970-491-7492
Fax: 970-491-7742

Benton, Eric PhD
Eril Research Inc.
P.O. Box 150788
San Rafael CA 94915-0788
E-mail: eric@physics.usfca.edu
Work: 415-386-0254
Fax: 415-422-2469

Barger, Laura K. PhD
Graduate Student
Department of Neurobiology,
Physiology & Behavior
311 Franklin Street
Alexandria VA 22314
E-mail: lkbarger@ucdavis.edu
Work: 703-535-3284
Fax: 703-535-3284

Berkowitz, Dan E. MD
Assistant Professor
Johns Hopkins Medical Institutions
Dept. of Anesthesiology and
Critical Care Medicine
Tower 711
600 N. Wolfe Street
Baltimore MD 21287
E-mail: dberkowi@jhmi.edu
Work: 410-955-7519
Fax: 410-955--0994

Bartok-Olson, Cynthia PhD
Graduate Research Assistant
Department of Nutritional Sciences
University of Wisconsin
Room 340B, Nutritional Sciences
1415 Linden Drive
Madison WI 53706
E-mail: bolson@nutrisci.wisc.edu
Work: 608-263-5477

Bertocci, Loren A. PhD
Director of Biochemistry
Presbyterian Hospital of Dallas
Institute for Exercise and
Environmental Medicine
7232 Greenville Avenue, Suite 435
Dallas TX 75231
E-mail: bertoc1@phscare.org
Work: 214-345-4624
Fax: 214-345-4618

Beck, Thomas, ScD
Johns Hopkins Outpatient Center
Department of Radiology
601 N. Charles Street
Baltimore MD 21287-0849
E-mail: tjbeck@rad.jhu.edu
Work: 410-955-2684
Fax: 410-614-1977

Bielitzki, Joseph T. DVM
Chief Veterinary Officer
MS-261-1
NASA Ames Research Center
Building 261, Room 111
Moffett Field CA 94035-1000
E-mail:
jbielitzki@mail.arc.nasa.gov
Work: 650-604-1121
Fax: 650-604-0046

Bedford, Joel S. PhD
Professor
Colorado State University
Department of Radiological Health
Sciences
MRB Building, Rm 439
Fort Collins CO 80523-1673

Bikle, Daniel D. MD, PhD
 Professor of Medicine
 VA Medical Center
 Endocrine Unit (111N)
 4150 Clement St.
 San Francisco CA 94121
 E-mail: doctor@itsa.ucsf.edu
 Work: 415-221-4810 ext. 3338
 Fax: 415-750-6929

Black, F. Owen MD
 Director, Neurology Research
 Legacy Health System
 Legacy Good Samaritan Hospital
 P.O. Box 3950
 1225 NE 2nd Avenue (Federal
 Express)
 Portland OR 97232
 E-mail: bof@ix.netcom.com
 Work: 503-413-5353
 Fax: 503-413-5348

Blakely, Eleanor A. PhD
 Senior Staff Biophysicist
 MS 70A-1118
 Lawrence Berkeley National
 Laboratory
 One Cyclotron Road
 Berkeley CA 94720
 E-mail: eablakely@lbl.gov
 Work: 510-486-6595
 Fax: 510-486-4475

Blomqvist, C. Gunnar MDPhD
 Professor of Internal Medicine and
 Physiology
 Univ. Texas Southwestern Medical
 Center
 Cardiology 122
 5323 Harry Hines Boulevard
 H8.122
 Dallas TX 75235-9034
 E-mail:
 carl.blomqvist@email.swmed.edu
 Work: 972-648-3425
 Fax: 972-648-2036

Bloomberg, Jacob J. PhD
 Senior Research Physiologist
 SD3

NASA Johnson Space Center
 Bldg. 37, Room 164
 2101 Nasa Road One
 Houston TX 77058
 E-mail: jbloombe@ems.jsc.nasa.gov
 Work: 281-483-0436
 Fax: 281-244-5734

Bloomfield, Susan A. PhD
 Asst. Professor
 Mail Stop 4243
 Texas A&M University
 Dept. of Health and Kinesiology
 College Station TX 77843-4243
 E-mail: sbloom@tamu.edu
 Work: 409-862-1181
 Fax: 409-847-8987

Borak, Thomas PhD
 Professor
 Colorado State University
 Department of Radiological Health
 Sciences
 308 MRB
 Fort Collins CO 80523
 E-mail: tborak@vines.colostate.edu
 Work: 970-491-6450
 Fax: 970-491-0623

Brady, Joseph V. PhD
 Professor of Behavioral Biology
 Institutes for Behavior Resources,
 Inc. (IBR)
 The Johns Hopkins University School
 of Medicine
 333 Cassell Drive, Suite 2200
 Behavioral Biology Research center
 Baltimore MD 21224
 E-mail: jvb@jhmi.edu
 Work: 410-550-2779
 Fax: 410-550-2780

Brooks-Asplund, Esther PhD
 Proctoral Fellow
 The Johns Hopkins School of
 Medicine
 624 Traylor
 720 Rutland Avenue
 Baltimore MD 21205

E-mail: easplund@bme.jhu.edu
Work: 410-955-3239
Fax: 410-614-0019

Fax: 713-798-5019

Brown, Edward M. MD
Professor of Medicine
Brigham and Women's Hospital
Harvard Medical School
Endocrine-Hypertension Division
221 Longwood Avenue
Boston MA 02115
E-mail:
embrown@bics.bwh.harvard.edu
Work: 617-732-5661
Fax: 617-732-5764

Butler, Bruce D. Ph.D.
Professor, Director of Research
University of Texas - Houston
Medical School
Dept. of Anesthesiology
6431 Fannin
MSB 5020
Houston TX 77030
E-mail:
bbutler@anes1.med.uth.tmc.edu
Work: 713-500-6231
Fax: 713-500-0759

Brown, Emery N. MD, PhD
Harvard University School of
Medicine
Massachusetts General Hospital
Dept. of Anesthesia and Critical
Care
Clinics 3
32 Fruit Street
Boston MA 02114-2698
E-mail: brown@srlb.mgh.harvard.edu
Work: 617-726-8786
Fax: 617-726-8410

Caldwell, Barrett S. PhD
University of Wisconsin - Madison
Industrial Engineering
1513 University Avenue
Madison WI 53706
E-mail: caldwell@engr.wisc.edu
Work: 608-262-2414
Fax: 608-262-8454

Buderer, Mel C. PhD
SM3
NASA Johnson Space Center
2101 Nasa Road One
Bldg 36 Room 144
Houston TX 77058
E-mail: mbuderer@ems.jsc.nasa.gov
Work: 281-483-7338
Fax: 281-244-5332

Cardon, Lisa
Cleveland Clinic Foundation
Department of Cardiology F-15
9500 Euclid Avenue
Cleveland OH 44195

Butel, Janet S. PhD
Distinguished Service Professor
Mail Station 739E
Baylor College of Medicine
Head, Division of Molecular
Virology, BCMA-737E
One Baylor Plaza
Houston TX 77030
E-mail: jbutel@bcm.tmc.edu
Work: 713-798-3003

Cavanagh, Peter R. PhD
Distinguished Professor
Pennsylvania State University
Center for Locomotion Studies
29 Recreation Building
University Park PA 16802
E-mail: prc@psu.edu
Work: 814-863-0995
Fax: 814-863-4755

Chang, Polly PhD
SRI International
333 Ravenswood Avenue
Menlo Park CA 94025
E-mail: pchang@mail.sri.com
Work: 650-859-2549
Fax: 650-859-2889

Charles, Harry K. Jr, PhD
Assistant Department Head for
Engineering
Johns Hopkins University
Applied Physics Laboratory
Energy and Fabrication Branch
Office
Building 13-N312
11100 Johns Hopkins RD
Laurel MD 20823-6099
E-mail: harry_charles@jhuapl.edu
Work: 240-228-8050
Fax: 240-228-6119

Charles, John B. PhD
Manager, Planning and Integration
Mail Code SL
NASA Johnson Space Center
Discipline Scientist, Human Life
Sciences, STS-95
2101 NASA Road One
Houston TX 77058
E-mail:
john.b.charles1@jsc.nasa.gov
Work: 281-483-7224
Fax: 281-483-6636

Chatterjee, Alope PhD
Deputy Head, Life Sciences
MS 29-100
Lawrence Berkeley National
Laboratory
Life Sciences Division
One Cyclotron Road
Berkeley CA 94720
E-mail: A_chatterjee@lbl.gov
Work: 510-486-5415
Fax: 510-486-6949

Clark, Jonathan MD
SD2
NASA Johnson Space Center
2101 Nasa Road One
Houston TX 77058
E-mail: jbclark@ems.jsc.nasa.gov
Work: 281-483-7120
Fax: 281-244-7947

Clark, Laurel B. MD

Code CB
NASA Johnson Space Center
2101 NASA Road 1
Houston TX 77058
E-mail:
laurel.b.clark1@jsc.nasa.gov
Work: 281-244-8721
Fax: 281-244-8543

Clarke, Mark PhD
Staff Scientist
SD3/USRA
Division of Space Life Sciences
3600 Bay Area Boulevard
Houston TX 77058
E-mail:
mark.s.clarke1@jsc.nasa.gov
Work: 281-483-7253
Fax: 281-483-3058

Clement, Gilles PhD
UMR 5549 - Faculte De Medecine
CNRS Cerveau Et Cognition
133 Route de Narbonne
Toulouse Cedex 31062
France
E-mail: gclement@cerco.ups-tlse.fr
Work: 33-562-173-779
Fax: 33-562-17-28-09

Coats, Alfred MD
Director
USRA
Division of Space Life Sciences
3600 Bay Area Blvd.
Houston TX 77058
E-mail: coats@lpi.jsc.nasa.gov
Work: 281-486-2012
Fax: 281-244-2006

Cohen, Bernard MD
Morris Bender Professor of
Neurology
Mount Sinai School of Medicine
One Gustave L. Levy Place
Department of Neurology
Box 1135
One East 100th Street
New York NY 10029

E-mail: bcohen@smtplink.mssm.edu
Work: 212-241-7068
Fax: 212-831-1610

Cohen, Malcolm M. PhD
Research Scientist
Mail Stop 239-11
NASA-Ames Research Center
Life Sciences Division
Moffett Field CA 94035-1000
E-mail: mmcohen@mail.arc.nasa.gov
Work: 650-604-6441
Fax: 650-604-3954

Cohen, Richard J. MDPhD
Whitaker Professor of Biomedical
Engineering
Massachusetts Institute of
Technology
Division of Health Sciences and
Technology
Room E-25-335
77 Massachusetts Avenue
Cambridge MA 02139-4307
E-mail: rjcohen@mit.edu
Work: 617-965-9721
Fax: 617-253-3019

Conner, Margaret E. PhD
Assistant Professor of Molecular
Virology
Baylor College of Medicine
One Baylor Plaza
Room 936
Houston TX 77030
E-mail: mconner@bcm.tmc.edu
Work: 713-798-3590
Fax: 713-798-3586

Conrad, Kevin MD
Physician
Ochsner Clinic
1514 Jefferson Highway
New Orleans LA 70121
E-mail: kmconrad@earthlink.net
Work: 504-488-8234

Convertino, Victor A. PhD
Research Physiologist
US Army Institute of Surgical
Research
3400 Rawley E. Chambers Avenue
Bldg. 3611
Fort Sam Houston TX 78234-6315
E-mail:
victor.convertino@cs.amedd.army.mil
Work: 210-916-5633
Fax: 210-227-8502

Cornish, Kurtis G. PhD
Associate Professor of Physiology
University of Nebraska College of
Medicine
Dept. Physiology and Biophysics
600 South 42nd Street
Omaha NE 68198-4575
E-mail: kgcornis@mail.unmc.edu
Work: 402-559-4372
Fax: 402-559-4438

Cowings, Patricia S. PhD
Research Scientist
Mail Stop 239-16
NASA Ames Research Center
Life Sciences Division
Gravitational Research Branch
Moffett Field CA 94035-1000
E-mail: pcowings@mail.arc.nasa.gov
Work: 415-604-5724
Fax: 415-604-1484

Crandall, Craig G. PhD
Assistant Professor
Institute for Exercise and
Environmental Medicine
Presbyterian Hospital of Dallas
7232 Greenville Avenue
Dallas TX 75231
E-mail: Crandall@utsw.swmed.edu
Work: 214-345-4623
Fax: 214-345-4618

Crouch, Roger PhD
Lead Scientist, Office of Life and
Microgravity Sciences
Code U

NASA Headquarters
300 E. Street SW
Washington DC 20546
E-mail: rcrouch@hq.nasa.gov
Work: 202-358-0689
Fax: 202-358-2886

Cucinotta, Francis A. PhD
Senior Research Scientist
SN3
NASA Johnson Space Center
Division of Space Life Sciences
2101 Nasa Road One
Bldg. 31 Room 266
Houston TX 77058
E-mail: FCucinot@ems.jsc.nasa.gov
Work: 281-483-0968
Fax: 281-483-5276

Czeisler, Charles A. PhDMD
Professor of Medicine
Harvard Medical School/Brigham &
Women's Hospital
Circadian Neuroendocrine & Sleep
Disorders Section
221 Longwood Avenue, Room 438A
Boston MA 02115
E-mail:
caczeisler@grc.bwh.harvard.edu
Work: 617-732-4013
Fax: 617-732-4015

Daunton, Nancy G. PhD
Mail Stop 261-3
NASA Ames Research Center
Gravitational Research Branch
Moffett Field CA 94035-1000
E-mail: ndaunton@mail.arc.nasa.gov
Work: 650-604-4818
Fax: 650-604-0046

Davis, Brian L. PhD
Associate Staff
MC WB3
The Cleveland Clinic Foundation
Department of Biomedical
Engineering
9500 Euclid Avenue
Cleveland OH 44195

E-mail: davis@bme.ri.ccf.org
Work: 216-444-1055
Fax: 216-444-9198

Dawson, David L. MD
NASA Johnson Space Center
2101 Nasa Road One
Houston TX 77058
E-mail: dldawson@ems.jsc.nasa.gov
Work: 281-483-7329
Fax: 281-483-2224

Devereaux, Ann PhD
MS 238-420
Jet Propulsion Laboratory
4800 Oak Grove Drive
Pasadena CA 91109-8099
E-mail: devereaux@jpl.nasa.gov
Work: 818-354-5154
Fax: 818-354-6825

Diamond, Shirley G. PhD
Research Associate
UCLA School of Medicine
Department of Neurology, RNRC
710 Westwood Plaza
Los Angeles CA 90095-1769
E-mail: diamond@psych.ucsb.edu
Work: 310-825-6578
Fax: 310-825-0930

Dicello, John F. PhD
Director of Medical Physics
The Johns Hopkins University School
of Medicine
Division of Radiation Oncology
Center
Room B1-170
600 North Wolfe Street
Baltimore MD 21287-8922
E-mail: diceljo@jhmi.edu
Work: 410-614-4194
Fax: 410-955-3691

Dinges, David F. PhD
Professor and Director
University of Pennsylvania School
of Medicine
Unit for Experimental Psychiatry

Department of Psychiatry
 1013 Blockley Hall
 423 Guardian Drive
 Philadelphia PA 19104
 E-mail: dinges@mail.med.upenn.edu
 Work: 215-898-9949
 Fax: 215-573-6410

DiZio, Paul PhD
 MS 033
 Ashton Graybiel Spatial Orientation
 Laboratory
 Vler Center for Complex Systems
 Brandeis University
 Waltham MA 02254-9110
 E-mail: dizio@brandeis.edu
 Work: 781-736-2033
 Fax: 781-736-2031

Duncan, Randall L. PhD
 Assistant Professor of Orthopaedic
 Surgery
 Indiana University School of
 Medicine
 Department of Orthopaedic Surgery
 Clinical Building, Suite 600
 541 Clinical Drive
 INDIANAPOLIS IN 46202-5111
 E-mail: rduncan@iupui.edu
 Work: 317-278-3482
 Fax: 317-278-3483

Durban, Elisa M. Ph.D.
 Associate Professor
 University of Texas Houston HSC
 Dental Branch
 Division of Oral Biology,
 Room 4.131
 Department of Stomatology
 P. O. Box 20068
 Houston TX 77035
 E-mail:
 edurban@mail.db.uth.tmc.edu
 Work: 713-500-4414
 Fax: 713-500-4416

Eckberg, Dwain L. MD
 Professor of Medicine & Physiology
 Veterans Affairs Medical Center,

Richmond
 Medical College of Virginia at
 Virginia Commonwealth University
 Hunter Holmes McGuire Department of
 Veterans Affairs Medical Center
 1201 Broad Rock Boulevard
 Research 151, Room 3C-126
 Richmond VA 23249
 E-mail: deckberg@aol.com
 Work: 804-675-5776
 Fax: 804-231-4493

Epstein, Henry F. MD
 Professor of Neurology
 Mail Stop NB302
 Baylor College of Medicine
 Department of Neurology
 Neurosensory Center B413
 One Baylor Plaza
 Houston TX 77030
 E-mail: hepstein@bcm.tmc.edu
 Work: 713-798-4629
 Fax: 713-798-3771

Feedback, Daniel L. PhD
 Head, Muscle Research Laboratory
 Mail Code SD3
 NASA Johnson Space Center
 Bldg. 37, Room 1117
 2101 Nasa Road One
 Houston TX 77058
 E-mail:
 daniel.l.feedback1@jsc.nasa.gov
 Work: 281-483-7189
 Fax: 281-483-2888

Ferrando, Arny A. PhD
 Associate Professor, Surgery
 University of Texas Medical Branch
 Metabolism, Shriners Burn Institute
 Department of Surgery
 815 Market Street
 Galveston TX 77550
 E-mail: aferrand@sbi.utmb.edu
 Work: 409-770-6612
 Fax: 409-770-6825

Fitts, Robert H. PhD
 Professor of Biology

Marquette University
 Biology Department
 Wehr Life Sciences Building
 P. O. Box 1881
 Milwaukee WI 53201-1881
 E-mail: fittsr@vms.csd.mu.edu
 Work: 414-288-7354
 Fax: 414-288-7357

Fax: 937-275-5420

Friedericks, Charlie
 Mail Stop 213-2
 NASA Ames Research Center
 Moffett Field CA 94035-1000
 E-mail:
 cfriedericks@mail.arc.nasa.gov
 Work: 650-604-4116
 Fax: 650-961-8472

Flynn, Kevin
 Electronics Engineer
 MS 213-2/N-213
 NASA Ames Research Center
 Moffett Field CA 94035-1000
 E-mail: kflynn@mail.arc.nasa.gov
 Work: 650-604-4062
 Fax: 650-604-3913

Fuller, Charles A. PhD
 Professor
 University of California, Davis
 Section of Neurobiology, Physiology
 & Behavior
 One Shields Avenue
 Davis CA 95616-8519
 E-mail: cafuller@ucdavis.edu
 Work: 530-752-2979
 Fax: 530-752-5851

Fox, George E. PhD
 Professor
 University of Houston
 Department of Biochemical and
 Biophysical Sciences
 4800 Calhoun Road
 Houston TX 77204-5934
 E-mail: fox@uh.edu
 Work: 713-743-8363
 Fax: 713-743-8351

Gevins, Alan S. DSc
 Director, EEG Systems Laboratory
 EEG Systems Laboratories
 One Rincon Center
 101 Spear Street #204
 San Francisco CA 94105
 E-mail: alan@eeg.com
 Work: 415-957-1600 x 133
 Fax: 415-546-7121

Frangos, John A. PhD
 Professor
 Mail Code 0412
 University of California San Diego
 Department of Engineering
 9500 Gillman Avenue
 La Jolla CA 92093-0412
 E-mail: frangos@ucsd.edu
 Work: 619-534-0421
 Fax: 619-822-0240

Gillette, Edward L. PhD
 Professor and Chairman
 Colorado State University
 Department of Radiological Health
 Sciences
 Fort Collins CO 80523
 E-mail:
 gillette@cvms.colostate.edu
 Work: 970-491-1276
 Fax: 970-491-1254

Frey, Mary Anne PhD
 Professor, Dept. Community Health
 (Aerospace Med.)
 Wright State University School of
 Medicine
 P.O. Box 927
 Dayton OH 45401
 E-mail: mary.frey@wright.edu
 Work: 937-276-8338

Goldberg, Alfred MD
 Professor of Cell Biology
 Harvard School of Medicine
 Building C1-415

240 Longwood Avenue
 Boston MA 02115
 E-mail:
 agoldber@bcmp.med.harvard.edu
 Work: 617-432-1855
 Fax: 617-232-0173

Goldberger, Ary L. MD
 Associate Professor of Medicine
 Harvard Medical School
 Beth Israel Deaconess Medical
 Center
 Department of Medicine
 330 Brookline Avenue
 GZ-435
 Boston MA 02215
 E-mail:
 ary@astro.bidmc.harvard.edu
 Work: 617-667-4199
 Fax: 617-667-7268

Greenberg, Neil L. PhD
 Project Scientist
 Cleveland Clinic Foundation
 Department of Cardiology, F-15
 9500 Euclid Avenue
 Cleveland OH 44195
 E-mail: ngreen@bmc.ri.ccf.org
 Work: 216-445-7286
 Fax: 216-445-7306

Greenisen, Michael PhD
 Mail Code SD-3
 NASA Johnson Space Center
 2101 NASA Road One
 Houston TX 77058
 Work: 281-483-3874
 Fax: 281-483-2888

Greenleaf, John PhD
 Research Physiologist
 MS 239-11, N239
 NASA-Ames Research Center
 Gravitational Research Branch
 Moffett Field CA 94035-1000
 E-mail:
 jgreenleaf@mail.arc.nasa.gov
 Work: 650-604-6604
 Fax: 650-604-3954

Grigoriev, Anatoly I MD
 Director
 Institute of Biomedical Problems
 76-A Khoroshevskoye shosse
 123007 Moscow
 Work: 7-095-195-2363
 Fax: 7-095-195-2253

Grund, Ellen M.S.
 Research Associate
 University of California, San
 Francisco
 VA Medical Center (116A)
 4150 Clement Street
 San Francisco CA 94121
 E-mail: grund@itsa.ucsf.edu
 Work: 415-476-7636
 Fax: 415-502-7296

Halloran, Bernard P. PhD
 Professor of Med
 Mail Code 111 N
 University of California San
 Francisco
 Endocrine Unit
 Department of Medicine
 4150 Clement Street
 San Francisco CA 94121-1598
 E-mail:
 halloran.bernard_p@sanfrancisco.
 va.gov
 Work: 415-750-6928
 Fax: 415-750-6929

Hardin, Tonya
 SD3
 Universities Space Research
 Association (USRA)
 Division of Space Life Sciences
 3600 Bay Area Boulevard
 Houston TX 77058
 E-mail: hardin@lpi.jsc.nasa.gov
 Work: 281-244-2009
 Fax: 281-244-2006

Hargens, Alan R. PhD
 Professor
 239-11
 University of California San Diego

Department of Orthopaedics
350 Dickinson Street
San Diego CA 92103-8894
E-mail: ahargens@ucsd.edu
Work: 619-543-6805
Fax: 619-543-2540

Harm, Deborah L. PhD
Senior Research Scientist
SD-3
NASA Johnson Space Center
Bldg. 37, Room 166
2101 Nasa Road One
Houston TX 77058
E-mail:
deborah.l.harm1@jsc.nasa.gov
Work: 281-483-7222
Fax: 281-244-5734

Hatton, Daniel C. PhD
L470
Oregon Health Sci. University
Division of Nephrology, Hypotension
& Clin. Pharmacol.
3181 SW San Jackson Pk Road
Portland OR 97201
E-mail: hattond@ohsu.edu
Work: 503-494-2013
Fax: 503-494-6877

Hines, John W.
Manager, Sensors 2000 Program (FZ)
MS 213-2
NASA Ames Research Center
Research and Development Services
Directorate
Bldg. 213, Room 155
Moffett Field CA 94035-1000
E-mail: john.hines@arc.nasa.gov
Work: 650-604-5538
Fax: 650-961-8472

Holland, Albert W. PhD
SD2
NASA Johnson Space Center
2101 Nasa Road One
Houston TX 77058
E-mail:
albert.w.holland1@jsc.nasa.gov

Work: 281-483-8482
Fax: 281-483-3396

Holmes, Ross P. PhD
Wake Forest University School of
Medicine
Department of Urology
Medical Center Boulevard
Winston-Salem NC 27157
E-mail: rholmes@bgsm.edu
Work: 336-716-2426
Fax: 336-716-0174

Holton, Emily M. PhD
Chief SLR
239-11
NASA Ames Research Center
Moffett Field CA 94035-1000
E-mail: EHolton@mail.arc.nasa.gov
Work: 650-604-5471
Fax: 650-604-3954

Hughes-Fulford, Millie PhD
Mail Code 151F
University of California San
Francisco
Lab of Cell Growth
4150 Clement Street
San Francisco CA 94121
E-mail: milliehf@aol.com
Work: 415-221-4810 ext. 2749
Fax: 415-476-1267

Huso, David L. DVM, PhD
Johns Hopkins University School of
Medicine
Division of Comparative Medicine
5501 Hopkins Bayview Circle
Room LA7
Baltimore MD 21224
E-mail: dhuso@jhmi.edu
Work: 410-550-2524
Fax: 410-550-2115

Ingalls, Christopher P. Ph.D.
Assistant Research Scientist
Texas A&M University

Muscle Biology Laboratory
 Department of Health and
 Kinesiology
 College Station TX 77843-4243
 E-mail: ingalls@unix.tamu.edu
 Work: 409-862-4808
 Fax: 409-862-4808

Jacobs, Ron PhD
 Senior Research Scientist -
 Biomechatronics
 Intelligent Inference Systems (IIS)
 Corp.
 NASA Ames Research Center
 West 333 Maude Avenue
 Suite 107
 Sunnyvale CA 94086
 E-mail: rjacobs@iiscorp.com
 Work: 408-730-8345
 Fax: 408-730-8550

Jan, Darrell L. PhD
 Program Coordinator AEMC
 MS 125-224
 Jet Propulsion Laboratory
 4800 Oak Grove Drive
 Pasadena TX 91109-8099
 E-mail: darrell.l.jan@jpl.nasa.gov
 Work: 818-354-4542
 Fax: 818-393-4057

Johnson, Roger B. DDS, PhD
 University of Mississippi
 School of Dentistry
 2500 North State Street
 Jackson MS 39216-4505
 E-mail: drrogerb@fiona.umsmed.edu
 Work: 601-984-6115
 Fax: 601-984-6014

Johnston, Carl PhD
 Box EHSC
 The University of Rochester
 Department of Environmental
 Medicine
 A 225 Annex Medical Center
 575 Elmwood Avenue
 Rochester NY 14642
 Work: 716-275-3804

Fax: 716-256-2631

Jones, Terri K
 SD3
 Universities Space Research
 Association
 Division of Life Sciences
 3600 Bay Area Blvd
 Houston TX 77058
 E-mail: jones@lpi.jsc.nasa.gov
 Work: 281-244-2010
 Fax: 281-244-2006

Kanas, Nick A. MD
 Professor of Psychiatry
 University of California, San
 Francisco
 Psychiatry Service
 Mail Code 116A
 Veterans Affairs Medical Center
 4150 Clement Street
 San Francisco CA 94121
 E-mail: nick21@itsa.ucsf.edu
 Work: 415-750-2072
 Fax: 415-502-7296

Kanwar, Samina PhD
 Mail Station 3-2372
 Baylor College of Medicine
 Pediatrics Leukocyte Biology
 Childrens Nutrition Research Center
 One Baylor Plaza
 Room CNRC 6014
 Houston TX 77030
 E-mail: skanwar@bcm.tmc.edu
 Work: 713-770-4358
 Fax: 713-770-4366

Kaufmann, Horacio C. MD
 Associate Professor of Neurology
 Mount Sinai Medical Center
 ANS Laboratory, Box 1052
 Department of Neurology
 1 Gustav Levy Place
 New York NY 10029-6574
 E-mail:
h_kaufmann@smtplink.mssm.edu
 Work: 212-241-7315
 Fax: 212-987-3301

Kavros, Perry
Electronics Technician
MS 221-5, Bldg. N221
NASA Ames Research Center
Systems Engineering Division
Moffett Field CA 94035-1000
Work: 650-604-0187
Fax: 650-604-0071

Khalsa, Sat Bir S. PhD
Harvard Medical School
Brigham and Women's Hospital
Circadian Section
221 Longwood Avenue
Boston MA 02115
E-mail:
khalsa@gcrc.bwh.harvard.edu
Work: 617-732-7994
Fax: 617-732-4015

Kozlovskaya, Inessa B. MD
Head of Department
SRC Institute of Biomedical
Problems
76A Khoroshevskoye shosse
123007 Moscow
Russia
E-mail: ikozlovs@mmcc.ibmp.rssi.ru
Work: 7-095-195-2375
Fax: 205-961-6504

Kronenberg, Amy PhD
Staff Scientist
MS 70A-1118
Lawrence Berkeley National
Laboratory
Life Sciences Division
One Cyclotron Road
Berkeley CA 94720
E-mail: A_Kronenberg@lbl.gov
Work: 510-486-6449
Fax: 510-486-4475

Lambertsen, Christian J. MD
University of Pennsylvania Medical
Center
Institute for Environmental
Medicine
1 John Morgan Building 6068

3620 Hampton Walk
Philadelphia PA 19104-6068
E-mail:
clambert@ebdc.med.upenn.edu
Work: 215-898-8692
Fax: 215-898-6120

Lane, Helen W. PhD
SA
NASA Johnson Space Center
Medical Sciences Division
2101 Nasa Road One
Bldg 1
Houston TX 77058
E-mail: hlane@ems.jsc.nasa.gov
Work: 281-483-7165
Fax: 281-483-2086

Layne, Charles PhD
Professor
University of Houston
Department of Health and Human
Performance
104C Garrison Gym
Houston TX 77204
E-mail: clayne2gbayou.uh.edu
Work: 713-743-9868
Fax: 713-743-9860

LeBlanc, Adrian PhD
Mail Code NB1-004
Baylor College of Medicine
Neurosensory Bldg
Methodist Hospital
6501 Fannin Street
Houston TX 77030
E-mail: aleblanc@bcm.tmc.edu
Work: 713-790-2761
Fax: 713-790-1341

Leonard, Joel PhD
Program Scientist
Uniformed Services University of
Health Science
Department of Physiology
NASA Life Sciences Data Archives,
Dept. of Physiology
4301 Jones Bridge Road
Bethesda MD 20814

E-mail: jleonard@hq.nasa.gov
Work: 301-295-3520
Fax: 301-295-3772

Leveton, Lauren PhD
6904 Lillie Mae Way
Annandale VA 22003
E-mail: lleveton@bellatlantic.net
Work: 703-916-0643
Fax: 703-642-2893

Levine, Benjamin D. MD
Associate Professor of Medicine &
Director
Institute for Exercise and
Environmental Medicine
HO8.116F
University of Texas Southwestern
Medical Center
Presbyterian Hospital of Dallas
7232 Greenville
Dallas TX 75231
E-mail:
benjamin.levine@email.swmed.edu
Work: 214-345-4619
Fax: 214-345-4618

Liskowsky, David PhD
Program Scientist
Code UL
NASA Headquarters
Life Sciences Division
300 E. Street SW
Washington DC 20546
E-mail:
david.liskowsky@hq.nasa.gov
Work: 202-358-1963
Fax: 202-358-4168

Lisle, John T PhD
Montana State University
Department of Microbiology
109 Lewis Hall
Bozeman MT MT 59717
E-mail: umbjl@montana.edu
Work: 406-994-5028
Fax: 406-994-5028

Locke, James MD
Aerospace Medicine Resident
SD26
NASA Johnson Space Center
Houston TX 77058
E-mail: jplocke@utmb.edu
Work: 281-218-9575
Fax: 281-244-2006

Low, Phillip A. MD
Professor of Neurology
Mayo Clinic
Department of Neurology
811 Auggenheim
Rochester MN 55905
E-mail: low@mayo.edu
Work: 507-284-3375
Fax: 507-284-3133

Mack, Gary W. PhD
Associate Fellow
Yale University
The John B. Pierce Laboratory
290 Congress Avenue
New Haven CT 06519
E-mail: mack@jbpierce.org
Work: 203-562-9901
Fax: 203-624-4950

Maida, James C. PhD
MC SP3
NASA Johnson Space Center
2101 Nasa Road One
Houston TX 77058
E-mail: jim.maida@jsc.nasa.gov
Work: 281-483-1113
Fax: 281-483-1847

Mains, Richard PhD
Mains and Associates
2039 Shattuck Avenue, Suite 402
Berkeley CA 94704
E-mail: rmains@mainsgate.com
Work: 510-548-1262
Fax: 510-548-1263

Mark, Roger G. PhD
 Distinguished Professor of Health
 Sciences & Technology
 Room E25-505
 Massachusetts Institute of
 Technology
 77 Massachusetts Avenue
 Cambridge MA 02139
 E-mail: rgmark@mit.edu
 Work: 617-253-7818
 Fax: 617-253-7498

Markham, Charles H. MD
 Professor Emeritus of Neurology
 UCLA School of Medicine
 Department of Neurology
 710 Westwood Plaza
 Los Angeles CA 90095-1769
 E-mail: cmarkham@ucla.edu
 Work: 310-825-6578
 Fax: 310-825-0930

Maurer, Richard H. PhD
 Principal Staff Physicist
 Johns Hopkins University
 Applied Physics Laboratory
 Dept. of Reliability and Quality
 Assurance - SOR
 Building 23-IT
 11100 Johns Hopkins RD
 Laurel MD 20723-6099
 E-mail:
 maurerh1@spacemsg.jhuapl.edu
 Work: 443-778-6482
 Fax: 443-778-6696

McCarthy, Thomas L. PhD
 (FMB) 211
 Yale University School of Medicine
 Department of Surgery
 333 Cedar Street
 P. O. Box 208041
 New Haven CT 06520-8041
 E-mail: thomas.mccarthy@yale.edu
 Work: 203-785-4927
 Fax: 203-785-5714

McClain, Bonnie J.
 Life Sciences Education Programs

Coordinator
 NASA
 Colorado State University Grantee
 300 D. Street SW, Suite 801
 Washington DC 20024
 E-mail: bjm@usra.edu
 Work: 202-488-5123
 Fax: 202-479-2613

McDonald, P. Vernon PhD
 Vice President
 NASCENT Technologies
 15806 Spring Forest Drive
 Houston TX 77059
 E-mail:
 vmcdonald@nascent-technologies.com
 Work: 281-461-8275
 Fax: 281-461-8275

McGinnis, Patrick MD
 SD26
 NASA Johnson Space Center
 2101 Nasa Road One
 Houston TX 77058
 E-mail:
 patrick.j.mcginnis1@jsc.nasa.gov
 Work: 281-483-2492
 Fax: 281-483-3392

McIntire, Larry V. PhD
 Prof. of Chem. and Biomedical Eng.
 and Director
 Rice University
 NSCORT in Gravitational Biology
 MS-144
 6100 Main Street
 P. O. Box 1892
 Houston TX 77005-1892
 E-mail: mcintire@rice.edu
 Work: 713-527-4903
 Fax: 713-285-5154

McKee, Patrick MD
 Director, Warren Medical Research
 Institute
 University of Oklahoma Health
 Sciences Center
 Building 921 S.L. Young Boulevard
 P.O. Box 26901

Basic Science Education Building,
Room 321
Oklahoma City OK 73126-0901
E-mail: patrick-mckee@ouhsc.edu
Work: 405-271-5645
Fax: 405-271-3195

Merrell, Ronald C. MD
Yale University School of Medicine
Chairman & Lampman Professor
Department of Surgery
P.O. Box 208062
330 Cedar Street, FMB 102
New Haven CT 06510-8047
E-mail: ronald.merrell@yale.edu
Work: 203-785-2697
Fax: 203-737-2116

Metaxas, Dimitris PhD
Associate Professor
University of Pennsylvania
Computer and Information Science
200 South 33rd Street
Philadelphia PA 19104-6389
Work: 215-898-0945
Fax: 215-898-0587

Metting, Noelle F. ScD
Sr. Research Scientist
MS P7-56/331 Bldg.
Pacific Northwest National
Laboratory
P.O. Box 999
Richland WA 99352
E-mail: nf.metting@pnl.gov
Work: 509-376-3348
Fax: 509-376-9449

Miller, Jack Ph.D.
Staff Scientist
MS 29-100
Lawrence Berkeley National
Laboratory
One Cyclotron Road
Berkeley CA 94720
E-mail: j_miller@lbl.gov
Work: 510-486-7130
Fax: 510-486-7934 or 6949

Mishra, Saroj K. PhD
Universities Space Research
Association
3600 Bay Area Boulevard
Houston TX 77058
E-mail: mishra@lpi.jsc.nasa.gov
Work: 281-244-2020
Fax: 281-244-2006

Monk, Timothy H. DSc
Professor
University of Pittsburgh
WPIC E1123
3811 Ohara St
Pittsburgh PA 15213
E-mail: monkth@msx.upmc.edu
Work: 412-624-2246
Fax: 412-624-2841

Moore, Steven PhD
Research Associate
Mount Sinai School of Medicine
Department of Neurology
1 East 100th Street
Box 1135
New York NY 10029
E-mail: steve.moore@mssm.edu
Work: 212-241-7068
Fax: 212-831-1610

Mosier, Dennis R. MDPhD
Mail Station NB302
Baylor College of Medicine
Department of Neurology
Neurosensory Center NB 403
Houston TX 77030
E-mail: dmosier@bcm.tmc.edu
Work: 713-798-8158
Fax: 713-798-3853

Mount, Frances E.
Manager, Space Human Factors
Laboratory
SP3
NASA Johnson Space Center
2101 Nasa Road One
Houston TX 77058

E-mail:
frances.e.mount1@jsc.nasa.gov
Work: 281-483-3723
Fax: 281-483-1847

Mullington, Janet PhD
Harvard Medical School
Beth Israel Deaconess Medical
Center
Room 433, Kirstein Bldg.
330 Brookline Avenue
Boston MA 02215
E-mail: jmulling@bidmc.harvard.edu
Work: 617-667-0434
Fax: 617-975-5506

Mundt, Carsten PhD
Mail Stop 213-15
Sverdrup Technology/NASA Ames
Research Center
Moffett Field CA 94035-1000
E-mail: cmundt@mail.arc.nasa.gov
Work: 650-604-0936
Fax: 650-961-8472

Murthy, Gita PhD
University of California, Berkeley
Department of Environmental Health
Ergonomics Laboratory
1301 South 46th Street
Building 112
Richmond CA 94804
E-mail: gita@uclink4.berkeley.edu
Work: 650-604-0073
Fax: 650-604-3954

Nelson, Dana
Universities Space Research
Association
Division of Space Life Sciences
3600 Bay Area Blvd.
Houston TX 77058
E-mail: nelson@lpi.jsc.nasa.gov
Work: 281-244-2015
Fax: 281-244-2006

Nelson, Gregory PhD

Director, Radiobiology Program
Loma Linda University Radiobiology
Program
11175 Campus Street
Chan Shun Pavillion, Room A-1010
Loma Linda CA 92354
E-mail: gnelson@dominion.llumc.edu
Work: 909-558-8366
Fax: 909-558-0825

Neville, Craig PhD
CVRC Mail Code 149-4201
Harvard Medical School
4th Floor
149 13th Street
Charlestown MA 02129-2060
E-mail:
neville@helix.mgh.harvard.edu
Work: 617-724-9562
Fax: 617-724-9561

Newman, Dava J. PhD
MS 33-119
College of Engineering
Aeronautics and Astronautics
Massachusetts Institute of
Technology
77 Massachusetts Avenue
Cambridge MA 02139
E-mail: dnewman@mit.edu
Work: 617-258-8799
Fax: 617-253-4196

Nicogossian, Arnauld E. MD
HQ8F32/ Code U
NASA Headquarters
Code U
Two Independence Square
300 E. Street SW
Washington DC 20546
E-mail: nicogossian@hq.nasa.gov
Work: 202-358-0215

Norfleet, William MD
Mail Code SD2
NASA Johnson Space Center
Sonny Carter Training Facility
Building SCTF3
13000 Space Center Boulevard
Houston TX 77058
E-mail: wnoflee@ems.jsc.nasa.gov

Work: 281-483-2225
Fax: 281-483-3396

Nute, Kay
USRA
Division of Space Life Sciences
3600 Bay Area Blvd.
Houston TX 77058
E-mail: nute@lpi.jsc.nasa.gov
Work: 281-244-2019
Fax: 281-244-2006

Nygren, Richard
Associate Director, Space & Life
Sciences
Mail Code SA
NASA Johnson Space Center
2101 Nasa Road One
Building 1, Room 850L
Houston TX 77058
E-mail: rnygren@ems.jsc.nasa.gov
Work: 281-483-3879
Fax: 281-483-6089

Oberdoerster, Gunter PhD
Professor of Toxicology
Box EHSC, A225 Annex, Medical
The University of Rochester
575 Elmwood Avenue
Rochester NY 14642
E-mail:
havalackj@envmed.rochester.edu
Work: 716-275-3804
Fax: 716-256-2631

Ohshima, Hiroshi PhD, MD
NASDA
Tsukuba Space Center
2-1-1 Sergen
Tsukuba Ibaraki 305
Japan
E-mail:
Ohshima.Hiroshi@nasda.go.jp
Work: 0298 54 3951
Fax: 0298 50 2232

Oman, Charles M. PhD

Director
Massachusetts Institute of
Technology
Man Vehicle Laboratory
Center for Space Research
77 Massachusetts Avenue
Room 37-219
Cambridge MA 02139
E-mail: cmo@space.mit.edu
Work: 617-253-7508
Fax: 617-253-0861

Osborn, Mary Jane PhD
3205
University of Connecticut Health
Center
Dept. Microbiology
Farmington CT 06030
E-mail: osborn@sun.uhc.edu
Work: 860-679-2318
Fax: 860-679-1239

Pacetti, Gail
SD3
Universities Space Research
Association
Division of Space Life Sciences
3600 Bay Area Blvd
Houston TX 77058-1113
E-mail: pacetti@lpi.jsc.nasa.gov
Work: 281-244-2016
Fax: 281-244-2006

Palinkas, Lawrence A. PhD
University of California, San Diego
Division of Family Medicine
Department of Family and Preventive
Medicine
9500 Gilman Drive
La Jolla CA 92093-0807
E-mail: lpalinka@ucsd.edu
Work: 619-543-5493
Fax: 619-543-5996

Paloski, William H. PhD
Chief, Life Sciences Research
Laboratories
SD3
NASA Johnson Space Center

Bldg. 37, Room 160
2101 Nasa Road One
Houston TX 77058
E-mail: wpaloski@jsc.nasa.gov
Work: 281-244-5315
Fax: 281-244-5734

Pantalos, George M. PhD
The University of Utah
Department of Surgery
Department of Bioengineering
Artificial Heart Laboratory
803 North 300 West
Salt Lake City UT 84103-1414
E-mail:
George.Pantalos@m.cc.utah.edu
Work: 801-595-7229
Fax: 801-581-4044

Parker, Donald E PhD
Professor
University of Washington
Department of Otolaryngology-HNS
School of Medicine
Box 356515
Seattle WA 98195-6515
E-mail: deparker@u.washington.edu
Work: 206-285-7528
Fax: 206-217-9044

Partridge, Nicola C. PhD
Professor
Saint Louis University
School of Medicine
Dept. of Pharmacological and
Physiological Science
1402 South Grand Boulevard
St. Louis MO 63104
E-mail: partrinc@slu.edu
Work: 314-577-8551
Fax: 314-577-8554

Pawelczyk, James A PhD
Pennsylvania State University
Noll Physiological Research Center
119 Noll Laboratory
University Park PA 16802
E-mail: jap18@psu.edu
Work: 814-865-3453

Fax: 814-865-4602

Pendergast, David R.
Professor of Physiology and
Biophysics
University at Buffalo
124 Sherman Hall South Campus
3435 Main Street
Buffalo NY 14214
E-mail:
dpenderg@ubmedh.buffalo.edu
Work: 716-829-3830
Fax: 716-829-2384

Peterka, Robert J. PhD
Associate Scientist
Neurological Sciences Institute
Oregon Health Sciences University
1120 NW 20nd Avenue
Portland OR 97209
E-mail: peterka@nsi.lhs.org
Work: 503-413-6558
Fax: 503-413-7229

Pierre, Lizanna
Environmental Engineer
SD2
Wyle Laboratories
1290 Hercules, Suite 120
Houston TX 77058
E-mail:
lizanna.m.pierrel@jsc.nasa.gov
Work: 281-483-5724
Fax: 281-483-3058

Pierson, Duane L. PhD
Microbiologist
SD3
NASA Johnson Space Center
Bldg. 37, Room 1119A
2101 Nasa Road One
Houston TX 77058
E-mail:
duane.l.pierson1@jsc.nasa.gov
Work: 281-483-7166
Fax: 281-483-3058

Pilmanis, Andrew A. Ph.D.

Air Force Research Laboratory
 2504 Gillingham Drive Suite 25
 Brooks Air Force Base TX 78235-5104
 E-mail:

andrew.pilmanis@afrlars.brooks.af.mi
 1

Work: 210-536-3247
 Fax: 210-536-4712

Pisacane, Vincent L. PhD
 Assistant Director for Research &
 Exploratory Development
 Johns Hopkins University
 Applied Physics Laboratory
 Building 1-5103A
 11100 Johns Hopkins RD
 Laurel MD 20723-6099
 E-mail: vince.pisacane@jhuapl.edu
 Work: 443-778-5100
 Fax: 443-778-5995

Pollitt, Julie A.
 221-5
 NASA Ames Research Center
 Moffett Field CA 94035-1000
 E-mail: jpollitt@mail.arc.nasa.gov
 Work: 650-604-0187
 Fax: 650-604-0000

Pool, Sam L. MD
 SA
 NASA Johnson Space Center
 2101 Nasa Road One
 Houston TX 77058
 E-mail: sam.l.pool1@jsc.nasa.gov
 Work: 281-483-7109
 Fax: 281-483-2224

Poth, Merrily Poczik Morgan
 Professor of Pediatrics
 Uniformed Services University of
 the Health Sciences
 Department of Pediatrics
 4301 Jones Bridge Road
 Bethesda MD 20814
 E-mail: mpoth@usuhs.mil
 Work: 301-295-0220
 Fax: 301-295-6441

Powell, Michael R. PhD
 Head, Environmental
 Physiology/Biophysics
 SD3
 NASA Johnson Space Center
 Building 37, Room 154
 2101 Nasa Road One
 Houston TX 77058
 E-mail:
 michael.r.powell1@jsc.nasa.gov
 Work: 281-483-5413
 Fax: 281-483-2888

Purdy, Ralph E. PhD
 University of California, Irvine
 College of Medicine
 Department of Pharmacology
 Irvine CA 92697-4625
 E-mail: repurdy@uci.edu
 Work: 949-824-7653
 Fax: 949-824-4855

Putcha, Lakshmi PhD
 Senior Pharmacologist
 SD3
 NASA Johnson Space Center
 2101 Nasa Road One
 Houston TX 77058
 E-mail: lputchal@ems.jsc.nasa.gov
 Work: 281-483-7760
 Fax: 281-483-3058

Pyle, Barry H. PhD
 Associate Research Professor
 Montana State University
 Microbiology Department
 109 Lewis Hall
 Bozeman MT 59717
 E-mail: barryp@montana.edu
 Work: 406-994-3041
 Fax: 406-994-4926

Rabin, Bernard M. PhD
 Professor
 University of Maryland
 Department of Psychology
 Baltimore County

1000 Hilltop Circle
Baltimore MD 21250
E-mail: rabin@umbc2.umbc.edu
Work: 410-455-2430
Fax: 410-455-1055

Radford, Nina B. MD
NK01.410
University of Texas Southwestern
Medical Center
The Rogers Magnetic Resonance
Center
Department of Internal Medicine
5801 Forest Park Drive
Dallas TX 75235
E-mail: radford@ryburn.swmed.edu
Work: 214-648-5863
Fax: 214-648-5881

Ramsdell, Craig MD
Massachusetts Institute of
Technology
Room E25-335
77 Massachusetts Avenue
Cambridge MA 02139
E-mail:
ramsdel@etherdome.mgh.harvard.edu
Work: 617-253-7430
Fax: 617-732-5764

Raven, Peter B. PhD
Chair, Department of Integrated
Physiology
University of North Texas Health
Science Center
3500 Camp Bowie Boulevard
Fort Worth TX 76107-2699
E-mail: praven@hsc.unt.edu
Work: 817-735-2074
Fax: 817-735-5084

Reschke, Millard F. PhD
Director, Neurosciences Laboratory
SD3
NASA Johnson Space Center
Bldg. 37, Room 146
2101 Nasa Road One
Houston TX 77058
E-mail: mreschke@ems.jsc.nasa.gov

Work: 281-483-7210
Fax: 281-244-5734

Robinson, Judith L. PhD
SL
NASA Johnson Space Center
2101 Nasa Road One
Bldg 1 Room 350A
Houston TX 77058
E-mail:
judith.l.robinson1@jsc.nasa.gov
Work: 281-483-1165
Fax: 281-483-6636

Rubin, Clinton T PhD
Professor and Director
H.S.C. T18-030
State University of New York
Center for Biotechnology
130 Life Sciences
Stony Brook NY 11794-5208
E-mail: clinton.rubin@sunysb.edu
Work: 516-632-8521
Fax: 516-632-8577

Russell, Patricia L. PhD
Universities Space Research
Association
300 D Street, SW
Suite 801
Washington DC 20024
E-mail:
patricia.russell@hq.nasa.gov
Work: 202-488-5142
Fax: 202-488-2613

Rydberg, Bjorn E. PhD
MS 934-47A
Lawrence Berkeley National
Laboratory
Life Sciences Division
One Cyclotron Road
Berkeley CA 94720
E-mail: Berydberg@lbl.gov
Work: 510-486-7045 or 7346
Fax: 510-486-5735

Sams, Clarence F. PhD
Research Biochemist
Mail Code SD-3
NASA Johnson Space Center
Life Science Research Laboratories
2101 NASA Road 1
Houston TX 77058
E-mail: csams@ems.jsc.nasa.gov
Work: 281-483-7160
Fax: 281-483-0402

Sauer, Richard L. PE
SD2
NASA Johnson Space Center
Medical Operations
2101 Nasa Road One
Houston TX 77058
E-mail:
richard.l.sauer1@jsc.nasa.gov
Work: 281-483-7121
Fax: 281-483-3058

Sawin, Charles F. PhD
SA
NASA Johnson Space Center
Life and Sciences Directorate
2101 Nasa Road One
Bldg. 1, Room 850B
Houston TX 77058
E-mail: csawin@ems.jsc.nasa.gov
Work: 281-483-7202
Fax: 281-483-6089

Schimmerling, Walter PhD
Program Scientist
CODE UL
NASA Headquarters
NASA Space Radiation Health and
Radiation Biology Programs
300 E. Street SW
Washington DC 20546-0001
E-mail: wschimmerling@hq.nasa.gov
Work: 202-358-2205
Fax: 202-358-4168

Schneider, Suzanne PhD
Research Physiologist
Mail Code SD3
NASA Johnson Space Center

2101 NASA Road One
Houston TX 77058
E-mail: sschneid@ems.jsc.nasa.gov
Work: 281-483-7213
Fax: 281-483-4181

Schonfeld, Julie
Mail Stop 213-2
NASA Ames Research Center
Building N213
Moffett Field CA 94035-1000
E-mail:
jschonfeld@mail.arc.nasa.gov
Work: 650-604-6504
Fax: 650-961-8472

Schultheis, Lex MD, PhD
Johns Hopkins University
Tower 711
The Johns Hopkins Hospital
600 North Wolfe Street
Baltimore MD 21287
E-mail:
lschulth@welchlink.welch.jhu.edu
Work: 410-955-8005
Fax: 410-955-0994

Schultz, Edward PhD
University of Wisconsin Medical
School
Department of Anatomy
1300 University Avenue
Madison WI 53706
E-mail: eschult1@facstaff.wisc.edu
Work: 608-263-2894
Fax: 608-262-7306

Schwartz, Robert J. PhD
Professor
Baylor College of Medicine
Department of Cell Biology
BCM Cullen Building 145EA
Houston TX 77030
E-mail: schwartz@bcm.tmc.edu
Work: 713-798-6649
Fax: 713-798-7799

Shackelford, Linda C. MD
SD3
NASA Johnson Space Center
Life Sciences Research Laboratories
2101 Nasa Road One
Bldg 37 Room 106
Houston TX 77058
E-mail:
linda.c.shackelford1@jsc.nasa.gov
Work: 281-483-7100
Fax: 281-483-2888

Shapiro, Jay R. MD
Walter Reed Army Medical Center
Building 2, Ward 64, Room 6433
Washington DC 20307-5001
E-mail:
j_shapiro@wramc1-amedd.army.mil
Work: 202-782-8933
Fax: 202-782-3539

Sharp, M. Keith PhD
University of Utah
Department of Civil and
Environmental Engineering
160 Central Campus Drive, Room 104
Salt Lake City UT 84112-0561
E-mail: m.k.sharp@m.cc.utah.edu
Work: 801-581-6955
Fax: 801-585-5477

Shearer, William T. MD, PhD
Professor and Chief, Section of
Allergy and Immunology
1-3291
Texas Children's Hospital
6621 Fannin Street
Houston TX 77030
E-mail: wshearer@bcm.tmc.edu
Work: 713-770-1274
Fax: 713-770-7131

Shelhamer, Mark J. ScD
Johns Hopkins University School of
Medicine
Depts. of Otolaryngology and
Biomedical Engineering
Room 2-210 Pathology
720 Rutland Avenue

Baltimore MD 21205
E-mail: mjs@ishtar.med.jhu.edu
Work: 410-955-7345
Fax: 410-614-1746

Shepanek, Marc PhD
Program Scientist
Code UL
NASA Headquarters
300 E. Street SW
Washington DC 20546
E-mail: mshepanek@hq.nasa.gov
Work: 202-358-2201
Fax: 202-358-4168

Sherman, Derin PhD
Massachusetts Institute of
Technology
Room E25-335
77 Massachusetts Avenue
Cambridge MA 02139
E-mail: derin@mit.edu
Work: 617-258-7082
Fax: 617-253-3019

Shiota, Taka MD
Project Scientist
Cleveland Clinic Foundation
Department of Cardiology, F-15
9500 Euclid Avenue
Cleveland OH 44195
E-mail: shiotat@cesntp.ccf.org
Work: 216-445-7287
Fax: 216-445-4419

Shoemaker, J. Kevin PhD
Assistant Professor
MC H047
Penn State College of Medicine
Section of Cardiology
P.O. Box 850
Hershey PA 17033
E-mail:
kshoemak@gcrc.hmc.psghs.edu
Work: 717-531-1799
Fax: 717-531-1792

Sienko, Kathleen H. PhD
Massachusetts Institute of
Technology
Department of Aeronautics and
Astronautics
Room 37-219
77 Massachusetts Avenue
Cambridge MA 02139-4307
E-mail: sienko@mit.edu
Work: 617-258-7552
Fax: 617-258-8111

Sinden, Richard R. PhD
Associate Professor
MailStop 3303
Texas A&M University
Institute of Biosciences and
Technology
2121 West Holcombe Blvd.
Houston TX 77030-3303
E-mail: Rsinden@ibt.tamu.edu
Work: 713-677-7664
Fax: 713-677-7689

Skidmore, Michael
Mail Stop 213-2, Bldg 213 Room
NASA Ames Research Center
Moffett Field CA 94035-1000
E-mail:
mskidmore@mail.arc.nasa.gov
Work: 650-604-6069
Fax: 650-961-8472

Smith, Michael L. PhD
Associate Professor
University of North Texas Health
Science Center
Department of Integrative
Physiology
3500 Camp Bowie Boulevard
Fort Worth TX 76107
E-mail: msmith@hsc.unt.edu
Work: 817-735-2514
Fax: 817-735-5084

Smith, Scott M. PhD
Research Nutritionist
SD3
NASA Johnson Space Center

Life Science Research Laboratories
2101 Nasa Road One
Houston TX 77058
E-mail:
s.m.smith1@ems.jsc.nasa.gov
Work: 281-483-7204
Fax: 281-483-2888

Sonnenfeld, Gerald PhD
Department of Microbiology and
Immunology
Morehouse School of Medicine
720 Westview Drive
Atlanta GA 30310-1495
E-mail: gsonnenfe@carolinas.org
Work: 404-752-1586
Fax: 404-752-1179

Souza, Kenneth A.
Chief, Life Sciences Division
240A-3
NASA Ames Research Center
Org. SP
Bldg. N240A, Room 144
Moffett Field CA 94035-1000
E-mail: ksouza@mail.arc.nasa.gov
Work: 650-604-5736
Fax: 650-604-4503

Stegemoeller, Charles
SA
NASA Johnson Space Center
2101 Nasa Road One
Bldg. 1 Room 376E
Houston TX 77058
E-mail:
charles.stegemoeller1@jsc.nasa.gov
Work: 281-483-0576
Fax: 281-483-6636

Stein, T. P. PhD
Professor of Surgery
University of Medicine and
Dentistry of NJ
Dept. of Surgery Science Center
2 Medical Center Drive
Room 109A, Science Ctr
Stratford NJ 08084
E-mail: TPSTEIN@UMDNJ.EDU

Work: 609-566-6036
Fax: 609-566-6040

Stowe, Raymond P. III PhD
Route 0609
UTMB
Department of Pathology
Galveston TX 77555
E-mail: rpstowe@marlin.utmb.edu
Work: 281-483-6762
Fax: 281-483-3058

Stuster, Jack W. Ph.D.
Vice President and Principal
Scientist
Anacapa Sciences, Inc.
P. O. Box 519
Santa Barbara CA 93101
E-mail:
jstuster@anacapasciences.com
Work: 805-966-6157
Fax: 805-966-7713

Suleiman, Ahmad A. Ph.D.
Southern University
Department of Chemistry
Baton Rouge LA 70813
Work: 504-771-3990
Fax: 504-771-3992

Sulzman, Frank M. PhD
Deputy Director
Code UL
NASA Headquarters
300 E. Street SW
Washington DC 20546-0001
E-mail: fsulzman@hq.nasa.gov
Work: 202-358-0220
Fax: 202-358-4168

Sundby, Grete PhD
Brigham and Women's Hospital
Endocrine/Hypertension Division
221 Longwood Avenue
Boston MA 02115
Work: 617-732-5500 ext. 1132
Fax: 617-732-5764

Sytkowski, Arthur J. MD
Harvard Med. School
Burlington Building, Room 548
Beth Israel Deaconess Medical
Center
Laboratory for Cell and Molecular
Biology
One Deaconess Road, West Campus
Boston MA 02215
E-mail: asytkows@bidmc.harvard.edu
Work: 617-632-9980
Fax: 617-632-0401

Thomas, James D. MD
Director of Cardiovascular Imaging
Cleveland Clinic Foundation
Cardiology F-15
Department of Cardiology
9500 Euclid Avenue
Cleveland OH 44195
E-mail: thomasj@cesmtp.ccf.org
Work: 216-445-6312
Fax: 216-445-7306

Tidball, James G. PhD
Professor of Physiological Science
University of California, Los
Angeles
Department of Physiological Science
5833 Life Science Building
Los Angeles CA 90024-1527
E-mail: jtidball@physci.ucla.edu
Work: 310-206-3395
Fax: 310-206-9184

Tomko, David L. PhD
Enterprise Scientist
Code UL
NASA Headquarters
Biomedical Research and
Countermeasures
300 E Street SW
Washington DC 20546-0001
E-mail: dtomko@hq.nasa.gov
Work: 202-358-2211
Fax: 202-358-4611

Turner, Ronald E. PhD
Principal Physicist
ANSER
1215 Jefferson Davis Highway,
Suite 800
Arlington VA 22202-3251
E-mail: turnerr@anser.org
Work: 703-416-3264
Fax: 703-416-3474/or 3264

Turner, Russell T. PhD
Professor of Orthopaedics
Mayo Clinic
Orthopedic Research
Medical Science Building, Room 3-69
200 First Street, SW
Rochester MN 55905
E-mail: rolbiecki.lori@mayo.edu
Work: 507-284-4062
Fax: 507-284-5075

Ueno, Toshiaki
NASDA
2-1-1 Sengen
Tsukuba Ibaraki 305-8505
Japan
E-mail: ueno.toshiaki@nasda.go.jp
Work: 81-298-54-3938
Fax: 81-298-50-1480

Vandenburgh, Herman H. PhD
Brown University
The Miriam Hospital
Pathology and Laboratory Medicine
164 Summit Avenue
Providence RI 02906
E-mail:
herman_vandenburgh@brown.edu
Work: 401-793-4273
Fax: 401-751-2398

Vann, Richard D. Ph.D.
Director of Applied Research
Duke University Medical Center
F.G. Hall Hypo/Hyperbaric Center
Department of Anesthesiology
Box 3823
Durham NC 27710
E-mail: vann0001@mc.duke.edu
Work: 919-684-3305

Fax: 919-684-6002

Vernikos, Joan PhD
Director, Life Sciences Division
Code UL
NASA Headquarters
300 E. Street, S.W.
Washington DC 20546-0001
E-mail: jvernikos@hq.nasa.gov
Work: 202-358-2192
Fax: 202-358-4168

Wade, Charles E. PhD
Mail Stop 239-11
NASA Ames Research Center
Moffett Field CA 94035
E-mail: cwade@mail.arc.nasa.gov
Work: 650-604-3943
Fax: 650-604-3954

Waldren, Charles A. Ph.D.
Professor
MRB
Colorado State University
Department of Radiology and
Radiobiology
Fort Collins CO 80523
E-mail:
CWaldren@cumbs.colostate.edu
Work: 970-491-0580
Fax: 970-491-0623

Walsworth, Ronald L. PhD
Physicist
Mail Stop 59
Harvard Smithsonian Center for
Astrophysics
Atomic and Molecular Physics
Division
60 Garden Street
Cambridge MA 02138
E-mail: rwalsworth@cfa.harvard.edu
Work: 617-495-7274
Fax: 617-496-7690

Warters, Raymond L. PhD
University of Utah Health Sciences

Center

Division of Experimental Oncology
 Department of Radiation Oncology
 50 North Medical Drive
 Salt Lake City UT 84132-1001
 E-mail: ray.warters@hsc.utah.edu
 Work: 801-581-8344
 Fax: 801-585-3502

Waters, Wendy PhD
 SD3/NSBRI
 NASA Johnson Space Center
 2101 Nasa Road One
 Building 261
 Houston TX 77058
 E-mail: wwaters@ems.jsc.nasa.gov
 Work: 281-483-2726
 Fax: 281-483-4181

Welage, Lynda S. PhD
 Associate Professor of Pharmacy
 University of Michigan
 College of Pharmacy
 428 Church Street
 Ann Arbor MI 48109-1065
 E-mail: lswelage@umich.edu
 Work: 734-763-9783
 Fax: 734-763-2022

Welch, Robert B PhD
 Mail Stop 239-11
 NASA Ames Research Center
 Life Sciences Division
 Moffett Field CA 94035
 E-mail: rwelch@mail.arc.nasa.gov
 Work: 650-604-5749
 Fax: 650-604-3954

Wenzel, Elizabeth PhD
 MS 262-2
 NASA Ames Research Center
 Human Information Processing
 Research Branch
 Moffett Field CA 94035-1000
 E-mail: bwenzel@mail.arc.nasa.gov
 Work: 650-604-6290
 Fax: 650-604-3729

Whalen, Robert T. PhD
 Research Scientist
 Mail Stop 239-11
 NASA Ames Research Center
 Life Sciences Division
 Moffett Field CA 94035
 E-mail:
 robert_whalen@qmgate.arc.nasa.gov
 Work: 650-604-3280
 Fax: 650-604-3954

White, Ronald J. PhD
 Room NA425
 National Space Biomedical Research
 Institute
 One Baylor Plaza
 Houston TX 77030-3498
 E-mail: rwhite@bcm.tmc.edu
 Work: 713-798-7412
 Fax: 713-798-3403

Whitmore, Mihriban
 C81
 Lockheed Martin
 NASA Johnson Space Center
 2101 Nasa Road One
 Houston TX 77058
 E-mail:
 mihriban.whitmore1@jsc.nasa.gov
 Work: 281-483-9725
 Fax: 281-244-5271

Williams, Gordon H. MD
 Harvard University School of
 Medicine
 Brigham & Women's Hospital
 Chief, Endocrine Hypertension
 Division
 221 Longwood Avenue
 Boston MA 02115
 E-mail:
 ghwilliams@bics.bwh.harvard.edu
 Work: 617-732-5661
 Fax: 617-732-5764

Williams, Jerry R. ScD
 Professor of Oncology
 Johns Hopkins University School of

Medicine

600 North Wolfe Street
Room 2-121 Oncology
Baltimore MD 21287

E-mail:

jwil@welchlink.welch.jhu.edu
Work: 410-955-8777
Fax: 410-955-8780

Williams, Richard S. MD
Code UO

NASA Headquarters
300 E Street SW
Room 8013
Washington DC 20546-0001
E-mail: rwillia3@hq.nasa.gov
Work: 202-358-2461
Fax: 202-358-4174

Wilson, John W. PhD
Senior Research Scientist
Mail Stop 188B
NASA Langley Research Center
8 West Taylor Road
Hampton VA 23681-0001
E-mail:
John.W.Wilson@larc.nasa.gov
Work: 757-864-1414
Fax: 757-864-7730

Wood, Joanna PhD
NL/37
Wyle Life Sciences
1290 Hercules, Suite 120
Houston TX 77058
E-mail: jwood@wahine.jsc.nasa.gov
Work: 281-244-5524
Fax: 281-244-5734

Woolford, Barbara J.
Human Factors Research Manager
SP3
NASA Johnson Space Center
2101 Nasa Road One
Houston TX 77058
E-mail:
barbara.J.woolford1@jsc.nasa.gov
Work: 281-483-3701
Fax: 281-244-5773

Wright, Kenneth P. PhD
Harvard Medical School/Brigham &
Women's Hospital
Circadian, Neuroendocrine & Sleep
Disorders Section
221 Longwood Avenue, Room 438A
Boston MA 02115
E-mail:
kwright@gcrc.bwh.harvard.edu
Work: 617-732-8782
Fax: 617-732-4015

Wu, Honglu PhD
Mission Radiation Health Specialist
Mail Code SD23
Kelsey-Seybold Clinic
Building 229
2101 Nasa Road One
Houston TX 77058
E-mail: hwu@ems.jsc.nasa.gov
Work: 281-483-6470
Fax: 281-483-3395

Yamauchi, Mitsuo DDSPhD
Professor
CB 7455
University of North Carolina at
Chapel Hill
Dental Research Center
Collagen Biochemistry Laboratory
Room 212
Chapel Hill NC 27599-7455
E-mail:
mitsuo-yamauchi@dentistry.unc.edu
Work: 919-966-3441
Fax: 919-966-1231

Yost, Bruce
IPT Manager
Mail Stop 240 A-4
NASA Ames Research Center
Moffett Field CA 94035-1000
E-mail: byost@mail.arc.nasa.gov
Work: 650-604-6839
Fax: 650-604-6605

Young, Laurence R. ScD
Apollo Program Professor of
Astronautics
Massachusetts Institute of
Technology (MIT)
77 Massachusetts Avenue
Bldg. 37 Room 219
Cambridge MA 02139-4307
E-mail: lry@mit.edu
Work: 617-253-7759
Fax: 617-258-8111

Zerwekh, Joseph E. MD
Professor, Internal Medicine
8885
University of Texas Southwestern
Medical Center at Dallas
5323 Harry Hines Boulevard
Dallas TX 75235-8885
E-mail:
Joseph.Zerwekh@mail.swmed.edu
Work: 214-648-3872
Fax: 214-648-2526

Author Index

Abdellatif, M.	Cardiovascular	257	Bishop, P.A.	Muscle	377
Abell, G.A.	Radiation	513	Bjornstad, K.A.	Radiation	484
Adams, G.	Muscle	363	Black, F.O.	Neurovestibular	409
Adolf, J.	BPFH II	182	Blakely, E.A.	Radiation	484
Albert, M.S.	Technol Dev	590	Bloomberg, J.J.	Neurovestibular	411, 418
Alfrey, C.P.	Immunol	327	Bloomfield, S.A.	Bone	200, 234
Amidon, G.L..	Nutrition	468	Bobbe, L.	Immunol	345
Amir, A.	BPFH II	173	Boda, W.L.	Muscle	378
Angelaki, D.E.	Neurovestibular	407	Bodell, P.	Muscle	363
Antoine, M.	Technol Dev	582	Boorman, G.I.	Muscle	369
Archambeau, J.O.	Radiation	513	Booth, F.W.	Muscle	370, 388
Armstrong, R.B.	Muscle	385	Bourne, D.W.A.	Nutrition	462
Arnaud, S.B.	Bone	192, 243	Braby, L.A.	Radiation	521
Arshi, A.	Neurovestibular	409	Brady, J.V.	BPFH I	139
Asplund, E.	Cardiovascular	259	Broadaway, S.C.	Immunol	340, 350
Assimos, D.G.	Nutrition	456	Brown, E.M.	Bone	184, 218
Babcock, E.E.	Cardiovascular	303	Brown, E.N.	Sleep/Circad	541
Bachelard, C.	BPFH I	162	Brown, H.	BPFH II	173
Badhwar, G.D.	Radiation	477	Bryden, W.A.	Technol Dev	582
Baicu, C.F.	Cardiovascular	258	Butel, J.S.	Sleep/Circad	561
Bailliard, F.	Immunol	354	Butel, J.S.	Immunol	338
Bain, J.L.W.	Muscle	371	Butler, B.D.	Barophysiology	116
Balcer-Kubiczek, E.K.	Radiation	478	Buyse, D.J.	Sleep/Circad	559
Baldwin, K.M.	Muscle	359, 363	Byrne, B.J.	Immunol	327
Baldwin, K.M.	Plenary	57	Cajochen, C.	Sleep/Circad	547
Ballard, R.E.	Muscle	378	Caldwell, B.S.	BPFH II	167
Barcellos-Hoff, M.H.	Radiation	480	Callini, G.	Sleep/Circad	543
Barger, L.K.	Sleep/Circad	538	Cardon, L.	Technol Dev	587
Barnes, M.	Cardiovascular	258	Carlin, M.	Sleep/Circad	561
Barnes, P.R.	Cardiovascular	278	Carter III, R.	Sleep/Circad	565
Baroni, G.	BPFH II	173	Cavanagh, P.R.	Bone	224
Barrett, A.D.T.	Immunol	356	Centrella, M.	Bone	215
Bates, R.	Immunol	354	Chang, E.	Radiation	484
Beall, A.	Neurovestibular	429	Chang, P.Y.	Radiation	484, 485
Beck, S.	BPFH II	173	Chapman, J.	Cardiovascular	282
Beck, T.J.	Bone	202, 232	Charles, J.B.	Plenary	80
Bedford, J.S.	Radiation	511	Charles, Jr., H.K.	Bone	202
Bednarczyk, E.	Cardiovascular	297	Chatterjee, A.	Radiation	488
Benghuzzi, H.A.	Bone	211	Chen, Y.	Bone	215
Benton, E.R.	Radiation	483, 515	Cherbonnel-Lasserre, C.	Radiation	493
Benton, E.V.	Radiation	483, 515	Chmielewski, C.	BPFH II	170, 182
Berens, K.L.	BPFH I	148	Choe, S.	Nutrition	468
Berens, K.L.	Nutrition	462	Chou, J.L.	Cardiovascular	278
Bergula, A.P.	Bone	194	Chutjian, A.	Technol Dev	579
Berkowitz, D.	Cardiovascular	259	Clark, J.M.	Barophysiology	120
Berman, A.	BPFH II	182	Clark, R.	Neurovestibular	416
Bertocci, L.A.	Muscle	386	Clark, S.	Bone	214
Betcher, R.A.	Bone	211	Clement, G.	Neurovestibular	425
Biaggioni, I.	Neurovestibular	416	Cohen, B.	Neurovestibular	416, 425
Bikle, D.D.	Bone	198	Cohen, H.S.	Neurovestibular	411
Billy, B.D.	Sleep/Circad	559			

Cohen, M.	Neurovestibular	403	Epstein, H.F.	Muscle	370
Cohen, R.J.	Cardiovascular	290, 293	Erkman, L.	Sleep/Circad	563
Cohen, R.J.	Technol Dev	570, 585	Ertl, A.C.	Muscle	378
Conner, M.E.	Immunol	329	Essig, S.M.	Sleep/Circad	543
Convertino, V.A.	Cardiovascular	260	Etzel, R.A.	Cardiovascular	267
Cooper, P.K.	Radiation	511, 520	Fainchtein, R.	Radiation	500
Cornish, K.G.	Cardiovascular	263	Farach-Carson, M.C.	Bone	205
Corson, N.	Immunol	340	Farhi, L.	Cardiovascular	297
Cory, D.G.	Technol Dev	590	Fedarko, N.	Bone	234
Costa, F.	Neurovestibular	416	Feedback, D.L.	Muscle	374
Costill, D.L.	Muscle	371	Feiveson, A.	Bone	235
Cotter, R.J.	Technol Dev	582	Feldmesser, H.S.	Bone	202
Coutrakon, G.A.	Radiation	513	Ferrando, A.A.	Nutrition	455
Cowings, P.	BPFH I	142	Ferrigno, G.	BPFH II	173
Crandall, C.G.	Cardiovascular	267	Finkelstein, J.N.	Immunol	340
Cress, A.E.	Radiation	526	Fitts, R.H.	Muscle	371
Cucinotta, F.A.	Plenary	100	Fleischman, K.O.	Muscle	369
Cucinotta, F.A.	Radiation	490, 529	Flynn, K.	Technol Dev	581
Cunningham, J.T.	Cardiovascular	279	Ford, J.R.	Radiation	521
Czeisler, C.A.	Sleep/Circad	535, 541, 544,	Foster, M.	Immunol	354
		567	Fotedar, L.K.	Muscle	374
Dai, X.	Bone	211	Fowler, N.A.	Immunol	354
D'Alonzo, R.C.	Bone	222	Fox, G.E.	Immunol	335
D'Andrea, S.E.	Muscle	365	Frangos, J.A.	Bone	194
Darrech, M.	Technol Dev	579	Frank, A.L.	Radiation	483
D'Aunno, D.S.	Cardiovascular	274	Freeman-Perez, S.	Cardiovascular	274
Davis, B.L.	Muscle	365	Friedricks, C.	Technol Dev	576, 577
Davis, K.L.	Immunol	357	Fritsch-Yelle, J.M.	Cardiovascular	274
Deaver, D.R.	Muscle	368	Fulford, M.H.	Bone	208
Del Tatto, M.	Muscle	400	Fuller, C.A.	Sleep/Circad	538, 554, 563
Demerritt, J.	Cardiovascular	282	Gaffney, D.K.	Radiation	526
DeRoshia, C.	BPFH I	142	Garcia, M.J.	Technol Dev	587
Devereaux, A.S.	Technol Dev	573	Gauny, S.	Radiation	493
Diamond, S.G.	Neurovestibular	420	Geary, G.G.	Cardiovascular	300
Dicello, J.F.	Radiation	490, 528	Gelein, R.	Immunol	340
Diedrich, A.	Neurovestibular	416	George, K.	Radiation	533
Dierckx, J.	Cardiovascular	282	Gerth, W.A.	Barophysiology	132
Dijk, D-J.	Sleep/Circad	544, 547, 555	Gevins, A.	BPFH II	173
Ding, Y.	Cardiovascular	300	Gilbertson, V.	Bone	208
Dinges, D.F.	Immunol	351	Gillars, K.J.	Cardiovascular	310
Dinges, D.F.	Sleep/Circad	535, 551, 561	Gizzi, M.	Neurovestibular	416
Diorotto, M.L.	Muscle	368	Goldberg, A.L.	Muscle	376
DiZio, P.	Neurovestibular	413	Goldberg, J.	Neurovestibular	443
DiZio, P.	Plenary	106	Goldberger, A.L.	Cardiovascular	276
Doerr, F.	Cardiovascular	260	Goldsten, J.O.	Radiation	500
Draghia-Akli, R.	Muscle	368	Gonzales, D.	Muscle	393
Dresser, E.T.	Bone	200	Gonzalez, R.	Cardiovascular	308
Duckles, S.P.	Cardiovascular	300	Gooch, C.L.	Muscle	388
Duncan, R.L.	Bone	205	Gordon, S.	Muscle	370, 388
Durban, E.M.	Immunol	331	Gottschalk, F.	Bone	245
Eckberg, D.L.	Cardiovascular	271	Goulet, C.	Muscle	369
Eddy, D.R.	BPFH I	145, 154, 158	Green, L.M.	Radiation	513
Edgerton, V.R.	Muscle	369	Greenberg, N.L.	Technol Dev	587
Elayan, N.	Immunol	334	Greenisen, M.C.	Muscle	377
Elliott, A.R.	Sleep/Circad	544	Greenleaf, J.E.	Cardiovascular	278, 308
Engelke, K.A.	Cardiovascular	260	Gridley, D.S.	Radiation	490, 513

Grindeland, R.	Bone	243	Johnston, C.J.	Immunol	340
Gronowicz, G.	Bone	214	Jolesz, F.A.	Technol Dev	590
Groves, J.A.	Bone	200	Jones, J.A.	Bone	242
Grund, E.	BPFH I	150	Joseph, J.A.	Radiation	517
Grzesik, W.	Bone	243	Kalajic, I.	Bone	214
Gunderson, E.K.E.	BPFH I	152	Kamm, R.D.	Cardiovascular	283
Gushin, V.	BPFH I	150	Kanas, N.	BPFH I	135, 150
Haddad, F.	Muscle	363	Kannan, N.	Barophysiology	124
Haight, V.	Cardiovascular	282	Kanwar, S.	Immunol	336
Hakenewerth, A.M.	Immunol	354	Kapoor, S.	Sleep/Circad	561
Halloran, B.	Bone	198, 209	Karmon, D.	Technol Dev	579
Hargens, A.R.	Muscle	378, 390	Kaufman, G.D.	Neurovestibular	432
Harm, D.L.	BPFH I	148, 164	Kaufmann, H.	Neurovestibular	416
Harm, D.L.	Nutrition	462	Kavouras, S.A.	Cardiovascular	288
Harrison, G.H.	Radiation	478	Kazarians, G.	Radiation	515
Hartman, P.	Radiation	515	Kelly, T.H.	BPFH I	139
Hasser, E.M.	Cardiovascular	279	Kennedy, K.S.	Sleep/Circad	559
Hatton, D.	Cardiovascular	282	Kern, R.	Radiation	515
Heesch, C.M.	Cardiovascular	279	Kessler, P.D.	Immunol	327
Heher, D.	Sleep/Circad	543	Khalsa, B.S. S.	Sleep/Circad	555
Hei, T.	Radiation	497	Kim, M.Y.	Radiation	529
Heilbronn, L.	Radiation	507	Kinnison, J.D.	Radiation	500
Heldt, T.	Cardiovascular	283	Klerman, E.B.	Sleep/Circad	567
Hersman, F.W.	Technol Dev	590	Ko, H.	Technol Dev	582
Hess, B.J.M.	Neurovestibular	407	Kornilova, L.	BPFH I	142
Hienz, R.D.	BPFH I	139	Koslovskaya, I.	BPFH I	142
Hines, J.	Technol Dev	578	Kostenuik, P.	Bone	198
Hinton, D.P.	Technol Dev	590	Kourentzi, K.	Immunol	335
Hlavacek, A.	Radiation	515	Kozerenko, O.	BPFH I	150
Hoffmann, D.	Technol Dev	590	Kozlovskaya, I.B.	Neurovestibular	411, 418, 441
Hogan, H.A.	Bone	200	Krause, D.N.	Cardiovascular	300
Holland, A.W.	BPFH I	152	Krause, K.M.	Barophysiology	124
Holley, W.R.	Radiation	488	Krebs, D.E.	Neurovestibular	447
Holmes, R.P.	Nutrition	456	Kronauer, R.E.	Sleep/Circad	567
Holton, E.M.	Bone	198, 209	Kronenberg, A.	Radiation	471, 493, 497
Hopkin, E.	Barophysiology	120	Lackner, J.R.	Neurovestibular	413
Houming, Z.	Radiation	528	Lambertsen, C.J.	Barophysiology	120
Howard, I.	Neurovestibular	429	Lane, H.W.	Nutrition	452, 461, 466
Howard, S.P.	Radiation	490	Larios-Sanz, M.	Immunol	335
Huang, W.	Bone	194	Layne, C.S.	Neurovestibular	411, 418
Hughes, K.	Cardiovascular	263	Leach, C.S.	Nutrition	461
Hughes, R.J.	Sleep/Circad	544	LeBlanc, A.	Bone	232, 235
Hunter, J.B.	Nutrition	459	Lecker, S.	Muscle	376
Hurst, J.E.	Muscle	371	Lednický, J.	Immunol	338
Huso, D.L.	Radiation	471, 490	Lee, D.H.	Muscle	376
Hutchinson, K.J.	Muscle	378	Lee, P.	Muscle	400
Hysong, S.J.	BPFH I	164	Lee, S.M.C.	Cardiovascular	308
Ingalls, C.P.	Muscle	385	Lee, S.M.C.	Muscle	377, 378
Iyengar, N.	Technol Dev	570	Lehman, S.	Muscle	390
Jackson, C.G.R.	Cardiovascular	278	Lenarczyk, M.	Radiation	497
Jan, D.	Technol Dev	579	Leonardo, M.	Technol Dev	582
Jewett, M.E.	Sleep/Circad	567	Levine, B.D.	Cardiovascular	286, 295
Ji, C.	Bone	215	Lewicki, D.	Radiation	515
Johnson, J.C.	BPFH I	152	Li, J.L.	Cardiovascular	303
Johnson, R.B.	Bone	211	Li, K.	Cardiovascular	303
Johnsrud, C.K.	Immunol	350	Liang, M.T.C.	Bone	192

Ling, P.D.	Immunol	338	Mullen, T.J.	Cardiovascular	290, 293, 317
Lisle, J.T.	Immunol	340	Mullen, T.J.	Technol Dev	570
Little, T.	Barophysiology	116	Mullington, J.L.	Sleep/Circad	561
Liu, W.	Radiation	493	Mullington, J.L.	Immunol	351
Loeblich, M.	Radiation	511	Mundt, C.	Technol Dev	580
Lugg, D.J.	BPFH I	164	Murakami, D.M.	Sleep/Circad	563
Lugg, D.J.	Immunol	348, 351	Murphy, J.C.	Immunol	335
Luithardt, H.H.	Sleep/Circad	541	Murthy, G.	Muscle	378, 390
Lujan, B.F.	Muscle	386	Nagashima, K.	Cardiovascular	288
Lutze-Mann, L.	Radiation	485	Navidi, M.	Bone	192
Mack, G.W.	Cardiovascular	288	Nelson, G.A.	Radiation	513, 515
Mack, K.	Bone	214	Neri, D.F.	Sleep/Circad	544
Magee, T.C.	Bone	202	Neudec, B.L.	Nutrition	468
Maida, J.C.	BPFH II	175, 182	Neville, C.	Muscle	393
Mair, R.W.	Technol Dev	590	Newman, D.	BPFH II	173
Mapta, A.	Bone	214	Newman, D.	Bone	232
Mark, R.G.	Cardiovascular	283	Nicogossian, A.E.	Plenary	4
Markham, C.H.	Neurovestibular	420	Nilan, K.	Cardiovascular	282
Marmar, C.	BPFH I	150	Nimmagudda, R.	Nutrition	462
Marshburn, T.	Muscle	374	Norenberg, K.M.	Muscle	371
Marucci, L.	Cardiovascular	259	Novak, G.R.	Radiation	490
Maurer, R.H.	Radiation	500	Nyhan, D.	Cardiovascular	259
McCall, G.E.	Muscle	369	Oberdörster, G.	Immunol	340
McCarron, D.	Cardiovascular	282	O'Brien, K.O.	Nutrition	466
McCarthy, T.L.	Bone	215	Ochs, H.D.	Immunol	351
McCrary, J.L.	Bone	224	Oden, M.	Bone	232
McCue, S.	Muscle	363	Oganov, V.	Bone	235
McDonald, P.V.	Neurovestibular	411, 418, 421	Olszowka, A.	Cardiovascular	297
McEvoy, L.	BPFH II	173	O'Malley, B.W.	Bone	218
McFeters, G.A.	Immunol	340, 350	Oman, C.	Neurovestibular	403, 429
McIntire, L.V.	Immunol	341	Orlando, T.	Muscle	365
McNamara, M.P.	Radiation	484	Osborn, M.J.	Plenary	71
Mehta, S.K.	Immunol	348	Otsuka, K.	Cardiovascular	282
Meir, J.	Muscle	400	Pak, C.Y.C.	Bone	245
Mercer, P.	Immunol	340	Palinkas, L.A.	BPFH I	152
Merkle, L.A.	Neurovestibular	411	Paloski, W.H.	Neurovestibular	432, 441, 443
Metaxas, D.	BPFH II	176	Paloski, W.H.	Plenary	38
Metting, N.F.	Radiation	503	Pandya, A.	BPFH II	182
Mian, I.S.	Radiation	488	Pantalos, G.M.	Cardiovascular	310
Miller, C.	BPFH I	152	Parker, D.E.	Neurovestibular	435
Miller, E.S.	Immunol	354	Parsell, D.E.	Bone	211
Miller, J.	Radiation	471, 507	Partridge, N.C.	Bone	222
Miller, N.	BPFH I	142	Patz, S.	Technol Dev	590
Minor, L.B.	Neurovestibular	443	Pavalko, F.M.	Bone	205
Moffitt, J.A.	Cardiovascular	279	Pawelczyk, J.A.	Cardiovascular	295
Monk, T.H.	Sleep/Circad	559	Pedotti, A.	BPFH II	173
Moore, A.	Muscle	377	Peled, S.	Technol Dev	590
Moore, S.T.	Neurovestibular	425	Pendergast, D.	Cardiovascular	297
Moreadith, R.W.	Cardiovascular	303	Peng, R.S.	Immunol	338
Morton, D.	Immunol	354	Perusek, G.	Muscle	365
Mosier, D.R.	Muscle	388	Peterka, R.J.	Neurovestibular	437
Moyers, M.M.	Radiation	483, 513	Peterman, M.	Bone	224
Mozdiak, P.E.	Muscle	395	Peterson, K.	Cardiovascular	310
Muenter, N.	Sleep/Circad	565	Petropoulos, L.J.	Barophysiology	124
Muhlmann-Diaz, M.C.	Radiation	511	Phanouvong, T.	Cardiovascular	282
Mulavara, A.P.	Neurovestibular	411, 418	Piazza, S.	Bone	224

Pierre, L.M.	Immunol	345	Ruff, C.B.	Bone	232, 234
Pierson, D.L.	Immunol	338, 348, 351, 356	Ruiz, J.	Bone	234
Pietrzyk, R.A.	Bone	242	Ruml, L.A.	Bone	245
Pilmanis, A.A.	Barophysiology	124	Rydberg, B.	Radiation	511, 520
Pisacane, V.L.	Bone	202	Salnitskiy, V.	BPFH I	150
Pisacane, V.L.	Technol Dev	582	Sams, C.F.	Immunol	351
Pollitt, J.	Technol Dev	581	Sams, C.F.	Bone	242
Pomeroy, V.	Technol Dev	590	Sangha, S.D.	Cardiovascular	300
Pornprasertsuk, S.	Bone	243	Sauer, R.L.	Immunol	345
Potember, R.S.	Technol Dev	582	Sawin, C.F.	Plenary	19
Powell, M.R.	Barophysiology	113, 127	Schifflett, S.G.	BPFH I	145, 154, 158
Price, N.	Sleep/Circad	561	Schimmerling, W.	Radiation	529
Prisk, G.K.	Sleep/Circad	544	Schlegel, R.E.	BPFH I	145, 154, 158
Protasov, N.N.	Immunol	345	Schneider, M.D.	Cardiovascular	257
Pruett, C.J.	Neurovestibular	418	Schneider, S.M.	Cardiovascular	308
Purdy, J.	Muscle	393	Schneider, S.M.	Muscle	378
Purdy, R.E.	Cardiovascular	300	Schoeller, D.A.	Nutrition	464
Putcha, L.	BPFH I	148	Scholl, P.	Technol Dev	582
Putcha, L.	Muscle	378	Schonfeld, J.	Technol Dev	584
Putcha, L.	Nutrition	462	Schranck, D.	Radiation	515
Pyle, B.H.	Immunol	340, 350	Schubert, W.	Radiation	515
Qin, A.	Muscle	363	Schultheis, L.	Bone	234
Qin, L.	Muscle	363	Schultz, E.	Muscle	395
Quast, M.J.	Muscle	374	Schultz, J.R.	Immunol	345
Rabin, B.M.	Radiation	517	Schwartz, R.J.	Muscle	368
Radford, N.B.	Cardiovascular	303	Schwartz, R.J.	Sleep/Circad	561
Rajadurai, H.	Muscle	370	Sekula, B.K.	BPFH I	148
Ramsdell, C.D.	Cardiovascular	290, 293, 317	Shackelford, L.C.	Bone	232, 235
Ramsdell, C.D.	Technol Dev	570	Shaffner, G.	Bone	232
Raphan, T.	Neurovestibular	425	Shapiro, J.	Muscle	400
Ravani, S.A.	Radiation	480	Shapiro, J.	Bone	184, 234
Raven, P.B.	Cardiovascular	305	Sharkey, N.A.	Bone	224
Rempel, D.	Muscle	390	Sharp, M.K.	Cardiovascular	310
Reschke, M.F.	Neurovestibular	441	Shearer, W.T.	Immunol	320, 351
Reuben, J.M.	Immunol	351	Shearer, W.T.	Sleep/Circad	561
Rhie, J.	Nutrition	468	Shebilske, W.	Neurovestibular	429
Rianon, N.	Bone	232	Shehab, R.L.	BPFH I	145, 154, 158
Ricart-Arbona, R.	Radiation	490	Shelhamer, M.	Neurovestibular	443
Riccio, G.E.	Neurovestibular	421	Sherman, D.A.	Technol Dev	585
Rice, B.L.	Nutrition	461	Shim, E.B.	Cardiovascular	283
Rice, L.	Immunol	327	Shiota, T.	Technol Dev	587
Richman, A.	Cardiovascular	303	Shoemaker, J.K.	Cardiovascular	314
Riley, D.A.	Muscle	371	Shoukas, A.	Cardiovascular	259
Roberts, J.C.	Radiation	497, 526	Shukitt-Hale, B.	Radiation	517
Ronda, J.M.	Sleep/Circad	544	Shykoff, B.	Cardiovascular	297
Rosenblatt, H.M.	Immunol	351	Siklós, L.	Muscle	388
Rosenfeld, M.G.	Sleep/Circad	563	Simonson, S.R.	Cardiovascular	278
Rosenthal, N.	Muscle	393	Sinden, R.R.	Radiation	521
Roth, D.R.	Radiation	500	Sinoway, L.I.	Cardiovascular	314
Roulet, C.	Cardiovascular	282	Sinyak, Y.E.	Immunol	345
Roulet, J.	Cardiovascular	282	Skidmore, M.	Technol Dev	586
Rowe, D.	Bone	214	Skuratov, V.M.	Immunol	345
Roy, R.R.	Muscle	369	Slater, J.M.	Radiation	513
Rubin, C.	Bone	228	Sled, A.	BPFH I	150
Rubin, R.H.	Technol Dev	585	Smith, C.L.	Bone	218
			Smith, C.W.	Immunol	336, 351

Smith, E.O.	Immunol	351	Voustaniuk, A.	Neurovestibular	416
Smith, M.E.	BPFH II	173	Wade, S.W.	Neurovestibular	409
Smith, M.L.	Sleep/Circad	565	Waldren, C.	Radiation	497
Smith, S.M.	Nutrition	461, 466	Walker, V.	Radiation	485
Smolen, J.E.	Immunol	336, 351	Wall III, C.	Neurovestibular	447
Solomon, V.	Muscle	376	Walsworth, R.L.	Technol Dev	590
Sonnenfeld, G.	Immunol	320, 354	Wan, B.	Cardiovascular	303
Souza, K.A.	Plenary	46	Wang, C.	Radiation	480
St. John, K.R.	Bone	211	Warren, G.L.	Muscle	385
Stegemoeller, C.	Plenary	12	Warters, R.L.	Radiation	497, 526
Stein, T.P.	Nutrition	452, 467	Wasmund, S.L.	Sleep/Circad	565
Storey, C.S.	Cardiovascular	303	Wasmund, W.L.	Sleep/Circad	565
Storfa, R.T.	Immunol	350	Wastney, M.E.	Nutrition	466
Stowe, R.P.	Immunol	356	Watanabe, M.	Cardiovascular	282
Strandberg, J.D.	Radiation	490	Watenpaugh, D.E.	Muscle	378
Stuart, C.S.	Nutrition	455	Watenpaugh, D.E.	Sleep/Circad	565
Stuster, J.	BPFH I	162	Waters, W.W.	Cardiovascular	274
Suedfeld, P.	BPFH I	162	Webb, J.T.	Barophysiology	124
Suleiman, A.	Immunol	334	Weider, T.	Bone	209
Sundby, G.	Cardiovascular	290, 293	Weigel, N.L.	Bone	218
Sundby, G.	Technol Dev	570	Weiss, B.	Immunol	340
Sytkowski, A.J.	Immunol	357	Weiss, D.	BPFH I	150
Szcepaniak, L.	Cardiovascular	303	Welage, L.S.	Nutrition	468
Szuba, M.	Sleep/Circad	561	Welch, R.B.	Neurovestibular	449
Szumski, A.	Cardiovascular	259	West, J.B.	Sleep/Circad	544
Taube, J.	Neurovestibular	429	Whalen, R.	Bone	239
Taylor, B.	BPFH I	142	Whitmore, M.	BPFH II	170, 182
Terzic, J.	Bone	214	Whitson, P.A.	Bone	242
Thai, D.K.	Radiation	526	Wibbenmeyer, J.	Immunol	335
Theegala, C.	Immunol	334	Widrick, J.J.	Muscle	371
Thierry-Palmer, M.	Bone	234	Wiese, C.	Radiation	493
Thomas, J.D.	Technol Dev	587	Wilde, H.	Radiation	515
Thompson, A.K.	Radiation	500	Williams, G.H.	Cardiovascular	290, 293, 317
Tidball, J.G.	Muscle	397	Williams, J.	Muscle	377
Torous, D.	Radiation	485	Williams, J.R.	Radiation	488, 528
Toscano, W.	BPFH I	142	Williams, W.J.	Cardiovascular	308
Townsend, L.W.	Radiation	524	Willrich, L.M.	Sleep/Circad	559
Trappe, S.W.	Muscle	371	Willson, R.C.	Immunol	335
Trappe, T.A.	Muscle	371	Wilson, J.W.	Radiation	529
Trial, J.	Immunol	327	Winchester, S.K.	Bone	222
Tsao, A.K.	Bone	211	Winegar, R.A.	Radiation	485
Tseng, C.H.	Technol Dev	590	Winters, B.	Cardiovascular	259
Tucci, M.A.	Bone	211	Wolfe, R.R.	Nutrition	455
Turner, J.H.	Cardiovascular	258	Wolinsky, I.	Bone	192
Turner, R.	Radiation	525	Wong, G.P.	Technol Dev	590
Turner, R.T.	Bone	236	Wood, J.	BPFH I	164
Tyring, S.K.	Immunol	348	Wood, S.J.	Neurovestibular	432
Ueno, A.	Radiation	497	Woolford, B.	BPFH II	135, 182
Uzawa, K.	Bone	243	Wright, Jr., K.P.	Sleep/Circad	541, 567
Van Dongen, H.P.A.	Sleep/Circad	551	Wu, H.	Radiation	533
Vandenburgh, H.H.	Muscle	400	Wyatt, J.K.	Sleep/Circad	544
Vann, R.D.	Barophysiology	113, 132	Xu, J.F.	Radiation	478
Vannais, D.	Radiation	497	Xu, Y.	Immunol	334
Vaziri, N.D.	Cardiovascular	300	Xue, H.	Cardiovascular	282
Vazquez, M.E.	Radiation	490	Yamauchi, M.	Bone	243
Visnjic, D.	Bone	214	Yang, T.C.	Radiation	533

Yang, Y.	Bone	222
Yeh, J.	Bone	214
Yost, B.	Technol Dev	593
Young, L.R.	Neurovestibular	443
Young, L.R.	Plenary	94
Young, L.R.	Sleep/Circad	543, 544
Young, V.D.	Cardiovascular	258
Yue, Q.	Cardiovascular	282
Zardiackas, L.D.	Bone	211
Zee, D.S.	Neurovestibular	443
Zeitlin, C.	Radiation	507
Zeng, M.	Muscle	363
Zerwekh, J.E.	Bone	245
Zhang, Y.	Radiation	490, 528
Zhou, H.	Radiation	490
Zhou, X.F.	Radiation	478
Zile, M.R.	Cardiovascular	258
Zung, Y.	Muscle	393

Index

- abdominal aorta, 300-302
 absorptiometry, 192, 194, 202, 227, 232, 455
 acetylcholine, 282, 300
 actigraphy, 546, 557, 568
 adaptability, 243, 408
 adynamia, 129, 131, 133
 agent, 207, 216, 234, 280, 464, 498, 555, 577
 aging, 186, 191-192, 201, 228, 233, 240-241, 370
 aldosterone, 249-250, 288, 317-318, 461
 alendronate, 190, 235
 alertness, 167-168, 535-537, 544, 547, 549, 551, 556, 559-560, 567
 alpha adrenoceptor, 300-302
 alpha particle, 473, 502
 ambient light, 544-546, 555, 557, 567
 ambulatory, 142, 159, 192, 196, 243, 245, 260-261, 278, 286, 397, 545, 548
 ambulatory control, 192, 397
 ambulatory monitoring, 142
 aminothiols, 474-475, 526-527
 animal model, 115, 191, 209, 234, 286, 320, 328, 341, 351, 386, 431, 490, 535
 dog, 116
 mouse, 187, 189, 214, 218, 222, 252, 303, 324, 329, 332, 360, 385, 474-476, 480, 482, 490, 514, 522, 535, 563
 knockout mouse, 535, 563
 rat, 187, 192, 194-196, 200, 209-211, 215, 218, 220, 222, 227, 230, 232, 233, 234, 238, 243, 251, 254-255, 259, 300-302, 320, 354, 361, 371-373, 376, 384, 386, 389, 397, 430, 474, 476, 482, 491-492, 514, 518, 523, 528, 563, 589, 590-591
 rodent, 117, 186, 285, 321, 324, 331, 336, 373, 388, 592
 Sprague Dawley, 192, 194, 279, 300, 363
 Antarctic, 151-153, 162, 164, 320, 322, 348-349, 351
 anthropometry, 137, 171, 176
 antibody (ies), 206, 220, 243, 321-323, 325, 329-330, 340, 353, 356, 480, 497, 504, 526
 antibody production, 351
 antibody-FITC conjugate, 334
 anti-gravity muscle, 114, 211, 361
 anti-orthostatic suspension, 321-322, 329, 336, 352
 aorta, 259, 300-302, 386
 aortic pressure, 269, 311-312
 apoptosis, 352, 376, 398-399, 493-495
 argon, 115, 124-125
 arm, 289, 305-308, 372, 390-391, 405, 413, 415, 444-445, 465, 565
 arm acceleration, 418-419
 arm fatigue, 124
 arm movement, 404, 414, 418-419
 short arm centrifugation, 434
 arterial
 arterial baroreflex, 249-250, 255, 279, 281, 284
 arterial blood pressure, 252, 255, 261, 282, 289-291, 305, 315, 383, 565-566, 569
 arterial pressure, 267, 269, 271, 273-274, 279-280, 287, 305-306, 312-313, 316, 379, 565
 artificial gravity, 251, 254, 256, 406, 413-415, 446
 atrial, 269, 303,
 atrial pressure, 311-312, 587
 atrophy, 211, 249, 254-256, 259, 286, 295-296, 359-360, 365, 368, 370-371, 373, 376, 386-387, 389, 394, 400, 418, 461, 582, 584
 attention, 137, 145, 154-155, 158-159, 168, 173-174, 191, 351, 369, 454, 567
 Australian National Antarctic Research Expedition, 164, 351
 autonomic, 136, 142, 144, 251, 253, 255, 260, 271, 273, 277, 287, 291-292, 309, 406, 417, 563-564, 569

- bacteria (ial), 320, 324-325, 329, 334-335, 340, 350
- balance, 189, 191-192, 237-238, 250, 262, 263-266, 331, 423, 432, 440, 452-453, 455, 465, 467
- baroreceptor, 250, 259-260, 267, 269, 279, 280-281, 284, 291, 293
- baroreflex, 249-250, 252-253, 255, 260-266, 269, 279-281, 284, 287, 290-292, 295, 305-307, 406, 565
- basement membrane, 480-481
- bed rest (bedrest), 137, 156, 158-161, 185, 186, 187, 189, 190, 221, 233, 235, 245-247, 249-250, 253, 259, 269, 276-277, 286, 292, 295-296, 308, 314-318, 362, 370-371, 378, 380, 452, 455, 467, 587
- bioartificial muscle, 400-401
- biomechanical, 138, 175, 186, 191, 201-203, 226-228, 230, 239-240, 365
- bioreactor, 218, 220, 324, 357, 400-401
- bioregenerative life support, 454, 459-460
- Biosatellite III, 554
- biosensor, 325, 577
- blastogenesis, 354, 355
- blood, 116-117, 132, 218, 245, 284-286, 312, 321-323, 338, 352, 356, 359, 485, 583, 587, 590
- blood flow, 129-130, 250, 267-269, 289, 297-299, 302, 308-309, 314-316, 341, 373, 379, 390-391, 416, 565, 585, 592
- blood lymphocyte, 473
- blood monocyte, 218
- blood potassium, 461
- blood pressure, 144, 182, 251-253, 262, 264, 278, 282, 287, 289, 290-291, 298, 302, 307, 314-315, 383, 390-391, 416, 462, 565-566, 570
- blood sample, 245, 322, 339, 561
- blood vessel, 301, 310, 314, 321, 379-380
- blood volume, 250, 255, 259-260, 263, 265, 271, 284-285, 297, 305, 310, 453, 461, 592
- red blood cell, 323, 590-591
- white blood cell, 117, 356
- body, 114, 116, 124, 127-128, 130, 137, 172, 175, 182, 186, 190, 195, 201-203, 205, 224, 228-229, 232, 234-235, 240, 251, 260, 268-271, 277, 284, 288, 300, 302, 305, 307, 309, 312, 317, 331, 351, 359, 379, 384, 391, 406, 413, 415, 421-422, 462, 467, 471, 480-481, 507, 535, 582, 585
- body cell mass, 464
- body composition, 452, 464
- body fat, 464
- body fluid volume, 242, 279
- body kinematics, 432
- body mass, 368, 440, 452, 455, 461, 464
- body orientation, 449
- body parts, 176, 177, 447
- body sway, 437, 438, 440
- body temperature, 308, 535, 538-540, 546, 552, 554, 556-559, 563-564, 568, 580, 584
- body water, 255, 461, 464-465
- body weight, 132, 192, 195, 224, 234, 240, 295, 308, 364, 366, 368, 371, 378, 380, 461, 464
- bone
- bone cell metabolism, 238
- bone density, 186-187, 189, 212, 215, 221, 228, 235, 239-240, 583
- bone formation, 187-188, 190, 198-199, 205, 209-210, 214-215, 217-218, 220, 228-230, 232, 234, 236-238, 246-247, 331, 365, 453
- bone fracture, 202, 214, 236
- bone fragility, 202, 232
- bone geometry, 201, 203, 232-233
- bone growth, 186, 188, 194, 198-199, 214-215, 229, 238
- bone histology, 187, 246
- bone histomorphometry, 236, 238, 245
- bone loss, 185-192, 195-196, 209-210, 217-218, 221, 224, 226, 228, 230, 232, 234-236, 238-239, 242, 247, 365, 453, 466, 535
- bone marrow, 188, 196, 199, 218, 320, 354, 486
- bone mass, 185-187, 191, 193, 196, 198, 202-203, 209-210, 213, 215, 224, 227-228, 232-234, 236, 466

- bone matrix, 190, 236-238
- bone mechanics, 224
- bone metabolism, 209, 215, 239-240, 245, 466
- bone mineral, 188, 191-192, 194, 200-202, 209, 224, 234-235, 245, 282, 362, 466
- bone mineral content, 188, 192
- bone mineral density, 191, 194, 200-202, 224, 234-235, 362
- bone mineral metabolism, 466
- bone mineralization, 282
- bone models, 202
- bone morphometry, 200
- bone recovery, 235
- bone remodeling, 185, 188, 194, 196-197, 215, 234, 239, 583
- bone resorption, 187, 190, 218, 220, 234, 236-237, 246, 255, 331, 453, 466, 583
- bone strain, 185, 224-226, 234, 362, 365-367
- bone strength, 198, 200-201, 203, 209, 211, 233
- bone turnover, 186-187, 214, 218, 236, 238, 245-247
- bone volume, 196, 209, 214, 229-230, 236-237
- brain, 173, 297, 299, 300, 314, 383, 390, 416, 425, 485, 517, 535, 548, 585, 590
- caffeine, 173, 453, 468, 561
- calcaneus, 187, 189, 211, 239-240, 362, 366-367
- calcium, 185, 205, 218, 242, 255, 346, 385, 454, 456, 458
 - calcium absorption, 245, 453, 457, 466
 - calcium balance, 189, 192
 - calcium channel, 188, 301
 - calcium homeostasis, 187, 245, 246, 466
 - calcium kinetics, 453, 466
 - calcium loss, 190, 453
 - calcium metabolism, 282
 - calcium resorption, 466
 - calcium supplementation, 192
 - intracellular calcium, 118, 188, 205, 251, 282
- canal-otolith feedback, 432, 434
- cancellous, 190, 196, 209, 227, 229, 236-239, 246
- cancer, 376, 475, 481, 483, 497, 500-501, 521-522, 532
- canine, 116, 117, 587
- carcinogenesis, 322, 471, 473-476, 481, 490, 492, 497-498
- cardiac, 251-252, 257-258, 260-262, 279, 291, 293-294, 305, 313-314
 - cardiac atrophy, 249, 254-256, 286, 295-296
 - cardiac deconditioning, 276
 - cardiac mass, 286, 296
 - cardiac output, 130, 144, 250, 253, 259, 267, 274-275, 297-299, 310-312, 589, 592
 - cardiac preload, 586
- cardiopulmonary baroreceptors, 267, 289
- cardiopulmonary reflex, 284
- cardiovascular deconditioning, 253, 263, 379, 565
- cardiovascular system identification, 290, 570
- carotid, 250, 252, 259-261, 284, 300-301, 305-307
- carotid artery, 250, 301
- catecholamine, 234
- cell
 - B-cell, 321
 - bone cell, 188, 198, 215, 218-219, 221, 236, 238
 - cell activity, 325, 352
 - cell culture, 215, 236, 258, 484, 529, 576
 - cell cycle, 475, 505, 520
 - cell function, 188, 198, 219, 328, 331
 - cell glycogen, 373
 - cell interactions, 336, 480
 - cell line, 185, 205, 218-220, 323, 333, 357, 475, 478, 493, 495, 503, 514, 521, 522-523, 526
 - cell membrane, 320
 - cell type, 475, 481, 484, 506, 528
 - cellular adhesion, 352
 - cellular protein, 527
 - fixed cell, 526-527
 - irradiated cell, 504-506, 522, 526, 527

- muscle cell, 214, 258, 324, 341, 360, 393, 397-400
- mutant cell, 493, 498
- neoplastic cell, 481
- red blood cell, 323, 589-590
- red cell, 323, 327-328
- satellite cell, 361, 395-396
- stem cell, 303
- T-cell, 321, 351
- tumor cell, 479, 514, 528
- white blood cell, 117, 356
- central venous pressure, 250, 267, 269, 297, 299, 305-306, 311, 591
- centrifugation, 216, 298, 331, 378-379, 406, 425-427, 432-444, 538, 554, 563
- centrifuge, 211, 251-252, 256, 278, 324, 331, 379, 425, 432-433, 444, 515, 539
- cerebellar disorders, 441-442
- cerebral, 132, 250-251, 298, 384, 416, 592
 - cerebral blood velocity, 297, 299
 - cerebral circulation, 297, 301, 384
 - cerebral perfusion, 297, 299, 300, 302, 314, 585
 - cerebral perfusion pressure, 299, 300, 302, 314
- chondrocytes, 198, 222-223
- chromosomal damage, 473, 486
- chromosome aberration, 473, 476, 515, 528
- chronobiotic, 555, 557
- circadian, 331, 538, 546, 551-552, 561
 - circadian amplitude, 539, 541-542, 547-548, 550
 - circadian clock, 555
 - circadian entrainment, 537, 567-568
 - circadian misalignment, 567
 - circadian pacemaker, 535-537, 541, 544, 547, 549, 555-558, 567
 - circadian phase, 541-542, 547-550, 555, 557, 567
 - circadian rhythm, 116-118, 136-137, 147, 198, 290, 318, 535-536, 538, 540, 547, 551-552, 555, 558-560, 563-564, 568
 - circadian system, 403, 535-537, 540-541, 545, 559, 567
 - circadian timing system, 535, 546-547, 554-556
- clearance, 288-289, 317, 321, 329-330, 351
- cognitive, 138-139, 141, 145, 168, 405, 430, 517, 551
 - cognitive impairment, 173-174
 - cognitive load, 137, 173-174
 - cognitive performance, 137, 145, 147, 154, 158, 161, 518, 536, 544, 549
 - cognitive process (ing), 154-155, 168
 - cognitive psychology, 136
 - cognitive speed, 551
 - cognitive state, 164
 - cognitive strategies, 430
 - cognitive throughput, 535, 547
- cold pressor test, 315-316
- collagen, 188-189, 198, 215-217, 237, 243, 245, 252, 257-258, 324, 332-333, 400, 476, 480-482, 582
- colon, 478, 526
- colony stimulating factor, 320, 354, 355
- computer model, 224, 254, 310, 312
- condensate, 325, 345-346
- confinement, 153, 162-164, 260, 286
- context cue, 405, 443-444
- core body temperature, 552, 556-559, 568
- coriolis (Coriolis), 403, 405, 406
 - Coriolis effect, 434
 - Coriolis force, 413-415, 444
- cortical thickness, 189, 211-213
- cortisol, 317-318, 356, 452, 455, 535-536, 557, 560-562, 567
- cosmic radiation, 471, 490
- cosmonaut, 143-144, 232-233, 411
- COSMOS 1514, 554
- creatinine, 368, 456, 582
- cross-coupling, 415, 436
- cyclic strain, 341-342
- cytogenetic damage, 485-486
- cytokine, 320, 352-353, 475
- cytoskeleton, 188, 205, 257
- decompression sickness, 114, 116, 124, 127, 128-129, 132-133
- deformable model, 176-178
- delayed-type hypersensitivity, 321, 336
- dextran, 263, 265, 305-306
- diastolic blood pressure, 144, 314, 416
- diastolic suction, 253, 286

- diet, 140, 245, 251, 282, 317, 453-457, 459, 464
 dietary salt, 190, 192
 Digit Symbol Substitution Task, 140-141
 disorientation, 414, 429, 443-444
 disuse atrophy, 386-387
 diuresis, 263, 265
 DNA, 222, 348-349, 368, 488-490, 493, 495, 505, 512, 520, 522
 DNA binding sequence, 217
 DNA chip hybridization, 335
 DNA damage, 473-475, 485-486, 500, 502, 511, 521, 526
 DNA lesions, 528
 DNA polymerase, 216
 DNA probe, 216, 325
 DNA repair protein, 503-504
 DNA repeat, 521
 DNA sequence, 476, 521
 DNA synthesis, 506
 DNA unit, 395-396
 viral DNA, 322, 561
 dopaminergic system, 474, 517-518
 Doppler, 132, 253, 256, 290, 299, 314, 379, 586-588
 Doppler flow, 263, 308, 379
 dose rate, 473, 477, 514, 521, 528, 529
 double strand break, 488-489, 496, 503, 511
 E protein, 359, 393
 E. coli, 216, 325, 335, 340, 485, 515
 early antigen, 323, 356
 echocardiograph, 133, 586
 edema, 115-118, 196, 297, 299, 344, 374
 ejection fraction, 293, 587
 elbow, 362, 369
 electrocardiogram (ECG), 256, 267, 274, 276, 291, 293, 298, 416, 565-566, 579, 585
 electrocardiographic, 253, 271, 276
 electrocardiography, 293
 electroencephalogram (EEG), 137, 167, 173-174, 537, 544, 546-549, 552, 558
 electromyogram (EMG), 226, 360, 366, 369, 388, 404, 418-419, 546
 electrooculogram (EOG), 444, 537, 546-549
 emboli, 115-116, 125
 end-diastolic volume, 298, 303
 energy intake, 452, 461, 467
 entrainment, 536-537, 542, 546, 555, 557, 567
 environmental chamber, 322, 348-349
 epithelial cell, 332, 333, 476, 503, 528
 Epstein-Barr virus, 321, 338, 356
 erythropoietin, 323, 328, 357
 estradiol, 219, 582
 estrogen, 190, 218-220, 236, 238, 274-275, 478
 estrogen receptor, 190, 218-219, 478
 ethylene, 325, 346
 exercise, 114, 125, 129-131, 140, 155, 158, 214, 218, 224, 237-238, 240, 250, 252, 261, 269, 271, 276, 293-294, 305, 313, 374, 378-379, 381, 467, 566, 570
 aerobic exercise, 452
 arm exercise, 306, 307
 bed rest exercise, 249
 dynamic exercise, 255, 260, 306
 exercise capacity, 387, 565
 exercise countermeasure, 232, 367, 370, 372
 exercise device, 380
 exercise metabolism, 386
 exercise protocol, 144, 288, 308, 375
 exercise regimen, 187, 189, 262, 365, 380
 forearm exercise, 565
 in-flight exercise, 226
 isometric exercise, 360, 371, 372, 373
 isotonic exercise, 371, 372, 373
 jumping exercise, 362, 365, 366, 367
 locomotor exercise, 224
 prebreathe exercise, 132, 133, 134
 resistive exercise, 189, 235, 362
 supine exercise, 278
 tethered jumping exercise, 365
 zero-G exercise, 225
 extracellular matrix, 208, 222, 476, 480, 482, 484, 514
 extravehicular activity (EVA), 114-116, 119, 124-125, 127, 129, 131-133, 137, 172, 175, 305, 308, 361, 374, 403-404, 407, 421-423, 471, 573-574, 578

- eye, 403-406, 425, 427, 436-437, 441, 443-445, 449-450, 514, 549
- fat, 202, 368, 456, 464, 468, 584
fatty acid, 371, 372, 386, 387
- fatigue, 124, 137, 140, 145, 154, 156, 158, 168, 170, 173, 175, 260, 308, 361, 371, 373-375, 380, 390-392, 422, 535, 544, 560, 565
- fatty acid, 371-372, 386-387
- Fe-ion irradiation, 478-479
- femoral, 188, 192, 200-201, 209, 224, 245, 259, 279-280, 300
femoral artery (ies), 251, 259, 300-302
femoral neck, 187, 189, 200, 201, 209, 245
femoral vein, 194, 196
femoral vessel, 455
- fibroblast, 237, 503, 511, 520
- filling pressure, 295, 303, 311
- finite element model, 232, 233, 239
- fluid, 116, 128, 196, 317, 346, 384, 453, 592
body fluid, 114, 242, 279, 331, 379
extracellular fluid, 464
fluid exchange dynamic, 361, 374
fluid intake, 189, 242, 261, 262, 461
fluid regulating system, 288
fluid shear, 188, 194, 205, 207, 216
fluid shift, 198, 286, 300, 302, 310, 311, 312, 336, 382, 391, 452, 540, 563
fluid volume, 242, 265, 279
interstitial fluid flow, 188, 194, 341
- fluorescent, 189, 325, 327-328, 340
- food, 136, 158, 192, 262, 324, 388, 452, 454, 456, 459, 461, 468, 515, 538-539, 563
food processing, 459
- foot, 179, 225, 239, 379, 404, 414, 418-419, 430, 513
foot pressure, 418-419
- forearm, 261, 267, 268, 269, 308, 316, 361, 374, 390, 391, 561, 565
forearm muscle, 361, 374
forearm vascular resistance, 261, 269, 565, 566
- fracture, 185-187, 200, 202, 204, 209, 245
- gait, 225, 227, 239, 379-380
gait assessment, 448
gait cycle, 412
- galactic cosmic ray, 477, 507, 521, 525
- gamma ray, 474, 491, 501, 503, 505, 514, 528
- gamma-radiation, 480, 481
- gas, 114-116, 124-125, 127-130, 343-344, 473, 501, 590-592
- gastric, 331, 452, 478
gastric emptying, 453, 468, 469
gastric motility, 468
- gastrocnemius, 364, 366-367, 371-372, 386, 388-389, 418
- gastrointestinal, 329, 452-453, 468, 478, 567
- gaze, 405, 429, 443, 445, 567
gaze fixation, 411
gaze stabilization, 412, 441
- gender difference, 201, 538
- gene, 215, 230, 238, 322, 352, 368, 475, 479, 486, 493, 497, 526, 527, 563, 564
gene activation, 216, 320
gene conversion, 523
gene expression, 188, 205, 207, 216, 219, 236, 237, 252, 341, 342, 359, 363, 364, 393, 394, 474, 478, 484, 514
gene function, 323
marker gene, 189, 214, 220
reporter gene, 216, 219, 222, 485, 522
- genome, 322, 338-339, 521-523
- genomic instability, 474, 481, 486, 521-522
- glomerular filtration rate, 288-289
- glucose, 324, 368, 373
- glycogen, 361, 371, 373, 387
- glycol, 325, 346
- ground reaction force, 187, 190, 225-226, 228, 234, 239-240, 366-367
- growth factor, 187-188, 215, 218, 237-238, 258, 331-333, 341, 360, 400, 482, 582-583
- growth hormone, 188, 238, 359, 362, 368, 400-401, 535, 537, 551, 553, 567
- head, 143, 172, 200, 211, 213, 255, 268, 293, 382, 416, 421, 425, 435
head direction cells, 404, 430
head down tilt, 159, 249, 380, 384, 464
head injury, 409

- head movement, 403, 405, 407-408, 411-415, 432-434, 441, 444
- head rest, 438
- head rotation, 445
- head stabilization, 443, 446
- head trauma, 381, 383
- head up tilt, 249, 284
- head-down tilt, 132, 260, 267, 269, 286, 292, 295, 298-299, 314, 383, 464
- head-eye coordination, 414
- head-out immersion, 298
- heads-up display, 572-573
- head-up tilt, 260, 278, 292, 295, 314, 379, 383
- heart, 130, 257, 286, 303, 310, 311, 317, 589
 - heart beat, 585
 - heart function, 255
 - heart rate, 143, 249-250, 252-253, 255-256, 259, 261, 267, 271, 274-280, 284, 287, 290-293, 296-298, 305-306, 308, 314, 406, 416-417, 462, 538-539, 554, 563, 565-566, 569, 583
 - heart rate dynamics, 253, 276-277
- heat stress, 256, 267, 269
- heavy charged particles, 471-472, 507
- heavy ion interaction, 474, 507, 509
- heavy particles, 517, 519
- heel, 239-240, 343-344, 366
 - heel-strike, 225, 412
- high LET, 483, 486, 489, 506
- high-LET radiation, 533
- hindlimb, 187
 - hindlimb elevation, 198, 237, 243
 - hindlimb suspended, 190, 194, 196, 385, 387
 - hindlimb suspension, 188, 360, 373, 385-387, 395, 397
 - hindlimb unloading, 201, 279, 281, 370-371, 385, 388-389, 398
 - hindlimb unweighted, 243, 279
 - hindlimb unweighting, 300, 373
- hip, 203, 224, 232-233, 235, 245
- human
 - human B-lymphoblastoid cell line, 493, 495
 - human body model, 176
 - human centrifugation, 298
 - human factors, 136-138, 170-172, 176
 - human lens epithelial, 484
 - human-environment interaction, 421
 - human-powered centrifuge, 278
- Human Research Facility (HRF), 158, 577, 580, 588
- humerus, 232, 234, 354
- humidity, 345-346
- hydraulic model, 310, 312
- hyperbaric, 114, 116-117, 133-134
- hypercalciuria, 246, 461
- hypergravity, 324, 331-332, 432, 434, 540
- hypertrophy, 252, 257, 259, 370
- hypobaric, 116, 125, 127, 134
- hypotension, 249-250, 259-263, 265-266, 271, 274, 280, 286-287, 302, 314-315
- hypovolemia, 262, 286, 296, 540
- HZE, 490, 510
 - HZE experiments, 491
 - HZE exposure, 480, 529
 - HZE Fe, 497, 520
 - HZE particle, 480, 490, 520, 521
 - HZE radiation, 486, 529
- ibandronate, 186, 190, 232-233
- illusory self-motion, 435
- image analysis, 331, 332, 480, 481
- immunofluorescence, 206, 208, 480, 484, 526
- immunoglobulin, 353-354
- immunosuppression, 325, 339, 350-351
- impact load, 365, 367, 380
- indomethacin, 194, 195, 301
- infectious disease, 338, 350, 561
- inflammation, 116, 336, 344, 351-352, 397-399
- insomnia, 536, 556
- instantaneous lung volume, 290-291
- insulin-like growth factor-I (IGF-I), 198-199, 215-217, 583
- interferon-gamma production, 354-355
- internal temperature, 250, 267, 269
- International Space Station (ISS), 114, 124, 127, 132-133, 150, 164, 170-172, 179-182, 185, 191, 235, 340, 345, 347, 404, 418, 430, 452-453, 459, 466, 472, 477,

- 483, 515, 529, 531, 558-559, 565, 568, 572, 576, 579, 587-589, 591, 593
 Human Research Facility (HRF), 158, 576, 588
 interstitial fluid flow, 188, 194, 341
 intracellular, 118, 188, 205-207, 251, 282, 325, 331-333, 340, 385, 388, 455, 464, 484, 526, 527
 intracellular physiology, 526
 intracellular water, 464
 intracranial pressure, 381-384
 intrathoracic pressure, 292, 311
 isolation, 139, 153, 162-164, 208, 254, 348, 351, 537
 isometric exercise, 360, 371-373
 isotonic exercise, 371-373
 jumping exercise, 362, 365-367
 kidney stone, 245, 456
 kinase, 215, 257, 301, 323, 331, 359, 370, 493
 kinematics, 175, 179, 225, 404, 411-412, 432-433
 Ku protein, 503, 505-506
 laminin, 476, 480-481
 laser-polarized, 589, 590-591
 latent virus, 321-322, 338, 348, 352, 561
 launch and entry suit, 309, 361
 leg movement, 405, 413-414
 leukocyte, 321, 336, 352, 355-356
 leukocyte blastogenesis, 355
 leukocyte infiltration, 336-337
 leukocyte recruitment, 336, 352
 leukocyte-endothelial cell interaction, 336
 light, 133, 180, 211, 259, 413, 415, 432, 449, 452, 539, 551, 555, 557, 568, 578
 light exposure, 545-546, 548
 light illumination cycle, 403
 light intensity, 537, 544
 light ions, 509
 light levels, 536, 541-542, 545
 light source, 390
 light-dark cycle, 537, 540-541, 556, 567
 linear acceleration, 405, 417, 420, 425, 427-428
 linear energy transfer (LET), 474, 483, 486, 489, 494, 497, 503-504, 506, 520, 529, 531-532
 high LET, 483, 486, 489, 506
 high-LET radiation, 533
 low LET, 489, 503-504, 529
 lithium, 288, 517-518
 liver, 189, 215, 230, 354, 476, 480-481, 485
 load, 116, 130, 137, 173-174, 179-180, 200-202, 215, 218, 224, 226, 252-253, 257, 278, 286, 288, 305, 338-339, 370-371, 473, 493, 587
 load cell, 179-180
 locomotion, 187, 190, 225-227, 361, 377, 381, 404, 411-412, 418, 447
 long duration space flight, 145, 224, 235, 239-240, 293, 405, 441, 453-454, 488, 547
 long duration space mission, 152, 368, 507
 lower body negative pressure (LBNP), 251, 260-261, 270, 276-277, 284-285, 295, 305-307, 313, 362, 378-379, 384, 566
 lumbar spine, 187, 189, 235, 245
 lumbar sympathetic, 250, 279
 lung, 592
 lung imaging, 591
 lung injury, 119, 343
 lung lavage, 344
 lung tissue, 117
 lung tumor, 514
 lung vasculature, 297, 299
 lung ventilation, 590
 lung volume, 290, 291, 298
 macrophage, 327, 398-399
 malignancy, 320, 325, 351
 mammary cell, 523, 528
 mammary gland, 331, 333, 475-476, 480-482
 marrow, 188, 195-196, 199, 218-219, 234, 320, 354, 486
 marrow pressure, 195-196
 Mars, 114-115, 124, 164, 185-186, 356, 403, 483, 517, 524-525, 536, 558, 567-568
 Martian, 115, 124, 537
 mathematical modeling, 120, 239-240, 466
 model of cardiovascular function, 283

- matrix protein, 190, 205, 236, 237, 238, 257
maturation of oocytes, 331
mechanical, 120, 190, 204, 214, 216, 227, 229, 231, 236-238, 258, 287, 359, 398
 mechanical damage, 397
 mechanical demand, 194, 224
 mechanical effect, 121, 292
 mechanical forces, 128
 mechanical hemodynamics, 341
 mechanical load, 186-187, 189, 191, 197, 205, 210, 215, 217-218, 234, 240, 243, 252, 257, 360, 399
 mechanical performance, 303
 mechanical properties, 200-201, 291, 373
 mechanical stimulus (stimuli), 187, 196, 202, 205, 207, 217, 228, 230, 232, 239, 367, 370, 435-436
 mechanical strain, 187, 190-191, 194, 196, 205, 215-217, 227-229, 234, 237-238
 mechanical stress, 214, 231
 mechanical testing, 200-201
 mechanical unloading, 237
 mechanical usage, 236, 238
 mechanical work, 359
melatonin, 249-250, 535, 537, 544, 546-547, 549, 555, 556-558, 560-561, 567
microbial, 320, 324-325, 345
 microbial monitoring, 335
microenvironment, 218, 480-481
micronuclei, 127-129, 486
microvasculature, 474, 584
mineralization, 188, 198, 211, 243, 282
Mir, 137, 150, 170-171, 181, 185-186, 190, 232-233, 235, 242, 271, 276-277, 293, 324, 345-346, 348, 380, 411, 418, 441, 452, 466, 472, 477, 483, 515, 535
 Mir 18, 461
Mission
 COSMOS 1514, 554
 D2, 467
 International Microgravity Laboratory (IML-1), 145, 154, 158, 516
 Life and Microgravity Spacelab, 145, 154, 158, 371
 Neurolab, 171, 271, 272, 295-296, 405, 425, 428, 543-546, 557, 581, 584
 Second International Microgravity Laboratory (IML-2), 145, 146, 154, 156, 158
 Skylab, 235, 348, 467
 SLS1, 467
 SLS2, 467
 Spacelab-3, 554
 STS, 139, 168, 170, 209, 224, 425
 STS-76, 473, 515
 STS-78, 145, 369, 371, 559
 STS-90, 170, 171, 295-296, 535, 537, 544-546, 583
 STS-95, 535, 537, 544, 545-546
mission control, 137-138, 150, 167, 169
mitochondrial, 257, 303, 373, 387-388
monitoring, 136, 139, 140, 142, 151, 167, 168, 177, 192, 202, 204, 239, 240, 256, 276, 293, 313, 318, 324, 325, 335, 340, 345, 347, 374, 382, 453, 468, 471, 502, 537, 547, 549, 552, 558, 573, 576-577, 580, 584-585
mood assessment, 142, 154
moon, 114, 124
Morris water maze, 474, 519
motion
 motion analysis, 176, 177, 179-180, 411
 motion sickness, 144, 253, 299, 403, 420, 423, 429, 433, 453-454, 462-463, 551, 584
motor
 motor control, 161, 172, 420-421, 432
 motor performance, 388
mucosal immune response, 321, 329-330
mucosal immune system, 321, 329
muscle, 186, 189, 203, 211, 213, 223, 225, 227, 242, 256, 259, 270, 279, 303, 363, 369, 372, 388, 401, 454, 535, 551, 582
 muscle activation, 374, 404, 419
 muscle atrophy, 359-360, 365, 368, 370-371, 373, 386, 389, 394, 400, 418, 461, 582
 muscle blood flow, 267
 muscle cell, 214, 258, 324, 341, 360, 393, 397-400

- muscle contraction, 116, 362, 387
- muscle deoxygenation, 380, 390, 392
- muscle development, 393, 396
- muscle fatigue, 252, 361, 374, 390-391
- muscle fiber injury, 397-399
- muscle fiber necrosis, 397-398
- muscle function, 282, 361, 371, 375
- muscle glycogen, 371, 373
- muscle groups, 226, 390
- muscle growth, 359, 361, 364, 395
- muscle loading, 170, 397, 399
- muscle mass, 185, 202, 232, 252, 305, 376, 385, 452, 465, 583
- muscle oxygenation, 361, 390-391
- muscle plasticity, 370
- muscle protein, 360, 452, 455
- muscle size, 233
- muscle strength, 190, 212, 359, 380
- muscle structure, 158
- muscle sympathetic nerve activity, 249, 251, 254, 271, 295, 314, 406, 416
- muscle tissue, 129-130, 195-196, 368, 374, 585
- muscle twitch force, 391
- mutagenicity, 497-498
- mutation, 222, 252, 303, 475, 485-486, 493-495, 498, 515-516, 521, 529-532
- myocardial, 258, 286, 304
 - myocardial ATP, 303
 - myocardial oxygen consumption, 252
- myofiber, 360, 395-396, 400
- myogenic tone, 251, 300-302
- myonuclear accretion, 395-396
- myosin heavy chain, 359, 363, 370, 393, 400
- natriuretic peptide, 288, 317
- neurobehavioral performance, 536, 545, 547-548, 551-552, 557, 568
- Neurolab, 171, 271-272, 295-296, 405, 425, 428, 543-546, 557, 581, 584
- neuromuscular activation, 418-419
- neuromuscular junction, 360, 388-389
- neutron, 477, 492, 502, 509
 - neutron detector, 500
 - neutron spectrometer, 473, 501
- neutrophil, 117, 356, 398-399
- nifedipine, 206, 207, 301
- NIH.R1, 211, 354
- nitric oxide, 115-118, 194, 250-251, 275, 300-302, 324, 341, 361, 398-399
- nitrogen balance, 465, 467
- nitroglycerin, 275, 299
- nitroprusside, 263, 265, 275, 279, 282, 565
- norepinephrine, 249, 251, 259, 261, 282, 300, 318
- nuclear fragmentation, 507, 508
- nuclear magnetic resonance, 303, 386, 590
- Number Recognition Task, 140-141
- nystagmus, 404, 416, 441
- ocular counterroll, 409, 445
- optokinetic, 404, 407-408
- orientation, 151, 159, 171, 208, 321, 404, 405, 407, 412, 421, 423, 426, 429-430, 432, 435, 437-438, 440-443, 449-450, 559, 589
- orthostatic, 278, 292, 329-330
 - anti-orthostatic suspension, 321-322, 329, 336, 352
 - orthostatic hypotension, 249, 260-263, 265, 274, 286-287
 - orthostatic intolerance, 144, 254, 260, 275, 279, 281, 283, 287, 290, 295-296, 313, 315, 382, 453
 - orthostatic stress, 259, 275, 283-285, 287, 295-296, 315, 379, 416
 - orthostatic syncope, 271
 - orthostatic tolerance, 252, 262, 274-275, 288, 290, 292, 296, 314-315, 378, 403, 406, 565-566
- osteoblast, 187-188, 191, 198, 208-209, 214, 218, 222, 236, 246, 257
- osteocalcin, 188, 198-199, 219-220, 237, 245-246
- osteoclast, 187, 191, 214, 218, 246
- osteopenia, 190, 209-210, 218, 228, 236-237, 243
- osteoporosis, 185, 189, 192, 204, 215, 224, 226, 242
- otolith, 403, 405, 406, 407, 416, 417, 420, 425, 427, 429, 434, 443-444
- oxalate, 189, 242, 453, 456-458
- oxygen consumption, 131, 133, 252, 298, 303, 308, 378

- oxygen uptake, 252, 278, 306
p53 protein, 493, 526-527
parabolic flight, 382, 404, 414, 420, 429-431, 443
parathyroid hormone, 215, 238, 245
particle, 343-344, 471-474, 477, 480, 485-486, 488-491, 493-495, 500, 502-507, 509, 515, 520-521, 525, 529, 532
passive upright tilt, 271, 274
pattern recognition, 174, 180
performance assessment, 154, 167, 545
Performance Assessment Workstation, 137, 145, 154, 158
performance measures, 147, 155-156
perfusion pressure, 299-300, 302, 314
peripheral resistance, 249, 274-275, 279, 290, 292, 297-298, 302, 314
personality, 152, 164
pharmacodynamics, 360, 452-453, 462
phenylephrine, 251, 259, 263, 279, 300, 565
photon, 192, 227, 390, 491
pitchroom, 449-450
plasma, 117, 269, 285-286, 295, 321, 327, 331, 453, 468, 561-562, 590, 591
 plasma cortisol, 356, 557
 plasma renin activity, 289
 plasma volume, 249, 251, 254-255, 260-262, 267, 288-289, 297, 381
plasmid DNA, 368, 485
polymorphism, 493, 516
porcine, 368, 386
porosity, 211-213, 591
postflight, 140, 145-146, 172, 191, 260, 262, 276, 308-309, 313, 322, 345-347, 373, 404, 406, 411-412, 441
posture, 158-159, 161, 170, 172, 249-250, 252, 253, 260, 284, 288-289, 310-312, 314, 317-318, 378, 380, 384, 390-391, 404, 413, 415-416, 418, 420, 422-423, 432-433, 444, 535, 547, 557
postural behavior, 179, 421, 440
postural control, 404, 421-423, 432, 437-440
postural intolerance, 300, 302
postural stability, 404, 422, 432-434, 439
postural sway, 415
prebreathe, 114, 127, 129-134, 377
preflight, 132, 138, 142-146, 189, 191, 235, 276, 308-309, 322, 356, 404-406, 420, 429-430, 441, 466
pressure, 114-117, 120-121, 124-125, 127-128, 132, 144, 182, 187-188, 190, 194-196, 215, 250-255, 257, 259-260, 262-264, 267-271, 273-274, 277, 279-280, 282, 284-287, 289-292, 295, 297-303, 305-307, 310-316, 324, 341-342, 377-384, 390-391, 404, 416, 418-419, 462, 547, 565-566, 569, 580, 587-589, 592
pressure suit, 124-125
presyncope, 251, 261, 275, 314-315, 384
Profile of Mood States, 139, 150, 154
programmed cell death, 493, 514
promethazine, 137, 148, 403-404, 453, 462
proprioceptor
 proprioceptive feedback, 563
 proprioceptive input, 369
prostaglandin, 194, 205, 215
protease, 216, 341
 proteasome inhibitor, 376, 393
protein, 116-118, 188-189, 198, 215-216, 218, 220, 252, 257-258, 323-324, 329, 331, 341-342, 359-360, 363-364, 370, 372-373, 376, 393, 398, 452-453, 456, 464, 467, 475, 484, 493, 503-506, 526-527, 563, 583
 protein metabolism, 455
 protein synthesis, 205, 208, 217, 236, 252, 360, 400, 452, 455
proteoglycans, 188, 243
proteolysis, 360, 376
proton, 361, 374-375, 472, 475, 491-492, 502, 513, 591
 proton beam, 483, 514
 proton radiation, 473, 484, 513
psychomotor performance, 138-140, 462
psychosocial, 150, 348, 535
PTFE fumes, 343-344
pulmonary, 121, 287, 295
 pulmonary arterial pressure, 312
 pulmonary blood flow, 250, 297-298
 pulmonary blood volume, 297
 pulmonary circulation, 297, 310

- pulmonary edema, 115-117, 344
- pulmonary mechanical function, 120
- pulmonary membrane, 592
- pulmonary tissue, 590, 591
- pulmonary vascular resistance, 250, 299
- pulmonary vasodilation, 118
- pulmonary ventilation, 278
- quality factor, 529, 531-532
- radiation, 322, 484, 486, 489-491, 503, 509, 513, 515-517, 529-533, 582
 - ionizing radiation, 474, 478-481, 483, 487, 493, 496, 497, 500, 511-512, 520-521, 526
 - radiation damage, 475, 488, 501, 511
 - radiation detectors, 472-473, 483
 - radiation dose, 186, 508
 - radiation environment, 471, 476-477, 485, 487, 493, 495, 500, 521, 524-525
 - radiation exposure, 322, 474-475, 513, 529
 - radiation hazards, 471, 507
 - radiation limits, 524
 - radiation protection, 471, 483, 524, 532
 - radiation response, 474-475, 484, 514-515
- radius, 115, 127, 245, 278, 406, 413, 415, 432
- reaching error, 414, 429
- Recommended Dietary Allowance (RDA), 461
- recycled water, 325, 345-347
- red cell, 323, 327-328
 - red cell age, 327
 - red cell mass, 327
- remodeling, 185, 188, 194, 196-197, 214-215, 229, 234, 239, 245, 254, 324, 342, 388, 480-482, 583
- remote manipulator system (RMS), 156-157, 159, 170, 172, 403
- renal, 263, 279, 452
 - renal artery, 259
 - renal blood flow, 250, 288-289
 - renal function, 261
 - renal hemodynamics, 317
 - renal plasma flow, 288
 - renal response, 265
 - renal sodium, 252, 288
 - renal stone, 185, 189, 242, 453-454
 - renal sympathetic, 279, 280, 289
 - renal tissue repair, 331
- renin-angiotensin, 261, 291, 318
- Repeated Acquisition Task, 140-141
- resistance exercise, 237-238, 373
- respiratory exchange, 278
- rest-activity cycle, 541, 545-547
- restraint, 170-172, 179, 182, 263, 287
- rodent, 117, 186, 285, 321, 324, 331, 336, 373, 388, 593
- roll tilt, 425-427, 432-434
- rotating room, 413-415
- rotation, 155, 203, 220, 403, 406-408, 413-416, 425, 427, 433-434, 444-445
- rotational stimuli, 405, 407
- rotavirus, 321, 329-330
- R-R interval, 255, 260, 271, 273
- running, 187, 190, 224, 226, 239-240, 343-344, 362, 378, 403
- saliva, 148, 322, 348-349
 - salivary flow rate, 453, 462
 - salivary gland, 331
- satellite cells, 361, 395
- secondary particle, 500, 521
- self-orientation, 429, 435
- serum, 185, 187, 198, 215-217, 238, 245-247, 327, 329, 333, 354-355, 368, 398, 497
- shielding, 471-472, 477, 483, 490, 500, 507-509, 521, 531-532, 592
- skeleton (skeletal), 185, 192, 196, 203, 205, 210, 218, 224, 228-229, 232-233, 236-240, 571
 - skeletal growth, 188, 214-215, 245
 - skeletal muscle, 202, 279, 303, 314, 359, 361, 363, 370-371, 373, 376, 385-386, 393, 395, 399-401, 452, 455, 585
 - skeletal muscle mass, 385
 - skeletal unloading, 189-190, 198-199, 243, 245-246
- skin, 270, 336, 429, 503, 546, 583, 585-586
 - skin blood flow, 267, 268, 269, 308, 309
 - skin conductance, 143
 - skin conductance level, 143
 - skin grafting, 331

- skin reaction, 321
- skin surface, 369, 390
- skin temperature, 143, 267, 268, 270, 308
- skin test, 348
- Skylab, 235, 348, 467
- sleep, 136-137, 140, 167, 276, 454, 535, 558-559, 568
 - sleep cycle shift, 555
 - sleep deprivation, 139, 292, 317-318, 320-321, 323, 547-549, 561
 - sleep disruption, 318, 544, 560
 - sleep duration, 536-537, 551, 552, 560
 - sleep efficiency, 544, 546, 556
 - sleep loss, 173, 536-537, 546-547, 551, 553, 561
 - sleep restriction, 536, 551, 565-566
 - sleep time, 545-546, 551, 553
 - sleep/wake cycle, 555-557
 - sleepiness, 462, 544, 548-550
 - sleep-wake cycle, 547, 554-556, 567
- smooth muscle, 116, 214, 256, 259, 282, 324, 341
 - smooth muscle hypertrophy, 259
- sodium intake, 453, 461
- solar
 - solar cycle, 472, 521
 - solar particle event, 471, 477, 490, 521, 525
 - solar particle radiation, 525
- soleus muscle, 212-213, 360, 364, 370-371, 373, 385, 389, 397
- Space Shuttle (shuttle), 114, 116, 124, 132, 137, 139, 142, 148, 150, 157, 170-172, 181-182, 188, 208, 221, 235, 242, 271-272, 276, 282, 297, 322-323, 340, 345-346, 348, 350, 354, 361, 363, 377, 400, 441, 459, 461-462, 467, 472, 500, 515, 535, 537, 544-546, 555-556, 558-559, 572, 575, 578, 583
 - D2, 467
 - IML-1, 516
 - IML-2, 145, 146, 154, 156, 158
 - Life and Microgravity Spacelab, 145, 154, 158, 371
 - Second International Microgravity Laboratory, 145, 154, 158
 - SLS1, 467
 - SLS2, 467
 - Spacelab-3, 554
- space sickness, 276, 403
- spatial, 144, 154, 158, 425, 480
 - spatial cognition, 435
 - spatial correlation, 488
 - spatial disorientation, 414
 - spatial distribution, 521
 - spatial learning, 404, 430, 474, 518, 519
 - spatial memory, 403, 404, 430
 - spatial organization, 407, 408
 - spatial orientation, 429, 432, 435, 441, 442, 450
 - spatial perception, 449
 - spatial processing, 145, 432
 - spatial resolution, 186, 203, 591
 - spatial rotation, 155
- spine, 187, 189-190, 203, 235, 245
- spleen, 321, 354, 485
- Stanford Sleepiness Scale, 148, 462
- static tilt, 404, 410, 425-427
- stimulus, 141, 155, 196, 202, 205, 207, 228, 230, 232, 239, 260, 278, 286, 287, 370, 382, 403, 405-409, 427, 429, 436, 438, 442, 444-445, 517-518
- strength, 128, 137, 175, 185, 190, 198, 200-203, 209, 211-212, 221, 228, 233, 359, 380, 385, 565-567
- stress, 116, 119, 121, 128-129, 136-137, 161, 168, 198, 205, 207, 214, 220, 231, 234, 239-240, 250, 256, 259, 267-269, 275, 283-287, 293, 295-296, 308, 315, 317, 320, 323-325, 336, 341-342, 348-349, 352, 356, 378-379, 416, 467, 514, 551, 562, 565-566
- stroke volume, 249, 255, 274-275, 286-287, 290, 295-296, 298, 305, 312, 314, 592
- structural analysis, 201-202
- sudden cardiac death, 253, 293-294
- supine exercise, 278
- sweat loss, 308-309
- sympathetic nerve activity, 249-251, 254-255, 271, 273, 279, 281, 289, 295, 314, 406, 416
- sympathetic nervous system, 252, 279, 314

- syncope, 142, 262, 271, 302
- systolic blood pressure, 282, 314-315, 390, 566
- tachycardia, 250, 263-265, 276-277, 293
- tail suspension, 198, 232, 243, 388
- T-cell, 321, 351
- telemetry, 168, 308, 538, 572, 581, 583
- tendon-bone junction, 189, 211-213
- thymidine, 354, 493
- thyroid, 474, 514
 - thyroid hormone, 359, 363, 364, 535
- tibia, 211, 224-225, 229-230, 236, 238
- Time Estimation Task, 140-141
- tissue, 127-128, 132, 188, 202, 222-224, 227-228, 240, 253, 321, 331, 361, 391, 399, 473-475, 478-479, 483, 485-486, 501, 521, 529, 591
 - connective tissue, 129, 185, 214
 - lung tissue, 117
 - muscle tissue, 129-130, 195-196, 368, 374, 585
 - myocardial tissue, 303
 - tissue culture, 354, 357, 400-401, 522
 - tissue dysfunction, 336
 - tissue engineering, 401
 - tissue equivalent material, 471-472
 - tissue imaging, 586-588
 - tissue integration, 474
 - tissue level metabolism, 361, 374
 - tissue loading, 240
 - tissue microenvironment, 480-481
 - tissue necrosis factor, 514
 - tissue perfusion, 129, 380, 584, 589
 - tissue plasminogen, 324, 341
 - tissue plasminogen activator, 341
 - tissue site, 532
 - tissue stress, 239
 - tissue type, 130
- total blood volume, 284-285, 461
- total body potassium, 461
- total body volume, 317
- total body water, 255, 461, 464
- total body weight, 368
- total organic carbon, 325, 346
- total peripheral resistance (TPR), 249, 255, 274-275, 287, 292, 297-298, 314
- trabecular density, 196, 233
- track structure, 488, 520, 529-532
- transcription, 188-189, 208, 217, 222-223, 257, 352, 359, 393, 478, 484, 526-527
- transforming growth factor, 188, 332-333, 341, 482
- transgene, 214, 393, 486
 - transgenic mice, 214, 222, 482, 485
- translation, 188, 202-203, 208, 257, 405, 416, 425, 427, 435, 445-446
- trapped particles, 473, 477
- treadmill exercise, 224, 237, 378
- trefoil peptide, 475, 478-479
- tricarboxylic acid cycle, 371, 373
- trunk rotation, 444-445
- tyrosine kinase, 301, 331
- ubiquitin-proteasome pathway, 360, 376, 393
- unweighting, 250, 280, 300, 311, 361, 371, 373, 395-396
- up-regulation, 300, 504-506
- upright tilt, 271, 274
- urine, 116-117, 148, 185, 192, 245, 250, 262-264, 322, 331, 348, 356, 456, 462, 466, 539, 557, 559, 561, 582-583
- urinary calcium, 189-190, 242, 246, 457
- urine catecholamine, 234
- urine output, 189, 242, 261, 264, 540
- Valsalva maneuver, 251, 261
- Valsalva straining, 271, 273
- vascular, 256, 259, 265, 267-268, 279, 282, 291, 300-302, 310, 315, 318, 324, 336, 342-343, 361, 379, 535
- vascular dilation, 316
- vascular resistance, 117-118, 250, 260, 261-262, 269, 287, 295, 297, 299, 314, 565
- vascular smooth muscle cells, 214, 341
- vascular tone, 116, 314-315, 416
- vasoconstriction, 116, 249, 255, 261-262, 270, 275, 297, 299, 301, 314, 316, 379
- vasoconstrictive responses, 254, 274
- vasopressin, 261, 289
- vastus lateralis, 366-367, 455

- venous, 116-117, 187-188, 194-196, 245, 250, 263, 267, 269, 279-280, 299, 305-306, 310-313, 315, 590, 592
- venous return, 275, 292, 297
- venous transmural pressure, 284-285
- ventilation, 252, 278, 297, 590
- ventricle, 286, 310-311, 382, 587
- ventricular arrhythmias, 293
- ventricular fibrillation, 293
- ventricular tachycardia, 276, 277, 293
- ventricular volume, 286-287, 312, 588-589
- ventrolateral medulla, 250, 280
- vestibular, 403-404, 406-408, 413-415, 422-423, 425, 429, 432, 435-438, 440, 444, 447, 535, 540, 563-564
- vestibular deficit, 409
- vestibular loss, 409
- vestibular-autonomic reflex, 416
- vestibulo-ocular reflex, 405, 407
- viral capsid antigen, 323, 356
- viral infection, 321, 325, 338, 352
- virtual reality, 136, 176, 182-183, 429
- virus shedding, 322, 329-330
- visual reorientation illusion, 404, 429
- visually perceived, 405, 449, 450
- visually perceived eye level, 405, 449
- volume, 128, 143, 171, 180, 189, 196, 202, 209, 214, 229-230, 236-237, 240, 242, 249, 251, 254, 259-260, 262, 264, 267, 271, 274-275, 284-287, 290-291, 295-298, 303, 305, 310-312, 314, 318, 323, 327, 378, 381, 383, 387-388, 396, 453, 461, 464, 494, 539, 589, 592
- volume expansion, 250, 252, 255, 263, 265, 288, 289
- volume homeostasis, 317
- walking, 114, 128, 187, 190, 224-226, 239-240, 361-362, 377, 411-412, 449
- water, 128, 194, 240, 252, 255, 262-264, 266, 268, 298, 334-335, 340, 346-347, 388, 452-453, 461, 464, 465, 474, 488, 517-519, 563, 589
- water immersion, 132, 250, 265, 308
- water reclamation, 324, 345
- water system, 325, 350
- weight bearing, 202, 209-210, 232, 234, 238, 359, 364
- weight bearing activity, 359, 364
- white blood cell (WBC) count, 117, 356
- whole body surface cooling, 255, 305
- whole body vibration, 228, 229
- work, 127, 130, 133-134, 136, 138-139, 164, 169, 179, 204, 215, 226, 228-229, 231, 241, 254-255, 260, 262, 278, 286, 290, 296, 302-303, 308, 323-324, 335, 359, 361, 370, 377-378, 390-391, 399, 418, 424, 429, 443, 446-447, 461, 466, 474, 490, 500, 509, 514, 537, 551, 558, 565
- work environment, 173
- Work Environment Scale, 150
- work performance, 309, 343-344, 373
- work/rest schedule, 147, 560
- workload, 162, 167, 252, 305
- workstation, 159, 170-172, 581
- X-ray, 186, 202-203, 216, 521



